

**INTERNATIONAL CONFERENCE
DAYS ON DIFFRACTION 2016**

ABSTRACTS



June 27 – July 1, 2016

St. Petersburg

ORGANIZING COMMITTEE

V. M. Babich /Chair/, A. S. Kirpichnikova /Secretary/,
T. V. Vinogradova /Visas/, N. V. Zalesskaya /Accommodation/,
I. V. Andronov, P. A. Belov, L. I. Goray, A. Ya. Kazakov, N. Ya. Kirpichnikova,
A. P. Kiselev, M. A. Lyalinov, O. V. Motygin, M. V. Perel, A. M. Samsonov,
V. P. Smyshlyaev, R. Stone, N. Zhu

Conference e-mail: diffract16@gmail.com

Web site: <http://www.pdmi.ras.ru/~dd/>

The conference is organized and sponsored by



St. Petersburg
Department
of V.A. Steklov
Institute of Mathematics



St. Petersburg State
University



The Euler International
Mathematical Institute



ITMO University



Russian Foundation
for Basic Research



IEEE Russia (Northwest)
Section AP/ED/MTT
Joint Chapter



Russian Academy
of Sciences



The Federal Agency
for Scientific
Organizations

FOREWORD

“Days on Diffraction” is an annual conference taking place in May–June in St. Petersburg since 1968. The present event is organized by St. Petersburg State University, St. Petersburg Department of the Steklov Mathematical Institute, the Euler International Mathematical Institute and the ITMO University.

The abstracts of 280 talks to be presented at oral and poster sessions during 5 days of the Conference form the contents of this booklet. The author index is located on the last pages.

Full-length texts of selected talks will be published in the Conference Proceedings. They must be prepared in \LaTeX format and sent not later than 14 July 2016 to diffraction16@gmail.com. Format file and instructions can be found at <http://www.pdmi.ras.ru/~dd/proceedings.php>. The final judgement on accepting the paper for the Proceedings will be made by the Organizing Committee after peer reviewing.

As always, it is our pleasure to see in St. Petersburg active researchers in the field of Diffraction Theory from all over the world.

Organizing Committee

List of talks

Abramian A.K., Vakulenko S.A.	
Localized waves and modes in beams connecting to nonlinear elastic foundation	19
Eugeny G. Abramochkin, Evgeniya V. Razueva	
Three-Airy beams and Fresnel transform	19
Aero E.L., Bulygin A.N., Pavlov Yu.V.	
Methods of construction of exact analytical solutions of nonautonomous nonlinear Klein–Fock–Gordon equation	20
Altaisky M.V.	
Renormalization group and wavelet transform	21
Andronov I.V., Bilous P.Yu.	
Currents induced on the surface of a strongly elongated spheroid	21
Lutz Angermann, Vasyl V. Yatsyk, Mykola V. Yatsyk	
A mathematical model for resonance scattering and generation of oscillations by nonlinear layered or grating-like media	22
Anikin A.Yu.	
Non-commutative normal forms and inverse spectral problems	22
Astrakhantseva A.A., Chebotarev A.Yu., Grenkin G.V., Kovtanyuk A.E.	
Numerical analysis of the complex heat transfer in a layered medium	23
S.A. Avdonin, A.S. Blagoveshchensky, A. Choque Rivero, V.S. Mikhaylov	
Dynamical inverse problem for two-velocity systems on finite trees	24
Babnikov M.B., Krivtsov A.M., Tsvetkov D.V.	
Heat transfer in a harmonic crystal on an elastic foundation	25
Andrey Badanin, Evgeny Korotyaev	
Trace formulas for fourth order operators on unit interval	26
Bagaev A.A., Pis'mak Yu.M.	
The 0D quantum field theory: Multiple integrals via background field formalism	26
Bagmutov A.S., Popov I.Yu.	
Current-voltage characteristics for two quantum waveguides, connected to quantum resonators	27
Baskin L.M., Kabardov M.M., Sharkova N.M.	
Electron transport in a multi-resonator system formed by constrictions of a quantum waveguide	28
Belyaev A.K., Lobachev A.M., Modestov V.S., Semenov A.S., Shtukin L.V., Tretyakov D.A., Polyanskiy V.A., Yakovlev Yu.A.	
Propagation of sound waves in stressed elasto-plastic material	28
Belyayev Yu.N., Bozhok E.V., Malyshkin D.S.	
Coefficients of elastic waves conversion in crystal indium	29
Belyayev Yu.N., Malyshkin D.S.	
Dependences spectra of elastic waves on thickness of the scattering layer	30
Belyayev Yu.N., Malyshkin D.S., Zhibalova Yu.A.	
Coefficients of elastic waves conversion by the crystal of BaTiO ₃	30
Alexander S. Blagoveshchensky, Aleksei P. Kiselev	
A relation between two simple localized solutions of the wave equation	31

A.S. Blagoveshchensky, F.N. Podymaka	
On the Cauchy problem for the wave equation with data on a non-spatially oriented plane .	32
Blokhin A.M., Tkachev D.L.	
The problem of flow about infinite plane wedge with inviscous non-heat-conducting gas.	
Linear stability of a weak shock wave	32
Ya.L. Bogomolov, M.A. Borodov, A.D. Yunakovsky	
Method of discrete sources as an effective solver for waveguides with sharp corners	33
Borzov V.V., Damaskinsky E.V.	
On the spectrum of a discrete Schrödinger equation in one-dimensional perturbation	34
H. Boumaza, O. Lafitte	
Precised description of the spectral bands for a 2D periodic Schrödinger operator	34
Bratov V.A., Kaplunov J., Prikazchikov D.A.	
On steady-state moving load problems for elastic half-space	35
Budylin A.M., Koptelov Ya.Yu., Levin S.B.	
To the question of absolutely continuous spectrum eigenfunctions asymptotics for the case	
of three three-dimensional dissimilarly charged quantum particles scattering problem	35
Budylin A.M., Levin S.B.	
To the question of absolutely continuous spectrum eigenfunctions asymptotics justification	
for the case of three one-dimensional quantum particles scattering problem with the short-	
range pare potentials.	36
Bulatov V.V., Vladimirov Yu.V.	
Uniform asymptotics of far internal gravity waves fields from pulsating sources	36
Tsu-Chi Chang, Ying-Yu Lai, Yu-Hsun Chou, Tien-Chang Lu	
Lasing characteristics in a ZnO microcavity with designable shape fabricated by focused	
ion beam milling	37
Chebotarev A.Yu., Kovtanyuk A.E., Grenkin G.V., Prokhorov I.V.	
Analysis of a diffraction problem for equations of complex heat transfer	38
Chugainova A.P.	
Uniqueness of self-similar solutions obeying the problems of arbitrary discontinuity disintegration	
for the generalized Hopf equation with a complex nonlinearity	39
Vitalii N. Chukov	
On the Laue–Bragg–Wulff scattering of the acoustic Rayleigh wave by surface roughness . . .	40
Tomasz Danek, Michael A. Slawinski	
On elasticity-tensor symmetries: material symmetry, symmetry-group average and spatial	
average	42
Delitsyn A.L.	
Mode matching method for resonance scattering and mode localization	42
Demin D.B., Kyurkchan A.G., Kleev A.I.	
Modeling of electromagnetic scattering on small particles by means of pattern equation	
method	43
Denisova I.V., Solonnikov V.A.	
Solvability of interface problems for the compressible and incompressible Navier–Stokes	
equations near the equilibrium	44
B. Despres, L.M. Imbert-Gerard, O. Lafitte	
The hybrid resonance plasma of ions and electrons with imposed magnetic field understood	
through Bessel functions.	45

Lyudmila A. Dmitrieva, Yuri A. Kuperin, Nikolai M. Smetanin, German A. Chernykh Method of calculating Lyapunov exponents for time series using artificial neural networks committees	46
Dobrokhotov, S.Yu. Caustics, focal points, and tsunami wave problems	46
Dobrokhotov S., Klevin A., Cardinali A., Tirozzi B. High frequency Gaussian beams for cold plasma in a toroidal domain	47
Dobrokhotov S.Yu., Nazaikinskii V.E., Tirozzi B. Homogenization in the Cauchy problem for a wave equation with rapidly varying coefficients	48
Dorodnyi M.A., Suslina T.A. Homogenization of hyperbolic-type equations	49
Eglit M.E., Yakubenko T.A., Yakubenko A.E. Averaged equations of higher order for microinhomogeneous media	50
Roman O. Evstigneev, Mikhail Yu. Medvedik, Marina A. Moskaleva, Aleksei A. Tsupak The numerical solution of the problem of electromagnetic wave diffraction by a system of free located bodies screens and wires	50
Faleeva M.P., Popov I.Y. Bound state for dielectric waveguide with locally perturbed core	51
A. Fedotov, E. Shchetka Complex WKB method for difference equations in unbounded domains	51
A. Fedotov On difference equations with meromorphic coefficients	52
A. Fedotov On the reflection coefficient for the Stark–Wannier equation	52
Filippenko G.V. The energy flux analysis of the “shell” type waves in the infinite cylindrical shell filled with acoustical fluid	52
Plamen Fiziev New approach to the connection problem for general Heun’s functions	53
Garbuzov F.E., Gula I.A., Samsonov A.M., Semenov A.A. The mathematical model of a longitudinal deformation wave propagation in multilayered structures	53
Gavrilov S.N., Mochalova Yu.A., Shishkina E.V. Trapped modes of oscillation and localized buckling of a tectonic plate as a possible reason of an earthquake	54
Gerasimov D.A., Popov I.Yu., Popov A.I. Resonant states for quantum ring with two infinite leads	55
Glushkov E.V., Glushkova N.V., Miakisheva O.A. Guided waves and energy flows in the coupled structure: monopole source – acoustic liquid – immersed laminate plate	56
Golub M.V., Fomenko S.I., Alexandrov A.A., Chen A.L., Wang Y.S., Zhang Ch. Band-gaps and low transmission pass-bands in layered functionally graded piezoelectric phononic crystals	57

Golub M.V., Shpak A.N., Müller I., Fritzen C.-P. Numerical simulation of Lamb wave excitation by the partially debonded rectangular strip-like piezoelectric actuator based on the integral approach and hp-FEM	58
Goray L.I. Generalization of energy balance for diffraction by randomly rough lossy 2D surfaces	59
D. Grigoriev, S. Vakulenko, J. Reinitz, A. Weber Genetic networks can learn fitness landscape	60
Gusev V.A. Oblique incidence and propagation of intense acoustic beams in a fluid layer with bubbles	61
Kuo-Bin Hong, Chun-Chieh Yang, Tien-Chang Lu GaAs-based high index contrast photonic crystal surface emitting lasers	61
Shen-Che Huang, Kuo-Bin Hong, Tien-Chang Lu, Sailing He Design of hybrid realization of high-index contrast gratings reflectors on silicon-on-insulator platform	62
Il'yasov Kh.Kh., Nazaikinskii V.E., Sekerzh-Zen'kovich S.Ya., Tolchennikov A.A. Asymptotic estimate of the 2011 tsunami source parameters on the basis of mareograms recorded by the South Iwate GPS Buoy and the DART 21418 station	63
A.M. Ishkhanyan Single-confluent Heun solutions of the one-dimensional stationary Schrödinger equation	64
A.M. Ishkhanyan, M.V. Hakobyan, T.A. Ishkhanyan Bi-confluent Heun potentials solvable in terms of confluent hypergeometric functions	64
A.Ya. Kazakov Confluent Heun equation with single added apparent singularity: elementary, gauge and integral symmetries	65
Kholodova S.E., Peregudin S.I. On the problem of propagation of MHD waves	65
Khusnutdinova K.R., Tranter M.R. Modelling of nonlinear bulk strain waves in inhomogeneous layered bars	66
Anna Kirpichnikova Fock–Leontovich parabolic equation method on prolonged bodies with Neumann boundary conditions	67
Kirpichnikova N.Ya., Popov M.M., Semtchenok N.N. Shortwave diffraction by prolate bodies of revolution. Results of numerical experiments	67
Kiselev A.D., Plutenko D.O. Optical-force-induced dynamics of Mie scatterers in Laguerre–Gaussian beams and near-field structures	68
Kislin D.A., Kozlov S.A. Self-action features of nonparaxial optical pulses in a medium with cubic nonlinearity	69
Klushin A.M., Kurin V.V., Shereshevskii I.A., Vdovicheva N.K. Simulation of Josephson antenna in 3D space	70
Kniazev M.A., Kozlov S.A., Dolgaleva K. Noncollinear interaction of few-cycle optical waves in dispersive nonlinear medium	70
Kazuya Kobayashi Wiener–Hopf analysis of the radar cross section of a finite parallel-plate waveguide with four-layer material loading	71

Kolonitskii S.B.	
Multiplicity of solutions of the Dirichlet problem with fractional p -Laplacian in spherical annulus	72
E. Korotyaev, A. Badanin	
Resonances of fourth order operators	73
Kovtanyuk A.E., Prokhorov I.V., Chebotarev A.Yu.	
A method of diagnostics of layered biological tissues	73
Kozitskiy S.B., Trofimov M.Yu., Zakharenko A.D.	
Boundary layers and normal mode parameters in a system with double-diffusive convection at large Rayleigh numbers	73
Vladimir Kozlov	
Age-structured population model on several patches	74
V. Kozlov, U. Wennergren, S. Vakulenko	
Hamiltonian methods for complex food webs	75
Krasnov I.P.	
On electromagnetic forces and works, connected with it	75
Kravchenko O.V., Kravchenko V.F., Churikov D.V.	
Application of $ch_{a,n}$ atomic basis to numerical simulation of wave propagation problem	76
Vladislav V. Kravchenko	
Efficient construction of transmutations and a new representation for solutions of Sturm–Liouville equations, uniform with respect to the spectral parameter	77
Vladislav V. Kravchenko, Sergii M. Torba, Raúl Castillo-Pérez	
Analysis of graded-index optical fibers by the spectral parameter power series method	78
A.V. Kudrin, T.M. Zaboronkova, A.S. Zaitseva, C. Krafft	
Electrodynamic characteristics of a loop antenna located on the surface of a uniaxial anisotropic cylinder	79
Kurseeva V.Yu., Valovik D.V.	
On the infinitely many electromagnetic TE eigenmodes in a plane layered waveguide filled with nonlinear medium: analytical results	80
Kuzmina E.A., Shestopalov Y.V.	
Existence of complex waves in Goubau line: mathematical aspects	81
Kuznetsov E.V., Merzlikin A.M.	
Scattering of a surface wave on a controlled inhomogeneity	81
Nikolay Kuznetsov	
On the Benjamin–Lighthill conjecture for water waves with vorticity	82
Nikolay Kuznetsov, Oleg Motygin	
Freely floating bodies trapping time-harmonic waves in water covered by brash ice	83
A.G. Kyurkchan, S.A. Manenkov	
Application of the modified method of discrete sources to the solution of the problem of a flow of a compact body and periodically rough surface	83
B.A. Lagovsky, A.B. Samokhin, V.I. Nefedov	
Superresolution based on interpolation and extrapolation of received signals	84
Liu T., Solntsev A.S., Neshev D.N., Sukhorukov A.A., Boes A., Mitchell A.	
Bidirectional adiabatic light transfer in coupled waveguides	85

Hanen Louati, Michel Rouleux Semiclassical quantization rules for a periodic orbit of hyperbolic type	86
Tien-Chang Lu Wide-bandgap optoelectronics with micro/nano-scale architectures	86
Lyalinov M.A., Polyanskaya S.V. Eigenoscillations in a water-wave problem for an infinite pool of special form	88
Machikhin A.S., Burmak L.I. Calculation of interference pattern after diffraction of two interfering image-carrying beams by acoustic wave in uniaxial crystal	88
Makin V.S., Makin R.S., Pestov Yu.I. Abnormal spatial nanogratings formation by long pulse durations laser radiation on condensed matter surfaces	90
Maly S.V., Arlova H.S. A technique of multichannel scattering matrices calculation in solving electrodynamic and acoustic problems by the minimal autonomous blocks method	90
Mamaikin M.S., Komissarova M.V., Zakharova I.G. Propagation of light bullets in media with quadratic nonlinearity	91
Vasily Maximov, Sergey Kshevetskii Numerical simulation of internal waves generation by the flow over uneven bottom in the stratified liquid	92
Melnikov A.S., Shereshevskii I.A., Vdovicheva N.K. On Bogoliubov – de Gennes equation for Kitaev chain	93
Fabian L. Müller, Christoph Schwab Finite elements for linear wave propagation in polygonal domains	93
Nakonechny A.G., Podlipenko Y.K., Shestopalov Y.V. Guaranteed estimation of solutions to Helmholtz problems from pointwise noisy observations	95
Sergei A. Nazarov Transmission conditions in a one-dimensional model of bifurcating arteria	95
Neely S.T., Rasetshwane D.M. Acoustic reflectance probes the inner ear	96
Grigory Panasenko, Konstantin Pileckas Asymptotic analysis of the non-steady Navier–Stokes equations in thin structures	97
Svetlana Pastukhova Homogenization of “double porosity” models for fourth order equations. Spectral problems	98
Peregudin S.I., Kholodova S.E. Long waves above the deformable bottom	98
Perel M.V., Sidorenko M.S. Asymptotic study of two-scale electromagnetic field in layered periodic structure	99
Pereskokov A.V. New type of semiclassical asymptotics eigenstates near the boundaries of spectral clusters for Schrödinger-type operators	100
Petrov P.S., Petrova T.N. On sound propagation in a shallow-water acoustical waveguide with variable bottom slope	100
Petrova Y.P. Spectral asymptotics in some problems with integral constraints	101

Boris Plamenevskii, Aleksandr Poretskii	
Electromagnetic waveguides with several cylindrical ends and non-homogeneous filling	101
Agnieszka Popiołek-Masajada, Jan Masajada, Łukasz Płociniczak	
Optical vortex microscope-analytical model	102
A. Popov, I. Prokopovich, D. Edemskii	
Experimental implementation of microwave subsurface holography	103
Evelina V. Prozorova	
Influence of dispersion and structure molecules on time relaxation	104
Pryanishnikova E.A., Belyaeva N.A., Stolin A.M., Stelmakh L.S.	
Mathematical model of the flow of compressible material in cylindrical channel with variable cross section	104
Puzyrev D.N., Kozlov S.A.	
Diffraction spectrum change in few-cycle wave structure	105
Vladimir Rabinovich, Josue Hernandez-Juarez	
Effective methods of numerical estimates of acoustic fields in the stratified ocean generated by moving airborne sources	106
Rastegaev N.V.	
On spectral asymptotics of the tensor product of operators with almost regular marginal asymptotics	107
Evgeniya V. Razueva, Eugeny G. Abramochkin	
Integral representation of spiral light beams	108
Rudnitsky A.S.	
Phase-shifting exposure in photolithography using a Gaussian beam of an odd order	109
Rushchitsky J.J., Yurchuk V.N.	
Approximate approach to description of evolution of plane nonlinear elastic wave with different types of initial profile	110
Saburova N.Yu., Korotyaev E.L.	
Magnetic Schrödinger operators on periodic discrete graphs	111
A.B. Samokhin, A.S. Samokhina	
FFT techniques for numerical solution of volume singular integral equations of electromagnetics	112
Saritskaya Zh.Yu.	
Stability of inverse coefficient problems' solutions for semilinear equations	112
Valeriia Sedaikina	
Acoustical imaging in semi-geodesic coordinates	113
Sergeev S.A.	
Formulas of van Vleck type for the Cauchy problem for differential and pseudodifferential equations in the one-dimensional case	113
Shafarevich A.I., Tsvetkova A.V.	
The Laplacian on a homogeneous tree with general matching conditions. The wave equation	114
Shanin A.V.	
Dispersion diagrams and first arriving signals in layered waveguides	114
Shanin A.V., Korolkov A.I.	
Diffraction by an impedance strip in parabolic approximation	115

Shchelik G.S., Sofronov I.L.	
Application of semi-analytical finite element method (SAFE) to inversion of acoustic logging data in non-cylindrical boreholes in anisotropic formation	116
Shestakov P.Yu., Marchenko S.V.	
Tunneling of Gaussian light pulses in chirped Bragg grating	117
Skvortsov D.S., Konobeeva N.N., Belonenko M.B.	
Ultrashort optical pulses in germanene in the 3D case	118
Sloushch V.A.	
Estimates for the singular numbers of the sandwiched Airy transformation	119
Smolkina M.O., Popov I.Y.	
Nodal count theorem for quantum tree graphs with δ -coupling	119
Irina A. So, Aleksei P. Kiselev, Alexandr B. Plachenov	
Gaussian beam in a gradual transition from a waveguide to an antiwaveguide	120
Spiridonov A.O., Karchevskii E.M.	
Mathematical and numerical analysis of the spectral characteristics of dielectric micro-cavities with active regions	121
Ivan A. Starkov, Alexander S. Starkov	
Impact of conical points on the object's scattered field	122
Suslina T.A.	
Homogenization of high-order elliptic equations	123
Trofimov M.Yu., Kozitskiy S.B., Zakharenko A.D.	
Weak shear modulus in the acoustic mode parabolic equation	124
Ul'yanov S.V.	
Light scattering from smectic C* film with anisotropic electrostatic interaction	125
Utkin A.B.	
Spacetime triangle diagram technique for sectoral horn waveguides	125
Vasilchuk V.	
Asymptotic distribution of the spectrum of some symmetric polynomials of unitary invariant random matrix ensembles	126
Wojda P., Kshevetskii S.P.	
The finite difference methods of computation of X-rays propagation through a system of many lenses	127
N.F. Yashina, T.M. Zaboronkova, C. Krafft	
Interaction of nonsymmetric electromagnetic waves guided by an anisotropic cylinder	127
V. Zalipaev, V. Vialov	
Electromagnetic guided waves on infinite periodic linear arrays of thin metallic conductors	128
German L. Zavorokhin	
A fractal graph model of capillary type systems	129
K. Zhelyazkova, M. Petrov, B. Katranchev, G. Dyankov	
Guided modes and surface plasmon exploration of cholesteric liquid crystal cell	130
Zhuchkova M.G.	
Wave propagation in a floating elastic plate with a periodic support	130
V. Zverzhcovsky, A. Bolotova, A. Kretushev, T. Vyshenskaya	
Phase images of living lymphocytes and its quantitative parameters obtained from optical model	131

Workshop on nanophotonics and metamaterials

Alekseev G.V., Lobanov A.V., Larkina O.S.	
Theoretical analysis of material body cloaking problems using the optimization method	133
Altaisky M.V., Kaputkina N.E., Krylov V.A.	
Advantages of quantum dot arrays for non-algorithmic information processing by quantum neural networks	134
Andryieuski A., Kuznetsova S.M., Odit M., Zhukovsky S.V., Kapitanova P., Kivshar Y.S., Lavrinenko A.V.	
Water based tunable all-dielectric microwave metamaterials	134
Babicheva V.E., Petrov M.I., Baryshnikova K.V., Belov P.A.	
Substrate-mediated antireflective properties of silicon nanoparticle array	135
J.D. Baena, S.B. Glybovski, J.P. del Risco, A.P. Slobozhanyuk, P.A. Belov	
Experimental characterization of microwave self-complementary metasurfaces for linear-to-circular polarization transform	136
D.A. Baranov, R. Malureanu, O. Takayma, A.K. Samusev, I.V. Iorsh, A.A. Bogdanov, A.V. Lavrinenko	
Attenuated total reflection spectroscopy of hybrid localized optical surface states in anisotropic metasurface	137
Baryshnikova K.V., Shalin A.S., Terekhov P.D., Khromova I.A., Evlyukhin A.B.	
Nonradiating anapole modes of dielectric nanoparticles in microwave range	138
Tobias Birr	
Time resolved ultrafast surface plasmon-polaritons	139
Benimetskiy F.A., Plekhanov A.I., Kuchyanov A.S., Parkhomenko R.G., Basova T.V.	
Characterization of the structure and stimulated emission of spherical and cylindrical spasers	140
Nicolas Bonod	
Silicon: an interesting material for optical antennas	141
Butko L.N., Anzulevich A.P., Pavlov D.	
Focusing of electromagnetic waves through the wired structure	141
V.S. Butylkin, Yu.N. Kazantsev, G.A. Kraftmakher, V.P. Mal'tsev	
Voltage controlled nonreciprocal metastructure ferrite/array of twice split rings with varactors	142
I.Yu. Chestnov, M.V. Charukhchyan, A.P. Alodjants, X. Ma, O.A. Egorov	
Nonlinear dynamics of coherent exciton polaritons in a periodic potential	143
P. Chhantyal, T. Birr, U. Zywietz, B.N. Chichkov, C. Reinhardt, S. Naskar, N. Bigall	
Quantum nanoparticles doped waveguide for light propagation	143
Yu-Hsun Chou, Tzy-Rong Lin, Chien-Chung Lin, Tien-Chang Lu	
Ag-based surface plasmon polariton nanolaser	144
E.D. Chubchev, A.A. Pukhov, A.P. Vinogradov	
Applicability of two-level approximation describing dynamics of spaser with four-level meta-molecule	145
Andrea Colombi, Richard V. Craster	
Full control of the A_0 mode in a plate using a locally resonant metamaterial	145
Dadoenkova N.N., Dadoenkova Yu.S., Panyaev I.S., Rozhleys I.A., Lyubchanskii I.L., Krawszyk M., Sannikov D.G.	
Complex photonic structure based on magneto-optic waveguide and photonic crystal	147

Dadoenkova Yu.S., Bentivegna F.F.L., Dadoenkova N.N., Lyubchanskii I.L., Lee Y.P. Goos–Hänchen shift of a light beam upon reflection from a magnetic film on a non-magnetic substrate: effect of misfit strain	148
Dadoenkova Yu.S., Bentivegna F.F.L., Dadoenkova N.N., Lyubchanskii I.L., Petrov R.V., Bichurin M.I. Electric and magnetic tuning of the Goos–Hänchen shift of a light beam upon reflection from a magneto-electric heterostructure	149
Bair Damdinov, Anton Demin, Tuyana Dembelova Viscoelastic properties of colloids	150
M. Danaeifar, N. Granpayeh Analysis of metasurface based structures by using equivalent conductivity method	150
V.I. Demidchik, R.V. Kornev The influence of non-uniformly scaled conducting inclusions on range properties of a layer of bi-isotropic composite material	152
Dmitriev P.A., Baranov D.G., Milichko V.A., Makarov S.V., Mukhin I.S., Samusev A.K., Krasnok A.E., Belov P.A., Kivshar Y.S. Enhancement of Raman scattering by magnetic resonances of crystalline silicon nanoparticles	153
Dolganov P.V., Dolganov V.K. Optical properties, density of photonic states and dispersion of light in liquid-crystalline photonic crystals	153
Dolganov P.V., Dolganov V.K., Gordeev S.O. Local optical anisotropy, diffraction and orientational order parameter in cholesteric photonic crystals	154
Doskolovich L.L., Bykov D.A., Bezus E.A. Optical implementation of differential operators with resonant nanophotonic structures	155
Vladimir P. Drachev Plasmonics from deep UV to far IR	156
Dyakov S.A., Gippius N.A., Dai J., Yan M., Qiu M. Bistability effect in near-field radiative heat transfer	157
Shanhui Fan Nanophotonics: controlling the flow of light and heat	158
Mathias Fink Wave control with space-time manipulations	158
Natalie Firsova Quantum description of nanoantenna properties of a graphene membrane	158
T. Fischer, U. Zywietz, T. Birr, A.B. Evlyukhin, C. Reinhardt, B.N. Chichkov Controlling light on the nanoscale by ultra-flat particle lenses	159
Fomenko S.I., Aleksandrov A.A. Simulation and analysis of wave propagation in periodic and aperiodic composites	160
Friziuk K.S., Krasnok A.E., Petrov M.I. Purcell enhanced Raman scattering from silicon nanoparticles	161
Friziuk K.S., Milichko V.A., Petrov M.I., Zuev D.A., Baranov A.V., Baranov M.A., Mukhin I.S., Makarov S.V., Krasnok A.E. Raman scattering governed by dark resonant modes in silicon nanoparticles	162

Galyamin S.N., Tyukhtin A.V., Peshkov A.A. Electromagnetic field of a charge flying into chiral isotropic medium	163
Pavel Ginzburg, Andrey A. Bogdanov, Aliaksandra Ivinskaya, Alexander S. Shalin Opto-mechanical metamaterials	164
Golenitskii K.U., Bogdanov A.A. Tamm–Langmuir surface waves	165
Golovan L.A., Kholodov M.M., Presnov D.E., Zaboltnov S.V., Efimova A.I., Timoshenko V.Yu., Neskromnaya A.V., Petrov G.I., Yakovlev V.V. Nonlinear-optical anisotropy of silicon nanowire arrays	166
Gorlach M.A., Poddubny A.N. Two-photon excitations in nonlinear topological Su–Schrieffer–Heeger model	167
Grachev A.A., Sadovnikov A.V., Beginin E.N., Sharaevskii Yu.P., Sheshukova S.E. Discrete diffraction and refraction of spin waves in magnonic waveguide lattice	168
Rachel Grange Enhancing nonlinear optical signal in Perovskite nanostructures	169
Hartmann M., Wohler M., Schühler M., Weisgerber L., Thielecke J., Heuberger A. A dual frequency antenna for RSSI-based DOA estimation: from theory to prototype	169
Hasan M., Iorsh, I.V., I.A. Shelykh Topological properties of the illuminated arrays of mesoscopic rings	170
A.A. Hurshkainen, S.B. Glybovski, I.V. Melchakova, I.J. Voogt, C.A.T. van den Berg, A.J.E. Raaijmakers Decoupling of antennas with wire metasurface structures: MRI applications	172
Ivanov A.V., Lagarkov A.N., Sarychev A.K. Metal-dielectric substrates for high-sensitive chemical detection	173
K.A. Ivanov, E.I. Girshova, S.J. Clark, M.A. Kaliteevski, A.J. Gallant Anharmonic Bloch oscillations in biased artificial and natural superlattices	174
Aliaksandra Ivinskaya, Pavel Ginzburg, Alexander S. Shalin Plasmonic substrates for optical tweezers	175
M.A. Kaliteevski, G. Pozina, E.V. Nikitina, D.V. Denisov, N.K. Polyakov, E.V. Pirogov, L.I. Goray, K.A. Ivanov, A.Yu. Egorov, S.J. Clark Coherent radiative mode in InAs-monolayer Bragg structures	176
M.A. Kaliteevski, V.A. Mazlin, K.A. Ivanov, A.R. Gubaydullin Quantization of electromagnetic field in an inhomogeneous medium based on scattering matrix formalism (S-quantization)	177
Chul Kang, Inhee Maeng, Chul Sik Kee, Jung Woo Leem, Jae Su Yu, Tae Heon Kim, Jong Seok Lee Strong emission of terahertz radiation from two dimensional arrays of nanostructures on Ge wafers	178
B. Kanté Bound state in the continuum nanophotonic laser	179
Kapitanova P.V., Song M., Belov P.A. Wireless power transfer system based on high-index dielectric resonators	180
Alexander B. Khanikaev Reconfigurable and all-dielectric photonic topological insulators	181

Yuri Kivshar

All-dielectric resonant nanophotonics and metasurfaces 183

Kolodny S.A., Yali Sun, Zuev D.A., Makarov S.V., Milichko V.A., Starikov S.V., Mukhin I.S., Morozov I.A., Belov P.A., Krasnok A.E.

Influence of fs-laser modification on coupling effects between hybrid nanoparticles 184

Kondratov A.V., Gorkunov M.V., Darinskii A.N.

Optical chirality of 2D- and 3D-chiral metal hole arrays 185

Konobeeva N.N., Ten A.V., Belonenko M.B.

About dipole moment in doped carbon nanotubes 186

Kononchuk R., Smith K., Chabanov A.A., Makri E., Kottos T., Vitebskiy I.

Hypersensitive transport in asymmetric photonic layered media 187

K.L. Koshelev, A.A. Bogdanov

Slow light in nonlocal anisotropic metamaterials 188

Kosulnikov S.Yu., Vovchuk D.A., Filonov D.S., Glybovski S.B., Mirmoosa M.S., Nefedov I.S., Tretyakov S.A., Belov P.A., Simovski C.R.

Wire media for molding electromagnetic fields 189

Kovrov A.E., Kadochkin A.S., Mukhin I.S., Voroshilov P.M., Simovski C.R., Shalin A.S.

Optically asymmetric structures for transparent electrodes 190

G.A. Kraftmakher, V.S. Butylkin, Yu.N. Kazantsev, V.P. Mal'tsev

Identifying microwave magnetic response of chiral elements through reflection for new applications 191

V.G. Kravets, F. Schedin, O.P. Marshall, A.N. Grigorenko

Nanoscale conductive filaments and quantized optical properties of plasmonic nanoarrays . . 191

Kruk S.S., Hopkins B., Kravchenko I., Miroshnichenko A., Neshev D.N., Kivshar Yu.S.

Broadband all-dielectric metasurfaces for polarization control with near-unity efficiency . . . 192

Kruk S.S., Wong Z.J., Pshenay-Severin E., O'Brien K., Neshev D.N., Zhang X., Kivshar Yu.S.

Magnetic hyperbolic dispersion in optical metamaterials 193

Lemoult F., Kaina N., Fink M., Lerosey G.

Locally resonant metamaterials beyond homogenization: subwavelength control of waves, negative refraction and other exotic phenomena 194

Ladutenko K.S., Belov P.A., Peña O., Mirzaei A., Miroshnichenko A.E., Shadrivov I.V.

Efficient absorption of light by nanoparticles designed by a stochastic optimizer 195

Mikhail Lapine

On the convergence from finite size and discrete structure towards homogeneous metamaterials 195

Lepeshov S.I., Zuev D.A., Makarov S.V., Miroshnichenko A.E., Krasnok A.E., Belov P.A.

Tuning of hybrid oligomers via fs-laser reshaping at nanoscale 196

Li S.V., Baranov D.G., Krasnok A.E., Belov P.A.

Chiral near-field formation with all-dielectric nanoantennas 197

Zhijie Ma, Stephen Hanham, Pablo Albella, Stefan Maier, Minghui Hong

Terahertz all-dielectric magnetic mirror metasurface 198

Stefan A. Maier

Applications of plasmonic and dielectric nanoantennas in nanophotonics 199

Mamonov E.A., Kolmychek I.A., Maydykovskiy A.I., Magnitskiy S.A., Murzina T.V. Chirality of planar G-shaped metamaterials evidenced by polarization-resolved SHG microscopy	200
Maslovski S.I. Metamaterial thermal superemitters and superabsorbers	201
Melik-Gaykazyan E.V., Zubyuk V.V., Shorokhov A.S., Kroychuk M.K., Shcherbakov M.R., Dolgova T.V., Fedyanin A.A., Choi D.-Y., Neshev D.N., Kivshar Y.S. Unidirectional second-harmonic generation from silicon nanoparticles	202
Merzlikin A.M., Puzko R.S. Self-averaging of effective refractive index in layered system	203
Miniaci M., Krushynska A.O., Bosia F., Pugno N.M. Large-scale mechanical metamaterials for seismic wave shielding	204
Mirmoosa M.S., Simovski C.R. Magnetic Purcell factor in polaritonic wire media	205
O. Mitrofanov, I. Khromova, T. Siday, R.J. Thompson, I. Brener, T.S. Luk, J.L. Reno THz near-field microscopy: application to spectroscopy of sub-wavelength resonators	206
I. Munina, P. Turalchuk, E. Kunakovskaya, I. Vendik, Michail Derkach Estimation of attenuation of EM waves propagating through interface biological tissue/free space	207
Nefedov I.S., Boardman A.D. Surface and leaky waves in a waveguide, filled with graphene-based hyperbolic metamaterial	207
A. Nikulin, S. Glybovski, I. Melchakova, P. Belov, B. Larrat, E. Georget, S. Enoch, R. Abdeddaim Tuning and matching of antennas for preclinical MRI with metamaterial structures	208
Mikhail Omelyanovich, Sergey Makarov, Valentin Milichko, Constantin Simovski Full broadband absorption of perovskite solar cells with plasmonic nanoparticles	209
Sergey Pasechnik, Dina Shmeliova, Anton Chopic, Denis Semerenko, Semen Charlamov, Alexander Dubtsov Electrically controlled porous polymer films filled with liquid crystals: new possibilities for photonics and THz applications	210
Dmitrii Pavlov, Leonid Butko, Anton Anzulevich Refraction angle of electromagnetic wave on a wired structure prism	211
Alexander Yu. Petrov, Pavel N. Dyachenko, Slawa Lang, Elisabeth W. Leib, Jefferson do Rosario, Sean Molesky, Zubin Jacob, Tobias Krekeler, Martin Ritter, Michael Störmer, Tobias Vossmeier, Horst Weller, Gerold Schneider, Manfred Eich Tungsten based metamaterials and photonic crystals for selective thermal emitters	212
Polischuk O.V., Popov V.V., Melnikova V.S. Wide-aperture superabsorption of terahertz radiation by plasmonic periodic array of graphene nanoribbons	213
Popov V.V., Novitsky A.V. Bianisotropic effective medium for subwavelength multilayers	214
Alexander Rusakov, Irina B. Vendik, Komsan Kanjanasit, Jiasheng Hong, Dmitry Filonov Ultra-wideband antenna with single- and dual-band notched characteristics based on electric ring resonator	215
Rustomji K., Abdeddaim R., Kuhlmeier B., Enoch S. Measurements of polarisation dependent Purcell factor in microwave metamaterials	216

M.V. Rybin, D.S. Filonov, K.B. Samusev, P.A. Belov, Y.S. Kivshar, M.F. Limonov Concept of phase transitions between photonic crystals and all-dielectric metamaterials	217
Mikhail V. Rybin, Mikhail F. Limonov Complex photonic band diagram and \mathcal{PT} -symmetry in periodic media	218
Mikhail V. Rybin, Sergei F. Mingaleev, Mikhail F. Limonov, Yuri S. Kivshar Purcell effect and Lamb shift for photonic modes	219
Sadrieva Z.F., Sinev I.S., Samusev A.K., Iorsh I.V., Bogdanov A.A., Lavrinenko A.V. Optical bound state in the continuum in one-dimensional photonic crystal slab: theory and experiment	219
K.B. Samusev, A.D. Sinelnik, M.V. Rybin, S.Y. Lukashenko, Y.S. Kivshar, M.F. Limonov Transition from photonic crystals to metasurfaces in optical Laue diffraction	220
Sarychev A.K., Vergeles S.S., Tartakovsky G. Transducer of light to longitudinal electric field in sub-wavelength volume	221
Savelev R.S., Yulin A.V., Krasnok A.E. Solitary waves in chains of silicon nanoparticles	222
Shadrivov, I.V. Liquid metamaterials	223
Shchelokova, A.V., Melchakova, I.V., Belov, P.A., Slobozhanyuk, A.P. Metasurfaces for magnetic resonance imaging	224
Shcherbakov, M.R., Vabishchevich, P.P., Shorokhov, A.S., Fedyanin, A.A., Chong, K.E., Choi, D.-Y., Staude, I., Miroshnichenko, A.E., Neshev, D.N., Kivshar, Yu.S. Ultrafast semiconductor metasurfaces: all-optical switching beyond free carriers	225
Shishkov V.Yu., Andrianov E.S., Pukhov A.A., Vinogradov A.P. Canonical quantization of surface plasmon polaritons	225
Shorokhov A.S., Melik-Gaykazyan E.V., Shcherbakov M.R., Fedyanin A.A., Smirnova D.A., Hopkins B., Chong K.E., Choi D.-Y., Miroshnichenko A.E., Neshev D.N., Kivshar Y.S. Third-harmonic generation spectroscopy of magnetic Fano resonances in oligomers of silicon nanoparticles	226
K.V. Shulga, M.V. Fistul, I. Besedin, S. Butz, E. Il'ichev, A.V. Ustinov Magnetically induced transparency of superconducting qubits array	227
Simovski C.R., Albooyeh M., Tretyakov S.A. Electromagnetic characterization of $p - m$ metasurfaces	228
Sinev I.S., Iorsh I.V., Bogdanov A.A., Permyakov D.V., Komissarenko F.E., Mukhin I.S., Samusev A.K., Miroshnichenko A.E., Kivshar Y.S. Light scattering and localization by silicon nanoparticle on metal	230
Smirnov Yu.G., Derevyanchuk E.D. Rotation method for the reconstruction of anisotropic electromagnetic characteristics of metamaterials	231
Spivak Yu.E. Numerical analysis of 2D approximate cloaking problem with using M layered shell	232
Ivan A. Starkov, Alexander S. Starkov Application of the matrix homogenization method to the Maxwell equations	233
A.A. Starovoytov, T.A. Vartanyan, V.I. Belotitskii, Yu.A. Kumzerov, A.A. Sysoeva, N.O. Alexeeva, V.G. Solovyev Emission of cyanine dye embedded in nanopores of anodic alumina matrix	234

Yue Sun, Andrey E. Miroshnichenko, Andrey A. Sukhorukov Opto-mechanical interactions in silicon nanoparticles	235
Sylgacheva D.A., Khokhlov N.E., Kalish A.N., Belotelov V.I., Dagesyan S.A., Shaposhnikov A.N., Berzhansky V.N. Magneto-optical nonreciprocity of the waveguide modes of photonic crystals in transverse magnetic field	236
Treviño C., Kononchuk R., Smith K., Vitebskiy I., Chabanov A.A. Induced transmission and enhanced Faraday rotation in ferromagnetic thin films	237
Tribelsky M.I., Miroshnichenko A.E. Light scattering by particles with high refractive index	238
Pavel Turalchuk, Irina Munina, Vladimir Yashenko, Orest Vendik Two-mode loop antenna with doubled gain	239
Vavulin D.N., Sukhorukov A.A. Generation of photon pairs through spontaneous four-wave mixing in nonlinear waveguides with the account of losses	240
Irina Vendik, Orest Vendik, Vladimir Pleskachev, Vitaly Kirillov Modeling and experimental investigations of on-body electromagnetic wave propagation ...	241
Voytova T.A., Makarov S.V., Tsyarkin A.N., Milichko V.A., Mukhin I.S., Yulin A.V., Putilin S.E., Baranov M.A., Krasnok A.E., Belov P.A. Third harmonic generation from the silicon self-organized nanostructured surface	242
Yermakov O.Y., Bogdanov A.A., Iorsh I.V., Lavrinenko A.V. New degrees of freedom of spin-optonics implemented by using hybrid surface waves localized at hyperbolic metasurface	243
Zagursky D.Yu., Trofimov V.A., Zakharova I.G. Enrichment of few-cycle pulse spectrum by non-linear interaction with medium	244
Zharov A.A., Zharov A.A. Jr., Zharova N.A. On the influence of the thermal disorientation of meta-atoms on electromagnetic properties of liquid metacrystals	245
Alexander A. Zharov Jr., Alexander A. Zharov, Nina A. Zharova Manipulations with surface plasmon excitation via the scattering of light by a nanoparticle: scanning and switching	245
Zharova N.A., Zharov A.A., Zharov A.A., Jr. Spectral diffusion of light in deformed (conformally squeezed and stretched) hyperbolic metamaterial	246
D.V. Zhirihin, S.B. Glybovski, P.A. Belov, C.R. Simovski, S.A. Tretyakov A perfectly absorbing mushroom metasurface for two arbitrary angles of incidence	247
Zograf G.P., Makarov S.V., Zuev D.A., Milichko V.A., Mukhin I.A., Krasnok A.E., Belov P.A. Novel method for fabrication of high-index metal-dielectric core-shell nanoparticles for advanced optical applications	248
Zuev D.A., Makarov S.V., Milichko V.A., Krasnok A.E., Belov P.A., Baranov D.G., Miroshnichenko A.E., Mukhin I.S., Morozov I.A. Reversible and non-reversible tuning of hybrid optical nanoresonators	248
U. Zywiets, T. Fischer, T. Birr, A.B. Evlyukhin, C. Reinhardt, B.N. Chichkov Laser printed nanoparticles to control light on the nanoscale	249

Localized waves and modes in beams connecting to nonlinear elastic foundation

Abramian A.K., Vakulenko S.A.

Institute for Problems in Mechanical Engineering of the Russian Academy of Sciences, V.O., Bolshoj pr. 61, St. Petersburg, Russia

e-mails: andabr55@gmail.com, vakulenfr@mail.ru

In some beams connected to nonlinear elastic foundation the formation and interaction of localized modes and waves are possible. These systems can describe, for example, nonlinear dissipative or elastic media with inclusions. The investigation of a nonlinear evolution of such modes shows the possibility of coherent structures formation. The slow time evolution of coherent structures is defined by an integrable Hamiltonian system with the single degree of freedom for the case of a single localized mode. The interaction of a fluid and a nonlinear elastic structure in which a solitary wave is propagate lead to formation of a soliton like wave propagating in a fluid. As examples the following problems are considered: 1. the interaction of an oscillating beam with nonlinear and linear inclusions and a fluid; 2. waves caused by a soliton moving along an elastic structure at the surface of the fluid. The second problem has the following physical background. In the process of an earthquake the interaction of an elevation of the sea bottom with a fluid is an issue. The sea bottom is modeled as an elastic plate, subjected to tension at its edges (the plate is subjected in perpendicular to the mentioned edges direction to the action of compression forces). The fluid is assumed to be compressible, so it is possible to take both gravity and acoustics effects into account. This model is reduced to the nonlinear equation for an imaginary beam-strip cut out of the central part of the plate. The beam-strip lies on a nonlinear elastic foundation and interacts with a fluid. The solution of that equation can be done analytically for two asymptotic cases: when soliton has a large or narrow width. The investigation shows that the coherent structures lead to slowly damping quasiperiodic waves (with slowly oscillating amplitudes) which can exist in the beam and the fluid. The nontrivial structures occur as a result of the interaction of localized modes through their tails. Geometric nonlinearity of an elastic foundation causes quasiperiodic and chaotic regimes. For the shallow water case the fluid action reduces to a change of tension of a beam and also act as an added mass. For an infinite volume of fluid a fluid acts as a dissipative media.

Three-Airy beams and Fresnel transform

Eugeniy G. Abramochkin, Evgeniya V. Razueva

Lebedev Physical Institute, Samara, 443011, Russia

e-mail: ega@fian.smr.ru

It is well known [1] that the propagation of a paraxial light field in free space along z axis obeys the equation

$$\left(\frac{\partial^2}{\partial x^2} + \frac{\partial^2}{\partial y^2} + 4i\frac{\partial}{\partial z}\right)F(x, y, z) = 0, \quad (1)$$

where F is the field complex amplitude and x, y, z are normalized (dimensionless) variables. If the field initial distribution is known, $F(x, y, 0) = F_0(x, y)$, then the solution of the paraxial wave equation (1) is the Fresnel transform of the initial field:

$$F(x, y, z) = \mathbf{FR}_z[F_0(\xi, \eta)](x, y) = \frac{1}{\pi iz} \iint_{\mathbb{R}^2} \exp\left(\frac{i}{z}[(x - \xi)^2 + (y - \eta)^2]\right) F_0(\xi, \eta) d\xi d\eta. \quad (2)$$

Three-Airy beams are a kind of solutions of the equation (1) whose initial field distribution is defined as a product of three Airy functions with linear arguments:

$$F_0(x, y) = t\text{Ai}(x, y; c) = \text{Ai}\left(\frac{x\sqrt{3} - y}{2} + c\right)\text{Ai}\left(\frac{-x\sqrt{3} - y}{2} + c\right)\text{Ai}(y + c). \quad (3)$$

Here c is the displacement parameter determining the shape of the field intensity.

It is known [2] that the Fourier image of these beams has a cubic phase and a radially symmetric intensity with super-Gaussian decrease:

$$\iint_{\mathbb{R}^2} e^{-i(x\xi+y\eta)} \text{tAi}(\xi, \eta; c) d\xi d\eta = \frac{2}{3^{5/6}} \exp\left(-\frac{2i}{27}(3x^2y - y^3)\right) \text{Ai}\left(3^{2/3}c + \frac{2}{3^{4/3}}(x^2 + y^2)\right). \quad (4)$$

We simplify the Fresnel transform of the field (3),

$$\mathbf{FR}_z[\text{tAi}(\xi, \eta; c)](x, y) = \frac{1}{\sqrt{\pi}} \exp\left(\frac{9icz}{8} + \frac{9iz^3}{512} + \frac{\pi i}{4}\right) \int_{\mathbb{R}} e^{-it^2} \text{tAi}\left(x, y; c + t\sqrt{\frac{z}{2} + \frac{9z^2}{64}}\right) dt \quad (5)$$

and consider some corollaries of this result.

References

- [1] M. B. Vinogradova, O. V. Rudenko, A. P. Sukhorukov, *Wave theory*, Nauka, Moscow (1979).
- [2] E. Abramochkin, E. Razueva, *Optics Letters*, **36**, 3732–3734 (2011).

Methods of construction of exact analytical solutions of nonautonomous nonlinear Klein–Fock–Gordon equation

Aero E.L., Bulygin A.N., Pavlov Yu.V.

Institute for Problems in Mechanical Engineering of Russian Academy of Sciences, St. Petersburg, Russia

e-mail: yuri.pavlov@mail.ru

Methods of finding of exact analytical solutions are given for the nonautonomous nonlinear Klein–Fock–Gordon equation

$$U_{xx} + U_{yy} + U_{zz} - \frac{U_{tt}}{v^2} = p(x, y, z, t) F(U). \quad (1)$$

Here $F(U)$ and $p(x, y, z, t)$ are arbitrary functions, and the subscript means the derivative with respect to the corresponding variable. We seek for the solution of the equation (1) in the form of complex function $U = \Psi(W)$. The equations for definition of the functions $\Psi(W)$ and W are suggested. The function $\Psi(W)$ is given by inversion of integral which is defined by the function $F(U)$. Function W is found by method of the construction of functionally invariant solutions of the partial differential equations. H. Bateman has developed this method for the theory of distribution of electromagnetic waves [1]. Functionally invariant solutions of the autonomous nonlinear Klein–Fock–Gordon equation and sine-Gordon equation are found by authors [2]–[5].

The function W has a form of arbitrary function, which depends of one $\tau(x, y, z, t)$ ($W = f(\tau)$) or two $\alpha(x, y, z, t)$, $\beta(x, y, z, t)$ ($W = f(\alpha, \beta)$) specially constructed functions. They are called ansatzes. Ansatzes (τ, α, β) are defined as solutions of some special equations (algebraic or the mixed, algebraic and differential with partial derivatives). These equations contain arbitrary functions depending on (τ, α, β) . The offered methods allow to find the solutions for special, but wide class of the nonautonomous nonlinear Klein–Fock–Gordon equations. The general methods are illustrated by the examples of some exact solutions.

References

- [1] H. Bateman, *The Mathematical Analysis of Electrical and Optical Wave–Motion: On the Basis of Maxwell’s Equations*, Cambridge University Press, Cambridge (1915).
- [2] E. L. Aero, A. N. Bulygin, Yu. V. Pavlov, *Theor. Math. Phys.*, **158**, 313–319 (2009).
- [3] E. L. Aero, A. N. Bulygin, Yu. V. Pavlov, *Differential Equations*, **47**, 1442–1452 (2011).
- [4] E. L. Aero, A. N. Bulygin, Yu. V. Pavlov, *Appl. Math. Comput.*, **223**, 160–166 (2013).
- [5] E. L. Aero, A. N. Bulygin, Yu. V. Pavlov, *Theor. Math. Phys.*, **184**, 961–972 (2015).

Renormalization group and wavelet transform

Altaisky M.V.

Space Research Institute RAS, Profsoyuznaya 84/32, Moscow 117997, Russia

e-mail: altaisky@mx.iki.rssi.ru

The renormalization group (RG), initially discovered by Stueckelberg and Petermann as a group of reparametrizations of the S matrix, emerging after cancellation of divergences, has further evolved into a powerful mathematical method that enables the study of the collective (large-scale) degrees of freedom of complex nonlinear systems by iteratively integrating out the small scales modes with appropriate rescaling of the fields and the parameters of the system. The physical relevance of the RG method is in a good deal due to the Kadanoff blocking procedure, which assumes that the coarse-grained blocks of the system degrees of freedom behave similarly to their sub-blocks. This assumption is too strong from mathematical point of view, and implies that the details lost in each step of the coarse graining, when applying RG transform, are not very significant. In this paper we show that the Kadanoff hypothesis in its strong form can be lifted and a finite Euclidean field theory can be constructed by using the wavelet expansion of each field from large scale to the small scale, rather than in inverse direction. The RG then becomes a natural group structure of the field theory defined on the affine group.

Currents induced on the surface of a strongly elongated spheroid

Andronov I.V., Bilous P.Yu.

St. Petersburg State University, Russia

e-mail: ivandronov@gmail.com

High-frequency diffraction by elongated bodies has its specifics which results in the requirement for the frequency to be extremely high in order Fock asymptotics be applicable. This forms the gap between the problem that can be effectively solved with numerical tools and those where high-frequency approximations can be used. To fill in this gap the asymptotic approach to diffraction by strongly elongated bodies was developed [1, 2, 3]. This approach is based on the assumption that the longitudinal size of the body and the square of its transverse cross-section are both large quantities of the same order.

The parabolic equation approximation in the boundary layer near the surface yields an effective approximation for the electromagnetic field. With the use of Green's formula (Stratton–Chu formula in electromagnetics) one can derive then the approximations for the far field [4]. However, the analysis of the currents on the surface of a perfectly conducting spheroid which takes into account not only the forward wave process, but also the backward wave which is formed when the forward wave encircles the shaded ending of the spheroid, was performed only in the case of axial incidence [5].

In this paper we extend the analysis to skew incidence. We compare our asymptotic results with the results of numerical computations obtained with the use of ANSYS and HFSS package. This enables us to investigate the applicability conditions for the derived asymptotics and to understand the limitations of HFSS package, i. e. to find out up to which values of the frequency and other parameters the computations performed with that package are accurate.

References

- [1] I. V. Andronov, High-frequency asymptotics for diffraction by a strongly elongated body, *Antennas and Wireless Propagation Letters, IEEE*, 2009, **8**, pp. 872.
- [2] I. V. Andronov, D. Bouche, M. Duruflé, High-frequency diffraction of plane electromagnetic wave by an elongated spheroid, *IEEE AP Transactions*, 2012, **60**(11), pp. 5286–5295.

- [3] I. V. Andronov, Diffraction of a high-frequency electromagnetic wave incident at a small angle to the axis of a strongly elongated body, *J. of Communic. Technol. and Electronics*, 2014, **59**(2), pp. 130–138.
- [4] I. V. Andronov, D. A. Shevnin, High-frequency scattering by perfectly conducting prolate spheroids, *J. of Electromagnetic Waves and Applications*, 2014, **28**(11), p. 1388–1396.
- [5] I. V. Andronov, D. Bouche, Forward and backward waves in high-frequency diffraction by an elongated spheroid, *Progress in Electromagnetics Research B*, 2011, **29**, pp. 209–231.

A mathematical model for resonance scattering and generation of oscillations by nonlinear layered or grating-like media

Lutz Angermann¹, Vasyl V. Yatsyk², Mykola V. Yatsyk³

¹Clausthal University of Technology, Department of Mathematics, Erzstraße 1, D-38678 Clausthal-Zellerfeld, Federal Republic of Germany

²O. Ya. Usikov Institute for Radiophysics and Electronics of the National Academy of Sciences of Ukraine, 12 Ac. Proskura Str., Kharkiv, 61085, Ukraine

³Kharkiv National University of Radio Electronics, 14 Nauky Ave., Kharkiv, 61166, Ukraine

e-mails: lutz.angermann@tu-clausthal.de, vasy1.yatsyk@gmail.com, vasy1.yatsyk@meta.ua, nikolaiyatsyk@gmail.com

The present work focuses on the development of a mathematical model, an effective algorithm and a self-consistent numerical analysis of the multifunctional properties of resonant scattering and generation of oscillations by nonlinear, cubically polarizable transversely layered and longitudinally periodic structures. The proposed mathematical model allows to investigate the properties of a nonlinear layered and periodic object in a unified way. Note that, depending on the method of excitation, the nonlinear medium can be transformed into a nonlinear layered or grating-like structure with quasihomogeneous and quasiperiodic scattered and generated fields, respectively. The work presents results of the numerical analysis characterizing the type-conversion of the generation/scattering oscillations of the nonlinear layered structures for one/two-sided acting fields at the generation/scattering frequency were taken into account and could be observed. These effects were observed at a symmetry violation of the nonlinear problem [1, 2].

References

- [1] L. Angermann, V. V. Yatsyk, M. V. Yatsyk, The type-conversion of oscillations at the excitation of nonlinear layered media, *Bulletin of V. Karazin Kharkiv National University. Series “Mathematical Modelling. Information Technology. Automated Control Systems”*, Issue 27, pp. 13–21 (2015).
- [2] L. Angermann, V. V. Yatsyk, M. V. Yatsyk, The dynamics of type-conversion of oscillations by nonlinear layered media, *Proceedings of the XX-th International Seminar/Workshop on Direct and Inverse Problems of Electromagnetic and Acoustic Wave Theory (DIPED-2015)*, Lviv, Ukraine, September 21–24, pp. 29–32 (2015).

Non-commutative normal forms and inverse spectral problems

Anikin A. Yu.

Ishlinski Institute for Problems in Mechanics of the Russian Academy of Sciences, 101 Prospekt Vernadskogo, bld. 1, 119526, Moscow, Russia

e-mail: anikin83@inbox.ru

We discuss a method for calculating low lying eigenvalues of a Schrödinger operator by means of a non-commutative Birkhoff normal form [1, 2] in a framework [3]. The approach is close to

[4, 5] but differs in important technical details. We show that the presented method may be useful for different reasons. Firstly, it enables to estimate a growth rate of eigenvalues asymptotic series expansion coefficients, and secondly it may be more convenient from the computational viewpoint. We illustrate the second point by strengthening a one-dimensional inverse spectral result from [6, 7]. Namely, we show that under some restrictions the knowledge of asymptotic series for any pair of low lying eigenvalues is enough to recover the potential.

References

- [1] A. Anikin, *Regular and Chaotic Dynamics*, **13**: 5, 337–402 (2008).
- [2] A. Yu. Anikin, *Theoretical and Mathematical Physics*, **160**, 1274–1291 (2009).
- [3] D. V. Treschev, *Proc. Steklov Inst. Math.*, **250**, 211–244 (2005).
- [4] J. Sjöstrand, *Asymptotic Analysis*, **6**, 29–43 (1992).
- [5] L. Charles, S. Vũ Ngọc, *Duke Mathematical Journal*, **143**(3), 463–511 (2008).
- [6] Y. Colin de Verdière, V. Guillemin, A semi-classical inverse problem I: Taylor expansions, arXiv:0802.1605 [math-ph].
- [7] H. Hezari, *Comm. Math. Phys.*, **288**(3), 1061–1088 (2009).

Numerical analysis of the complex heat transfer in a layered medium

Astrakhantseva A.A.¹, Chebotarev A.Yu.^{1,2}, Grenkin G.V.^{1,2}, Kovtanyuk A.E.^{1,2}

¹Far Eastern Federal University, 8 Sukhanova st., 690950 Vladivostok, Russia

²Institute for Applied Mathematics, FEB RAS, 7 Radio st., 690041 Vladivostok, Russia

e-mails: astra92293@gmail.com, chebotarev.ayu@dvmfu.ru, glebgrenkin@gmail.com,

kovtanyuk.ae@dvmfu.ru

The study of the complex (coupled) heat transfer [1, 2] where the radiative and conductive contributions are simultaneously taken into account is important for many engineering applications. Here, the following examples can be mentioned: modeling the heat transfer in combustion chambers and industrial furnaces, estimating the efficiency of cooling systems, predicting heat transfer in glass manufacturing, control of thermal processes in optical fiber production, etc.

The nonlinear radiative-conductive heat transfer model consists of two differential equations: an equation of the radiative heat transfer and an equation of the conductive heat exchange. The boundary-value problem for participating layered medium is considered. The boundary conditions describe effects of reflection and transmission at inner boundaries, and reflection, absorption and emission at external boundaries of the layered medium.

Currently, there are known effective numerical algorithms to solve the boundary-value problem for single layer medium with reflecting (external) boundaries (see e. g. [3, 4]). The development of numerical algorithm to solve the boundary-value problem for multilayered medium with reflecting and refracting boundaries is an open problem.

For the computation of solutions of this problem, two approaches based on iterative techniques are considered. First, a recursive algorithm based on some modification of the Monte Carlo method is proposed. Second, the P_1 (diffusion) approximation of the radiative-conductive heat transfer model is utilized. Implementation of the diffusion approximation does not require large computational costs. It can be successfully applied to various heat transfer problems which do not require obtaining high accuracy. Compared with P_1 approximations, the proposed Monte Carlo algorithm allows us to obtain more precise results, because it deals with the exact model, whereas P_1 approximation utilizes simplified equations. Besides, the Monte Carlo algorithm is well appropriate for parallelization. Thus, it allows us to get a good accuracy in a reasonable computational time.

References

- [1] M. N. Ozisik, *Radiative Transfer and Interaction with Conduction and Convection*, John Wiley, New York, 1973.
- [2] M. F. Modest, *Radiative Heat Transfer, 2nd ed.*, Academic Press, New York, 2003.
- [3] C. E. Siewert, *J. Quant. Spectrosc. Radiat. Transfer*, **54**, 599–605 (1995).
- [4] A. E. Kovtanyuk, N. D. Botkin, K.-H. Hoffmann, *Int. J. Heat Mass Transfer*, **55**, 649–654 (2012).

Dynamical inverse problem for two-velocity systems on finite trees

S.A. Avdonin¹, A.S. Blagoveshchensky², A. Choque Rivero³, **V.S. Mikhaylov**^{4,2}

¹Department of Mathematics and Statistics, University of Alaska Fairbanks, Fairbanks, AK 99775-6660, USA

²St. Petersburg State University, Faculty of Physics, University Embankment 7-9, St. Petersburg 199034, Russia

³Instituto de Física y Matemáticas, Universidad Michoacana de San Nicolás de Hidalgo, C.P. 58040 Morelia, Mich., México

⁴St. Petersburg Department of V. A. Steklov Institute of Mathematics of the Russian Academy of Sciences, 7 Fontanka, St. Petersburg 191023, Russia

e-mails: s.avdonin@alaska.edu, v.mikhaylov@spbu.ru

We consider the dynamical inverse problem for the two-velocity system on a tree, as the inverse data we use the response operator, i. e. the dynamical Dirichlet-to-Neumann map, on finite time interval. The corresponding inverse spectral problem was considered in [1]. As we consider the problem on the finite time interval, we cannot go from the dynamical problem to spectral one by a simple trick (for example by Fourier transform). We suggest two ways to overcome this difficulty. Using the controllability of the dynamical system, we extract the spectral data from the dynamical one. Then we can write down the kernel of the response operator in terms of the spectral data and pass to the Titchmarsh–Weyl function which is a inverse data for the spectral problem. On the other hand, using the controllability of the system, we can extend the response operator by operator technique, developed by M. I. Belishev in [3], thus reducing the problem to known one. In [2] the authors treated the dynamical inverse problem for the Schrödinger equations on finite trees by a different method, without passing to a spectral problem.

References

- [1] S. A. Avdonin, A. Choque Rivero, G. Leugering, V. S. Mikhaylov, On the inverse problem of the two-velocity tree-like graph, *ZAMM – Journal of Applied Mathematics and Mechanics*, **95**(12), 1490–1500 (2015).
- [2] S. A. Avdonin, V. S. Mikhaylov, K. B. Nurtazina, On inverse dynamical and spectral problems for the wave and Schrödinger equations on finite trees. The leaf peeling method, *Mathematical problems in the theory of wave propagation. Part 45, Zap. Nauchn. Sem. St. Petersburg. Otdel. Mat. Inst. Steklov (POMI)*, **438**, 7–21 (2015).
- [3] M. Belishev, On a relation between data of dynamic and spectral inverse problems, *Mathematical problems in the theory of wave propagation. Part 32, Zap. Nauchn. Sem. St. Petersburg. Otdel. Mat. Inst. Steklov (POMI)*, **297**, 30–48 (2003); translation in *J. Math. Sci. N.Y.*, **127**(6), 2353–2363 (2005).

Heat transfer in a harmonic crystal on an elastic foundation

Babnikov M.B.^{1,2}, **Krivtsov A.M.**^{1,2}, **Tsvetkov D.V.**^{1,2}

¹Peter the Great Saint Petersburg Polytechnic University, St. Petersburg, Russia

²Institute for Problems in Mechanical Engineering, Russian Academy of Sciences, St. Petersburg, Russia

e-mails: mikhail.babnikov@gmail.com, akrivtsov@bk.ru, dvtsvetkov@ya.ru

Non-Fourier heat conduction processes in ideal crystal structures have been intensively studied in the recent decades. The literature is surveyed in the review papers [1, 2]. In this work we consider a one-dimensional crystal in the form of a chain of identical particles with mass m that are connected by linear springs with each other and with a fixed base, described by the following equations of motion:

$$\ddot{u}_n = \omega_0^2(u_{n-1} - (2 + \epsilon)u_n + u_{n+1}), \quad \epsilon = C_1/C_0, \quad \omega_0 = \sqrt{C_0/m} \quad (1)$$

where u_n is the displacement of the n -th particle, m is the particle mass, C_0 is the stiffness of the interparticle bond, C_1 is the stiffness of the bond between a particle and the fixed base, and dots denote partial time derivatives. The crystal is infinite: the index n is an arbitrary integer.

The initial conditions for (1) are $u_n|_{t=0} = 0$, $\dot{u}_n|_{t=0} = \sigma(x)\varrho_n$, where ϱ_n are independent random values with zero expectation and unit variance; $\sigma^2(x)$ is a variance of the initial velocities, which is a slowly varying function of the spatial coordinate $x = na$, where a is the lattice constant. These initial conditions correspond to an instantaneous temperature perturbation, which can be induced in crystals, for example, by an ultrashort laser pulse.

We adopt an approach based on the covariance analysis [3, 4] for the velocities \dot{u}_i to obtain a closed equation system determining unsteady thermal processes. The nonlocal temperature $\theta_n(x)$ is introduced as [4, 5]:

$$k_B(-1)^n \theta_n(x) = m\langle \dot{u}_i \dot{u}_j \rangle, \quad (2)$$

where k_B is the Boltzmann constant, $n = j - i$ is the covariance index, $x = \frac{i+j}{2}a$ is the spatial coordinate, a is the lattice constant. If $n = 0$ then $i = j$ and quantity θ_n coincides with the kinetic temperature T : $\theta_0(x, t) = T(x, t) = \frac{m}{k_B} \langle \dot{u}_i^2 \rangle$, where $i = x/a$. The use of the correlation analysis [4, 5] and the long wavelength approximation allows to formulate the initial value problem for kinetic temperature $T(x, t)$ in a simple form:

$$\ddot{T} + \frac{1}{t}\dot{T} = c_*^2 T'', \quad T|_{t=0} = T_0(x), \quad \dot{T}|_{t=0} = 0, \quad (3)$$

where $c_* = c(\sqrt{\epsilon + 4} - \sqrt{\epsilon})/2$ is the velocity of a heat wave propagating in a harmonic crystal with a substrate potential, $c = \omega_0 a$ is the sound velocity in a simple harmonic crystal.

References

- [1] F. Bonetto, J. L. Lebowitz, L. Rey-Bellet, Fourier's law: a challenge to theorists, in *Mathematical Physics 2000*, Eds.: A. Fokas et al., Imperial College Press, London, 2000, p. 128–150.
- [2] S. Lepri, R. Livi, A. Politi, Thermal conduction in classical low-dimensional lattices, *Phys. Rep.*, Vol. **377**, pp. 1–80, 2003.
- [3] Z. Rieder, J. L. Lebowitz, E. Lieb, Properties of a harmonic crystal in a stationary nonequilibrium state, *J. Math. Phys.*, Vol. **8**, pp. 1073–1078, 1967.
- [4] A. M. Krivtsov, Heat transfer in infinite harmonic one-dimensional crystals, *Doklady Physics*, Vol. **60**(9), pp. 407–411, 2015.
- [5] A. M. Krivtsov, On unsteady heat conduction in a harmonic crystal, arXiv:1509.02506, 2015.

Trace formulas for fourth order operators on unit interval

Andrey Badanin, Evgeny Korotyaev

St. Petersburg State University, Universitetskaya nab. 7/9, St. Petersburg, 199034 Russia
e-mails: a.badanin@spbu.ru, korotyaev@gmail.com, e.korotyaev@spbu.ru

We consider a self-adjoint operator H on $L^2(0, 1)$ given by $Hy = (\partial^4 + 2\partial p\partial + q)y$, under the boundary conditions $y(0) = y''(0) = y(1) = y''(1) = 0$, the functions p, q are real and satisfy $p, q \in L^1(0, 1)$.

The standard applications of the fourth order differential equations are bending vibrations of thin beams and plates described by the Euler–Bernoulli equation. Moreover, these equations arise in many other physical models: hydrodynamic stability (Orr–Sommerfeld equation), kinetic of liquid phase (Cahn–Hilliard equation), elastic buckling, dewetting in micro and nanoscopic liquid films and so on.

It is well known that the spectrum of the operator H consists of real eigenvalues $\mu_n, n \in \mathbb{N}$, of multiplicity ≤ 2 labeled by $\mu_1 \leq \mu_2 \leq \mu_3 \leq \dots$, counted with multiplicities. We prove the following trace formulas, similar to the Gelfand–Levitan formulas for second order operators [GL].

Theorem 1. [BK] *Let $p, p'''' , q, q'' \in L^1(0, 1)$, $\int_0^1 q(x)dx = 0$. Then the following trace formula holds true:*

$$\sum_{n \geq 1} (\mu_n - ((\pi n)^2 - p_0)^2 + \frac{1}{2}(P + p_0^2)) = -\frac{1}{4}(P - p_0^2 + V(0) + V(1)),$$

where the series converge absolutely and uniformly in p, q ,

$$p_0 = \int_0^1 p(t)dt, \quad P = \int_0^1 (p''(t) + p^2(t))dt, \quad V = q - \frac{p''}{2}.$$

The work is supported by the RSF grant No 15-11-30007.

References

- [BK] A. Badanin, E. Korotyaev, Trace formula for fourth order operators on unit interval. II, *Dynamics of PDE*, Vol. **12**(3), 217–239 (2015).
[GL] I. M. Gelfand, B. M. Levitan, On a simple identity for eigenvalues of a second order differential operator, *Dokl. Akad. Nauk SSSR*, **88**(4), 593–596 (1953).

The 0D quantum field theory: Multiple integrals via background field formalism

Bagaev A.A., Pis'mak Yu.M.

St. Petersburg State University, 7–9 Universitetskaya nab., St. Petersburg, 199034, Russia
e-mails: a.bagaev@spbu.ru, ypismak@yahoo.com

A variant of “0D field theory” is proposed. As is known, there is an alternative of 0D quantum field theory — the theory of random matrices. That was some success in respective fields of physics and mathematics. However, some new approach has been developed and the authors mean that as more common and more simple. The Feynman’s path integrals are directly replaced by usual multiple Riemannian ones over finite-dimensional real Euclidean space. The obtained field theory, firstly, is real, secondly, is divergence-free and thirdly, all the quantum quantities are defined without any ambiguities. In this scheme we realized L. D. Faddeev’s version of background field formalism [3]. All its attributes such as generating functionals, special boundary conditions and quantum equations

of motions are correctly defined. As an example a model with quadruple self-interaction (also known as φ^4 model) is discussed. Necessary Feynman diagram techniques is constructed. If diagrams in each order of the perturbation theory (or the loop expansion) will be calculated, so we will have an asymptotic series for S-matrix generating functional. There is an idea, that method allows calculation of asymptotic expansions for special kind of integrals and it can aid that more simple.

This work is supported by RFBR grant 16-02-00943-a.

References

- [1] A. Bagaev, Yu. Pis'mak, *Vestnik of Saint-Petersburg University. Series 4. Physics. Chemistry*, **1**(59), 464–472 (2014).
- [2] A. Bagaev, Yu. Pis'mak, *Vestnik of Saint-Petersburg University. Series 4. Physics. Chemistry*, **2**(60), 327–334 (2015).
- [3] L. Faddeev, *Theoretical and Mathematical Physics*, **148**, 133–142 (2006).

Current-voltage characteristics for two quantum waveguides, connected to quantum resonators

Bagmutov A.S., Popov I.Yu.

Department of Higher Mathematics, ITMO University, Saint Petersburg 197101, Russia

e-mail: Bagmutov94@mail.ru

We investigate several quantum systems, consisting of waveguides and resonators, connected through small apertures. We use zero-width slits model, in which apertures considered infinitely-small. For the systems, in the framework of model, exact solutions are found and scattering problem is solved. Results then used to calculate current-voltage characteristics of suggested devices. Obtained characteristics have interesting properties. Parameters of systems, for which effects are still observable, calculated. The results may be useful in constructing electronic devices.

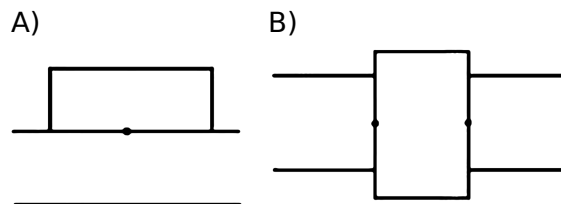


Fig. 1: Schematics of considered systems.

References

- [1] S. Datta, *Electronic Transport in Mesoscopic Systems*, Cambridge University Press, Cambridge (1995).
- [2] V. Adamyan, B. Pavlov, A. Yafyasov, *Operator Theory: Adv. and Appl.*, **190**, 3–26 (2009).
- [3] G. B. Lesovik, I. A. Sadovskyy, *Physics-Uspekhi (Advances in Physical Sciences)* **54**, 1007–1059 (2011).
- [4] U. Wulf, M. Krahlisch, J. Kučera, H. Richter, J. Höntschel, *Nanosystems: Physics, Chemistry, Mathematics*, **4**(6), 800–809 (2013).
- [5] I. Yu. Popov, S. L. Popova, *Europhys. Lett.*, **24**(5), 373–377 (1993).
- [6] I. Yu. Popov, S. L. Popova, *Phys. Lett. A*, **173**(6), 484–488 (1993).

Electron transport in a multi-resonator system formed by constrictions of a quantum waveguide

Baskin L.M., Kabardov M.M.

The Bonch-Bruевич Saint Petersburg State University of Telecommunications, 22, Prospekt Bolshevnikov, St. Petersburg, 193232, RUSSIA

e-mails: lev.baskin@mail.ru, kabardov@bk.ru

Sharkova N.M.

Saint Petersburg State University, 7-9, Universitetskaya nab., St. Petersburg, 199034, RUSSIA

e-mail: n.sharkova@spbu.ru

Resonant tunneling is known [1] to emerge in ballistic electron transport in a quantum waveguide with two narrows (constrictions). Here we present the results of numerical simulations of electron transport in a system consisting of two identical resonators produced by three narrows in a quantum waveguide. It is shown, that at small electron energies the resonance peaks of one-resonator system split, and the peaks width and their separation depends on the diameter (width) of the narrows. The processes of high energy electron transport, where the role of multichannel scattering with changes of transverse channels (quantum states) becomes substantial, have been investigated [2]. In addition, resonant tunneling in a quantum waveguide with $N + 1$ delta potential barriers, which produce N resonators, has been considered. Numerical simulations show formation of zones and the zones parameters' dependence on the potential barriers, which confirm the possibility of making quasi-one-dimensional crystal in a quantum waveguide with a number of narrows. The results of the study may find potential applications in designing various resonance devices based on quantum waveguides.

References

- [1] N. Ashcroft, N. Mermin, *Solid State Physics*, V. 1, M.: Mir (1979).
- [2] L. Baskin, P. Neittaanmaki, B. Plamenevskii, O. Sarafanov, *Resonant Tunneling: Quantum Waveguide of Variable Cross-Section, Numerics, and Asymptotics*, Springer International Publishing, Switzerland (2015).

Propagation of sound waves in stressed elasto-plastic material

Belyaev A.K., Lobachev A.M., Modestov V.S., Semenov A.S., Shtukin L.V., Tretyakov D.A.

Peter the Great Saint-Petersburg Polytechnic University, 29, Polytechnicheskaya, St. Petersburg, 195251, Russia

e-mail: vice.ipme@gmail.com

Polyanskiy V.A., Yakovlev Yu.A.

Institute for Problems in Mechanical Engineering RAS, V.O., Bolshoj pr., 61, St. Petersburg, 199178 Russia

e-mail: vapol@mail.ru

The analysis of ultrasonic longitudinal and transverse waves of different polarization in solids is widely used for the technical diagnostics. One of the important applications is the method of acoustoelasticity. Theoretical substantiation of this method are based upon the study of the propagation of transverse ultrasonic waves in Murnaghan's nonlinear elastic material [1]. The method allows one to measure mechanical stresses in terms of Δa which is the relative difference in velocities of two transverse waves polarized orthogonally to each other.

The acoustoelasticity method is able to uniquely determine the value of the principal stress in the case of no plastic deformation. The report provides a number of experimental facts which demonstrate that the plastic deformation causes a change in Δa that nonlinearly depends on the value of plastic deformation.

In this case the methods for evaluating the contribution of plastic strain in the value of acoustic anisotropy are required for technical diagnostics.

In order to develop these methods we take a model of viscoplastic material with hardening. The problem of propagation of a plane acoustic wave in a homogeneous prismatic elastic-plastic body that is uniaxially prestressed in the direction perpendicular to the wave propagation direction in presence of plastic deformation. The problem is posed with account for the kinematic continuity on the wave front in terms of jumps.

The system of equations for the relative jumps in acceleration of the medium particles at the wave front is derived. The solutions are analyzed for different approximations in terms of the first and second order of smallness.

It was found that in contrast to the non-linear elastic wave in the zero-order approximation there is a strong dependence of the velocity of propagation of longitudinal wave from the hardening factor and component of the deviatoric stress tensor. This is the essential difference between an elastic-plastic material from the nonlinear elastic one.

In the first and second approximation we obtain the dependence of the propagation velocity of transverse sound waves of different polarization from the hardening factor and components of the deviatoric stress tensor.

The expressions are obtained for the main direction of propagation of the waves which are no longer mutually orthogonal when the external mechanical stress exceeds the yield limit.

The study provides a number of dependences required for solving the practical problem of technical diagnostics of structures in the cases in which the external load is higher than the yield limit.

The mathematical model of viscoplastic material and the study carried out enable us to substantiate the dependence of the propagation velocity of longitudinal ultrasonic wave on the magnitude of plastic deformation. The phenomenon has been observed in tests, cf. [2].

References

- [1] D. S. Hughes, J. L. Kelly, *Physical Review*, **92**(5), 1145 (1953).
- [2] L. B. Zuev, B. S. Semukhov, K. I. Bushmeleva, *Technical Physics*, **44**(12), 1489–1490 (1999).

Coefficients of elastic waves conversion in crystal indium

Belyayev Yu.N., Bozhok E.V., Malyshkin D.S.

Syktvykar State University, Oktyabrskii pr. 55, Syktvykar-167001, Russia

e-mails: ybelyayev@mail.ru, kat.bozh@gmail.com, prorid3r@gmail.com

Converting of elastic waves due to their scattering by crystalline layer indium is investigated. In particular, the possibility rotation of the polarization plane of the shear wave as a result of wave reflection (or transmission) is considered.

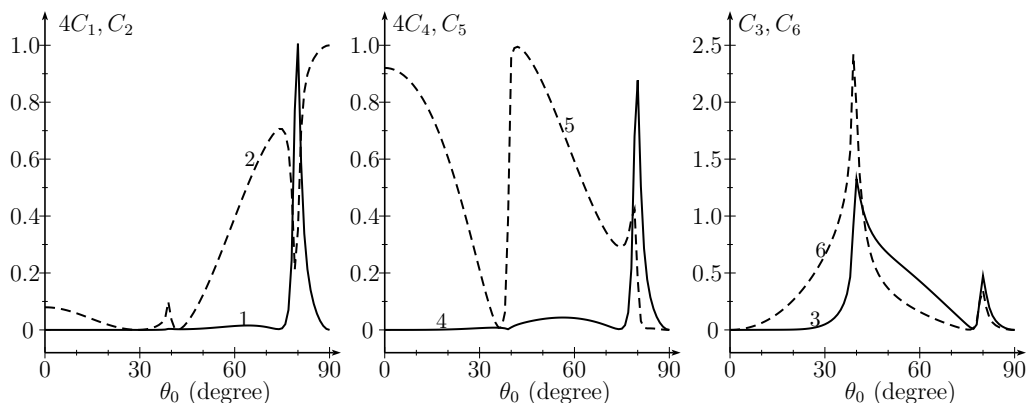


Fig. 1: The conversion coefficients of SV wave. θ_0 is the angle between incident wave vector and axis $0x_3$ which is perpendicular to the surface of the crystal.

Conversion coefficients $C_j = |\mathcal{A}_j/\mathcal{A}_0|^2$ was computed by means of the transfer matrix method [1]. Here $\mathcal{A}_0, \mathcal{A}_1, \dots, \mathcal{A}_6$ are amplitudes of incident wave, reflected SH, SV, P waves and transmitted SH, SV, P waves accordingly.

Modeling of scattering spectra of elastic waves on a layer of indium is performed. Spectra $C_j(\theta_0, \alpha)$ for three type of incident wave (SH, SV, P) for different layer thicknesses d and frequencies ν are considered. For example, the spectra in Figure 1 correspond to scattering on the surface (001) when the angle between axis [001] and the plane of incidence is equal to $\alpha = 23^\circ$ and parameter $\nu d = 2080 \text{ Hz}\cdot\text{m}$; isotropic half-spaces that limit crystalline layer, are characterized by identical parameters: density $\rho_0 = \rho_d = 2.65 \cdot 10^3 \text{ kg/m}^3$, Lamé parameters $\lambda_0 = \lambda_d = 1.67 \cdot 10^{10} \text{ N/m}^2$ and $\mu_0 = \mu_d = 3.27 \cdot 10^{10} \text{ N/m}^2$.

References

- [1] Yu. N. Belyayev, *Proc. Intern. Conf. Days on Diffraction 2015*, 37–42 (2014).

Dependences spectra of elastic waves on thickness of the scattering layer

Belyayev Yu.N., Malyshkin D.S.

Syktyvkar State University, Oktyabrskii pr. 55, Syktyvkar-167001, Russia
e-mails: ybelyayev@mail.ru, prorid3r@gmail.com

The scattering of SH, SV and P waves by layered structure (isotropic medium-crystal-isotropic medium) are investigated. In general case, the crystalline layer can produce six waves: SH-type with amplitude \mathcal{A}_1 , SV-type with amplitude \mathcal{A}_2 , P-type with amplitude \mathcal{A}_3 in the region of reflection and SH-type with amplitude \mathcal{A}_4 , SV-type with amplitude \mathcal{A}_5 , P-type with amplitude \mathcal{A}_6 in the region of transmission. The values of these amplitudes depend on the elastic parameters of the media, the angles of incidence θ_0 (angle between direction of incident wave vector \vec{k}_0 and the axis x_3 , perpendicular to the surface of crystalline layer) and α (angle between plane of incidence and coordinate plane x_1x_3), frequency of incident wave ν and the thickness of the crystal layer d .

Conversion coefficients $C_j = |\mathcal{A}_j/\mathcal{A}_0|^2$, $j = 1, \dots, 6$, are calculated using the transfer matrix method [1]. Here \mathcal{A}_0 is amplitude of incident wave. The results of calculations of the spectra $C_j(\theta_0, \alpha)$ for the crystal PbMoO_4 , when parameter $\nu d \in (10, 10^4)$, are presented.

The program of visualization of dependencies of scattering spectra on the parameter νd is developed and demonstrated.

References

- [1] Yu. N. Belyayev, *Proc. Intern. Conf. Days on Diffraction 2015*, 37–42 (2014).

Coefficients of elastic waves conversion by the crystal of BaTiO_3

Belyayev Yu.N., Malyshkin D.S., Zhibalova Yu.A.

Syktyvkar State University, Oktyabrskii pr. 55, Syktyvkar-167001, Russia
e-mails: ybelyayev@mail.ru, prorid3r@gmail.com, zhibalova2012@yandex.ru

Converting of elastic waves due to their scattering by crystalline layer barium titanate is studied.

In general case, the wave (amplitude A_0) incident on the crystal layer $0 \leq x_3 \leq d$ can produce SH wave (amplitude A_1), SV wave (amplitude A_2), P wave (amplitude A_3) in the region $x_3 < 0$ and similar waves with amplitudes A_4, A_5, A_6 in the region $x_3 > d$. Conversion coefficients $C_j = |\mathcal{A}_j/\mathcal{A}_0|^2$ was computed by means of the transfer matrix method [1]. Examples of dependences $C_j(\theta_0)$ are shown in Figure 1. It correspond to scattering on the surface (001) when the angle between axis [001] and the plane of incidence is equal to $\alpha = 21^\circ$ and parameter $\nu d = 8050 \text{ Hz}\cdot\text{m}$; isotropic half-spaces that

limit crystalline layer, are characterized by identical parameters: density $\rho_0 = \rho_d = 2.65 \cdot 10^3 \text{ kg/m}^3$, Lamé parameters $\lambda_0 = \lambda_d = 1.67 \cdot 10^{10} \text{ N/m}^2$ and $\mu_0 = \mu_d = 3.27 \cdot 10^{10} \text{ N/m}^2$.

Spectra $C_j(\theta_0, \alpha)$ for three type of incident wave (SH, SV, P) for different layer thicknesses d and frequencies ν are presented and discussed.

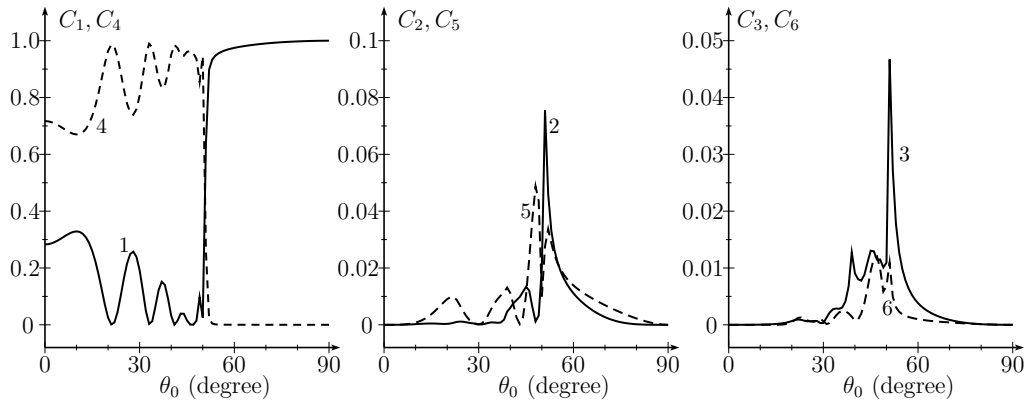


Fig. 1: The conversion coefficients of SH wave. θ_0 is the angle between incident wave vector and axis $0x_3$ which is perpendicular to the surface of the crystal.

References

[1] Yu. N. Belyayev, *Proc. Intern. Conf. Days on Diffraction 2015*, 37–42 (2015).

A relation between two simple localized solutions of the wave equation

Alexander S. Blagoveshchensky¹, Aleksei P. Kiselev^{1,2,3}

¹St. Petersburg State University, St. Petersburg, Russia

²Steklov Mathematical Institute, St. Petersburg Department, St. Petersburg, Russia

³Institute of Mechanical Engineering RAS, St. Petersburg, Russia

e-mails: a.blagoveshchensky@spbu.ru, kiselev@pdm.ras.ru

We are concerned with establishing a relation between two simple solutions of the wave equation

$$u_{xx} + u_{yy} + u_{zz} - c^{-2}u_{tt} = 0, \quad c = \text{const.} \tag{1}$$

The first one, found by Sheppard and Saghafi [1] shows a Gaussian-beam asymptotic behavior. It was much discussed in connection with the theory of “complex source”(see, e. g., [2]). It satisfies the Helmholtz equation $u_{xx} + u_{yy} + u_{zz} + k^2u = 0$, $k = \omega/c$, obtained from (2) by the substitution $U = u(x, y, z)e^{-i\omega t}$, and is given by

$$U(\omega; \rho, z) := \sin(kR_*)/R_*, \quad R_* = \sqrt{\rho^2 + (z - ia)^2}, \quad \rho = x^2 + y^2, \tag{2}$$

with $a > 0$ a free constant. The other solution under consideration is

$$u(t; \rho, z) = 1 / [c^2t^2 - \rho^2 - z^2 - 2ia(ct - z)], \tag{3}$$

with the same constant a . It was recently introduced in [3] as an example of a function having a singularity at a running point $\{x = y = 0, z = ct\}$, but satisfying the homogeneous equation (2) in the whole space–time $\mathbb{R}^3 \times \mathbb{R}$.

We establish that

$$\hat{u}(\omega; \rho, z) = \begin{cases} 2(\pi c)^{-1}e^{-ka}U(\omega; \rho, z) & \text{if } \omega > 0, \\ 0 & \text{if } \omega \leq 0, \end{cases} \tag{4}$$

where $\hat{u}(\omega; \rho, z) := \int_{-\infty}^{\infty} u(t; \rho, z) e^{+i\omega t}$ is the Fourier transform.

The research was supported by grants from RFBR No. 14-01-00535 and from St. Petersburg University No. 11.38.263.2014.

References

- [1] C. J. R. Sheppard, S. Saghafi, *Phys. Rev. A*, **57**, 2971–2979 (1998).
- [2] A. M. Tagirdzhanov, A. P. Kiselev, *Opt. Spectr.*, **119**, 271–281 (2015).
- [3] A. S. Blagoveshchensky, A. M. Tagirdzhanov, A. P. Kiselev, *Zap. Nauch. Sem. POMI*, **438**, 73–82 (2015); English translation to appear in *J. Math. Sci.*

On the Cauchy problem for the wave equation with data on a non-spatially oriented plane

A.S. Blagoveshchensky¹, F.N. Podymaka²

¹St. Petersburg State University, St. Petersburg, Russia

²State School n. 2, Sosnovy Bor, Russia

e-mail: a.blagoveshchensky@spbu.ru

We consider the Cauchy problem for the wave equation

$$u_{xx} + u_{yy} + u_{zz} = u_{tt}, \quad x > 0, \quad (1)$$

with the data

$$u|_{x=0} = \varphi(y, z, t), \quad u_x|_{x=0} = 0. \quad (2)$$

As is known, see, e. g. [1], this problem is ill-posed: for an arbitrary $\varphi(y, z, t)$ its solution not necessarily exists. If it exists, then the function $\varphi(y, z, t)$ must satisfy rather strong conditions. More precisely, $\varphi(y, z, t)$ is uniquely determined by its values in an arbitrarily thin cylinder $x^2 + y^2 < \varepsilon^2$, $-\infty < t < \infty$, see [1]. A solution of the problem (1)–(2) is unique.

We present an explicitly described operator B , which maps the function $\varphi(y, z, t)$ into a solution $u(x, y, z, t)$ of the the problem (1)–(2), provided it exists. If solution does not exist, $B\varphi$ is a certain function not being a solution of (1)–(2). If A is the operator mapping an arbitrary solution u of (1), satisfying the second condition (2) (that is, $Au = \varphi$) to φ , then B is the left inverse to A , $BA = I$, where I is the identity operator.

References

- [1] R. Courant, D. Hilbert, *Methods of Mathematical Physics v. 2*, Interscience, New York (1962).

The problem of flow about infinite plane wedge with inviscous non-heat-conducting gas. Linear stability of a weak shock wave

Blokhin A.M., Tkachev D.L.

Sobolev Institute of Mathematics 630090, Novosibirsk, Russia; Novosibirsk State University 630090, Novosibirsk, Russia

e-mails: blokhin@math.nsc.ru, tkachev@math.nsc.ru

As is well-known [1], on stationary supersonic gas flow over infinite plane wedge (angle σ at the point of the wedge is small enough, $\sigma < \sigma_{\text{lim}}$) theoretically there are two possible stationary solutions: one of them corresponds to strong shock wave when gas speed beyond the shock is less than the speed of sound, i. e. $u_0^2 + v_0^2 < c_0^2$ (u_0, v_0 are components of the speed vector, c_0 is the speed of sound), and the other corresponds to the weak shock wave, when, generally speaking, $u_0^2 + v_0^2 > c_0^2$ (figure illustrates the position of the shocks, θ_s, θ_w are angular coordinates of the strong and the weak shocks accordingly).

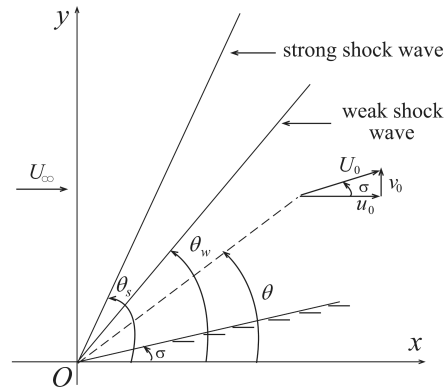


Fig. 1: Sketch for weak and strong shock waves.

However, in numerous physical and computational experiments if there is no additional information, for example about the value of the pressure down the flow, the case of weak shock wave is realized. As of today there is no strict mathematical explanation why this is happening. R. Courant and K. O. Friedrichs noticed in their monograph [1], that there is an opinion that strong shock wave is unstable by Lyapunov while weak shock wave is on the contrary stable.

In previous work of this talk authors [2], this assumption was grounded on the linear level in assumption that strong Lopatinski condition is satisfied on the shock. Current work again studies the case of a weak shock wave [3] but now in assumption that only Lopatinski condition holds on the shock, i. e. in corresponding linear problem there are plane waves [4].

References

- [1] R. Courant, K. O. Friedrichs, *Supersonic flow and shock waves*, N.Y.: Interscience Publ. Inc. (1948).
- [2] A. M. Blokhin, D. L. Tkachev, L. O. Baldan, Study of the stability in the problem on flowing around a wedge. The case of strong wave, *J. Math. Anal. Appl.*, **319**, 248–277 (2006).
- [3] A. M. Blokhin, D. L. Tkachev, Stability of a supersonic flow about a wedge with weak shock wave, *Mat. Sb.*, **200**, 3–30 (2009).
- [4] A. M. Blokhin, D. L. Tkachev, Stability of a supersonic flow over a wedge containing a weak shock wave satisfying the Lopatinski condition, *J. Hyperbolic Differential Equations*, **11**, 215–248 (2014).

Method of discrete sources as an effective solver for waveguides with sharp corners

Ya.L. Bogomolov, M.A. Borodov, A.D. Yunakovsky

Institute of Applied Physics, Russian Academy of Sciences, Nizhny Novgorod, Russia

e-mail: bogomol@appl.sci-nnov.ru

In recent years many electromagnetic waveguides with complicated structures have appeared. Sometimes these structures contain sharp corners. The discretization of the initial problem, which leads to a set of linear algebraic equations (SLAE), can be obtained by a variety of methods: the finite difference method, the finite element method, the pseudospectral method, etc. Nevertheless, it is very difficult to find suitable numerical method, due to the field singularities at the corners. In the case of sharp boundaries the resulting matrices are often very large, that is why the most numerical algorithms are time consuming and the accuracy may be limited. The method of discrete sources (MDS) seems to be the most promising one in such the case.

The model plane scattering problem in a strip region with a sharp ledge is considered. The problem is governed by the Helmholtz equation together with the Neumann condition on the boundary and the radiation condition in infinity.

To solve such the problem effectively, the MDS is used. An unknown solution is sought as a linear combination of the Green (source) functions of the infinite strip domain. Substitution of such an anzats into the boundary condition leads to a SLAE.

Effectiveness of the MDS depends essentially on the way of source placement. The original scheme of source allocation for sharp-pointed domains were suggested in [1], [2]. In this paper a new “dipole” source allocation in the neighbourhood of the sharp points is suggested. Numerical results demonstrate the effectiveness of the idea proposed.

References

- [1] Ya. L. Bogomolov, A. D. Yunakovsky, Scattering of electromagnetic waves in a channel with a step-like boundary, *Proceedings of Int. seminar “Days on Diffraction”*, 2001, pp. 26–37.
- [2] Ya. L. Bogomolov, M. A. Borodov, A. D. Yunakovsky, Scattering of electromagnetic waves in a plane channel with sharp corners, *Proceedings of Int. seminar “Days on Diffraction”*, 2014, pp. 43–47.

On the spectrum of a discrete Schrödinger equation in one-dimensional perturbation

Borzov V.V.¹, Damaskinsky E.V.²

¹Mathematical Department, The Bonch-Bruевич SPbGUT, Russia

²Mathematical Department, VI(IT) affiliated to VA MTO, Russia

e-mails: borzov.vadim@yandex.ru, evd@pdmi.ras.ru

We consider the spectrum of a discrete Schrödinger equation in finite-dimensional perturbation. We obtain the explicit form of scattering matrices for one-dimensional perturbations. In some cases, proved the absence of discrete spectrum and singular continuous part of the spectrum. The proof is based on solving the moment problem for the corresponding Jacobian matrix. Case of an arbitrary finite-dimensional perturbations is considered in less detail.

Precised description of the spectral bands for a 2D periodic Schrödinger operator

H. Boumaza¹, O. Lafitte^{1,2}

¹LAGA, UMR 75 39, Université Paris 13, 99 Av J.B. Clément, F-93430 Villetaneuse

²CEA, DM2S, 91191 Gif-sur-Yvette CEDEX

e-mails: boumaza@math.univ-paris13.fr, lafitte@math.univ-paris13.fr

Let L_0 and L be two characteristic lengths and V_0 a reference potential. We describe the spectral bands of the periodic Schrödinger operator acting on $H^2(\mathbb{R}^2)$, $H = -\frac{\hbar^2}{2m}\Delta + V$, associated with the periodic potential V whose unit cell is $[-L_0, L_0] \times [-L, L]$ and given on it by $V(x, y) = \left(\frac{|x|}{L_0} - 1\right)V_0 \times \text{sign}(y)$. We set \tilde{V} the $2L_0$ -periodic potential equal to $\left(\frac{|x|}{L_0} - 1\right)V_0$ on $[-L_0, L_0]$.

This potential has also been studied in the context of photonic crystals where, instead of the Schrödinger equation, the wave propagation is described by the Helmholtz equation (see [T]).

Bloch modes are obtained by Fourier analysis in y as functions $\psi : (x, y) \mapsto \sum_{n \in \mathbb{Z}} a_n^\pm(x) e^{i\frac{2n\pi}{L}y}$, where \pm is the sign of y and, for every $n \in \mathbb{Z}$, a_n^\pm is a solution on $[-L_0, L_0]$ of the equation :

$$-\frac{\hbar^2}{2m} \frac{d^2}{dx^2} a_n^\pm \pm \tilde{V}(x) \cdot a_n^\pm = \left(E - \frac{\hbar^2}{2m} \frac{4n^2\pi^2}{L^2} \right) a_n^\pm, \quad E \in \mathbb{R}. \quad (1)$$

together with conditions that ensure that ψ is in the domain of H and with quasiperiodic boundary conditions : $a_n^\pm(-L_0) = e^{i\omega\frac{\pi}{L_0}} a_n^\pm(L_0)$, $\omega \in [0, L_0]$.

Let $P_{\pm} = -\frac{\hbar^2}{2m} \frac{d^2}{dx^2} \pm \tilde{V}$ acting on $H^2(\mathbb{R})$. Since for every $x \in \mathbb{R}$, $-\tilde{V}(x) = \tilde{V}(x + L_0) + V_0$, we get that $\sigma(P_-) = V_0 + \sigma(P_+)$. But, as presented in [OL1], $\sigma(P_+)$ is a union of spectral bands $[E_{\min}^i, E_{\max}^i]$ for $i \geq 0$. Precised description of these spectral bands is detailed in [OL2] along with estimates on the length of the spectral bands and of the gaps.

Since H is a periodic Schrödinger operator, it has a band spectrum. With (1), the previous considerations lead to the following inclusion on the spectrum of H :

$$\sigma(H) \subset \bigcup_{i,j \geq 0} \bigcup_{(n,p) \in \mathbb{Z}^2} \left([E_{\min}^i, E_{\max}^i] + \frac{\hbar^2}{2m} \frac{4n^2\pi^2}{L^2} \right) \cap \left([E_{\min}^j, E_{\max}^j] + V_0 + \frac{\hbar^2}{2m} \frac{4p^2\pi^2}{L^2} \right). \quad (2)$$

A straightforward analysis shows that the gaps may close, by superposition of translated bands. Two dimensionless parameters appear : $\delta_0 = \frac{\hbar^2}{2mL_0^2V_0}$ and $\delta = \frac{\hbar^2}{2mL^2V_0}$. The results on the superposition of the bands will be linked with the relative order of magnitude of δ_0 and δ .

References

- [OL1] H. Boumaza, O. Lafitte, An exactly solvable non C^1 periodic potential, *Proceedings of the International Conference "Days on Diffraction 2015"*, St. Petersburg, Russia, IEEE, 62–66 (2015).
- [OL2] H. Boumaza, O. Lafitte, Explicit band spectrum for an exactly solvable non C^1 periodic potential, In preparation.
- [T] J. Tausch, Computing Floquet–Bloch modes in biperiodic slabs with boundary elements, *J. Comput. Appl. Math.*, **254**, 192–203 (2013).

On steady-state moving load problems for elastic half-space

Bratov V.A.¹, Kaplunov J.², Prikazchikov D.A.²

¹Saint-Petersburg State University, Department of Elasticity

²School of Computing and Mathematics, Keele University, Keele, Staffordshire, ST5 5BG, UK

e-mails: vladimir.bratov@gmail.com, j.kaplunov@keele.ac.uk, d.prikazchikov@keele.ac.uk

The steady-state regimes of moving loads on elastic half-plane are addressed. It is shown that the solution can be expressed through a single harmonic function, originally proposed in [1] for travelling surface waves. The examples of steadily moving vertical force and rigid punch are investigated. The extension for a beam resting on elastic half-plane is also discussed.

References

- [1] P. Chadwick, *Journal of Elasticity*, **6**, 73–80 (1976).

To the question of absolutely continuous spectrum eigenfunctions asymptotics for the case of three three-dimensional dissimilarly charged quantum particles scattering problem

Budylin A.M., Koptelov Ya.Yu., Levin S.B.

St. Petersburg State University, Universitetskaja nab. 7/9

e-mails: budylin@math.nw.ru, kopya239@yandex.ru, s.levin@spbu.ru

We suggest an approach with the main idea to propose the explicit formulas for the asymptotic behavior of the eigenfunctions of the continuous spectrum (like scattered plane perturbed waves) describing them up to the simple diverging waves with a smooth amplitude.

For one-dimensional particles with quickly decreasing at infinity pair potentials we can use for the description of the mentioned asymptotic behavior the analogy between the stated problem and the

classical problem of the diffraction of the plane waves by the set of semi-transparent infinite screens. This analogy was already used in [1, 2, 3, 4]. In case of long range potentials we are able to treat the diffraction problem analogously with the replacement of the classical plane waves by plane waves that are appropriately deformed by the long range tails of the Coulomb potentials.

References

- [1] V. S. Buslaev, S. P. Merkur'ev, *Dokl. Akad. Nauk SSSR*, **189**, 269–272 (Russian); translated as *Soviet Physics Dokl.*, **14**, 1055–1057 (1969).
- [2] V. S. Buslaev, S. P. Merkuriev, S. P. Salikov, *Probl. Mat. Fiz.*, Leningrad. Univ., Leningrad, **9**, 14–30 (1979).
- [3] V. S. Buslaev, S. P. Merkuriev, S. P. Salikov, *Zap. Nauchn. Sem. Leningrad. Otdel. Mat. Inst. Steklov (LOMI)*, **84**, 16–22 (1979).
- [4] V. S. Buslaev, S. B. Levin, *Amer. Math. Soc. Transl. (2)* **225**, 55–71 (2008).

To the question of absolutely continuous spectrum eigenfunctions asymptotics justification for the case of three one-dimensional quantum particles scattering problem with the short-range pare potentials

Budylin A.M., Levin S.B.

St. Petersburg State University, Universitetskaja nab. 7/9
e-mails: budylin@math.nw.ru, s.levin@spbu.ru

We consider the quantum scattering problem of three one-dimensional particles with repulsive short-range pair potentials. For clarity we restrict ourself by the case of finite pair potentials. The absence of singular continuous spectrum of the corresponding Schroedinger operator for the broad class of pair potentials was proved earlier in known works [1, 2]. Nevertheless the Mourre techniques do not allow to describe the asymptotics of absolutely continuous spectrum eigenfunctions. In our work we prove the existence of the resolvent limit values on absolutely continuous spectrum regardless of Mourre results and construct them explicitly. It allows us following the known procedure to derive the absolutely continuous spectrum eigenfunctions asymptotics, offered earlier in [3]. Our approach, ideologically close to the foundational work of L. D. Faddeev devoted to three-dimensional particles [4], specifically uses the ideas of Schwarz alternating method [5, 6].

References

- [1] E. Mourre, *Commun. Math. Phys.*, **78**, 391–408 (1981).
- [2] P. Perry, I. M. Sigal, B. Simon, *Annals of Mathematics*, **114**, 519–567 (1981).
- [3] V. S. Buslaev, S. B. Levin, *Amer. Math. Soc. Transl. (2)*, **225**, 55–71 (2008).
- [4] L. D. Faddeev, *Mathematical aspects of the three-body problem of the quantum scattering theory*, Daniel Davey and Co., Inc. (1965).
- [5] K. Moren, *Methods of Hilbert spaces*, PWN, Warszawa (1967).
- [6] A. M. Budylin, V. S. Buslaev, *St. Petersburg Math. J.*, **7**(6), 925–942 (1996).

Uniform asymptotics of far internal gravity waves fields from pulsating sources

Bulatov V.V., Vladimirov Yu.V.

Institute for Problems in Mechanics RAS, 119526, Moscow, pr. Vernadskogo 101-1
e-mail: internalwave@mail.ru

One of the main mechanisms of excitation of internal gravity waves in natural stratified media (ocean, atmosphere) is the wave generation by non-stationary sources of perturbations, different in

physical nature, both of natural (moving typhoons, flow about ocean relief irregularities, leeward mountains, etc.) and anthropogenic (sea technological structures, collapse of turbulent mixing regions, underwater explosions, etc.) origin [1, 2]. In the linear approximation, the far wave fields can be investigated, for example, using various asymptotics [3–6]. The analytical expressions constructed make it possible to obtain, using, for example, methods of computer mathematics, asymptotic representations of wave fields with account for the realistic inhomogeneity and non-stationarity of the parameters of natural stratified media. The present study is aimed at constructing asymptotic solutions that can describe the far fields of the internal gravity waves excited by a pulsating localized source of perturbations in finite-depth stratified medium flow. The problem of constructing uniform asymptotics for the far fields of internal gravity waves generated by a pulsating localized source of perturbations in finite-depth stratified medium flow is considered. The solutions obtained describe the wave perturbations both inside and outside the wave fronts and can be expressed in terms of the Airy function and its derivatives. Numerically calculated wave patterns of the excited wave fields are presented. The uniform asymptotic problem solutions obtained enabled us to describe the far fields of the internal gravity waves from a localized pulsating source of perturbations in finite-thickness stratified medium flow both outside and inside the corresponding wave fronts. It is shown that the far field asymptotics make it possible to efficiently calculate the main characteristics of the wave fields and to qualitatively analyze the solutions obtained. This opens wide opportunities for studying wave patterns as a whole, which is important for correctly constructing the mathematical models of gas dynamics, including for express-estimating in natural measurements of wave fields. Note that such wave patterns can be observed in the remote probing and observation of the internal gravity waves excited by various sources of perturbations in both the ocean and Earth's atmosphere [5, 6]. The results presented in the paper have been obtained by research performed under projects supported by the Russian Foundation for Basic Research (No. 14-01-00466).

References

- [1] V. Bulatov, Yu. Vladimirov, *Internal gravity waves: theory and applications*, Nauka Publishers, Moscow (2007).
- [2] V. Bulatov, Yu. Vladimirov, *Wave dynamics of stratified mediums*, Nauka Publishers, Moscow (2012).
- [3] V. Bulatov, Yu. Vladimirov, *Russian Journal of Mathematical Physics*, **17**, 400–412 (2010).
- [4] V. Bulatov, Yu. Vladimirov, *Journal of Engineering Mathematics*, **69**, 243–260 (2011).
- [5] V. Bulatov, Yu. Vladimirov, *Atmospheric and Oceanic Physics*, **51**, 609–614 (2015).
- [6] V. Bulatov, Yu. Vladimirov, *Fluid Dynamics*, **50**, 741–747 (2015).

Lasing characteristics in a ZnO microcavity with designable shape fabricated by focused ion beam milling

Tsu-Chi Chang¹, Ying-Yu Lai¹, Yu-Hsun Chou^{1,2}, Tien-Chang Lu¹

¹Department of Photonics, National Chiao Tung University, 1001 University Road, Hsinchu 300, Taiwan

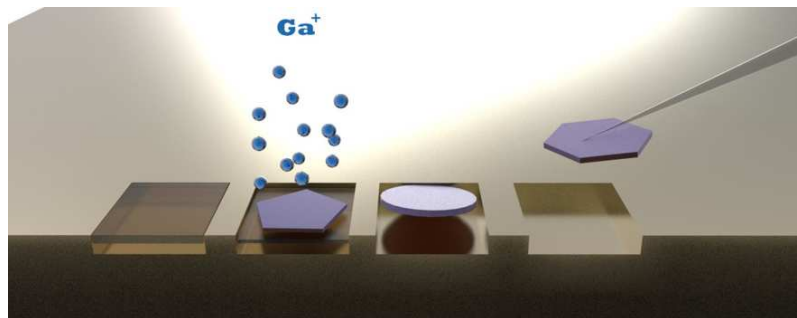
²Institute of Lighting and Energy Photonics, National Chiao Tung University, 301 Gaofa 3rd Road, Guiren District, Tainan 71150, Taiwan

e-mail: tsuchi.eo02g@g2.nctu.edu.tw

ZnO has a wide band-gap energy of 3.37 eV and a significantly large exciton binding energy of 60 meV at room temperature. Therefore, ZnO are recognized as potential light emitters in the blue and UV spectral regions. The ZnO attracted considerable attention because of various interesting optical confinement and laser cavities. ZnO nanocrystals can be synthesized by several methods, including chemical vapor deposition (CVD) [1], hydrothermal [2, 3], pulsed laser deposition (PLD).

There are many reports on various kinds of ZnO nanocrystals such as nanosheets [4], nanowires [5] and nanodisks [6, 7]. Most of the previous reports discussed the lasing mechanisms in a single ZnO nanowire and microdisks [8]. They were synthesized by bottom-up methods with high material quality. On the other hand, up to now, lasing characteristics on a top-down synthesis approach was difficult to fabricate a single ZnO nanostructure. Further investigations of lasing characteristics and clarification of lasing mechanisms on a single ZnO nanostructure are needed.

We show a three-dimensional membrane cavity fabrication technique and corresponding lasing characteristics of the fabricated rectangular ZnO membrane microcavity (MC) using optical injection. The ZnO membrane was cut from a single crystalline ZnO substrate by using a focused ion beam, and was then placed onto a SiO₂ substrate by using a glass tip. The micro-photoluminescence measurement performed on the fabricated ZnO membrane MC at 77 K showed an obvious feature of lasing action including non-linear increasing of intensity and linewidth narrowing. By using this fabrication approach, various MCs with desired shapes can be made.



References

- [1] S. Ruhle, L. K. van Vugt, H. Y. Li, N. A. Keizer, L. Kuipers, D. Vanmaekelbergh, *Nano Letters*, Vol. **8**, pp. 119–123, 2008.
- [2] C. Czekalla, C. Sturm, R. Schmidt-Grund, B. Q. Cao, M. Lorenz, M. Grundmann, *Applied Physics Letters*, Vol. **92**, 2008.
- [3] L. Du, H. B. Mao, X. Q. Luo, J. Q. Wang, Z. Remes, *Physica B. Condensed Matter*, Vol. **434**, pp. 74–77, 2014.
- [4] K. Okazaki, D. Nakamura, M. Higashihata, P. Iyamperumal, T. Okada, *Optics Express*, Vol. **19**, pp. 20389–20394, 2011.
- [5] M. H. Huang, S. Mao, H. Feick, H. Q. Yan, Y. Y. Wu, H. Kind, *et al.*, *Science*, Vol. **292**, pp. 1897–1899, 2001.
- [6] R. Chen, B. Ling, X. W. Sun, H. D. Sun, *Advanced Materials*, Vol. **23**, pp. 2199, 2011.
- [7] C. X. Xu, J. Dai, G. P. Zhu, G. Y. Zhu, Y. Lin, J. T. Li, *et al.*, Vol. **8**, pp. 469–494, 2014.
- [8] J. Dai, C. X. Xu, R. Ding, K. Zheng, Z. L. Shi, C. G. Lv, *et al.*, *Applied Physics Letters*, Vol. **95**, 2009.

Analysis of a diffraction problem for equations of complex heat transfer

Chebotarev A.Yu., Kovtanyuk A.E., Grenkin G.V., Prokhorov I.V.

Institute for Applied Mathematics, FEB RAS, 7 Radio st., 690041 Vladivostok, Russia;

Far Eastern Federal University, 8 Sukhanova st., 690950 Vladivostok, Russia

e-mail: cheb@iam.dvo.ru, kovtanyuk.ae@dvfu.ru, glebgrenkin@gmail.com, prh@iam.dvo.ru

The interest in studying problems of complex heat transfer (where the radiative and conductive contributions are simultaneously taken into account) is motivated by their importance for many engineering applications. Problems of diffraction type for complex heat transfer equations arise in scattering media with a piecewise constant refractive index. The use of steady-state P_1 approximation

(diffusion model) of the radiative heat transfer leads to special conjugation problems for nonlinear elliptic systems.

Let us consider a bounded domain Ω consisting of two subdomains Ω_i , $i = 1, 2$, that is $\Omega = \Omega_1 \cup \overline{\Omega_2}$. Suppose that $\partial\Omega_1 \cap \partial\Omega_2 = \emptyset$. So, Ω_1 is called an outer subdomain, Ω_2 an inner subdomain. The governing equations of complex heat transfer in each subdomain Ω_i have the following normalized form [1–3]:

$$-a\Delta\theta_i + b(|\theta_i|\theta_i^3 - \varphi_i) = 0, \quad -\alpha\Delta\varphi_i + \beta(\varphi_i - |\theta_i|\theta_i^3) = 0. \quad (1)$$

Here, φ_i is the normalized radiation intensity averaged over all directions, θ_i is the normalized temperature in the subdomain Ω_i . The parameters a, b, α and β are given, and they are constant in each domain. Let n be the refractive index. Denote $a = a_i$, $b = b_i$, $\alpha = \alpha_i$, $\beta = \beta_i$, and $n = n_i$ in the subdomain Ω_i . The following boundary conditions on $\Gamma := \partial\Omega$ are assumed:

$$a\partial_n\theta_1 + c(\theta_1 - \Theta_0) = 0, \quad \alpha\partial_n\varphi_1 + \gamma(\varphi_1 - \Theta_0^4) = 0, \quad (2)$$

where c and γ are given positive functions defined on Γ , and the symbol ∂_n denotes the derivative in the outward normal direction. Conditions at the inner boundary $\Gamma_0 := \partial\Omega_2$ are of the form:

$$\theta_1 = \theta_2, \quad a_1\partial_n\theta_1 = a_2\partial_n\theta_2, \quad \alpha_1n_1^2\partial_n\varphi_1 = \alpha_2n_2^2\partial_n\varphi_2, \quad \varphi_2 - \varphi_1 = h\partial_n\varphi_1. \quad (3)$$

Here h is a given positive parameter depending on the reflective properties of Γ_0 , ∂_n is the normal derivative inside Ω_2 .

In this talk, a priori estimates of temperature and radiation intensity in the space $L^\infty(\Omega)$ ensuring the unique solvability of the problem (1)–(3) are presented. The theoretical analysis is illustrated by numerical examples.

References

- [1] M. F. Modest, *Radiative Heat Transfer*, Academic Press (2003).
- [2] A. E. Kovtanyuk, A. Yu. Chebotarev, N. D. Botkin, K.-H. Hoffmann, *J. Math. Anal. Appl.*, **409**, 808–815 (2014).
- [3] A. E. Kovtanyuk, A. Yu. Chebotarev, N. D. Botkin, K.-H. Hoffmann, *Commun. Nonlinear Sci. Numer. Simulat.*, **20**, 776–784 (2015).

Uniqueness of self-similar solutions obeying the problems of arbitrary discontinuity disintegration for the generalized Hopf equation with a complex nonlinearity

Chugainova A.P.

Steklov Mathematical Institute RAS, Moscow, Russia
 e-mail: anna_ch@mi.ras.ru

Solutions of the problems of disintegration of an arbitrary discontinuity of the generalized Hopf equation are under analysis. These solutions are constructed from the sequence of non-tipping Riemann waves and shock waves having the stable stationary or non-stationary structure.

In [1, 2], devoted to investigation of the solutions of the Hopf equations with complex nonlinearity, for selection of discontinuities, which have been used for construction of the solution, the request of existence of the stationary structure of the discontinuity has been posed. The structure of discontinuities has been described by the generalized (in the sense of nonlinearity) Korteweg–de Vries–Burgers equation. Appearance of the recent works [3, 4], in which spectral stability of the solutions describing the structure is investigated, makes it possible to include effectively in the notion of the permissible discontinuity the claim of stability of its structure and from this point of view revise before obtained results. We call admissible (i. e. realizable in practice for disintegration of an arbitrary discontinuity) discontinuities with structure, having stability property.

Introduction of the request of stability of the structure in the notion of admissibility of discontinuities results in cutting down the set of admissible discontinuities, described in [1, 2], and eliminate non-uniqueness of the solution of the problem about disintegration of the arbitrary shock, discovered in previous investigations [1]. Furthermore, for construction of the solution of the problem we have used the discontinuities with structure, containing the internal periodic oscillations (non-stationary structures). Variation of the quantities in such discontinuities may not coincide with variation of the quantities in any discontinuities with stationary structure. It has been shown that the solution of the problem of disintegration of the arbitrary discontinuity in this setting always uniquely exists.

References

- [1] A. G. Kulikovskii, A. P. Chugainova, Modeling the influence of small-scale dispersion processes in a continuum on the formation of large-scale phenomena, *Computational Mathematics and Mathematical Physics*, **44**, No 6, 1062–1068 (2004).
- [2] A. G. Kulikovskii, A. P. Chugainova, Classical and nonclassical discontinuities and their structures in nonlinear elastic media with dispersion and dissipation, *Russian Math. Surveys*, **63**, Suppl. 2, 283–350 (2008).
- [3] A. T. Il'ichev, A. P. Chugainova, V. A. Shargatov, Spectral stability of special discontinuities, *Dokl. Math.*, **91**, No 3, 347–351 (2015).
- [4] A. P. Chugainova, V. A. Shargatov, Stability of a discontinuity structure described by the generalized KdV–Burgers equation *Computational Mathematics and Mathematical Physics*, **56**, No 2, (2016).

On the Laue–Bragg–Wulff scattering of the acoustic Rayleigh wave by surface roughness

Vitalii N. Chukov

N. M. Emanuel Institute of Biochemical Physics RAS, Center of Acoustic Microscopy, Kosygin Str. 4, Moscow, 119334, Russia
e-mail: chukov@chph.ras.ru

The modulation of the surface acoustic Rayleigh wave [1] Laue–Bragg–Wulff scattering [2]–[11] by a deterministic cylindrically symmetrical roughness occupying finite size region of an isotropic solid surface is considered in the Born (the Rayleigh–Born [1]) approximation of the perturbation theory in roughness amplitude in detail.

It is a short-wavelength scattering, when a wavelength of the incident Rayleigh wave $\lambda = 2\pi\bar{\lambda}$ is more less than a radius of the surface rough region d , i. e. $\bar{\lambda} \ll d$. This limit of the wave scattering is well-known in the theories and experiments on the scattering of the Rontgen x-rays in the crystals and amorphous media. For the macroscopic crystals the Laue conditions of the discrete point maxima in diffraction pattern of the x-rays beam incident on the crystal due to the interference of the scattered waves are known and are confirmed by the experimental Lauegrams [2]–[9]. W. L. Bragg [2, 4] proposed to consider x-rays scattering in crystals as mirror reflections from a system of the atoms parallel planes. A corresponding condition of the interference maxima in a reflection pattern is named the Bragg condition of scattering [2]–[11].

Both Laue and Bragg conceptions of the Rontgen rays scattering in crystals are used in the x-rays crystallography and microscopy [2]–[9].

Russian professor of crystallography George V. Wulff considered [3] the physical results of the Laue, Friedrich and Knipping on x-rays scattering in crystals and noted that scattered waves propagate only along discrete directions according to the Laue conditions of the interference maxima.

Scattering of the Rontgen waves in amorphous media gives rise to the Lauegrams with a system of diffraction rings – scattered waves intensity continuous space oscillations, i. e. Bragg short-wavelength oscillations [7]. Space structure of the scattering media and definite space configurations of scatterers, that is form-factor of the scattering media, can violate the Bragg condition of scattering [7].

For scattering of the surface acoustic Rayleigh wave by a single deterministic roughness in the limit $\bar{\lambda} \ll d$, considered in the present work [10, 11], conditions of scattering maxima and minima are obtained. These conditions are named the generalized Laue–Bragg–Wulff conditions, and corresponding oscillations of the scattered Rayleigh wave intensity are named Laue–Bragg–Wulff oscillations. The short-wavelength scattering is named the Laue–Bragg–Wulff scattering.

The system of the linear independent functions describing the scattering indicatrix in dependence on radius of a rough region to wavelength ratio $d/\bar{\lambda}$ is constructed for the Laue–Bragg–Wulff $d \gg \bar{\lambda}$ limit of scattering. Each function of this system, i. e. each scattering indicatrix, corresponds to the Rayleigh wave scattering by the roughness of a definite form and has its own dependence on the $d/\bar{\lambda}$ ratio.

In the Laue–Bragg–Wulff limit this system is determined by the roughness topological characteristic of the second kind $d^m f(x)/dx^m$, where $m = 0, 1, \dots$, — derivatives of a roughness profile in the end and discontinuity points [10, 11].

A possibility of this system construction is a mathematical expression of a physical strong modulation of scattering, obtained in the present work, by a roughness form-factor in the Laue–Bragg–Wulff limit of scattering.

This phenomenon gives the new laws of scattering violating the Laue–Bragg–Wulff laws of scattering, obtained in the present work [10, 11], for the short-wavelength $\bar{\lambda} \ll d$ limit.

The new strong dependence of the scattering indicatrix frequency and scattering angular oscillations on the roughness form-factor in the Laue–Bragg–Wulff limit $\bar{\lambda} \ll d$ is obtained. The new phenomena of the Laue–Bragg–Wulff oscillations reduction, straightening and construction of an arbitrary frequency and scattering angular spectrum of scattering indicatrix, defined beforehand, due to a strong modulation of the Laue–Bragg–Wulff scattering by the roughness form-factor are obtained.

The results obtained in the present work can be used in the acoustoelectronics, solid state physics, geophysics and acoustic microscopy.

References

- [1] Lord Rayleigh, *The theory of sound*, Vols. I, II, Dover, New York (1945).
- [2] W. L. Bragg, *Proc. Camb. Philos. Soc.*, **17**, 43–57 (1913).
- [3] G. V. Wulff, *Priroda*, **1**, 27–38 (1913) (in Russian).
- [4] W. H. Bragg, W. L. Bragg, *X Rays and Crystal Structure*, G. Bell and Sons, LTD, London (1915).
- [5] Max Von Laue, *History of Physics*, Academic Press Inc., New York (1950).
- [6] I. K. Robinson, D. J. Tweet, *Rep. Prog. Phys.*, **55**, 599–651 (1992).
- [7] J. S. Blakemore, *Solid State Physics*, Cambridge University Press (1985).
- [8] J. M. Cowley, *Diffraction Physics*, Elsevier (1995).
- [9] O. H. Seeck, B. M. Murphy, *X-ray diffraction. Modern Experimental Techniques*, CRC Press, Taylor & Francis Group (2014).
- [10] V. N. Chukov, *Days on Diffraction 2011. International Conference*, Saint Petersburg, May 30 – June 3, 2011, Abstracts, p. 29.
- [11] V. N. Chukov, *Proceedings of the International Conference Days on Diffraction 2011*, Saint Petersburg, May 30 – June 3, 2011, p. 55–62.

On elasticity-tensor symmetries: material symmetry, symmetry-group average and spatial average

Tomasz Danek, Michael A. Slawinski

Memorial University of Newfoundland

e-mail: mslawins@mac.com

We examine three concepts that are pertinent to studies in continuum mechanics. They are material symmetry, symmetry-group average and spatial average. Each concept is a consequence of certain properties of the elasticity tensor.

Material symmetry is invariance given by

$$\begin{aligned} C &= \tilde{A}_1^{\text{sym}} C \tilde{A}_1^{\text{sym}T} \\ &\vdots \\ C &= \tilde{A}_n^{\text{sym}} C \tilde{A}_n^{\text{sym}T}, \end{aligned} \tag{1}$$

where n is the number of elements in the symmetry group, and \tilde{A}_i^{sym} is a rotation. C satisfying system (1) of equation is C^{sym} , which is an elasticity tensor of a given symmetry class of a Hookean solid.

A symmetry-group average is given by an orthogonal projection,

$$C_{\text{eff}}^{\text{sym}} := \int_{G^{\text{sym}}} (g \circ C) d\mu(g), \tag{2}$$

where the integration is over the symmetry group, G^{sym} , whose elements are g , with respect to the invariant measure, μ , normalized so that $\mu(G^{\text{sym}}) = 1$. Integral (2) reduces to a finite sum for the classes whose symmetry groups are finite, which are all classes except isotropy and transverse isotropy. For such symmetries, we can write integral (2) as

$$C_{\text{eff}}^{\text{sym}} = \frac{1}{n} \left(\tilde{A}_1^{\text{sym}} C \tilde{A}_1^{\text{sym}T} + \dots + \tilde{A}_n^{\text{sym}} C \tilde{A}_n^{\text{sym}T} \right).$$

If the tensor to be averaged, C , is generally anisotropic, its orientation is implicitly contained within its twenty-one components; hence, not only the averaged elasticity parameters, but also the corresponding optimal orientation of the symmetry axes or planes is obtained.

A spatial average is a moving average defined by

$$\bar{f}(x_3) = \int_{-\infty}^{\infty} w(\xi - x_3) f(\xi) d\xi,$$

where the weight, $w(x_3)$, allows us the use of many functions, since the conditions imposed on it are not restrictive; w is required to be a continuous nonnegative function tending to zero at infinities.

Each concept needs to be examined in the scope of the empirical accuracy of a given mathematical model. A relation between mathematical models and experiments, subject to measurement errors and limited resolution, might be accommodated within these concepts.

Mode matching method for resonance scattering and mode localization

Delitsyn A.L.

M. V. Lomonosov Moscow State University, Physical Dept., Moscow, Leninskie Gory, 2

e-mail: delitsyn@mail.ru

There are different methods for investigation resonance scattering problem in waveguide. The most of them are connected with consideration of Green function poles with small imaginary part.

In general this methods are not elementary. Our aim to present for the problem of scattering on two barriers in the waveguide the elementary approach which use only mode matching method. This method may be applied for mode localization problem in resonators of simple geometry.

We consider the problem

$$\begin{aligned} \Delta u + k^2 u &= 0, \quad (x, y, z) \in Q, \\ u|_{\partial Q} &= 0, \end{aligned}$$

in $Q = ((x, y) \in \Omega, z \in (-\infty, \infty))/\Gamma_i, i = 1, 2$, where Γ_i are infinite thin barriers at $z = z_i, i = 1, 2$ with small aperture. The radiation conditions corresponds to scattering of the mode on such obstacle:

$$\begin{aligned} u &= e^{i\gamma_1 z} \psi_1(x, y) + c_1 e^{-i\gamma_1 z} \psi_1(x, y) + \sum_{n=2}^{\infty} c_n e^{\gamma_n z} \psi_n(x, y), \quad z < z_1, \\ u &= d_1 e^{i\gamma_1 z} \psi_1(x, y) + \sum_{n=2}^{\infty} d_n e^{-\gamma_n z} \psi_n(x, y), \quad z > z_2, \end{aligned}$$

where

$$\begin{aligned} -\Delta_{\perp} \psi_n &= \lambda_n \psi_n, \quad (x, y) \in \Omega, \\ \psi_n|_{\partial\Omega} &= 0, \\ \gamma_1 &= \sqrt{k^2 - \lambda_1}, \quad \gamma_n = \sqrt{\lambda_n - k^2}, \quad n = 2, \dots \end{aligned}$$

We prove that for frequency close to the frequency of resonator obtained when barriers are without aperture the transition coefficient is close to 1 when diameter of aperture tend to 0. The boundary problem is reformulated as some problem in the aperture. This method may be applied for mode localization problem in resonators with barrier:

$$\begin{aligned} -\Delta u &= k^2 u, \quad (x, y) \in Q, \\ u|_{\partial Q} &= 0, \end{aligned}$$

in $Q = ((x, y) \in \Omega, z \in [z_1, z_2]/\Gamma)$.

The estimates of rate of convergence for mode localization in subdomains and eigenvalues convergence are obtained.

References

- [1] A. L. Delitsyn, *Computational Mathematics and Mathematical Physics*, **52:7**, 1289–1293 (2012).

Modeling of electromagnetic scattering on small particles by means of pattern equation method

Demin D.B.¹, **Kyurkchan A.G.**¹, **Kleev A.I.**²

¹Moscow Technical University of Communications and Informatics, 8a Aviamotornaya str., Moscow 111024, Russian Federation

²P. L. Kapitza Institute for Physical Problems RAS, 2 Kosygina str., Moscow 119334, Russian Federation

e-mails: dbdemin@gmail.com, agkmtuci@yandex.ru, kleev@kapitza.ras.ru

When solving a number of applied problems in various fields of science and technology, building an adequate model of radiation interaction with small particles is of paramount importance [1]. In particular, this problem is quite relevant with regard to intensive research into negative media (metamaterials) electrodynamics [2, 3]. For the time being, Rayleigh approximation is virtually the only

mathematical model used while solving this problem [4]. This approach is sufficiently detailed in literature for special cases of scattering, including multi-layer confocal [5] and non-confocal ellipsoid [6]. It should be noted that such a traditional approach has well-known drawbacks. In particular, use of dipole approximation does not provide required accuracy of energy balance achievement [7]. It should be pointed out that the existing methods of solving the relevant electrostatic problem have a number of crucial limitations [8].

This paper develops alternative technique based on the usage of pattern equation method (PEM) [9]. To date it has been established that PEM has important advantages over numerous multi-purpose techniques and is quite efficient for solving a wide range of problems. When building a new approach to the analysis, we used a high speed of PEM convergence which allowed obtaining explicit formulae for integral scattering characteristics applied for complex-shape scatterers. The calculation results are compared with the data obtained by means of other methods. It is demonstrated that the accuracy of calculations controlled by calculating the balance of power flows for incident and scattered waves (checking the accomplishment of optical theorem) is quite sufficient for practice.

References

- [1] M. I. Mishchenko, J. W. Hovenier, L. D. Travis, *Light Scattering by Nonspherical Particles*, Academic Press, San Diego (2000).
- [2] I. Vendik, O. Vendik, I. Kolmakov, N. Odit, *Opto-Electronics Review*, **14**, 176–186 (2006).
- [3] X. Cai, R. Zhu, G. Hu, *Metamaterials*, **2**, 220–226 (2008).
- [4] L. D. Landau, E. M. Lifshitz, *Electrodynamics of Continuous Media*, Pergamon, Oxford and New York (1984)
- [5] V. G. Farafonov, *Optics and Spectroscopy*, **88**, 441–443 (2000).
- [6] B. Posselt, V. G. Fafaronov, V. B. Il'in, M. S. Prokopjeva, *Measur. Sci. Technol.*, **13**, 256–262 (2002).
- [7] R. E. Collin, *IEEE Transactions on Antennas and Propagation*, **AP-29**, 795–798 (1981).
- [8] V. G. Farafonov, V. I. Ustimov, *Optics and Spectroscopy*, **118**, 445–459 (2015).
- [9] A. G. Kyurkchan, N. I. Smirnova, *Mathematical Modeling in Diffraction Theory Based on A Priori Information on the Analytic Properties of the Solution*, Elsevier, Amsterdam (2015).

Solvability of interface problems for the compressible and incompressible Navier–Stokes equations near the equilibrium

Denisova I.V.

Institute for Problems in Mechanical Engineering, Russian Academy of Sciences, 61 Bol'shoy prosp., V.O., St. Petersburg, 199178, Russia
e-mail: denisovairinavlad@gmail.com

Solonnikov V.A.

St. Petersburg Department of Steklov Math. Institute, Russian Academy of Sciences, 27 Fontanka, St. Petersburg, 191023, Russia
e-mail: solonnik @pdmi.ras.ru

The study is concerned with interface problems for the Navier–Stokes equations governing viscous compressible flows. The main difficulty of such problems is due to the fact that the interface between the fluids is unknown. The problem on the motion of two compressible capillary fluids separated by a closed interface was studied in anisotropic Sobolev–Slobodetskiĭ [1] and Hölder spaces [3] where local solvability was obtained in both cases with restrictions on the fluid viscosities. These restrictions are discussed and a way to eliminate them is presented.

Next, the problem on the evolution of a bubble in an incompressible continuum is analyzed in the spaces $W_2^{l,l/2}$. A local existence theorem for the problem is proved in the case of non-negative surface

tension without restrictions on the viscosities and the densities imposed in [2]. The case where a drop is surrounded by a gas may be studied in the same way. Finally, the global unique solvability is obtained for the problem without surface tension forces on the interface and with small data, the liquids being located in a container of finite volume. The proof is based on an exponential global estimate for a generalized energy in a linear problem.

References

- [1] I. V. Denisova, Problem of the motion of two compressible fluids separated by a closed free interface, *Zap. Nauchn. Semin. Petersburg. Otdel. Mat. Inst. Steklov. (POMI)*, **243**, 61–86 (1997); English transl.: *J. Math. Sci.*, **99**(1), 837–853 (2000).
- [2] I. V. Denisova, Evolution of compressible and incompressible fluids separated by a closed interface, *Interface Free Bound*, **2**(3), 283–312 (2000).
- [3] I. V. Denisova, Solvability in weighted Hölder spaces for a problem governing the evolution of two compressible fluids, *Zap. Nauchn. Semin. Petersburg. Otdel. Mat. Inst. Steklov. (POMI)*, **295**, 57–89 (2003); English transl.: *J. Math. Sci.*, **127**(2), 1849–1868 (2005).

The hybrid resonance plasma of ions and electrons with imposed magnetic field understood through Bessel functions

B. Despres

LJLL, Université Pierre et Marie Curie, 1 place Jussieu 75005 Paris
 e-mail: despres@ann.jussieu.fr

L.M. Imbert-Gerard

CIMS, New York University, 251 Mercer Street, New York, NY 10012-1185
 e-mail: imbert@cims.nyu.edu

O. Lafitte

LAGA, UMR 75 39, Université Paris 13, 99 Av J.B. Clément, F-93430 Villetaneuse
 e-mail: lafitte@math.univ-paris13.fr

Consider an electroneutral plasma of ions and electrons (the density of electrons being $n_e(x)$ for all $(x, y, z) \in \mathbb{R}^3$) under the action of an imposed magnetic fields $\vec{B}_0(\vec{x}) = B_0(x)\vec{e}_z$. The cyclotron (resp. plasma) frequency of this plasma is $\omega_c(x) = \frac{eB_0(x)}{m_e}$ (resp. $\omega_p(x) = \sqrt{e^2 n_e(x) \epsilon_0 m_e}$). The electrons satisfy the fluid equations with dissipation at frequency ω (see [1]).

We are able to describe exactly the solution of the coupled Maxwell-fluid equations in the neighborhood of the point x_h of the so-called hybrid resonance $\omega_h(x_h) = \sqrt{\omega_c^2(x_h) + \omega_p^2(x_h)}$. It is a singular solution at $\nu = 0$ that can be expressed through Bessel functions, generalizing [3].

The system of Maxwell equations is $\nabla \wedge E = i\omega B$, $c^2 \nabla \wedge B = -i\omega E + \epsilon_0^{-1} \vec{j}$. It is coupled with the definition of current $\vec{j} = -en_e(x)\vec{v}_e + en_e(x)\vec{v}_I$ and the fluid equations $m_{e,I}(-i\omega + \nu)\vec{v}_{e,I} = eZ_{e,I}(E + v_{e,I} \wedge B)$. The traditional approach is to replace \vec{v}_e and \vec{v}_I in the equation on the magnetic field to deduce the effective dielectric tensor; instead we keep this system as a first order PDE system.

A Fourier mode in the transverse to \vec{B}_0 direction y is considered. The solutions write $\vec{E}(x)e^{iky}$, $\vec{B}(x)e^{iky}$, $\vec{v}_e(x)e^{iky}$, $kc = \omega$ and one obtains the system

$$\begin{aligned} \frac{d}{dx} E_2(x) &= a_\nu(x) E_2(x) + b_\nu(x) c B_3(x), \\ \frac{d}{dx} (c B_3)(x) &= c_\nu(x) E_2(x) - a_\nu(x) (c B_3)(x) \end{aligned}$$

with coefficients behaving as $(x - x_h^\nu)^{-1}$. Introducing $y := (-c_\nu(x))^{-\frac{1}{2}} c B_3(x)$, y is solution of

$$y''(x) = \left(-\frac{1}{4(x - x_h^\nu)^2} + \frac{R_\nu(x)}{(x - x_h^\nu)} \right) y$$

where R_ν is regular, non zero, in a complex neighborhood of x_h^ν . General solutions of this equation are $A(x)\sqrt{\rho_\nu(x)}J_0(\lambda\sqrt{\rho_\nu(x)}) + B(x)\sqrt{\rho_\nu(x)}Y_0(\lambda\sqrt{\rho_\nu(x)})$, where $\rho_\nu(x)$ is a *stretching function* and A and B are smooth in a neighborhood of x_h^ν , which allows us to compute the energy deposited by the magnetic field in the plasma [2].

References

- [1] F. F. Chen, R. B. White, Amplification and absorption of electromagnetic waves in overdense plasmas, *Plasma Phys.*, 16565 (1974); anthologized in *Laser Interaction with Matter, Series of Selected Papers in Physics*, ed. by C. Yamanaka, Phys. Soc. Japan (1984).
- [2] B. Despres, L. M. Imbert-Gerard, O. Lafitte, Solutions to the coldplasma model at resonances (accepted for publication at JEP, 2016).
- [3] B. Després, L.-M. Imbert-Gerard, R. Weder, Hybrid resonance of Maxwell's equations in slab geometry, *Journal de Mathématiques Pures et Appliquées*, Volume **101**(5), pp. 623–659 (2014).
- [4] F. da Silva, S. Heurax, E. Z. Gusakov, A. Popov, A numerical study of forward- and backscattering signatures on Doppler-reflectometry signals, *IEEE Transactions on Plasma Science*, **38**(9) pp. 2144–2149 (2010).

Method of calculating Lyapunov exponents for time series using artificial neural networks committees

Lyudmila A. Dmitrieva, Yuri A. Kuperin, Nikolai M. Smetanin, German A. Chernykh

Saint Petersburg State University, Russia, 199034, Saint Petersburg, Universitetskaya nab. 7/9
e-mails: l.dmitrieva@spbu.ru, y.kuperin@spbu.ru, smtnm@ya.ru, g.chernykh@spbu.ru

The aim of this work is to develop a method for calculating all Lyapunov exponents from time series with high accuracy. To achieve this goal we propose a new method for determining the local and global Lyapunov exponents for a given time series. The method is based on the results of studies [1, 2]. A special feature of the proposed method is the use of neural networks committee for the approximation of a dynamic system, generating the time series. Approximation model of a dynamical system is a trained neural network. The committees of neural networks are used to improve the accuracy of calculation of local and global Lyapunov exponents. In order to test the proposed method, we used time series that have been generated by the chaotic logistic map, Henon map and the X-component of the Lorenz system. As a result of numerical experiments we have shown that for the model time series the proposed method determines all the Lyapunov exponents of listed above dynamic systems with good accuracy. We have also considered the examples of real world time series such as physical, financial and electroencephalogram examples.

References

- [1] V. I. Oseledets, A multiplicative ergodic theorem. Lyapunov characteristic numbers for dynamical systems, *Moscow Math. Soc.*, **19**, 197–231 (1968).
- [2] A. Maus, J. C. Sprott, Evaluating Lyapunov Exponent Spectra with Neural Networks, *Chaos, Solitons & Fractals*, **51**, 13–21 (2013).

Caustics, focal points, and tsunami wave problems

Dobrokhotov, S. Yu.

A. Ishlinsky Institute for Problems in Mechanics of the Russian Academy of Sciences, Moscow;
Moscow Institute of Physics and Technology (Technical University), Dolgoprudnyi, Moscow Oblast
e-mail: dobr@ipmnet.ru

We discuss the role of caustics and focal points in tsunami wave propagation and the run-up problem. We assume that tsunami waves in the open ocean are described by solutions of the linearized

2D shallow water equations with spatially localized sources. We show that the initial perturbation contains a focal point appearing in the asymptotic solution from the very beginning. Then focal space-time caustics can appear over underwater banks and ridges, thus producing nonstationary trapped waves propagating in the form of wave trains. We show that the coastline in linear theory is a caustic of a special type as well, and hence the behavior of the asymptotic solution near the coastline is related to these type of objects. The passage to the nonlinear run-up problem is based on the Carrier–Greenspan transform, which allows one to compute the uprush distance on the beach. All these results are described by several closed-form analytical expressions and illustrated by pictures based on these expressions. No special prior knowledge is needed for understanding the talk.

Let us say several words about the method for constructing asymptotic solutions of the linearized 2D shallow water equations with spatially localized sources. It is based on a modification of Maslov’s canonical operator and, in spite of the fairly complicated original constructions, produces simple, efficient formulas for the waves and vortices propagating in a basin with a nonuniform bottom. The final formulas include minimum reasonable physical information about the problem and take into account the presence of focal points and caustics and the degeneration of the depth function on the coastline, which corresponds to the well-known run-up problem. As we said above, the coastline is viewed as a caustic of a special type, and the construction of Maslov’s canonical operator near this line is based on the Fock quantization of appropriate classical canonical transformations. It is these formulas given by the method that describe how nonstationary waves trapped by underwater banks and ridges are generated, in what way the curvature of the Earth surface affects the wave amplitude, why and where the wave profiles are influenced by weak dispersion effects caused by “standard water dispersion” as well as by the dispersion due to rapidly oscillating parts of the bottom, what the linear run-up effects look like, etc. Then we use the Carrier–Greenspan transformation for nonlinear shallow water equations to generalize the 1D Pelinovskii–Mazova formulas for the long-wave uprush to the 2D case and present formulas relating the initial source characteristics to the uprush distance on the beach.

The talk is based on joint research with J. Brüning, V. Grushin, D. Lozhnikov, D. Minenkov, V. Nazaikinskii, S. Sekerzh-Zenkovich, S. Sergeev, A. Shafarevich, B. Tirozzi, A. Tolchennikov, T. Tudorovskii, C. Vargas, and B. Volkov. The research was supported by RFBR grants nos. 05-01-00968, 08-01-00726, 11-01-00973, and 14-01-00521 (Russia), DFG project SFB 647/3 (Germany), and the RITMARE program of CINFAI (Italy).

High frequency Gaussian beams for cold plasma in a toroidal domain

Dobrokhotov S., Klevin A.

Ishlinsky Institute for Problems in Mechanics of the Russian Academy of Sciences, Moscow, Russia;
Moscow Institute of Physics and Technology (Technical University), Dolgoprudnyi, Moscow oblast,
Russia

e-mails: dobr@ipmnet.ru, klyovin@mail.ru

Cardinali A., Tirozzi B.

Laboratori Enea, Frascati, Italy

e-mails: alessandro.cardinali@enea.it, alessandro.cardinali@enea.it

We consider a system of linear PDE describing a cold plasma in a toroidal domain in three-dimensional space. This system simulates the passage of a laser beam through the TOKAMAK, it consists of 9 equations for the electric field and the velocities of electrons and ions in a given magnetic field.

Asymptotic solutions describing high-frequency Gaussian beams are constructed with the help of the Maslov complex germ theory in a fairly effective form. The solutions of the system are localized in the neighborhood of the beam passing through the toroidal domain (the camera). The equations for a ray take into account the density of particles in the camera and do not “feel” the presence

of the magnetic field because of the high frequency of the Gaussian beam; the dependence on the magnetic field is contained in the amplitude of the electric field. Before the TOKAMAK camera the amplitude of the Gaussian beam is the same as in free space, but after the camera the amplitude vector rotates under the influence of the magnetic field, and the formula for the angle of rotation is given explicitly. Using the asymptotic formulas for the Gaussian beams and the Radon transform we also construct the analytical-numerical algorithm to analyze the parameters of the magnetic field in the TOKAMAK.

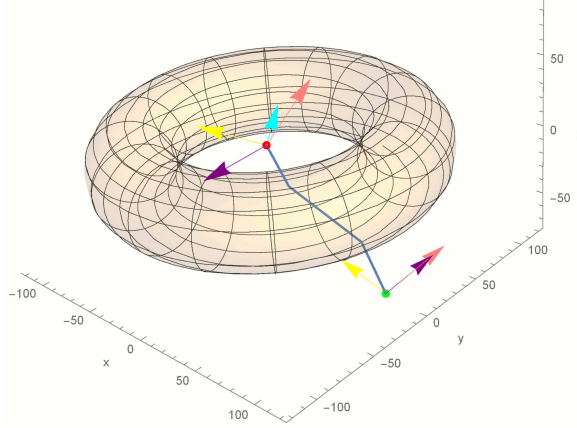


Fig. 1: The ray and the vector-amplitude before and after toroidal domain.

This work was supported by RFBR (grants No. 14-01-00521, No. 16-31-00442).

Homogenization in the Cauchy problem for a wave equation with rapidly varying coefficients

Dobrokhotov S.Yu.^{1,2}, Nazaikinskii V.E.^{1,2}, Tirozzi B.³

¹A. Ishlinsky Institute for Problems in Mechanics of Russian Academy of Sciences, Moscow, Russia

²Moscow Institute of Physics and Technology (Technical University), Dolgoprudny, Russia

³Centro Ricerche Enea, Frascati, Rome, Italy

e-mails: doobr@ipmnet.ru, nazaikinskii@yandex.ru, brunellotirozzi@gmail.com

We say that a smooth function $f(x, \varepsilon)$ of $x \in \mathbf{R}^n$ arbitrarily depending on the small parameter $\varepsilon > 0$ is *averageable* if $|\partial_x^\alpha f(x, \varepsilon)| \leq C_\alpha \varepsilon^{-|\alpha|}$, $|\alpha| = 0, 1, 2, \dots$, as $\varepsilon \rightarrow 0$ and the convolution

$$[\varphi *_{\gamma} f](x, \varepsilon) := \int_{\mathbf{R}^n} f(x - \varepsilon^\gamma \xi, \varepsilon) \varphi(\xi) d\xi,$$

together with all of its x -derivatives, is uniformly bounded as $\varepsilon \rightarrow 0$ for any function $\varphi(x)$ in the Schwartz class $\mathcal{S}(\mathbf{R}^n)$ of rapidly decaying function and any $\gamma \in (0, 1)$. We define the *average* \bar{f} of an averageable function f as $\bar{f} = \varphi *_{\gamma} f$ for arbitrary $\gamma \in (0, 1)$ and $\varphi \in \mathcal{S}(\mathbf{R}^n)$ such that

$$\int_{\mathbf{R}^n} \varphi(x) dx = 1, \quad \int_{\mathbf{R}^n} x^\alpha \varphi(x) dx = 0 \quad \text{for } |\alpha| > 0;$$

this is well-defined (more precisely, independent modulo $O(\varepsilon^\infty)$ of the specific choice of φ and γ).

Consider the Cauchy problem for the wave equation with localized initial data

$$u_{tt} - \langle \nabla, c^2(x, \delta, \varepsilon) \nabla \rangle u = 0, \quad u|_{t=0} = h^{1-n/2} V\left(\frac{x}{h}\right), \quad u_t|_{t=0} = 0, \quad (1)$$

where $V(y) \in \mathcal{S}(\mathbf{R}^n)$, $c^2(x, \delta, \varepsilon) = c_0^2(x) + \delta f(x, \varepsilon)$, the function $c_0^2(x) \geq C > 0$ is bounded together with all derivatives, $f(x, \varepsilon)$ belongs to an algebra of averageable functions, and the small parameters

ε , δ , and h are related by $h \sim \delta \sim \sqrt{\varepsilon}$. The initial data in (1) are normalized in such a way that the energy integral of the solution, which is equivalent to $\|\partial_x u\|_{L_2(\mathbf{R}^n)}^2 + \|\partial_t u\|_{L_2(\mathbf{R}^n)}^2$, is of the order of 1 as $h \rightarrow 0$. Along with problem (1), consider the *homogenized problem*

$$v_{tt} - \langle \nabla, \bar{c}^2(x, \delta, \varepsilon) \nabla \rangle v = 0, \quad v|_{t=0} = h^{1-n/2} V \left(\frac{x}{h} \right), \quad v_t|_{t=0} = 0, \quad (2)$$

where $\bar{c}^2(x, \delta, \varepsilon) = c_0^2(x) + \delta \bar{f}(x, \varepsilon)$, which can be solved asymptotically by known methods (see the survey [1]).

Theorem. *Let u and v be the solutions of problems (1) and (2), respectively. Then*

$$\|u - v\|_{W_2^1(\mathbf{R}^n)} + \|u_t - v_t\|_{L_2(\mathbf{R}^n)} = O(\delta^{1-\kappa})$$

locally uniformly with respect to t for any $\kappa > 0$.

We will discuss classes of averageable functions, the relations between this result and other approaches to homogenization (see the references in [1, 2]), various generalizations, and possible applications to modeling tsunami wave propagation. A preliminary version of the result was announced in [2]. The research was supported by RFBR project 14-01-00521 and the CINFAI-RITMARE project.

References

[1] S. Yu. Dobrokhotov, V. E. Nazaikinskii, in *50 Years of Ishlinsky Institute for Problems in Mechanics of Russian Academy of Sciences*, Nauka, Moscow (2015), pp. 98–139 [Russian].
 [2] S. Yu. Dobrokhotov, V. E. Nazaikinskii, B. Tirozzi, *Dokl. Akad. Nauk*, **461**:5, 516–520 (2015).

Homogenization of hyperbolic-type equations

Dorodnyi M.A., Suslina T.A.

St. Petersburg State University, Universitetskaya nab. 7/9, St. Petersburg, 199034, Russia
 e-mails: st023864@student.spbu.ru, t.suslina@spbu.ru

In $L_2(\mathbb{R}^d; \mathbb{C}^n)$, we consider a selfadjoint strongly elliptic operator A_ε , $\varepsilon > 0$, given by the differential expression $b(\mathbf{D})^* g(\mathbf{x}/\varepsilon) b(\mathbf{D})$. Here $g(\mathbf{x})$ is a periodic bounded and positive definite $(m \times m)$ -matrix-valued function, and $b(\mathbf{D}) = \sum_{l=1}^d b_l D_l$ is a first order differential operator. It is assumed that b_l , $l = 1, \dots, d$, are constant $(m \times n)$ -matrices, $m \geq n$, and the symbol $b(\boldsymbol{\xi})$ has maximal rank.

We study the behavior of the operator $\cos(tA_\varepsilon^{1/2})$, $t \in \mathbb{R}$, for small ε . It is proved that, as $\varepsilon \rightarrow 0$, $\cos(tA_\varepsilon^{1/2})$ converges to $\cos(t(A^0)^{1/2})$ in the norm of operators acting from the Sobolev space $H^s(\mathbb{R}^d; \mathbb{C}^n)$ (with a suitable s) to $L_2(\mathbb{R}^d; \mathbb{C}^n)$. Here $A^0 = b(\mathbf{D})^* g^0 b(\mathbf{D})$ is the effective operator. In [1], the following sharp order error estimate was obtained:

$$\|\cos(tA_\varepsilon^{1/2}) - \cos(t(A^0)^{1/2})\|_{H^2(\mathbb{R}^d) \rightarrow L_2(\mathbb{R}^d)} \leq (C_1 + C_2|t|)\varepsilon. \quad (1)$$

Also, by interpolation, $\|\cos(tA_\varepsilon^{1/2}) - \cos(t(A^0)^{1/2})\|_{H^s \rightarrow L_2} = O(\varepsilon^{s/2})$ for $0 \leq s \leq 2$.

Now we obtain more subtle results [2]. From one hand, we confirm that (1) is sharp: in the general case the estimate $\|\cos(tA_\varepsilon^{1/2}) - \cos(t(A^0)^{1/2})\|_{H^s(\mathbb{R}^d) \rightarrow L_2(\mathbb{R}^d)} = O(\varepsilon)$ is not true if $s < 2$. The supporting examples are given.

From the other hand, we distinguish conditions on the operator under which the result can be improved:

$$\|\cos(tA_\varepsilon^{1/2}) - \cos(t(A^0)^{1/2})\|_{H^{3/2}(\mathbb{R}^d) \rightarrow L_2(\mathbb{R}^d)} \leq (\tilde{C}_1 + \tilde{C}_2|t|)\varepsilon,$$

and then also $\|\cos(tA_\varepsilon^{1/2}) - \cos(t(A^0)^{1/2})\|_{H^s \rightarrow L_2} = O(\varepsilon^{2s/3})$ for $0 \leq s \leq 3/2$. In particular, this is the case for the scalar elliptic operator $A_\varepsilon = -\text{div } g(\mathbf{x}/\varepsilon) \nabla$, where the matrix $g(\mathbf{x})$ has real entries.

The results are applied to study the behavior of the solution $\mathbf{v}_\varepsilon(\mathbf{x}, t)$ of the Cauchy problem for the hyperbolic-type equation $\partial_t^2 \mathbf{v}_\varepsilon = -A_\varepsilon \mathbf{v}_\varepsilon$. Applications to the acoustics equation and the system of elasticity theory are given.

Similar results for the Schrödinger-type equations have been obtained in [3]. We develop the approach of [1] and [3]. The method is based on the scaling transformation, the Floquet–Bloch theory and the analytic perturbation theory.

References

- [1] M. Sh. Birman, T. A. Suslina, Operator error estimates in the homogenization problem for non-stationary periodic equations, *St. Petersburg Math. J.*, **20**, no. 6, 873–928 (2009).
- [2] M. A. Dorodnyi, T. A. Suslina, Homogenization of hyperbolic-type equations with periodic coefficients, in preparation.
- [3] T. A. Suslina, Homogenization of nonstationary Schrödinger type equations with periodic coefficients, Preprint (2015), arXiv:1508.07641 [math.AP].

Averaged equations of higher order for microinhomogeneous media

Eglit M.E.¹, Yakubenko T.A.², Yakubenko A.E.²

¹Lomonosov Moscow State University, Moscow 119991, Russia

²Institute of Mechanics, Lomonosov Moscow State University, Moscow 119991, Russia

e-mails: m.eglit@mail.ru, yakubta@mail.ru, yakub@imec.msu.ru

Dynamic processes in periodic inhomogeneous anisotropic elastic media as well as in thin plates and bars are considered. The ratio ε of the medium inhomogeneity scale or the thickness of plates and bars to the typical wave length is supposed to be small. The mathematical homogenization method based on two-scale asymptotic expansions on ε is used to derive the averaged effective equations [1]. Commonly, the averaged equations in zeroth approximation on ε only are derived. However, the equations of higher order of accuracy on ε are also needed, e.g., to describe dispersion of waves in microinhomogeneous media, to take into account the scale effect, i.e., the dependence on the inhomogeneity scale, to study processes in narrow domains, e.g., the structure of shock waves in composites, to calculate the coefficients of models in couple-stress elasticity by information of the medium structure and to study rather short waves and processes in relatively thick plates and bars. In this paper various asymptotically equivalent versions of the higher order effective equations are derived and investigated.

References

- [1] N. S. Bakhvalov, G. P. Panasenko, *Homogenization. Averaging Processes in Periodic Media. Mathematical Problems in Mechanics of Composite Materials*, Nauka, Moscow (1984), Kluwer Academic Publishers, Dordrecht-Boston-London (1989).

The numerical solution of the problem of electromagnetic wave diffraction by a system of free located bodies screens and wires

Roman O. Evstigneev, Mikhail Yu. Medvedik, Marina A. Moskaleva, Aleksei A. Tsupak

Department of Mathematics and Supercomputer Modeling, Penza State University, 40, Krasnaya street, Penza, Russia

e-mails: mmm@pnzgu.ru, _medv@mail.ru, m.a.moskaleva1@gmail.com

The three-dimensional vector problem of electromagnetic wave diffraction by systems of free located bodies, screens and wires is considered. The original boundary value problem for Maxwell's

equations is reduced to a system of integro-differential equations. The system of linear algebraic equations is obtained using the Galerkin method with compactly supported basis functions. The subhierarchical method is applied to solve the diffraction problem by scatterers of irregular shapes. Several results are presented.

Bound state for dielectric waveguide with locally perturbed core

Faleeva M.P., Popov I.Y.

ITMO University, Kronverkskiy, 49, Saint Petersburg 197101, Russia
e-mails: faleeva.masha@gmail.com, popov1955@gmail.com

Optical fibers with high contrast in permittivity are widely used (see, e.g., [1, 2, 3, 4]). We consider a cylindrical dielectric waveguide (permittivity $\epsilon = \epsilon_1 > 1$ with a core (permittivity $\epsilon = \epsilon_2 \gg \epsilon_1$) in a vacuum (permittivity $\epsilon = 1$). The core has single small gap filled with a material with permittivity $\epsilon = \epsilon_1$). Analysis of electromagnetic waves reduces to the investigation of the scalar equation for the electric field. We show that a bound state below the bottom of the continuous spectrum exists for the system. Variational approach is used. We construct the trial function and obtain the necessary estimate. The technique is analogous to that in [4].

References

- [1] W. Axmann, P. Kuchment, L. Kunyansky, *J. Light. Tech.*, **17**, 1996–2007 (1999).
- [2] A. Tip, A. Moroz, J.M. Combes, *J. Phys. A: Math. Gen.*, **33**, 6223–6252 (2000).
- [3] I. Y. Popov, A. I. Trifanov, E. S. Trifanova, *Comp. Math. Math. Phys.*, **50** (11), 1830–1836 (2010).
- [4] O. P. Melnichuk, I. Y. Popov, *J. Math. Phys.*, **46**, 073501 (2005).

Complex WKB method for difference equations in unbounded domains

A. Fedotov, E. Shchetka

St. Petersburg State University, 3, Ulyanovskaya st., St. Petersburg, 198504, Russian Federation
e-mails: fedotov.s@mail.ru, shchetka.ekaterina@mail.ru

In the complex plane, we consider the difference Schrödinger equation

$$\psi(z+h) + \psi(z-h) + v(z)\psi(z) = E\psi(z), \quad z \in \mathbb{C}, \quad (1)$$

where $h > 0$ and $E \in \mathbb{C}$ are parameters, and v is a trigonometric polynomial, i.e., $v(z) = \sum_{k=-m}^n c_k e^{ikz}$, $m, n > 0$, $c_n, c_{-m} \neq 0$.

If $v = 2 \cos z$, equation (1) is called Harper equation. This equation appeared as a model to study the spectrum of a Bloch electron in a crystal placed in a weak constant magnetic field. V. Buslaev and A. Fedotov studied quasiclassical asymptotics of solutions of Harper equation on the complex plane (see [1]). It turns out that solutions have the standard quasiclassical behavior for sufficiently small h on certain canonical domains on the complex plane.

We generalize their result to the case where the potential v is a trigonometric polynomial and provide a relatively simple proof of the main theorem of the method.

References

- [1] V. S. Buslaev, A. A. Fedotov, The complex WKB method for Harper's equation, *St. Petersburg Math. J.*, **6**(3), 495–517 (1995).

On difference equations with meromorphic coefficients

A. Fedotov

St. Petersburg State University, 3, Ulyanovskaya st., St. Petersburg, 198504, Russian Federation
e-mails: fedotov.s@mail.ru, a.fedotov@spbu.ru

In the complex plane, consider a difference Schrödinger equation of the form

$$\psi(z+h) + \psi(z-h) + v(z)\psi(z) = E\psi(z) \quad z \in \mathbb{C}, \quad (1)$$

where v is a periodic entire or meromorphic function, and h is a positive constant. Such equations arise in particular in the framework of Sommerfeld–Malyuzhinets method and in solid state physics. There are solutions to (1) playing a very important role in applications. These are its minimal solutions. If v is entire, they are entire solutions growing as slowly as possible simultaneously as $\text{Im } z \rightarrow \pm\infty$. If v is meromorphic, then, in addition, the set of the poles of a minimal solution has to be the smallest possible. The minimal entire solutions were first introduced and studied by V. Buslaev and A. Fedotov in the case where v is a trigonometric polynomial. For $v(z) = \cot(\pi z)$, A. Fedotov and F. Sandomirski have constructed minimal meromorphic solutions. Now, we turn to the case, where that v has a finite number of poles on its period, and tends to constant limits as $\text{Im } z \rightarrow \pm\infty$. We plan to discuss briefly applications of our results to physical problems.

On the reflection coefficient for the Stark–Wannier equation

A. Fedotov

St. Petersburg State University, 3, Ulyanovskaya st., St. Petersburg, 198504, Russian Federation
e-mails: fedotov.s@mail.ru, a.fedotov@spbu.ru

One of the models for an electron in a crystal placed in a constant electric field is the Stark–Wannier equation

$$-\psi''(x) + (v(x) - \epsilon x)\psi(x) = E\psi(x), \quad x \in \mathbb{R}, \quad (1)$$

where v is a periodic *potential* describing the internal field of the crystal, ϵ is a parameter proportional to the electric field, and E the *energy of the electron*. For this equation, in a natural way, one can define a reflection coefficient r . It appears to be ϵ -periodic in E , and its zeros are the well-known Stark–Wannier resonances. They are located in the lower half-plane of the complex plane. We describe the asymptotics of the Fourier coefficients r_n of r as $n \rightarrow +\infty$. This allows us to study the asymptotics of the resonances far from the real axis.

The talk is based on a joint work with F. Klopp.

The energy flux analysis of the “shell” type waves in the infinite cylindrical shell filled with acoustical fluid

Filippenko G.V.

Institute for Problems in Mechanical Engineering, V.O., Bolshoj pr., 61, St. Petersburg, 199178, Russia
e-mails: g.filippenko@gmail.com, g.filippenko@spbu.ru

The problem of oscillations of the systems containing pipelines filled with the liquid is one of the actual problems of modern techniques. It is important to estimate the parameters of vibrations and acoustical fields of such objects in order to provide the construction from damaging, but calculation of these complicated systems demands major computing resources. Therefore the consideration of simple model problems which have exact analytical solution [1] is actual. On these models it is possible to analytically explore main effects and also to use them as the test problems for computing

packages. The problem of joint oscillations of infinite thin cylindrical shell with ideal acoustical fluid inside it is considered. The “shell” type waves are explored. The propagating waves and energy flux are analyzed in the system shell-liquid. The comparison of different mechanisms of energy transmission in the shell and input of the energy flux in the water is fulfilled.

References

- [1] G. V. Filippenko, Energy aspects of wave propagation in an infinite cylindrical shell fully submerged in liquid, *Vycisl. Meh. Splos. Sred — Computational Continuum Mechanics*, **7**(3), 295–305 (2014).

New approach to the connection problem for general Heun’s functions

Plamen Fiziev

JINR, Dubna

e-mail: fiziev@theor.jinr.ru

New geometrical approach to the connection problem of local solutions to the general Heun equation is developed and described in details.

The mathematical model of a longitudinal deformation wave propagation in multilayered structures

Garbuzov F.E., Gula I.A., Samsonov A.M., Semenov A.A.

The Ioffe Physical Technical Institute of the Russian Academy of Sciences, 26, Polytekhnicheskaya st., St. Petersburg, 194021 Russia

e-mail: gula@mail.ioffe.ru

Since the 1960–70th the study of strain wave motion in non-homogeneous solids has taken considerable attention. Among aims are the possibility to estimate the elastic properties of composite materials, a determination of wave parameters in one layer using known wave parameters from another one etc.

In [1] the authors developed linear theory of longitudinal wave propagation in a two-layered cylinder made of different materials. The model is represented by two governing equations:

$$\begin{aligned}\rho F_{tt}(x, t) &= m F_{xx}(x, t), \\ \rho G_{tt}(x, t) - m G_{xx}(x, t) &= A F_{xxx}(x, t),\end{aligned}$$

where ρ , m , A are constants, depending on physical properties of both layers, and $F(x, t)$ and $G(x, t)$ are unknown functions, through which displacement fields are determined.

The model for nonlinear strain wave propagation in periodic composites was derived in [2]. The authors considered a composite consisting of an infinite number of layers. Corresponding power expansions for displacements:

$$\begin{aligned}u^{(1)} &= U_0(x, t) + y^2 U_1(x, t), \quad v^{(1)} = y V_0(x, t) + y^3 V_1(x, t), \\ u^{(2)} &= Q_0(x, t) + (y - h_1 - h_2)^2 Q_1(x, t), \quad v^{(2)} = (y - h_1 - h_2) W_0(x, t) + (y - h_1 - h_2)^3 W_1(x, t),\end{aligned}\tag{1}$$

where $u^{(i)}$ and $v^{(i)}$ are displacements along x and y axes in i -th layer, are hypothetical and are thought to be hardly applicable to the structures, consisting of a finite number of layers. The power expansions (1) are illustrated schematically in Fig. 1.

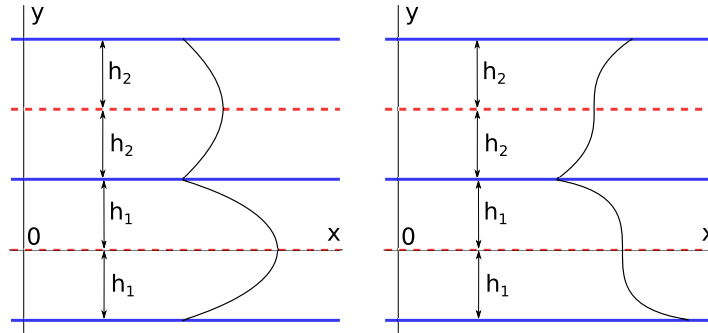


Fig. 1: Geometrical interpretation of power expansions (1) for displacements: the lateral one is to the left, the transversal one — to the right.

We developed mathematical models to describe propagation of nonlinear longitudinal deformation waves in three-layered rod with rectangular cross-section, two-layered cylindrical rod and three-layered semi-infinite plate. The refinements allow us to describe the waves in composites made of several layers and obtain the strain distribution.

References

- [1] M. Moulana, G. A. Nariboli, *Acta Mechanica*, **24**, 13–24 (1976).
- [2] A. V. Porubov, I. V. Andrianov, V. V. Danishevskyy, *International Journal of Solids and Structures*, **49**, 3381–3387 (2012).

Trapped modes of oscillation and localized buckling of a tectonic plate as a possible reason of an earthquake

Gavrilov S.N.^{1,2}, Mochalova Yu.A.¹, Shishkina E.V.¹

¹Institute for Problems in Mechanical Engineering RAS, St. Petersburg, Bolshoy pr. V.O., 61

²Peter the Great St. Petersburg Polytechnic University, St. Petersburg, Polytechnicheskaya str., 29
e-mails: serge@pdmi.ras.ru, yumochalova@yandex.ru, shishkina_k@mail.ru

We suggest a mechanical model describing buckling of a tectonic plate due to non-stationary longitudinal wave of compression that propagates along the plate. For low frequencies the interaction of a tectonic plate with its environment can be approximately described by means of the Winkler elastic foundation. Introducing the inhomogeneous Winkler foundation with weakened zone can lead to the existence of trapped modes of transversal oscillation in this mechanical system, and makes possible the localized buckling of the plate [1]. Such an instability can be considered as a possible reason of an earthquake. To describe this mechanism of an earthquake we need a coupled model that can describe both transversal and longitudinal motions of a tectonic plate.

At the beginning, to construct such a model we restrict ourselves with one-dimensional case and use the non-linear equations of the theory of elastic rods. In the framework of the model we deal with a straight extensible rod, while the shear deformations and the rotational inertia are neglected. The coupled nonlinear equations for longitudinal and transversal motions of the rod are derived. For the case, when the rod is subjected to the slowly varying in time longitudinal load, we proceed with the asymptotic reduction of the nonlinear equations. Finally, we obtain a problem on the evolution of a trapped mode of transversal oscillation in a weakly non-stationary system. If the frequency of the localized oscillation approaches zero, the amplitude of the oscillation can be a growing quantity. This is true for the solution of ODE describing oscillation of a one degree of freedom system with slowly varying stiffness (recall the Liouville–Green approximation). Nevertheless, we demonstrate that this classical result cannot be directly applied to a system with a trapped mode of oscillation. To consider the evolution of a trapped mode we plan to use the asymptotic approach proposed in study [2].

The further increasing of the longitudinal load results in the localized buckling of the tectonic plate that causes an earthquake.

We expect that the proposed model can explain the known experimental fact that ultra-low-frequency seismic pulses are registered before powerful earthquakes [3]. In [4] this was explained by beating between an oscillation eigenmode of a whole tectonic plate and a local eigenmode of an active zone.

References

[1] D. A. Indeitsev, T. S. Kuklin, Yu. A. Mochalova, *Vestnik St. Petersburg University. Mathematics*, **48**(1), 41–48 (2015).
 [2] S. N. Gavrilov, D. A. Indeitsev, *J. Appl. Math. Mech.*, **66**(5), 825–833 (2002).
 [3] E. M. Linkov, L. N. Petrova, K. S. Osipov, *Doklady Akademii Nauk, Physics of Earth*, **313**, 23–25 (1992).
 [4] V. V. Flambaum, B. S. Pavlov, *J. Seismology*, **20**(1), 385–392 (2016).

Resonant states for quantum ring with two infinite leads

Gerasimov D.A., Popov I.Yu., Popov A.I.

Department of Higher Mathematics, ITMO University, Saint Petersburg 197101, Russia
 e-mails: karlicoss@gmail.com, popov1955@gmail.com, popov239@gmail.com

Quantum graph is a widely used model of nanosystem [1–4]. If the graph Γ consists of finite number of edges of finite lengths, then the Hamiltonian has purely discrete spectrum and the eigenfunctions are complete in $L_2(\Gamma)$. If Γ contains semi-infinite edges, one has non-empty continuous spectrum and resonances generated by the eigenvalues of the Hamiltonian of finite graph. For many applications, it is important to know a space in which the resonant states form a complete system. In this paper we determine this space for a graph with two infinite leads and a loop (Fig. 1) using Sz.-Nagy model [5].

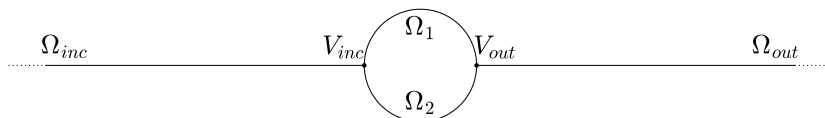


Fig. 1: Quantum graph Γ consisting of edges $\Omega_{inc}, \Omega_{out}, \Omega_1, \Omega_2$. Ω_1 and Ω_2 represent the 1D ring connected to lead Ω_{inc} via the vertex V_{inc} and to lead Ω_{out} via V_{out} .

We are interested in scattering of a wave with wavevector k incoming from the left lead to the right one. At vertices V_{inc}, V_{out} we impose Dirichlet boundary conditions for wavefunctions and δ -coupling boundary conditions with the coupling constant a for wavefunction’s derivative. After solving the system of equations, we obtain a closed-form expression for the S-matrix determinant:

$$\det S = \frac{((a^2 - 5k^2) \cos(kd) \sin(kd) - 4ak \sin^2(kd) + 2ak) + i(2ak \cos(kd) \sin(kd) - 4k^2 \sin^2(kd) + 2k^2)}{((a^2 - 5k^2) \cos(kd) \sin(kd) - 4ak \sin^2(kd) + 2ak) - i(2ak \cos(kd) \sin(kd) - 4k^2 \sin^2(kd) + 2k^2)}$$

To establish the completeness, we have to prove that S is a Blaschke–Potapov product [6], that is, $\lim_{r \rightarrow 1-0} \int_{L_r} \log |\det S(k)| \frac{dk}{(k-1)^2} = 0$, where L_r is the image of the curve $|\xi| = r$ ($r < 1$) under the map $k = i \frac{1+\xi}{1-\xi}$. Substituting $\det S$, which we calculated above, and estimating the integral, one obtains the desired result.

This work was partially financially supported by the Government of the Russian Federation (grant 074-U01), by Ministry of Science and Education of the Russian Federation (GOSZADANIE 2014/190, Projects No. 14.Z50.31.0031 and No. 1.754.2014/K), by grant MK-5001.2015.1 of the President of the Russian Federation and DFG Grant NE 1439/3-1.

References

- [1] P. Kuchment, *Waves in Random Media*, **12**(4), R1–R24 (2002).
- [2] I. S. Lobanov, A. I. Trifanov, E. S. Trifanova, *Nanosystems: Phys. Chem. Math.*, **3**(4), 512–523 (2013).
- [3] P. Exter, J. P. Keating, P. Kuchment, T. Sunada, A. Teplyaev (eds.), *Analysis on Graphs and Its Applications*, Proc. Symp. Pure Math., 77 (Providence, RI: Amer. Math. Soc.) (2008).
- [4] I. Yu. Popov, A. N. Skorydina, I. V. Blinova, *J. Math. Phys.*, **55**, 033504 (2014).
- [5] B. Sz.-Nagy, C. Foias, H. Bercoviuci, L. Kerchy, *Harmonic Analysis of Operators on Hilbert Space*, 2nd edition, Berlin: Springer (2010).
- [6] N. K. Nikolskii, *Treatise on the Shift Operator*, Berlin: Springer (1986).

Guided waves and energy flows in the coupled structure: monopole source – acoustic liquid – immersed laminate plate

Glushkov E.V., Glushkova N.V., **Miakisheva O.A.**

Institute for Mathematics, Mechanics and Informatics, Kuban State University, 350040, Russia
e-mails: evg@math.kubsu.ru, miakisheva.olga@gmail.com

Numerous technical applications ranging from the vibration isolation and noise control to the acoustic stealth of submarines assume the investigation of acoustic wave interaction with an elastic plate immersed in acoustic fluid (water or air). By now this classical problem of structural acoustic is well studied. However, it is still complicated to simulate wave processes in such fluid-loaded structures with a strict accounting for the wave source in a coupled source-structure problem. Especially, if a composite plate of complex anisotropic elastic properties is under investigation. Contemporary commercial finite-element packages are ample for such a simulation, but their use is often too expensive and so cannot provide fast parametric analysis required for the optimization of design and technology respects. More suitable for this purpose are semi-analytical solutions based on the Green's function of the source-fluid-plate structure as a whole.

The present work aims at the simulation and study of wave processes inherent to non-contact non-destructive testing (NDT) of laminate composite structures using air-coupled transducers. This is a cheaper practical alternative to the laser Doppler vibrometry that is, nevertheless, feasible and to control material properties of the plate and to detect flaws. Unlike the acoustic microscopy that utilizes bulk waves directly reflected from the plate, the air-coupled inspection of large structural areas is based on the generation of guide waves (GW) in the plate by incident ultrasound signals coming from the transducer and detection of acoustic waves re-radiated in the course of GW propagation over the plate. Hence, the questions of optimal GW excitation and source energy distribution among the incident and scattered waves are of prime concern.

Explicit integral representations for the generated and scattered wave fields have been derived using the Fourier transform technique. In the far-field, the bulk and guided waves are described by asymptotic representations obtained from those integrals using the stationary phase method and the residue technique. These representations make it possible to evaluate wave energy fluxes in the time-harmonic wave field generated by a given source. As a control of the numerical results, the energy balance has been calculated in the frequency range considered by comparing the source power with the amount of energy going away to infinity through the sphere surface of various radii. Numerical results obtained for the sources located at different distances from the plates of various material parameters have shown optimal frequency ranges for the generation of required GWs.

The work is supported by the Ministry of Education and Science of the Russian Federation (Project No. 1.189.2014K).

Band-gaps and low transmission pass-bands in layered functionally graded piezoelectric phononic crystals

Golub M.V., Fomenko S.I., Alexandrov A.A.

Institute for Mathematics, Mechanics and Informatics, Kuban State University, Krasnodar, 350040, Russian Federation

e-mails: sfom@yandex.ru, m_golub@inbox.ru, bright_sky@list.ru

Chen A.L., Wang Y.S.

Institute of Engineering Mechanics, Beijing Jiaotong University, Beijing 100044, PR China

e-mails: alchen@bjtu.edu.cn, yswang@bjtu.edu.cn

Zhang Ch.

Chair of Structural Mechanics, Department of Civil Engineering, University of Siegen, Paul-Bonatz Strasse 9-11, D-57076, Siegen, Germany

e-mail: c.zhang@uni-siegen.de

Owing to the possible advantages in a broad range of engineering applications, the wave propagation phenomena in periodic composites or phononic crystals are intensively studied in last decades [1]. In-plane wave propagation in layered piezoelectric phononic crystals composed of functionally graded interlayers arisen from the solid diffusion is considered in the present work. Wave transmission and band-gaps due to the material gradation and incident wave-field are investigated. A classification of band-gaps in layered piezoelectric functionally graded phononic crystals is proposed. The classification relies on the analysis of the eigenvalues of the transfer matrix for a unit-cell and the asymptotics derived for the transmission coefficient in the same manner as in [2]. Wave-fields, low transmission pass-bands and band-gaps are studied. The so-called low transmission pass-bands are introduced in order to identify frequency ranges, in which the wave transmission is sufficiently low for engineering applications, but it does not tend to zero exponentially as the number of the unit-cells tends to infinity. The influence of the driving parameters for electrodes on band-gaps and pass-bands is analyzed and discussed.

This work is supported by the Russian Foundation for Basic Research (Project 16-51-53043) and the grant of the President of the Russian Federation (MK-7154.2015.1).

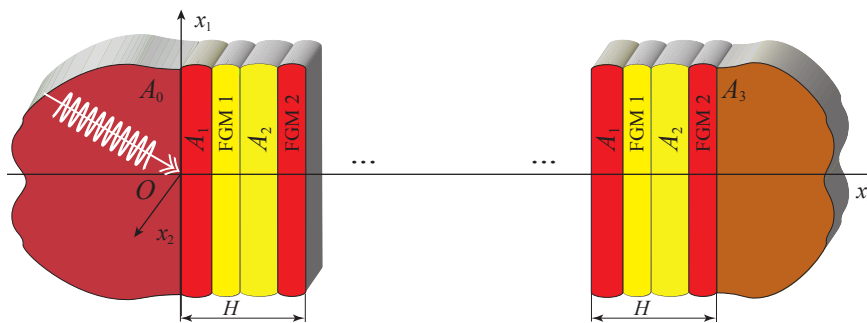


Fig. 1: Geometry of the problem considered.

References

- [1] A. Khelif, A. Adibi, *Phononic Crystals Fundamentals and Applications*, Springer-Verlag, New York (2016).
- [2] M. V. Golub, S. I. Fomenko, T. Q. Bui, C. Zhang, Y.-S. Wang, *International Journal of Solids and Structures*, **51**(13), 2491–2503 (2014).

Numerical simulation of Lamb wave excitation by the partially debonded rectangular strip-like piezoelectric actuator based on the integral approach and hp-FEM

Golub M.V., Shpak A.N.

Institute for Mathematics, Mechanics and Informatics, Kuban State University, Krasnodar, 350040, Russian Federation

e-mails: m_golub@inbox.ru, alisashpak7@gmail.com

Müller I., Fritzen C.-P.

Institute of Mechanics and Control Engineering-Mechatronics, University of Siegen, D-57076 Siegen, Germany

e-mails: inka.mueller@uni-siegen.de, Claus-Peter.Fritzen@uni-siegen.de

A two-dimensional coupled mathematical model for the dynamic behaviour of a rectangular piezoelectric actuator attached at the surface of an elastic layer is presented, see Fig. 1. Two contact problems are studied: perfect/imperfect contact between bottom of the actuator and the layer ($S_d = \emptyset$) and partially debonded actuator ($S_d \neq \emptyset$). A solution is constructed in a frequency domain, and then Laplace transform is used to obtain a non-stationary solution. Lamb wave propagation in the elastic layer is described by integral representations based on the integral approach [1]. The solution is obtained in the form of convolution of the Fourier transforms of Green's matrix and the surface load. Stress functions defined at S_c are determined as a solution of the coupled problem taking into account interaction between the layer and the piezoelectric actuator with given electric potentials V_1 and V_2 at the top and bottom surfaces. All other external boundaries of the actuator and the layer (except for S_c) are assumed free of normal and tangential stresses. The dynamic behavior of the piezoelectric sensor is simulated using the high precision finite element method also called the spectral element method [2]. Coupling between the piezoelectric actuator and the elastic layer is given by spring boundary conditions [3] used to simulate perfect and imperfect contact. In order to verify the developed coupled model an experiment has been conducted. An experimental setup with elongated rectangular perfectly glued and debonded piezoelectric actuator attached at the surface of an aluminum plate has been used. Velocities of Lamb waves at the top of the elastic layer have been measured by a laser Doppler vibrometer on the surfaces of the plate. A good correspondence between numerical and experimental results are shown.

The work is supported by the Russian Foundation for Basic Research (Projects 14-08-00370 and 16-51-53043).

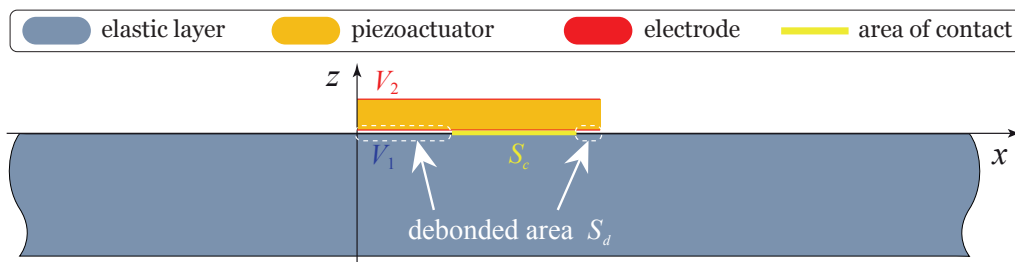


Fig. 1: Geometry of the problem considered.

References

- [1] E. V. Glushkov, N. V. Glushkova *Journal of Computational Acoustics*, **9**(3), 889–898 (2001).
- [2] R. Schulte, C.-P. Fritzen, *AIP Conference Proceedings*, **1281**, 1753–1756 (2010).
- [3] M. V. Golub, O. V. Doroshenko, A. Boström, *International Journal of Solids and Structures*, **81**, 141–150 (2016).

Generalization of energy balance for diffraction by randomly rough lossy 2D surfaces

Goray L.I.

Saint Petersburg Academic University, Khlopin 8/3, L. A, St. Petersburg, 194021, Russia;
Institute for Analytical Instrumentation, Rizhsky Prospect 26, St. Petersburg, 190103, Russia
e-mail: lig@pcgrate.com

Some surfaces are deterministic, e.g., perfect gratings, and some are random, e.g., polished mirrors. Some surfaces are 1D, e.g., one-periodic (classical) gratings or vicinal crystal surfaces, but most are 2D, e.g., bi-periodic gratings (bigratings), ocean surfaces or surfaces with atomic scale roughness. Any complex diffraction structure, e.g., butterfly wings or coronas can be represented as a combination of the described above types. There are two classical and equivalent approaches in electromagnetics, with some restrictions in each of them, to model rigorously — with rigorous boundary conditions (boundary-continuous tangential components of the full field) and radiation conditions — randomly-rough 1D and 2D surfaces. The most general and time consuming one is to use large surface lengths of many wavelengths. In this approach some window functions and tapered (narrowing) beams can be used to restrict the illuminated range and avoid numerical difficulties at endpoints. The second widely-explored approach is to use periodic boundary conditions (quasi-periodicity of Floquet–Bloch modes). This method uses an infinite beam (plane wave) and assumes that the random rough surface lengths repeats itself for given large periods having some numbers of random asperities. That means using infinite grating samples and their periodicity together with intensive Monte-Carlo simulations. From the theoretical and numerical reasons we thought it convenient to use the large-periods-grating model. So one uses the model in which an uneven surface is represented by a bigrating with large periods of d_x, d_y in perpendicular planes, which include appropriate numbers of random asperities with correlation lengths of ξ_x, ξ_y , respectively. We analyze a complex structure which, while being the bigrating from a mathematical viewpoint, is actually the rough surface for $d_x, d_y \gg \xi_x, \xi_y$. If ξ_x, ξ_y about a wavelength λ and the number of orders is large, the continuous angular distribution of the energy reflected or transmitted from randomly rough boundaries can be described by a discrete distribution $\tilde{\eta}_{n,m}$ in orders $(n, m) \in \mathbb{Z}^2$ of a bigrating, similar to [1] for classical gratings. Here the author describes an approach applicable for general 2D surfaces that generalizes the methods [1, 2] developed to study the scattering intensity (diffraction efficiency), absorption and energy balance of 1D rough surfaces and perfect bigratings.

A study of the scattering intensity starts with obtaining any statistical realizations of profile boundaries of the structure to be analyzed, after which one calculates the differential reflection coefficient (DRC) ζ (analogous of a bistatic scattering coefficient) for each realization. For $\lambda/d \ll 1$ the discrete order efficiencies is an approximation of DRC for a continuum of scattered angles θ_n^\pm, ϕ_m^\pm in the upper, +, and lower (if exist), –, mediums. Then, DRCs are averaged out over all realizations to obtain a mean DRC:

$$\sum_{\gamma_{n,m}^\pm > 0} \eta_{n,m}^\pm = \left\langle \int_{-\pi/2}^{\pi/2} \int_{-\pi/2}^{\pi/2} \zeta(\theta_n^\pm, \phi_m^\pm) d\theta_n^\pm d\phi_m^\pm \right\rangle, \quad (1)$$

where $\gamma_{n,m}^{\pm 2} = k_\pm^2 - \alpha_n^2 - \beta_m^2$, $\alpha_n = \alpha + 2\pi n/d_x$, $\beta_m = \beta + 2\pi m/d_y$ and $k = 2\pi/\lambda$. By selecting large enough samples and numbers of sampling points, one comes eventually to properly averaged properties of the rough surface; however, this approach does not involve approximations, including averaging by the Monte Carlo method [3, 4]. In the lossy case, one needs an independently calculated absorption quantity A_2 that is especially important in the x-ray and EUV ranges and also for plasmonics and metamaterials applications, where absorption plays a predominant role. For a study of the absorption one follows the similar procedure starting from one realization of A_2 , e.g., by direct calculus of A_2 using a surface integral for the Poynting vector component over the closed grating

region $\partial\Omega$, to end with A_2 averaged out over all realizations to obtain a mean value [1]

$$A = \frac{\frac{1}{2}Z_v\sqrt{\mu^+/\epsilon^+}}{d_x d_y \cos\theta} \left\langle \operatorname{Re} \int_{\partial\Omega} \mathbf{E} \times \overline{\mathbf{H}} \mathbf{n} ds \right\rangle, \quad (2)$$

where \mathbf{n} refers to the exterior unit vector normal to the surface $\partial\Omega$ enclosing Ω , Z_v is the vacuum impedance, θ is the incidence angle and ϵ , μ are electric and magnetic permittivities, respectively. Finally, the generalization of the normalized energy balance for rough lossy 2D surfaces can be represented as

$$\sum_{\gamma_{n,m}^\pm > 0} \eta_{n,m}^\pm + A = 1. \quad (3)$$

Besides being physically meaningful (3) is very useful as one of numerical accuracy tests for computational codes.

References

- [1] L. Goray, G. Schmidt, in *Gratings: Theory and Numeric Applications*, Ch. 12, pp. 447–536, Presses universitaires de Provence (2014).
- [2] L. I. Goray, Energy balance for weak formulation of diffraction by lossy anisotropic inhomogeneous gratings, *Proc. of the Int. Conf. Days on Diffraction 2015*, IEEE, pp. 123–129 (2015).
- [3] K. F. Warnick, W. C. Chew, Numerical simulation methods for rough surface scattering, *Waves Random Media*, **11**, pp. R1–R30 (2001).
- [4] M. Saillard, A. Sentenac, Rigorous solutions for electromagnetic scattering from rough surfaces, *Waves Random Media*, **11**, pp. R103–R137 (2001).

Genetic networks can learn fitness landscape

D. Grigoriev

CNRS, Mathématiques, Université de Lille, Villeneuve d’Ascq, 59655, France

e-mail: dmitry.grigoryev@math.univ-lille1.fr

S. Vakulenko

Institute for Mechanical Engineering Problems, Russian Academy of Sciences, Saint Petersburg, Russia and ITMO University, Saint Petersburg, Russia

J. Reinitz

University of Chicago, Dept. of Ecology and Evolution, Chicago, USA

A. Weber

Bonn University, Computer Dept., Bonn, Germany

We consider evolution of a large population, where fitness of each organism is defined by many phenotypical traits. These traits result from expression of many morphogenes. In turn, we assume that the morphogene expression is controlled by a number of morphogenes and by a gene regulatory network with a memory, which creates a feedback between that morphogenes and other genes. Under general assumptions on the fitness we prove that organisms having such a regulation are capable, to some extent, to recognize the fitness landscape. This fact leads to acceleration of evolution the number of mutations necessary for adaptation decreases. However, this acceleration leads to an additional risk since learning procedure can produce errors. Finally evolution acceleration reminds races on a rugged highway: when you speed up, you have more chances to crash. Results can be used to explain recent experimental data on anticipation of environment changes by some organisms.

Oblique incidence and propagation of intense acoustic beams in a fluid layer with bubbles

Gusev V.A.

Lomonosov's Moscow State University, Physical Faculty, Department of Acoustics, Russia, 119991, Moscow, Leninskie gori
e-mail: vgusev@bk.ru

The problem of the high intensity bounded acoustical beam fall at large angle to the boundary of the liquid layer with bubbles is studied. Usually bounded beams are described by evolutions equations such as Khokhlov–Zabolotskaya equation and its modifications. But these equations are set up for normal propagation with regard to initial plane. When the wave falls at some not small angle it is necessary to set up new evolution equation. The standard method to be applied is the Taylor expansion for spatial spectrum of wave. But this approach allows to derive evolution equation which is good enough only for relatively small angles. For larger angles it can be used only for waves with narrow spatial spectrum so the larger angle of incidence the more narrow spectrum we can consider. In this work the another approach is developed. The new approximation of the spatial spectrum of wave is based on quality coincidence with exact one as a whole and fulfillment of some conditions. As a result new evolution equation for the oblique propagation of nonlinear acoustic beams is set up. This equation is generalized for description of acoustic beams in the liquid layer with bubbles. The wave profile distortion and transversal wave form of beam in such medium is obtained. This work was supported by Russian Science Foundation (project 14-22-00042).

GaAs-based high index contrast photonic crystal surface emitting lasers

Kuo-Bin Hong, Chun-Chieh Yang, Tien-Chang Lu

Department of Photonics and Institute of Electro-Optical Engineering, National Chiao Tung University, 1001 University Road, Hsinchu, Taiwan
e-mail: timtclu@mail.nctu.edu.tw

In this article, we experimentally and numerically discussed the optical characteristics of a deeply-etched InGaAs/GaAs photonic crystal surface emitting layers (PCSELS) with different air hole filling factors (FFs). There are a lot of works about the optical characteristics of photonic crystal with high index contrast in the literature [1, 2]. In addition, the feature of quality factor as a function of filling factor have been discussed by FDTD calculation [3, 4]. However, emission features of PCSELS with smaller and larger filling factors appear particular phenomena.

The epitaxial wafer was grown by molecular beam epitaxy (MBE) which include GaAs substrate, AlGaAs etching stop layer, 3 pairs of InGaAs/GaAs multiple quantum wells (MQWs), AlGaAs cladding layer and GaAs layer. The PC pattern with square lattice was fabricated by E-beam lithography. The photonic bands for different guided modes calculated by the plane wave expand method (PWEM) and the operating frequency near at Γ point was picked out to meet the Bragg's condition. The targeted lasing wavelength and lattice constant were set to 950 nm and 285 nm, respectively. Moreover, air hole filling factors of 0.17 and 0.49 are also included.

In measurement, the out coupling of different guided modes was observed by the angular-resolved photoluminescence system. For $FF = 0.17$, both TE_0 and TE_2 guided modes were observed for below the threshold condition. when incident pumping power increased above the threshold condition, the lasing mode was dominated by the TE_0 mode. Interestingly, for $FF = 0.49$, room temperature lasing characteristics show that the lasing wavelength would jump from 950 nm to 880 nm when the filling factor increased to 0.49 because the lasing mode was then changed to the higher order guided mode. High index contrast photonic crystals with deeper and larger air holes were more favorable for higher order guided modes and the output emission is highly influenced by out coupling effect.

The overall concluded that further systematic studies of etching depth and filling factor of air holes could be achieved for improving the development of laser devices in the future.

References

- [1] S. H. Kwon, S. H. Kim, S. K. Kim, Y. H. Lee, S. B. Kim, *Opt. Express*, **12**, 5356–5361 (2004).
- [2] S. Kim, S. Ahn, J. Lee, H. Jeon, *Opt. Express*, **193**, 2105–2110 (2011).
- [3] D. Ohnishi, T. Okano, M. Imada, S. Noda, *Opt. Express*, **128**, 1562–1568 (2004).
- [4] M. Yokoyama, S. Noda, *Opt. Express*, **138**, 2869–2880 (2005).

Design of hybrid realization of high-index contrast gratings reflectors on silicon-on-insulator platform

Shen-Che Huang¹, Kuo-Bin Hong¹, **Tien-Chang Lu**¹, Sailing He²

¹Department of Photonics, National Chiao Tung University, Hsinchu 30010, Taiwan

²Department of Electromagnetic Engineering, Royal Institute of Technology, Stockholm 11428, Sweden

e-mail: timtclu@mail.nctu.edu.tw

High-index contrast gratings (HCGs) which composed of a thin planar higher refractive index layer surrounded by distinct lower refractive index substances [1] bring about a large stopband reflected spectra, polarization control and light mass for fast tuning of cavity modes; moreover, these structures are being widely used in several applications [2–5]. To compare with the distributed Bragg reflectors (DBRs) structure, HCG is employed the destructive interference in the in-plane direction. These gratings also can have superior performance with polarization-independent to that of DBRs.

In this study, here we report the realization of a novel hybrid silicon-compatible two-dimension grating reflectors, which could enhance the laser properties and perform the much lower cost of the integrated optoelectronic device. The optimized realistic nanoscale fabricated structure in details with various geometry-dependent designs was employed to prove the structural parameters inclusive of grating periods and duty-cycles by utilizing three-dimension computer-aided software. Based on the optimized calculated results, the optimized structure was obtained high-quality stopband spectra with reflectivity greater than 90%. The HCG designed reflector with a highly reflective stopband of over 200 nm through the monochromator system to record the reflectivity spectra was fabricated on a SOI wafer with a 220 nm silicon layer by electron-beam lithography and inductively coupled plasma process. The measured result was almost in good agreement with calculated one. We believe this accomplishment should have an influence on several photonic devices operating in the telecommunication wavelength range or even visible-infrared region of the light sources and fruitful contribution to the integrated blue-violet HCG VCSELs in the near future.

References

- [1] C. F. R. Mateus, *et al.*, *IEEE Photon. Technol. Lett.*, **16**(7), 1676–1678 (2004).
- [2] Y. Zhou, *et al.*, *IEEE J. Sel. Top. Quantum Electron.*, **15**(5), 1485–1499 (2009).
- [3] M. Shokooh-Saremi, *et al.*, *Opt. Lett.*, **35**(8), 1121–1123 (2010).
- [4] Y. Wang, *et al.*, *IEEE J. Sel. Top. Quantum Electron.*, **21**(4), 2700706 (2015).
- [5] M. C. Y. Huang, *et al.*, *Nat. Photonics*, **1**(2), 119–122 (2007).

Asymptotic estimate of the 2011 tsunami source parameters on the basis of mareograms recorded by the South Iwate GPS Buoy and the DART 21418 station

Il'yasov Kh.Kh.¹, Nazaikinskii V.E.^{1,2}, Sekerzh-Zen'kovich S.Ya.^{1,3}, Tolchennikov A.A.^{1,2}

¹A. Ishlinsky Institute for Problems in Mechanics of Russian Academy of Sciences, Moscow, Russia

²Moscow Institute of Physics and Technology (Technical University), Dolgoprudny, Russia

³Financial University under the Government of the Russian Federation, Moscow, Russia

e-mails: ilyasov@ipmnet.ru, nazaikinskii@yandex.ru, sekerzh@gmail.com,

tolchennikovaa@gmail.com

For the 2011 Tohoku tsunami, we consider a very simple four-parameter model in which the tsunami wave propagation is described in the linear approximation by the wave equation

$$\eta_{tt}(\mathbf{x}, t) - g(D(\mathbf{x})\eta_x(\mathbf{x}, t))_x - g(D(\mathbf{x})\eta_y(\mathbf{x}, t))_y = 0 \quad (1)$$

for the free surface elevation $\eta(\mathbf{x}, t)$ (where $D(\mathbf{x})$ is the depth at the point $\mathbf{x} = (x, y)$ and g is the free fall acceleration) and the tsunami is generated according to the piston model with initial data

$$\eta(\mathbf{x}, 0) = A(1 + (x - x_0)^2/R^2 + (y - y_0)^2/R^2)^{-3/2}, \quad \eta_t(\mathbf{x}, 0) = 0. \quad (2)$$

We compute the epicenter coordinates (x_0, y_0) in the geometric optics approximation from the leading crest wave arrival times at the DART 21418 station and the South Iwate GPS Buoy, use Maslov's canonical operator method [1, 2] for the approximate solution of problem (1), (2), and finally find the characteristic radius R and the free surface elevation A at the epicenter from the condition of best fit with the mareogram produced by the DART 21418 station. It turns out that the resulting solution fits very well with the mareogram produced by the South Iwate GPS Buoy. (See the figure. Only the leading crest wave is taken into account in both cases, because the dispersion-free equation (1) cannot adequately describe tail oscillations.) In the talk, we discuss the advantages and drawbacks of our model, make comparison with other studies, and outline possible implications and applications. This study continues the research in [3], where a very coarse constant-depth model with the same four-parameter source (2) was used. The talk is based on the paper [4].

The research was supported by RFBR project 14-01-00521.

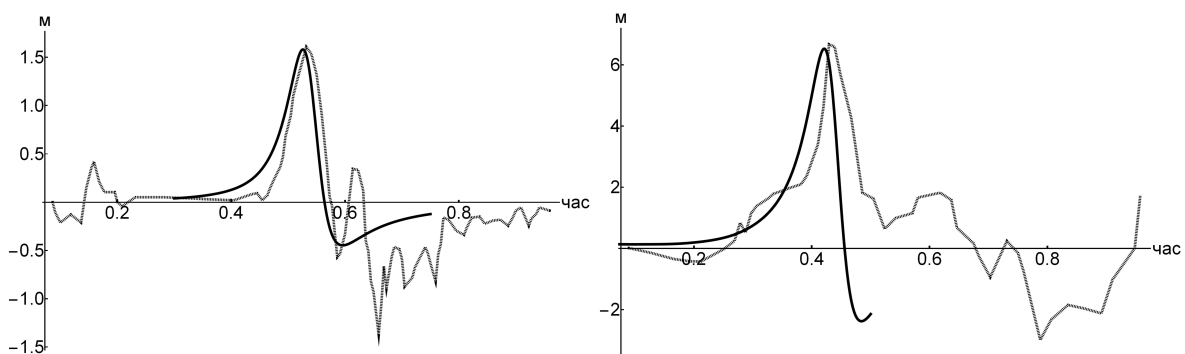


Fig. 1: (see [4]) Mareograms for DART 21418 (left) and South Iwate GPS buoy (right), shown by dotted lines. Solid lines depict the mareograms produced by the model.

References

- [1] V. P. Maslov, *Perturbation Theory and Asymptotic Methods*, Izd. MGU (1965).
- [2] S. Yu. Dobrokhotov, B. Tirozzi, A. A. Tolchennikov, *Russ. J. Math. Phys.*, **21**:4, 430–449 (2014).
- [3] S. Ya. Sekerzh-Zen'kovich, *Russ. J. Math. Phys.*, **21**:4, 504–508 (2014).
- [4] Kh. Kh. Il'yasov, et al., *Dokl. Akad. Nauk* (2016), to appear.

Single-confluent Heun solutions of the one-dimensional stationary Schrödinger equation

A.M. Ishkhanyan

Institute for Physical Research, NAS of Armenia, 0203 Ashtarak, Armenia
e-mail: aishkhanyan@gmail.com

We present fifteen possible choices for the coordinate transformation that provide energy-independent potentials that are proportional to an energy-independent continuous parameter and have a shape independent of that parameter and for which the one-dimensional Schrödinger equation is solved in terms of the single-confluent Heun functions. Because of the symmetry of the confluent Heun equation with respect to the transposition of its regular singularities only nine of the potentials are independent [1]. No confluent Heun potential can in general be transformed into another one by specifications of the involved parameters.

Five of the independent potentials present distinct generalizations of either a hypergeometric or a confluent hypergeometric classical potential, one potential possesses sub-cases of both hypergeometric types, and three others possess particular five-parametric conditionally integrable confluent hypergeometric sub-potentials. We present an explicit solution for one of the latter potentials belonging to the confluent Heun Lambert-W potential.

We show that there are other exactly or conditionally integrable sub-potentials the solution for which is written in terms of simpler special functions. However, these are solutions of different structure. For instance, there are sub-potentials for which each of the two fundamental solutions of the Schrödinger equation is written in terms of irreducible combinations of hypergeometric functions [2–4]. Several such potentials are derived with the use of extended Heun equations [5]. A complementary approach is the termination of the hypergeometric series expansions of the solutions of the Heun equations (e.g., [6]).

References

- [1] A. M. Ishkhanyan, Schrödinger potentials solvable in terms of the confluent Heun functions, *Theor. Math. Phys.* (2016), in press.
- [2] A. M. Ishkhanyan, Exact solution of the Schrödinger equation for the inverse square root potential V_0/\sqrt{x} , *Eur. Phys. Lett.*, **112**, 10006 (2015).
- [3] A. M. Ishkhanyan, The Lambert-W step-potential — an exactly solvable confluent hypergeometric potential, *Phys. Lett. A*, **380**, 640–644 (2016).
- [4] A. M. Ishkhanyan, A conditionally exactly solvable generalization of the inverse square root potential, arXiv:1511.03565 (2016).
- [5] A. Ya. Kazakov, S. Yu. Slavyanov, Euler integral symmetries for the confluent Heun equation and symmetries of the Painlevé equation PV, *Theor. Math. Phys.*, **179**, 543 (2014).
- [6] A. M. Ishkhanyan, The third exactly solvable hypergeometric quantum-mechanical potential, arXiv:1602.07685 [quant-ph] (2016).

Bi-confluent Heun potentials solvable in terms of confluent hypergeometric functions

A.M. Ishkhanyan¹, M.V. Hakobyan², T.A. Ishkhanyan^{1,3}

¹Institute for Physical Research, NAS of Armenia, Ashtarak, 0203 Armenia

²Yerevan State University, 1 Alex Manookian, Yerevan, 0025 Armenia

³Moscow Institute of Physics and Technology, Dolgoprudny, 141700 Russia

e-mail: mane.hakobian@gmail.com

We introduce a hierarchy of exactly and conditionally exactly solvable potentials for which the solution of the one-dimensional Schrödinger equation is written in terms of the confluent hyperge-

ometric functions. The presented potentials belong to the bi-confluent family of the Heun class of potentials. This family is distinguished in that it includes four of the five presently known exactly solvable confluent hypergeometric potentials that are proportional to an energy-independent parameter and have a shape that is independent of that parameter. Three of these four potentials are the classical ones — the harmonic oscillator (plus inverse square) [1], the Coulomb (plus inverse square) [1] and the Morse [2] potentials. The fourth one is the inverse square root potential reported very recently [3]. The hierarchy we introduce possesses several conditionally exactly solvable potentials including the two well-known Stillingner ones [4] as well as many quasi-exactly solvable ones. Apart from the general interest, the presented list includes several particular potentials that deserve a detailed examination because of their relevance to the modern trends such as the applications in graphene systems and the Dirac equation. The approach we apply for deriving the presented hierarchy can be extended to other Heun equations, e. g. to the general Heun equation [5, 6].

References

- [1] E. Schrödinger, Quantisierung als Eigenwertproblem (Erste Mitteilung), *Annalen der Physik*, **76**, 361–376 (1926).
- [2] P. M. Morse, Diatomic molecules according to the wave mechanics. II. Vibrational levels, *Phys. Rev.*, **34**, 57–64 (1929).
- [3] A. M. Ishkhanyan, Exact solution of the Schrödinger equation for the inverse square root potential, *EPL*, **112**, 10006 (2015).
- [4] F. H. Stillinger, Solution of a quantum mechanical eigenvalue problem with long range potentials, *J. Math. Phys.*, **20**, 1891–1895 (1979).
- [5] A. M. Ishkhanyan, The third exactly solvable hypergeometric quantum-mechanical potential, arXiv:1602.07685 [quant-ph] (2016).
- [6] A. M. Ishkhanyan, Schrödinger potentials solvable in terms of the general Heun functions, arXiv:1601.03360 [quant-ph] (2016).

Confluent Heun equation with single added apparent singularity: elementary, gauge and integral symmetries

A. Ya. Kazakov

St. Petersburg State University of Technology and Design;
St. Petersburg State University of Aerospace Instrumentation
e-mail: a-kazak@mail.ru

Confluent Heun equation with single added apparent singularity (CHE1AP) is under consideration. This equation is a natural bridge between linear and nonlinear special functions of mathematical physics. It can be generated at reduction of different systems of linear differential equations. These generating systems can be exploited for the deducing of the gauge symmetries and Euler, Laplace and hypergeometric integral symmetries for the solutions of CHE1AP and corresponding symmetries of the monodromy group.

On the problem of propagation of MHD waves

Kholodova S.E.¹, **Peregudin S.I.**²

¹National Research University ITMO, 49 Kronverksky Pr., St. Petersburg, 197101 Russia

²Saint Petersburg State University, 7/9 litera A, Universitetskaya emb., St. Petersburg, 199034 Russia
e-mails: kholodovase@yandex.ru, peregudinsi@yandex.ru

The system of nonlinear partial differential equations describing the dynamics of a rotating layer of an ideal conducting incompressible fluid is difficult to investigate because of its vector character. Therefore, it is natural to try to reduce it to equivalent scalar equations for auxiliary functions.

We consider the nonlinear system of partial differential equations that model perturbations in a layer of an ideal conducting rotating fluid bounded by spatially and temporally varying surfaces with allowance for inertial forces and diffusions of magnetic field. The purpose of this study is to reduce this system to a scalar equation and to construct analytical solutions to the corresponding boundary value problems.

The accounting of diffusive members is necessary when studying dynamics of waves of more local character, i. e., when the horizontal scale of change of hydromagnetic sizes much less than a radius of a considered layer, and also at very great time scales. It would be desirable to see influence of diffusion of a magnetic field on its generation. Whether there will be able to be a magnetic field as much as long time and whether it will exist at shutdown of an inoculating field.

The motion of a conducting fluid in a magnetic field causes electric currents. These currents change the magnetic field. At the same time, the forces acting on the currents in the magnetic field can change the character of the fluid motion. Hence, hydrodynamic motion and electromagnetic phenomena are interrelated. This relation is described by the joint system of field equations and the equations of motion of a fluid. According to the works by the well-known Swedish physicist and astrophysicist G. Alfven, the interrelation between electromagnetic and hydrodynamic phenomena strengthens as the linear scale of a phenomenon increases. For large-scale phenomena, this interrelation can be rather strong. For example, this is true of star interiors and the Earth's liquid core.

In this study, we assume that the boundaries of the layer are not stationary but vary in space and time. Furthermore, the inertial forces are taken into account in the equation of motion.

References

- [1] S. E. Kholodova, S. I. Peregudin, *Modelling and analysis streams and waves in liquid and granulars medias*, Saint Petersburg State University, Saint Petersburg (2009).

Modelling of nonlinear bulk strain waves in inhomogeneous layered bars

Khusnutdinova K.R., Tranter M.R.

Department of Mathematical Sciences, Loughborough University, Loughborough LE11 3TU, UK
e-mails: k.khusnutdinova@lboro.ac.uk, m.tranter@lboro.ac.uk

In this talk we will discuss the modelling of nonlinear waves in inhomogeneous layered elastic bars with different types of bonding between the layers. In particular, we model the dynamics of a long longitudinal strain solitary wave in a symmetric perfectly bonded layered bar with delamination [1]. The previously developed analytical approach [2], based on matching two asymptotic multiple-scale expansions and the integrability theory of the KdV equation by the Inverse Scattering Transform, is used to develop an effective semi-analytical numerical approach for these types of problems. We also employ a direct finite-difference method and compare the numerical results with each other, and with the analytical predictions. The numerical modelling confirms that delamination causes fission of an incident solitary wave and, thus, can be used to detect the defect (see also [2, 3]). We then extend our approaches to the modelling of the waves in a layered bar with a soft bonding layer, described by a system of coupled Boussinesq equations [4].

References

- [1] K. R. Khusnutdinova, M. R. Tranter, Modelling of nonlinear wave scattering in a delaminated elastic bar, *Proc. Roy. Soc. A*, **471**, 20150584 (2015).
[2] K. R. Khusnutdinova, A. M. Samsonov, Fission of a longitudinal strain solitary wave in a delaminated bar, *Phys. Rev. E*, **77**, 066603 (2008).

- [3] G. V. Dreiden, K. R. Khusnutdinova, A. M. Samsonov, I. V. Semenova, Splitting induced generation of soliton trains in layered waveguides, *J. Appl. Phys.*, **107**, 034909 (2010).
- [4] K. R. Khusnutdinova, A. M. Samsonov, A. S. Zakharov, Nonlinear layered lattice model and generalized solitary waves in imperfectly bonded structures, *Phys. Rev. E*, **79**, 056606 (2009).

Fock–Leontovich parabolic equation method on prolonged bodies with Neumann boundary conditions

Anna Kirpichnikova

Liverpool Hope University, Hope Park, Liverpool, L16 9JD, UK
e-mail: kirpica@hope.ac.uk

We consider a diffraction problem where the scatterer is a strictly convex and prolonged body of revolution. The incident plane wave radiates along the revolution axis. The wave field is constructed in the vicinity of the shadow-light (penumbra, Fock’s region) zone and in the shadow zone.

Fock’s zone plays a crucial role in calculating a diffraction field, because it works as an origin of the field for the shadow region and in the vicinity of the creeping rays cone. Moreover the diffracted field can be described in terms of the Ray Method in the lighted part of a scatterer in case of the both curvature radii of the surface are much greater than the incident wavelength.

Shortwave diffraction by prolate bodies of revolution. Results of numerical experiments

Kirpichnikova N.Ya., Popov M.M., Semtchenok N.N.

Steklov Mathematical Institute, Saint-Petersburg, Fontanka 27
e-mails: nkirp@pdmi.ras.ru, mpopov@pdmi.ras.ru, semtchenok@gmail.com

In our previous papers [1, 2] we suggested and developed a new approach to shortwave diffraction by prolate convex bodies of revolution (axis-symmetrical case). It is based on the method of matching of local asymptotics ascending actually from papers by B. A. Fock [3] and also on the method of two-scaled asymptotic expansions. The oblongness of the scatterer is characterized by the parameter $\Lambda = \frac{\rho}{\rho_t}$, where ρ is the curvature radius along the geodesics (meridians), and ρ_t represents a curvature radius in the transversal direction (latitudes). It appears in the diffraction problems under consideration as an additional large parameter with respect to large Fock parameter $M = (\frac{k\rho}{2})^{1/3}$, where k is the wave number.

In the asymptotic formulae for the diffracted wave field it appears in the following combination $\kappa = \frac{\Lambda}{M^2}$. Thus for strongly elongated bodies when $\kappa = O(1)$ as $M \rightarrow \infty$, it compensates influence of Fock parameter in corresponding terms of asymptotics and Leontovich–Fock method fails. Exactly for this case we suggest and use the new boundary layer in the vicinity of the light-shadow zone, see [4].

In order to examine influence of the oblongness of a scatterer on the diffracted wave field and to compare our approach with ones available in the literature, we carried out numerical experiments.

In this report we demonstrate results of those experiments.

The research was supported by RFBR grant 14-01-00535-a.

References

- [1] N. Ya. Kirpichnikova, M. M. Popov, Leontovich–Fock parabolic equation method in the problems of short-wave diffraction by prolate bodies, *Zap. Nauch. Semin. POMI*, Vol. **409**, no. 42, pp. 55–79 (2012).
- [2] M. M. Popov, N. Ya. Kirpichnikova, On problems of applying the parabolic equation to diffraction by prolate bodies, *Acoustical Physics*, Vol. **60**(4), pp. 365–372 (2014).

- [3] V. A. Fock, *Electromagnetic Diffraction and Propagation Problems*, Pergamon Press (1965).
- [4] N. Ya. Kirpichnikova, M. M. Popov, Diffraction by strongly elongated bodies and matching of the asymptotics in illuminated part of the light-shadow boundary, *Proc. Intern. Conf. "Days on Diffraction 2014"*, St. Petersburg, 124–127 (2014).

Optical-force-induced dynamics of Mie scatterers in Laguerre–Gaussian beams and near-field structures

Kiselev A.D.

St. Petersburg National Research University of Information Technologies, Mechanics and Optics, Kronverskiy Prospekt, 49, 197101 St. Petersburg, Russia

e-mail: alexei.d.kiselev@gmail.com

Plutenko D.O.

Institute of Physics of National Academy of Sciences of Ukraine, Prospekt Nauki, 46, 03680 Kiev, Ukraine

e-mail: dmplutenko@gmail.com

Using a T -matrix approach in the form described in [1, 2] we study the light scattering problem for optically isotropic spherical scatterers illuminated with Laguerre–Gaussian (LG) beams. Our method uses the remodelling procedure in which the far-field matching method [2] is combined with the results for nonparaxial propagation of LG beams. Scattering of such beams can be described in terms of the far-field angular distributions that determine the outgoing parts of the incident and scattered waves [3]. In particular, these distributions give the differential cross-sections and the optical (radiation) force acting upon the Mie scatterer.

The theoretical results are used to analyze the optical-force-induced dynamics of the scatterer near the trapping points represented by the equilibrium (zero-force) positions. The regimes of linearized dynamics are described in terms of the stiffness matrix spectrum and the damping constant of the ambient medium. For non-vortex LG beams characterized by vanishing azimuthal mode number, $m_{\text{LG}} = 0$, the stiffness matrix is symmetric and hence the dynamics being locally conservative appears to be essentially independent of the ambient medium. The latter is no longer the case when the LG beams are purely azimuthal and represent optical vortex beams. For such beams, the dynamics in the transverse plane is non-conservative, so that the dynamical regimes governed by the ambient medium may take place.

The optical field in the near-field region is analyzed for the purely azimuthal LG beams. It is shown that the morphology of photonic nanojets significantly varies depending the mode number and the scatterer characteristics. The cases of negative index metamaterial and metallic Mie scatterers are discussed. The near-field structure of optical vortices associated with the components of the electric field being highly sensitive to the mode number is found to be determined by the twofold rotational symmetry.

A. D. K. acknowledges partial financial support from the Government of the Russian Federation (Grant No. 074-U01), from the Ministry of Education and Science of the Russian Federation (Grant No. GOSZADANIE 2014/190, Project No. 14.Z50.31.0031, and ZADANIE Grant No. 1.754.2014/K), through a grant from the Russian Foundation for Basic Research, and through a grant from the President of Russia (Grant No. MK-2736.2015.2).

References

- [1] A. D. Kiselev, V. Y. Reshetnyak, T. J. Sluckin, *Phys. Rev. E*, **65**, 056609 (2002).
- [2] A. D. Kiselev, D. O. Plutenko, *Phys. Rev. A*, **89**, 043803 (2014).
- [3] M. I. Mishchenko, L. D. Travis, A. A. Lacis, *Scattering, Absorption and Emission of Light by Small Particles*, Cambridge University Press, NY (2004).

Self-action features of nonparaxial optical pulses in a medium with cubic nonlinearity

Kislin D.A., Kozlov S.A.

ITMO University, St. Petersburg, Russia

e-mails: kislin.dmitriy@gmail.com, kozlov@mail.ifmo.ru

In this paper, we show main effects simulated by the system of spectral equations describing the diffraction dynamics of TM polarized nonparaxial waves in a dielectric media with inertialless cubic nonlinearity in the form

$$\begin{cases} \frac{\partial^2 g_x}{\partial z^2} + (k^2 - k_x^2)g_x = -\frac{\varepsilon_{nl}}{n^2(\omega)} \left((k^2 - k_x^2)\Phi_x + ik_x \frac{\partial \Phi_z}{\partial z} \right), \\ \frac{\partial g_z}{\partial z} + ik_x g_x = -\frac{\varepsilon_{nl}}{n^2(\omega)} \left(ik_x \Phi_x + \frac{\partial \Phi_z}{\partial z} \right), \end{cases} \quad (1)$$

where $g_{x,z}$ are the Cartesian components of the radiation spectrum; ω , k_x are the frequencies of temporal and spatial spectra, respectively; $n(\omega)$ is the frequency-dependent refractive index of the medium; $k(\omega) = \omega n(\omega)/c$ is the wave number; c is the speed of light in vacuum; ε_{nl} is the nonlinear susceptibility; z is the direction of radiation propagation,

$$\begin{aligned} \Phi_x &= F \left[F^{-1}[g_x]^3 + F^{-1}[g_z]^2 F^{-1}[g_x] \right], \\ \Phi_z &= F \left[2F^{-1} \left[\frac{\partial g_x}{\partial z} \right] F^{-1}[g_x] F^{-1}[g_z] + (F^{-1}[g_x]^2 + 3F^{-1}[g_z]^2) (-ik_x F^{-1}[g_x]) \right], \end{aligned}$$

whereas F , F^{-1} are the operators of direct and inverse Fourier transform.

Present work covers a range of effects arising in longitudinal and transverse components in the nonparaxial beam. The figures below show simulation result of the longitudinal component dynamics of initially a one-cycle TM polarized terahertz wave (central wavelength is 0.3 mm) in a crystal of lithium niobate ($N_0 = 4.73$, $a = 2.22 \cdot 10^{-38}$ s cm², $n_2 = 5.4 \cdot 10^{-12}$ cm²/W, $I = 1.0 \cdot 10^{10}$ W/cm²) with a nonlinear additive to the refractive index $\Delta n_{nl} = 10^{-2}$. The beam variance can not be ignored in such case for the one-period beam where the carrier frequency is 1 THz. its power of influence becomes comparable to the non-linear effects.

Figures show that the nonlinear medium gives rise to two special major effect in the longitudinal component of the electric field. The wavelength increases significantly approximately one and a half to two times and half periods of the pulse is modulated in intensity and spatial width.

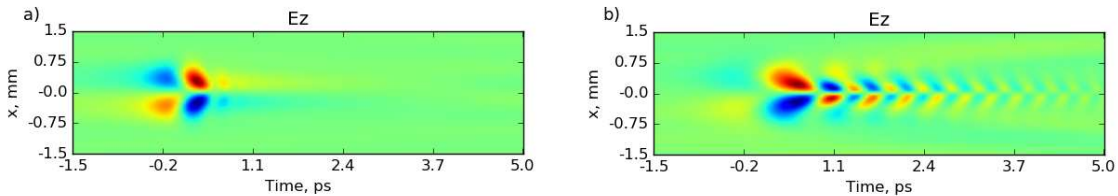


Fig. 1: (a) dependence of the longitudinal component of the electric field on the transverse coordinate x and time t at the input of the medium $z = 0.01$ mm and (b) its output $z = 2$ mm.

References

- [1] A. Ezerskaya, D. Ivanov, S. Kozlov, Yu. Kivshar, Spectral approach in the analysis of pulsed terahertz radiation, *Journal of Infrared, Millimeter and Terahertz Waves*, **33**(9), 926–942 (2012).
- [2] A. Drozdov, A. Sukhorukov, S. Kozlov, Spatio-temporal dynamics of single-cycle optical pulses and nonlinear frequency conversion, *Int. J. Mod. Phys. B*, **28**, 1442007 (2014).

Simulation of Josephson antenna in 3D space

Klushin A.M.¹, Kurin V.V.^{1,2}, Shereshevskii I.A.^{1,2}, Vdovicheva N.K.¹

¹Institute for Physics of Microstructures RAS, 603950, GSP-105, Russia

²Nizhnii Novgorod State University

e-mail: ilya@ipmras.ru

We present the mathematical model and algorithm for simulation of active Josephson antenna, which consists of a few lumped Josephson junctions, connected by perfectly conducting wires of different radius's with the source of a.c. bias current and placed on dielectric substrate. First we discuss some problems, connected with the formulation of mathematical models of the considered system. We suggest a system of equations which contains the discrete model of Maxwell equations, known as *Yee scheme* [2, 3], the equations for the dynamics of lumped Josephson junctions biased by a.c. current, and conditions which connect current and voltage on the junctions with electromagnetic field in the waveguide. We use so-called *Perfectly Matched Layer* boundary conditions [2, 4] to avoid the reflection of electromagnetic waves at the artificial boundary of calculating domain. To simulate the dynamic of electromagnetic field we use the known FDTD explicit method [2] and semi-implicit scheme for the Josephson equations. We also discuss the implementation of suggested algorithm. We present the current-voltage characteristics of junctions and calculate the 3D antenna diagram at the Josephson frequency using near-to-far field transformation [1, 2].

References

- [1] J. D. Jackson, *Classical Electrodynamics*, New York: Wiley (1975).
- [2] A. Taflov, S. C. Hagness, *Computational Electrodynamics The Finite-Difference Time-Domain Method*, 3rd ed., Artech House, Inc. (2005).
- [3] K. S. Yee, *IEEE Trans. Antennas Propagat.*, **14**, 302–307 (1966).
- [4] J. P. Berenger, *J. Computational Physics*, **127**, 363–379 (1996).

Noncollinear interaction of few-cycle optical waves in dispersive nonlinear medium

Kniazhev M.A., Kozlov S.A.

ITMO University, St. Petersburg 197101, Russia

e-mails: knyazhev.michael@gmail.com, kozlov@mail.ifmo.ru

Dolgaleva K.

School of Electrical Engineering and Computer Science and the Department of Physics, University of Ottawa, Ottawa, ON Canada

e-mail: ksenia.dolgaleva@uottawa.ca

Analysis of the interaction of intense light waves propagating in an optical medium at an angle to each other is a classic problem of nonlinear optics [1]. Usually it is solved for the case of quasi-monochromatic radiation [2]. In the present work, we consider a self-consistent problem of a non-collinear interaction of two few-cycle waves in a nonlinear dispersive optical medium. We used the spectral method of describing the dynamics of radiation [3]:

$$\frac{\partial^2 g}{\partial z^2} + [k(\omega)^2 - k_x^2] g = -\frac{\omega^2 \epsilon_{nl}}{c^2} \frac{1}{(2\pi)^4} \int \int \int \int_{-\infty}^{\infty} g(\omega - \omega', k_x - k'_x, z) \times g(\omega' - \omega'', k'_x - k''_x, z) g(\omega'', k''_x, z) d\omega' dk'_x d\omega'' dk''_x. \quad (1)$$

where g is a spectral density of the radiation, ω and k_x are the angular and spatial frequencies, respectively, $k(\omega) = \omega n(\omega)/c$ is the wave number, $n(\omega) = N_0 + a\omega^2$ is the refractive index, ϵ_{nl} is the

dielectric permittivity, c is the speed of light in vacuum, z is the spatial coordinate along which one of the waves propagates.

The primary wave with a fixed intensity serves as a source for the third-harmonic generation (THG); the other wave with a varying intensity (acting wave) interacts with the primary wave and influences the conversion efficiency of the THG process. We show that, similar to the case of quasi-monochromatic radiation, for the few-cycle waves, propagating and interacting in isotropic dielectric media with an instantaneous third-order nonlinearity, there is no energy redistribution between the interacting incoming waves. Nevertheless, the interaction between the incoming waves could lead to a significant enhancement of the third-harmonic generation in the primary wave. The interaction with the acting wave accompanied by a spectral broadening and reshaping (see figure).

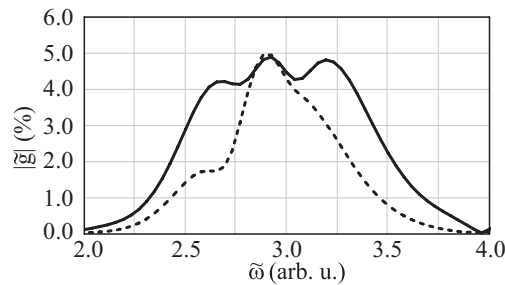


Figure. The spectrum of the third harmonic of the primary wave (by dashed line is shown spectrum without the interaction).

References

- [1] J. A. Armstrong, N. Bloembergen, J. Ducuing, *et al.*, *Phys. Rev.*, **127**, 1918–1939 (1962).
- [2] R. W. Boyd, *Nonlinear Optics*, 3rd ed., Academic Press (2008).
- [3] A. A. Ezerskaya, D. V. Ivanov, S. A. Kozlov, *et al.*, *J. Infrared, Millimeter, and Terahertz Waves*, **33**, 926–942 (2012).

Wiener–Hopf analysis of the radar cross section of a finite parallel-plate waveguide with four-layer material loading

Kazuya Kobayashi

Department of Electrical, Electronic, and Communication Engineering, Chuo University, 1-13-27 Kasuga, Bunkyo-ku, Tokyo 112-8551, Japan
e-mail: kazuya@tamacc.chuo-u.ac.jp

The analysis of electromagnetic scattering by open-ended metallic waveguide cavities is an important subject in the prediction and reduction of the radar cross section (RCS) of a target. This problem serves as a simple model of duct structures such as jet engine intakes of aircrafts and cracks occurring on surfaces of general complicated bodies. Some of the diffraction problems involving two- and three-dimensional cavities have been analyzed thus far based on high-frequency techniques and numerical methods. It appears, however, that the solutions due to these approaches are not uniformly valid for arbitrary dimensions of the cavity. Therefore it is desirable to overcome the drawbacks of the previous works to obtain solutions which are uniformly valid in arbitrary cavity dimensions. The Wiener–Hopf technique is known as a powerful, rigorous approach for analyzing scattering and diffraction problems involving canonical geometries. In this paper, we shall consider a finite parallel-plate waveguide with four-layer material loading as a geometry that can form cavities, and analyze the plane wave diffraction rigorously using the Wiener–Hopf technique. Both E and H polarizations are considered.

Introducing the Fourier transform of the scattered field and applying boundary conditions in the transform domain, the problem is formulated in terms of the simultaneous Wiener–Hopf equations.

The Wiener–Hopf equations are solved via the factorization and decomposition procedure leading to the exact solution. However, this solution is formal since infinite series with unknown coefficients and infinite branch-cut integrals with unknown integrands are involved. For the infinite series with unknown coefficients, we shall derive approximate expressions by taking into account the edge condition. For the branch-cut integrals with unknown integrands, we assume that the waveguide length is large compared with the wavelength and apply a rigorous asymptotics. This procedure yields high-frequency asymptotic expressions of the branch-cut integrals. Based on these results, an approximate solution of the Wiener–Hopf equations, efficient for numerical computation, is explicitly derived, which involves a numerical solution of appropriate matrix equations. The scattered field in the real space is evaluated by taking the inverse Fourier transform and applying the saddle point method. Representative numerical examples of the RCS are shown for various physical parameters, and the far field scattering characteristics of the waveguide are discussed in detail. The results presented here are valid over a broad frequency range and can be used as a reference solution for validating other analysis methods such as high-frequency techniques and numerical methods.

Multiplicity of solutions of the Dirichlet problem with fractional p -Laplacian in spherical annulus

Kolonitskii S.B.

Saint-Petersburg State University

e-mail: sergey.kolonitskii@gmail.com

Let $n \geq 2$, $\Omega_R = B_{R+1}(0) \setminus B_{R-1}(0) \subset \mathbb{R}^n$ and consider the problem

$$(-\Delta)_p^s u = u^{q-2} \text{ in } \Omega_R; \quad u = 0 \text{ in } \mathbb{R}^n \setminus \Omega_R. \quad (1)$$

Here $p \in (1, \infty)$, $q \in (p, p^{*,s})$, where $p^{*,s} = \frac{np}{n-sp}$ for $n > sp$, $p^{*,s} = +\infty$ for $n \leq sp$ and

$$(-\Delta)_p^s u(x) = 2 \lim_{\varepsilon \rightarrow 0^+} \int_{\mathbb{R}^n \setminus B_\varepsilon(x)} \frac{|u(x) - u(y)|^{p-2} (u(x) - u(y))}{|x - y|^{n+sp}} dy$$

is the fractional p -Laplacian (see, e.g. [2]). Let \mathcal{G} be a finite subgroup of $O(n)$. The set M on the unit sphere is a locally minimal set if

- there exists such $C > 0$ that for any $z \in M$ $\#\mathcal{G}z = C$;
- there exists such an open set $V \supset M$ and $\gamma > 0$ that for any $x \in V \setminus M$ $\#\mathcal{G}x \geq C + \gamma$.

By adapting the concentration-compactness approach (see, e.g. [1]) to quasilinear fractional-derivative setting the following theorems are proved:

Theorem 1. *Let \mathcal{G} be a finite subgroup of $O(n)$ and let M be a \mathcal{G} -invariant locally minimal set. Then*

1. *the boundary problem (1) has a weak \mathcal{G} -invariant positive solution $u_{R,\mathcal{G}}$;*
2. *$\|u_{R,\mathcal{G}}\|_q$ concentrates in the neighbourhood of $R \cdot M$ as $R \rightarrow \infty$.*

Theorem 2. *Let $N > 0$. Then there exists such $R_0 = R_0(n, p, q, s, K)$ such that:*

1. *the boundary problem (1) has at least N weak positive solutions $u_{R,1}, \dots, u_{R,N}$;*
2. *for any $R > R_0$ and any $1 \leq i, j \leq N$ the solutions $u_{R,i}$ and $u_{R,j}$ are not rotationally equivalent, i.e. there exists no such rotation $g \in O(n)$ that $u_{R,i}(x) = u_{R,j}(gx)$.*

References

- [1] J. Byeon, *J. Diff. Eq.*, **136**, 136–165 (1997).
- [2] A. Iannizzotto, S. Liu, K. Perera, M. Squassina, *Advances in Calculus of Variations* **2**, 101–126 (2016).

Resonances of fourth order operators

E. Korotyaev, A. Badanin

Mathematical Physics Department, St. Petersburg State University, Russia

e-mail: korotyaev@gmail.com

There are a lot of results about resonances for second order operators. In our talk we consider resonances for fourth order ordinary differential operator with compactly supported coefficients on the half-line and the line. We determine a resonance as a pole of a perturbed resolvent on the non-physical sheets of the Riemann surface. We determine asymptotics of counting function of resonances in complex discs at large radius. Moreover, we obtain different properties of the resonances and in particular we express the trace formula in terms of resonances only.

Furthermore, we consider the resonances for Euler–Bernoulli operators $Eu = (1/b)(au'')''$. We show the following results. Let the coefficients a, b be positive and constants outside finite interval. Then the operator E has a finite number of resonances iff a, b are constants everywhere.

A method of diagnostics of layered biological tissues

Kovtanyuk A.E., Prokhorov I.V., Chebotarev A.Yu.

Institute for Applied Mathematics, FEB RAS, 7 Radio st., 690041 Vladivostok, Russia

Far Eastern Federal University, 8 Sukhanova st., 690950 Vladivostok, Russia

e-mails: kovtanyuk.ae@dvmfu.ru, prh@iam.dvo.ru, cheb@iam.dvo.ru

Imaging of biological tissue to detect tumors and other inclusions can be carried out by determining the refraction indices of the medium. The problem of optical diagnostics of layered biological medium is studied by methods of the radiation transfer theory. The polarized radiation transfer equation with generalized matching conditions is chosen as a basic mathematical model [1]. This problem can be considered as a problem of the diffraction type.

The problem of determination of the refraction indices of a multilayered medium by the measurement of outgoing radiation is examined. The solution of the posed problem is based on the use of the total internal reflection phenomena arising at boundaries of layers. Also, polarization properties of radiation flux are taken into account. To solve this problem, smoothness properties of the solution of the boundary-value problem for the polarized radiation transfer equation are used. In particular, the proposed formulas determining the refraction indices are based on singularities of the derivative of the outgoing radiation at certain values of the angular variable. The numerical experiments corresponding to imaging of human skin were performed. The efficiency of the proposed method of reconstruction was shown.

References

- [1] A. E. Kovtanyuk, I. V. Prokhorov, *J. Comp. Appl. Math.*, **235**, 2006–2014 (2011).

Boundary layers and normal mode parameters in a system with double-diffusive convection at large Rayleigh numbers

Kozitskiy S.B., Trofimov M.Yu., Zakharenko A.D.

Il'ichev Pacific Oceanological Institute, 43 Baltiiskaya St., Vladivostok, 690041, Russia

e-mails: skozi@poi.dvo.ru, trofimov@poi.dvo.ru, zakharenko@poi.dvo.ru

We consider two-dimensional double-diffusive convection [1] in a horizontally infinite layer of water at large Rayleigh numbers. Governing equations in this case are the equations of hydrodynamics of

the liquid mixture in the gravity field, which can be written in a singular disturbed form:

$$\begin{aligned}\Delta\psi &= w, \\ (\partial_t - \sigma\epsilon^2\Delta)w + (\partial_x\xi - (1 - N^2)\partial_x\theta) &= -J(\psi, w), \\ (\partial_t - \epsilon^2\Delta)\theta - \partial_x\psi &= -J(\psi, \theta), \\ (\partial_t - \tau\epsilon^2\Delta)\xi - \partial_x\psi &= -J(\psi, \xi).\end{aligned}\tag{1}$$

Here we have introduced small parameter $\epsilon = 1/(\sigma R_S)^{1/4}$ (R_T and R_S are the Rayleigh numbers), buoyancy frequency $N = (1 - R_T/R_S)^{1/2}$. Vector of the dependent variables $\vec{\varphi}(t, x, z) = (w, \psi, \theta, \xi)$ describes variations of the state of the liquid relative to the basic state with zero velocity field and linear vertical profiles of the temperature and (for example) salinity.

To investigate linear stability problem for system (1) we omit nonlinear terms in the right parts and seek solution in the form of normal convective mode $\vec{\varphi}(x, z, t) = \vec{\Phi}(z)e^{\lambda t} \begin{Bmatrix} \sin kx \\ \cos kx \end{Bmatrix}$, where k is horizontal wave number. Then for $\vec{\Phi}(z) = (W, \Psi, \Theta, \Xi)$ we have system ($\Delta_0 = \partial_z^2 - k^2$)

$$\begin{aligned}\Delta_0\Psi(z) &= W(z), & (\lambda - \sigma\epsilon^2\Delta_0)W(z) - k[\Xi(z) - (1 - N^2)\Theta(z)] &= 0, \\ (\lambda - \epsilon^2\Delta_0)\Theta(z) - k\Psi(z) &= 0, & (\lambda - \tau\epsilon^2\Delta_0)\Xi(z) - k\Psi(z) &= 0,\end{aligned}\tag{2}$$

with boundary conditions $\Psi = 0$, $\partial_z W + a_1 W = 0$, $\partial_z \Theta + a_2 \Theta = 0$, $\partial_z \Xi + a_3 \Xi = 0$ at $z = \pm 1/2$.

According to multiscale expansions method introduce quick variable $\eta = z/\epsilon$, prolonged derivative $\partial_z \rightarrow \partial_z + \epsilon^{-1}\partial_\eta$ and express variables $\vec{\Phi}$ and λ as series in ϵ : $\vec{\Phi} = \sum_{n=0}^{\infty} \epsilon^n \vec{\Phi}_n(z, \eta)$, $\lambda = \sum_{n=0}^{\infty} \epsilon^n \lambda_n$. Substitute it in system (2) and collect terms at the same powers in ϵ . Equations at ϵ^{-2} and ϵ^{-1} lead to $\vec{\Phi}_0$ depends only on z , equations at ϵ^0 lead to the internal wave solution for $\vec{\Phi}_0$: $\vec{\Phi}_0(z) = \vec{A} \cos(\pi z)$, $\lambda_0 = i\omega$, where $\omega^2 = N^2 k^2 / (k^2 + \pi^2)$. Thus traveling waves of double-diffusive convection at large Rayleigh numbers look like usual internal waves with constant buoyancy frequency N . The explored system loses stability via the Hopf bifurcation with frequency ω .

Equations at ϵ^1 give formulas for the double-diffusive boundary layers of the form $B \cosh(\eta\sqrt{i\omega})$, also $\lambda_1 = 0$. Thus one can see, that boundary layers thickness h_m is of the order of ϵ . It can be estimated as $h_m \approx (\pi/13)(\delta T/h)^{-1/4}$ through the temperature difference δT and the thickness h of convective layer. In real situations often $h_m \approx 1-2$ cm. Equations at ϵ^2 define λ_2 :

$$\lambda_2 = \frac{k^2 + \pi^2}{2N^2} (1 + \sigma) \left(\frac{1 - \tau}{1 + \sigma} - N^2 \right).$$

This value describes increment of the traveling convective waves. When N^2 is less than $N_0^2 = (1 - \tau)/(1 + \sigma)$, the mode amplitude increases.

In this work we obtain asymptotic estimates for boundary layers and increment parameters for general type boundary conditions at large Rayleigh numbers, usual for oceanography.

References

- [1] T. Radko, *Double-diffusive convection*, Cambridge University Press, New York (2013).

Age-structured population model on several patches

Vladimir Kozlov

Linköping University, Sweden

e-mail: vladimir.kozlov@liu.se

We consider an age-structured population that lives on N patches in variable environments. The balance law is obtained from the age-structured logistic equation by adding the dispersion term. In

this way for the part of population that lives on patch k , where $1 \leq k \leq N$, we have the following balance equation:

$$\frac{\partial n_k(a, t)}{\partial t} + \frac{\partial n_k(a, t)}{\partial a} = -\mu_k(a, t)n_k(a, t) \left(1 + \frac{n_k(a, t)}{L_k(a, t)} \right) + \sum_{j=1}^N D_{kj}(a, t)n_j(a, t), \quad (1)$$

where $n_k(a, t)$ is the number of individuals in the age class a at time t in the k th patch. The boundary and initial conditions are

$$n_k(0, t) = \int_0^\infty m_k(a, t)n_k(a, t) da, \quad \text{for } t > 0, \quad \text{and} \quad n_k(a, 0) = f_k(a), \quad \text{for } a > 0, \quad (2)$$

where $m_k(a, t)$ and $\mu_k(a, t)$ are the birth and the death rate of population on patch k of age a at time t , $f_k(a)$ is the initial distribution of population in age classes on patch k , $L_k(a, t)$ is the carrying capacity of age-class a at time t on patch k . For $j \neq k$ nonnegative coefficients $D_{kj}(a, t)$ represent dispersion i.e. a proportion of population $n_k(a, t)$ that from patch j goes to patch k . Contrary to this, coefficient $D_{kk}(a, t) \leq 0$ describe a proportion of population $n_k(a, t)$ that leaves patch k .

We prove that the model (1)–(2) has a unique non-negative solution. We study the behaviour of solution for large time in three cases:

- (i) Coefficients of the problem are time independent;
- (ii) Coefficients of the problem are time periodic functions;
- (iii) Arbitrary coefficients.

In the cases (i) and (ii) we introduce a so called *net reproductive number* and *characteristic equation*, which is a fixed point equation for positive vectors in the case (i) and for positive periodic functions in the case (ii). We show that if the net reproductive number is less than or equal to 1 then populations in all patches vanish as time tends to infinity. If the net reproductive number is greater than 1 then the new born population distribution tends to the fixed point of the characteristic equation. In the case (iii) we present two sides estimates for the population distribution function. Biological interpretation of the results obtained is given.

This is a joint work with Sonja Radosavljevic, Vladimir Tkachev and Uno Wennergren (Linköping University).

Hamiltonian methods for complex food webs

V. Kozlov¹, U. Wennergren², S. Vakulenko³

¹Linköping University, Math Dept.; ²Linköping University Ecological. Dept.; ³IPME RAS and ITMO University

e-mail: vakulenfr@mail.ru

In this paper we show that catastrophic events in complex food webs can be studied by methods of mechanics and physics. In particular, there are possible soliton and kink solutions, which can describe ecological catastrophes, chaos and quasiperiodic oscillations. Moreover, we state results on global stability of random foodwebs.

On electromagnetic forces and works, connected with it

Krasnov I.P.

Krylov State Research Centre, Saint Petersburg, Russia

e-mail: i3349@yandex.ru

The problem associated with determination of forces acting on substance and works, connected with this forces, is not still finally solved in classical electrodynamics [1, 2, 3]. One can consider the possibility construction of solution of this problem on the basis of examining the integrals of Maxwell's

equations that connected with the energy-momentum tensors. For this purpose Maxwell's equations are used in general form:

$$\operatorname{rot} \mathbf{H} = \frac{1}{c} \frac{\partial}{\partial t} \mathbf{D} + \frac{1}{c} \mathbf{j}, \quad \operatorname{div} \mathbf{D} = \rho, \quad \operatorname{rot} \mathbf{E} = -\frac{1}{c} \frac{\partial}{\partial t} \mathbf{B}, \quad \operatorname{div} \mathbf{B} = 0; \quad \mathbf{D} = \mathbf{E} + \mathbf{P}, \quad \mathbf{B} = \mathbf{H} + \mathbf{J}. \quad (1)$$

This equations permit four versions of description of electromagnetic fields, and correspondingly four formulation of Maxwell's equations, that connected with the choice of the couple of vectors of the field among four couples: \mathbf{E} and \mathbf{H} , \mathbf{D} and \mathbf{B} , \mathbf{D} and \mathbf{H} , \mathbf{E} and \mathbf{B} . Each version has its own form of expression for the densities of electromagnetic forces \mathbf{f} and works f_0 produced by \mathbf{f} in unit of time and own energy-momentum tensor [4, 5].

The values \mathbf{f} and f_0 form the 4-vector in Minkowsky space, that is equal to the 4-divergence of energy-momentum tensor $T_{\alpha\beta}$ [4, 5]:

$$(\mathbf{f} + if_0) \equiv \mathbf{f}_\alpha = \frac{\partial}{\partial x_\beta} T_{\alpha\beta}, \quad \mathbf{x}_\beta = (\mathbf{x} + ict). \quad (2)$$

Formulae (2) is different for each couple of vectors of the field. The region V , that contains the substance, consist of $n \geq 2$ bodies occupying regions V_k with the boundaries S_k , ($k \leq n$). Main result is obtained by integration of formulae (2) over the region V_k for each version:

$$\begin{aligned} \mathbf{F}_k(\mathbf{E}, \mathbf{H}) + \frac{1}{c} \frac{\partial}{\partial t} \int_{V_k} [\mathbf{E}, \mathbf{H}] dV &= \mathbf{F}_k(\mathbf{D}, \mathbf{B}) + \frac{1}{c} \frac{\partial}{\partial t} \int_{V_k} [\mathbf{D}, \mathbf{B}] dV = \mathbf{F}_k(\mathbf{D}, \mathbf{H}) + \frac{1}{c} \frac{\partial}{\partial t} \int_{V_k} [\mathbf{D}, \mathbf{H}] dV \\ &= \mathbf{F}_k(\mathbf{E}, \mathbf{B}) + \frac{1}{c} \frac{\partial}{\partial t} \int_{V_k} [\mathbf{E}, \mathbf{B}] dV = \Phi_k \equiv \int_{S_k} \left(\mathbf{n} \frac{1}{2} (E^2 + H^2)^- - \mathbf{E}^- E_n^- - \mathbf{H}^- H_n^- \right) dV; \quad (3) \end{aligned}$$

$$\begin{aligned} F_k^0(\mathbf{E}, \mathbf{H}) + \frac{1}{c} \frac{\partial}{\partial t} \int_{V_k} \frac{1}{2} (E^2 + H^2) dV &= F_k^0(\mathbf{D}, \mathbf{B}) + \frac{1}{c} \frac{\partial}{\partial t} \int_{V_k} \frac{1}{2} (D^2 + B^2) dV = F_k^0(\mathbf{D}, \mathbf{H}) \quad (4) \\ + \frac{1}{c} \frac{\partial}{\partial t} \int_{V_k} \frac{1}{2} (D^2 + H^2) dV &= F_k^0(\mathbf{E}, \mathbf{B}) + \frac{1}{c} \frac{\partial}{\partial t} \int_{V_k} \frac{1}{2} (E^2 + B^2) dV = \Phi_k^0 \equiv \int_{S_k} (\mathbf{n}, [\mathbf{E}^-, \mathbf{H}^-]) dS, \end{aligned}$$

where \mathbf{F}_k are the electromagnetic forces caused by the density \mathbf{f} and by Maxwell's stress-tensor $T_{\alpha\beta}$ ($\alpha, \beta \leq 3$), F_k^0 are the works, produced by \mathbf{F}_k in unit of time.

References

- [1] V. P. Makarov, A. A. Rukhadze, *Phys. Usp.* Vol. **52**, pp. 995–1001, 2009.
- [2] S. Bobbio et al., *IEEE Trans. Magn.*, Vol. **36**, pp. 663–666, 2000.
- [3] I. P. Krasnov, *Proc. of "Days on Diffraction 2011"*, pp. 98–102, 2011.
- [4] I. P. Krasnov, *Proc. of "Days on Diffraction 2012"*, pp. 145–151, 2012.
- [5] I. P. Krasnov, *Proc. of "Days on Diffraction 2014"*, pp. 162–167, 2014.

Application of $\mathbf{ch}_{a,n}$ atomic basis to numerical simulation of wave propagation problem

Kravchenko O.V.^{1,2,3}, Kravchenko V.F.^{1,2,3}, Churikov D.V.^{2,3,4}

¹Bauman Moscow State Technical University, 2nd Baumanskaya, 5, 105005 Moscow, Russia

²Kotel'nikov Institute of Radio Engineering and Electronics of RAS, Mokhovaya 11-7, 125009 Moscow, Russia

³Scientific and Technological Center of Unique Instrumentation of RAS, Butlerova str., 15, 117342 Moscow, Russia

⁴Moscow Institute of Physics and Technology, Institutskiy per., 9, Dolgoprudny, 141700 Moscow Region, Russia

e-mails: ok@bmstu.ru, olekravchenko@cplire.ru, kvf-ok@mail.ru, cdv@cplire.ru

Recently, a family $\mathbf{ch}_{a,n}$ of infinitely differentiable finite functions [1]–[5] on the basis of atomic functions [1]–[6] have been introduced and applied [2] to numerical solution of a hyperbolic linear

scalar equation. It has been noticed that the advantage of the resulting scheme is that the algorithm is very simple and it is very easy to implement. In fact, proposed technique include interpolation process over grid points.

On the other hand, it seems to be an open question how to spread such approach on linear vector problems. From such a point of view, let us consider a linear wave propagation problem [7] in general form

$$\begin{aligned} \partial_t P + \kappa \nabla \cdot \mathbf{v} &= \mathbf{0}, \\ \partial_t \mathbf{v} + \rho^{-1} \nabla P &= 0. \end{aligned} \tag{1}$$

Here, P is a pressure, κ is bulk modulus, $\nabla = (\partial_x, \partial_y)$, \mathbf{v} is particle velocity, and ρ is a density. Eq. (1) correspond to the characteristic equations that describe the acoustic wave propagation in two-dimensional space. First equation is a continuity equation and second one is the equation of motion in an acoustic medium.

It is considered how the proposed approach could be adopted for such a problem. The usage of family $ch_{a,n}$ function provides a good noise immunity of the computational scheme, as well as a reasonable calculation speed.

References

- [1] Ya. Yu. Konovalov, O. V. Kravchenko, *Days on Diffraction 2014*, 132–138 (2014).
- [2] O. V. Kravchenko, *Days on Diffraction 2015*, 170–176 (2015).
- [3] V. F. Kravchenko, O. V. Kravchenko, Ya. Yu. Konovalov, V. I. Pustovoi, D. V. Churikov, *Journal of Communications Technology and Electronics*, **60**(7), 707–736 (2015).
- [4] V. F. Kravchenko, Ya. Yu. Konovalov, V. I. Pustovoi, *Journal of Communications Technology and Electronics*, **60**(9), 986–998 (2015).
- [5] V. F. Kravchenko, Ya. Yu. Konovalov, V. I. Pustovoi, *Doklady Physics*, **60**(5), 197–202 (2015).
- [6] *Digital Signal and Image Processing in Radio Physical Applications*, Ed. V.F. Kravchenko, Moscow, Fizmatlit (2007).
- [7] K. Shiraiishi, T. Matsuoka, *Commun. Comput. Phys.*, **3**(1), 121–135 (2008).

Efficient construction of transmutations and a new representation for solutions of Sturm–Liouville equations, uniform with respect to the spectral parameter

Vladislav V. Kravchenko

Department of Mathematics, Center for Research and Advanced Studies of the National Polytechnic Institute, Campus Queretaro, Mexico

e-mail: vkravchenko@math.cinvestav.edu.mx

Let $q \in C[-b, b]$ be a complex valued function. Consider the Sturm–Liouville equation

$$Ay := y'' - q(x)y = -\omega^2 y. \tag{1}$$

It is well known (see, e.g., [2]) that there exists a Volterra integral operator T called the transmutation (or transformation) operator defined on $C[-b, b]$ by the formula

$$Tu(x) = u(x) + \int_{-x}^x K(x, t)u(t)dt$$

such that for any $u \in C^2[-b, b]$ the following equality is valid

$$ATu = Tu''$$

and hence any solution of (1) can be written as $y = T[u]$ where $u(x) = c_1 \cos \omega x + c_2 \sin \omega x$ with c_1 and c_2 being arbitrary constants.

The transmutation kernel K is a solution of a certain Goursat problem for the hyperbolic equation

$$\left(\frac{\partial^2}{\partial x^2} - q(x) \right) K(x, t) = \frac{\partial^2}{\partial t^2} K(x, t).$$

In the talk I present an exact representation for K in the form of a Fourier–Legendre series with explicit formulas for the coefficients. As a corollary of this result, a new representation of solutions to equation (1) is obtained. For every x the solution is represented as a Neumann series of Bessel functions depending on the spectral parameter ω . Due to the fact that the representation is obtained using the corresponding transmutation operator, a partial sum of the series approximates the solution uniformly with respect to ω which makes it especially convenient for the approximate solution of spectral problems. The numerical method based on the proposed approach allows one to compute large sets of eigendata with a nondeteriorating accuracy. The talk is based on [1].

References

- [1] V. V. Kravchenko, L. J. Navarro, S. M. Torba, Representation of solutions to the one-dimensional Schrödinger equation in terms of Neumann series of Bessel functions. Submitted for publication, available at arxiv:1508.02738.
- [2] V. A. Marchenko, *Sturm–Liouville Operators and Applications*. Birkhäuser, Basel (1986).

Analysis of graded-index optical fibers by the spectral parameter power series method

Vladislav V. Kravchenko¹, Sergii M. Torba¹, Raúl Castillo-Pérez²

¹Departamento de Matemáticas, CINVESTAV del IPN, Unidad Querétaro, Libramiento Norponiente #2000, Fracc. Real de Juriquilla, Querétaro, Qro. C.P. 76230 Mexico

²SEPI, ESIME Zacatenco, Instituto Politécnico Nacional, Av. IPN S/N, C.P. 07738, Ciudad de México, Mexico

e-mails: vkravchenko@math.cinvestav.edu.mx, storba@math.cinvestav.edu.mx,
rcastillo@ipn.mx

In this work an approach for analysis of optical fibers with inhomogeneous refractive index profiles was introduced based on the recently developed SPPS (Spectral Parameter Power Series) Method ([1, 2]). A new technique has been created for solving the associated linear differential equations and spectral problems. The computation of the guided modes for different kinds of fibers is done through the characteristic equation of the eigenvalue problem obtained in an analytical form in terms of SPPS. Consideration of the approximate characteristic equation obtained from the truncated series gives us an efficient numerical method for solving the problem. The results have been compared with those of other available techniques revealing clear advantages for the SPPS approach, in particular, with regards to accuracy. Based on the solution of the eigenvalue problem, the group velocity, dispersion coefficient, group index and other relevant parameters of the fibers are computed.

References

- [1] V. V. Kravchenko, A representation for solutions of the Sturm–Liouville equation, *Complex Var. Elliptic Equ.*, **53**, pp. 775–789, 2008.
- [2] V. V. Kravchenko, R. M. Porter, Spectral parameter power series for Sturm–Liouville problems, *Math. Methods Appl. Sci.*, **33**, pp. 459–468, 2010.

Electrodynamic characteristics of a loop antenna located on the surface of a uniaxial anisotropic cylinder

A.V. Kudrin, T.M. Zaboronkova, A.S. Zaitseva

University of Nizhny Novgorod, 23 Gagarin Ave., Nizhny Novgorod 603950, Russia
e-mails: kud@rf.unn.ru, t.zaboronkova@rambler.ru, anaze@yandex.ru

C. Krafft

Laboratoire de Physique des Plasmas, École Polytechnique, 91128 Palaiseau Cedex, France
e-mail: catherine.krafft@lpp.polytechnique.fr

Radiation from loop antennas in anisotropic and gyrotropic homogeneous media has received much careful study (see, e.g., [1] and references therein). The electrodynamic characteristics of a loop antenna excited by a time-harmonic given voltage and located on the surface of a magnetized plasma column in free space have recently been considered in [2, 3]. In this work, we study the current distribution and input impedance of a strip loop antenna located on the surface of a uniaxial anisotropic cylinder surrounded by a homogeneous isotropic background medium. The interest in this problem is stimulated by various practical applications such as the radiation from a loop antenna in the presence of a strongly magnetized plasma column or a cylinder filled with uniaxial metamaterial.

We consider an antenna having the form of an infinitesimally thin, perfectly conducting narrow strip, which is coiled into a circular loop. The antenna is located coaxially on the surface of a uniform uniaxial anisotropic cylinder aligned with the anisotropy axis and placed in an isotropic medium. The medium inside the cylinder is described by a dielectric tensor with nonzero frequency-dependent diagonal elements and zero off-diagonal elements. The antenna current is excited by a time-harmonic external voltage creating an electric field with the only azimuthal component in a narrow gap of the strip. We employ Fourier series expansions with respect to the azimuthal angle for both an unknown antenna current and the voltage supplied to the antenna. Using the boundary conditions for the tangential components of the electromagnetic field on the cylinder surface and the antenna surface, we derive singular integral equations for the angular harmonics of the surface current density.

We solve the obtained integral equations in the case of a hyperbolic metamaterial for which the diagonal elements of the dielectric tensor have opposite signs. On the basis of the solutions of these equations, it is shown that the current distribution and input impedance of the antenna are significantly influenced by the presence of an infinite number of propagating quasiolelectrostatic eigenmodes that are guided by a such cylinder. The radiation characteristics of the considered antenna have been studied analytically and numerically, and the results of their calculation will be reported in cases of interest.

This work was supported by the Russian Science Foundation (project No. 14-12-00510) and the Government of the Russian Federation (project No. 14.B25.31.0008).

References

- [1] A. V. Kudrin, E. Yu. Petrov, T. M. Zaboronkova, *J. Electromagn. Waves Appl.*, **15**, 345–378 (2001).
- [2] A. V. Kudrin, A. S. Zaitseva, T. M. Zaboronkova, C. Krafft, G. A. Kyriacou, *PIER B*, **51**, 221–246 (2013).
- [3] A. V. Kudrin, A. S. Zaitseva, T. M. Zaboronkova, S. S. Zilitinkevich, *PIER B*, **55**, 241–256 (2013).

On the infinitely many electromagnetic TE eigenmodes in a plane layered waveguide filled with nonlinear medium: analytical results

Kurseeva V. Yu., Valovik D.V.

Department of Mathematics and Supercomputing, Penza State University, Penza, Russia, 440026
e-mails: NoelleDestler@yandex.ru, dvalovik@mail.ru

We consider the propagation of a monochromatic TE wave $\mathbf{E}e^{-i\omega t}$, $\mathbf{H}e^{-i\omega t}$ of the form

$$\mathbf{E} = (0, E_y(x)e^{i\gamma z}, 0)^\top, \quad \mathbf{H} = (H_x(x)e^{i\gamma z}, 0, H_z(x)e^{i\gamma z})^\top, \quad (1)$$

along the boundaries of the double-layer dielectric waveguide $\Sigma = \Sigma_1 \cup \Sigma_2$, where

$$\Sigma_1 := \{(x, y, z) \in \mathbb{R}^3 : 0 \leq x \leq h_1\}, \quad \Sigma_2 := \{(x, y, z) \in \mathbb{R}^3 : h_1 \leq x \leq h_1 + h_2\}$$

and \mathbf{E} , \mathbf{H} are the complex amplitudes; ω is a circular frequency; $(\cdot)^\top$ is the transposition operation; γ is an unknown (real) propagation constant; E_y, H_x, H_z are unknown functions,

The waveguide Σ is located in the Cartesian coordinate system $Oxyz$. In the half-space $x < 0$ the permittivity is constant and equal to $\varepsilon_s > 0$. At the boundary $x = h_1 + h_2$ the waveguide has a perfectly conducted wall. In the layers the permittivity is described by the formula

$$\varepsilon = \begin{cases} \varepsilon_1 + \alpha_1 |\mathbf{E}|^2, & 0 \leq x < h_1, \\ \varepsilon_2 + \alpha_3 |\mathbf{E}|^2, & h_1 \leq x \leq h_1 + h_2, \end{cases}$$

where $\varepsilon_1, \varepsilon_2, \alpha_1, \alpha_2$ are real positive constants. We assume that $\varepsilon_s \geq \varepsilon_0$, where ε_0 is the permittivity of free space, and $\varepsilon_s < \varepsilon_1 < \varepsilon_2$. There are no sources in the entire space. Everywhere $\mu = \mu_0$, where μ_0 is the magnetic permeability of free space.

Complex amplitudes (1) satisfy Maxwell's equations

$$\begin{cases} \operatorname{rot} \mathbf{H} = -i\omega\varepsilon\mathbf{E}, \\ \operatorname{rot} \mathbf{E} = i\omega\mu\mathbf{H}; \end{cases} \quad (2)$$

the continuity condition for the tangential components of the field at the boundaries $x = 0$ and $x = h_1$, and the radiation condition at infinity: the electromagnetic field decays as $O(|x|^{-1})$ when $x \rightarrow \infty$. The tangential components of \mathbf{E} vanishes at the $x = h_1 + h_2$.

A rigorous analytical approach is suggested. It is proved that under some restrictions there exists an infinite number of propagation constants and guided modes, whereas the corresponding linear problem has only a finite number of solutions. It is shown that perturbation methods do not allow one to determine new propagation constants. Numerical results are also presented, comparison with the linear cases is given. Results for similar problems see in [1, 2, 3, 4].

References

- [1] V. Yu. Kurseeva, D. V. Valovik, *Proceedings of the International Conference DAYS on DIFFRACTION 2014*, 177–180 (2014).
- [2] V. Yu. Kurseeva, D. V. Valovik, *Proceedings of the International Conference DAYS on DIFFRACTION 2015*, 189–195 (2015).
- [3] Yu. G. Smirnov, D. V. Valovik, *Physical Review A*, **91**, 013840-1–6 (2015).
- [4] D. V. Valovik, *PIERS Proceedings (Moscow)*, 122–126 (2012).

Existence of complex waves in Goubau line: mathematical aspects

Kuzmina E.A.

Moscow State University of Information Technologies, Radioengineering and Electronics (MIREA),
Moscow, Russia

e-mail: ekaterina.kuzm@gmail.com

Shestopalov Y.V.

University of Gävle, Gävle, Sweden

e-mail: yuyshv@hig.se

In this work we investigate a homogeneous Goubau line (GL) covered with a lossy dielectric. A systematic study is made of the dispersion equation $F_G = 0$ for symmetric waves in the complex domain with respect to the problem parameters. We present a mathematical proof of the existence of radially symmetric complex waves using continuation with respect to the imaginary part of the permittivity of the dielectric cover $t = \Im\epsilon$ and reduction to the Cauchy problem

$$d\gamma/dt = -(\partial F_G/\partial t)/(\partial F_G/\partial \gamma); \quad \gamma(0) = \gamma_n, \quad (1)$$

where $\gamma = \gamma(t)$ denotes the longitudinal wavenumber of the running symmetric wave. Using the technique developed in [1, 2] we prove [3] that Cauchy problem (1) is uniquely solvable. This implies that complex zeros of $F_G = F_G(\gamma, t)$ constitute regular perturbations of its real zeros γ_n . Also, we calculate linear approximations of complex zeros of $F_G(\gamma, t)$ in the form of segments of Taylor series.

As we find out introduction of a small imaginary part of the permittivity of the GL makes it possible to study certain anomalous behavior and regimes of complex eigenwaves. We show in particular that longitudinal wavenumbers of complex waves are regular perturbations of the propagation constants of eigenwaves of lossless GL, weakly depend on the imaginary part of permittivity of the cover, and that attenuation in GL is low at higher losses. This reveals a new property of lossy GLs.

Generally, the developed mathematical technique applied for the study of GLs covered with lossy dielectric is the first and necessary step to the analysis of complex waves in open metal-dielectric waveguides.

References

- [1] Y. Shestopalov, E. Kuzmina, *Proceedings of Progress in Electromagnetics Research Symposium (PIERS)*, Guangzhou, China, 2605–2609 (2014).
- [2] Y. Shestopalov, E. Kuzmina, A. Samokhin, *Forum for Electromagnetic Research Methods and Application Technologies (FERMAT)*, Vol. 5 (2014).
- [3] E. Kuzmina, Y. Shestopalov, *The 10th European Conference on Antennas and Propagation (EuCAP)*, Davos, Switzerland (2016).

Scattering of a surface wave on a controlled inhomogeneity

Kuznetsov E.V.^{1,2}, Merzlikin A.M.^{1,2,3}

¹All-Russia Research Institute of Automatics, Moscow 101000, Russia

²Institute for Theoretical and Applied Electrodynamics, Moscow 125412, Russia

³Moscow Institute of Physics and Technology, Moscow 117303, Russia

e-mail: evgenykuznet@gmail.com

Manipulating of an electromagnetic radiation is one of the most actual problems of electrodynamics. Many devices such as optical filters, blockers, beam-splitters, spatial light modulators, etc., have been proposed [1–3]. Spatial light modulators are used for spatial modulation of an incident plane wave transmittance, which means it is practically an amplitude-phase lattice. The most widespread spatial modulator is a matrix which elements are Fabri–Perot resonators [3]. The central layer of the

element is made of electrooptical crystal and thus may be operated by external static electric field, which results in Fabri–Perot modes shifting. If this shift exceeds mode width then one can switch on or switch off the element of the matrix. That makes a pixel of an image. Let a light beam incident on that matrix. The transmitted light will give an image on a screen.

The size of elements is limited due to restriction on Fabri–Perot resonator quality factor and cannot be less than several wavelengths. In order to create a controlled subwavelength element we propose to use a nearfield scattering. Let us consider a layer of an electrooptical material deposited on a surface of a photonic crystal. The surface wave is excited on the boundary between an electrooptical material and a photonic crystal. Propagation of surface wave on PC boundary is very sensitive to changes of dielectric permittivity of surrounding medium [4]; therefore we expect that we will be able to operate scattering even at minor changes of system parameters. Control of surface wave propagation is carried out by a subwavelength electrodes grid injected into an electrooptical layer.

We have shown that applying voltage to electrodes in this system allows changing of a dielectric permittivity in a certain point of an electrooptical layer in a controlled way. Such inhomogeneities of a dielectric permittivity are subwavelength. That allows to control surface wave scattering and its radiation outside the system at each cell of a spatial modulator. We have shown that scattered field intensity in its maximum is 25 times more than incidence field intensity. The scattering on a dielectric permittivity is stronger than scattering on surface defects.

References

- [1] M. Gilo, Design of a nonpolarizing beam splitter inside a glass cube, *Appl. Opt.*, **31**(25), 5345 (1992).
- [2] C. K. Madsen, J. H. Zhao, *Optical Filter Design and Analysis: A Signal Processing Approach*, John Wiley & Sons, New York (1999).
- [3] L. J. Hornbeck, Digital light processing for high-brightness, high-resolution applications, *Proc. SPIE 3013, Projection Displays III*, **27** (May 8, 1997).
- [4] E. Alieva, D. Dolgy, E. Olshansky, S. Sekatskii, G. Dietler, Registration of long-range surface plasmon resonance by angle-scanning feedback and its implementation for optical hydrogen sensing, *New Journal of Physics*, **11** (2009).

On the Benjamin–Lighthill conjecture for water waves with vorticity

Nikolay Kuznetsov

Laboratory for Mathematical Modelling of Wave Phenomena
 Institute for Problems in Mechanical Engineering, Russian Academy of Sciences
 V.O., Bol'shoy pr. 61, 199178 St Petersburg, Russian Federation
 e-mail: nikolay.g.kuznetsov@gmail.com

We analyse the nonlinear problem of steady gravity-driven waves on the free surface of a two-dimensional flow of an incompressible fluid (say, water). The flow is assumed to be unidirectional of finite depth and the water motion is supposed to be rotational with a Lipschitz continuous vorticity distribution. We verify the Benjamin–Lighthill conjecture for flows whose Bernoulli's constant is close to the critical one. For this purpose it is shown that every wave, whose slope is bounded by a fixed constant, is either a Stokes or a solitary wave. It is proved that the whole set of these waves is uniquely (up to translation) parametrised by the flow force which varies between its values for the supercritical and subcritical shear flows of constant depth. There exists another parametrisation for waves; it involves wave heights varying between the constant depth of the subcritical shear flow and the solitary wave height.

These results are obtained in collaboration with Vladimir Kozlov and Evgeniy Lokharu (Linköping University, Sweden).

Freely floating bodies trapping time-harmonic waves in water covered by brash ice

Nikolay Kuznetsov, Oleg Motygin

Laboratory for Mathematical Modelling of Wave Phenomena, Institute for Problems in Mechanical Engineering of the Russian Academy of Sciences, V.O., Bol'shoy pr. 61, 199178 Saint Petersburg, Russian Federation

e-mails: nikolay.g.kuznetsov@gmail.com, o.v.motygin@gmail.com

We study a mechanical system consisting of infinitely deep water covered by brash ice and surface-piercing bodies floating freely. The water is assumed to be inviscid and incompressible and the coupled motion is of small amplitude. The corresponding linear setting for time-harmonic oscillations reduces to a spectral problem whose parameter is the frequency of oscillations. A constant that characterizes the brash ice divides the set of frequencies into two subsets where the problem has essentially different properties. For every frequency belonging to the finite interval adjacent to zero, we prove that the total energy of motion is finite and the equipartition of energy holds for the whole system. For every frequency from this interval, we prove the existence of structures supporting trapped modes and consisting of arbitrary finite number of bodies. The structures are constructed by virtue of the semi-inverse procedure and it can be done so that any subset of bodies is motionless whence other bodies are heaving at the same frequency as water.

Application of the modified method of discrete sources to the solution of the problem of a flow of a compact body and periodically rough surface

A.G. Kyurkchan, S.A. Manenkov

Moscow Technical University of Communication and Informatics, Aviamotornaya Street 8A, 111024, Moscow, Russia

e-mail: mail44471@mail.ru

The problem of a flow by a stream of incompressible liquid of motionless compact body and periodically rough surface is considered. As it is known the problem of the flow is reduced to the solution of the Laplace equation with a Neumann boundary condition on the rough surface or the body border [1]. The method of conformal mapping is applied to the solution of similar problems earlier [1]. This method is applied to the problem of the flow of a circular cylinder, a thin plate, etc. Thus, the method of conformal mapping is applicable in the case of the solution of the problem of the flow of the simple geometry bodies. In more difficult cases use of other approaches is required. In the present work for the solution of the problem of the flow of compact body and periodically rough surface the modified method of discrete sources (MMDS) which is successfully applied earlier to the solution of the problems connected with the solution of the equations of Maxwell, Helmholtz's equations and Laplace's equation is used [2–5]. In the latter case the electrostatic problem for a body of revolution is considered.

MMDS is based on two ideas. First, the integral equation to which the initial boundary problem is reduced, has the solution corresponding to the initial problem if and only if the auxiliary surface on which the unknown function is distributed, covers the set of singularities of analytical continuation of the field inside the area occupied by the body. Secondly, the choice of the auxiliary surface should be made by means of analytical deformation of the boundary of the body [2–5]. In this work the problem of the flow is reduced to the solution of the integral equation of the first kind, relative some unknown function distributed on the auxiliary surface which is taken by the way stated above. The integral equation is solved by the collocation method. The numerical results given in the paper belong to the problem of the flow of the sinusoidal surface and the surface in the form of the cycloid as well as

the Chebyshev particle. We have plotted the lines of fluid flow and the curves of distribution of the pressure versus the distance from the body.

References

- [1] A. N. Tikhonov, A. A. Samarskii, *Equations of mathematical physics*, Mos. Gos. Univ., Moscow (1999); Pergamon Press, Oxford (1964).
- [2] A. P. Anyutin, A. G. Kyurkchan, S. A. Manenkov, S. A. Minaev, About 3D solution of diffraction problems by MMDS, *Journal of Quantitative Spectroscopy & Radiative Transfer*, v. **100**, pp. 26–40 (2006).
- [3] A. G. Kyurkchan, S. A. Manenkov, The application of a modified method of discrete sources for solving the problem of wave scattering by group of bodies, *Journal of Quantitative Spectroscopy & Radiative Transfer*, v. **109**, pp. 1430–1439 (2008).
- [4] A. G. Kyurkchan, S. A. Manenkov, The electrostatic approximation in the problem of diffraction of a plane wave by a group of coaxial small scatterers, *J. Commun. Technol. Electron*, v. **57**, pp. 353–362 (2012).
- [5] A. G. Kyurkchan, S. A. Manenkov, Application of different orthogonal coordinates using modified method of discrete sources for solving a problem of wave diffraction on a body of revolution, *Journal of Quantitative Spectroscopy & Radiative Transfer*, v. **113**, pp. 2368–2378 (2012).

Superresolution based on interpolation and extrapolation of received signals

B.A. Lagovsky, A.B. Samokhin, V.I. Nefedov

Moscow Technological University, 78, Vernadsky av., 119454, Moscow, Russia
e-mail: absamokhin@yandex.ru

Increasing angular resolution is the important way of radar development. We consider the problem of obtaining the angular superresolution using smart antennas. Forming radio images with super-resolution reduced to the solution of inverse problems on the basis of Fredholm integral equations. The signals received by each radiator of the smart antennas can be recorded digitally. This makes it possible combined digital processing of all the information received. The new signal processing method is based on the interpolation and extrapolation of the signals received by each element of the smart antennas. Extrapolation of the signals beyond the real aperture enables you to create synthesized aperture much larger size. Thus it becomes possible to obtain a synthesized the receiving narrow beam that provides superresolution. The quality of the extrapolation depends on the number and density of distribution the initial points of extrapolated function. To increase the number of initial points within the real aperture proposed to interpolate the received antenna array signals. Interpolation allows obtaining continuous distribution of the received signal at the location of the antenna array. As a result, the accuracy of angular measurements and angular resolution increases.

The algorithm without the interpolation predicts the values of the signals for the aperture array 5–10 times higher than the original one with a negligible error. Numerical studies have shown that the Rayleigh criterion in this problem is exceeded by 4–7 times. More complex algorithm with the interpolation predicts the values of the signals for the aperture array 8–10 and even more — up to 20 times higher than the original one.

An important characteristic of solutions is a minimal signal/noise ratio (SNR) with which a superresolution image reconstruction is still possible. Stability of solutions and quality of image reconstruction were examined using a mathematical model. The results of numerical studies show that the angular resolution is increased 5–12 times under SNR 12–13 dB, which is lower than that achieved by the known methods.

The proposed new method of signal processing based on digital aperture synthesis significantly improves the accuracy of angle measurements and provides a stable restoration of detailed images of the objects with superresolution in the presence of small distortions.

Bidirectional adiabatic light transfer in coupled waveguides

Liu T., **Solntsev A.S.**, Neshev D.N., Sukhorukov A.A.

Nonlinear Physics Centre and Centre for Ultrahigh Bandwidth Devices for Optical Systems, Research School of Physics and Engineering, Australian National University, Canberra, ACT 2601, Australia
e-mail: alexander.solntsev@anu.edu.au

Boes A., Mitchell A.

Centre for Ultrahigh Bandwidth Devices for Optical Systems, School of Engineering, RMIT University, Melbourne, VIC 3001, Australia

The analogy between quantum systems and optical waveguide structures make the latter not only a favorable tool for emulating quantum phenomena but also a powerful platform for the development of photonic devices. One of such quantum-inspired photonic devices is the adiabatic three-waveguide coupler, which is a reminiscent of the celebrated Stimulated Raman Adiabatic Passage technique (STIRAP) [1]. This adiabatic process is inherently tolerant to variations of structure parameters and exhibits broadband coupling, based on so-called dark state switching, see Fig. 1(a) [2].

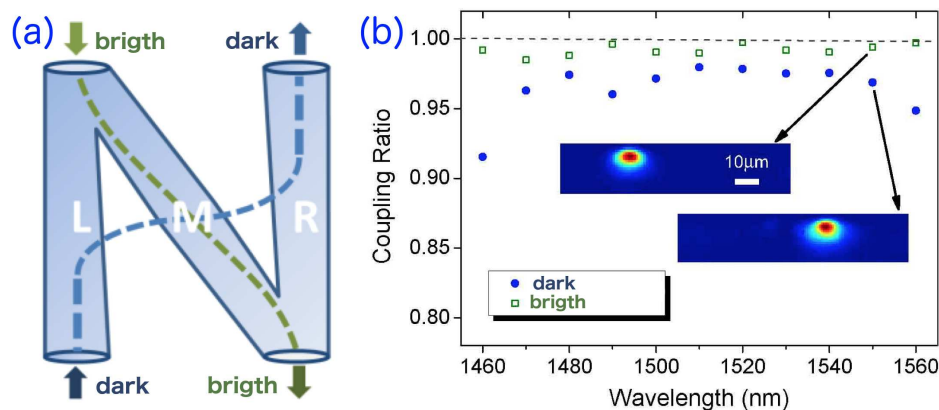


Fig. 1: (a) The scheme of the 3-waveguide structure showing dark- and bright-state coupling. (b) Experimental broadband dark- and bright-state coupling ratio, inserts show output modes.

We propose and demonstrate a novel type of optical waveguide couplers consisting of three adiabatically coupled waveguides arranged in a unique N-shaped geometry. Unlike conventional adiabatic three-waveguide couplers mimicking STIRAP which utilize solely the dark state and thus work only in one direction, in our newly designed structure, nearly complete bidirectional light transfer between two waveguides can be achieved through a dark state and a bright state of the system respectively [see Fig. 1(a)]. Such N-type adiabatic waveguide coupler exhibits high coupling ratios in both directions over a wide wavelength range [see Fig. 1(b)]. Our results may shed new light on the design of integrated photonic devices for both classical and quantum applications [3].

References

- [1] U. Gaubatz, P. Rudecki, S. Schieman, K. Bergmann, *J. Chem. Phys.*, **92**, 5363 (1990).
- [2] C. Ciret, V. Coda, A. Rangelov, D. Neshev, G. Montemezzani, *Phys. Rev. A*, **87** (2013).
- [3] C. W. Wu, A. S. Solntsev, D. N. Neshev, A. A. Sukhorukov, *Opt. Lett.*, **39**, 953 (2014).

Semiclassical quantization rules for a periodic orbit of hyperbolic type

Hanen Louati^{1,2,3}, Michel Rouleux^{2,3}

¹Université de Tunis El-Manar, Département de Mathématiques, 1091 Tunis, Tunisia

²Aix Marseille Université, CNRS, Centre de Physique Théorique, UMR 7332, 13288 Marseille, France

³Université de Toulon, CNRS, CPT, UMR 7332, 83957 La Garde, France

e-mails: louatihanen42@yahoo.fr, rouleux@univ-tln.fr

We consider semi-excited resonances for a Pseudo-Differential Operator $H(x, hD_x; h)$ on $L^2(M)$ induced by a periodic orbit of hyperbolic type at energy $E = 0$, as arises when $M = \mathbf{R}^n$ and $H(x, hD_x; h)$ is Schrödinger operator with AC Stark effect, or $H(x, hD_x; h)$ is the geodesic flow on an axially symmetric manifold M , extending Poincaré example of Lagrangian systems with 2 degree of freedom. We generalize the framework of [GeSj], in the sense that we allow for hyperbolic and elliptic eigenvalues of Poincaré map, and look for (excited) resonances with imaginary part of magnitude h^s , with $0 < s < 1$.

It is known [NoSjZw], [FaLoRo] that these resonances are given by the zeroes of a determinant associated with Poincaré map. We make here this result more precise, in providing a first order asymptotics of Bohr–Sommerfeld quantization rule in terms of the (real) longitudinal and (complex) transverse quantum numbers, including the action integral, the sub-principal 1-form and Gelfand–Lidskii index.

To this aim we bring the operator to its Birkhoff normal form microlocally near the periodic orbit, and construct Poisson operator as an oscillatory integral that assigns to a transverse data a semi-classical distribution (of WKB type) in the microlocal kernel of $H - E$. The fibre bundle $K_h(E)$ of such WKB solutions is endowed with Hermitian structure by means of the “flux norm” introduced by Helffer and Sjöstrand. This allows to build up the monodromy operator $\mathcal{M}(E)$ as a h -FIO microlocalized on a Poincaré section, which is unitary for real energies. Breaking this unitarity according to the usual procedure of “complex scaling”, we disclose discrete spectrum E on the second sheet in energy complex plane, which is precisely the set of resonances of H near 0. The residue of the phase function defining $\mathcal{M}(E)$ modulo exact forms gives the generalized action integral and we obtain the quantization condition by expressing that $K_h(E)$ should be trivial whenever E is a resonance.

References

- [GeSj] C. Gérard, J. Sjöstrand, Semiclassical resonances generated by a closed trajectory of hyperbolic type, *Comm. Math. Phys.*, **108**, p. 391–421 (1987).
- [FaLoRo] H. Fadhlou, H. Louati, M. Rouleux, Hyperbolic Hamiltonian flows and the semiclassical Poincaré map, *Proceedings “Days of Diffraction 2013”*, Saint-Petersburg, pp. 53–58 (2013), doi: 10.1109/DD.2013.6712803.
- [NoSjZw] S. Nonnenmacher, J. Sjöstrand, M. Zworski, From open quantum systems to open quantum maps, *Comm. Math. Phys.*, **304**, pp. 1–48 (2011).

Wide-bandgap optoelectronics with micro/nano-scale architectures

Tien-Chang Lu

Department of Photonics, National Chiao Tung University 1001, University Rd., Hsinchu 30050, Taiwan

e-mail: timtclu@mail.nctu.edu.tw

Wide bandgap materials have been attracted much attention due to their potential for development of optoelectronic devices in the wide wavelength region, especially ranging from UV to visible bands. In addition, the excellent exciton features in GaN-based or ZnO-based materials enables them

to be applied in high efficiency light emitting devices. On the other hand, one and two dimensional photonic crystal incorporated of periodic structures with its unique optical properties, have been widely adopted to many optoelectronic devices including light emitting diodes (LEDs) and photonic crystal (PC) lasers [1–4]. These wide-bandgap optoelectronics with micro or nano-scale architectures are developed rapidly due to the recent advances in processing and manufacturing technology.

One dimensional (1D) PC have been utilized on various functional devices by using the focused ion beam (FIB), e-beam lithography and inductively coupled plasma (ICP) dry etching. In recent years, sub-wavelength high contrast gratings (HCG) as being one form of the 1D PC have been widely investigated owing to their advantageous optical properties. By changing of HCG parameters such as grating period, height and width, high reflectivity reflectors with broad stopband width and specific polarization characteristics could be obtained and are useful for many applications. Based on the superior properties, HCGs not only serve as high reflectivity reflectors for vertical cavity surface-emitting lasers (VCSELs) but also provide unique characteristics including polarization selection, wavelength tuning and fast modulation speed. We have demonstrated GaN-based high contrast grating (HCG) as an optical reflector in blue region [5] and GaN-based HCG surface-emitting lasers [6], which have the great potential for accomplishment of low threshold, high power short wavelength coherent light sources in the near future.

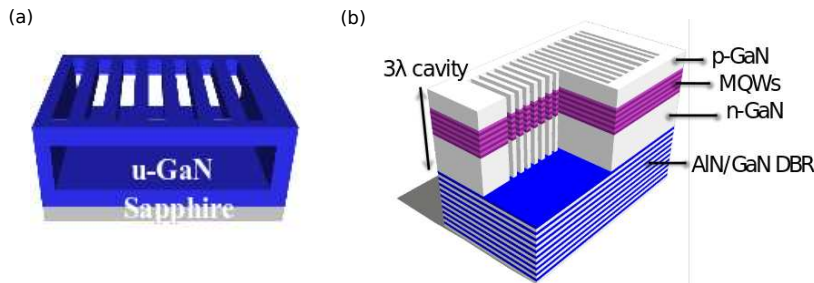


Fig. 1: (a) GaN-based high contrast grating reflector and (b) surface emitting lasers.

For two dimensional (2D) PC structures, two kinds of 2D PC lasers such as band-edge lasers and defect type lasers have been proposed and investigated during the past decade. In this part, we have demonstrated the GaN-based band-edge PC lasers, so called photonic crystal surface emitting lasers (PCSELs) operated at room temperature [7]. The laser characteristics of PCSELs at different band-edge modes and with different lattice types have been fabricated and analyzed. And their characteristics are calculated by the multiple scattering method. For defect type PC lasers, owing to the photonic band gap effect in the in-plane direction and total internal reflection in the vertical direction to the thin membrane, highly localized laser oscillations usually can be observed in the defect cavities to achieve small modal volume with a high quality factor and strong-coupling effect. We have fabricated the high Q GaN-based non-polar defect nanocavity [8] and observed localized lasing mode in GaN-based quasi-periodic nanopillars [9].

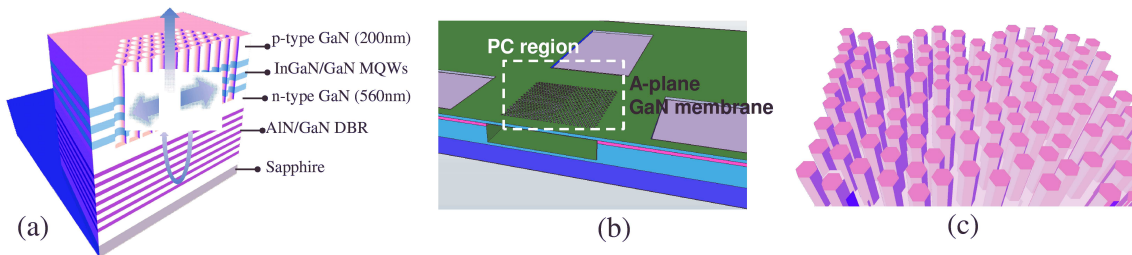


Fig. 2: (a) GaN-based PCSEL (b) Non-polar GaN-based H1 defect type PC lasers and (c) GaN Quasi Periodic nanopillar lasers.

References

[1] M. C. Y. Huang, Y. Zhou, C. J. Chang-Hasnain, *Nat. Photonics*, **1**, 119 (2007).

- [2] O. Painter, R. K. Lee, A. Scherer, A. Yariv, J. D. O'Brien, P. D. Dapkus, I. Kim, *Science*, **284**, 1819 (1999).
- [3] H. Matsubara, S. Yoshimoto, H. Saito, Y. Jianglin, Y. Tanaka, S. Noda, *Science*, **319**, 445 (2008).
- [4] T. C. Lu, S. W. Chen, L. F. Lin, T. T. Kao, C. C. Kao, P. Yu, H. C. Kuo, S. C. Wang, S. H. Fan, *Appl. Phys. Lett.*, **92**, 011129 (2008).
- [5] T. T. Wu, Y. C. Syu, S. H. Wu, T. C. Lu, S. C. Wang, H. P. Chiang, D. P. Tsai, *Optics Express*, **20**(18), 20551–20557 (2012).
- [6] T. T. Wu, S. H. Wu, T. C. Lu, S. C. Wang, *Appl. Phys. Lett.*, **102**, 081111 (2013).
- [7] T. T. Wu, P. H. Weng, J. J. Hou, T. C. Lu, *Appl. Phys. Lett.*, **99**, 221105 (2011).
- [8] T. T. Wu, S. Y. Lo, T. C. Lu, S. C. Wang, *Appl. Phys. Lett.*, **102**, 191106 (2013).
- [9] T. T. Wu, C. C. Chen, H. W. Chen, T. C. Lu, S. C. Wang, C. H. Kuo, *IEEE J. Select. Topics Quantum Electron.*, **19**(4), 4900206 (2013).

Eigenoscillations in a water-wave problem for an infinite pool of special form

Lyalinov M.A.

Department of Mathematical Physics, Physics Faculty, Saint-Petersburg University, 7/9 Universitet-skaya nab., Saint-Petersburg, 199034, Russia
e-mail: lyalinov@yandex.ru

Polyanskaya S.V.

Department of Mathematics, North-West Academy of Municipal and State Management, Sredniy ave. 57, Saint-Petersburg, Russia

In the framework of the assumptions of the linearized theory of small-amplitude water waves the eigenfunctions of the point spectrum are studied for the boundary-value problems in an infinite domain. Special type of the 3D infinite water pool characterised by cone-shaped bottom and bounded in the azimuthal directions is considered. By means of the incomplete separation of variables, exploiting the Mellin transform, we reduce construction of the eigenmodes to the study and solution of the problems for some functional difference equations with meromorphic coefficients. The behaviour of the eigenmodes at a singular point of the boundary and the rate of their decay at infinity are also discussed.

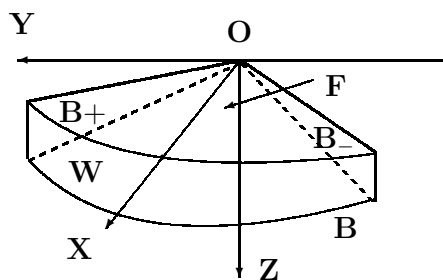


Fig. 1: An infinite pool with the conical bottom B and vertical walls B_{\pm} .

Calculation of interference pattern after diffraction of two interfering image-carrying beams by acoustic wave in uniaxial crystal

Machikhin A.S., Burmak L.I.

Scientific and Technological Center of Unique Instrumentation RAS, 117342, Moscow, Butlerova 15
e-mails: aalexanderr@mail.ru, burmakliu@yandex.ru

Acousto-optic (AO) image filtration is based on the diffraction of image-carrying light beam by an acoustic wave [1]. Because of rather high spectral and spatial resolution, random spectral access,

programmability and other advantages, AO tunable filters (AOTFs) are widely used for spectral imaging in microscopy, endoscopy and remote sensing. Recently, imaging AOTFs are being in use in optical coherence tomography [2] and profilometry [3] for simultaneous spectral filtration of two interfering light beams. Up to now, the efficiency of such approach has been demonstrated only experimentally. In this paper, we show the calculation of interference pattern after diffraction of two interfering image-carrying light beams by an acoustic wave in uniaxial crystal and its comparison to the experimental data.

If the intensities of two interfering beams are equal ($I_0 = I_1 = I_2$), the following equation can be used to calculate the interference pattern [4]:

$$I \sim 2I_0 \left\{ 1 + \exp \left[- \left(\frac{\Delta}{l_c} \right)^2 \right] \cos \left[\frac{2\pi}{\lambda} \Delta \right] \right\},$$

where Δ is path-length difference between the beams, λ is wavelength, $l_c = \lambda^2/\delta\lambda$ is coherence length, $\delta\lambda$ is spectral channel width, which for an AOTF can be approximately calculated as $\delta\lambda = \alpha\lambda^2/(\pi L\Delta n)$, α denotes coefficient depending on the configuration of AO interaction, L is length of AO interaction, $\Delta n = n_e - n_o$ is difference in refractive indices for extraordinary and ordinary waves in the crystal.

We used a wide-angle non-collinear imaging AOTF made of TeO₂ uniaxial crystal, placed in the output channel of Michelson interferometer for spectral filtration of light from a low-coherence wideband light source. The AOTF has a tuning range of 450–750 nm and spectral resolution $\delta\lambda$ of 2.5 nm (at $\lambda = 532$ nm). Fig. 1 shows the real and calculated interference patterns at $\lambda = 532$ nm obtained experimentally from a test-object (grating with 100 μm period and 9.7 μm depth).

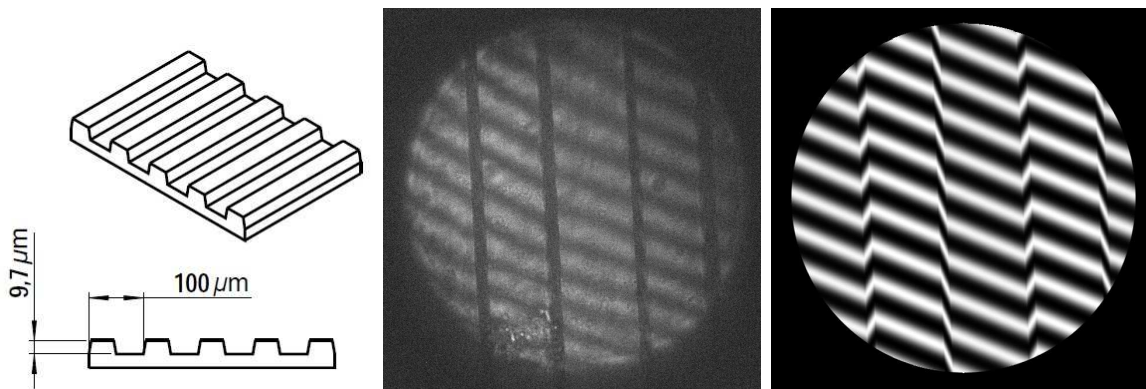


Fig. 1: (a) test-object, (b) experimental data, (c) calculated pattern.

This study was supported by Russian Foundation for Basic Research (grant 16-07-00393) and President grant MK-4296.2015.8.

References

[1] A. Goutzulis, D. Rape, *Design and Fabrication of Acousto-Optic Devices*, Marcel Dekker, New York (1994).
 [2] A. S. Machikhin, V. E. Pozhar., A. V. Viskovatykh, L. I. Burmak, *Applied Optics*, **54(25)**, 7508–7513 (2015).
 [3] A. V. Viskovatykh, A. S. Machikhin, V. E. Pozhar, V. I. Pustovoit, *Instruments and Experimental Techniques*, **58(1)**, 114–117 (2015).
 [4] V. V. Lychagov, V. P. Ryabukho, A. L. Kalyanov, I. V. Smirnov, *Journal of Optics*, **14(1)**, 015702 (12 pp) (2012).

Abnormal spatial nanogratings formation by long pulse durations laser radiation on condensed matter surfaces

Makin V.S.¹, Makin R.S.², Pestov Yu.I.¹

¹Public Limited Company “Scientific Research Institute for Opto-Electronic Measurement Engineering”, Sosnovy Bor City, Leningrad oblast’, Russia

²National Research Nuclear University “MEPHI”, Moscow, Russia

e-mail: makin@sbor.net

In experiments with laser-matter interaction of ultrashort pulse durations (UPD) the formation of the gratings (\vec{g}) of normal orientation ($\vec{g} \parallel \vec{E}$, $d \leq \lambda$) and abnormal one ($\vec{g} \perp \vec{E}$, $d \ll \lambda$) have been observed [1]. Here d is the period of grating and λ is the laser radiation wavelength. The origin of their formation has been suggested based on the channel (wedge) surface plasmon polaritons excitation and participation in interference [1] in framework of universal polariton model. Here we consider the residual gratings resulted after irradiated zone was cooling-down. The spatial periods of abnormal gratings usually are as small as $d \approx \lambda/10$. There is an opinion that abnormal grating formation is the peculiarity of UPD regime. One of the physical restrictions for such small scale grating production is their thermal smoothing. The rough inequality governing their survival after long-pulse duration irradiation is

$$d \geq \ell = \sqrt{a\tau}, \quad (1)$$

where a is temperature conductivity, ℓ is the heat diffusion length, τ is the duration of laser pulse. Here we consider one more cause which hinder from heat diffusion length according to inequality (1) due to non-Gaussian processes of heat transfer [2] along the direction of forming grating. This is due to phonons [3] and electrons scattering on temporal grating of small period. The estimations of heat diffusion reduction for such cases were made. An experimental examples illustrating abnormal oriented nanograting formation under the interaction of normally incident nanosecond pulses of linear polarized laser radiation with metals, semiconductors, and dielectrics for regimes near the melting or ablation material thresholds were listed. For these cases the inequality (1) is not valid.

At the excess number of laser pulses (the final stage of abnormal grating formation) the local bumps of abnormal gratings on the ridges of the main resonance relief are transformed into the nanoconical-shaped gratings. The height of the cone depends on the wavelength of laser radiation (and the abnormal grating period) and the radius of curvature of cone’s tip was near 1÷4 nm. The surface density of so self-assembled nanostructures may be equaled to $(d_0d)^{-1} \approx 10^{10} \text{ cm}^{-2}$ for $\lambda \sim 250 \text{ nm}$.

Hence the abnormal grating formation was theoretically predicted and confirmed by experiments with linear polarized laser radiation of nanosecond duration.

References

- [1] V. S. Makin, R. S. Makin, *Optics and Spectroscopy*, V. **120**(4), p. 610 (2016).
- [2] L. M. Zelenyi, A. V. Milovanov, *Physics – Uspekhi*, V. **47**, pp. 749–788 (2004).
- [3] R. Anufriev, J. Ma, M. Nomura, *Phys. Rev. B*, V. **93**, p. 045411 (2016).

A technique of multichannel scattering matrices calculation in solving electrodynamic and acoustic problems by the minimal autonomous blocks method

Maly S.V., Arlova H.S.

Belarusian State University, Minsk, Belarus

e-mail: malaya.rfe@gmail.com

The minimal autonomous blocks (MAB) method has large potential in solving wide range of problems of applied electrodynamics and acoustics [1–4]. There exist several techniques for its implementation: recompositional, iterative and hybrid algorithms.

A multichannel scattering matrices formalism for spatial domains of different wave sizes and shapes is successfully used for solving important applied problems such as description of metamaterials and composites characteristics; estimation of radiolocating and acoustic perceptibility of objects, including invisibility and imitation; description of absorbing coatings and frequency-selective surfaces characteristics for arbitrary irradiation modes; modeling of systems with multiscale inner structure organization. Algorithms of metamaterials and composites synthesis can be constructed on the basis of multichannel scattering matrices. For calculation of these matrices, the MAB method involves the use of recompositional algorithm. It has a high computational complexity limiting the size of domains wave properties of which are described by multichannel matrices.

A technique of multichannel scattering matrices calculation based on solving systems of linear algebraic equations with sparse matrices is proposed. Its implementation includes the following steps:

- decomposition of the investigated domain into a system of blocks;
- scattering matrices calculation for blocks with different sizes and material parameters;
- solution of the system of linear algebraic equations with sparse matrix; right-hand sides of the system are formed by sequential excitation of all outer channels at the boundary of the domain;
- formation of multichannel scattering matrix from the solutions of the system derived at the previous step.

A comparative analysis of accuracy and computational efficiency of the technique proposed and the recompositional algorithm is carried out.

The peculiarities of using the proposed technique in problems of multivariant analysis and synthesis are considered.

References

- [1] V. V. Nikolskii, T. I. Nikolskaja, *Decompositional approach to problems of electrodynamics*, Nauka, Moscow, 1983 (in Russian).
- [2] S. V. Maly, Homogenization of metamaterials on the basis of average scattering matrices, *Abstracts on International conference DAYS ON DIFFRACTION 2010*, Saint Petersburg, June 8 – 11, p. 114, 2010.
- [3] S. V. Maly, The electrodynamic analysis of composites and metamaterials on the basis of the method of minimal autonomous blocks, *Abstracts of the International conference DAYS ON DIFFRACTION 2011*, Saint Petersburg, May 30 – June 3, p. 145, 2011.
- [4] S. V. Maly, A. S. Malaya, A. S. Rudnitsky, Modeling of acoustic processes in structurally nonuniform mediums by the method of minimal autonomous blocks, *Abstracts of the International conference DAYS ON DIFFRACTION 2013*, Saint Petersburg, May 27 – 31, p. 129, 2013.

Propagation of light bullets in media with quadratic nonlinearity

Mamaikin M.S., Komissarova M.V., Zakharova I.G.

Lomonosov Moscow State University, Faculty of Physics, Leninskie Gory 1, 119991, Moscow, Russia
e-mails: mamaikinms@gmail.com, komissarova@physics.msu.ru, zaharova@phys.msu.ru

Spatiotemporal optical solitons or light bullets are well investigated for media with either cubic or quadratic nonlinearities [1]. However, most of the results for solitons in quadratic media were obtained by numerical simulations. Analytical methods were used mostly to derive different approximate solutions [2, 3] or to estimate parameters of solitons and to analyze their stability [4].

In the present work an investigation of coupled spatiotemporal solitons in a medium with quadratic nonlinearity is based on the application of aberrationless approximation [5]. We solve the following system of nonlinear equations for complex amplitudes of harmonics A_1 and A_2 :

$$i \frac{\partial A_1}{\partial z} - \frac{c}{2n\omega} \frac{\partial^2 A_1}{\partial x^2} + \frac{k_2}{2} \frac{\partial^2 A_1}{\partial \tau^2} - \gamma A_1^* A_2 = 0; \quad (1)$$

$$i\frac{\partial A_2}{\partial z} - \frac{c}{4n\omega} \frac{\partial^2 A_2}{\partial x^2} + k_2 \frac{\partial^2 A_2}{\partial \tau^2} - \frac{\gamma}{2} A_1^2 = 0. \quad (2)$$

We search the solution in the form

$$A_1 = (E_{01}/\sqrt{f_{x_1}f_{\tau_1}}) \exp[-x^2/(a_1^2 f_{x_1}^2) - \tau^2/(T_1^2 f_{\tau_1}^2) - i\psi_1]; \quad (3)$$

$$A_2 = (E_{02}/\sqrt{f_{x_2}f_{\tau_2}}) \exp[-x^2/(a_2^2 f_{x_2}^2) - \tau^2/(T_2^2 f_{\tau_2}^2) - i\psi_2]. \quad (4)$$

Substituting (3)–(4) into (1)–(2) we derive a system of ordinary differential equations for bullet width f_x and pulse duration f_τ . Then we compare the numerical solution of this aberrationless system with the numerical solution of the original system (1)–(2). In particular, to verify our results we used the known approximate soliton solution given in [3]. We demonstrated that optical bullet consisted of two coupled wave pulses propagates about 10–15 diffraction lengths.

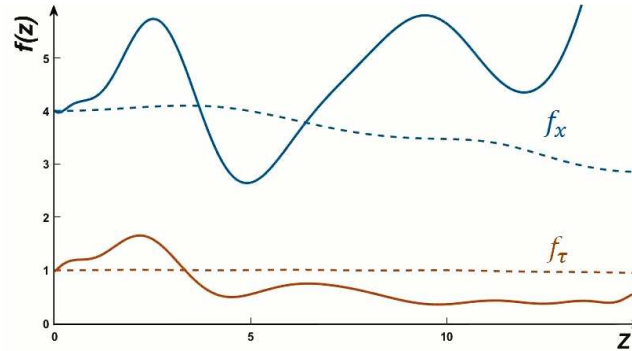


Fig. 1: The soliton width f_x and pulse duration f_τ versus propagation distance: comparison of numerical simulation (solid) and aberrationless (dashed) approach.

References

- [1] Y. S. Kivshar, G. P. Agrawal, *Optical Solitons: From Fibers to Photonic Crystals*, Academic (2003).
- [2] D. Mihalache, D. Mazilu, B. A. Malomed, L. Torner, *Optics communications*, **169**, 341–356 (1999).
- [3] S. V. Sazonov, D. Yu. Zagursky, I. G. Zakharova, M. V. Komissarova, *Theses of the School-Seminar “Waves-2015”*, Section 6, 54–56.
- [4] I. N. Towers, B. A. Malomed, *Physical Review Letters*, **90**, 123902-1–123902-4 (2003).
- [5] A. Churilova, N. Sukhorukov, *Izvestia Akademii Nauk SSSR Seriya Fizicheskaya*, **61**, 2439–2441.

Numerical simulation of internal waves generation by the flow over uneven bottom in the stratified liquid

Vasily Maximov¹, **Sergey Kshevetskii**²

¹Saint-Petersburg State University, Faculty of Applied Mathematics & Control Processes, Saint-Petersburg, Russian Federation

²Kant Baltic Federal University, Theoretical Physics, Kaliningrad, Russian Federation

e-mails: wmaximov@mail.ru, spkshev@gmail.com

The problem of internal wave generation by incident flow interacting with an uneven bottom is considered.

The full Euler equations for the numerical simulation of this process are used. The full-conservative numerical method of the second order is used to solve the problem under consideration. Three types of liquid stratification increasing with depth are proposed: 1. exponential growth, 2. linear increase, 3. piecewise linear increase.

Characteristics of internal waves depending on the flow velocity are studied. The flow function, the density, the horizontal and vertical velocity as the functions of time are simulated and examined.

The dynamics of vortex structures arising from the flow over the seamount is also studied.

Some conclusions about the effect of the type of stratification of the liquid on the transformation of internal waves are derived.

References

- [1] S. P. Kshevetskii, Analytical and numerical investigation of nonlinear internal gravity waves, *Non-linear Proc. Geophys.*, Vol. **8**, pp. 37–53 (2001).
- [2] S. P. Kshevetskii, Study of vortex breakdown in a stratified fluid, *Computational Mathematics and Mathematical Physics*, Vol. **46**(11), pp. 1988–2005 (2006).
- [3] V. V. Maximov, S. P. Kshevetskii, Numerical simulation of internal waves generated by the flow and an isolated seamount in the stratified liquid, *Geophysical Research Abstracts*, Vol. **17**, EGU2015-6609, Vienna: EGU General Assembly (2015).

On Bogoliubov – de Gennes equation for Kitaev chain

Melnikov A.S.^{1,2}, **Shereshevskii I.A.**^{1,2}, Vdovicheva N.K.¹

¹Institute for Physics of Microstructures RAS, 603950, GSP-105, Russia

²Nizhnii Novgorod State University

e-mail: ilya@ipmras.ru

We discuss the properties of simple model of “p-wave” superconducting wire [4] is known as Kitaev chain [1]. This system is described by the discrete self-consistent Bogoliubov – de Gennes equation. This equation is usually solved numerically by iteration procedure. To avoid the calculation of spectrum of big matrix at the each iteration step, we use the method of calculation of operator function [5] suggested in the series of work, see e. g., [2]. We have founded numerically that there exist several solutions of considered equation at given values of parameters. This may have an essential effect on behaviour of physical system contained “p-wave” superconducting wires. We present some analytic results on the existence of solutions based on the abstract fixed point theorems [3]. We also analyse some common properties of the solutions, in particular, free energy [4].

References

- [1] A. Yu. Kitaev, *Usp. Fiz. Nauk (Suppl.)*, **171**(10) (2001).
- [2] Y. Nagai, Y. Shinohara, Y. Futamura, Y. Ota, T. Sakurai, *Journal of the Physical Society of Japan*, **82**(9), 094701 (2013).
- [3] V. I. Danilov, *Lectures on fixed points*, Russian economy school, Moscow (2006) (Russian).
- [4] A. V. Svidzinskii, *Space-inhomogeneous problems in the theory of superconductivity*, Nauka, Moscow (1982) (Russian).
- [5] N. I. Akhiezer, I. M. Glazman, *The theory of linear operators in Hilbert spaces*, Nauka, Moscow (1966) (Russian).

Finite elements for linear wave propagation in polygonal domains

Fabian L. Müller, Christoph Schwab

Seminar for Applied Mathematics, ETH Zurich, Rämistrasse 101, 8092 Zürich

e-mails: muelfabi@ethz.ch, christoph.schwab@sam.math.ethz.ch

When dealing with propagation phenomena of acoustic or seismic waves, second-order linear wave equations provide a physical model widely used in the applications. The method of lines is a popular

simulation technique. There, the partial differential equation (PDE) is discretized in space first, followed by a time-stepping scheme solving the resulting ordinary differential equation.

The convergence order of this method strongly depends on the regularity of the solution. When dealing with a PDE posed on a polygonal domain or in the presence of piecewise smooth (material-dependent) coefficients, the solution exhibits strongly singular behaviour in the neighbourhood of an isolated point set (see [1]), implying very slow convergence of the Finite Element method on quasi-uniform meshes. This is an intrinsic defect of polynomial approximations on uniform meshes and cannot be improved without significant changes to the underlying mesh and/or the choice of ansatz function.

In [2] and [3], the authors have proved that optimal convergence rates can be restored using locally refined mesh families. The presented results hold for the h-version of the Finite Element Method in polygonal domains and with arbitrarily high local polynomial degree. They are applicable to acoustic and elastic wave equations in homogeneous media, and the acoustic wave equation in the presence of piecewise smooth wavespeeds.

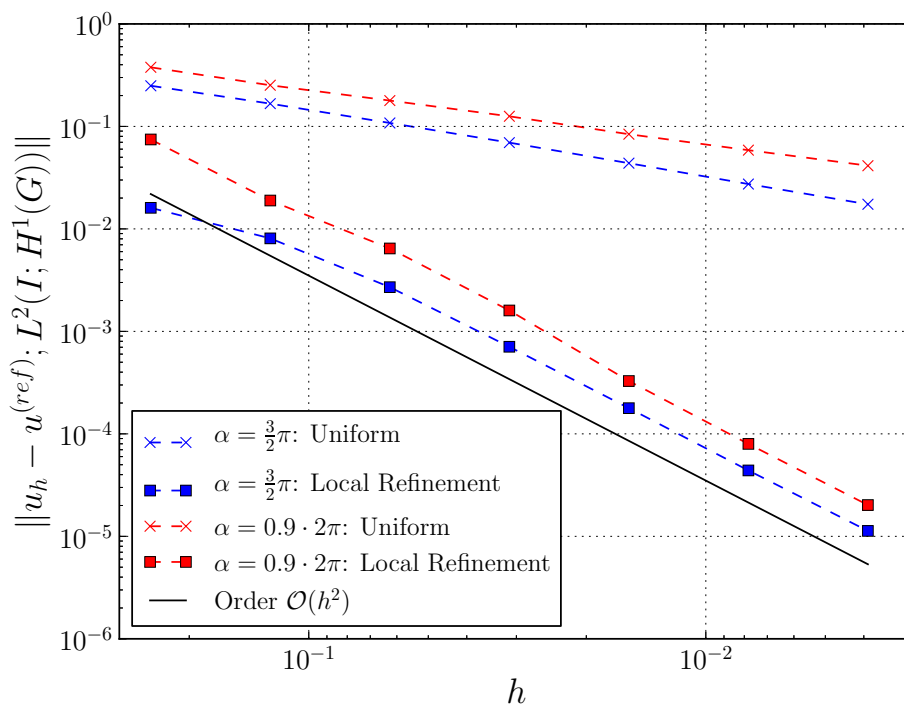


Fig. 1: Results of convergence tests using piecewise linear Finite Elements. The angle $\alpha \in (0, 2\pi)$ denotes the interior opening angle of a polygonal corner in the domain. Due to insufficient regularity of the solution u , uniform meshes cannot approximate u with optimal convergence rates. In both cases, local refinement towards the polygonal corner is necessary to restore full convergence rates.

References

- [1] S. I. Matyukevich, B. A. Plamenevskĭ, On dynamic problems in the theory of elasticity in domains with edges, *Algebra i Analiz*, Vol. **18**(3), pp. 158–233 (2006).
- [2] F. L. Müller, Ch. Schwab, Finite elements with mesh refinement for wave equations in polygons, *Journal of Computational and Applied Mathematics*, Vol. **283**, pp. 163–181 (2015).
- [3] F. Müller, Ch. Schwab, Finite elements with mesh refinement for elastic wave propagation in polygons, *Mathematical Methods in the Applied Sciences*, doi: 10.1002/mma.3355.

Guaranteed estimation of solutions to Helmholtz problems from pointwise noisy observations

Nakonechny A.G.¹, Podlipenko Y.K.¹, Shestopalov Y.V.²

¹Taras Shevchenko National University of Kyiv, Kyiv, Ukraine

²University of Gävle, Gävle, Sweden

e-mails: a.nakonechniy@gmail.com, yourip@mail.ru, yuyshv@hig.se

We study the optimal reconstruction (estimation) of values of linear continuous functionals defined on solutions to the exterior or interior Helmholtz problems from pointwise noisy observations of the form

$$y_i = \varphi(x_i) + \xi_i, \quad i = 1, \dots, N,$$

where $\varphi(x)$ is the unknown solution of the Helmholtz problem, x_i , $i = 1, \dots, N$, is a given system of points belonging to the considered domain, and ξ_i are estimation errors that are realizations of random variables $\xi_i = \xi_i(\omega)$ with zero expectations, $\mathbb{E}\xi_i = 0$, and finite second moments $\mathbb{E}|\xi_i|^2$. We assume that right-hand sides of the Helmholtz equation and the boundary data are not known, as well as the second moments of random noises in observations; the only available information is that they belong to given bounded sets in the appropriate functional spaces.

For linear (with respect to observations) estimation methods, this formulation leads to the necessity of introducing minimax statements of estimation problems when optimal estimates of the aforementioned functionals are defined as the estimates for which the dispersion of the estimation error calculated for the “worst” implementation of perturbations takes its minimal value. Such estimates are called guaranteed or minimax estimates (see [1, 2]).

We develop constructive methods for finding these estimates and the estimation errors which are expressed in terms of solutions to systems of special variational equations.

In particular, we find the representations for the guaranteed estimates of linear functionals from the unknown solutions to the Helmholtz problems which are expressed via solutions of certain systems of variational equations independent of the specific form of the functionals involved in the problem formulations. The latter implies that the solutions of the obtained variational equations can be taken as good estimates for the unknown solutions of the Helmholtz problems under consideration.

In the case of domains for which the Green functions of the corresponding Helmholtz problems are known in the explicit form, we reduce the solution of the estimation problems to solving some systems of linear algebraic equations.

References

- [1] A. Nakonechny, *Proceedings of 2010 URSI International Symposium on Electromagnetic Theory*, 515–516 (2010).
- [2] Y. Podlipenko, Y. Shestopalov, V. Prishlyak, *Proceedings of 2010 URSI International Symposium on Electromagnetic Theory*, 621–623 (2010), arXiv:0910.2331 [math.AP] (2009).

Transmission conditions in a one-dimensional model of bifurcating arteria

Sergei A. Nazarov

St. Petersburg State University and Institute of Mechanical Engineering Problems, St. Petersburg, Russia

e-mail: srgnazarov@yahoo.co.uk

This work was done in cooperation with V.A. Kozlov (Linköping University, Sweden).

Development of adequate one-dimensional models of circulatory blood system meets several serious obstacles and we will discuss one very particular question related to bifurcation nodes of the arterial tree. Although the blood vessel walls are strongly elastic [1] and blood is a viscoelastic

liquid [2], we consider the Stokes (or Navier–Stokes) equations in a junction of three ($\alpha = 0, \pm$) thin, of radius h , finite tubes with rigid walls meeting each other inside a small, of diameter $O(h)$, node. Neglecting the elastic properties of walls for a while, see discussion of those in [3], we employ the standard Reynolds one-dimensional model of flow in the tubes, that is, a second-order ordinary differential equation on the intervals $\Upsilon_\alpha = (0, L_\alpha) \ni z_\alpha$. The necessary transmission conditions at the junction point with the local coordinates $z_\alpha = 0$ are found with the help of the method of matched asymptotic expansions and by means of the pressure drop matrix [4] describing the boundary layer phenomenon in the vicinity of the three-dimensional bifurcation node of the arteria. As a result, we obtain transmission conditions which provide the error estimate of order $e^{-\delta/h}$, $\delta > 0$, but differ from the classical Kirchhoff conditions supporting only a poor proximity order h . At the same time, based on the concept [5] of one-dimensional asymptotic images of thin spacial objects, we introduce the effective length $L_\alpha^h = L_\alpha + hl_\alpha$ of vessels such that solving the Reynolds equations in the intervals $\Upsilon_\alpha^h = (0, L_\alpha^h)$ with the Kirchhoff transmission conditions keeps the same approximation order $e^{-\delta/h}$. The length increments hl_α are expressed in terms of the above-mentioned matrix of pressure drops and a computational scheme for this matrix will be discussed as well.

References

- [1] V. A. Kozlov, S. A. Nazarov, Asymptotic models of the blood flow in arterias and veins, *Zap. Nauchn. Sem. St. Petersburg Otdel. Mat. Inst. Steklov*, V. **406**, pp. 80–106 (2012); English transl.: *Journal of Math. Sci.*, V. **194**, no. 1, pp. 44–57 (2013).
- [2] V. A. Kozlov, S. A. Nazarov, One-dimensional model of viscoelastic blood flow through a thin elastic vessel, *Probl. Mat. Analiz.*, No. 78, pp. 123–140 (2015); English transl.: *Journal of Math. Sci.*, V. **207**, no. 2, pp. 249–269 (2015).
- [3] V. A. Kozlov, S. A. Nazarov, The transmission conditions in the one-dimensional model of a bifurcating arteria with elastic walls, *Zap. Nauchn. Sem. St. Petersburg Otdel. Mat. Inst. Steklov*, V. **438**, pp. 138–177 (2015).
- [4] S. A. Nazarov, K. Pileckas, Asymptotics of solutions to Stokes and Navier–Stokes equations in domains with paraboloidal outlets to infinity, *Rend. Semin. Mat. Univ. Padova*, V. **99**, pp. 1–43 (1998).
- [5] S. A. Nazarov, Two-term asymptotics of solutions of spectral problems with singular perturbations, *Mat. sbornik*, V. **181**, no. 3, pp. 291–320 (1990); English transl.: *Math. USSR. Sbornik*, V. **69**, no. 2, pp. 307–340 (1991).

Acoustic reflectance probes the inner ear

Neely S.T., Rasetshwane D.M.

Boys Town National Research Hospital, 555 North 30th Street, Omaha, Nebraska, USA 68131
 e-mails: Stephen.Neely@boystown.org, Daniel.Rasetshwane@boystown.org

Sound travels through an acoustic waveguide as a plane wave if (and only if) the waveguide has a uniform cross section. Any deviation in the cross-sectional area of the waveguide generates a reflection that travels back from the location of that deviation toward the origin of the sound. Acoustic reflectance is defined as the ratio of the reflected pressure wave to the forward pressure wave when expressed as complex functions of frequency. An inverse Fourier transform of reflectance renders time-domain reflectance, which is equivalent to an impulse response that describes acoustic reflections as a continuous function of time. When a miniature sound source and microphone are placed in a human ear canal, measurements of reflectance can provide clinically-useful information. Most of the sound energy that is delivered to an ear canal is reflected by the eardrum. The sound reflected from the eardrum contains information about the status of the middle ear (see Fig. 1A). Ear-canal reflectance is currently used in audiology clinics to diagnose middle-ear pathologies. Time-domain reflectance (see Fig. 1B) may be used to estimate the cross-sectional area of the ear canal

by solving a mathematical inverse problem [1]. Finally, ear-canal reflectance includes a very small component due to reflections from beyond the middle ear, from the portion of the inner ear that is called the cochlea. Cochlear reflectance [2] has the potential to aid in the clinical evaluation of inner-ear status. Current research is further developing methods to exploit the information about the status of all three portions ear (i. e., ear-canal, middle ear, and cochlea) that is contained in measurements of ear-canal reflectance.

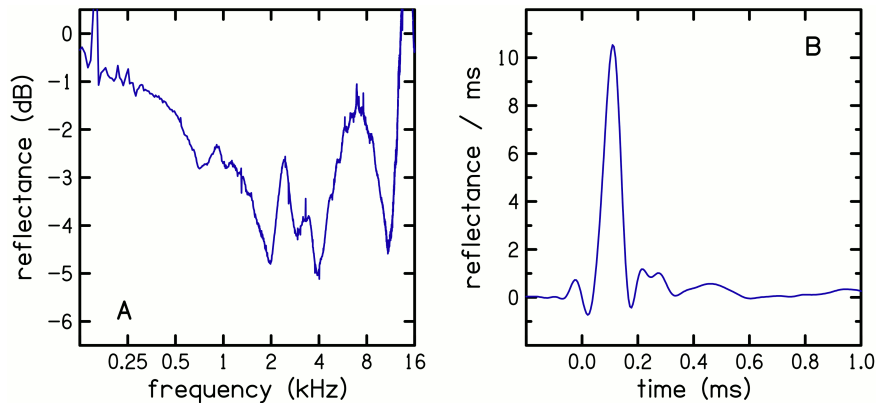


Fig. 1: Ear-canal reflectance measurement in the frequency domain (A) and time-domain (B).

References

- [1] D. M. Rasetshwane, S. T. Neely, *Journal of the Acoustical Society of America*, **130**, 3873–3881 (2011).
- [2] D. M. Rasetshwane, S. T. Neely, *Journal of the Association for Research in Otolaryngology*, **13**, 591–607 (2012).

Asymptotic analysis of the non-steady Navier–Stokes equations in thin structures

Grigory Panasenko¹, Konstantin Pileckas²

¹Institute Camille Jordan UMR CNRS 5208, PRES University of Lyon/ University of Saint Etienne, France and Moscow Power Energy Institute (Technical University), Moscow, Russia

²Vilnius University

e-mail: grigory.panasenko@univ-st-etienne.fr

Thin structures are some finite unions of thin rectangles (in 2D settings) or cylinders (in 3D settings) depending on small parameter $\epsilon \ll 1$ that is, the ratio of the thickness of the rectangle (cylinder) to its length. We consider the non-steady Navier–Stokes equations in thin structures with the no-slip boundary condition at the lateral boundary and with the inflow and outflow conditions with the given velocity of order one. The steady state Navier–Stokes equations in thin structures were considered in [1–3]. The asymptotic expansion of the solution is constructed. The error estimates for high order asymptotic approximations are proved. Asymptotic analysis is applied for an asymptotically exact condition of junction of 1D and 2D (or 3D) models. These results are presented in [4–8]. The present work is supported by the grant number 14-11-00306 of Russian Scientific Foundation executed in Moscow Power Energy Institute (Technical University).

References

- [1] G. P. Panasenko, Asymptotic expansion of the solution of Navier–Stokes equation in a tube structure, *C. R. Acad. Sci. Paris*, t. **326**, Série IIb, pp. 867–872 (1998).
- [2] G. P. Panasenko, Partial asymptotic decomposition of domain: Navier–Stokes equation in tube structure, *C. R. Acad. Sci. Paris*, t. **326**, Série IIb, pp. 893–898 (1998).

- [3] G. P. Panasenko, *Multi-Scale Modelling for Structures and Composites*, Springer, Dordrecht (2005).
- [4] G. Panasenko, K. Pileckas, Asymptotic analysis of the nonsteady viscous flow with a given flow rate in a thin pipe, *Applicable Analysis*, **91**(3), pp. 559–574 (2012).
- [5] G. Panasenko, K. Pileckas, Divergence equation in thin-tube structure, *Applicable Analysis* (2014), doi: 10.1080/00036811.2014.933476.
- [6] G. Panasenko, K. Pileckas, Flows in a tube structure: equation on the graph, *Journal of Mathematical Physics*, **55**, 081505 (2014).
- [7] G. Panasenko, K. Pileckas, Asymptotic analysis of the non-steady Navier–Stokes equations in a tube structure. I. The case without boundary layer-in-time, *Nonlinear Analysis, Series A, Theory, Methods and Applications*, **122**, pp. 125–168 (2015).
- [8] G. Panasenko, K. Pileckas, Asymptotic analysis of the non-steady Navier–Stokes equations in a tube structure, II. General case, *Nonlinear Analysis, Series A, Theory, Methods and Applications*, **125**, pp. 582–607 (2015).

Homogenization of “double porosity” models for fourth order equations. Spectral problems

Svetlana Pastukhova

Moscow Technological University (MIREA)

e-mails: pas-se@yandex.ru

We study in \mathbb{R}^d a fourth order operator $A_\varepsilon = D^* a^\varepsilon(x) D$, where $D\varphi = \nabla^2 \varphi = \left\{ \frac{\partial^2 \varphi}{\partial x_i \partial x_j} \right\}_{i,j=1}^d$ is a matrix of second order derivatives and $D^* = \nabla^* \nabla^* = \text{div div}$ is conjugate to D . We assume that $a^\varepsilon(x) = \varepsilon^4 a(\frac{x}{\varepsilon})$ on F_ε and $a^\varepsilon(x) = a(\frac{x}{\varepsilon})$ on $\mathbb{R}^d \setminus F_\varepsilon$, where $a(y)$ is 1-periodic tensor acting in a space of symmetric matrices and is subordinate to conditions of ellipticity. Here, $\varepsilon \in (0, 1)$, $F_\varepsilon = \varepsilon F$ is a contraction of 1-periodic set F , \mathbb{R}^d is endowed with Lebesgue measure dx . So, the space \mathbb{R}^d is divided into soft and stiff phases, F_ε being a soft one.

Other “double porosity” models for fourth order equations can be considered, they correspond to measures on \mathbb{R}^d which are singular with respect to the measure dx . These are models on a singular network or in the space reinforced with a singular network.

We find the limit operator $A = \lim_{\varepsilon \rightarrow 0} A_\varepsilon$ in the sense of so-called strong two-scale resolvent convergence. We investigate the spectrum of the limit operator. Thereby, we prove in this way some spectral properties of the initial operator A_ε , among them band-gap structure of the spectrum.

Long waves above the deformable bottom

Peregudin S.I.

Saint Petersburg State University, 7/9 litera A, Universitetskaya emb., St Petersburg, 199034 Russia

e-mail: peregudinsi@yandex.ru

Kholodova S.E.

National Research University ITMO, 49 Kronverksky Pr. St. Petersburg, 197101 Russia

e-mail: kholodovase@yandex.ru

We consider the problem of motion of two layers of an ideal heavy incompressible fluid above the deformable bottom and simulate the media as a three-layer one — two layers over non-uniform liquid soil. The lower liquid has a density ρ_1 , the upper — ρ_2 . Waves are formed on the interface between the upper layer – the air (free surface) and in the section of water surface layers. At motion of the lower layer, liquid react with the soil particles of the bottom layer and they are set to move.

The motion of an ideal incompressible homogeneous fluid in a layer is described by the equations [1]

$$\frac{\partial \rho_j}{\partial t} + \mathbf{v}_j \cdot \nabla \rho_j = 0, \quad \operatorname{div} \mathbf{v}_j = 0, \quad \rho_j \frac{d\mathbf{v}_j}{dt} = \mathbf{g} \rho_j - \nabla p_j, \quad \mathbf{g} = (0, 0, -g)$$

with appropriate boundary conditions on the surface intersection liquid – ground

$$\frac{\partial \eta}{\partial t} + \mathbf{v}_{1h} \cdot \nabla \eta = w_1, \quad \frac{\partial \eta}{\partial t} + \frac{\partial Q_x}{\partial x} + \frac{\partial Q_y}{\partial y} = 0, \quad z = -H_0 + \eta(x, y, t),$$

at the interface of liquid media

$$\frac{\partial \eta_1}{\partial t} + \mathbf{v}_{jh} \cdot \nabla \eta = w_j, \quad p_1 = p_2, \quad z = \eta_1(x, y, t)$$

and on the free surface

$$\frac{\partial \eta_2}{\partial t} + \mathbf{v}_{2h} \cdot \nabla \eta_2 = w_2, \quad p_2 = p_\alpha, \quad z = H_2 + \eta_2(x, y, t).$$

The problem is to determine the function $\mathbf{v}_j, \rho_j, p_j$, satisfying the equation of motion and the boundary conditions. If this problem is solved, then profiles of the free surface and the interfaces may be determined from boundary conditions.

Assuming the motion of the fluid in each layer is potential and using long-wave approximation, we can obtain specific problems in the case of small-amplitude waves, such as linear model without dispersion and with dispersion, non-linear model without dispersion. In the first case we have

$$\begin{cases} \zeta_t(x, t) - \eta_t(x, t) + H_0 w_x(x, t) = 0, \\ \zeta_x(x, t) + w_t(x, t) = 0, \\ \zeta_t(x, t) + \kappa w_x(x, t) = 0 \end{cases}$$

and converted into the wave equation for the vertical velocity $w(x, t)$.

References

- [1] S. I. Peregudin, *Wave Motion in Liquid and Granular Medias*, Saint Petersburg State University, Saint Petersburg (2004).

Asymptotic study of two-scale electromagnetic field in layered periodic structure

Perel M.V.

St. Petersburg State University, 7/9 Universitetskaya nab., St. Petersburg 199034, Russia
e-mail: m.perel@spbu.ru

Sidorenko M.S.

Krylov State Research Centre, 44 Moskovskoe shosse, St. Petersburg 196158, Russia
e-mail: m-sidorenko@yandex.com

The propagation of monochromatic electromagnetic field in the dielectric layered periodic medium is studied by the method of two-scale asymptotic expansions. The frequency of the field is assumed to be close to the frequency of the stationary point of the dispersion surface. It is established that the principal term of expansion is a linear combination of two differently polarized Floquet–Bloch solutions with slowly varying envelopes. The envelopes are governed by a system of either hyperbolic or elliptic equations. The type of equations is determined by the type of the stationary point. The equations are independent only in the planar case. All the terms of the asymptotic expansion are found.

New type of semiclassical asymptotics eigenstates near the boundaries of spectral clusters for Schrödinger-type operators

Pereskokov A.V.

National Research University “Moscow Power Engineering Institute”, Krasnokazarmennaya 14, Moscow, 111250 Russia

e-mail: pereskokov62@mail.ru

We consider the eigenvalue problem for a two-dimensional perturbed oscillator in $L^2(\mathbb{R}^2)$

$$\left(-\frac{\hbar^2}{2} \left(\frac{\partial^2}{\partial q_1^2} + \frac{\partial^2}{\partial q_2^2} \right) + \frac{q_1^2 + q_2^2}{2} + \varepsilon V \right) \psi = \lambda \psi, \quad \|\psi\|_{L^2(\mathbb{R}^2)} = 1, \quad (1)$$

where $V(q_1, q_2)$ is an arbitrary polynomial of degree 4 and $\hbar > 0$, $\varepsilon > 0$ are small parameters with $\varepsilon \ll \hbar$. In [1], an example of problem (1) was used to propose a method for finding a series of asymptotic eigenvalues near the boundaries of spectral clusters which are formed around the eigenvalues of the unperturbed equation (at $\varepsilon = 0$). This method is based on a new integral representation.

Applying the operator averaging and coherent transformation to problem (1) on the l -th irreducible representation of the algebra of symmetries of the unperturbed operator, we obtain the eigenvalue problem in the space \mathcal{P}_ℓ of polynomials of degree less than or equal to ℓ . Here the number ℓ is of the order of \hbar^{-1} . The desired polynomial satisfies a second-order differential equation. We first study the multiple-point spectral problem in the class of antiholomorphic functions with zero characteristic exponents at finite singular points. Further, we obtain the asymptotics of the desired polynomial by using the operation of projection on the space \mathcal{P}_ℓ .

In the subsequent papers [2, 3], this method was used to obtain asymptotics of a series of eigenvalues of the hydrogen atom in a magnetic field near the lower boundaries of spectral clusters and series of asymptotic eigenvalues of the Hartree-type operator near the boundaries of spectral clusters.

References

- [1] A. V. Pereskokov, *Mat. Zametki*, **92**(4), 583–596 (2012).
- [2] A. V. Pereskokov, *Tr. Mosk. Mat. Obs.*, **73**(2), 277–325 (2012).
- [3] A. V. Pereskokov, *Teoret. Mat. Fiz.*, **178**(1), 88–106 (2014).

On sound propagation in a shallow-water acoustical waveguide with variable bottom slope

Petrov P.S.^{1,2}, Petrova T.N.²

¹V. I. Il'ichev Pacific Oceanological Institute, 43 Baltiyskaya str., Vladivostok, 690041, Russia

²Far Eastern Federal University, 8 Sukhanova str., 690950, Vladivostok, Russia

e-mails: petrov@poi.dvo.ru, petrova.tn@dvfu.ru

Sound propagation in the cross-slope direction in a shallow-water acoustical waveguide with tilted bottom is considered. The bottom slope angle that is varying with range is assumed to be small. The modal expansion is used to reduce the problem to the coupled system of elliptic equations for the mode amplitudes. For sufficiently small bottom tilt angles the adiabaticity assumption can be used to uncouple the system.

Each elliptic equation of the uncoupled system is approximated via the narrow-angle parabolic equation (known as mode parabolic equation in this context). For the cross-slope propagation the mode parabolic equations can be solved analytically using the technique of Wei and Norman [1]. Similar adiabatic approximation was studied in the work [2], and it was shown that it is sufficiently accurate for the case of the propagation in a 3D wedge (i. e. for constant bottom slope).

The properties and features of the obtained solution are studied, and the numerical example is presented.

References

[1] J. Wei, E. Norman, *J. Math. Phys.*, **4**, 575–581 (1963).
 [2] P. Petrov, F. Sturm, *J. Acoust. Soc. Am.*, **139** (2016).

Spectral asymptotics in some problems with integral constraints

Petrova Y.P.

Saint Petersburg State University, Russia, Saint Petersburg, Universitetskaya nab., 7–9
 e-mail: delafer21@gmail.com

We discuss the asymptotics of eigenvalues of the boundary value problem

$$(-1)^p u^{(2p)}(t) = \lambda^{(n,p)} u(t) + \mathcal{P}_{n-2p}(t), \quad \int_0^1 t^i u(t) dt = 0, \quad i = 0 \dots n - 1, \quad (1)$$

where $n, p \in \mathbf{N}$, $n > 2p$, and $\mathcal{P}_{n-2p}(t)$ is a polynomial of degree less than $(n - 2p)$ with unknown coefficients.

We reduce this problem to the following eigenvalue problem:

$$(-1)^p y^{(2n)}(t) = \mu^{(n,p)} y^{(2n-2p)}(t), \quad y^{(j)}(0) = y^{(j)}(1) = 0, \quad j = 0 \dots n - 1. \quad (2)$$

Note that the smallest eigenvalue of the problem (2) gives the sharp constant in the embedding theorem $\overset{\circ}{W}_2^n(0, 1) \hookrightarrow \overset{\circ}{W}_2^{n-p}(0, 1)$.

The obtained results are applied to the problem of small ball deviations in L_2 -norm for some Gaussian processes.

The work is supported by RFBR grant (No 16-01-00258a).

Electromagnetic waveguides with several cylindrical ends and non-homogeneous filling

Boris Plamenevskii, Aleksandr Poretskii

St. Petersburg State University, Universitetskaya nab. 7-9, 199034 Saint Petersburg, Russia
 e-mails: b.plamenevskii@spbu.ru, st036768@student.spbu.ru

A waveguide occupies a 3D domain G coinciding, outside a large ball, with the union of finitely many semicylinders $\Pi_+^r = \{(y^r, t^r) : y^r \in \Omega^r, t^r > 0\}$, $r = 1, \dots, T$. A dielectric permittivity ε and a magnetic permeability μ are matrix-valued functions in \overline{G} that are smooth and positive definite. For $x = (y^r, t^r) \in \Pi_+^r$ and $t^r \rightarrow +\infty$, the matrices $\varepsilon(y^r, t^r)$ and $\mu(y^r, t^r)$ tend, at exponential rate, to $\varepsilon^r(y^r)$ and $\mu^r(y^r)$, respectively; the ε^r and μ^r can be arbitrary matrix-valued functions being smooth and positive definite on $\overline{\Omega^r}$.

In such a waveguide we consider the stationary Maxwell system with a real spectral parameter and conductive boundary conditions. We propose and justify a well-posed statement of the boundary value problem with intrinsic radiation conditions and describe asymptotics of solutions to the problem at infinity. Moreover, on the problem continuous spectrum we introduce a scattering matrix and prove that it is unitary.

To establish the results we extend the Maxwell system to an elliptic boundary value problem. The solution of the elliptic problem with a right-hand-side, subject to some compatibility conditions, provides a solution to the original problem. The scattering matrix of the elliptic problem turns out

to be block-diagonal and one of its blocks plays the role of the scattering matrix for the original Maxwell system.

The results generalize and develop those in [1], where empty electromagnetic waveguides were considered.

References

- [1] B. A. Plamenevskii, A. S. Poretskii, The Maxwell system in waveguides with several cylindrical ends, *St. Petersburg Math. J.*, **25**(1), 63–104 (2014).

Optical vortex microscope-analytical model

Agnieszka Popiołek-Masajada, Jan Masajada

Faculty of Fundamental Problems of Technology, Wrocław University of Technology, Wybrzeże Wyspiańskiego 27, 50-370 Wrocław, Poland
e-mail: Agnieszka.Masajada@pwr.edu.pl

Łukasz Płociniczak

Faculty of Pure and Applied Mathematics, Wrocław University of Technology, Wybrzeże Wyspiańskiego 27, 50-370 Wrocław, Poland

We consider an microscopic optical system in which the optical vortex is embedded within the Gaussian beam and focused to the observation/sample plane (Fig. 1). Additionally, optical vortex can be shifted inside the beam allowing fine scanning of the sample. We provide the analytical solution of the whole path of the beam in such system—from the vortex lens to the observation plane situated on the CCD camera. The calculations are performed step by step from one optical element to the next. We show that at each step, the expression for light complex amplitude has the same form with only four coefficients modified. We also derive a simple expression for the vortex trajectory for small vortex displacements. The analytical solutions are verified by the experimental results.

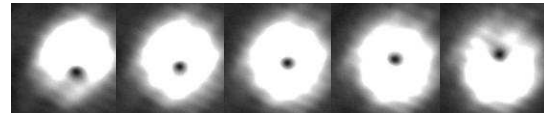
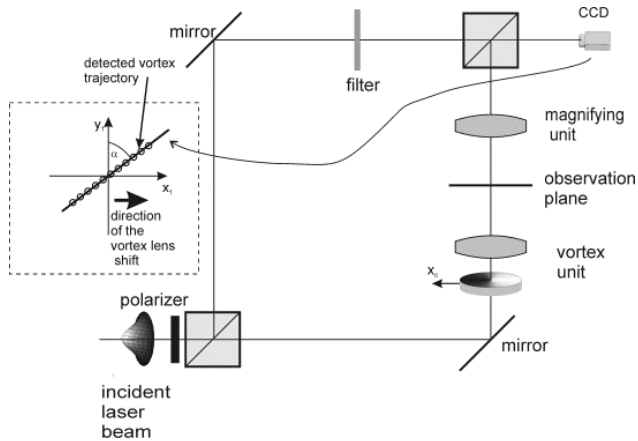


Fig. 1: Optical Vortex Microscopy setup. Shifting of the vortex plate within the Gaussian beam causes the vortex point (dark point) movement inside the beam, allowing scanning of the sample inserted into the observation plane. The vortex trajectory, magnified by the magnifying unit is observed on the CCD camera.

References

- [1] I. Augustyniak, A. Popiołek-Masajada, J. Masajada, S. Drobczyński, *Appl. Opt.*, **51**, C117–C124 (2012).
- [2] A. Popiołek-Masajada, B. Sokolenko, I. Augustyniak, J. Masajada, A. Khoroshun, M. Bacia, *Opt. and Lasers in Eng.*, **55**, 105–112 (2014).
- [3] Ł. Płociniczak, A. Popiołek-Masajada, M. Szatkowski, D. Wojnowski, *Opt. Las. Technol.*, **81**, 127–136 (2016).
- [4] Ł. Płociniczak, A. Popiołek-Masajada, J. Masajada, M. Szatkowski, *App. Opt.*, **55**, B20–B27 (2016).

Experimental implementation of microwave subsurface holography

A. Popov, I. Prokopovich, D. Edemskii

Pushkov Institute of Terrestrial Magnetism, Ionosphere and Radio Wave Propagation IZMIRAN, Troitsk, Moscow, 142190 Russia

e-mail: popov@izmiran.ru

Attempts of subsurface object visualization by means of microwave holography started in the 60-ies of the last century. Those times, possibilities of measurement and computation were not enough to perform this task. Recently a substantial progress was made in the problem of radio-frequency wave monitoring of closed rooms and identification of moving objects [1]. This work is aimed at another important practical problem — visualization of subsurface environment and embedded contrast objects. Here, a number of basic difficulties are encountered: unfavorable relationship between the wavelength, object dimensions, probing range and antenna array aperture; EM wave attenuation in subsurface matter, and strongly interfering interface reflection. These problems are partially mitigated by scanning the material surface with a combined microwave transceiver [2]. However, this method essentially hinders and complicates the process of subsurface RF-vision and limits the range of practical applications.

In this work, we apply another scheme of registration and processing of the subsurface probing data. The object of interest, embedded in a dielectric half-space, is illuminated from outside with harmonic microwave radiation. The amplitude and phase distribution of the scattered signal is captured by a multi-element receiver array separated from the material surface. Imaging of the scattering object is performed via mathematical wave front inversion using “anti-Kirchhoff” approximation. The synthetic aperture approach allowing one to radically increase spatial resolution was described in our previous paper [3]. Here, we outline the generalization to the case of a stratified non-uniform medium, experimental implementation of subsurface imaging, and an efficient method of eliminating the interfering reflections from the material boundary. The numerical examples given below illustrate the main moments of localization and visualization of a buried test object (metallic stencil of letter “R”).

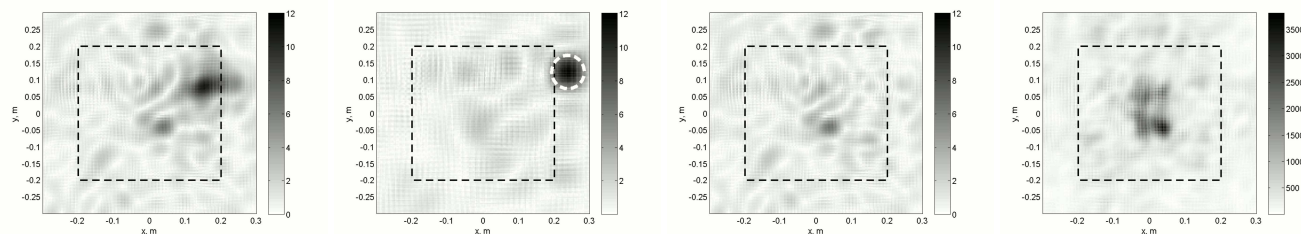


Fig. 1

Fig. 2

Fig. 3

Fig. 4

Fig. 1: Attempt of direct object reconstruction from the primary digital hologram; Fig. 2: Localization of the interfering source image in the specular reflection plane $z = 80$ cm; Fig. 3: Cleared image in the object plane $z = 50$ cm; Fig. 4: Image improvement by energy summation of inverted wave fields with different source positions.

Experimental images were obtained with a prototype of subsurface holographic radar provided by JSC VNIISMI.

References

- [1] F. Adib, C.-Y. Hsu, H. Mao, D. Katabi, F. Durand, *ACM J., Trans. on Graphics*, **34**, Article No. 219 (2015).
- [2] A. Zhuravlev, S. Ivashov, I. Vasiliev, V. Razevig, *Proc. 14th Intern. Conf. on Ground Penetrating Radar*, Shanghai, 68–71 (2012).
- [3] A. Popov, I. Prokopovich, V. Kopeikin, D. Edemskii, *Proc. Int. Conf. “DAYS on DIFFRACTION 2014”*, St. Petersburg, 192–197 (2014).

Influence of dispersion and structure molecules on time relaxation

Evelina V. Prozorova

Mathematics and Mechanics Faculty, St. Petersburg State University, University av. 28, Peterhof, 198504, Russia

e-mail: prozorova@spbu.ru

The influence of the angular momentum and the delay are investigated in the mechanics for: the interaction of many-particles, kinetic theory, the structural of molecules. Attention is drawn to the delay process, which is important in describing the discrete space. The analysis of the recording of the Lagrangian function for the collective interaction of the particles with the change of the center of inertia of the moving particles and the effect influence angular momentum are made. Elementary volume can rotate around the axis of inertia or to be involved in the rotational movement. In both cases the flow density varies across the border on the value $\frac{d(\rho u)}{dr} \cdot (r' - r) + \dots$ by the rotation of the elementary volume. For rarefied gas the second term (on space) in integral of collision of the Boltzmann equation is taken into account to calculate the self-diffusion and thermo-diffusion that was foretold by S. Vallander. It should be noted that for the kinetic theory (the Boltzmann equation) the law of conservation of angular momentum does not hold. Macroscopic parameters are determined in the equilibrium function of the Chapman–Enskog distribution in which used parameters of the Euler equations. From this implies for the Chapman–Enskog distribution function formally we have values (density, linear moment and energy) with the first-order error. This fact was noted by Hilbert without further use and correction. The Boltzmann equation is invariant with respect to the choice of macro parameters. Therefore, the coincidence of the Navier–Stokes equations and the construction is of formal nature, order of approximation for the parameters in a locally equilibrium distribution function different. The Hilbert paradox was being solved. To solve this problem the iteration procedure was suggested. The new stress tensor is obtained for the molecules with their rotations and oscillations. Delay effect is due to the nature of the definition of derivative as the limit, while rarefied gas is discrete with large distances among molecules. It turns out that for recording the time derivative in the final terms we take into account only the high-speed components, as slow collisions do not have time to occur. Therefore there is a need on a second term of a Taylor series for inclusion in the work of the other component or to use the mean value of the time derivative, i. e. we have to take averages over time for all the terms in the equations, averages in space due to the withdrawal are defined. For the compound molecules is obtained the equal relaxation time and delay of interaction molecules in rarefied gas. This situation is typical for discrete environment because the transition from discrete to continuous environment is a key to the issue of mechanics. Summary records of all effects lead to a cumbersome system of equations and therefore require the selection of main effects in a particular situation. Study is continued of the problem of Faulkner–Scan with a constant vorticity at the outer edge of the boundary layer and with changing the vorticity. The emergence of “banded” structures revealed under certain conditions of flow at the outer edge.

Mathematical model of the flow of compressible material in cylindrical channel with variable cross section

Pryanishnikova E.A.¹, **Belyaeva N.A.**¹, **Stolin A.M.**², **Stelmakh L.S.**²

¹Syktyvkar State University named after Pitirim Sorokin, Syktyvkar, 167000 Russia

²Institute of Structural Macrokinetics and Material Science of Russian Academy of Science, Chernogolovka, 142432 Russia

e-mails: pryaysh@inbox.ru, belyaevana@mail.ru, amstolin@ism.ac.ru, stelm@ism.ac.ru

The flow of compressible material in cylindrical channel with variable cross section under the effect of one-sided pressure is considered. The movement is completely described by the equations

$$\frac{\partial \rho}{\partial t} + \operatorname{div}(\rho \vec{V}) = 0, \quad (1)$$

$$\rho \left(\vec{F} - \frac{d\vec{V}}{dt} \right) + \operatorname{div}(\Pi) = 0, \tag{2}$$

$$\Pi = \left[-p + \left(\xi - \frac{2}{3}\mu \right) \operatorname{div}(\vec{V}) \right] I + 2\mu\Phi, \tag{3}$$

where (1) is the continuity equation for density of the material ρ , flow velocity \vec{V} , (2) are Navier–Stokes equations, Π is the stress tensor, (3) is Newton’s law of viscosity, μ, ξ are the dynamic and volume viscosity, respectively.

To solve the system (1)–(2) the method of averaging over the radius of the cross section is applied by using the formula

$$\overline{f(r)} = \frac{2}{R^2} \int_0^R r f(r) dr. \tag{4}$$

The averaged system is solved numerically using the method of finite difference schemes. The influence of friction and slip velocity on the side of the boundary surface in the behavior parameters (density, components of stress tensor, components of velocity) of the moving material. The analysis of numerical solutions, the comparison with the results of experimental studies [1, 2] is conducted. The dependence of the slip velocity from the average velocity at the inlet of the channel is approximated by a cubic polynomial. The resulting functional dependence of slip velocity and friction can be used to describe the flow of viscous and visco-elastic materials.

References

[1] I. I. Ivitsky, *Technology audit and production reserves*, **5/3**(19), 8–11 (2014).
 [2] A. Perrot, D. Ranged, Y. Melinge, F. Micaelli, P. Estelle, C. Lanos, *Rheologica Acta*, **51/8**, 743–754 (2012).

Diffraction spectrum change in few-cycle wave structure

Puzyrev D.N., Kozlov S.A.

ITMO University, Saint-Petersburg 197101, Russia

e-mail: puzurev.danila@niuitmo.ru

Paper reports the theoretical analysis of spectral structure features of paraxial few-cycle initially Gaussian beams at their diffraction in the air. Based on the analytical expressions it is shown that frequency of the maximum spectral density increases on the beams axis as more as less is number of oscillation in the wave packet. For initially one cycle beam it multiplies by 1.4 times. Ratio of value on the axis to the value on the periphery the frequency of the maximum spectral density depends on initial number of oscillation in wave packet with generally monotonically change.

Based on the Helmholtz equation solution for propagation of spectral component of paraxial wave with arbitrary initial temporal profile in homogeneous and isotropic medium spatial distribution of frequency of the maximum spectral density in diffracted originally Gaussian beam is derived:

$$\omega(x, y, z) = \frac{\omega_0 \sqrt{3}}{6L\pi} \sqrt{2 \cosh \left(\left| \frac{\varphi(x, y, z)}{3} \right| \right) \sqrt{(z^2 + L^2)^2 - \frac{3z^2 L^2}{2N-1} \left(\frac{x^2 + y^2}{\rho^2} 2 - 1 \right)} - (2z^2 - L^2)}, \tag{1}$$

where

$$\varphi(x, y, z) = \operatorname{arcosh} \left(\frac{2(z^2 + L^2)^3 + \frac{9z^2 L^2}{2N-1} \left(z^2 + L^2 + \frac{x^2 + y^2}{\rho^2} 2(2z^2 - L^2) \right)}{2 \left((z^2 + L^2)^2 - \frac{L^2}{2N-1} \left(1 - \frac{x^2 + y^2}{\rho^2} 2 \right) \right)^{3/2}} \right),$$

x, y, z are coordinates of Cartesian axes, ρ is the radial transverse width at waist of beam, L is the Rayleigh distance for frequency of the maximum spectral density ω_0 at $z = 0$, N is the number of oscillation in initial wave packet.

The initial spatial-temporal distribution of the electric field strength on radiation source was used in the form

$$E(t, x, y) = (-1)^{2N} E_0 \exp\left(-\frac{x^2 + y^2}{\rho^2}\right) H_{2N-1}\left(\frac{t\omega_0}{\sqrt{2(2N-1)}}\right) \exp\left(-\frac{(t\omega_0)^2}{2(2N-1)}\right), \quad (2)$$

where t is time, E_0 is the initial amplitude of electric field strength of wave and H_n is the Hermite polynomials

Fig. 1a shows spatial distribution of the frequency of the maximum spectral density for initial one-cycle beam. Fig. 1b and fig. 1c present changes of the frequency of the maximum spectral density on beams axis and at distance ρ from axis for different number of oscillation in initial wave packet. In figures $\rho = 0.3$ mm, frequency of the maximum spectral density at source of radiation is $\omega_0 = 1$ THz, $R = \sqrt{x^2 + y^2}$.

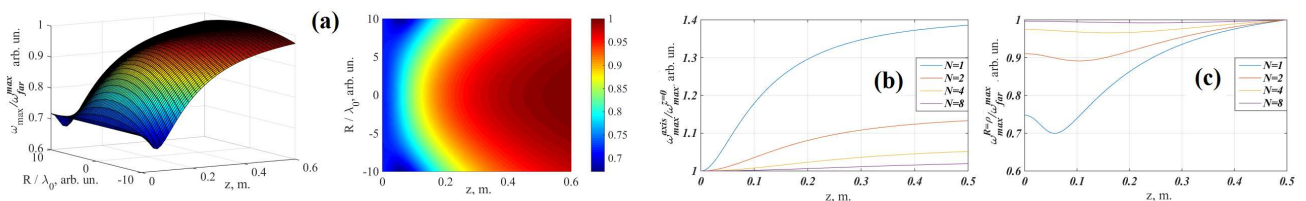


Fig. 1: Spatial distribution of the frequency of the maximum spectral density for initial one-cycle beam (a). Dynamic of the frequency of the maximum spectral density on the beam axis (b) and on the distance ρ from the beam axis. Normalization was performed by value of frequency on beam axis in far field region of diffraction (a, c) and by value of frequency on radiation source (b).

References

- [1] A. A. Ezerskaya, D. V. Ivanov, Y. S. Kivshar', S. A. Kozlov, *Journal of Infrared, Millimeter and Terahertz Waves*, No. 33, pp. 926–942 (2012).

Effective methods of numerical estimates of acoustic fields in the stratified ocean generated by moving airborne sources

Vladimir Rabinovich, **Josue Hernandez-Juarez**

National Polytechnic Institute of Mexico, ESIME Zacatenco, Av. IPN, S/N, C.P. 07738, Mexico City
e-mails: vladimir.rabinovich@gmail.com, jhernandezj0903@alumno.ipn.mx

The underwater acoustic wave propagation in the stratified ocean produced by moving airborne sources is investigated. We construct the asymptotics of the acoustic pressure in the ocean on large horizontal distances between a moving in the air source and a receiver located in the ocean. Our study is based on the representation of the acoustic field $P(t, \mathbf{x}, z)$ generated by a moving airborne source of the form of a time-frequency integral

$$P(t, \mathbf{x}, z) = \frac{1}{2\pi} \iint_{\mathbb{R}^2} a(\tau) g(\omega, \mathbf{x} - \mathbf{x}_0(\tau), z, z_0(\tau)) e^{i\omega(t-\tau) - i\omega_0\tau} d\omega d\tau, \quad (1)$$

where $g(\omega, \mathbf{x}, z, z_0)$ is the Green function of the stationary problem (see for instance [2, 3]).

For the numerical implementations we use the method of spectral parameter power series (SPPS method). This method is an effective tool of solutions of some problems of Mathematical Physics

reduced to the solution of the spectral Sturm–Liouville problem (see for instance [1] and references cited there). Note also our previous papers [4, 5] devoted to the application of the SPPS method for the numerical study of underwater waves propagation in the ocean generated by underwater stationary and moving sources.

In the talk we present the asymptotic constructions of the acoustic fields in the ocean generated by an airborne moving source, give formulas for modes frequency and time Doppler effects. We illustrate these results by calculations for some practical example.

References

- [1] R. Castillo-Perez, V. V. Kravchenko, H. Oviedo-Galdeano, V. S. Rabinovich, Dispersion equation and eigenvalues for quantum wells using spectral parameter power series, *Journal of Mathematical Physics*, **52**, 043522, 2011.
- [2] V. I. Il'ichev, V. S. Rabinovich, E. A. Rivelis, U. V. Hoha, Acoustic field of a moving narrow-band source in oceanic waveguides, *Dokl. Akad. Nauk SSSR*, **304**(5), 1123–1127, 1989 (in Russian).
- [3] O. A. Obresanova, V. S. Rabinovich, Acoustic field generated by moving sources in stratified waveguides, *Wave Motion*, **27**, 155–167, 1998.
- [4] V. S. Rabinovich, J. Hernandez-Juarez, Method of the spectral parameter power series in problems of underwater acoustics of the stratified ocean, *Mathematical Methods in the Applied Science*, **38**(10), 1990–1999, 2015.
- [5] V. S. Rabinovich, J. Hernandez-Juarez, Effective methods of estimates of acoustic fields in the ocean generated by moving sources, *Applicable Analysis*, **95**(1), 124–137, 2016.

On spectral asymptotics of the tensor product of operators with almost regular marginal asymptotics

Rastegaev N.V.

Chebyshev Laboratory, St. Petersburg State University, 199178, 14th Line 29B, Vasilyevsky Island, St. Petersburg, Russia;

St. Petersburg Department of V. A. Steklov Institute of Mathematics, 191023, 27 Fontanka, St. Petersburg, Russia

e-mail: rastmusician@gmail.com

Operators with almost power spectral asymptotics naturally arise, for example, when considering an ordinary differential operator with singular self-similar weight. The asymptotic of eigenvalue counting function in that case takes the form

$$N(\lambda) = \lambda^D \cdot (s(\ln \lambda) + o(1)), \quad \lambda \rightarrow +\infty,$$

where s is a positive continuous periodic function, dependent on the choice of the weight. Some properties of function s are described in [1, 2] (in particular, the fine structure of s is established for certain classes of weights). For the sake of generality we also consider almost regular asymptotics of the form

$$N(\lambda) = \lambda^D \cdot \varphi(\lambda) \cdot (s(\ln \lambda) + o(1)), \quad \lambda \rightarrow +\infty,$$

where φ is a slowly varying function.

As a part of the currently intensive development of the theory of small deviations of Gaussian random functions, tensor products of compact operators with almost regular marginal asymptotics containing periodic functions are considered for asymptotic analysis. We extend for this case the mode of proof developed in [3].

We infer that the same asymptotic behavior persists for the tensor product. It is also almost regular containing a periodic function. If the asymptotics of the operators are of different powers, it will resemble the stronger of two, with a difference only in the periodic term. If the powers coincide,

the slowly varying function will be the convolution of the original ones (in the case, when slowly varying functions are constant, it means the emergence of a logarithmic term). We establish the cases, where new periodic function could be shown to be non-degenerate under certain circumstances. We also establish cases, where it is guaranteed to degenerate into constant.

Author was supported by RFBR grant 16-01-00258a and by “Native towns”, a social investment program of PJSC “Gazprom Neft”.

References

- [1] A. A. Vladimirov, I. A. Sheipak, On the Neumann problem for the Sturm–Liouville equation with Cantor-type self-similar weight, *Functional Analysis and Its Applications*, V. **47**, no. 4, pp. 261–270 (2013).
- [2] N. V. Rastegaev, On spectral asymptotics of the Neumann problem for the Sturm–Liouville equation with self-similar generalized Cantor type weight, *Journal of Mathematical Sciences (New York)*, V. **210**, no. 6, pp. 814–821 (2015).
- [3] A. Karol’, A. Nazarov, Ya. Nikitin, Small ball probabilities for Gaussian random fields and tensor products of compact operators, *Transactions of the American Mathematical Society*, V. **360**, no. 3, pp. 1443–1474 (2008).

Integral representation of spiral light beams

Evgeniya V. Razueva, Eugeny G. Abramochkin

Lebedev Physical Institute, Samara, 443011, Russia

e-mail: dev@fian.smr.ru

Spiral light beams are paraxial wave fields whose intensity retain its shape up to scale and rotation during propagation of the field in free space. Various aspects of spiral beam theory are presented and discussed in [1]. In particular, it has been proven that rotation of a spiral beam is determined by the function $\theta(z) = \theta_0 \arctan z$, where θ_0 is an arbitrary real number. Then the total rotation angle of the field intensity during propagation is

$$\theta(+\infty) - \theta(0) = \frac{\pi\theta_0}{2},$$

and the rotation velocity goes to zero when z goes to infinity:

$$\left| \frac{d\theta(z)}{dz} \right| = \frac{|\theta_0|}{1+z^2}.$$

The most famous spiral beams are

$$F(x, y, z) = \frac{1}{1+iz} \exp\left(-\frac{x^2+y^2}{1+iz}\right) f\left(\frac{x+iy}{1+iz}\right), \quad (1)$$

where $f(z)$ is an arbitrary entire analytic function such that $F(x, y, 0) \in L_2(\mathbb{R}^2)$. In this case, the rotation parameter is $\theta_0 = -1$. During the propagation of such beam its intensity rotates over $\pi/2$ radians. These beams turned out to be useful for the creation of high-efficiency diffraction phase elements, which allow obtaining the intensity distribution in focusing plane in the shape of a predefined planar curve.

The natural question occurs: Is it possible to find an analytic expression, which is similar to Eq. (1) but for spiral beams with a large value of θ_0 ? Such beams, whose intensity rotates with a large velocity are a subject of interest in optical microscopy [2].

When the rotation parameter θ_0 is an integer, $\theta_0 \neq 0$, we obtain the following integral representation of corresponding spiral beam:

$$F(x, y, 0) = \exp(x^2 + y^2) \iint_{\mathbb{R}^2} \exp(-\xi^2 - \eta^2 + 2\sqrt{2}i(x\xi + y\eta)) f(W) d\xi d\eta, \quad (2)$$

where W is determined by the value of θ_0 :

$$\begin{aligned} \text{if } \theta_0 = \pm 2N, & \quad \text{then } W = (\xi^2 + \eta^2)^{2N-1}(\xi \mp i\eta)^2, \\ \text{if } \theta_0 = \pm(2N + 1), & \quad \text{then } W = (\xi^2 + \eta^2)^N(\xi \mp i\eta). \end{aligned}$$

Here, as above, $f(z)$ is an arbitrary entire analytic function that does not destroy the square integrability of the function $F(x, y, 0)$. If $\theta_0 = -1$, then Eq. (2) is reduced to Eq. (1) easily.

References

[1] E. G. Abramochkin, V. G. Volostnikov, *Modern optics of Gaussian beams*, Fizmatlit, Moscow (2010).
 [2] S. R. P. Pavani, R. Piestun, *Optics Express*, **16**, 3484–3489 (2008).

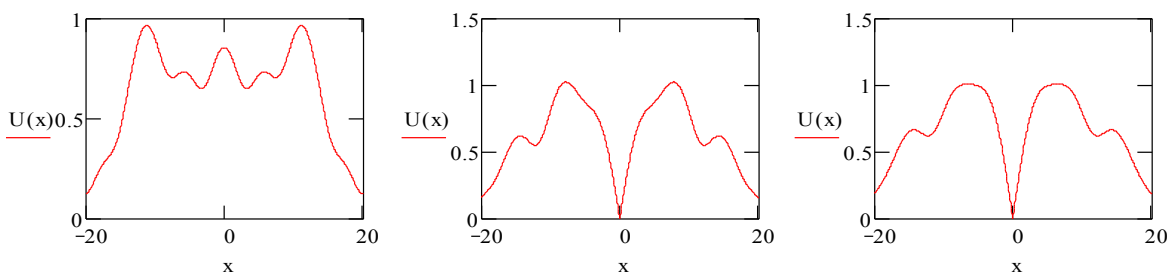
**Phase-shifting exposure in photolithography
using a Gaussian beam of an odd order**

Rudnitsky A.S.

Belarusian State University, Minsk, Belarus
 e-mail: rudnitsky@bsu.by

Every stage of photolithography is accompanied by agents deforming the prototype mask pattern. One of them is the diffraction of radiation at its propagation through a mask [1], that is one of the principal phenomena, limiting minimal dimensions of image elements in photolithography. One of the methods to increase resolution and to decrease dimensions in photolithography is utilizing of phase-shifting masks. There are several methods of phase-shifting mask realization, which differ by configuration of elements in the masking layer [1]. The more simple technique for improving of resolution is exposure with the off-axis illumination. In this case, the phase shift is provided by specific choice of the angle of incidence, when adjacent lines are illuminated by rays with opposite phases. This work is devoted to consideration of the phase-shifting exposure technique using a Gaussian beam of an odd order. As an example, a two-dimensional Gaussian beam of the first order is used. We consider the most simple mathematical model of the wave diffraction by an opaque screen with two parallel slits placed in the plane $z = 0$. The diffraction field is computed at the distance $z = h$ from a screen using the Rayleigh–Zommerfeld formula:

$$\begin{aligned} \nu(x, y) &= \int_{-c}^{-d} \left[\nu(\xi) \frac{\partial G}{\partial \zeta} \right]_{\zeta=0} d\xi + \int_d^c \left[\nu(\xi) \frac{\partial G}{\partial \zeta} \right]_{\zeta=0} d\xi, \quad \nu(\xi) = 2\sqrt{2} \frac{\xi}{\rho} \exp\left(-\frac{\xi^2}{\rho^2}\right), \\ G(x, \xi, z, \zeta) &= \frac{i}{2} H_0^{(2)} \left(k \sqrt{(x - \xi)^2 + (z - \zeta)^2} \right), \quad u(x) = |\nu(x)| \end{aligned}$$



The graphs represent the results of field amplitude computation at the following values of parameters (in the wavelengths) $n = 13$, $d = 3$, $h = 130$, $\rho = 9$, when a phase-shifting mask is exposed by a plane wave (the second graph), a simple mask is also exposed by a plane wave (the first graph) and by a Gaussian beam (the third graph).

As one can see from the first graph, diffraction causes the interference of light fluxes in gaps between elements and the confluence of topological details. Resolution of those is achieved by using a phase-shifting mask or by utilizing a Gaussian beam of an odd order, as the second and third graphs demonstrate.

References

- [1] R. P. Seisyan, Nanolithography in microelectronics. A review, *Technical Physics*, Vol. **56**(8), pp. 1061–1073 (2011).

Approximate approach to description of evolution of plane nonlinear elastic wave with different types of initial profile

Rushchitsky J.J., Yurchuk V.N.

S. P. Timoshenko Institute of Mechanics, Nesterov str. 3, Kiev, 03680, Ukraine

e-mail: rushch@inmech.kiev.ua

Let nonlinearity of deformation of the wave propagation medium is described by the Murnaghan's elastic potential [1]. Choose the model, in which the potential is presented by only the second and third powers of the displacements gradients, and assume that displacements depend only on one spatial coordinate x_1 and time t . Then the form of potential simplifies and the nonlinear wave equations for plane waves can be written in the simple form too. The equation for longitudinal wave is as follows [1]:

$$\begin{aligned} \rho u_{1,tt} - (\lambda + 2\mu)u_{1,11} &= N_1 u_{1,11} u_{1,1} + N_2 (u_{2,11} u_{2,1} + u_{3,11} u_{3,1}), \\ N_1 &= [3(\lambda + 2\mu) + 2(A + 3B + C)], \quad N_2 = \lambda + 2\mu + (1/2)A + B, \end{aligned} \quad (1)$$

where λ , μ , A , B , C are the elastic constants. Restrict further an analysis to the problem, when only the longitudinal wave is initially excited in a material [1]. Then equation (1) is simplified

$$\rho u_{1,tt} - (c_L)^2 u_{1,11} = (N_1/\rho) N_1 u_{1,11} u_{1,1}, \quad (2)$$

where $c_L = \sqrt{(\lambda + 2\mu)/\rho}$ is the velocity of linear P-wave. Represent equation (2) in the form

$$u_{1,tt} - (1 + \alpha u_{1,1})(c_L)^2 u_{1,11} = 0, \quad \alpha = [N_1/(\lambda + 2\mu)]. \quad (3)$$

Let the wave initial profile is described by the sufficiently smooth function $u(x_1, t = 0) = F(x_1)$ and the wave propagates in the form $u(x_1, t) = F(x_1 - vt)$, $v = \sqrt{1 - \alpha u_{1,1}} c_L$. Suppose the initial wave profile in the form of three functions: 1. $F(x_1) = \cos k_L x_1$ or $F(x_1) = e^{-k_L x_1}$ (harmonic wave); 2. $F(x_1) = e^{-(ax_1)^2/2}$ (solitary wave); 3. $F(x_1) = W_{0,0}(ax_1)$. Assume further

$$|\alpha u_{1,1}| \ll 1 \quad (4)$$

and represent the wave in the form

$$u(x_1, t) = F[x_1 - c_L t - (1/2)\alpha u_{1,1} t]. \quad (5)$$

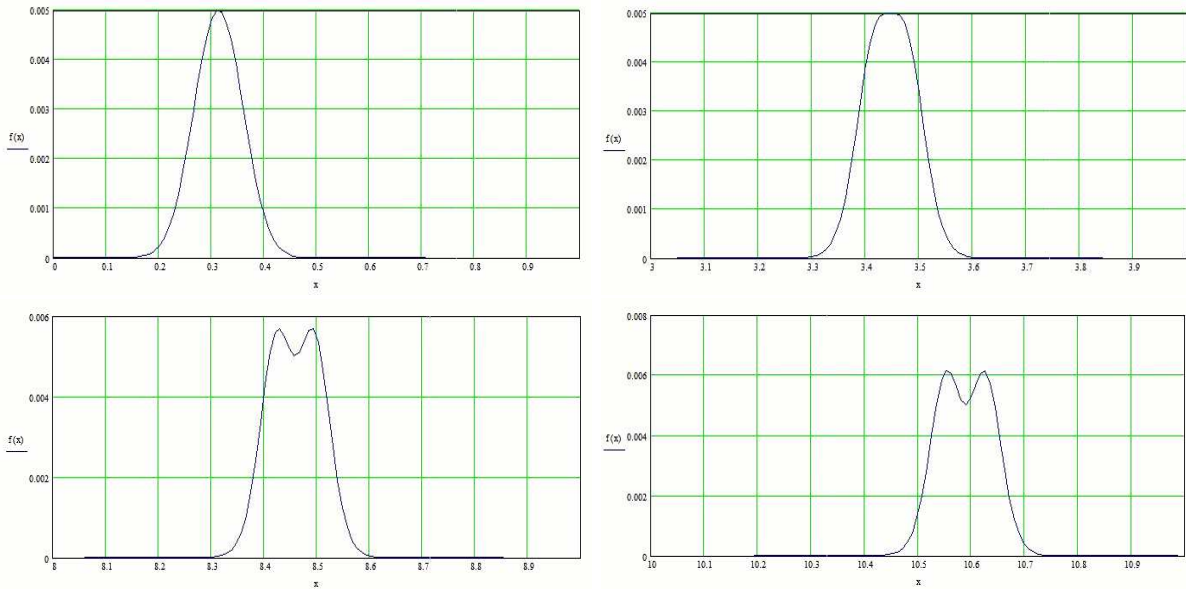
Denote the wave phase with the constant phase velocity by $\sigma = x_1 - C_L t$ and the additional small parameter by $\delta = -(1/2)\alpha c_L u_{1,1} t$. Represent now the solution (5) in the form of the Taylor series and restrict an analysis by the two first members owing to the smallness δ . Then relation (5) with

allowance for $u_{1,1}(x_1, t) \approx F_{\sigma}(\sigma + \delta)\sigma'_{x_1} = F_{\sigma}(\sigma + \delta)(1 - (1/2)\alpha c_L u_{1,1} t) \approx F_{\sigma}$ can be written in the form

$$u_{1,1}(x_1, t) \approx F(\sigma) - (1/2)\alpha c_L t [F'(\sigma)]^2. \tag{6}$$

The approximate representation of solution (6) has the general character. For different concrete functions (6) describes the nonlinear wave phenomenon — an appearance of the second harmonic or the similar new constituents and distortion of the wave initial profile. The numerical analysis that is realized for the mentioned above three types of waves, three kinds of metallic materials (aluminum, copper, steel) and certain range of changing the wave parameters (wave length or the wave bottom, maximal amplitude of initial profile showed that the proposed approximate approach describes the essential distortion of initial profile.

The pictures show an example of distortion for the wave with profile of Gauss function (bell-shaped wave).



References

[1] J.J. Rushchitsky, *Nonlinear Elastic Waves in Materials*, Springer, Heidelberg (2014).

Magnetic Schrödinger operators on periodic discrete graphs

Saburova N.Yu.

Northern (Arctic) Federal University, Northern Dvina emb. 17, Arkhangelsk, 163002, Russia
 e-mail: n.saburova@gmail.com

Korotyaev E.L.

St. Petersburg State University, Universitetskaya nab. 7/9, St. Petersburg, 199034, Russia
 e-mail: korotyaev@gmail.com

We consider magnetic Schrödinger operators with periodic magnetic and electric potentials on periodic discrete graphs. The spectrum of the operators consists of an absolutely continuous part (a union of a finite number of non-degenerate bands) plus a finite number of flat bands, i. e., eigenvalues of infinite multiplicity. We estimate the Lebesgue measure of the spectrum in terms of the Betti numbers and show that these estimates become identities for specific graphs. We estimate a variation of the spectrum of the Schrödinger operators under a perturbation by a magnetic field in terms of magnetic fluxes. The proof is based on Floquet theory and a precise representation of fiber magnetic Schrödinger operators constructed in the paper.

FFT techniques for numerical solution of volume singular integral equations of electromagnetics

A.B. Samokhin¹, A.S. Samokhina²

¹Moscow Technological University, 78, Vernadsky av., 119454, Moscow, Russia

²Institute of Control Sciences of RAS, 65, Profsoyznaya st., 117997, Moscow, Russia

e-mail: absamokhin@yandex.ru

We consider two family of problems of electromagnetics: (i) the medium in a finite 3D domain Q is characterized by a dielectric permittivity tensor function and constant outside Q , the permeability is constant everywhere; (ii) the same domain Q lies over perfectly conducting plane. The problem is to find electromagnetic field excited in the medium by an external field. These problems can be reduced to the volume singular integral equations (VSIEs) with respect of electric field in domain Q .

To solve the integral equation numerically, one reduce it to a system of linear algebraic equations (SLAE). It is clear that we must apply only iteration methods. Number T of arithmetic operations that guarantees the required accuracy of solution and memory volume M required for the implementation of the algorithm are the main efficiency criteria for any numerical algorithm. Multiplication of matrix SLAE by vector is the most laborious operation of the iteration method. Taking into account that the kernels of VSIEs depend only on the difference and sum of arguments and using regular grid we reduce integral equations to SLAE with matrix having properties of symmetry. Then memory volume M is proportionally the dimension of SLAE. Further using FFT techniques we construct fast algorithm for the multiplication of matrix SLAE by vector. Thus we can solve SLAE with matrix of huge dimension.

Stability of inverse coefficient problems' solutions for semilinear equations

Saritskaya Zh. Yu.

Far Eastern Federal University, 8 Sukhanova St., Vladivostok, Russia

e-mail: zhsar@icloud.com

The stationary nonlinear convection–diffusion–reaction equation is studied in the bounded domain $\Omega \subset R^3$ as a semilinear elliptic model

$$-\lambda\Delta\varphi + \mathbf{u} \cdot \nabla\varphi + k(\varphi, \mathbf{x})\varphi = f \quad \text{in } \Omega \quad (1)$$

with mixed-boundary conditions

$$\varphi = 0 \quad \text{on } \Gamma_D, \quad -\lambda\partial\varphi/\partial n + \alpha(\varphi, \mathbf{x})\varphi = \chi \quad \text{on } \Gamma_N. \quad (2)$$

Here Γ_D and Γ_N are open segments of the boundary $\partial\Omega$, such as $\partial\Omega = \bar{\Gamma}_D \cup \bar{\Gamma}_N$, φ is a concentration of polluting substance, \mathbf{u} is a given vector of velocity, f is a volume density of external sources of substance, λ is a constant diffusion coefficient, function $k = k(\varphi, \mathbf{x})$ means a reaction coefficient, function α , given on Γ_N , has the meaning of a mass-transfer coefficient.

Under the assumption that the mentioned coefficients depend nonlinearly and rather commonly either on the solution φ of the problem (1), (2), or on the spatial variable $\mathbf{x} \in \Omega$, global solvability of the problem(1), (2) and local uniqueness of its solution are proved.

The identification problem for function $\beta(\mathbf{x})$, which is multiplicatively included in reaction coefficient $k(\varphi, \mathbf{x}) = \beta(\mathbf{x})\check{k}(\varphi)$, conducted with the help of the additional information about substance's concentration in some subdomain $Q \subset \Omega$, can be interpreted as one of the examples of inverse coefficient problems. The stated inverse problem can be reduced to the corresponding multiplicative control problem. In the common case its solvability is proved, and for particular functions $\check{k}(\varphi)$ stability estimates are obtained for its solutions regarding to disturbances of cost functional and of the given functions from model (1), (2). See [1] about such problems' studying.

See [2, 3] about similar coefficient problems of acoustics and electromagnetics, such as identification problems of refraction coefficient and boundary impedance. The method of studying nonlinear boundary value and extremal problems, which was developed in this paper, can be applied to complicated nonlinear acoustics and electromagnetics models, in which main coefficients can depend on not only spatial variables as in [2, 3], but also on acoustic pressure and electromagnetic field correspondingly.

This work was supported by the Russian Foundation for Basic Research (project no. 16-01-00365 A).

References

- [1] G. V. Alekseev, R. V. Brizitskii, Zh. Yu. Saritskaya, Stability estimates of extremum problem's solutions for nonlinear convection–diffusion–reaction equation, *J. Applied and Industrial Math.*, **19**, 3–16 (2016).
- [2] G. V. Alekseev, A. V. Lobanov, Stability estimates for the solutions to inverse extremal problems for the Helmholtz equation, *J. Applied and Industrial Math.*, **7**, 1–13 (2013).
- [3] G. V. Alekseev, R. V. Brizitskii, Stability estimates for solutions of control problems for the Maxwell equations with mixed boundary conditions, *Differential Equations*, **49**, 963-974 (2013).

Acoustical imaging in semi-geodesic coordinates

Valeriia Sedaikina

Research Institute of Applied Informatics and Mathematical Geophysics of Immanuel Kant Baltic Federal University

e-mail: VSedaikina@kantiana.ru

The wave equation in two-dimensional Euclidian space with variable velocity is considered (Marmousi model). A set of sources is located at the part of the boundary of lower half space. First we solve the forward problem. Then the obtained synthetic data (inverse data) are used for model's imaging in semi-geodesic coordinates under assumption that the velocity is unknown. The imaging is based on the Boundary Control method: from the inverse data we obtain the waves in semi-geodesic coordinates and then use some imaging condition.

Formulas of van Vleck type for the Cauchy problem for differential and pseudodifferential equations in the one-dimensional case

Sergeev S.A.

Institute for Problems in Mechanics of the Russian Academy of Sciences, Moscow, Russia;

Moscow Institute for Physics and Technology (Technical University), Dolgoprudny, Russia

e-mail: sergeevse1@yandex.ru

Consider the pseudodifferential equation

$$ihu_t = L\left(x, -ih\frac{\partial}{\partial x}\right)u, \quad x \in R, \quad t > 0, \quad (1)$$

with symbol $L(x, p)$, where h is a small parameter. For this equation, we pose the Cauchy problem with localized initial data

$$u|_{t=0} = V\left(\frac{x - x_0}{h}\right). \quad (2)$$

Using Maslov's canonical operator, we construct an asymptotic solution of the Cauchy problem (1), (2).

This formula resembles the van Vleck formula, but in some examples (e. g., the linearized Korteweg–de Vries equation) for small time it can be expressed via the Airy function.

Further, if the Fourier transform of the initial function tends to unity as $h \rightarrow 0$, then we obtain the Green function of the Cauchy problem (1), (2).

References

- [1] V. P. Maslov, M. V. Fedoryuk, *Semiclassical approximation for equations of quantum mechanics*, Moscow, Nauka (1978).
- [2] S. Yu. Dobrokhotov, G. N. Makrakis, V. E. Nazakinskii, Maslov's canonical operator, Hörmander's formula, and localization of the Berry–Balazs solution in the theory of wave beams, *Theoretical and Mathematical Physics*, **180**:2, 894–916 (2014).

The Laplacian on a homogeneous tree with general matching conditions. The wave equation

Shafarevich A.I., Tsvetkova A.V.

Lomonosov Moscow State University, GSP-1, Leninskie Gory, Moscow, 119991, Russian Federation
e-mails: shafarev@yahoo.com, annatsvetkova25@gmail.com

In the present work we study the spectral properties of the Laplacian with general matching conditions on a homogeneous rooted metric tree Γ with the branching number b . Along with this problem we consider the Cauchy problem for the wave equation on Γ .

In the paper [1] the Laplacian was represented by a family of the operators $-\frac{d^2}{dx^2}$ on edges of this tree, complemented by the Kirchhoff matching conditions at vertices. We consider general matching conditions: namely, for every vertex v

$$\begin{aligned} f(e_v^-) &= \frac{1}{\gamma} f(e_v^1) = \frac{1}{\gamma} f(e_v^2) = \dots = \frac{1}{\gamma} f(e_v^b), \\ f'(e_v^-) &= \gamma(f(e_v^1) + f(e_v^2) + \dots + f(e_v^b)). \end{aligned}$$

Here $\gamma > 1$ is a real constant, e_v^- is the edge terminating at v , e_v^1, \dots, e_v^b are edges emanating from v .

We obtain the spectrum of the Laplacian. Also we find the solution of the Cauchy problem and study the behaviour of the wave energy in case time tends to infinity. We show that the share of the energy remains at the initial section of the graph.

References

- [1] A. V. Sobolev, M. Solomyak, Shrödinger operators on homogeneous metric trees: spectrum in gaps, *Rev. Math. Phys.*, Vol. **14**, pp. 421–468 (2002).

Dispersion diagrams and first arriving signals in layered waveguides

Shanin A.V.

Moscow State University, Department of Physics, Leninskie gory, Moscow, Russia, 119992
e-mail: a.v.shanin@gmail.com

Consider a layered 2D acoustic waveguide, which is homogenous in the x -direction and has a sandwich structure in the y -direction. The media constituting the waveguide can be elastic, liquid or gaseous. Waves in such a waveguide are described by a dispersion diagram in the (k, ω) coordinates (k is the wavenumber in the x -direction, ω is the temporal circular frequency). Usually the dispersion diagram is a graph consisting of several branches (curves). Each point of the dispersion diagram is characterized by phase velocity and group velocity.

It is known empirically that one can observe the *first arriving signal* (FAS) propagating with the velocity of the fastest medium in the structure of the waveguide. In the case of a single elastic isotropic medium the velocity of the FAS is close to the velocity of the longitudinal waves. In some cases the velocity of the FAS is bigger than any of the group velocities provided by the dispersion diagram. The FAS pulse decays with propagation distance unlike the pulses corresponding to usual modal pulses.

In the talk it is shown that FAS is related to *pseudo-branches* of the dispersion curve. An example of the pseudo-branch is shown in the figure. The pseudo-branch is composed of fragments of branches of the dispersion curve. One can approximate the pseudo-branch by a linearly transformed tangent function and estimate the integral describing the transient wave in the waveguide. As the result, one can obtain the velocity and the decay of FAS.

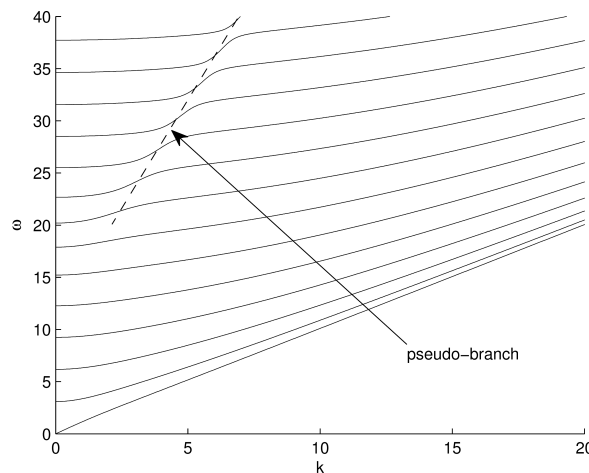


Fig. 1: A pseudo-branch.

The formulae obtained in the talk are compared with results of numerical modeling.

The work is supported by Russian Scientific school grant 7062.2016.2 and the Russian Foundation for Basic Research grant 14-02-00573.

Diffraction by an impedance strip in parabolic approximation

Shanin A.V., Korolkov A.I.

Moscow State University, Moscow, 119992 Russia

e-mails: a.v.shanin@gmail.com, korolkov@physics.msu.ru

A 2D stationary problem of acoustic wave scattering by a segment bearing impedance boundary conditions is considered (see Fig. 1). The impedances of the sides are assumed to be equal. Consideration is held in parabolic approximation which is applicable in case of diffraction of high-frequency grazing wave [1]. As it is known, the scattered field u^{sc} can be represented as

$$u^{sc}(r, \theta) = S(\theta, \theta^{in}) \sqrt{\frac{k_0}{2\pi ir}} e^{ik_0 r} + o(e^{ik_0 r} (k_0 r)^{-1/2}). \tag{1}$$

Here $\theta = \arctan(y/x)$, $r = \sqrt{x^2 + y^2}$, k_0 is a wave number, $S(\theta, \theta^{in})$ is the directivity of the scattered field.

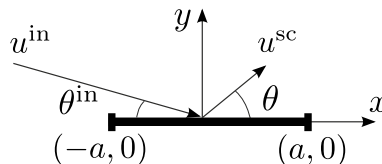


Fig. 1: Geometry of the problem.

A simple expression in a single quadratures is derived for the directivity in parabolic approximation:

$$S(\theta, \theta^{\text{in}}) = \exp \left\{ ik_0 a \frac{(\theta^{\text{in}})^2 + \theta^2}{2} \right\} \left(-Y(-\theta, \theta^{\text{in}}) - \frac{\eta + ik_0 \theta^{\text{in}}}{\eta - ik_0 \theta^{\text{in}}} Y(-\theta, -\theta^{\text{in}}) \right. \\ \left. - Y(\theta, -\theta^{\text{in}}) - \frac{\eta - ik_0 \theta^{\text{in}}}{\eta + ik_0 \theta^{\text{in}}} Y(\theta, \theta^{\text{in}}) + \frac{2\eta}{\eta - ik_0 \theta^{\text{in}}} Y(i\eta/k_0, -\theta) + \frac{2\eta}{\eta + ik_0 \theta^{\text{in}}} Y(-i\eta/k_0, \theta) \right), \quad (2)$$

where

$$Y(\theta_1, \theta_2) = \frac{1}{2ik_0(\theta_1 - \theta_2)} \left(\exp\{-ik_0 a \theta_1^2\} \operatorname{erfc} \left(\theta_1 \sqrt{\frac{k_0 a}{i}} \right) - \exp\{-ik_0 a \theta_2^2\} \operatorname{erfc} \left(\theta_2 \sqrt{\frac{k_0 a}{i}} \right) \right), \quad (3)$$

$\operatorname{erfc}(z)$ is the complementary error function, η is impedance of the strip, a is a half-width of the segment.

References

- [1] S. N. Vlasov, V. I. Talanov, *Radiophys. and Quantum Electronics*, **38**, 1–12 (1995).

Application of semi-analytical finite element method (SAFE) to inversion of acoustic logging data in non-cylindrical boreholes in anisotropic formation

Shchelik G.S.^{1,2}, Sofronov I.L.^{1,2}

¹Moscow Institute of Physics and Technology, 9 Institutskiy per., Dolgoprudny, 141700, Russia

²Schlumberger, 13, Pudovkina street, Moscow, 119285, Russia

e-mails: german.schelik@phystech.edu, isofronov@slb.com

Conventional processing algorithms for acoustic cross-dipole and logging-while-drilling measurements are largely based on propagation analysis of guided modes in a borehole. The development of oilfield technologies increases the relevance of such measurements in formations with complex anisotropy or geological structure. However, there is no common approach for inversion of formation parameters considering these effects.

Assuming the homogeneity of formation and borehole geometry along axial direction z , the direct problem of elastic waves propagation reduces to a set of two-dimensional problems in (r, θ) -plane. Using standard finite element discretization in frequency domain each of 2D problems transforms to a generalized eigenvalue problem and is solved numerically. The considered approach is referred as semi-analytical finite element method [1].

In this study logging measurements are approximated with sum of a finite number of numerically obtained eigenfunctions. The high-accurate 3D simulations by spectral element method [2] are taken as reference logging data. The chosen approximation by small number of eigenfunctions is proved to be valid for fluid-filled boreholes with non-cylindrical cross-section in typical transversely anisotropic formations.

The residual of approximated and initial solution is shown to be sensitive to both compressional and shear wave velocities and Thomsen anisotropic parameters (ϵ, δ) . The gradient of the residual can be calculated with a adjoint-state method [3] and used for the solution of inverse problem. The key feature of the proposed inverse problem formulation is the simultaneous analysis of data from all receivers both along borehole axis and in cross-sectional plane.

The residual functional between approximated and reference solutions is shown to be sensitive to both compressional and shear wave velocities and Thomsen anisotropic parameters (ϵ, δ) when

the data collected from all receivers both along borehole axis and in cross-sectional plane is used. Therefore a conventional inverse problem approach is formulated. The gradient of the functional is evaluated with adjoint-state method [3]. The key feature of the proposed inverse problem formulation is a usage of a small number of eigenfunctions for good approximation accuracy in considered typical formations.

References

- [1] T. V. Zharnikov, D. E. Syresin, *The Journal of the Acoustical Society of America*, **137(6)**, EL396–EL402 (2015).
- [2] D. Komatitsch, J. Tromp, *Geophysical Journal International*, **139**, 806–822 (1999).
- [3] R.-E. Plessix, *Geophysical Journal International*, **167(2)**, 495–503 (2006).

Tunneling of Gaussian light pulses in chirped Bragg grating

Shestakov P.Yu., Marchenko S.V.

Lomonosov Moscow State University, Russian Federation, 119991, Moscow, GSP-1, Leninskie gory, 1, bld. 2

e-mail: iveage@physics.msu.ru

Reflective properties of chirped Bragg gratings (CBG) allow effectively compress and stretch light pulses. Tunneling which also takes place in such structures can be considered as a side effect while using chirped gratings as devices with negative dispersion. This phenomenon is of an independent interest, for example, for the finding of the traversal time of Gaussian pulses (or group delay) through a chirped periodic structure in the forbidden gap.

Special properties of tunneling in the present paper are studied with the help of numerical methods on the basis of a two component dielectric structure. The period of the structure changes linearly $d(z) = d_0 \pm \alpha(z - L_{gr}/2)$, where d_0 is the period in the center of the grating, α is the chirp parameter, L_{gr} is the grating length. Period variation leads to a deviation of a local Bragg wavelength ($\lambda_{br}(z) = 2n_0d(z)$, n_0 is the mean refractive index of the CBG). Hence, different spectral components of an incident pulse reflect back from different points of the CBG. Such behavior results in the frequency modulation of a reflected pulse.

Spatial size of the photonic barrier in the CBG is important for the transmitted pulse. Its value is determined by $L_{br} = 2\kappa/\beta$, where κ is a coupling constant, $\beta = -\alpha\pi/d_0^2$ [1]. The output pulse is not modulated since optical paths of various spectral components before and after the photonic barrier in CBG are equal to each other.

Profiles of transmitted pulses with different durations are calculated. It was shown that minimal losses related to tunneling in schemes of stretching and compressing take place when the value κL_{br} is large enough.

Group delays of narrow band pulses are calculated as $d\phi_{tr}/d\omega$, where ϕ_{tr} is a phase of a transmission coefficient. Our simulations show that the phase is distorted in the forbidden gap. That is why group delay has a lower value compared to the propagating time in a homogeneous medium. Note that the group delay of narrow band pulses also saturates with the increasing of the photonic barrier as well as in a Bragg grating without chirp [2].

References

- [1] S. Kaim, S. Mokhov, et al, *SPIE Optical Engineering*, **53(5)**, 051509(1–7) (2014).
- [2] H. Winful, *IEEE J. Sel. Top. Quant. Electron.*, **9(17)**, 17–29 (2003).

Ultrashort optical pulses in germanene in the 3D case

Skvortsov D.S.¹, Konobeeva N.N.¹, Belonenko M.B.^{1,2}

¹Volgograd State University, Volgograd, Russia

²Volgograd Institute of Business, Volgograd, Russia

e-mails: yana_nn@inbox.ru, mbelonenko@yandex.ru

In recent years, increasing effort has been devoted to studying nonlinear propagation of ultrashort optical pulses in different materials. This interest is associated with the prospects of using nonlinear optical effects in practical applications [1]. Here, we consider the dynamics of electromagnetic pulses propagating in germanene in three-dimensional case. Germanene is rather new material. It is a single layer of germanium atoms like graphene is a monolayer of carbon atoms. It should be noted that the magnitude of the spin-orbit coupling is significantly larger in germanene than in graphene and silicone, and can not be neglected as it is a materials property. At the same time there are open issues related to going beyond the one-dimensional approximation. Taking into account these circumstances, it is important to study the evolution of 3D ultrashort optical pulses in germanene, which is expected to reveal new effects with a broad range of practical applications.

In a long-wavelength approximation, a Hamiltonian for germanene can be written as:

$$H = \nu(\xi k_x \sigma_x + k_y \sigma_y) - 0.5\xi \Delta_{SO} \tau_z \sigma_z + 0.5\Delta_z \sigma_z, \quad (1)$$

where ξ is the sign of the valley for two Dirac dots, ν is the Dirac electron velocity, (k_x, k_y) is the quasi-momentum of electrons, Δ_{SO} is the spin-orbit gap width, Δ_z is the potential on a lattice site, and $\Delta_z = E_z d$, E_z is the electric field strength, d is the distance between two sublattice planes, σ_i, τ_i are the Pauli matrices.

The eigenvalues of matrix form of Hamiltonian allow us to define the current density of electrons in germanene. The Maxwell equations in cylindrical coordinates can be written as:

$$A_{tt} = \frac{1}{r} \frac{\partial}{\partial r} \left(r \frac{\partial A}{\partial r} \right) + \frac{\partial^2 A}{\partial z^2} + \frac{1}{r^2} \frac{\partial^2 A}{\partial \phi^2} + 4\pi j(A), \quad (2)$$

where A is the vector-potential, j is the current density in germanene. Evolution of ultrashort optical pulses (consist of two electric field oscillations) is presented in Figure 1.

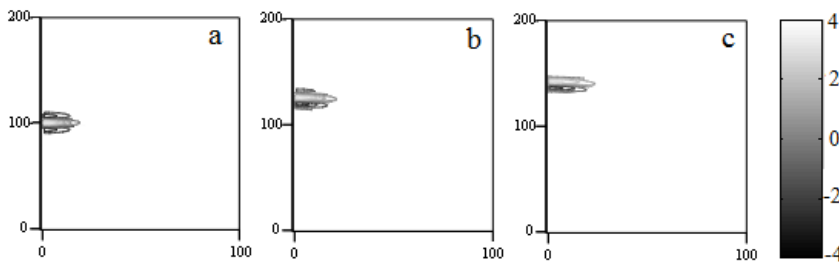


Fig. 1: The intensity of 3D optical pulse at the different times: a) $t = 0$ s; b) $t = 3.0 * 10^{-13}$ s; c) $t = 5.0 * 10^{-13}$ s.

This study was supported by the Ministry of Education and Science of the Russian Federation, project no. MK-4562.2016.2.

References

- [1] T. Yu. Astakhova, O. D. Gurin, M. Menon, G. A. Vinogradov, *Phys. Rev. B*, V. **64**, p. 035418, 2001.

Estimates for the singular numbers of the sandwiched Airy transformation

Sloushch V.A.

St. Petersburg State University, 7/9 Universitetskaya nab., St. Petersburg, 199034 Russia
e-mails: v.slouzh@spbu.ru, vsloushch@list.ru

In $L_2(\mathbb{R})$ we consider the unitary integral Airy transformation T defined by

$$Tu(x) := \int_{\mathbb{R}} \text{Ai}(y-x)u(y)dy, \quad u \in L_2(\mathbb{R}) \cap L_1(\mathbb{R}).$$

Here $\text{Ai}(z) = \frac{1}{\pi} \int_0^\infty \cos(\frac{t^3}{3} + zt)dt$, $z \in \mathbb{R}$, is the Airy function. We study the compactness conditions and estimates for the singular numbers of the operator fTg for suitable functions $f, g \in L_{2,\text{loc}}(\mathbb{R})$. The results of such type can be useful for investigation of the spectrum of the Stark operator $H = -\frac{d^2}{dx^2} + x$ perturbed by a decaying potential.

More precisely, we discuss conditions ensuring that the operator fTg belongs to the standard \mathcal{S}_p -class or to the Lorentz class $\mathcal{S}_{p,q}$. For $p > 2$ these conditions were established in [1]. This talk concerns the case where $p \in (0, 2)$ and $q \in (0, +\infty]$. In particular, we discuss the conditions ensuring that the operator fTg belongs to the trace class.

References

- [1] V. A. Sloushch, Generalizations of the Cwikel estimate for integral operators, *Proceedings of the St. Petersburg Mathematical Society. Vol. XIV, Amer. Math. Soc. Transl. Ser. 2*, vol. **228**, pp. 133–155, Amer. Math. Soc., Providence, RI (2009).

Nodal count theorem for quantum tree graphs with δ -coupling

Smolkina M.O., Popov I.Y.

ITMO University, Kronverkskiy, 49, Saint Petersburg 197101, Russia
e-mails: vega14@mail.ru, popov1955@gmail.com

The Courant theorem provides an upper bound for the number of nodal domains of eigenfunctions of a wide class of Laplacian-type operators (see, e.g. [1]). In particular, it holds for generic eigenfunctions of a quantum graph. The theorem states that after ordering the eigenvalues as a non-decreasing sequence the number v_n of nodal domains of the n^{th} eigenfunction is bounded from above by n . Here we obtain the analogous theorem for special type quantum graphs. A quantum tree with the Schrödinger operator defined at the edges and δ -type coupling conditions is suggested.

Let Γ be a quantum tree, $V(\Gamma)$ is a set of its vertices and $E(\Gamma)$ is a set of its edges. We assume the following equation at the edges:

$$(H - \lambda I)u(x) = -u''(x) - (\lambda - q(x))u(x) = 0. \tag{1}$$

We deal with the Dirichlet boundary condition at the boundary vertices of the graph and δ -type coupling at the internal graph vertices:

$$\sum_{e \in E_v} \frac{du}{dx_e}(v) = \beta_v u(v), \quad \beta_v > 0, \quad x \in V(\Gamma), \tag{2}$$

where u is continuous on Γ , $V(\Gamma)$ is a set of vertices of Γ , E_v is a set of edges containing vertex v , $\frac{du}{dx_e}(v)$ is a derivative of the solution at the vertex v of the edge e in the outgoing direction from the vertex, $\beta_v, \beta_v > 0$, are some real positive numbers.

Theorem. Let the following conditions take place:

$$y_0(x), y_1(x), \dots, y_k(x), \dots \quad (3)$$

where $y_0(x), y_1(x), \dots, y_k(x), \dots$ are the eigenfunctions;

$$n_0 < n_1 < \dots < n_k < \dots \quad (4)$$

where n_0, n_1, n_k, \dots are the number of zeroes;

$$\lambda_0 < \lambda_1 < \dots < \lambda_k < \dots \quad (5)$$

where $\lambda_0, \lambda_1, \dots, \lambda_k, \dots$ are the eigenvalues. Then the $y_k(x)$ has exactly k zeroes, i. e. $n_k = k$ in the inequality (4).

To prove the Theorem authors used already obtained in previous works the Molchanov-type condition that guarantees the discreteness of the spectrum [2] and had to prove some properties about the behavior of eigenfunctions.

References

- [1] P. D. Karageorge, U. Smilansky, *J. Phys. A*, **41**(20), 205102 (2008).
 [2] M. O. Kovaleva, I. Y. Popov, *Rep. on Math. Phys.*, **76**, 171–178 (2015).

Gaussian beam in a gradual transition from a waveguide to an antiwaveguide

Irina A. So¹, Aleksei P. Kiselev^{2,3,4}, Alexandr B. Plachenov^{5,6}

¹Nevinpat, Pirogova 7, St. Petersburg, Russia

²PDMI RAS, Russia; ³St. Petersburg State University, Russia; ⁴IPME RAS, St. Petersburg, Russia

⁵MIREA, Moscow, Russia; ⁶SUAI, St. Petersburg, Russia

e-mails: irene_so@mail.ru, kiselev@pdmi.ras.ru, a_plachenov@mail.ru

From time immemorial, propagation of paraxial Gaussian beams has attracted attention of researchers working in different areas of the theory of diffraction (see, e.g., [1, 2]). For optics, of particular interest is the propagation of beams in axisymmetric structures with a straight axis. We are concerned with high-frequency beams in a structure with a smooth refraction index described by $n(x, y, z) = n_0 - n_2(z)(x^2 + y^2)/2$, where $n_2(z) > 0$ as $z < 0$ (which corresponds to a waveguide), and $n_2(z) < 0$ as $z > 0$ (which corresponds to an antiwaveguide).

The parabolic equation for the amplitude U reads as follows:

$$2ikn_0U_z + U_{xx} + U_{yy} - k^2n_0n_2(z)(x^2 + y^2)U = 0, \quad (1)$$

where k is the wavenumber in vacuum, which can be regarded as a formal large parameter. The fundamental mode has the form

$$U = a(z) \exp\{ik(x^2 + y^2)/2q(z)\}, \quad (2)$$

where $a(z)$ and $q(z)$ can be described in an explicit form (see, e.g., [2]).

As shown in [3], a mode transversely localized at some $z = z_0$ (that is, $\text{Im } q(z_0) < 0$) remains such for all values of z . In particular, a mode localized in a waveguide is also localized after a transition to an antiwaveguide. We numerically simulated wavefields in a vicinity of the transition point $z = 0$. By analogy with [4], we considered higher-order modes as well.

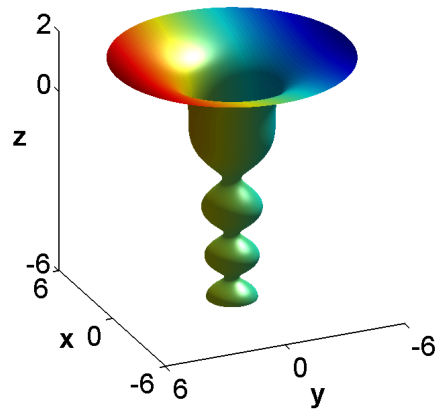


Fig. 1: Half-width of the fundamental mode.

References

- [1] V. M. Babich, V. S. Buldyrev, *Short-Wavelength Diffraction Theory*, Springer, NY (1991).
- [2] H. Kogelnik, *Appl. Opt.*, **4**, 1562–1569 (1965).
- [3] V. M. Babich, M. M. Popov, *Acoust. Zh.*, **27**, 828–834 (1981).
- [4] A. P. Kiselev, A. B. Plachenov, *JOSA A*, **33**, 663–666 (2016).

Mathematical and numerical analysis of the spectral characteristics of dielectric microcavities with active regions

Spiridonov A.O., Karchevskii E.M.

Department of Applied Mathematics, Kazan Federal University, Russia
 e-mails: aospiridonov@gmail.com, ekarchev70@gmail.com

We study electromagnetic fields and emission thresholds of two-dimensional dielectric microcavities solving the lasing eigenvalue problem (LEP) proposed in [1]. We solve the LEP for microcavities of arbitrary shape with active regions. Namely, we propose a new convenient formulation of the LEP as a nonlinear spectral problem for a Fredholm holomorphic operator-valued function, which includes weakly singular integral operators. On the base of the new formulation of the problem we investigate the qualitative properties of the characteristic set: the localization on the corresponding Riemann surface, the discreteness, the dependence of the characteristic values (eigenfrequencies) on the threshold gain and nonspectral parameters.

We reduce the original problem to the system of Muller boundary integral equations, which we solve numerically by the Nystrom method [2]. We prove a theorem on convergence of the Nystrom method. We get the following results. If there exists a solution to the set problem, then there exists a sequence of eigenvalues of the Nystrom method matrix, converging to the exact solution as a number of grid points increases. On the other hand, if there exists a converging sequence of the above mentioned eigenvalues, then it converges to the exact problem solution.

We propose a new computer implementation of the Nystrom method and calculate the spectral characteristics of new types of microcavities with active regions, having the following important for applications properties: the low thresholds of lasing and the sparseness of spectrum.

References

- [1] E. I. Smotrova, A. I. Nosich, *Optical and Quantum Electronics*, **36**, 213–221 (2004).
- [2] E. I. Smotrova, et al., *J. Opt. Soc. Am. B*, **30**, 1732–1742 (2013).

Impact of conical points on the object's scattered field

Ivan A. Starkov

Nanotechnology Center, St. Petersburg Academic University, Russian Academy of Sciences, Khlopin st. 8/3, St. Petersburg, Russia, 194021

e-mail: starkov@spbau.ru

Alexander S. Starkov

National Research University of Information Technologies, Mechanics and Optics, Kronverksky pr. 49, St. Petersburg, Russia, 197101

e-mail: ferroelectrics@ya.ru

The problem of scattering of acoustic, elastic, and electromagnetic waves from cavities or inclusions, whose dimensions are significantly smaller than the wavelength (so-called long-wave or Rayleigh approximation), is among the classical questions in wave theory. In the literature, only the cases with known analytical solutions of the corresponding dynamic problem have been usually studied. At the same time, the behavior of the long-wave asymptotic is determined from expressions representing this explicit solution. Of the many possible approaches to solve this problem in a general case, we consider only two. In the first one [1], two kinds of asymptotic expansions are employed. The wave field near the scatterer can be represented by the series whose coefficients are the result of consistent solutions of static problems. In turn, at long distances, the field is represented as an expansion in multipoles. The second approach is based on the derivation of the integral equation for the field in question and its solution by the method of successive approximations [2]. It is possible to conclude from the results of these studies that in the main approximation the scattered field at large distances is similar to the field of a point source placed at the inclusion location. The amplitude of this source is determined only by its volume. In this paper we use a combined method when the short-range solution is constructed by the method of [1] and an integral equation is used at the large distances. The spindle-like body (see Fig. 1) was treated as a scatterer for a model demonstration. The solution of the static problems is sought in the bispherical coordinate system as the Mehler–Fock integral. The field continuity conditions at the interface of the spindle lead to a difference equation for integrands that can be solved with the help of the Fourier transform.

The reported study was funded by RFBR, according to the research project No. 16-32-60189 mol_a_dk.

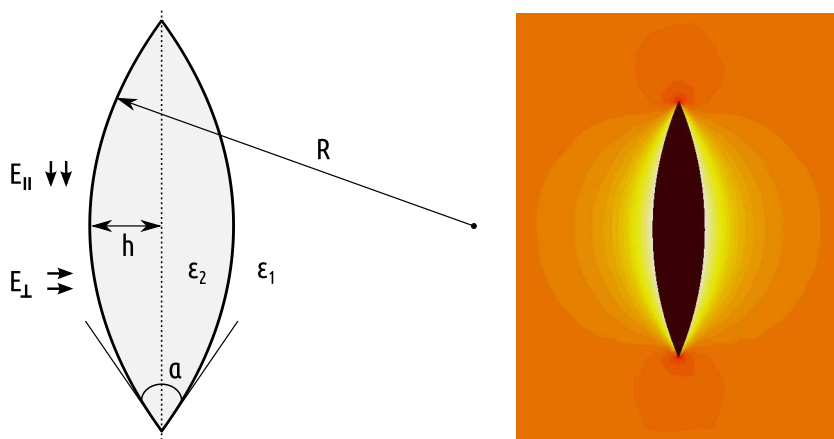


Fig. 1: The schematic representation of the spindle-like body.

References

- [1] V. Yu. Gotlib, *J. Sov. Math.*, **11**, 695–699 (1979).
- [2] N. Ya. Kirpichnikova, V. B. Philippov, *J. Math. Sci.*, **117**, 3936–3944 (2003).

Homogenization of high-order elliptic equations

Suslina T.A.

St. Petersburg State University, Universitetskaya nab. 7/9, St. Petersburg, 199034, RUSSIA
 e-mail: t.suslina@spbu.ru

In $L_2(\mathbb{R}^d; \mathbb{C}^n)$, we consider a selfadjoint strongly elliptic operator A_ε , $\varepsilon > 0$, given by the differential expression $b(\mathbf{D})^*g(\mathbf{x}/\varepsilon)b(\mathbf{D})$. Here $g(\mathbf{x})$ is a periodic bounded and positive definite $(m \times m)$ -matrix-valued function, $b(\mathbf{D}) = \sum_{|\alpha|=p} b_\alpha \mathbf{D}^\alpha$ is a differential operator of order p , and b_α are constant $(m \times n)$ -matrices. It is assumed that $m \geq n$ and that the symbol $b(\boldsymbol{\xi})$ has rank n for any $0 \neq \boldsymbol{\xi} \in \mathbb{R}^d$. The precise definition of A_ε is given in terms of the quadratic form. We study the behavior of the resolvent $(A_\varepsilon - \zeta I)^{-1}$, where $\zeta = |\zeta|e^{i\varphi} \in \mathbb{C} \setminus \mathbb{R}_+$, for small ε . It is proved that, as $\varepsilon \rightarrow 0$, the operator $(A_\varepsilon - \zeta I)^{-1}$ converges in the L_2 -operator norm to the resolvent of the effective operator $A^0 = b(\mathbf{D})^*g^0b(\mathbf{D})$. Here g^0 is the so called effective matrix. In [1], the following error estimate for $0 < \varepsilon \leq 1$ was obtained:

$$\|(A_\varepsilon - \zeta I)^{-1} - (A^0 - \zeta I)^{-1}\|_{L_2(\mathbb{R}^d) \rightarrow L_2(\mathbb{R}^d)} \leq C_1(\varphi)\varepsilon|\zeta|^{-1+1/2p}. \tag{1}$$

Also, in [1] approximation of the resolvent in the norm of operators acting from $L_2(\mathbb{R}^d; \mathbb{C}^n)$ to the Sobolev space $H^p(\mathbb{R}^d; \mathbb{C}^n)$ was obtained:

$$\|(A_\varepsilon - \zeta I)^{-1} - (A^0 - \zeta I)^{-1/2} - \varepsilon^p K(\varepsilon; \zeta)\|_{L_2(\mathbb{R}^d) \rightarrow H^p(\mathbb{R}^d)} \leq C_2(\varphi)\varepsilon(|\zeta|^{-1+1/2p} + |\zeta|^{-1/2+1/2p}). \tag{2}$$

Here the operator $K(\varepsilon; \zeta)$ is a corrector; it contains rapidly oscillating coefficients and so depends on ε ; herewith, $\|K(\varepsilon; \zeta)\|_{L_2 \rightarrow H^p} = O(\varepsilon^{-p})$. Estimates (1) and (2) are order-sharp for small ε . The constants $C_1(\varphi)$, $C_2(\varphi)$ are uniformly bounded in any sector $\varphi_0 \leq \varphi \leq 2\pi - \varphi_0$ with $\varphi_0 > 0$.

Now, let $\mathcal{O} \subset \mathbb{R}^d$ be a bounded domain with sufficiently smooth boundary. By $A_{D,\varepsilon}$ we denote the operator in $L_2(\mathcal{O}; \mathbb{C}^n)$ given by the expression $b(\mathbf{D})^*g(\mathbf{x}/\varepsilon)b(\mathbf{D})$ with the Dirichlet boundary condition. The precise definition of $A_{D,\varepsilon}$ is given in terms of the quadratic form. Let A_D^0 be the effective operator given by $b(\mathbf{D})^*g^0b(\mathbf{D})$ with the Dirichlet condition. In [2], the following error estimates are proved for $0 < \varepsilon \leq \varepsilon_0$ (ε_0 is sufficiently small) and $\zeta \in \mathbb{C} \setminus \mathbb{R}_+$, $|\zeta| \geq 1$:

$$\|(A_{D,\varepsilon} - \zeta I)^{-1} - (A_D^0 - \zeta I)^{-1}\|_{L_2(\mathcal{O}) \rightarrow L_2(\mathcal{O})} \leq C_3(\varphi) (\varepsilon|\zeta|^{-1+1/2p} + \varepsilon^2), \tag{3}$$

$$\|(A_{D,\varepsilon} - \zeta I)^{-1} - (A_D^0 - \zeta I)^{-1} - \varepsilon^p K_D(\varepsilon; \zeta)\|_{L_2(\mathcal{O}) \rightarrow H^p(\mathcal{O})} \leq C_4(\varphi) (\varepsilon^{1/2}|\zeta|^{-1/2+1/4p} + \varepsilon). \tag{4}$$

Here $K_D(\varepsilon; \zeta)$ is the corresponding corrector. Estimate (3) is order-sharp for small ε . The order of estimate (4) is worse than the order of (2) because of the boundary layer effect. The constants $C_3(\varphi)$, $C_4(\varphi)$ are uniformly bounded in any sector $\varphi_0 \leq \varphi \leq 2\pi - \varphi_0$ with $\varphi_0 > 0$.

The analogs of (3), (4) for $\zeta \in \mathbb{C} \setminus \mathbb{R}_+$, $|\zeta| < 1$, are also obtained, but the behavior of the right-hand sides with respect to ζ is different from (3), (4).

References

- [1] A. A. Kukushkin, T. A. Suslina, Homogenization of high-order elliptic operators with periodic coefficients, *Algebra i Analiz*, **28**, no. 1, 89–149 (2016).
- [2] T. A. Suslina, Homogenization of solutions of the Dirichlet problem for high-order elliptic equations with periodic coefficients, in preparation.

Weak shear modulus in the acoustic mode parabolic equation

Trofimov M.Yu., Kozitskiy S.B., Zakharenko A.D.

Il'ichev Pacific Oceanological Institute, 43 Baltiiskaya St., Vladivostok, 690041, Russia
e-mails: trofimov@poi.dvo.ru, skozi@poi.dvo.ru, zakharenko@poi.dvo.ru

Adiabatic acoustic mode parabolic equations appeared as a convenient tool for solving three-dimensional problems of ocean acoustics. Here by the multi-scale expansions method [1] we derive an elastic mode parabolic equation, which takes into account the effects of a weak elasticity on the acoustic field. As a small parameter a ratio of a typical wavelength to a typical size of horizontal inhomogeneities is chosen. The shear modulus is of the order of the small parameter.

We postulate the following expansions of the parameters of elasticity and the dependent variables (velocity) $\lambda = \lambda_0(X, z) + \epsilon\lambda_1(X, Y, z)$, $\mu = \epsilon\mu_1(X, Y, z)$, $\frac{1}{\rho} = \gamma_0(X, z) + \epsilon\gamma_1(X, Y, z)$, $(u, v, w) = ((u_0 + \epsilon u_1 + \dots), (\epsilon^{1/2}v_0 + \epsilon^{3/2}v_1 + \dots), (w_0 + \epsilon w_1 + \dots))e^{i\theta(X)/\epsilon}$. Stress tensor of the elasticity with the elasticity equations are:

$$\sigma_{ij} = \lambda \left(\sum_k \frac{\partial u_k}{\partial x_k} \right) \delta_{ij} + \mu \left(\frac{\partial u_i}{\partial x_j} + \frac{\partial u_j}{\partial x_i} \right), \quad -\rho\omega^2 u_k = \sum_j \frac{\partial \sigma_{kj}}{\partial x_j}, \quad k = 1, \dots, 3.$$

Without loss of generality we consider the only interface surface $z = h_0$.

With all this we expand the equations of elasticity. The solvability condition at the $O(\epsilon^1)$ in the case of piecewise constant γ_0 is the parabolic equation for amplitude A_m of the mode with number m :

$$2ik_m A_{mX} + ik_{mX} A_m + A_{mYY} + \alpha_m A_m = 0, \quad (1)$$

where α_m is given by the formula

$$\begin{aligned} \alpha_m = & \int_{-H}^0 \gamma_0 \nu \varphi_m^2 dz + \int_{-H}^0 \gamma_1 (n_0^2 - k_m^2) \varphi_m^2 dz - \int_{-H}^0 \gamma_1 (\varphi_{mz})^2 dz \\ & - 4 \int_{-H}^0 \gamma_0^2 n_0^2 \mu_{1z} \varphi_{mz} \varphi_m dz + 2 \int_{-H}^0 \gamma_0^2 \omega^2 n_0^4 \mu_1 \varphi_m^2 dz + 2 \int_{-H}^0 \gamma_0^2 (k_m^2 / \omega^2 - n_0^2) \mu_{1zz} \varphi_m^2 dz \\ & + h_1 \left\{ \varphi_{m+}^2 \left[k_m^2 (\gamma_{0+} - \gamma_{0-}) - (n_0^2 \gamma_0)_+ + (n_0^2 \gamma_0)_- \right] - (\gamma_0 \varphi_{mz})_+^2 \left[\left(\frac{1}{\gamma_0} \right)_+ - \left(\frac{1}{\gamma_0} \right)_- \right] \right\} \Big|_{z=h_0} \\ & + \frac{2}{\omega^2} \left\{ \varphi_{m+}^2 \left[k_m^2 ((\mu_z \gamma_0)_+ - (\mu_z \gamma_0)_-) - (\mu_z n_0^2 \gamma_0)_+ + (\mu_z n_0^2 \gamma_0)_- \right] + ik_m (\gamma_0 \varphi_{mz} \varphi_m)_+^2 (\mu_+ - \mu_-) \right\} \Big|_{z=h_0} \end{aligned}$$

Here point of interface $z = h_0$ is excluded from the integrals. Thus, in the case of low shear velocities, the problem reduces to the acoustic case with the correction in the form of three members, depending on μ . To illustrate the efficiency of our equation, we performed a numerical simulation of sound propagation, which shows that the elastic mode parabolic equation (1), despite the relatively small account of the shear modulus has the solution substantially different from the purely acoustic case.

The derived equation can be effectively used in seismoacoustics propagation problems, when the influence of elastic effects is essential.

References

- [1] A. H. Nayfeh, *Perturbation methods*, John Wiley and Sons, New York, London, Sydney, Toronto (1973).

Light scattering from smectic C* film with anisotropic electrostatic interaction

Ul'yanov S.V.

Saint Petersburg State University, Ul'yanovskaya, 1, Petrodvoretz, Saint Petersburg, 198504, Russia
e-mail: ulyanov_sv@mail.ru

This talk is devoted to description of light scattering from the thin freely standing smectic C* (Sm-C*) film or from the Sm-C* cell. Smectic C* liquid crystals are interesting due to their unusual physical properties and their possible practical applications [1]. The Sm-C* liquid crystals are formed by monomolecular layers composed by elongated molecules which are inclined relative to the normal to the layer. The averaged direction of preferred molecule orientation is given by the vector director \mathbf{n} , which is inclined at an angle θ relative to the normal \mathbf{N} to the smectic layers. At fixed temperature the angle θ is constant throughout the liquid crystal and each layer in Sm-C* can be regarded as two-dimensional liquid. All these properties are usual for the smectic C liquid crystals, but the symbol “*” means that the Sm-C* is formed by chiral molecules and additionally possesses spontaneous polarization. The polarization vector \mathbf{P} in each point of liquid crystal is perpendicular both to the normal \mathbf{N} , and the director \mathbf{n} . In a bulk Sm-C* when passing from layer to layer the vector \mathbf{P} rotates around the normal \mathbf{N} on definite angle, the same for all layers. The number of layers over which the vector \mathbf{P} obey the full rotation can vary from several to thousand layers in different Sm-C*. The director \mathbf{n} also uniformly rotates when passing from layer to layer forming a helical structure.

In thin free standing Sm-C* film or in thin cell the constant direction of polarization vector \mathbf{P} can be achieved by an external electric field or by small film thickness. These systems are considered here. The main contribution to the light scattering intensity arises from the director \mathbf{n} fluctuations which results in fluctuations of permittivity tensor $\varepsilon_{\alpha\beta}$. The provided calculations were based on the free energy of the film with taken into account not only the elastic energy and the interaction with weak external electric field, but also the anisotropic Coulomb interaction of polarization charges arising with the density $\rho = -\text{div } \mathbf{P}$ from the fluctuations of the polarization vector \mathbf{P} . For the correlation function of the director fluctuations it was obtained integro-differential equation which was solved by transformation to the system of differential equations. The angular dependencies of the light scattering intensity for various values of spontaneous polarization were calculated from the correlation function of director fluctuations. It was shown that the obtained results sufficiently depend on the anisotropy of the Coulomb interaction of polarization charges.

References

- [1] P. G. de Gennes, J. Prost, *The Physics of Liquid Crystals*, Clarendon Press, Oxford (1993).

Spacetime triangle diagram technique for sectoral horn waveguides

Utkin A.B.

INOV – Inesc Inovação, Rua Alves Redol 9, Lisbon 1000-029 Portugal;
CeFEMA, Instituto Superior Técnico, Technical University of Lisbon, Av. Rovisco Pais 1, 1049-001
Lisbon, Portugal
e-mails: andrei.utkin@inov.pt, andrei.outkine@gmail.com

Providing inherently causal solutions directly in the spacetime domain, the STTD (spacetime triangle diagram) technique has been successfully applied to solve a wide range of electromagnetic and scalar problems of wave motion. At the moment, the STTD methodology is developed for numerous models resulting in the wave and wave-like hyperbolic partial differential equations written in the Cartesian, cylindrical, and spherical coordinate systems [1]–[3]. In 2012, specific STTDs were constructed for the elliptic cylinder coordinate system [4], enabling the general solution to the causal

inhomogeneous problem of wave propagation in an elliptical waveguide to be found as an expansion in terms of transient Mathieu modes.

Based on preliminary theoretical considerations made by Borisov [1], the present study describes extension of the STTD technique to another practically important case (see, e.g., [5]) of the sectoral horn waveguide constrained top and bottom by two parallel planes (see Fig. 1).

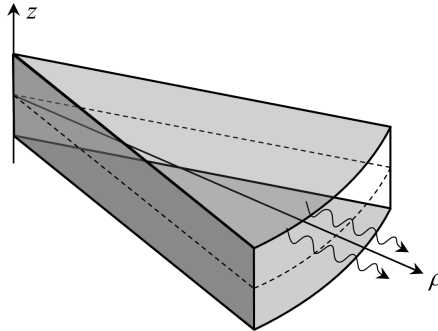


Fig. 1: Schematic representation of the sectoral horn waveguide.

The adopted methodology has the following specificity: (1) the consideration is carried out in the cylindrical (rather than spherical) coordinates (ρ, φ, z) , (2) the unseparated spatial variable is untraditional (coordinate ρ rather than z), (3) the model geometry does not possess angular symmetry, so the coordinate φ must be explicitly separated for any source configuration.

The modal expansions must match boundary conditions imposed on the lateral and top/bottom walls of the horn. Instantiation of these conditions depends on the physical meaning of the wavefunction, which may be an acoustic wave or an electromagnetic parameter resulted from some scalarization procedure.

References

- [1] V. V. Borisov, *Nonsteady-State Fields in Waveguides*, Leningrad State University Press, Leningrad (1991).
- [2] V. V. Borisov, *Electromagnetic Fields of Transient Currents*, Leningrad State University Press, Leningrad (1996).
- [3] A. B. Utkin, *Electromagnetic Waves Generated by Line Current Pulses*. In: *Wave Propagation*, InTech, Vienna, 483–508 (2011).
- [4] A. B. Utkin, *Wave Motion*, **49**, 347–363 (2012).
- [5] S. Pandey, R. A. Deshpande, S. Ranade, *IOSR Journal of Electronics and Communication Engineering*, **7**(6), 12–16 (2013).

Asymptotic distribution of the spectrum of some symmetric polynomials of unitary invariant random matrix ensembles

Vasilchuk V.

St. Petersburg State University of Architecture and Civil Engineering, 4, 2nd Krasnoarmeiskaya Str., St. Petersburg, 190005, Russia;

Peter the Great St. Petersburg Polytechnic University, 29, Polytechnicheskaya Str., St. Petersburg, 195251, Russia

e-mail: vvyu@yahoo.com

We consider the ensemble of $n \times n$ random matrices

$$H_n = (A_n + U_n^* B_n U_n)(A_n + U_n^* B_n U_n)$$

where A_n and B_n are hermitian random (or non-random), having the limiting Normalized Counting Measure (NCM) of eigenvalues, U_n is unitary, uniformly distributed over $U(n)$, and A_n , B_n and U_n

are mutually independent. By using the technique described in [1], we establish the convergence of NCM of ensemble H_n to the non-random limit and find the limiting NCM via its Stieltjes transform. The later is the unique solution of some system of functional equations written in terms of the Stieltjes transforms of the limiting NCM of A_n and B_n . We compare this result with the previous results obtained in [2] for the ensembles of commutator $i(A_n U_n^* B_n U_n - U_n^* B_n U_n A_n)$ and anticommutator $(A_n U_n^* B_n U_n + U_n^* B_n U_n A_n)$.

References

- [1] L. Pastur, M. Shcherbina, *Eigenvalue Distribution of Random Matrices*, Math. Surv. Monogr., **171**, RI: AMS (2011).
- [2] V. Vasilchuk, On the asymptotic distribution of the commutator and anticommutator of random matrices, *J. Math. Phys.*, **44**, 1882–1908 (2003).

The finite difference methods of computation of X-rays propagation through a system of many lenses

Wojda P.

Gdansk University of Technology, Gdansk, Poland
e-mail: pwojda@mif.pg.gda.pl

Kshevetskii S.P.

Baltic I. Kant Federal University, Kaliningrad, Russia
e-mail: spkshev@gmail.com

The propagation of X-ray waves through an optical system consisting of many beryllium X-ray refractive lenses is considered. In order to calculate the propagation of electromagnetic in the optical system, two differential equations are considered. First equation for an electric field of a monochromatic wave and the second equation derived for complex phase of the same electric field. For solving the problems, finite-difference methods are suggested and investigated.

It is shown that very small steps of the difference grid are necessary for reliable computation of propagation of X-ray waves through the system of lenses, when the first equation is used. The reason of such a result is that the electric field of the wave after passing through many lenses is a quickly oscillating function of coordinates. It is shown that much larger steps may be utilized if the second equation is used, because the phase of electric field after passing through many lenses is quickly increasing, but not oscillating function. We suggest and recommend using the equation for a phase function instead of the equation for an electric field. The error of simulation obtained for both equations is estimated mathematically and investigated.

Interaction of nonsymmetric electromagnetic waves guided by an anisotropic cylinder

N.F. Yashina, T.M. Zaboronkova

R. E. Alekseev State Technical University, 24 Minin St., Nizhny Novgorod 603950, Russia
e-mail: gematityash@rf.unn.ru

C. Krafft

Laboratoire de Physique des Plasmas, École Polytechnique, 91128 Palaiseau Cedex, France
e-mail: catherine.krafft@lpp.polytechnique.fr

Electromagnetic waves guided by cylindrical structures aligned with the gyrotropic axis have received much careful study (see, e.g., [1] and references therein). Parametric instability of axisymmetric waves guided by anisotropic cylinder in free space have been considered in [2, 3]. Here we

study the interaction of nonsymmetric waves guided by uniform anisotropic cylinder in the presence of an external electromagnetic wave. The interest in this problem is motivated by many practical applications ranging from ionospheric research to laboratory plasma experiments.

We consider the waves guided by an anisotropic infinitely extended cylinder filled with uniform magnetized plasma or a metamaterial. The cylinder is aligned with an anisotropic axis and surrounded by homogeneous isotropic medium. The medium inside the cylinder is described by a dielectric tensor with nonzero off-diagonal elements. The elements of the tensor are functions of frequency. The dispersion characteristics of guided waves whose fields depend on the azimuthal angle are analyzed. The instability of the guided waves propagating in the negative and positive directions of the z axis may be observed if the space-time and polarization conditions between the intense time-harmonic external electromagnetic field and the waves supported by cylinder take place. The equations for the amplitudes of interacted waves are obtained from the hydrodynamic and the Maxwell's equations. The expression for the instability increment of guided waves is found in the approximation of a weak nonlinearity. For the some practically interesting cases the results of the numerical calculations will be reported.

References

- [1] I. G. Kondrat'ev, A. V. Kudrin, T. M. Zaboronkova, *Electrodynamics of Density Ducts in Magnetized Plasmas*, Gordon and Breach, Amsterdam (1999).
- [2] N. F. Yashina, T. M. Zaboronkova, *Proceedings of the International Conference Days on Diffraction 2009*, 202–205 (2009).
- [3] N. F. Yashina, T. M. Zaboronkova, *Transactions of N. Novgorod State Technical University n.a. Alekseev*, **2**(109), 155–161 (2015).

Electromagnetic guided waves on infinite periodic linear arrays of thin metallic conductors

V. Zalipaev, V. Vialov

Krylov State Research Centre, St. Petersburg, Russia

e-mail: v.zalipaev1@lboro.ac.uk

Guided modes propagating along periodic structures have received considerable attention and, depending on the physical contexts, are known variously as edge waves [1], Rayleigh–Bloch surface waves [2], array-guided surface waves [3] or bound states. Most of this work has focused on two-dimensional problems. There have been previous studies of electromagnetic surface waves guided by periodic arrays, but these have concentrated on cases of spherical scatterers where the spheres can be modelled by some combination of electric and magnetic dipoles, see for example [4]. It is worth to mention an another example of guided electromagnetic waves propagating along one-dimensional arrays of dielectric spheres that was studied recently in [5] on the basis of a rigorous analysis of a wave field superposition of vector spherical wave functions.

In the paper guided electromagnetic waves propagating along one-dimensional periodic arrays of thin metallic conductors are studied semi-analytically. The conductors are assumed to be perfectly conducting, and their length is of the order of the wavelength. The approach makes extensive use of a well-known numerical analysis of method of integral equations in two different forms of Pocklington and Hallen integral formulations to make a comparison between results. An approximation being used in the analysis is based on the assumption of presence of low parameter, i. e. that the ratio conductor radius to wavelength is much less than one. The quasi-periodic wave field is constructed as a superposition of wave fields generated by linear electric currents that satisfies the boundary conditions on the surfaces of the conductors leading to an infinite system of real linear algebraic equations. The vanishing of the determinant of the associated infinite matrix provides the condition

for surface waves to exist and these are determined numerically. Our numerical analysis is based on the accurate and efficient computation of lattice sums.

The work described here is a complete analysis, based on the full Maxwell equations, of traveling electromagnetic waves propagating along linear arrays of thin metallic conductors in the absence of any incident field. We also demonstrate that a suitable truncation of the full system is precisely equivalent to the dipole approximation that has been used previously by other authors. Our goal is to provide a thorough study of the modes that can exist. The problem is a natural extension of the equivalent electromagnetic problem [5] and, as in that case, there is a cut-off frequency below which waves cannot radiate energy away from the array. The modes that we seek have frequencies below this cut-off and decay exponentially as one moves away from the array.

References

- [1] D. V. Evans, C. M. Linton, Edge waves along periodic coastlines, *Q. J. Mech. Appl. Math.*, **46**(4), 642–656 (1993).
- [2] R. Porter, D. V. Evans, Rayleigh–Bloch surface waves along periodic gratings and their connection with trapped modes in waveguides, *J. Fluid Mech.*, **386**, 233–258 (1999).
- [3] D. S. Janning, B. A. Munk, Effects of surface waves on the currents of truncated periodic arrays, *IEEE Trans. Antennas Propagat.*, **50**(9), 1254–1265 (2002).
- [4] R. A. Shore, A. D. Yaghjian, Traveling electromagnetic waves on linear periodic arrays of lossless penetrable spheres, *IEICE Trans. Commun.*, E88-B(6), 2346–2352 (2005).
- [5] C. M. Linton, V. Zalipaev, I. Thompson, Electromagnetic guided waves on linear arrays of spheres, *Wave Motion*, **50**(1), pp. 29–40 (2013).

A fractal graph model of capillary type systems

German L. Zavorokhin

PDMI RAS, St. Petersburg, Russia

e-mail: germanzavorokhin@rambler.ru

This work was done in cooperation with V. A. Kozlov (Linköping University, Sweden) and S. A. Nazarov (St. Petersburg State University and Institute for Problems in Mechanical Engineering, St. Petersburg, Russia).

The capillary system is modelled by a fractal graph attached to a blood vessel. It is supplied with differential equations obtained from three-dimensional model by the dimension-reduction procedure. The geometry and physical parameters of this system are described by a finite number of scaling parameters which allows for system to have self-reproducing solutions, solutions which are determined by their values on a certain finite piece of the fractal graph and are continued on the remaining part by using these scaling factors. We describe all self-reproducing solutions and, as a result we obtain a connection between the pressure and the flux at the junction point between the capillary system and blood vessel. This connection gives an artificial boundary condition at the junction in the blood vessel and allows to solve the problem for the flow in the blood vessel without solving it in the capillary system.

The present work is supported by Linköping University and RFBR grant 15-31-20600 mol-a-ved.

References

- [1] C. D’Angelo, G. Panasenko, A. Quarteroni, Asymptotic-numerical derivation of the Robin type coupling conditions for the macroscopic pressure at a reservoir-capillaries interface, *Appl. Anal.*, V. **92**(1), pp. 158–171 (2013).
- [2] S. A. Nazarov, K. I. Pileckas, Reynolds flow of a fluid in a thin threedimensional channel, *Litovsk. mat. sbornik*, V. **30**(4), pp. 772–783 (1990); English transl.: *Lithuanian Math. J.*, V. **30**(4), pp. 366–375 (1990).

- [3] S. A. Nazarov, J. H. Videman, Reynolds type equation for a thin flow under intensive transverse percolation, *Math. Nachr.*, Bd. 269/270, S. 189–209 (2004).
- [4] V. A. Kozlov, S. A. Nazarov, G. L. Zavorokhin, A fractal graph model of capillary type systems, arXiv:1511.05554 (2015).

Guided modes and surface plasmon exploration of cholesteric liquid crystal cell

K. Zhelyazkova¹, M. Petrov³, B. Katranchev³, G. Dyankov^{1,2}

¹Faculty of Physics, Plovdiv University “Paisii Hilendarski”, 24 Tzar Assen Str, 4000 Plovdiv, Bulgaria

²Institute of Optical Materials and Technologies, Bulgarian Academy of Sciences, 109 Acad. G. Bontchev Str., 1113 Sofia, Bulgaria

³Institute of Solid State Physics, Bulgarian Academy of Sciences, 72 Tzarigradsko shosse Blvd, 1784 Sofia, Bulgaria

e-mail: katiajeliyazkova@abv.bg

Optical excitation of guided modes and surface plasmon has been used for characterization nematic liquid crystal layer. In this theoretical study we apply this method, for the first time to our knowledge, to explore cholesteric liquid crystal layer. A series of guided modes and surface plasmon are excited at the condition of attenuated total reflection. The structure we consider consists in prism with a thin gold layer, the liquid crystal layer and a glass substrate. The prism has the highest refractive index, whereas the substrate — the lowest. The liquid crystal is uniaxial and specified by the permittivities parallel and perpendicular to the director. The theoretical study is performed with a general anisotropic multilayer modeling program.

The structure we consider has two main differences, compared with the nematic liquid crystal cell: i) the twist angle is a function of layer’s thickness; ii) the pitch of the helical structure defines how the wavelength “sees” the refractive index profile of the liquid crystal layer. Bearing in mind these special features we propose a new definition of the critical angles for extraordinary modes. We propose to use “effective critical angle” defined in terms of ratio pitch/wavelength. The effective critical angle explains very well the dependence of number of guided modes on tilt angle and on pitch.

The plasmon, excited on the surface gold/liquid crystal, depends on the director tilt and pitch of helical structure. On purpose to explain these dependences we introduce “effective refractive index” defined again in terms of ratio pitch/wavelength. Thereby a coupling plasmon-guided mode is explained. A theoretical comparison with different modeling methods confirms the correctness of our approach.

Our study shows that the guided modes structure in cholesteric liquid crystal layer and plasmon, excited on the boundary metal/liquid crystal are very sensitive to the cholesteric liquid crystal structure and can be used for exploration of anisotropic liquid-crystal layers.

Wave propagation in a floating elastic plate with a periodic support

Zhuchkova M.G.

Institute for Problems in Mechanical Engineering, Russian Academy of Sciences, V.O., Bolshoj pr., 61, St. Petersburg, 199178

e-mail: m.zhuchkova@list.ru

We consider a thin elastic plate floating on the surface of an ideal incompressible fluid. The plate is movably clamped along infinitely long parallel straight-lines periodically spaced in the horizontal coordinate with an equal separation. Time-harmonic flexural-gravitational waves propagating with-

out attenuation along the interface between the fluid and the plate are studied. The passing and stopping bands having been found under a thin fluid layer approximation are shown in Fig. 1.

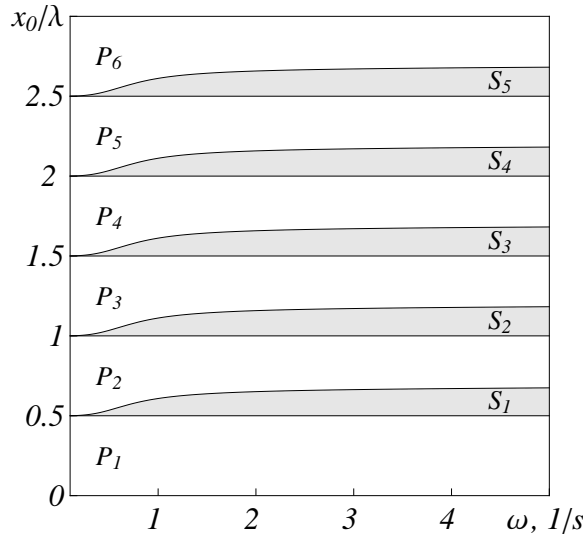


Fig. 1: The passing (P) and stopping (S) bands in relation to the frequency ω and the spacing x_0/λ between the movable clamps (λ is the wave length). The plate density $\rho = 917 \text{ kg/m}^3$, the Young's module $E = 4.2 \cdot 10^9 \text{ N/m}^2$, the Poisson ratio $\nu = 0.3$, the thickness of the plate $h = 1.6 \text{ m}$, the thickness of the fluid layer $h_1 = 50 \text{ m}$, the density of the fluid $\rho_1 = 1000 \text{ kg/m}^3$.

References

- [1] G. V. Filippenko, The bending waves in the beam with periodically located point masses, *Computational continuum mechanics*, Vol. **8**, no. 2, pp. 153–163 (2015).
- [2] E. Glushkov, N. Glushkova, J. Wauer, Wave propagation in an elastically supported string with point-wise defects: gap-band and pass-band effects, *Z. Angew. Math. Mech.*, Vol. **91**, issue 1, pp. 4–22 (2011).
- [3] A. V. Marchenko, Swell wave propagation in an inhomogeneous ice sheet, *Fluid Dynamics*, Vol. **31**, no. 5, pp. 761–767 (1996).
- [4] R. Porter, D. V. Evans, Scattering of flexural waves by multiple narrow cracks in ice sheets floating on water, *Wave Motion*, Vol. **43**, issue 5, pp. 425–443 (2006).
- [5] S. V. Sorokin, O. A. Ershova, Plane wave propagation and frequency band gaps in periodic plates and cylindrical shells with and without heavy fluid loading, *Journal of Sound and Vibrations*, Vol. **278**, issue 3, pp. 501–526 (2004).
- [6] M. G. Zhuchkova, D. P. Kouzov, The transmission of a flexural-gravitational wave through several straight obstacles in a floating plate, *J. Appl. Math. Mech.*, Vol. **78**, no. 4, pp. 359–366 (2014).

Phase images of living lymphocytes and its quantitative parameters obtained from optical model

V. Zverzhcovsky, A. Bolotova, A. Kretushev, T. Vyshenskaya
 Moscow technological university (MIREA)
 e-mail: andreevna@mail.ru

Phase microscopy is one of the most dynamically developing areas of optical microscopy. A number of features makes it promising to work with transparent biological objects (as living cells are), especially the possibility to determine the index of refraction of its internal structures in the phase image. Extracting this information and presentation in an easy to use form is an urgent task of phase microscopy. For this purpose, it can be used the following approach: the object is associated with the

optical model, for which the parameters of an object are determined. To determine the parameters of the internal structures of T-lymphocytes, the following method is used: T-lymphocytes are associated with a model objects, consisting of concentric spherical layers corresponding to the outer cytoplasm, dense cytoplasm, nucleus and nucleolus. Thus, from the phase image of T-lymphocytes can be obtained square, phase height and phasevolume of the organelles, the average refractive indices of the organelles, and a number of parameters that characterize the cell as a whole: the degree of cell energization, nuclear-cytoplasmic ratio, the degree of compaction of chromatin in the nucleus, cytoplasm density. The effectiveness of the methodology is illustrated by experimental results (CD4+ and CD8+ T-lymphocytes of donors and patients with multiple sclerosis).

Workshop on Nanophotonics and Metamaterials

Theoretical analysis of material body cloaking problems using the optimization method

Alekseev G.V.^{1,2}, Lobanov A.V.¹, Larkina O.S.²

¹Institute of Applied Mathematics FEB RAS, 7, Radio St., Vladivostok, 690041, Russia

²Far Eastern Federal University, D(20), pen. Ayaks, i. Russky, Vladivostok, 690922, Russia

e-mails: alekseev@iam.dvo.ru, alekslobanov1@mail.ru

In recent years significant research has focused on design of invisibility cloaking devices for material bodies. Beginning with pioneering papers [1, 2] the large number of publications was devoted to developing different methods of solving the cloaking problems. It should be emphasized that the technical realization of solutions obtained in these papers is connected with substantial difficulties. One of approaches of overcoming these difficulties consists of replacing the exact cloaking problem by approximate cloaking problem for which solutions admit simple technical realization. Another approach is based on using the optimization method of solving inverse problems. This method was applied in papers [3, 4] devoted to numerical analysis of 2D cloaking problems and in [5, 6] when studying impedance cloaking problems. The approach is based on introducing the cost functional under minimization which adequately corresponds to inverse problem of constructing a device for approximate cloaking. As a result initial cloaking problem is reduced to study of respective control problem using well known methods of theory of extremum problems. Optimization method is applied and in this paper for theoretical analysis of cloaking problems. More precisely: we consider control problems for the 2D electromagnetic field model describing scattering TM-polarized electromagnetic waves in unbounded homogeneous medium containing an inhomogeneous permeable obstacle with the boundary partially coated for masking. These problems are associated with solving cloaking problems for respective scattering model. Two functional parameters: variable refraction index and surface conductivity of the coated part of the boundary play the role of controls. Solvability of control problems is proved, the optimality system which describes the necessary conditions of extremum is derived, uniqueness and stability of optimal solutions are established, numerical algorithms based on analysis of optimality system are proposed. The similar results are obtained while theoretical analysis of acoustic cloaking problems in which the cloaking effect is achieved due choice of variable parameters of inhomogeneous isotropic liquid medium filling the acoustic cloaking shell.

This work was financially supported by the Russian Science Foundation (project no 14-11-00079) and Program of Fundamental Research of Far Eastern Branch of Russian Academy of Sciences “Far East” (project no 15-1-4-036).

References

- [1] L. S. Dolin, *Izvestiya Vuzov. Radiofizika*, **4**, 964–967 (1961).
- [2] J. B. Pendry, D. Shurig, D. R. Smith, *Science*, **312**, 1780–1782 (2006).
- [3] B.-I. Popa, S. A. Cummer, *Phys. Rev. A*, **79**, 023806 (2009).
- [4] Z. Yu, Y. J. Feng, X. F. Xu, J. M. Zhao, T. Jiang, *J. Phys. D: Appl. Phys.*, **44**, 185102 (2011).
- [5] G. V. Alekseev, *Dokl. Phys.*, **58**, 147–151 (2013).
- [6] G. V. Alekseev, *Appl. Anal.*, **93**, 254–268 (2014).

Advantages of quantum dot arrays for non-algorithmic information processing by quantum neural networks

Altaisky M.V.¹, Kaputkina N.E.², Krylov V.A.³

¹Space Research Institute RAS, Profsoyuznaya 84/32, Moscow 117997, Russia

²National University of Science and Technology “MISIS”, Leninsky prospect 4, Moscow 119049, Russia

³Joint Institute for Nuclear Research, Joliot Curie 6, Dubna 141980, Russia

e-mails: altaisky@mx.iki.rssi.ru, nataly@misis.ru, kryman@jinr.ru

The concept of quantum neural computation was first formulated by S. Kak in 1995 [1] as a model for animal intelligence, although the functioning model of brain as a quantum neural network (QNN) was given earlier in [2]. Later the concept of QNN have been developed by many authors, see [3] for a review. It was shaped into mathematical model of an artificial neural network, where each neuron is fed by a quantum state with certain phase and amplitude, rather than by a classical signal. The first commercial implementation of a scalable hardware for QNN was built on SQUID-based Hopfield network by D-wave Systems Ltd. [4]. The drawback of SQUID-based QNN is its low working temperature in the mK range, which demands kW of power for cooling. As alternative elements of QNN, which may substitute SQUIDS in future, the quantum dot (QD) arrays have been considered since 2000 [5]. The advantages of QDs, as prospective QNN elements, as well as for quantum information processing in general, are the high working temperature (up to $\sim 10^2$ K range), the acceptability of optical input signals, reliable output readout, fine tuning of QD parameters by external fields, and high density of QDs on substrate, if compared to SQUIDS.

In this paper we review some of our developments in simulation of QD based QNN [6], as well as other current developments aimed to *in silico* implementation of QNN working at room temperatures, and also the mathematical problems that can be efficiently solved by such devices due to inherent quantum parallelism.

References

- [1] S. Kak, On quantum neural computing, *Inf. Sci.*, **83**: 143–160, 1995.
- [2] V. Chavchanidze, On spatial-temporal quantum-wave processes in neural networks, *Soobshch. AN Gruzinskoi SSR*, **59**(1): 37–40, 1970.
- [3] M. V. Altaisky, N. E. Kaputkina, V. A. Krylov, Quantum neural networks: State of art and perspectives of development, *Physics of Particles and Nuclei*, **45**(6): 1013–1032, 2014.
- [4] M. W. Johnson *et al.*, Quantum annealing with manufactured spins, *Nature*, **473**: 194–198, 2011.
- [5] E. C. Behrman, L. R. Nash, J. E. Steck, V. G. Chandrashekar, S. R. Skinner, Quantum dot neural networks, *Inf. Sci.*, **128**: 257–269, 2000.
- [6] M. V. Altaisky, N. N. Zolnikova, N. E. Kaputkina, V. A. Krylov, Yu. E. Lozovik, N. S. Dattani, Towards a feasible implementation of quantum neural networks using quantum dots, *Appl. Phys. Lett.*, **108**(11), 2016.

Water based tunable all-dielectric microwave metamaterials

Andryieuski A.^{1,2}, Kuznetsova S.M.³, Odit M.⁴, Zhukovsky S.V.^{2,4}, Kapitanova P.⁴, Kivshar Y.S.^{4,5}, Lavrinenko A.V.²

¹Laserscom LLC, Minsk, Belarus

²DTU Fotonik, Technical University of Denmark, Kgs. Lyngby, Denmark

³Radiophysics Department, University of Nizhny Novgorod, Nizhny Novgorod, Russia

⁴Department of Nanophotonics and Metamaterials, ITMO University, St. Petersburg, Russia

⁵Nonlinear Physics Center, Australian National University, Canberra ACT, Australia

e-mails: andrandr@gmail.com, alav@fotonik.dtu.dk

In this talk we discuss an outstanding potential of water as a cheap and ecological high-refractive-index material for creating tunable all-dielectric [1] microwave structures and metamaterials. Water

being a dielectric liquid with large permittivity depending on temperature, however, has not been considered as a building material for microwave metamaterial until recently [2, 3]. We suggest various types of tuning transmission by mechanical compression or stretching, rotation and heating metamaterial's constitutive elements (Fig. 1). Numerical simulations are supported by transmission measurements in microwave range. The proposed water-based metamaterials can find applications not only as inexpensive and bio-friendly microwave devices, but also in optical and terahertz metamaterials prototyping and educational lab equipment.

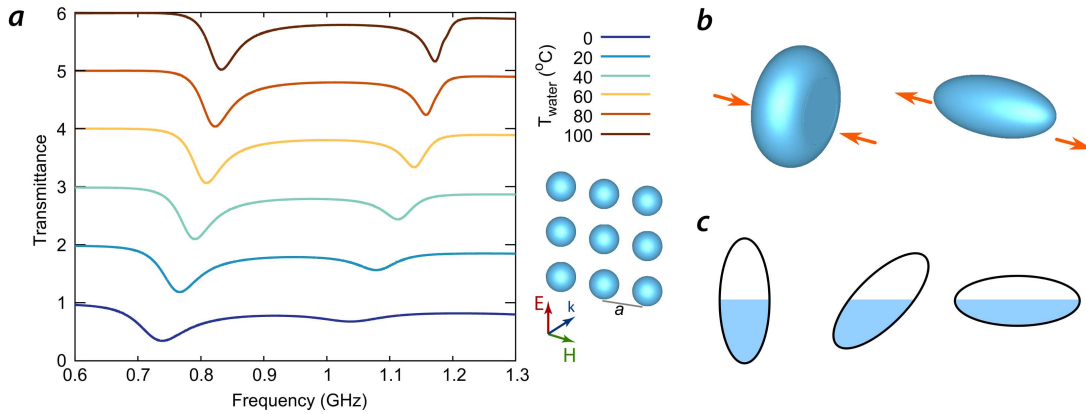


Fig. 1: (a) Example of tuning transmittance through a single layer of spherical water-filled cavities of the radius 2.2 cm arranged in a square lattice with the period 7.5 cm by changing their temperature from 0 to 100° C. Mechanical tunability can be achieved by compression or stretching (b) as well as rotation (c) of the metamaterials constitutive elements.

References

[1] A. Krasnok, S. Makarov, M. Petrov, R. Savelev, P. Belov, Y. Kivshar, *SPIE Optics + Optoelectronics*, **950203**, 950203-17 (2015).
 [2] A. Andryieuski, S.M. Kuznetsova, S.V. Zhukovsky, Yu.S. Kivshar, A.V. Lavrinenko, *Scientific Reports*, **5**, 13535 (2015).
 [3] M.V. Rybin, D.S. Filonov, K.B. Samusev, P.A. Belov, Y.S. Kivshar, M.F. Limonov, *Nature Communications*, **6**, 10102 (2015).

Substrate-mediated antireflective properties of silicon nanoparticle array

Babicheva V.E.^{1,2}, Petrov M.I.¹, Baryshnikova K.V.¹, Belov P.A.¹

¹ITMO University, Kronverkskiy, 49, St. Petersburg 197101, Russia

²Center for Nano-Optics, Georgia State University, P.O. Box 3965, Atlanta, GA 30302

e-mail: v.babicheva@phoi.ifmo.ru

We theoretically study silicon metasurfaces on the dielectric substrates with different permittivities [Fig. 1] and show that such system demonstrates broadband zero reflectance for wavelengths between the electric and magnetic dipole resonances. It originates from the destructive interference between the wave reflected from the substrate and the waves scattered by induced electric and magnetic dipole moments of the nanoparticles [1]. We show that this condition is satisfied for the wavelength between electric and magnetic dipole resonances, when their moments are shifted in phase by π . The anti-phase Kerker condition is opposite to more common in-phase condition, which results in strong forward scattering from metasurface, when electric and magnetic dipoles are in-phase.

The cumulative reflection of almost independent nanoparticle scatterers provides the antireflectance effect and makes it tolerant with respect to inter-particle distance distortions. In particular, we design the structure with disordered array of nanospheres and numerically demonstrated a broadband reflection suppression: the reflectance is less than 10% at 300–650 nm wavelength range, which

is better than standard quarter-wavelength layer of silicon nitride [Fig. 1(d)]. The main mechanism, namely the possibility of destructive interference between substrate-reflected and multipole-scattered waves, can be used to suppress reflection in either narrow or broad spectral bands [2].

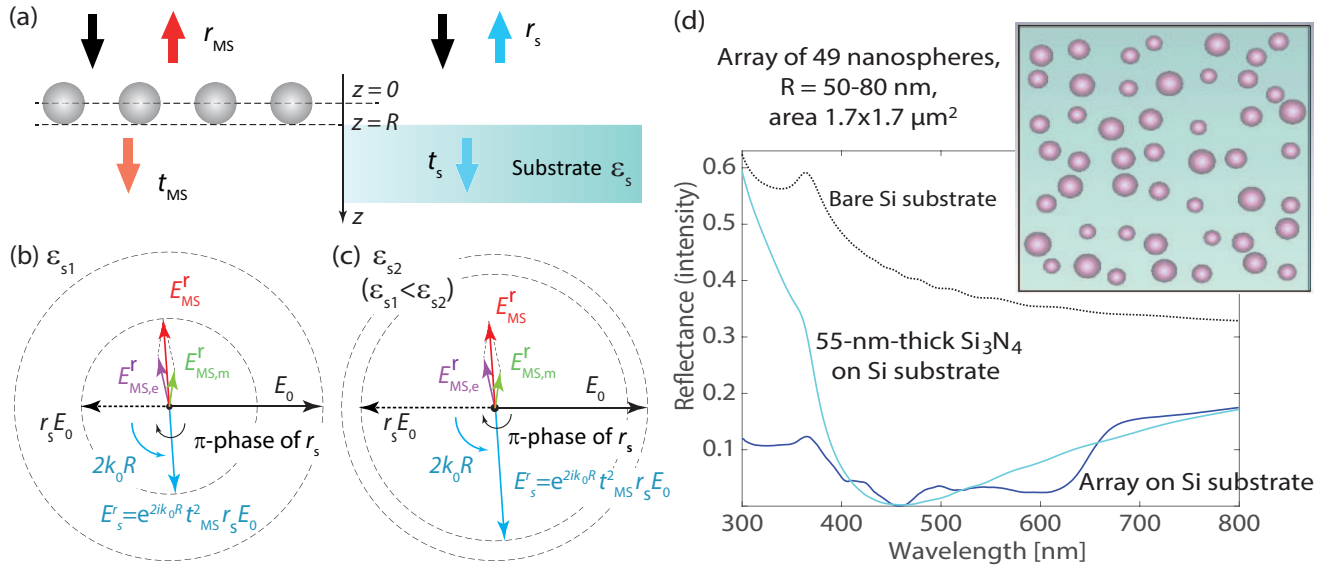


Fig. 1: (a) Decomposition of the structure into the metasurface: nanoparticle array and the substrate. (b), (c) Artistic view of vector diagrams depicting electric field of the incident wave E_0 and reflected field E_s^r for two different cases: (b) perfect match of reflected waves and near-zero reflectance and (c) non-zero reflectance. (d) Reflectance spectrum for disordered array of silicon nanospheres on top of Si substrate in comparison to reflectance from bare Si substrate and from 55-nm-thick Si₃N₄ layer on top of the Si substrate. Inset: top view on simulation domain with 49 nanospheres of radiuses $R = 50-80$ nm. 55-nm-thick Si₃N₄ layer is chosen as an optimal single-layer antireflective coating that provides reflectance minimum at wavelength 470 nm and matches reflection minimum of nanoparticle array under consideration.

References

- [1] M. Petrov, V. Babicheva, K. Baryshnikova, P. Belov, arXiv:1511.08473 [physics.optics] (2015).
- [2] K. V. Baryshnikova, M. I. Petrov, V. E. Babicheva, P. A. Belov, *Scientific Reports*, **6**, 22136 (2016).

Experimental characterization of microwave self-complimentary metasurfaces for linear-to-circular polarization transform

J.D. Baena¹, S.B. Glybovski², J.P. del Risco¹, A.P. Slobozhanyuk², P.A. Belov²

¹Universidad Nacional de Colombia, Bogota 111321, Colombia

²ITMO University, St. Petersburg 197101, Russia

e-mail: s.glybovski@metalab.ifmo.ru

Metasurfaces are artificial electromagnetic boundaries usually implemented as two-dimensional periodic arrays of engineered inclusions with sub-wavelength periodicity. Due to the capability to control electromagnetic field distributions electrically thin metasurfaces have recently become useful tools performing various manipulations with an incident wave front [1]. Therefore, design and characterization techniques for metasurfaces are of a high importance.

It was found by the authors that the transformation of a linearly-polarized plane wave into a circularly-polarized one can be easily achieved employing a broad class of self-complimentary metasurfaces with a negligible thickness [2]. Self-complimentary metasurfaces are thin metal sheets patterned

in such a way that these structures are identical to their complements (the inverse patterns), except for some translation smaller than the periodicity. The particular symmetry of self-complimentary patterns ensures linear-to-circular polarization conversion, which significantly simplifies the design of thin polarizers as compared to previous approaches. Advantageously, these self-complimentary polarization transformers require only a single patterned metal sheet. Therefore, the proposed design technique is unique for microwave, submillimeter and terahertz applications. In the microwave range self-complimentary metasurfaces can be realized by printing a periodic metal pattern on a dielectric substrate. By engineering the shape of the pattern's unit cells it is possible to obtain a required bandwidth, i.e. to make the polarization transform narrow- or wideband.

In this work we compare several practical designs of self-complimentary metasurfaces having different frequency responses and show their experimentally realized polarization transform properties. We stress on the influence of manufacturing constraints on their performance. Also we discuss the principles of their correct experimental characterization in the microwave range by measurements of complex reflection and transmission coefficients in an anechoic chamber (see Fig. 1).

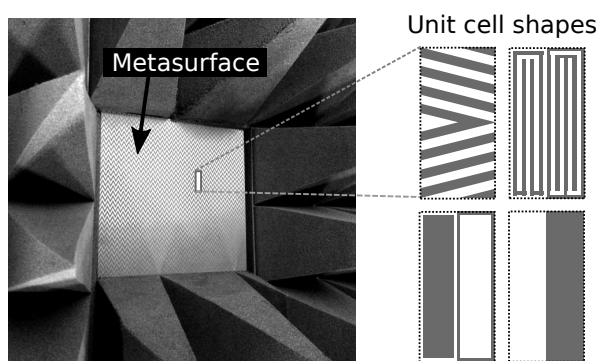


Fig. 1: Microwave experimental characterization (left) and various unit-cell designs (right) of self-complimentary metasurfaces.

References

- [1] N. Yu, F. Capasso, *Nat. Mater.*, **13**, 139 (2014).
- [2] J.D. Baena, J.P. del Risco, A.P. Slobzhanyuk, S.B. Glybovski, P.A. Belov, *Phys. Rev. B*, **92**, 245413 (2015).

Attenuated total reflection spectroscopy of hybrid localized optical surface states in anisotropic metasurface

D.A. Baranov¹, R. Malureanu², O. Takayma², A.K. Samusev¹, I.V. Iorsh¹, A.A. Bogdanov¹, A.V. Lavrinenko¹

¹ITMO University, 197101, St. Petersburg, Russia

²Technical University of Denmark, 2800 Kgs. Lyngby, Denmark

e-mail: dbaranov@metalab.ifmo.ru

Significant advance in the field of nanophotonics has been achieved with the help of metamaterials — artificially created composite structures, whose electromagnetic properties drastically differ from the properties of the natural materials. Engineering of the metamaterials allows one to control their optical properties. A compatible with modern planar fabrication two-dimensional analogue of a metamaterial is a metasurface, i.e. planar periodic structure with controllable electromagnetic properties in a predefined frequency band. Along with unprecedented control over propagation of bulk optical waves, metasurfaces can support surface waves [1].

In this work we have observed experimentally hybrid localized waves predicted and described in Ref. [2]. The dispersion relation derived in that work predicts the existence of unusual localized modes with hybrid polarization, which are surface-plasmon-like surface waves.

The considered metasurface consisted of a periodic array of gold nanocylinders on the fused silica substrate. Finite-difference time domain simulation technique was applied to optimize the anisotropic metasurface. The chosen method allows for reconstruction of the entire eigenspectrum of the structure in desired spectral range.

Solving eigenvalue-like problem for a unit cell, excited by randomly distributed point dipoles we have reconstructed the entire dispersion diagram in visible/near-infrared band and found the dispersion branches corresponding to the hybrid localized waves.

The fabricated optimized metasurface is a square periodic array of nanocylinders with an elliptical base covered by 200 nm layer of the photoresist with the index of refraction matched to one of SiO₂.

Using the hemi-cylindrical high-index prism we have measured the angular dependence of attenuated total internal reflection spectra of the high-index prism with coupled metasurface (so called, Otto geometry), which is a common method of surface waves observation.

We have performed the measurements in both TE and TM polarizations and both main directions of a metasurface unit cell. After, we have partially reconstructed the dispersion diagrams of localized surface states along two main axis. As the experimental results fitted well the dispersion diagram calculated by FDTD we were enabled to reconstruct the isofrequency contours of the anisotropic metasurface and have shown that the topological transition occurs at certain wavelength.

Our experimental results confirm that the anisotropic resonant metasurface supports both TE- and TM-polarized surface waves. We also observe a topological transition from elliptic to hyperbolic regime at certain wavelength. We believe that our results open new ways for application of hyperbolic metasurfaces in optical and optoelectronic devices.

References

- [1] Yu. Nanfang, F. Capasso, *Nature materials*, **13**(2), 139–150 (2014).
- [2] O. Y. Yermakov, A. I. Ovcharenko, M. Song, A. A. Bogdanov, I. V. Iorsh, Y. S. Kivshar, *Phys. Rev. B*, **91**, 235423 (2015).

Nonradiating anapole modes of dielectric nanoparticles in microwave range

Baryshnikova K.V.¹, Shalin A.S.¹, Terekhov P.D.¹, Khromova I.A.^{1,2,3}, Evlyukhin A.B.^{1,4}

¹ITMO University, Kronverkskii prospect 49, 197101 Saint-Petersburg, Russia

²Department of Physics, KCL, London, WC2R 2LS, U.K.

³Department of Electronic & Electrical Engineering, UCL, London, WC1E 7JE, U.K.

⁴Laser Zentrum Hannover e.V., Hollerithallee 8, D-30419 Hannover, Germany

e-mail: k.baryshnikova@metalab.ifmo.ru

Nonradiating current configurations attract attention of physicists and engineers for many years as possible systems for effective cloaking and camouflage. One intriguing example of such a nonradiating source is known as ‘anapole’. Recently, an anapole was suggested as a classical model of elementary particles describing dark matter in the Universe. The electrodynamics analogue of the anapole is a composition of electric and toroid dipole moments. The classical analogue of a stationary anapole is the toroidal nanoparticle. Toroidal moment irradiation can destructively interfere with the dipole one with total suppressing of far-field radiation [1, 2]. Recently it was shown that in dielectric nanocylinders anapole modes could be excited in the visible range [1].

Here we demonstrate that TiO₂ nanoparticles can exhibit a radiationless anapole mode in microwave range. We achieve the spectral overlapping of the toroidal and electric dipole modes through a geometry tuning, and observe a highly pronounced dip in the far-field scattering accompanied by the specific near-field distribution associated with the anapole mode. Possibility of toroidal and electric dipole modes overlapping at the resonant frequency with total suppressing of scattering spectral resonances is also considered.

The anapole physics provides a unique playground for the study of electromagnetic properties of nontrivial excitations of complex fields.

References

- [1] A. E. Miroshnichenko, *et al.*, Nonradiating anapole modes in dielectric nanoparticles, *Nat. Commun.*, **6**, 8069 (2015).
- [2] A. A. Basharin, *et al.*, Dielectric metamaterials with toroidal dipolar response, *Phys. Rev. X*, **5**, 011036 (2015).

Time resolved ultrafast surface plasmon-polaritons

Tobias Birr

Laser Zentrum Hannover e.V. Hollerithallee 8 30419 Hannover Germany
e-mail: t.birr@lzh.de

We present studies on ultrafast interactions of multiple coherently excited surface plasmon-polaritons (SPPs) in waveguiding systems and on plane metal films. SPPs are excited by local scattering of laser light on surface nanostructures consisting of polymeric or metallic ridges [1]. SPP interaction and scattering effects are investigated by temporally resolved leakage radiation microscopy. This technique enables to visualize and measure time resolved behavior of propagation effects, as the Gouy phase shift along a 2D Gaussian focus [2]. Further 2D scattering effects of dielectric nanoparticles, generated with laser induced transfer [3, 4], on plane metal films are presented. In addition, we demonstrate ultrafast interactions of coherently excited SPPs and light beams in complex dielectric waveguides [5]. Coherent control of SPP and light interactions further allow for the construction of ultrafast low-power SPP switches and all-optical gate structures [6]. These structures were investigated experimentally regarding their efficiency depending on their geometrical properties. The measurement results have been compared with FDTD simulations of the same structures and were used to design novel plasmonic half adders which functionality has been demonstrated experimentally [6].

References

- [1] C. Reinhardt *et al.*, *Appl. Phys. A*, **89**, pp. 321–325, 2007.
- [2] A. B. Evlyukhin, S. I. Bozhevolnyi, *Opt. Express*, **16**, pp. 17429–17440, 2008.
- [3] U. Zywietz *et al.*, *Nat. Commun.*, **5**, 3402, 2014.
- [4] U. Zywietz *et al.*, *Appl. Phys. A*, **114**, pp. 45–50, 2014.
- [5] T. Birr *et al.*, *Appl. Phys. B*, (accepted with minor revisions).
- [6] T. Birr *et al.*, *Optics Express*, **23**, pp. 31755–31765, 2015.

Characterization of the structure and stimulated emission of spherical and cylindrical spasers

Benimetskiy F.A.¹, Plekhanov A.I.¹, Kuchyanov A.S.¹, Parkhomenko R.G.², Basova T.V.²

¹Institute of Automation and Electrometry, 1 Acad. Koptug Ave., Novosibirsk, Russia, 630090

²Institute of Inorganic Chemistry, 3 Acad. Lavrentiev Ave., Novosibirsk, Russia, 630090

e-mail: benimetskiy@iae.nsk.su

Over the last decade, nanophotonics is undergoing rapid development. One of the main directions in the field of nanophotonics is the development of new classes of plasmonic structures and metamaterials as potential building blocks for advanced optical technologies, including processing, sharing and storing data, to create a new generation of cheap sensors with high sensitivity, the development of imaging techniques with nanoscale resolution, new concepts of energy conversion, including improved solar panels, as well as being for possible use in biomedical applications. One of the most promising areas of research is nano-sized optical light sources, allowing to overcome the diffraction limit. These sources are plasmonic nanolasers, known as Spaser (acronym for Surface Plasmon Amplification by Stimulated Emission of Radiation).

The spaser concept was first proposed by Mark Stockman and David Bergman in 200 [1]. Spasers have been proposed as a near-field generator and amplifier of nano-localized optical fields. And these nano-optical devices based on the surface plasmons (SP) when the free surface electrons collectively oscillate, driven by light. These oscillations display localized (localized surface plasmons, LSP) and propagating type (surface plasmon polaritons, SPP). Spasers have been realized for LSP [2] and SPP [3] themselves. In this feature article, we review mainly our studies on spaser which consists of a metal nano-particle, which plays the role of a laser resonator, and the active medium, which is the energy donor for the localized surface plasmons. Spasers due to the unique properties have many potential practical applications such as ultrasensitive detection, spectroscopy of chemical. They are potentially able to be a novel versatile biomedical tool [4], etc.

We have fabricated spherical and cylindrical spasers with gold core and silica dye-embedded shell and characterized them with the use of transmission electron microscopy, confocal microscopy and thermogravimetry. We have studied the stimulated emission of spherical and cylindrical spasers with the different aspect ratio, which allowed to significantly expand the spectral range of the spasing. We have shown that the stimulated emission threshold was about 250 kW/cm² for spherical spasers and some less for cylindrical ones. The spasing signature can be also seen from the concurrent onset of the line width narrowing plateau and the nonlinear kink of the “S”-shape L-L plot shows the output power of the spasing mode as a function of pump power. In addition, emission dynamics obtained for spherical spasers at a wavelength of 526 nm showed that the pulse is shortened at excess pumped critical threshold.

This work was supported by RFBR 15-03-03833 and 16-32-00710 mol_a.

References

- [1] D. J. Bergman, M. I. Stockman, *Phys. Rev. Lett.*, **90**, 027402 (2003).
- [2] M. A. Noginov, G. Zhu, A. M. Belgrave, R. Bakker, V. M. Shalaev, E. E. Narimanov, S. Stout, E. Herz, T. Suteewong, U. Wiesner, *Nature*, **460**, 1110–1112 (2009).
- [3] R. F. Oulton, V. J. Sorger, T. Zentgraf, R. M. Ma, C. Gladden, L. Dai, G. Bartal, X. Zhang, *Nature*, **461**, 629–632 (2009).
- [4] E. I. Galanzha, R. Weingold, D. A. Nedosekin, M. Sarimollaoglu, A. S. Kuchyanov, R. G. Parkhomenko, A. I. Plekhanov, M. I. Stockman, V. P. Zharov, *arXiv*, 1501.00342 (2015).

Silicon: an interesting material for optical antennas

Nicolas Bonod

CNRS, Aix Marseille Université, Centrale Marseille, Domaine Universitaire de Saint Jérôme, 13397 Marseille, France

e-mail: nicolas.bonod@fresnel.fr

The spontaneous emission of quantum emitters can be manipulated with optical antennas made of sub-wavelength photonics resonators. Most of the optical antennas are composed of noble metals like gold that can host localized surface plasmons. Recently, we synthesized, characterized and modeled DNA-templated 60 and 80 nm diameter gold nanoparticle dimers linked with a single fluorophore. These single photon sources feature emission lifetimes below 10 ps and typical quantum yields in a 45 ÷ 70% range [1].

Besides metallic nanostructures, dielectric particles host electromagnetic resonances, called morphologic or Mie resonances, that can yield to the same near field enhancements than those observed at the vicinity of plasmonic particles [2]. In the visible spectrum, the electric and magnetic low order Mie modes hosted by silicon particles can be used to enhance the electric or magnetic decay rates of quantum emitters [2]. In this context, quantifying the Purcell factor and the effective volume of such cavities is of high interest. We used the latest advances on this field of research [4] to derive the Purcell factor and the effective volume of a normal mode of spherical resonators [5]. Thanks to this numerical tool, we can calculate the averaged Purcell factor of a silicon particle homogeneously doped by quantum emitters with a random orientation of emission.

We also show that spherical silicon resonators are interesting to tailor the chirality of single emitters. In particular, dielectric optical antennas that host electric and magnetic resonances overperform those made of plasmonic materials. In particular, the chirality of the field emitted by the antenna can exceed the initial chirality emitted by the molecule. Thanks to the Mie theory formalism in the helicity basis, we show that the interplay between electric and magnetic modes of the resonator is required to tailor the chirality of light [6].

References

- [1] S. Bidault, A. Devilez, V. Maillard, L. Lermusiaux, J.-M. Guigner, N. Bonod, J. Wenger, Picosecond lifetimes with high quantum yields from single-photon emitting colloidal nanostructures at room temperature, *ACS Nano*, DOI:10.1021/acsnano.6b01729, (2016).
- [2] A. Devilez, X. Zambrana-Puyalto, B. Stout, N. Bonod, Mimicking localized surface plasmons with dielectric particles, *Phys. Rev. B*, **92**, 241412(R) (2015).
- [3] B. Rolly, B. Bebey, S. Bidault, B. Stout, N. Bonod, Promoting magnetic dipolar transition in trivalent lanthanide ions with lossless Mie resonances, *Phys. Rev. B*, **85**, 245432 (2012).
- [4] E. A. Muljarov, M. B. Doost, W. Langbein, Exact mode volume and Purcell factor of open optical systems, arXiv:1408.6877v2 (2014).
- [5] X. Zambrana-Puyalto, N. Bonod, Purcell factor of dielectric Mie resonators featuring electric and magnetic resonances, *Phys. Rev. B*, **91**, 195422 (2015).
- [6] X. Zambrana-Puyalto, N. Bonod, Tailoring the chirality of light emission with spherical Si-based antennas, *Nanoscale*, in press (2016).

Focusing of electromagnetic waves through the wired structure

Butko L.N., Anzulevich A.P., Pavlov D.

Chelyabinsk State University, Chelyabinsk, Russia

e-mail: lnbutko@yandex.ru

Numerical 2D simulation method based on the solution of Maxwell's equations shows that the ordered wire structure (Fig. 1 left) [1, 2] under certain conditions shows the properties of left media,

i. e. its external electrodynamic characteristics (reflection, absorption, and refraction) are similar to the characteristics of a homogeneous medium with simultaneously negative permeability. They had developed method (PMC/PEC Boundary Conditions method) for determining permeabilities in the investigated composite structure. It is shown that in a wide frequency range effective permeability are simultaneously negative and the investigated structure in this area showing the effects of the left media, such as the slab of wire structure under certain conditions is can focusing electromagnetic radiation (Fig. 1 right) i. e. it expresses the properties of the so-called Veselago lens.

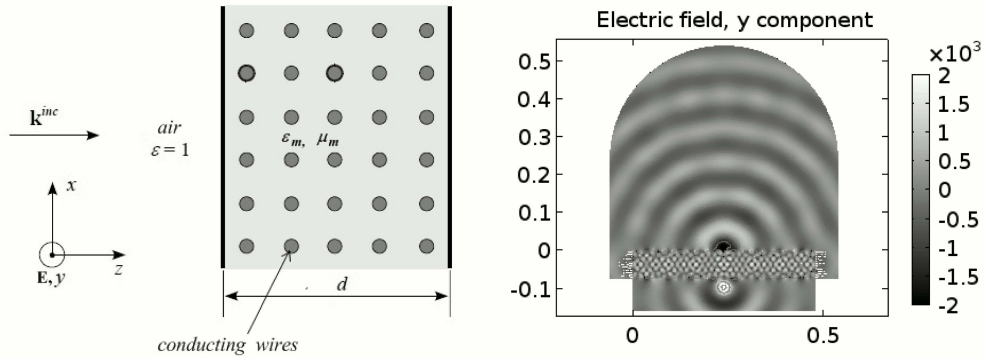


Fig. 1: 2D wire structure model (left) and a 2D picture of propagation of electromagnetic waves through a slab of wire structure. The color change corresponds to a change in the intensity of the electric field along OY (E_y).

References

- [1] J. Pendry *et al.*, *IEEE Trans. Microw. Theory Tech.*, **47**, 2075–2084 (1999).
- [2] P. Below, *Waves and Appl.*, **16**, 1153–1170 (2002).

Voltage controlled nonreciprocal metastructure ferrite/array of twice split rings with varactors

V.S. Butylkin*, Yu.N. Kazantsev, G.A. Kraftmakher, V.P. Mal'tsev

Kotelnikov Institute of Radioengineering & Electronics RAS, Moscow, Russia
e-mail: *vasebut@ms.ire.rssi.ru

Placed along propagation direction metastructure ferrite/array of resonant element shows unidirectional propagation of microwaves and acquires unique functionalities when regime of coupled ferromagnetic resonance (FMR) in ferrite and resonance in conductive elements is formed [1–5].

Here nonreciprocal effects in metastructure “ferrite plate/array of twice split rings loaded with a pair of varactors” are investigated by experiment and theory at microwaves. Metastructure shows two frequency bands of unidirectional microwave propagation which can be voltage controlled in the case when coupled ferromagnetic resonance in ferrite and resonance in split rings are formed. Mechanism of control is considered.

References

- [1] V. S. Butylkin, G. A. Kraftmakher, Giant nonreciprocal effect under conditions of mutual influence of ferromagnetic and chiral resonance, *Tech. Phys. Letters*, Vol. **32**, No. 9, 775–778, 2006.
- [2] G. A. Kraftmakher, V. S. Butylkin, Nonreciprocal amplitude-frequency resonant response of metasandwiches “ferrite plate – grating of resonant elements”, *Eur. Phys. J., Appl. Phys.*, Vol. **49**, No. 3, 33004, 2010.
- [3] G. A. Kraftmakher, V. S. Butylkin, Yu. N. Kazantsev, Electrically controlled frequency bands of nonreciprocal passage of microwaves in metastructures, *Tech. Phys. Letters*, Vol. **39**, No. 6, 505–508, 2013.

- [4] G. A. Kraftmakher, V. S. Butylkin, Yu. N. Kazantsev, Electrically controlled nonreciprocity inversion in a metastructure based on ferrite and a varactor-loaded dipole, *Tech. Phys. Letters*, Vol. **41**, No. 8, 723–726.
- [5] V. Butylkin, G. Kraftmakher, Yu. Kazantsev, In Re Electric Switching Sense of Microwave Magnetic Field Rotation near Varactor-loaded Dipole Excited by a Plane Wave, in Final Proceedings of PIERS 2015 (Progress In Electromagnetics Research Symposium), July 6–9, 2015, Prague, Czech Republic, 949–953.

Nonlinear dynamics of coherent exciton polaritons in a periodic potential

I.Yu. Chestnov¹, M.V. Charukhchyan¹, A.P. Alodjants², X. Ma³, O.A. Egorov³

¹Department of Physics and Applied Mathematics, Vladimir State University named after A. G. and N. G. Stoletovs, 87 Gorkii St., 600000 Vladimir, Russia

²National Research University of Information Technology, Mechanics and Optics, (ITMO) Saint Petersburg 197101, Russia

³Institute of Condensed Matter Theory and Solid State Optics, Abbe Center of Photonics, Friedrich-Schiller-Universität Jena, Max-Wien-Platz 1, 07743 Jena, Germany

e-mail: martin.charukhchyan@gmail.com

Here we describe the model of an exciton-polariton condensate formed in an incoherently pumped semiconductor microcavity coupled to an exciton reservoir in the strong coupling regime. We develop a mean-field model for coupled three spatial harmonics (TSH) and clarify fundamental features of nonequilibrium exciton-polariton condensates trapped in one-dimensional periodic potentials both in the center and at the boundaries of Brillouin zone. This simplified TSH model is a very convenient tool for obtaining important analytical relations for polaritonic eigenstates and band-structures of weak-contrast polaritonic lattices. Here we give a numerical analysis of different regimes of both relaxation and oscillatory dynamics governed by the Bloch eigenstates of coherent exciton polaritons trapped in the periodic lattice. In particular, we study the dynamics of condensate oscillations in the middle (‘zero-momentum state’) and at the boundaries (‘ π -states’) of the Brillouin zone separately. We also prove the existence and stability of the obtained nonlinear oscillations within the frame of the more general open-dissipative Gross–Pitaevskii model with external periodic potential. We have performed numerical modeling of π -state oscillations for different system parameters within the frame of the original GP model. The strong influence of dissipative effects is discussed and the feedback induced by the inhomogeneity of the incoherent reservoir on the dynamics of coherent polaritons. The calculations demonstrate a perfect agreement between the results obtained in both models [1].

References

- [1] X. Ma, I. Yu. Chestnov, M. V. Charukhchyan, A. P. Alodjants, O. A. Egorov, *Physical Review B*, **91**, 214301 (2015).

Quantum nanoparticles doped waveguide for light propagation

P. Chhantyal, T. Birr, U. Zywietz, B.N. Chichkov, C. Reinhardt

Laser Zentrum Hannover e.V., Hollerithallee 8, D-30419, Hannover, Germany

e-mail: p.chhantyal@lzh.de

S. Naskar, N. Bigall

Institute of Physical Chemistry, Leibniz University Hannover, Schneiderberg 39, 30167 Hannover, Germany

The unique optical properties of quantum nanoparticles doped polymer can have huge advantage in photonic applications [1]. In this research, we investigated different methods to acquire quantum

nanoparticles into photo curable polymers followed by producing waveguide structures (shown in Fig. 1) using photo lithography technique. Comparative studies of different quantum nanoparticles, such as dots, rods and plates were conducted. The optical properties were evaluated based on the concentration of the quantum nanoparticles and structural parameters of the polymers. Simultaneously, Rhodamine B was embedded into polymer for comparison [2]. Furthermore, lasing potential of the doped polymers was evaluated.

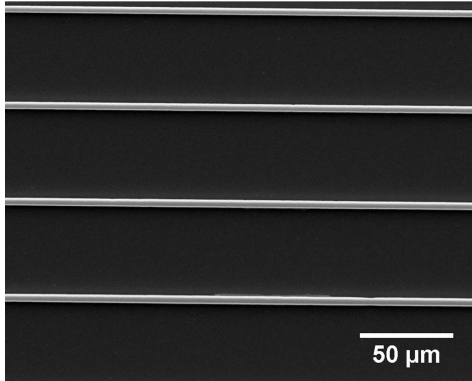


Fig. 1: SEM image of doped Ormocer.

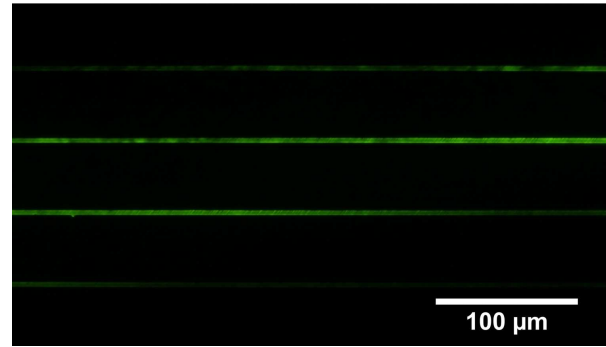


Fig. 2: Fluorescence of doped Ormocer.

References

- [1] H. Cheng, et al., Coupling quantum dots to optical fiber: Low pump threshold laser in the red with a near top hat beam profile, *Applied Physics Letter*, **106**, 081106 (2015).
- [2] P.H.D. Ferreira, et al., Femtosecond laser fabrication of waveguides in Rhodamine B-doped GPTS/TEOS-derived organic/silica monolithic xerogel, *Optical Materials*, **47**, 310–314 (2015).

Ag-based surface plasmon polariton nanolaser

Yu-Hsun Chou¹, **Tzy-Rong Lin**², **Chien-Chung Lin**¹, **Tien-Chang Lu**³

¹Institute of Lighting and Energy Photonics, National Chiao Tung University, Tainan, Taiwan

²Department of Mechanical and Mechatronic Engineering, National Taiwan Ocean University, Keelung, Taiwan

³Department of Photonics, National Chiao Tung University, Hsinchu, Taiwan

e-mail: t_n_chou@hotmail.com

The bottleneck of realizing a semiconductor laser with a size nearby/below the nano scale is the diffraction law, which limits the spatial resolution of light focusing in a conventional cavity to the scale of light wavelength by $(\lambda/2n)^3$. In last decade, this fundamental limit could be reached to wavelength scale or further smaller by using photonic crystal defect cavities [1], metal-clad cavities [2] and nanowire (NW) cavities [3]. These lasers, however, require the cavity size in the order of few $(\lambda/n)^3$ to sustain a proper mode profile with a reasonable cavity Q value. On view of this, surface plasmons provide another concept to localizing light into subwavelength scale. In 2009, Oulton et al. successfully demonstrated the first NW-based plasmonic laser by using the SIM structure, which is composited by CdS NW and silver [4]. Recently, Lu et al. demonstrated InGa_N NW plasmonic laser using a high quality epitaxial Ag film [5]. The aforementioned results are all locate at visible region, so far, there has no UV plasmonic nanolaser being demonstrated yet. With this concern, ZnO is an appropriate material for UV plasmonic lasing since it exhibits wide-direct-bandgap around 3.37 eV and robust excitonic behaviors such as large exciton binding energy and oscillator strength. These two properties make ZnO a very promising material system to probe the novel photonic devices in the blue/UV region, especially the ultra-low threshold laser. In this letter, we theoretically and experimentally demonstrate the laser action of surface plasmon polaritons by placing ZnO nanowires

on a high-quality Ag film with a thin SiO₂ spacer layer based on the semiconductor-insulator-metal (SIM) structure. The truly sub-wavelength-scale plasmonic laser device in blue/UV was realized.

References

- [1] H. Altug, D. Englund, J. Vuckovic, Ultrafast photonic crystal nanocavity laser, *Nat. Phys.*, **2**, 484–488 (2006).
- [2] M. T. Hill, Y. S. Oei, B. Smalbrugge, Y. Zhu, T. d. Vries, P. J. van Veldhoven *et al.*, Lasing in metallic-coated nanocavities, *Nat. Photonics*, **1**, 589 (2007).
- [3] J. C. Johnson, H. J. Choi, K. P. Knutsen, R. D. Schaller, P. Yang, R. J. Saykally, Single gallium nitride nanowire lasers, *Nat. Mater.*, **1**, 106–110 (2002).
- [4] F. Oulton, V. J. Sorger, T. Zentgraf, R. M. Ma, C. Gladden, L. Dai, G. Bartal, X. Zhang, Plasmon lasers at deep subwavelength scale, *Nature*, **461**, 629–632 (2009).
- [5] Y. J. Lu, J. Kim, H. Y. Chen, C. Wu, N. Dabidian, C. E. Sanders, C. Y. Wang, M. Y. Lu, B. H. Li, X. Qiu, *et al.*, Plasmonic nanolaser using epitaxially grown silver film, *Science*, **337**, 6093 (2012).

Applicability of two-level approximation describing dynamics of spaser with four-level metamolecule

E.D. Chubchev¹, A.A. Pukhov^{1,2}, A.P. Vinogradov^{1,2}

¹All-Russia Research Institute of Automatics, 22 Sushchevskaya, Moscow 127055, Russia

²Institute for Theoretical and Applied Electromagnetics, Russian Academy of Science, 13 Izhorskaya, Moscow 125412, Russia

e-mail: chubchev.evgeniy@physics.msu.ru

As it has been shown in [1, 2], a spaser consisting of a plasmonic nanoparticle and two-level system (TLS) may exhibit the Rabi oscillations after pulse excitation. Real quantum systems utilized for lasing and spasing should be typically described by means of either three-level or four-level schemes. Often these schemes are reduced to equivalent two-level scheme [3]. However, it seems that the Rabi oscillations predicted for TLS could not be observed for four-level system (FLS) due to the mismatch between the excitation and laser transition frequencies of FLS. Thus, in some cases the common transition from FLS system to TLS may be not quite correct.

We have shown that the Maxwell–Bloch equations for FLS can be reduced to two different systems of equations for TLS. These systems describe strong and weak coupling regimes. In addition, we show that in the case of strong coupling regime the Rabi oscillations predicted for TLS occur in FLS as well.

References

- [1] M. I. Stockman, *J. Opt.*, **12**, 024004 (2010).
- [2] E. S. Andrianov *et al.*, *Phys. Rev. B*, **85**, 035405 (2012).
- [3] Ya. I. Khanin, *Fundamentals of Laser Dynamics*, Cambridge International Science Publishing Ltd., Cambridge, 2006.

Full control of the A_0 mode in a plate using a locally resonant metamaterial

Andrea Colombi, Richard V. Craster

Dept. of Mathematics, Imperial College London, South Kensington Campus, London

e-mail: andree.colombi@gmail.com

In this talk, the exotic dispersion properties that characterize a locally resonant metamaterial for flexural waves (A_0 mode) in thin plates are in deep analysed [1]. A collection of closely spaced

aluminium rods attached to an aluminium plate (Fig. 1a) gives rise to bandgaps, slow waves and anisotropy [2]. The occurrence of these particular states is theoretically predicted either by homogenization or by applying Bloch theory on the irreducible Brillouin zone. Results from 3D time domain numerical simulations and laboratory experiments are shown to visually explore the most interesting regions of the dispersion curve in the 1–10 kHz frequency range (Fig. 1b). Two applicative examples of this metamaterial, aimed at controlling the propagation of the A_0 mode, are proposed. In the first, the slow wave branch of the dispersion curve (Fig. 1b), occurring right before the bandgap, is used to build a resonant metalens for flexural waves. The metalens is made of a circular cluster of closely spaced rods whose length depends on the distance from the center of the cluster and ultimately on the effective refraction index of the lens. Results from numerical simulations are shown for the Luneburg (Fig. 1c) and Maxwell lens type [3]. Both can be used to steer waves in particular directions. In the second examples, the height of the rods that compose the metamaterial increases progressively along one direction, thus realizing a wedge-shaped resonator cluster. The wedge spatially segregates (like an elastic rainbow) different frequency components of the incoming wavefield. When the waves are trapped their amplitude is drastically increased, a condition that could ease their absorption and hence the damping of vibrations in plates.

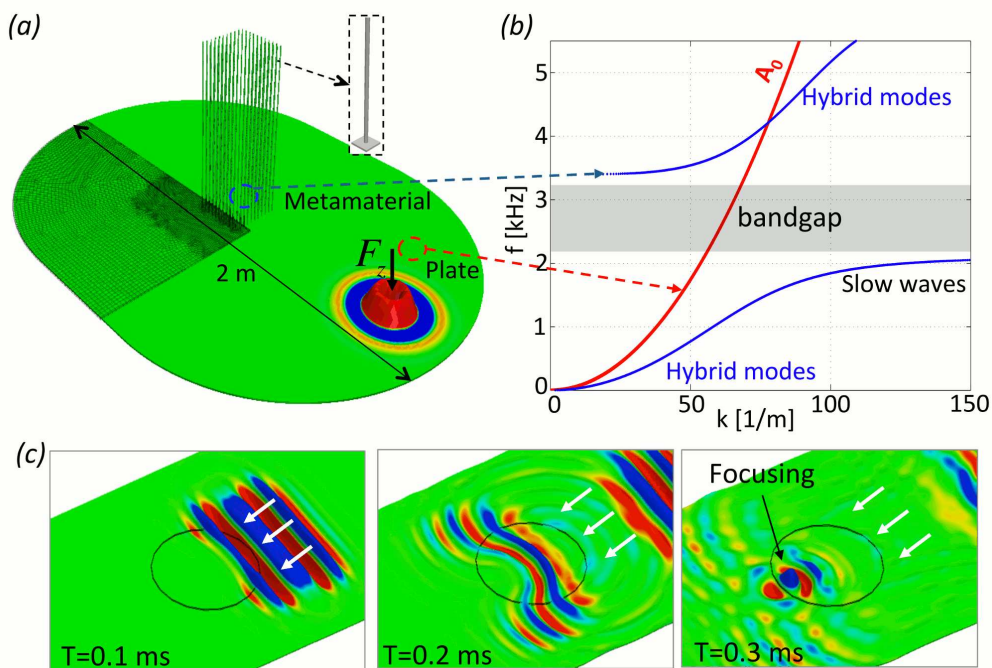


Fig. 1: (a) The numerical model of the metamaterial made with aluminium rods on a plate. (b) Dispersion curves of the metamaterial and bare plate in (a). (c) The Luneburg metalens obtained with a radially varying rods length profile.

References

- [1] M. Rupin, F. Lemoult, G. Lerosey, P. Roux, *Phys. Rev. Lett.*, **112**, 234301 (2014).
- [2] A. Colombi, P. Roux, S. Guenneau, M. Rupin, *J. Acoust. Soc. Am.*, **137**, 1783–9 (2015).
- [3] M. Sarbort, T. Tyc, *Journal of Optics*, **14**, 075705 (2012).

Complex photonic structure based on magneto-optic waveguide and photonic crystal

Dadoenkova N.N.^{1,2}, Dadoenkova Yu.S.^{1,2,3}, Panyaev I.S.¹, Rozhleys I.A.⁴, Lyubchanskii I.L.², Krawszyk M.⁵, Sannikov D.G.¹

¹Ulyanovsk State University, 432017, Ulyanovsk, Russian Federation

²Donetsk Physical and Technical Institute of NAS of Ukraine, 83114, Donetsk, Ukraine

³Novgorod State University, 173003, Veliky Novgorod, Russian Federation

⁴National Research Nuclear University MEPhI, Moscow, 115409, Russian Federation

⁵Adam Mickiewicz University in Poznan, 61-614, Poznan, Poland

e-mail: dadoenkova@yahoo.com

Magneto-optical (MO) waveguides and photonic crystals (PCs) are widely used in modern integrated optics [1] and magneto-photonics [2]. Recently the hybrid plasmonic waveguide modes localized in Bragg mirrors of the magnetophotonic crystal giving rise to MO effects are reported [3]. Combined structures based on MO waveguide and PCs can open new opportunities in possible application. In this communication, we present the results of theoretical study of waveguide properties of a heterostructure composed of MO yttrium-iron garnet (YIG) film on the SiO₂ substrate covered by one-dimensional (1D) dielectric PC on base of gadolinium-gallium garnet (GGG) and titanium oxide TiO₂: (SiO₂/YIG/(GGG/TiO₂)^N/vacuum) [Fig. 1(a)]. We investigate the influence of the geometrical parameters of the system (the YIG layer thickness L , the GGG and TiO₂ layers thicknesses d_1 and d_2) on the spectra of TE- and TM-modes. For the numerical calculations we take into account the refractive indices dispersion for all constituent media of the considered waveguide system and bigyrotropic properties of YIG in the near IR regime. We show the evolution of the dispersion curves with increase of the number of the PC's unit cells N . Presence of the dielectric periodic covering on top of the YIG layer leads to appearance of the gaps in the spectra of TE- and TM-modes [Figs. 1(b) and 1(c)] and the systems of minigaps. As well numerous degeneracy points (where TE- and TM-mode can coexist) appear in the spectra [Fig. 1(d)] with increasing N .

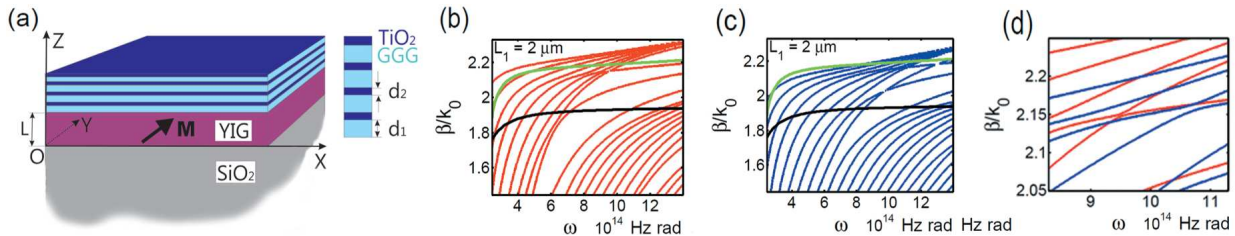


Fig. 1: (a) Schematic of the MO waveguide structure under consideration. The thick arrow shows the magnetization direction in the YIG layer. Dispersion curves for TE- (b) and TM-polarized modes (c) for the structure with $N = 7$ bilayers, $L = 2.0 \mu\text{m}$ and $d_1 = d_2 = 0.5 \mu\text{m}$. The black and green lines show the refractive index dispersion for GGG and YIG, respectively.

References

- [1] H. Dötsch, et al., *J. Opt. Soc. Am. B*, **22**, 240 (2005).
- [2] I. L. Lyubchanskii, et al., *J. Phys. D: Appl. Phys.*, **36**, R277 (2003).
- [3] N. E. Khokhlov, et al., *J. Phys. D: Appl. Phys.*, **48**, 095001 (2015).

Goos–Hänchen shift of a light beam upon reflection from a magnetic film on a non-magnetic substrate: effect of misfit strain

Dadoenkova Yu.S.^{1,2,3}, Bentivegna F.F.L.⁴, Dadoenkova N.N.^{2,3}, Lyubchanskii I.L.³, Lee Y.P.⁵

¹Ulyanovsk State University, 432017 Ulyanovsk, Russian Federation

²Novgorod State University, 173003 Veliky Novgorod, Russian Federation

³Donetsk Physical and Technical Institute of NAS of Ukraine, 83114 Donetsk, Ukraine

⁴Lab-STICC (UMR 6285), CNRS, UBL, ENIB, 29238 Brest Cedex 3, France

⁵q-Psi and Hanyang University, 04763 Seoul, South Korea

e-mail: dadoenkova@yahoo.com

The Goos–Hänchen shift (GHS) is an optical phenomenon, in which the reflected light beam exhibit a lateral shift from the position predicted by geometrical optics [1]. The amplitude of the GHS depends upon such parameters as the incidence angle, wavelength and state of polarization of the incident light, but it also strongly depends on the nature and anisotropy of the media forming the interface. The quality of the interfaces encountered by light can also be of importance. Indeed, it is well known that elastic strain takes place in the vicinity of interfaces in layered structures due to the crystalline lattice misfit between the neighboring materials [2]. As a consequence, atomic alignment on each side of the geometric interfaces is altered, and the thickness of the resulting deformed layers can reach values up to a few hundred ångströms. Such crystalline deformations near interfaces are known to affect the optical properties, notably the reflectivity, of the multilayers via the photoelastic interaction. The effect of interfacial strain on the transmittivity of a dielectric photonic crystal has been studied in [3].

In this Communication, we theoretically study the influence of the misfit strain on the GHS experienced by a near-infrared light upon reflection from the surface of a dielectric bilayer consisting of a magnetic yttrium-iron garnet film epitaxially grown on a non-magnetic gadolinium-gallium garnet substrate. We show that the mechanical strain near the geometrical film/substrate interface can be significant, and the GHS can reach values from a few tens to hundreds of incident light wavelengths at incidence angles close to the normal incidence, as well as at the pseudo-Brewster angle [4]. We demonstrate that the largest GHS, observed at small incidence angles, where the half-wave condition for both layers is nearly satisfied, is entirely induced by strain. If the half-wave condition is satisfied for an oblique incidence angle, the reflection coefficient turns to zero in the absence of strain, resulting in a large GHS near this incidence angle. In this case, unlike what is obtained at the pseudo-Brewster angle, the impact of strain is large and strain-induced contributions to the reflection coefficient and its phase result in a broadening of the GHS peak. For a TM-polarized incident wave, the variation of the GHS upon magnetization reversal (in the transverse magneto-optical configuration) is found to be only noticeable around the pseudo-Brewster angle for the unstrained structure, and around that angle and near normal incidence when strain is taken into account. No noticeable dependence of the GHS upon magnetization was observed for a TE-polarized wave.

References

- [1] F. Goos, H. Hänchen, *Ann. der Phys.*, **1**, 333–346 (1947).
- [2] J. M. Howe, *Interfaces in Materials*, Wiley (1997).
- [3] A. E. Zabolotin, N. N. Dadoenkova, F. F. L. Bentivegna, I. L. Lyubchanskii, A. L. Shyshmakov, Y. P. Lee, Y. G. Boucher, Th. Rasing, *J. Opt. Soc. Am. B*, **28**, 2216–2219 (2011).
- [4] Yu. S. Dadoenkova, F. F. L. Bentivegna, N. N. Dadoenkova, I. L. Lyubchanskii, Y. P. Lee, *J. Opt. Soc. Am. B*, **33**, 393–404 (2016).

Electric and magnetic tuning of the Goos–Hänchen shift of a light beam upon reflection from a magneto-electric heterostructure

Dadoenkova Yu.S.^{1,2,3}, Bentivegna F.F.L.⁴, Dadoenkova N.N.^{2,3}, Lyubchanskii I.L.³, Petrov R.V.¹, Bichurin M.I.¹

¹Novgorod State University, 173003 Veliky Novgorod, Russian Federation

²Ulyanovsk State University, 432017 Ulyanovsk, Russian Federation

³Donetsk Physical and Technical Institute of NAS of Ukraine, 83114 Donetsk, Ukraine

⁴Lab-STICC (UMR 6285), CNRS, UBL, ENIB, 29238 Brest Cedex 3, France

e-mail: yulidad@gmail.com

When a light beam impinges on an optical system, the reflected beam can exhibit a lateral shift relatively to the position predicted by geometric optics for ideal light rays — that is the Goos–Hänchen shift (GHS) [1]. In magneto-optical materials, the GHS can reach values up to several tens of light wavelengths [2]. Thus, the GHS should be taken into account for the precise design of integrated optical or magneto-optical devices. Furthermore, it is well-known that certain classes of magnetic materials possess magneto-electric (ME) properties [3], which result in the induction of a magnetization by an electric field or the induction of a dielectric polarization by a magnetic field. It has been shown that the linear ME interaction modifies the complex reflectivity of a magnetic/dielectric bilayer [4]. Thus the ME properties can also be expected to influence the GHS of light reflected from such a system.

In this Communication, we investigate theoretically the GHS upon light reflection from a three-component ME heterostructure consisting of an electro-optic slab deposited on a magnetic film, itself grown on a nonmagnetic dielectric substrate. External static magnetic and electric fields can be applied to the system in order to tune its optical characteristics. Our results show that the linear ME interaction in the magnetic slab leads to an about sixfold increase of the cross-polarized contribution to the GHS even in the absence of any applied electric field. However, the ME interaction alone is not strong enough to provide essential changes to the GHS when the external electric field is applied to the system without the electro-optic film. The latter, when present, enhances the influence of the electric field on the GHS. The amplitude of the GHS decreases when the magnitude of the applied electric field increases, and its angular position (in terms of incidence angle) can be shifted when the electric field is neither parallel to the plane of incidence of light nor perpendicular to it. On the other hand, inverting the direction of the external magnetic field, and thus reversing the initial magnetization of the magnetic film, inverts the direction of the GHS but non-symmetrically modifies its amplitude. Neglecting the ME interaction in the magnetic layer in the calculations, however, does not lead to noticeable change of the GHS, which means that the ME effect plays an essential part in the behaviour of the GHS upon magnetization reversal. As our results show, a well-chosen combination of applied electric and magnetic fields (amplitude and direction) makes it possible to use this interplay in order to efficiently control (enhance or reduce) the GHS in the ME heterostructure.

References

- [1] F. Goos, H. Hänchen, *Ann. der Phys.*, **1**, 333–346 (1947).
- [2] Yu. S. Dadoenkova, F. F. L. Bentivegna, N. N. Dadoenkova, I. L. Lyubchanskii, Y. P. Lee, *J. Opt. Soc. Am. B*, **33**, 393–404 (2016).
- [3] T. H. O’Dell, *The Electrodynamics of Magnetolectric Media*, Amsterdam: NorthHolland (1970).
- [4] Yu. S. Dadoenkova, I. L. Lyubchanskii, Y. P. Lee, Th. Rasing, *Eur. Phys. J. B*, **71**, 401–406 (2009).

Viscoelastic properties of colloids

Bair Damdinov, Anton Demin

Physical-Technical Department, Buryat State University, Russia
e-mail: bdamdinov@bsu.ru

Tuyana Dembelova

Molecular Structure Lab, Institute of Physical Materials Science, Russia
e-mail: tu_dembel@mail.ru

In this paper we present the result of measurement of the shear properties of liquid crystal mixed with various nanoparticles. Effective viscosity of the liquid crystal mixed with nanoparticles was measured by rheometrical method at various frequencies. Results obtained for different concentrations of the nanoparticles. It was shown that value of viscosity is not linearly dependent on the concentration and the value of viscosity to a certain point decreases with decreasing concentration.

Acknowledgements. Supported by RFBR grants 15-02-08204, 15-42-04319 r_sibir_a. Supported by BSU grant 3822.

Analysis of metasurface based structures by using equivalent conductivity method

M. Danaeifar, N. Granpayeh

Center of Excellence in Electromagnetics, Faculty of Electrical Engineering, K. N. Toosi University of Technology, Tehran, Iran
e-mails: danaeifar@mail.kntu.ac.ir, granpayeh@eetd.kntu.ac.ir

Equivalent conductivity method is presented to analysis the structures involving metasurfaces. In this method, a calculated equivalent conductivity is ascribed to the metasurface and this surface conductivity plays the interface role between two media in electromagnetics equations. Graphene and silver nanodisks are considered as metasurface's components in infrared and optical regime, respectively. Recently, metasurface as a new class of two dimensional metamaterials has been developed. This artificial medium known as a 'metasurface' is usually made by particles in a very thin host material [1]. In this work, we present the equivalent conductivity method (ECM) where a metasurface can easily be considered as a thin layer with equivalent conductivity (σ_e) for analytical evaluations. In a complex multilayer structure, σ_e is calculated separately for each metasurface, and finally these conductivities are considered in the comprehensive relation of the entire multi-layer structure. It is possible to consider the metasurface as a homogeneous surface with an effective σ_e instead of considering the structured surface including its detailed distribution of particles and their geometrical and physical properties. For a metasurface sandwiched between two media and exposed by a perpendicularly polarized plane wave with an incidence angle of θ_i (Fig. 1(a)) one can calculate σ_e [2]:

$$\sigma_e = \frac{\sqrt{\epsilon_{r1}} \cos \theta_t - \sqrt{\epsilon_{r2}} \cos \theta_i - r (\sqrt{\epsilon_{r1}} \cos \theta_t + \sqrt{\epsilon_{r2}} \cos \theta_i)}{\eta_0(1+r) \cos \theta_i}, \quad (1)$$

where θ_t is the transmittance angle ($\sqrt{\epsilon_{r2}} \sin \theta_t = \sqrt{\epsilon_{r1}} \sin \theta_i$), η_0 is the free-space wave impedance, ϵ_{r1} and ϵ_{r2} are the relative permittivities of up and down media, respectively. The reflection coefficient of r can be derived as [2, 3]:

$$r = \frac{i2\pi k}{\frac{A \cos \theta_i}{\alpha} - \frac{g \cos \theta_i}{p} + i \left(\frac{2A \cos \theta_i}{3} k^3 - 2\pi k \right)}, \quad (2)$$

where k is the free-space propagation constant, α is polarizability of metasurface's components, A is the unit cell area and g is the array arrangement constant. This reflection coefficient is derived when

the metasurface is embedded in vacuum and it should be amended with respect to dielectric effect in non-free space cases. The polarizability of α can be calculated as [3]:

$$\alpha(\omega) = \frac{3c^3\Delta}{\omega_0} \frac{1}{\omega_0^2 - \omega^2 - i2\Delta\omega^3/\omega_0^2}, \quad (3)$$

where c is speed light in vacuum, ω_0 is the peak frequency, and Δ is half of the linewidth of the resonance. To evaluate the method in infrared and optical regime, we consider graphene and silver nanodisks as metasurface's components. The polarizabilities of silver and graphene nanodisks are depicted in Fig. 1(b) and (c), respectively. A dielectric slab with the height of 200 nm and the relative permittivity of 2 are allocated under the metasurface (Fig. 2(a)). For this case, the permittivity of silver is calculated by Drude model and the conductivity values of graphene are calculated by random-phase approximation with the chemical potential of $\mu_c = 500$ meV.

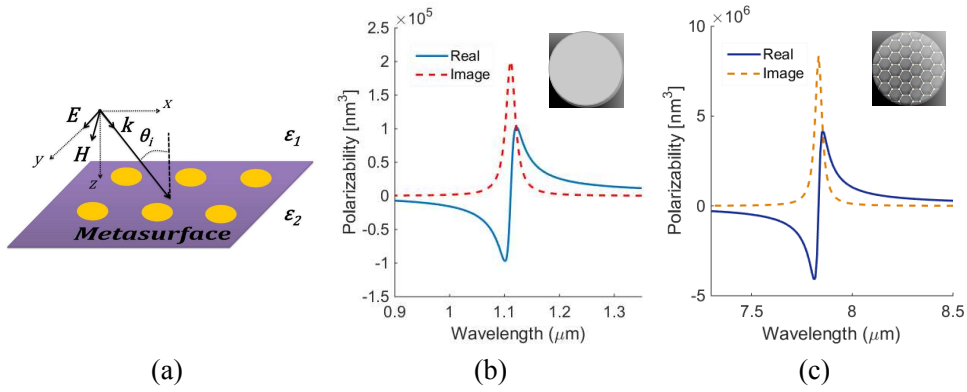


Fig. 1: (a) A metasurface sandwiched between two media that exposed by a perpendicularly polarized plane wave, polarizability of (b) silver nanodisk with the radius of $r_s = 20$ nm and the height of $h_s = 1$ nm, and (c) graphene nanodisk with the radius of $r_g = 40$ nm and the height of $h_g = 0.5$ nm.

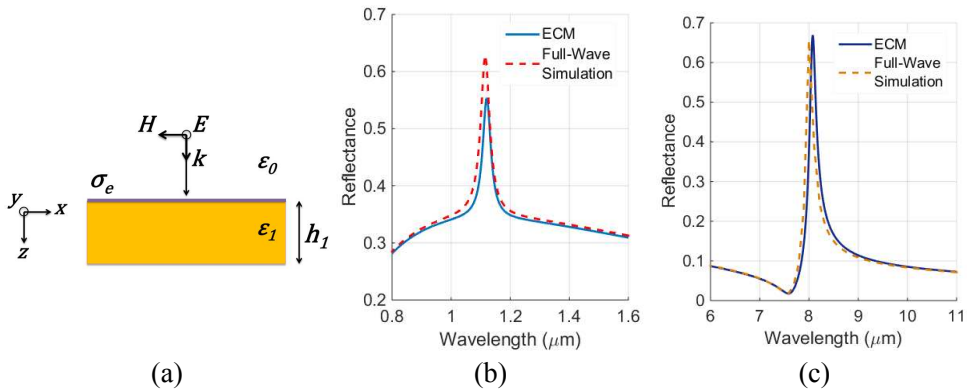


Fig. 2:(a) The metasurface on the dielectric slab, the reflection coefficient calculated by ECM and full-wave simulation for (b) silver based metasurface and (c) graphene based one.

For these two metasurfaces, the equivalent conductivities are calculated and these surface conductivities are considered as interface layers between ambient and the dielectric slab. Then the reflection coefficients are calculated analytically by ECM and compared with finite-element method (COMSOL Multiphysics) for metasurfaces involve graphene nanodisks (Fig. 2(b)) and silver nanodisks (Fig. 2(c)). So, the equivalent conductivity method establishes a straightforward approach for analytical analysis of multilayers and complicated metasurface assemblies. The ECM is a general method and can be applied to inhomogeneous metasurface [4] and the method has no limitations on nanoparticles' shape and material or frequency range.

References

- [1] N. Yu, P. Genevet, M. A. Kats, F. Aieta, J. Tetienne, F. Capasso, Z. Gaburro, *Science*, **334**, 333–337 (2011).
- [2] M. Danaeifar, N. Granpayeh, N. A. Mortensen, S. Xiao, *J. Phys. D*, **48**, 385106 (2015).
- [3] S. Thongrattanasiri, F. H. L. Koppens, F. J. G. d. Abajo, *Phys. Rev. Lett*, **108**, 047401 (2012).
- [4] M. Danaeifar, N. Granpayeh, *Opt. Lett*, **40**, 5666–5669 (2015).

The influence of non-uniformly scaled conducting inclusions on range properties of a layer of bi-isotropic composite material

V.I. Demidchik, R.V. Kornev

Belarusian State University, Minsk, Belarus

e-mail: demidvi@bsu.by

Electrodynamic properties of composite materials in the form of a dielectric matrix, filled with conducting fibers of definite geometry, depend substantially on geometric size, form, fiber concentration. The calculation of effective dielectric permittivity and magnetic permeability, medium chirality factor are generally based on analyzing the interaction between an electromagnetic wave (EMW) and a single particle. Moreover, similar media with chaotically dispersed inclusions of identical geometry and size possess resonant properties with a rather narrow resonance band.

The article describes the methods of defining effective electrodynamic parameters (EEP) of composite material in the form a dielectric matrix, containing a mixture of arbitrary oriented particles, having identical geometry, but different size, which are proportionally scaled-up one relative to another. The calculation of composite EEP was carried out using Maxwell–Garnett method, generalized for the case of chiral media. So far as EEP is defined by aggregate polarization factors (PF) of the particles, that constitute the matrix, the PF of separate particles of each geometry type are calculated first [2]. Afterwards the summarized PF are calculated as the sum of PFs of all particles having different geometry, considering their quantity in a volume unit, and effective parameters of a composite are defined.

On the basis of obtained values for effective parameters the interaction between electromagnetic wave and flat layer of such a composite material was investigated according to the methods, described in [3, 4]. As an example the calculation results for reflection factor of composite layer, located on metallic coating, are presented.

It was ascertained, that by varying the size of inclusions and their concentration in a multi-component mixture it is possible to achieve resonant bandwidth widening with a minimal reflection factor, as well as to obtain two and more resonances.

Analysis results can find application for designing selective microwave devices on the basis of bi-isotropic composite materials.

References

- [1] F. Guerin, P. Bannelier, M. Labeyrie, Scattering of electromagnetic waves by helices and application to the modeling of chiral composites. Maxwell Garnett treatment, *Journal of Physics D – Applied Physics*, no. 28, pp. 643–656 (1995).
- [2] V. T. Erofeenko, V. I. Demidchik, S. V. Malyi, R. V. Kornev, Penetration of electromagnetic waves through composite screens containing ideally conducting helices, *Journal of Engineering Physics and Thermophysics*, vol. **84**, no. 4, pp. 799–806 (2011).
- [3] V. A. Neganov, O. V. Osipov, Scattering of electromagnetic waves from plane chiral structures, *Izv. Vuzov SSSR. Ser. Radiofizika*, vol. **42**, no. 9, pp. 870–878 (1999).
- [4] O. V. Ivanov, D. I. Sementsov, Light propagation in stratified chiral media. The 4×4 matrix method, *Crystallography Reports*, vol. **45**, no. 3, pp. 487–492 (2000).

Enhancement of Raman scattering by magnetic resonances of crystalline silicon nanoparticles

Dmitriev P.A.¹, Baranov D.G.², Milichko V.A.¹, Makarov S.V.¹, Mukhin I.S.^{1,3}, Samusev A.K.¹, Krasnok A.E.¹, Belov P.A.¹, Kivshar Y.S.¹

¹ITMO University, St. Petersburg 197101, Russia

²Moscow Institute of Physics and Technology, Dolgoprudny 141700, Russia

³St. Petersburg Academic University, St. Petersburg 194021, Russia

⁴Nonlinear Physics Centre, Australian National University, Canberra ACT 2601, Australia

e-mail: pavel.a.dmitriev@gmail.com

Raman scattering of light is an electromagnetic effect which has found many different applications including sensing, optical amplification and lasing [1]. Traditionally, plasmonic nanoparticles have been used for applications requiring enhanced Raman scattering. However, recent studies in high-index dielectric nanoparticles have paved the way towards all-dielectric resonant nanodevices [2].

Many semiconductor materials, including crystalline silicon, demonstrate their own Raman signals. Also, crystalline silicon nanoparticles exhibit Mie-type electric and magnetic resonances [4], which can be used to enhance Raman scattering from the nanoparticles. However previous studies of Raman scattering by silicon nanostructures have only considered dense clusters of nanoparticles [3] or large bulk waveguide structures.

Here we present an experimental and theoretical studies of enhanced Raman scattering from single crystalline silicon nanoparticles, fabricated by our laser-transfer technique [4]. Comparison of Raman scattering from resonant particles to scattering from their non-resonant counterparts shows a 140-fold increase in Raman signal. We have shown theoretically and demonstrated experimentally, that the strongest enhancement of Raman scattering occurs in the vicinity of the nanoparticles' magnetic resonances. The efficiency of the enhancement is related to the different nanoparticles' resonances' Q-factor and electric field confinement in the bulk of the nanoparticle, which favors the magnetic dipole resonance.

References

- [1] W. Haye, R. Loudon, *Scattering of Light by Crystals*, Wiley (1978).
- [2] R. S. Savelev, S. V. Makarov, A. E. Krasnok, P. A. Belov, *Optics and Spectroscopy*, **119**(4), p. 551–568 (2015).
- [3] F. M. Liu, et al., *Chemical physics letters*, **382**(5), p. 502–507 (2003).
- [4] P. A. Dmitriev, S. V. Makarov, V. A. Milichko, I. S. Mukhin, A. S. Gudovskikh, A. A. Sitnikova, A. K. Samusev, A. E. Krasnok, P. A. Belov, *Nanoscale*, **8**, p. 5043–5048 (2016).

Optical properties, density of photonic states and dispersion of light in liquid-crystalline photonic crystals

Dolganov P.V., Dolganov V.K.

Institute of Solid State Physics RAS, 143432 Chernogolovka, Moscow Region, Russia

e-mails: pauldol@issp.ac.ru, dolganov@issp.ac.ru

Many liquid-crystalline phases composed by chiral molecules form one-dimensional and three-dimensional photonic crystals. Cholesterics and ferroelectrics are famous examples of one-dimensional photonic liquid crystals. A peculiar feature of one-dimensional chiral photonic crystals is strong dependence of their optical properties on the polarization of light. For light propagating along the helical axis the photonic stop band exists for light of only one circular polarization. Twisted structure leads to strong optical activity (rotation of the plane of polarization of light). In spite of intensive investigations, a number of questions related to properties of photonic liquid crystals

remain open. Due to unusual fundamental properties and possibility of different applications much effort is currently devoted to theoretical studies and experimental investigations of chiral photonic liquid crystals.

In this work optical investigations were performed on high-quality samples of cholesteric photonic crystals. It allowed to determine important optical characteristics and density of photonic states. We have measured diffraction, transmission spectra and rotation of the plane of polarization of light, their dependence on chirality and temperature. Spectra of rotation of the plane of polarization of light in high-quality samples show oscillations predicted by theory. The experimental results are analyzed on the basis of Maxwell equations and Kramers–Kronig relations [1].

We propose a method to determine experimentally density of photonic states in photonic liquid crystals from measurements of rotation of the plane of polarization of light [2]. The proposed method allowed to determine for the first time density of photonic states in cholesteric. In high-quality samples the experimentally determined density of states demonstrates peculiarities predicted by theory. Near the bandgap the density of states increases essentially, outside the bandgap oscillations in the density of states are observed. Group and phase velocity of light, dispersion relation $\omega(k)$ were determined from the experimental data. The group velocity of light in the pseudogap can become greater than speed of light in vacuum, which does not violate Einstein causality. Besides high-quality samples, we studied the influence of disorder on optical characteristics. The results of our studies demonstrate that universal approaches can be effectively applied for the description of optical properties of liquid-crystalline photonic crystals.

This work was supported in part by RFBR, grant No. 14-02-01130.

References

- [1] P. V. Dolganov, G. S. Ksyonz, V. E. Dmitrienko, V. K. Dolganov, *Phys. Rev. E*, **87**, 032506 (2013).
- [2] P. V. Dolganov, *Phys. Rev. E*, **91**, 042509 (2015).

Local optical anisotropy, diffraction and orientational order parameter in cholesteric photonic crystals

Dolganov P.V.¹, Dolganov V.K.¹, Gordeev S.O.^{1,2}

¹Institute of Solid State Physics RAS, 143432 Chernogolovka, Moscow Region, Russia

²M. V. Lomonosov Moscow State University, 119991, Moscow, Russia

e-mails: pauldol@issp.ac.ru, dolganov@issp.ac.ru

Liquid crystals are formed by orientationally ordered anisotropic organic molecules. Cholesteric liquid crystals are one-dimensional photonic crystals. In cholesterics the orientation of the long molecular axes periodically rotates in space forming a helical structure [1]. Period of the structure can be comparable with visible light wavelength. Spatial variation of the refractive index gives rise to a photonic stop band.

A number of important questions related to properties of liquid-crystalline photonic crystals are still not completely clear. These are, in particular, relation of macroscopic optical characteristics of the photonic crystal with macroscopic and microscopic properties of the liquid-crystalline structure, description of the temperature dependence of photonic characteristics and the orientational order parameter. It should be noted that experimental determination of the orientational order parameter in cholesteric photonic crystals and its variation with temperature constitutes a nontrivial task. Methods developed for determination of the order parameter in other liquid-crystalline phases cannot be directly employed in photonic structures.

We have performed optical investigations on high-quality samples of cholesteric photonic crystals [2, 3]. Diffraction and transmission spectra have been measured. The experimental spectra are well described by the theoretical dependence following from the analytical solution of Maxwell equations [4]. Temperature dependence of the characteristics of the photonic structure (i. e. spectral width

of the photonic stop band, optical anisotropy, etc.) is determined from diffraction and transmission measurements. The diffraction band halfwidth depends on properties of the sample surface and in samples with rigid boundary conditions for molecular orientation can change with temperature in a stepwise manner. On the contrary, the relative width of the photonic band has a universal character and does not depend on boundary conditions in the samples. We employ the relation between local optical anisotropy and the orientational order parameter of the photonic liquid crystal following from microscopic theory. In this manner temperature dependence of the orientational order parameter of the photonic liquid crystal was determined. The obtained results are compared with existing theories. It is shown that temperature dependence of the orientational order parameter can be described on the basis of Landau theory of phase transitions.

This work was supported in part by RFBR, grant No. 14-02-01130.

References

[1] P. G. de Gennes, J. Prost, *The Physics of Liquid Crystals*, 2nd edition, Clarendon Press, Oxford (1994).
 [2] P. V. Dolganov, G. S. Ksyons, V. E. Dmitrienko, V. K. Dolganov, *Phys. Rev. E*, **87**, 032506 (2013).
 [3] P. V. Dolganov, S. O. Gordeev, V. K. Dolganov, *JETP*, **118**, 891–895 (2014).
 [4] V. A. Belyakov, V. E. Dmitrienko, *Optics of Chiral Liquid Crystals*, Harwood Academic, London (1989).

**Optical implementation of differential operators
with resonant nanophotonic structures**

Doskolovich L.L., Bykov D.A., Bezus E.A.

Image Processing Systems Institute of the RAS, 151 Molodogvardeiskaya st., Samara, 443001, Russia
 Samara State Aerospace University (SSAU), 34 Moskovskoye shosse, Samara, 443086, Russia
 e-mails: leonid@smr.ru, bykovd@gmail.com, evgeni.bezus@gmail.com

Photonic devices performing required temporal and spatial transformations of optical signals are of great interest for a wide range of applications including all-optical information processing and analog optical computing. Among the most important operations of analog optical processing are the operations of temporal and spatial differentiation. Various types of resonant photonic structures performing these operations were previously proposed, such as Bragg gratings, waveguide resonant gratings, and nanoresonators [1–3].

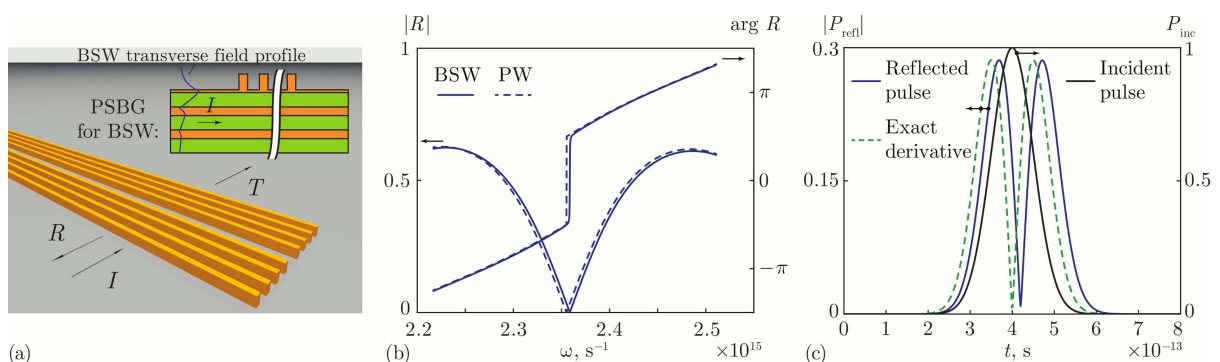


Fig. 1: (a) Geometry of a PSBG for BSW; (b) Reflection spectra of typical PSBG for BSW and plane waves (PSBG consist of two Bragg gratings with 4 periods on the each side of the defect); (c) Incident and reflected BSW pulses and the analytically computed derivative.

In the current work, we present an overview of our recent results dedicated to the design of nanophotonic structures for optical implementation of various differential operators. A special attention is paid to “spatiotemporal differentiation” of optical pulses implemented by waveguide reso-

nant gratings and phase-shifted Bragg gratings (PSBG) and to the design of their planar analogues for differentiation of surface electromagnetic waves. The latter is of interest due to the promising applications of surface waves in on-chip all-optical information processing. In particular, we consider a planar PSBG analogue for Bloch surface waves (BSW) propagating along the interfaces between a photonic crystal and a homogeneous medium (Fig. 1(a)). The reflection spectra of the proposed PSBG for BSW and conventional PSBG for plane waves are in good agreement (Fig. 1(b)) and therefore the proposed BSW PSBG can efficiently perform temporal differentiation of BSW pulses (Fig. 1(c)). For the considered example, the Pearson correlation coefficient between the reflected pulse envelope and the exact derivative exceeds 0.999.

This work was funded by the Russian Science Foundation grant 14-19-00796.

References

- [1] L. L. Doskolovich, D. A. Bykov, E. A. Bezus, V. A. Soifer, *Opt. Lett.*, **39**, 1278–1281 (2014).
- [2] D. A. Bykov, L. L. Doskolovich, V. A. Soifer, *Opt. Lett.*, **36**, 3509–3511 (2011).
- [3] N. L. Kazanskiy, P. G. Serafimovich, S. N. Khonina, *Opt. Lett.*, **38**, 1149–1151 (2013).

Plasmonics from deep UV to far IR

Vladimir P. Drachev

Department of Physics and Advanced Materials and Mechanical Processing Institute, University of North Texas, Denton, TX, USA;

Skolkovo Institute of Science and Technology, Skolkovo, Moscow region, Russia

e-mail: vladimir.drachev@unt.edu

The quality of the plasmon resonance in absorption and its correlation with superparamagnetic magnetization of Co nanoparticles will be discussed as well as the extremely broadband 0.5 -20 μm extinction of the Au fractal shells.

A variety applications of plasmonics requires ability to design a plasmon structure with its resonance in a broad spectral range from the deep ultra-violet (UV) to far infra-red (IR). The red shifted resonances can be obtained by the aspect ratio of nanoparticles, core/shell ratio, or by the nanoparticle aggregation. The UV resonances can be obtained only by using other materials.

We have found recently that Co nanoparticles with high quality crystal structure support an excellent plasmon resonance at about 275 nm, which is comparable with the noble metal in the visible range. It was observed also that the surfactant fluorescence is enhanced by factor of 10^3 . The quality of the resonance in optical response correlates with superparamagnetic magnetization of Co nanoparticles. In this talk we will discuss why the quality of the resonance does not correspond to the permittivity of the bulk Co from Johnson and Christy; possible mechanism of the correlation between magnetic and optical responses in the DUV.

Another set of observation is related to the broadband 0.5 -20 μm extinction of the core-shell submicron microspheres with Au fractal shells [1]. In contrast to the planar fractal films, where the absorption and reflection equally contribute to the extinction, the shells' extinction is caused mainly by the absorption, while the reflection and scattering are noticeably reduced. The Mie scattering resonance at 560 nm of a silica core with 780 nm diameter is strongly suppressed by and partially substituted by the absorption in the shell so that the total transmission is increased by factor of 1.6 due to the gold fractal shell. The characteristic feature of the silica core, vibrational stretching band at 9 μm in absorption, also disappears in the extinction spectrum, which is completely dominated by the shell absorption. Effective medium theory (EMT) describes the experimental spectra reasonably well and gives an epsilon-near-zero real part of the effective shell permittivity and approximately wavelength independent product of the imaginary part of the permittivity and light frequency over the broad spectral range. This product is responsible for the energy density dissipation rate of the plane wave. Applicability of the EMT and known scaling theories will be discussed.

References

- [1] V. C. De Silva, P. Nyga, V. P. Drachev, Scattering suppression in epsilon-near-zero plasmonic fractal shells, *Optical Materials Express*, **5**(11), 2491–2500 (2015).

Bistability effect in near-field radiative heat transfer

Dyakov S.A., Gippius N.A.

Skolkovo Institute of Science and Technology, Photonics and Quantum Materials Center, Nobel Street 3, 143026, Moscow, Russia
e-mail: s.dyakov@skoltech.ru

Dai J., Yan M.

KTH Royal Institute of Technology, Department of Materials and Nano Physics, School of Information and Communication Technology, Electrum 229, 16440 Kista, Sweden

Qiu M.

KTH Royal Institute of Technology, Department of Materials and Nano Physics, School of Information and Communication Technology, Electrum 229, 16440 Kista, Sweden;
Zhejiang University, Department of Optical Engineering, State Key Laboratory of Modern Optical Instrumentation, 310027 Hangzhou, China

We report the concept of a near-field thermal memory based on radiative bistability effect in the system of two closely separated parallel plates of SiO₂ and VO₂ which exchange heat by thermal radiation in vacuum. Using the approach of fluctuational electrodynamics [1, 2], we theoretically demonstrate that VO₂ plate, having metal-insulator transition at 340 K, has two thermodynamical steady-states. In this geometry, due to contactless near-field interaction between the plates, the driving heat exchange flux provides 5 ms switching time which more than 3 orders of magnitude faster than in the far field. In spite of the fact that 5 ms switching time is fairly slow, we believe that the discussed structure is a great example of radiative heat flux control by near field that could be useful for practical applications in information processing.

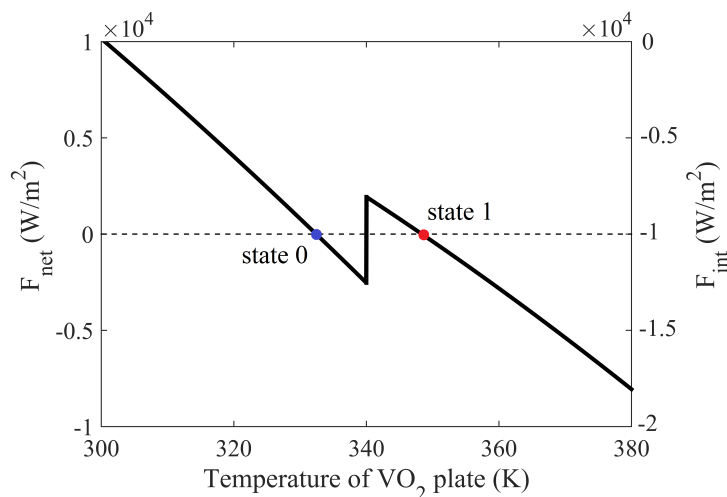


Fig. 1: The power of the heat transfer from SiO₂ plate to VO₂ plate due to the difference in their temperatures, $F_{int}(T_2)$, and the net power flux $F_{net}(T_2)$ of VO₂ plate as a function of the temperature of VO₂ plate. The graph illustrates the negative differential thermal conductance. $h = 50$ nm, $d = 50$ nm, $F_0 = 1.9 \times 10^4$ W/m², $T_{SiO_2} = 300$ K.

References

- [1] M. Francoeur, M. Pinar Mengüç, Role of fluctuational electrodynamics in near-field radiative heat transfer, *J. Quant. Spectrosc. Radiat. Transf.*, Vol. **109**, no. 2, pp. 280–293, 2008.

- [2] S. A. Dyakov, J. Dai, M. Yan, M. Qiu, Thermal radiation dynamics in two parallel plates: The role of near field, *Phys. Rev. B*, Vol. **90**, p. 045414, Jul 2014.

Nanophotonics: controlling the flow of light and heat

Shanhui Fan

Department of Electrical Engineering, Ginzton Laboratory, Stanford University, Stanford, California 94305, USA
e-mail: shanhui@stanford.edu

The use of nanophotonic structures provide new mechanisms to control the flow of light and heat. In this talk, we review some of our recent efforts in designing dynamic nanophotonic structures to create new topological effects in photonic structures. We also discuss the use of nanophotonic structures for the control of thermal radiation, leading to the possibility of passive air-conditioning without the use of electricity.

Wave control with space-time manipulations

Mathias Fink

Institut Langevin, ESPCI Paris Tech 1 rue Jussieu, 75005, Paris, France
e-mail: mathias.fink@espci.fr

Time-reversal processing is based on Huygens principles and on wavefield manipulation on spatial boundaries. It provided an elegant way to back propagate a wave field towards its initial source allowing to create, through any complex medium, a wave pattern of any required shape restricted only by diffraction limits.

Here we want to revisit these approaches by introducing another point of view, the one that Loschmidt proposed in his famous argument to create a time-reversal experiment by inverting instantaneously all velocities of the particles in a gas. The extension of this concept to wave will be discussed through the concept of time boundaries manipulation. Experiments, conducted with water waves, validating this approach will be presented. We show that sudden changes of the medium properties generate instant wave sources that emerge instantaneously from the entire space at the time disruption. The time-reversed waves originate from these “Cauchy sources” which are the counterpart of Huygens virtual sources on a time boundary. It allows us to revisit the holographic method and introduce a new approach for wave control in complex media.

In the second part of this talk, we will discuss another approach to manipulate a wave field in reverberating medium by introducing tunable metasurfaces as spatial boundaries and we will emphasize this concept for microwaves.

Quantum description of nanoantenna properties of a graphene membrane

Natalie Firsova

Institute for Problems of Mechanical Engineering, the Russian Academy of Sciences, St. Petersburg 199178, Bolshoy Prospect V.O. 61, Russia;
St. Petersburg Polytechnic University, St. Petersburg 195231, Politechnicheskaya 29, Russia;
A. F. Ioffe Physical-Technical Institute, the Russian Academy of Sciences, St. Petersburg, 194021, Politechnicheskaya 26, Russia
e-mail: nef2@mail.ru

The graphene membrane irradiated by weak activating periodic electric field in terahertz range was considered. The quantum approach based on the time-dependent density matrix method was

used. The exact solution was obtained for graphene membrane density matrix equation in linear on the external field approximation. On this basis the graphene electromagnetic response was studied i.e. the quantum formulae for the induced current and conductivity were found as functions of temperature. The found formula for the conductivity corrected the one obtained by V.P. Gusynin, S.G. Sharapov and J.P. Carbotte and allowed to see that the graphene membrane was an oscillating contour, its fundamental eigen frequency coinciding with a singularity point of the conductivity. This formula allowed us to calculate the graphene membrane quantum inductivity and capacitance. So the graphene membrane could be used as an antenna or a transistor. It was shown that its eigen frequency could be tuned by doping as its value was found to depend on electrons concentration. It was obtained that the eigen frequency could be tuned in a rather large frequency range 1–100 terahertz as electrons concentration in graphene may differ considerably. The found dependence on concentration correlates with experiments. The obtained corrected formula for conductivity can be used to correct the SPPs Dispersion Relation and the description of radiation process. It would be useful to take the obtained results into account when constructing devices containing graphene membrane nanoantenna allowing wireless communications among nanosystems. This could be promising research area of energy harvesting applications.

Controlling light on the nanoscale by ultra-flat particle lenses

T. Fischer, U. Zywietz, T. Birr, A.B. Evlyukhin, C. Reinhardt, B.N. Chichkov

Laser Zentrum Hannover e.V., Hollerithallee 8, D-30419 Hannover, Germany

e-mail: t.fischer@lzh.de

Spherical nanoparticles with diameters around 200 nm provide unique optical properties. They show characteristic resonances in the visible spectrum and strong directional scattering [1]. Arranged in a special geometry these features can be utilized in ultra-flat lenses as shown schematically in figure 1 [2]. We considered gold and silicon nanoparticles as building blocks for these lenses and designed the focussing properties by iterative optimization of the particle arrangement based on Mie theory calculations. After evaluating optimal geometries we were able to fabricate prototypes of ultra-flat particle lenses using a combination of prestructured material films and subsequent laser induced transfer. Experimental evaluation showed very good agreement with the theoretically calculated properties.

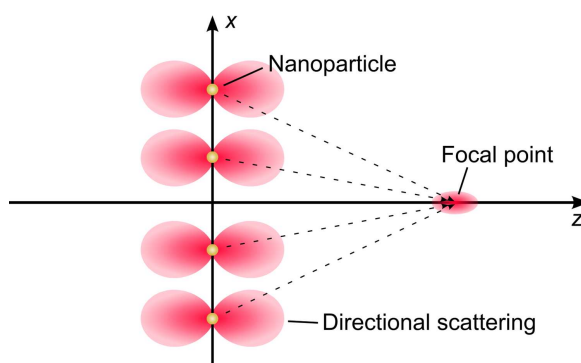


Fig. 1: Basic mechanism of an ultra-flat nanoparticle lens.

References

- [1] A.B. Evlyukhin, S.M. Novikov, U. Zywietz, R.L. Eriksen, C. Reinhardt, S.I. Bozhevolnyi, B.N. Chichkov, Demonstration of magnetic dipole resonances of dielectric nanospheres in the visible region, *Nano Lett.*, vol. **12**, no. 7, pp. 3749–3755 (2012).
- [2] N. Yu, F. Capasso, Flat optics with designer metasurfaces, *Nat. Mater.*, vol. **13**, no. 2, pp. 139–150 (2014).

Simulation and analysis of wave propagation in periodic and aperiodic composites

Fomenko S.I., Aleksandrov A.A.

Institute for Mathematics, Mechanics and Informatics, Kuban State University, Krasnodar, 350040, Russia

e-mails: evg@math.kubsu.ru, sfom@yandex.ru

Composite materials are gaining wider application in various fields of engineering, rocket production, shipbuilding, etc. Unlike traditional materials multilayered composites have lower weight, greater stiffness and high specific strength at a certain combination of layers. Periodic elastic composites that are frequently named phononic crystals have additional unique features such as frequency band-gaps, negative refraction of incident waves, energy transformation, etc. Therefore, the interest to phononic crystals is growing as for theoretical investigators so for engineers [1].

The present talk is a continuation of our previous researches of band-gaps in structures with layered phononic crystals [2, 3]. Now it is focused on a classification and a parametric study of various types of frequency ranges in wave dynamics of periodical composites consisted of anisotropic layers. The investigation of disturbance in the periodicity of phononic crystal cells is under special consideration. The aperiodicity in the cell structure of phononic crystals can arise with big probability during their production or exploitation.

The analysis is performed using transfer matrix method. The wave state vector of a phononic crystal with given finite number of cells is obtained in terms of an expansion by eigenvalues of transfer matrix. This representation has numerical stability for any number of cells as well as gives convenient tool for classification and analysis of band-gaps. The classification based on the localization factor, that is provided by the eigenvalues, and on the asymptotics of transmission coefficient as a number of cells tends to infinity. The classification gives three types of frequency ranges in which the wave transmission is sufficiently low: band-gaps of 1st and 2nd kinds and low transmission pass-band (LTPB). Interpretation of different types of frequency ranges is performed using dispersion analysis of Bloch waves. There are not any Bloch waves to propagate through the periodical structure in 1st band-gap while in other types of bands Bloch wave may be generated theoretically. Just only a single Bloch wave is excited in both of LTPB and 2nd band-gap. The wave amplitude is equal to zero in the 2nd band-gap while its amplitude is sufficiently small in the engineering sense in LTPB. Developed method provides the methodic for investigating aperiodic phononic crystals. The aperiodicity at given probability distribution law for a width of cell layers is studied using sampling statistics. Sufficient results of numerical parametric analysis of wave propagation in the phononic crystals will be presented for discussion.

The work is supported by grant of President of Russian Federation (MK-7154.2015.1), the Russian Foundation for Basic Research (16-51-53043) and the Ministry of Education Science of Russian Federation (1.189.2014K).

References

- [1] A. Khelif, A. Adibi, *Phononic Crystals Fundamentals and Applications*, Springer-Verlag, New York (2016).
- [2] S. I. Fomenko, M. V. Golub, T. Q. Bui, C. Zhang, Y.-S. Wang, *International Journal of Solids and Structures*, **51**(13), 2491–2503 (2014).
- [3] M. V. Golub, S. I. Fomenko, A. A. Alexandrov, *Proceedings of the International Conference Days on Diffraction 2014*, 83–89 (2014).

Purcell enhanced Raman scattering from silicon nanoparticles

Frziuk K.S.^{1,2}, Krasnok A.E.², Petrov M.I.²

¹Saint-Petersburg Polytechnic University, 29, Polytechnicheskaya str., St. Petersburg, Russia

²ITMO University, 49, Kronverksky Pr., St. Petersburg, Russia

e-mail: frzyuk@gmail.com

The growing interest in all-dielectric nanostructures as an alternative to plasmonic [1] requires a better understanding of their optical properties. Here we present the theoretical study of Raman scattering from spherical silicon nanoparticles as a building block of all-dielectric photonics. One of the major aspects of all-dielectric is that high refractive index nanoparticles have Mie resonances when the condition is satisfied $\lambda \approx 2nR$, where λ is the light wavelength, n is the refractive index, and R is the nanoparticle radius. Therefore, electromagnetic field is amplified on the resonant wavelength, resulting in resonances in Raman scattering. Here we apply simple analytical method based on Green's function approach. Implementing the properties of dyadic Green's function [2, 3], we show that Raman signal has additional enhancement on account of Purcell factor F_p [4]:

$$I \sim \int F_p(\mathbf{r}, \omega_s) |\mathbf{P}(\mathbf{r})|^2 dV, \quad F_p(\mathbf{r}, \omega_s) = \frac{6c}{\omega_s} \left(\mathbf{n}^*(\mathbf{r}) \cdot \text{Im} \left(\widehat{\mathbf{G}}(\mathbf{r}, \mathbf{r}, \omega_s) \right) \cdot \mathbf{n}(\mathbf{r}) \right),$$

where ω_s is the frequency of Stokes signal, $\mathbf{P}(\mathbf{r})$ is the Raman polarization vector, \mathbf{n} is the unit vector oriented along the Raman dipole transition vector, $\widehat{\mathbf{G}}(\mathbf{r}, \mathbf{r}, \omega_s)$ is the dyadic Green's function, and the integration is taken over nanoparticle volume. This method can be applied for calculating of Raman signal produced by substances with various phonon correlation length [5].

Additional resonant Purcell factor increases the quality factor of Raman scattering in comparison to elastic scattering as shown in Fig. 1. Moreover, the dark modes of silicon nanoparticles, which are not seen in the elastic scattering spectrum, can be clearly detected in Raman signal spectrum due to their resonant contribution into the Purcell factor.

The work has been supported by the project # RFMEFI58416X0018 of the Ministry of Education and Science of the Russian Federation.

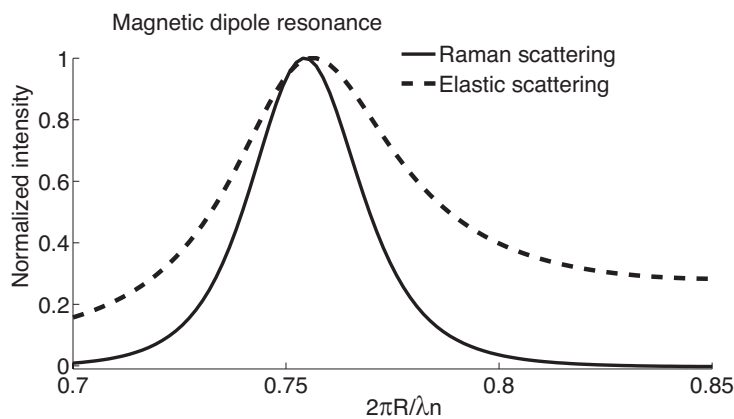


Fig. 1: Normalized intensity of elastic and Raman scattering from spherical dielectric nanoparticle.

References

- [1] S. Jahani, Z. Jacob, All-dielectric metamaterials, *Nat. Nanotechnol.*, vol. **11**, no. 1, pp. 23–36 (2016).
- [2] A. Krasnok, S. Makarov, M. Petrov, R. Savelev, P. Belov, Y. Kivshar, Towards all-dielectric metamaterials and nanophotonics, *Proc. SPIE 9502, Metamaterials X*, p. 950203 (2015).
- [3] L. Knoll, S. Scheel, D.-G. Welsch, QED in dispersing and absorbing media, *Coherence Stat. Photons Atoms*, p. 60 (2000).

- [4] E. Purcell, Spontaneous emission probabilities at radio frequencies, *Phys. Rev.*, vol. **69**, no. 11-12, pp. 674–674 (1946).
- [5] L. G. Cancado, R. Beams, A. Jorio, L. Novotny, Theory of spatial coherence in near-field Raman scattering, *Phys. Rev. X*, **4**(3), 031054 (2014).

Raman scattering governed by dark resonant modes in silicon nanoparticles

Friziuk K.S.^{1,2}, Milichko V.A.², Petrov M.I.², Zuev D.A.², Baranov A.V.², Baranov M.A.², Mukhin I.S.³, Makarov S.V.², Krasnok A.E.²

¹St. Petersburg Polytechnic University, Russia, 195251, St. Petersburg, Polytechnicheskaya, 29

²ITMO University, 49 Kronverksky Pr., St. Petersburg, 197101, Russia

³St. Petersburg Academic University, 8/3, Khlopina Str., St. Petersburg, 194021, Russia

e-mail: trisha.petrov@gmail.com

The interest of the optical community in all-dielectric nanophotonics rapidly grows for the last several years, which already gave a number of bright results in this field [1, 2]. The properties of high-index nanostructures manifest themselves in strong magnetic and electric resonances in the visible and near-infrared region for sufficiently subwavelength nanoparticles.

Currently, silicon is the the most common and prospective material of all-dielectric nanophotonics, having high refractive index over all visible range and relatively low optical losses. Silicon is one of the most widely used materials in optics and electronics, and, in particular, it is known for its pronounced Raman scattering properties. The lines of transversal and longitudinal optical phonons located at 520 cm^{-1} govern the Raman scattering spectra. In this work we suggest implementing Raman scattering for detection and investigation of optical modes in silicon nanostructures. We show that Raman scattering allows identification and imaging of dark modes not observed in elastic scattering spectrum. We observe intense scattering at magnetic quadrupole mode considering silicon nanoparticle placed over gold substrate [see Fig. 1(a)]. Gold substrate strongly modifies the spectrum of silicon nanoparticles due to surface plasmon coupling and to substrate induced bi-anisotropy [3]. At the magnetic quadrupole resonance the electrical dipole and toroidal modes cancel each other [4] allowing detection of magnetic quadrupole mode in its pure, non-mixed state [see Fig. 1(b)].

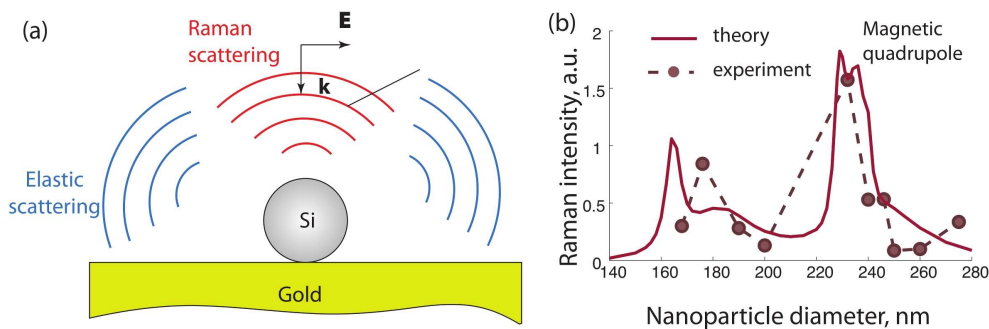


Fig. 1: (a) The geometry of the problem. (b) The measured Raman scattering intensity at pumping wavelength 632 nm depending on the nanoparticle diameter. The theoretical dependence is shown by solid line.

The demonstrated results prove that Raman scattering can be a powerful tool for detecting and imaging of silicon nanoparticles modal structure.

The work has been supported by the project # RFMEFI58416X0018 of the Ministry of Education and Science of the Russian Federation.

References

- [1] S. Jahani, Z. Jacob, All-dielectric metamaterials, *Nat. Nanotechnol.*, vol. **11**, pp. 23–36 (2016).
- [2] A. Krasnok, S. Makarov, M. Petrov, R. Savelev, P. Belov, Y. Kivshar, Towards all-dielectric metamaterials and nanophotonics, *Proc. SPIE 9502, Metamaterials X*, p. 950203 (2015).
- [3] A. E. Miroshnichenko, A. B. Evlyukhin, Y. S. Kivshar, B. N. Chichkov, Substrate-induced resonant magnetoelectric effects with dielectric nanoparticles, *ACS Photonics*, **2**, pp. 1423 (2015).
- [4] A. E. Miroshnichenko, A. B. Evlyukhin, Y. F. Yu, R. M. Bakker, A. Chipouline, A. I. Kuznetsov, B. Luk'yanchuk, B. N. Chichkov, Y. S. Kivshar, Nonradiating anapole modes in dielectric nanoparticles, *Nat. Commun.*, vol. **6**, p. 8069 (2015).

Electromagnetic field of a charge flying into chiral isotropic medium

Galyamin S.N., Tyukhtin A.V., Peshkov A.A.

Saint Petersburg State University, 7/9 Universitetskaya nab., St. Petersburg, 199034 Russia
e-mails: s.galyamin@spbu.ru, a.tyukhtin@spbu.ru

We analyze electromagnetic field of a point charge flying from vacuum into half-space filled with isotropic chiral medium. We continue the investigation performed in our previous paper [1] where we dealt with the field produced by uniformly moving charge in corresponding infinite medium. Moreover, we perform generalization of early paper [2], where the problem with half-space was considered in the specific case of slow charge motion. It should be also noted, that the interest to radiation of moving charged particles in media with chiral properties is connected with relatively new and prospective method for diagnostics of biological objects which uses the Cherenkov radiation — Cherenkov luminescence imaging [3]. Optical activity (chirality, gyrotropy) is typical of biological matter and is caused by mirrorless structure of molecules. Contrary to such gyrotropic medium as magnetized ionospheric plasma, aforementioned media are isotropic. One distributed model describing the frequency dispersion of isotropic chiral media is Condon model [4].

In this report, we deduce analytical expressions for Fourier components of electromagnetic field in both vacuum and medium for arbitrary charge velocity. Further, the main attention is paid to investigation of the far field in vacuum. The distinguishing feature of interface with chiral isotropic medium is that field in vacuum area contains both co-polarization (field with polarization coinciding with that of self-field of a charge) and cross-polarization (field with polarization orthogonal to that of self-field of a charge). With the use of steepest descent approach, we obtain asymptotic representations for the field components in the far-field zone for typical frequency ranges of Condon model. We also note that the lateral wave is generated in vacuum for certain parameters. The main contribution to the radiation at large distances is presented by two (co- and cross-) spherical waves of transition radiation. These waves are coherent and result in total spherical wave with elliptical polarization, with the polarization coefficient being determined by chirality of the medium. We present typical radiation patterns and ellipses of polarization.

Work is supported by the Grant of the Russian Foundation for Basic Research (No. 15-32-20985).

References

- [1] S. N. Galyamin, A. A. Peshkov, A. V. Tyukhtin, *Phys. Rev. E*, **88**, 013206 (2013).
- [2] N. Engheta, A. R. Mickelson, *IEEE Trans. Antennas Propag.*, **30**(6), 1213 (1982).
- [3] A. E. Spinelli, et al., *Nucl. Instr. Meth. Phys. Res. A*, **648**, S310 (2011).
- [4] E. U. Condon, *Rev. Mod. Phys.*, **9**, 432 (1937).

Opto-mechanical metamaterials

Pavel Ginzburg^{1,2*}, Andrey A. Bogdanov², Aliaksandra Ivinskaya², Alexander S. Shalin²

¹School of Electrical Engineering, Tel Aviv University, Tel Aviv 69978, Israel

²ITMO University, St. Petersburg, 197101, Russia

e-mail: *pginzburg@post.tau.ac.il

Control over mechanical motion of nanoscale particles is a valuable functionality desired in a variety of multidisciplinary applications, e.g. in biophysics, and it is usually achieved by employing optical forces. Hyperbolic metamaterials enable tailoring and enhancing electromagnetic scattering (e.g. [1]) and, as the result, could provide a platform for a new type of optical manipulation. A span of opto-mechanical phenomena, inspired by plasmonic structures and metamaterials will be discussed. For example, pulling forces acting on a small particle placed inside a hyperbolic metamaterial slab will be demonstrated. In order to attract particles to a light source, highly confined extraordinary modes of hyperbolic metamaterial were excited via scattering from an imperfection situated at the slab's interface. This type of structured illumination together with remarkable scattering properties, inspired by the hyperbolic dispersion in the metamaterial, creates optical attraction. Forces acting on high-, low-index dielectric, and gold particles were investigated and it was shown that the pulling effect emerges in all of the cases (Fig. 1) [2]. Furthermore, three-dimensional nanorod metamaterial platform, serving as an auxiliary tool for the optical manipulation, will be discussed. Its unique ability to support and control near-field interactions and generate both steep and flat optical potential profiles, will be presented. In particular, the impact of 'topological transitions' on optical forces will be revised [3].

The ability to control mechanical motion at nanoscale using auxiliary photonic structures paves the way for investigation of various phenomena, e.g. biochemical reactions, molecular dynamics, and more.

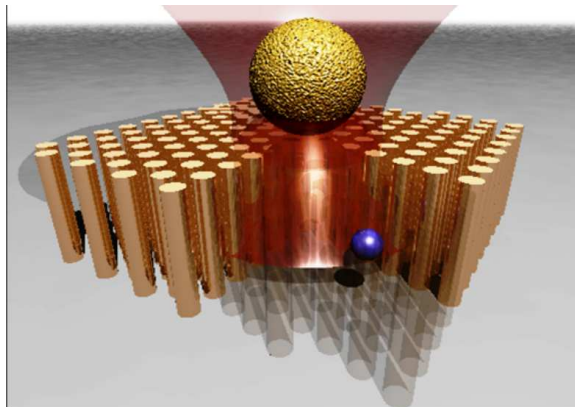


Fig. 1: Schematics of opto-mechanical manipulation with auxiliary metamaterials. Extraordinary highly localized waves in nanorods hyperbolic metamaterial are excited via scattering and enable controlling mechanical motion of embedded particles (blue sphere on the schematics).

References

- [1] I. V. Iorsh, A. N. Poddubny, P. Ginzburg, P. A. Belov, Y. S. Kivshar, Compton-like polariton scattering in hyperbolic metamaterials, *Phys. Rev. Lett.*, Vol. **114**, no. 18, p. 185501, 2015.
- [2] A. S. Shalin, S. V. Sukhov, A. A. Bogdanov, P. A. Belov, P. Ginzburg, Optical pulling forces in hyperbolic metamaterials, *Phys. Rev. A*, Vol. **91**, no. 6, p. 063830, 2015.
- [3] A. A. Bogdanov, A. S. Shalin, P. Ginzburg, Optical forces in nanorod metamaterial, *Sci. Rep.*, Vol. **5**, p. 15846, 2015.

Tamm–Langmuir surface waves

Golenitskii K.U.¹, Bogdanov A.A.²

¹Ioffe Institute, St. Petersburg, Russia

²ITMO University, St. Petersburg, Russia

e-mail: kirillgol@yandex.ru

Modern nano- and optoelectronics are based on planar multilayered structures. Due to the great number of interfaces, which can reach several thousands, electromagnetic properties of optoelectronic devices can be mainly determined by surface effects, in particular, by surface electromagnetic waves localized at the interfaces [1].

In this work we analyze electromagnetic waves localized at the interface of periodic metal-dielectric structures taking into account anisotropy of conducting layers [Fig. 1(a)]. Anisotropy of natural materials in the visible range usually is quite weak in contrast to the case of artificial media where a role of anisotropy can be crucial [2]. We show that strong anisotropy of electron spectrum in the metal layers lifts the degeneracy of plasma oscillation that results in appearance of the surface waves with singular density of optical states. We analyse nature of these waves, their dispersion, field distribution, and losses.

The spectrum of anisotropic metal-dielectric structure is shown in Fig. 1(b). One can see that along with surface plasmon polariton modes and optical Tamm waves able to propagate in the isotropic case there are infinite number of surface waves whose dispersion lies between plasma frequencies of anisotropic metal layers (Ω_{\parallel} and Ω_{\perp}) and degenerates in the isotropic case ($\Omega_{\parallel} = \Omega_{\perp}$) [3]. Dispersion and field distribution of these waves are very similar to the ones of the bulk Langmuir waves. So, it is naturally to call these modes *Tamm–Langmuir waves*. Dispersion of the Tamm–Langmuir waves can be easily tailored by the proper choice of design and materials of the structure. This makes them quite promising for on-chip photonics, optical communications, and biological sensing.

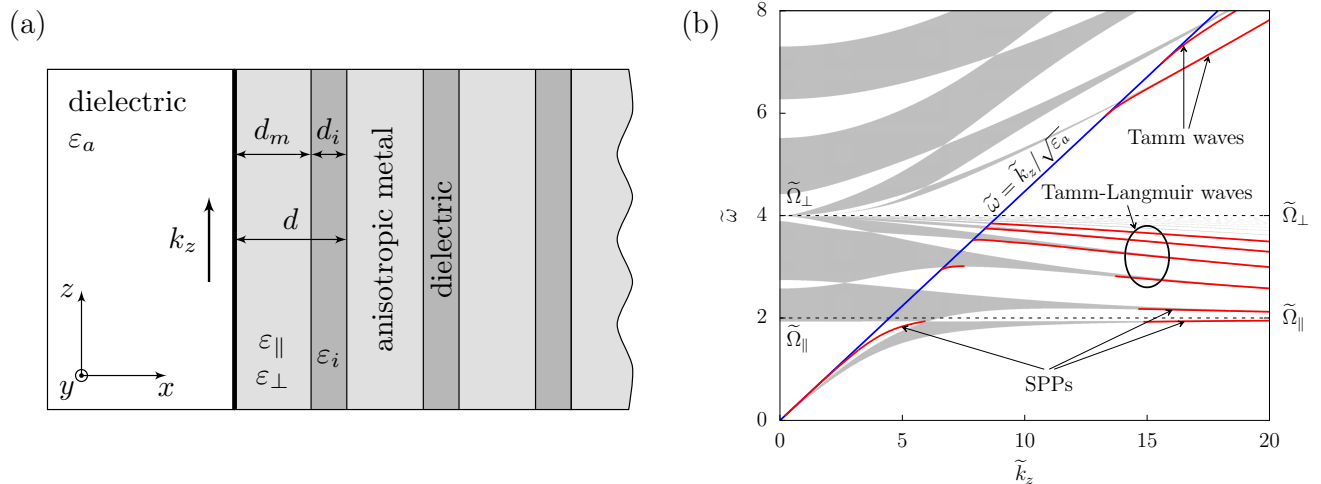


Fig. 1: (a) Investigated semi-infinite metal-dielectric structure with anisotropic conducting layers (b) Dependence of ω on k_z for surface waves on the interface of the structure. Gray areas correspond to the allow bands of the periodic structure.

References

- [1] J. Polo, A. Lakhtakia, *Laser & Photonics Reviews*, **5**, 234 (2011).
- [2] A. Poddubny, I. Iorsh, P. Belov, Y. Kivshar, *Nature Photonics*, **7**, 948 (2013).
- [3] A. Bogdanov, R. Suris, *JETP Letters*, **96**, 49 (2012).

Nonlinear-optical anisotropy of silicon nanowire arrays

Golovan L.A.¹, Kholodov M.M.¹, Presnov D.E.¹, Zobotnov S.V.¹, Efimova A.I.¹, Timoshenko V.Yu.¹, Neskromnaya A.V.², Petrov G.I.³, Yakovlev V.V.³

¹Physics Department, M. V. Lomonosov Moscow State University, 119991, Moscow, Russia

²Material Sciences Department, M. V. Lomonosov Moscow State University, Moscow 119991, Russia

³Department of Biomedical Engineering, Texas A & M University, College Station, TX 77843, USA
e-mail: golovan@physics.msu.ru

Nowadays, arrays of silicon nanowires (SiNW) of about 100 nm attract great interest due to their unique optical properties such as extremely high light absorption, enhanced spontaneous Raman scattering, third-harmonic generation, and infrared interband photoluminescence, which are often connected with the light trapping in SiNW arrays.

The SiNW sample was fabricated by means of metal-assisted chemical etching process [1] at (110) crystalline silicon (c-Si) wafer. The formed SiNWs are strongly prolate parallelepipeds of about 100 nm in diameter tilted to the surface at the angle of 45° with projection oriented along (1 $\bar{1}$ 0) direction (Fig. 1a). The SiNW arrays demonstrate effective light scattering, therefore linear reflectance measurements evidence no effect of the SiNW orientation. However, nonlinear-optical processes, e. g. third-harmonic generation and coherent anti-Stokes Raman (CARS) scattering, which strongly depend on the local fields could demonstrate their anisotropy. The broadband CARS signal was generated at the frequency $2\omega_1 - \omega_2$, where ω_1 and ω_2 were the frequencies of Nd:YVO₄ laser (1064 nm, 10 ps) radiation and continuum radiation generated in optical fiber, correspondingly. The third-harmonic generation was carried out with the help of Cr: forsterite laser (1250 nm, 80 fs). In all cases polarization dependences of the signals were obtained.

In contrast to spontaneous Raman, the SiNW arrays exhibit pronounced polarization dependences of the CARS signal. The resonant CARS signal in SiNW ensemble is an order of magnitude less than in c-Si in the case when pumping radiation propagates perpendicular to the SiNWs and the CARS signal is collected in the direction along SiNWs and two orders of magnitude less than in c-Si in another case. Although third-harmonic signal for SiNW array exhibits less expressed orientation dependence then for c-Si, it exceeds the latter one the case of the fundamental radiation incident perpendicular, whereas in the case of incident wave propagation along the SiNWs it falls several time in comparison with c-Si (Fig. 1b). Thus, found in experiments anisotropy of the nonlinear-optical signals evidences the sensitivity of the these techniques to the orientation of SiNWs in their highly scattering arrays.

This work is supported by the Russian Foundation for Basic Research grant no. 15-29-01185.

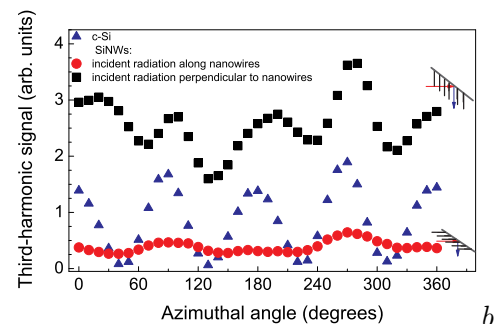
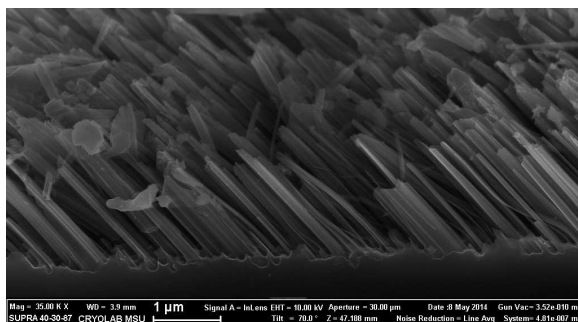


Fig. 1: (a) The SiNW sample cross-section in (100) plane. (b) Orientation dependence of the third-harmonic signals for c-Si and SiNW array in cases of fundamental radiation incident along and perpendicular to the nanowires.

References

- [1] V. A. Sivakov *et al.*, *J. Phys. Chem. C*, **114**, 3798–3803 (2010).

Two-photon excitations in nonlinear topological Su–Schrieffer–Heeger model

Gorlach M.A.¹, Poddubny A.N.^{2,1}

¹ITMO University, Saint Petersburg, 197101, Russia

²Ioffe Physical-Technical Institute, Saint Petersburg, 194021, Russia

e-mails: maxim.gorlach.blr@gmail.com, a.poddubny@phoi.ifmo.ru

Currently, there is a growing interest in the investigation of nonlinear systems with strong mutual interactions. In the case of optics, strong photon-photon interactions can be realized using nonlinearity of host medium [1]. Bose–Hubbard model provides a systematic way to describe nonlinearity in the framework of quantum theory. Recently it was demonstrated that in the presence of repulsive nonlinearity a pair of bosons can form a stable object that propagates as a single particle [2]. Such repulsively bound pairs further termed as doublons were also observed experimentally [2]. Advanced theoretical studies revealed that in the presence of defect in the chain doublons can form edge states [3]. However, to the best of our knowledge, the concept of topological edge states has not been extended to describe the topological properties of doublon edge states.

Inspired by the simplest example of topologically nontrivial system in the linear case, Su–Schrieffer–Heeger model, we consider a doubly periodic chain of optical resonators with Kerr-type nonlinearity coupled to each other as depicted in Fig. 1. We study the properties of two-photon excitations propagating in the systems as well as edge states formed by these photon pairs.



Fig. 1: Schematic view of a chain with two tunneling constants J_1 and J_2 .

According to our results, there are four main types of two-photon excitations in such system. The first type depicted in Fig. 2 by green color corresponds to almost noninteracting photons. Positions of such photons in nonlinear chain have almost no correlation. The second type corresponds to the situation when one photon is located at the edge of the chain, whereas the other one freely propagates in chain (blue color). The third type corresponds to repulsively bound photon pairs (red color) which exhibit nontrivial dispersion in the case of doubly periodic chain. Finally, the fourth type of two-photon excitations corresponds to two-photon edge states.

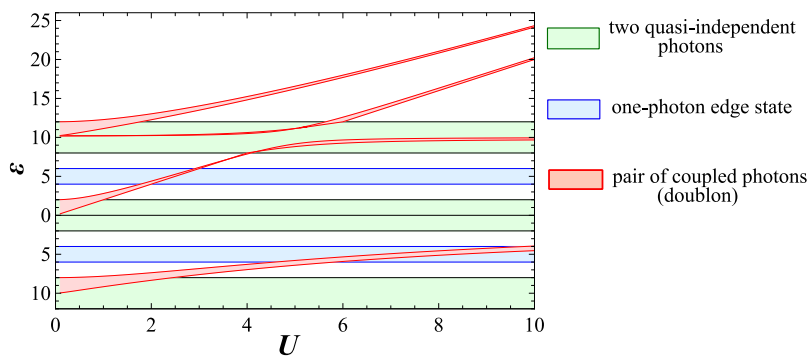


Fig. 2: Energy bands for different types of two-photon excitations in doubly periodic chain as a function of the nonlinearity parameter U . The ratio of hopping amplitudes is $J_2/J_1 = 5$.

References

- [1] I. Carusotto, C. Ciuti, *Reviews of Modern Physics*, **85**, pp. 299–366 (2013).
- [2] K. Winkler, G. Thalhammer, F. Lang, R. Grimm, J. H. Denschlag, A. J. Daley, A. Kantian, H. P. Buchler, P. Zoller, *Nature*, **441**, pp. 853–856 (2006).
- [3] S. Longhi, G. della Valle, *Journal of Physics: Condensed Matter*, **25**, p. 235601 (2013).

Discrete diffraction and refraction of spin waves in magnonic waveguide lattice

Grachev A.A., Sadovnikov A.V., Beginin E.N., Sharaevskii Yu.P., Sheshukova S.E.

Saratov State University, 410012, Saratov, Russia

e-mails: stig133@gmail.com, sadovnikovav@gmail.com

Discrete diffraction are studied in optics both theoretically and experimentally by scanning tunneling optical microscopy in arrays of equally spaced identical waveguide elements [1, 2]. Coupled Yttrium iron garnet (YIG) structures are of great interest at the modern time due to extremely small spin-wave loss in this material and the possibility of spin wave (SW) propagation control. Coupled YIG waveguides can be used as components in the tunable signal processing devices (nonlinear couplers, nonlinear switches, phase shifters).

This report shows the results of investigation of the spatio-temporal dynamics of magnetization in the laterally coupled planar YIG waveguide array by Brillouin light scattering (BLS) spectroscopy. The structure was fabricated from a sample of the YIG film thickness of 10 μm , grown on the basis of GaGd-garnet (GGG) thickness of 0.5 mm by laser cutting (Fig. 1, a). The structure was magnetized by an in-plane magnetic field of $H_0 = 1200 \text{ Oe}$ parallel to the microstrip antennas. The discrete diffraction of surface spin wave in a lateral coupled YIG waveguide array was demonstrated experimentally with BLS technique in planar waveguide geometry, when a single input channel with number $n = 0$ is excited.

Spin-wave diffraction in the array of side-coupled magnonic stripes was numerically studied using the discrete nonlinear Schrödinger equations. We show that increasing the amplitude of input signal the regime of spin wave diffraction is switched to the multi-channel discrete soliton-like propagation (Fig. 1, b). It was demonstrated also that the a highly localized single channel regime of signal propagation is a robust effect in the side-coupled magnonic array. The dependence of coupling between the waveguide channels on the parameters of spin wave (wavenumber, frequency, power) makes the continuous regulation of spin wave path possible.

This work was partially supported by the Grant from Russian Science Foundation (Project 14-19-00760), Grant of RFBR (project No. 16-37-60093, 16-37-00217), Scholarship of the President of RF (SP-313.2015.5) and Grant of the President of RF (MK-5837.2016.9).

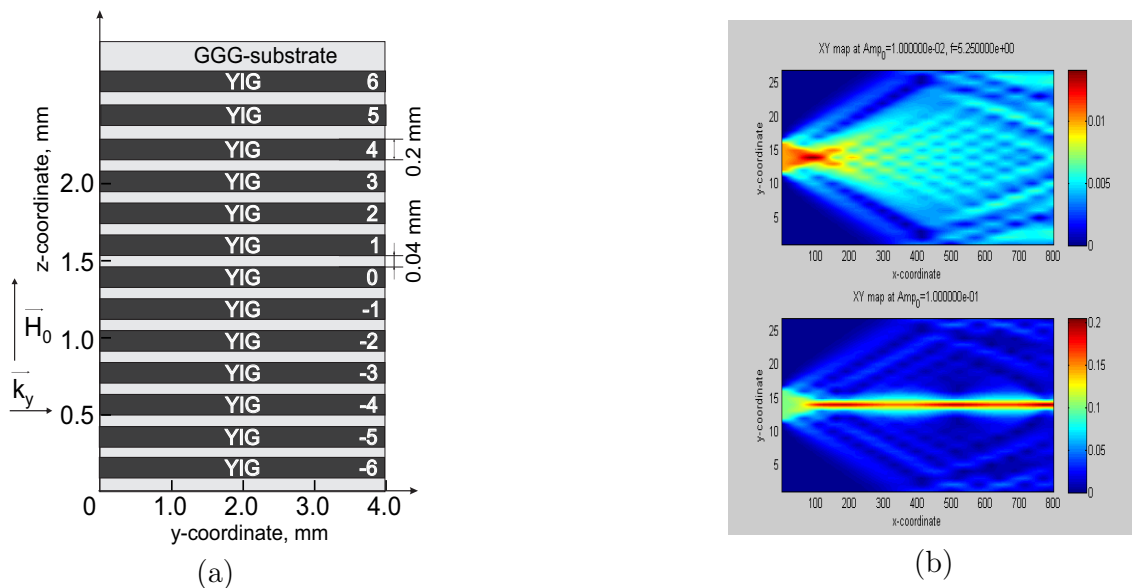


Fig. 1: (a) Geometry of YIG waveguides array. (b) Discrete diffraction as function of propagation distance.

References

- [1] F. Lederer, G.I. Stegeman, D.N. Christodoulides, *Phys. Rep.*, **463**, 1–126 (2008).

- [2] A. V. Sadovnikov, E. N. Beginin, S. E. Sheshukova, D. V. Romanenko, Yu. P. Sharaevskii, S. A. Nikitov, *Appl. Phys. Lett.*, **107**, 202405 (2015).

Enhancing nonlinear optical signal in Perovskite nanostructures

Rachel Grange

Optical Nanomaterial Group, Institute for Quantum Electronics, Department of Physics ETH Zürich, Switzerland

e-mail: grange@phys.ethz.ch

Nonlinear optical processes are known to be weak in bulk materials and extremely small at the nanoscale since they mainly scale with the volume. Here I will show how we enhance second-harmonic generation in few Perovskite nanomaterials.

First, I will present the core-shell approach for BaTiO₃ nanospheres [1], and KNbO₃ nanowires [2]. The originality of our work, compared to pioneering works on core-shell plasmonics, is that the core material (ABO₃-like) possess additional interesting properties than the usual silica spheres and the nanoshells is not only used to interact with the surrounding medium, for instance by local heating, but to enhance the incident infrared light. Thus, by adding functionality to a nanosystem, we offer new possibility of applications in nanomedicine or integrated devices. I will also discussed recent results taking advantage of various resonances of BaTiO₃ nanoparticles in the visible wavelength range. Contrary to plasmonics occurring in metallic nanostructures, those resonances take place in dielectric nanoparticles and they are well described by Mie scattering theory.

Besides chemically synthesized nanostructures, we developed lithography processes to obtain high aspect ratio lithium niobate (LiNbO₃) nanowaveguides. We demonstrate phase-matching and use it to increase the guided second-harmonic power by a factor of more than 40 [3]. We also increase non-phase-matched guided second-harmonic by engineering the nanowire length. Those bright nanostructures can serve for developing compact efficient nonlinear optical sources or waveguides.

References

- [1] E. Kim, A. Steinbrück, M. T. Buscaglia, V. Buscaglia, T. Pertsch, R. Grange, Second-harmonic generation of single BaTiO₃ nanoparticles down to 22 nm diameter, *ACS Nano*, **7**, 5343–5349 (2013).
- [2] J. Richter, A. Steinbrück, M. Zilk, A. Sergeev, T. Pertsch, A. Tünnermann, R. Grange, Core-shell potassium niobate nanowires for enhanced nonlinear optical effects, *Nanoscale*, **6**, 5200–7 (2014).
- [3] A. Sergeev, R. Geiss, A. S. Solntsev, A. A. Sukhorukov, F. Schrempel, T. Pertsch, R. Grange, Enhancing guided second-harmonic light in lithium niobate nanowires, *ACS Photonics*, **2**, 687–691 (2015).

A dual frequency antenna for RSSI-based DOA estimation: from theory to prototype

Hartmann M.¹, Wohler M.², Schühler M.², Weisgerber L.², Thielecke J.¹, Heuberger A.¹

¹Friedrich-Alexander-Universität Erlangen-Nürnberg (FAU), InformationTechnologies, 91058 Erlangen, Germany

²Fraunhofer Institute for Integrated Circuits (IIS), 91058 Erlangen, Germany

e-mail: markus.hartmann@fau.de

This paper presents a dual band antenna for Received Signal Strength (RSS)-based direction of arrival (DOA) estimation. Based on the RSS difference of two directional antennas the DOA is

inferred. Our targeted application is the measurement of flight trajectories of bats equipped with tiny transmitters.

Our design aims at a low-cost prototype antenna, providing suitable properties for RSS-DOA estimation. The full design process from the theoretical considerations and calculations up to simulations and a fully working prototype are presented. The influences due to the small separation configuration, e. g. additional side-lobes and impedance transformation, are compensated.

The fundamentals of field strength-based DOA estimation are briefly introduced in the paper. Our used DOA estimation is based on orthogonal antenna patterns. We present the theoretical basics for the antenna pattern design with multiple antenna elements, e. g. the array factor and the radiation pattern of single elements. Considering these basics, the arrangement of the single antenna elements w.r.t. the desired antenna pattern for the DOA estimation is computed. The main challenge is the mutual coupling between the antenna elements for the small separation configuration, resulting in additional side-lobes and an undesired impedance transformation. We address these challenges using a two-stage approach. Firstly, the shapes of the antenna elements are optimized. Secondly, the matching of the single elements is optimized to minimize coupling between the elements. Furthermore, our design focuses on the decoupling of the antenna elements for both operating frequency bands, i. e. 868 MHz and 2.4 GHz. For this propose, we designed a combined feeding and matching network. A prototype of the antenna has been manufactured.



Fig. 1: Prototype top-side, including two monopoles for the 868 MHz and 2.4 GHz frequency band.



Fig. 2: Prototype back-side, including matching.

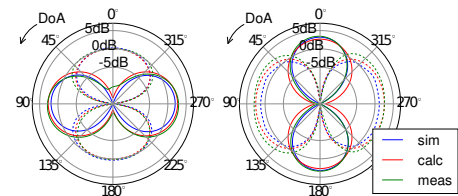


Fig. 3: Comparison of analytically calculated, simulated and measured antenna pattern for 868 MHz (left) and 2.4 GHz (right).

In the paper we present a dual frequency array prototype providing a suitable pattern for DOA estimation. Fig. 1 and Fig. 2 show the implemented antenna prototype including the feeding and matching network. The spatial distribution of the elements is optimized for the used small separation configuration. The side-lobes have been suppressed by a matching and decoupling network. Compared to phase-based approaches, a precise synchronization with coherent sampling on the antenna ports is not required. Hence, the proposed RSS-DOA antenna represents an excellent alternative to phase-based arrays, especially for energy-constrained and low-cost sensor networks.

Topological properties of the illuminated arrays of mesoscopic rings

Hasan M., Iorsh, I.V., I.A. Shelykh

ITMO University, St. Petersburg 197101, Russia

e-mail: m.hasan@metalab.ifmo.ru

The novel and rapidly emerging field of spinoptronics aims to find the way of the efficient optical control over the spin transport in nanostructures through the strong light-matter coupling. Exciton-polaritons [1], the quasiparticles originating from the strong light-matter coupling in microcavities, seem to be the most suitable platform for the realization of the spinoptronic devices. Exciton polaritons possess the spin degree of freedom, which can be flexibly controlled with the external light, exhibit strong nonlinearity and are characterized by much larger coherent propagation lengths than the carriers in semiconductors.

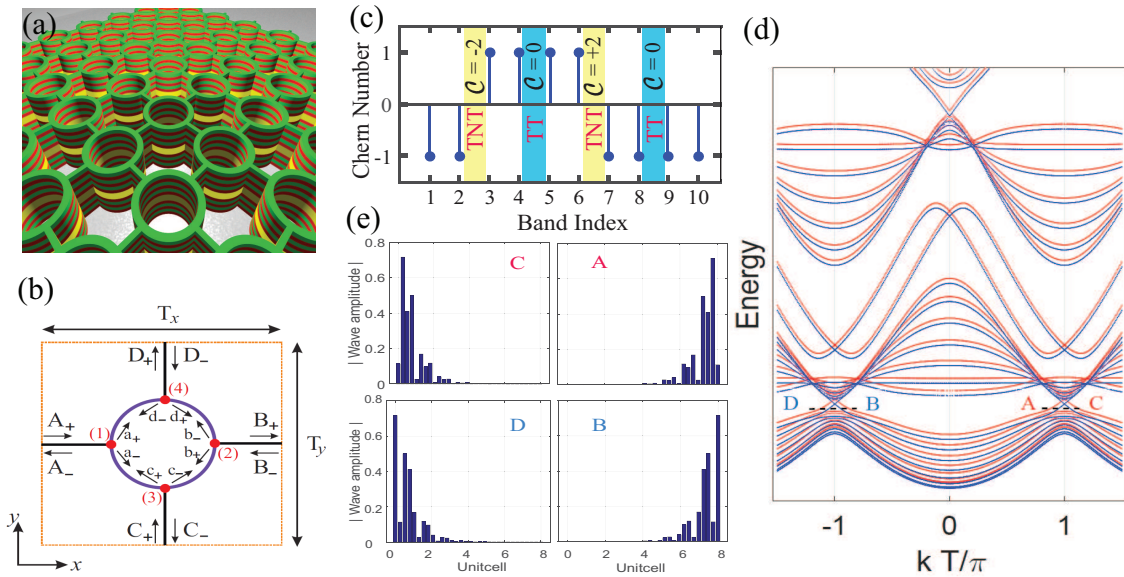


Fig. 1: (a) Geometry of the structure: two-dimensional square lattice of the exciton-polariton ring resonators; (b) Unit cell of the structure: polariton rings are connected via leads at quantum point contacts (QPCs) which are shown as red filled-dots. (c) the Chern numbers of each band. The Chern invariants at bulk gaps are $\mathcal{C} = \pm 2$ for topologically non-trivial (TNT) gaps and $\mathcal{C} = 0$ for topologically trivial (TT) gaps. (d) Band structure of the stripe consisting of the 8 periods in y directions. (e) Field profiles of the edge states marked at the band diagram.

Recently it has been shown that the Aharonov–Bohm effect can be optically induced in the mesoscopic rings. Motivated by the known connection between the Aharonov–Bohm effect and topology we studied the topological properties of the illuminated arrays of mesoscopic rings of various geometry. Firstly, we have demonstrated that a one-dimensional array of coupled rings can change the electronic properties under the illumination of circular polarized light [2]. The counter-propagating edge-currents in a one-dimensional chain manifestly show the similarity with the celebrated Haldane model [3], and thus suggests to increase the dimensionality by one and to look for topological non-trivial properties. We consider the two dimensional structure shown in Fig. 1(a): a two-dimensional square lattice of microcavity rings subject to the perpendicular magnetic field. The geometry of the unit cell is shown in Fig. 1(b). We have calculated the band structure and the Chern numbers of the system using the approach developed in [4]. For that, we have first derived the basis eigenfunctions both in the rings and in the leads. The polaritons both in the ring and in the lead experience a total magnetic field which is the combination of the real magnetic field aligned along the growth axis and the momentum dependent effective magnetic field originating due to the polariton TE-TM splitting. After that the scattering matrix of the single quantum point contact has been derived parametrized by a single parameter corresponding to the contact transparency. Finally, the scattering matrix of the single period of the structure has been obtained, from which we derived the dispersion equation. Topologically protected edge currents for both spins will be demonstrated. Finally we will discuss non-trivial properties of zigzag array of quantum rings.

To conclude, we have shown that a two-dimensional array of the polariton rings is characterized by the non-trivial Chern invariants and supports topologically protected chiral edge states analogously to the case of Quantum Spin Hall insulator. The topologically protected states carrying the specific spin projection would undoubtedly find its applications in the perspective spinoptronic devices.

References

[1] A. V. Kavokin, J. J. Baumber, G. Malpuech, F. P. Laussy, *Microcavities*, Oxford University Press (2007).

- [2] M. Hasan, I. V. Iorsh, O. V. Kibis, I. A. Shelykh, Optically controlled periodical chain of quantum rings, *Phys. Rev. B*, **93**(12), 125401 (2016).
- [3] F. D. M. Haldane, Model for a quantum hall effect without Landau levels: condensed-matter realization of the “parity anomaly”, *Physical Review Letters*, **61**(18), 2015–2018 (1988).
- [4] M. Pasek, Y. D. Chong, Network models of photonic Floquet topological insulators, *Phys. Rev. B*, **89**(7), 075113 (2014).

Decoupling of antennas with wire metasurface structures: MRI applications

A.A. Hurshkainen, S.B. Glybovski, I.V. Melchakova

ITMO University, St. Petersburg 197101, Russia

e-mail: a.hurshkainen@metalab.ifmo.ru

I.J. Voogt, C.A.T. van den Berg, A.J.E. Raaijmakers

University Medical Center Utrecht, 3584 CX, Netherlands

e-mail: A.Raaijmakers@umcutrecht.nl

High-impedance metasurfaces (HIS) are artificial periodic structures that have two important electromagnetic properties. The first one is total and in-phase reflection of an incident plane wave, while the second one is evanescent nature of all surface waves in certain frequency bands (electromagnetic bandgap effect) [1, 2]. This second feature allows HIS to be successfully employed for the decoupling of antennas located nearby the interface in the microwave range [2], which is particularly useful to reduce mutual coupling in antenna arrays with closely spaced elements.

Ultra-high frequency dipole antennas have recently become widely used tools in ultra-high field magnetic resonance imaging [3]. In such systems individually fed dipoles are elements of receive and transmit arrays for body imaging, particularly at the scanner permanent field strength of 7 Tesla. The number of elements in dipole MRI coil arrays is limited by the mutual coupling of adjacent antennas. Therefore, there is a strong need for simple and reliable decoupling techniques, which are specific for dipoles and are still not elaborated in the MRI domain.

In the previous work by the authors it was experimentally shown that metasurface structures of the mushroom type are very promising for strong isolation of body array coil elements (dipole antennas surrounding a human body) at 7 Tesla [4]. While the isolation improvement for the inter-element separation 0.03 of the wavelength reached -14 dB, the mushroom structure working at the 7 Tesla MRI Larmor frequency of 298 MHz is considerably thick (more than 40 mm). However, in practical body arrays it is attractive to apply the decoupling surfaces, which are very thin and flexible, in order to cover the whole circumference and arbitrary number of elements.

To solve this problem in this work we suggest and study metasurface-inspired periodic EBG structures composed of multiple thin and resonant wires. If the wire periodicity is small enough compared to the inter-element distance of an array, the structure enables strong isolation of adjacent dipoles. We discuss the simulated and measured decoupling characteristics of the dipoles in the presence of the proposed structure, as well as its effect on the radio-frequency field distribution inside a scanned subject.

References

- [1] F. Capolino, *Theory and phenomena of metamaterials. Metamaterials handbook*, CRC Press (2009).
- [2] D. Sievenpiper, L. Zhang, R. F. Jimenez Broas, N. G. Alexöpolous, E. Yablonovitch, High-impedance electromagnetic surfaces with a forbidden frequency band, *IEEE Transactions on Microwave Theory and Techniques*, **47**(11), pp. 2059–2074 (1999).

- [3] A. J. E. Raaijmakers, O. Ipek, D. W. J. Klomp, C. Possanzini, P. R. Harvey, J. J. W. Lagendijk, C. A. T. van den Berg, Design of a radiative surface coil array element at 7 T: The single-side adapted dipole antenna, *Magnetic Resonance in Medicine*, **66**(5), pp. 1488–1497 (2011).
- [4] A. A. Hurshkainen, T. A. Derzhavskaya, S. B. Glybovski, I. V. Melchakova, A. J. E. Raaijmakers, I. J. Voogt, C. A. T. van den Berg, Element decoupling of 7T dipole body arrays by EBG meta-surface structures: experimental verification, arXiv:1601.05314 (2016).

Metal-dielectric substrates for high-sensitive chemical detection

Ivanov A.V., Lagarkov A.N., Sarychev A.K.

Institute for Theoretical and Applied Electrodynamics of Russian Academy of Sciences, 13 Izhorskaya, Moscow 125412, Russia

e-mail: av.ivanov@physics.msu.ru

We theoretically investigate metal-dielectric metamaterials consisting of periodic dielectric blocks placed on the metallic substrate. We demonstrate the excitation of multiple plasmon and dielectric resonances within metamaterial, which can be tuned by variation of shape and size of the surface elements. We demonstrate the possibility of high-sensitive SERS detection by using proposed substrates in the example of dithionitrobenzoic acid (TNB).

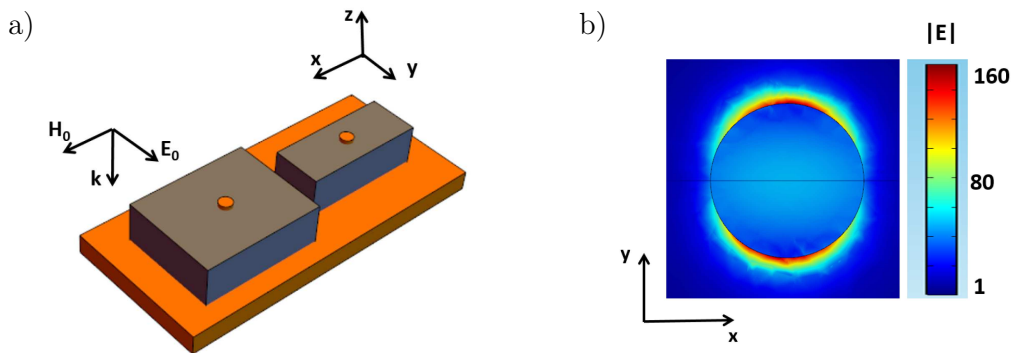


Fig. 1: (a) A single elementary cell of metal-dielectric substrate with metallic nanodisks (orange) embedded into each of dielectric parallelepipeds (gray). (b) Electric field distribution $|E/E_0|$ at the wavelength 785 nm, where E_0 is amplitude of the incident field. Normal incidence. The other parameters: $D_x = 817$ nm, $D_y = 698$ nm, $d_{x1} = d_{x2} = 704$ nm, $d_{y1} = 568$ nm, $d_{y2} = 284$ nm, $h = 148$ nm, $d_c = 50$ nm, $h_c/d_c = 1/14$ (d_c is diameter of nanodisk, h_c is length of nanodisk).

Let us consider the uniform dielectric layer with thickness d placed on the metallic substrate in x, y plane. The incident light has the electric field $\mathbf{E} = \mathbf{E}_0 \exp(ikz)$, where $k = 2\pi/\lambda$ is the wave vector, λ is the free-space wavelength. The surface electric field, which is result of the interference of the incident and reflected waves propagating along z axis, is given by the following equation

$$\mathbf{E}_{\text{surface}} = 2\mathbf{E}_0 \exp(-idk) / [1 + in \cot(dkn)], \quad (1)$$

where n is the refractive index. The condition $d = (2m + 1)\lambda/4n$ gives $\mathbf{E}_{\text{surface}} = 2\mathbf{E}_0$, where \mathbf{E}_0 is the incident electric field. That is the amplitude of the surface electric field is twice larger than the amplitude of the incident electric field. The value of SERS signal, described EF G is given by

$$G = \frac{\langle |\mathbf{E}_\omega(\mathbf{r})|^2 |\mathbf{E}_{\omega-\Delta\omega}(\mathbf{r})|^2 \rangle}{|\mathbf{E}_0|^4} \simeq \frac{\langle |\mathbf{E}_\omega(\mathbf{r})|^4 \rangle}{|\mathbf{E}_0|^4}, \quad (2)$$

where ω is the frequency of exciting radiation, $\Delta\omega$ is the frequency of the Stokes shift; the second equation holds for $\Delta\omega \ll \omega$. It follows from Eqs. (1) and (2) that the G factor reaches its maximum

$G = 16$. The SERS signal can be additionally increased by combination of plasmonic and dielectric resonators.

To increase the value of G factor we consider periodic dielectric structure fabricated from dielectric parallelepipeds (silicon dioxide (SiO_2)) with inserted metal nanodisks (gold and silver) placed on metallic substrate (gold and silver). The lattice constant is chosen to be anisotropic: dimension of lattice constant (D_x — along x axis, D_{y1}, D_{y2}) — along y axis, dimension of dielectric parallelepipeds (h is height along z axis, d_x is width along x axis, d_y is width along y axis). Helmholtz equation was solved by finite element method (FEM). As a result the Raman signal G reaches the value 10^9 for the case of metal-dielectric metamaterial with Ag emdedd nanodiscs. The resonance frequency determined by independent variation of D_x and D_y , for $(D_x - D_y) \ll D_x, D_y$. We tuned resonance frequencies to combine it to the Stocks shifts of dithionitrobenzoic acid (TNB): $\Delta\omega_1 = \omega_3 - \omega_1 = 1338 \text{ cm}^{-1}$, $\Delta\omega_2 = \omega_3 - \omega_2 = 326 \text{ cm}^{-1}$ ($\omega_1 = 11400 \text{ cm}^{-1}$, $\omega_2 = 12412 \text{ cm}^{-1}$, $\omega_3 = 12738 \text{ cm}^{-1}$).

Anharmonic Bloch oscillations in biased artificial and natural superlattices

K.A. Ivanov^{1,2*}, E.I. Girshova², S.J. Clark³, M.A. Kaliteevski^{1,2,4}, A.J. Gallant⁵

¹ITMO University, 49 Kronverksky pr., St. Petersburg, 197101, Russia

²St. Petersburg Academic University, 8/3 Khlopina st., St. Petersburg, 194021, Russia

³Department of Physics, Durham University, South Road, Durham, DH1 3LE, UK

⁴A. F. Ioffe Physico-Technical Institute, 26 Politekhnikeskaya, St. Petersburg, 194021, Russia

⁵School of Engineering and Computing Sciences, Durham University, South Road, Durham, DH1 3LE, UK

e-mail: *kivanov@corp.ifmo.ru

Bloch oscillations (BO) in THz range are important in the context of developing THz emitters. The phenomenon itself is a fundamentally quantum one and consists in radiative transitions between Wannier–Stark localized states that occur as a consequence of Stark effect when an electric field of magnitude F is applied to a periodic structure, typically a superlattice [1] (SL) with a period d . The energy gaps between these states are equal, so all the transitions have the frequency determined from $\hbar\omega = eFd$, where e is the elementary charge.

Although proposed quite a while ago [2], Bloch oscillations are still hard to experimentally observe or utilize in both crystals and artificial SLs. The structures of silicon carbide (SiC) provide a workaround for this problem. Its hexagonal polymorphs have minizone energy spectra and can thus be considered as natural SLs. Recently THz-radiation emission was demonstrated from a biased 6H-SiC at liquid helium temperature [3].

At present BO are thought to be harmonic, which means that they are accompanied by a single-frequency radiation. In analytical quantum consideration [4], this is indeed the case. However, numerical approaches such as transfer matrix method allow quantum consideration of a SL as a whole, in which case other matrix elements — for transition that leap across one, two or more Stark states — may become non-zero. If so, there may be a radiation emission with multiple Bloch frequencies.

The electron properties are given by its energy dispersion, and the branch adjacent to the conduction band minimum is responsible for transport properties, which in case of hexagonal SiC is the M-L branch. It is sufficient to pick a one-dimensional Kronig–Penney potential that would yield the same dispersion curve as was calculated by DFT for M-L

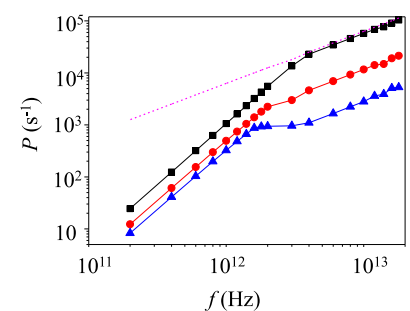


Fig. 1: Radiative transition probabilities for single (squares), double (circles) and triple (triangles) Bloch frequencies.

path. This idea was proposed in [5]. Having picked such a potential, one could find Wannier–Stark states using transfer matrix technique.

After the Wannier–Stark states' wave functions are calculated, dipole transition matrix elements can be found. It was shown by us [6] that the transitions between separated states are also accompanied by radiation emission at multiple Bloch frequencies. This means that the Bloch oscillations in SLs (both natural and artificial) can show anharmonic properties, when the rate of radiation at double and triple Bloch frequencies is an order and two orders of magnitude lower than at a Bloch frequency, respectively (see fig. 1).

References

- [1] L. Esaki, R. Tsu, *IBM J. Res. Dev.*, **14**, 61 (1970).
- [2] F. Bloch, *Z. Phys.*, **52**, 555 (1928).
- [3] V. I. Sankin, A. V. Andrianov, A. G. Petrov, A. O. Zakhar'in, *Appl. Phys. Lett.*, **100**, 111109 (2012).
- [4] A. M. Bouchard, M. Luban, *Phys. Rev. B*, **52**, 5105 (1995).
- [5] G. B. Dubrovskii, A. A. Lepneva, *Sov. Phys. Semiconductors*, **19**, 1252 (1977).
- [6] K. A. Ivanov, A. G. Petrov, M. A. Kaliteevski, A. J. Gallant, *Pis'ma v ZhETF*, **102**, 911–918 (2015).

Plasmonic substrates for optical tweezers

Aliaksandra Ivinskaya, Pavel Ginzburg, Alexander S. Shalin

ITMO University, St. Petersburg 197101, Russia

e-mail: ivinskaya@tut.by

A set of microfluidic, spectroscopic and bio-devices operate by employing optical forces, moreover, optical tweezers are vital for conducting quantum experiments on trapped atoms and ions [1]. While manipulation of microparticles and subnanometer-sized objects can be done with well-established approaches, new unexpected features are discovered for optical forces acting on nanoparticles. Recently not over complex environment such as planar metal or dielectric surface demonstrated interesting effects, for example, lateral forces on particles illuminated by circularly polarized light or linearly polarized plane wave breaking the symmetry of the system [2]. Pulling force towards the source is observed when surface plasmon is excited in the substrate [3].

Tightly focused Gaussian beam employed as optical tweezer can localize biological object or particle in space with high precision. At the same moment, radiation pressure along the beam axis requires another beam or substrate for 3D localization. Here we consider how optical tweezer operates when focused on planar substrates.

Green function formalism can be employed to find optical force acting on a dipole particle [3, 4]. The approach allows to analyze total optical force and contributions arising from different physical mechanisms. Figure 1 illustrates how optical tweezer stiffness changes depending on the choice of the substrate. The insert sketches the geometry of the problem: 2D Gaussian beam propagates along the z -axis and trapping of particle due to gradient force takes place along the x -coordinate. Incident wavelength corresponds to the condition of surface plasmon resonance excitation at air-silver interface.

Trapping force F_x is approximately 8 times stronger for metal (bold black line) compared to glass substrate (bold grey line), Fig. 1. If surface plasmon contribution is not taken into account, trapping at metal substrate becomes more than twice weaker (dashed black line). It appears that focus position of Gaussian beam plays crucial role in the efficiency of surface plasmon excitation. Depending on whether Gaussian beam is focused above or below the substrate tweezer stiffness can be increased or significantly decreased. It paves the way for various applications from improved trapping to particle sorting.

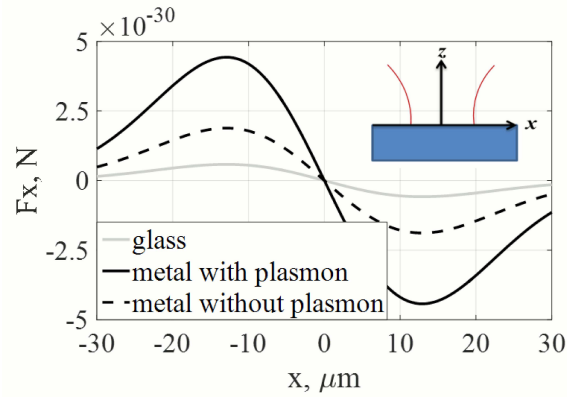


Fig. 1: Trapping of particle by Gaussian beam as the particle position changes across the beam. The beam is focused at 2.2 mm above the interface between air and substrate made of glass or silver. Dielectric bead of radius $R = 15$ nm and permittivity $\varepsilon = 3$ is placed a distance $z = 15$ nm above the substrate. The incident wavelength of radiation is 340 nm, Gaussian beam has waist of 10 μm and electric field of 1 V/m at the very center of the beam in free space.

References

- [1] O. M. Maragò, P. H. Jones, P. G. Gucciardi, G. Volpe, C. Ferrari, Optical trapping and manipulation of nanostructures, *Nature Nanotechnology*, Vol. **8**, pp. 807–19, 2013.
- [2] F. J. Rodriguez-Fortuno, N. Engheta, A. Martinez, A. V. Zayats, Lateral forces on circularly polarizable particles near a surface, *Nature Communications*, Vol. **6**, pp. 1–7, 2015.
- [3] M. I. Petrov, S. V. Sukhov, A. A. Bogdanov, A. Dogariu, A. S. Shalin, Surface plasmon polariton assisted optical pulling force, *Laser & Photonics Reviews*, Vol. **10**, pp. 116–122, 2016.
- [4] L. Novotny, B. Hecht, *Principles of Nano-Optics*, Cambridge University Press, 2006.

Coherent radiative mode in InAs-monolayer Bragg structures

M.A. Kaliteevski^{1,2,3}, G. Pozina⁴, E.V. Nikitina^{1,2}, D.V. Denisov^{1,2}, N.K. Polyakov¹, E.V. Pirogov¹, L.I. Goray¹, K.A. Ivanov¹, A.Yu. Egorov², S.J. Clark⁵

¹St. Petersburg Academic University, St. Petersburg, Russia

²Ioffe Physical-Technical Institute of Russian Academy of Science, St. Petersburg, Russia

³ITMO University, St. Petersburg, Russia

⁴IFM, Linköping University, Sweden

⁵Department of Physics, Durham University, South Road, Durham, UK DH1 3LE

e-mail: m.kaliteevski@mail.ru

Coherent interaction of an ensemble of emitters and the electromagnetic field can modify optical properties of emitters. This effect was theoretically investigated already in the 1950s by Dicke [1], who considered a system of emitters in the case when a spatial separation between them is much smaller than the wavelength of light, or in the Bragg quantum well (QW) structure [2]. In this work, we present the first experimental observations of superradiance in Bragg quantum well structure, formed by InAs single monolayers confined in GaAs matrix [3].

The 60-periods Bragg QW structure was grown by amolecular beam epitaxy, and time-resolved photoluminescence pattern were investigated.

It was shown that if the structure is excited by a laser pulse of the wavelength 400 nm (which is absorbed near the surface of the sample and excited only few quantum wells, there is only one luminescence line, corresponding to ground state in QW (see fig. 1a). If the structure is excited by a laser with the wavelength 800 nm, which excites the whole structure, additional line appears in

the spectra (see fig. 1b). This line has a maximal intensity when the Bragg condition is fulfilled, demonstrates superlinear dependence of luminescence intensity on pumping power and characterized by a increase of the probability of spontaneous emission with increasing power.

Such behaviour of additional line in the spectra indicate the the line is caused by superradiance effect. For the details see [3].

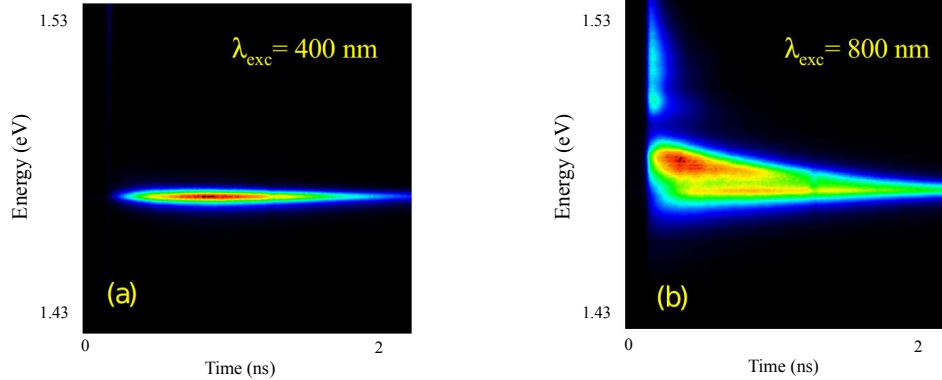


Fig. 1: Low-temperature (5 K) time-resolved photoluminescence images taken under excitation by the laser with the wavelength of 400 nm (a) and 800 nm (b). The emission angle is 50° in both cases. An average excitation power was kept to 30 mW in both cases.

References

- [1] R. H. Dicke, *Phys. Rev.*, **93**, 99–110 (1954).
- [2] E. L. Ivchenko, *et al.*, *Phys. Solid State*, **36**, 1156–1161 (1994).
- [3] G. Pozina, M. A. Kaliteevski, E. V. Nikitina, D. V. Denisov, N. K. Polyakov, E. V. Pirogov, L. I. Goray, A. R. Gubaydullin, K. A. Ivanov, N. A. Kaliteevskaya, A. Yu. Egorov, S. J. Clark, *Scientific Reports*, **5**, 14911 (2015).

Quantization of electromagnetic field in an inhomogeneous medium based on scattering matrix formalism (S-quantization)

M.A. Kaliteevski^{1,2,3}, V.A. Mazlin^{1,2,3}, K.A. Ivanov^{1,2,3}, A.R. Gubaydullin^{1,2,3}

¹St. Petersburg Academic University, St. Petersburg, 194021 Russia

²Ioffe Physical Technical Institute, Russian Academy of Sciences, St. Petersburg, 194021 Russia

³ITMO University, St. Petersburg, 197101 Russia

e-mail: m.kaliteevski@mail.ru

Photonic crystals can be used to control the rate of spontaneous emission. It was shown experimentally that in a heterogeneous environment, the probability of spontaneous emission can vary considerably [1]. In the case of an inhomogeneous medium, the method to study the mode structure of the field on the basis of periodical boundary conditions (BC) is not strict and self-consistent, since the presence of inhomogeneity can lead to a significant change in the mode structure, calculated on the basis of periodical BC, which can lead to inaccurate results in the analysis of systems of finite size. For example, for a finite Bragg reflector (BR) the density of states (DOS) in the photonic band gap (PBG) calculated on the basis of periodical BC is equal to zero, figure 1(b). However, it is evident that the emission from the BR of finite size in the region of PBG may occur and the DOS must be nonzero.

The purpose of this work is to develop methods of quantization of the electromagnetic field, which would allow to obtain the density of states and the spatial profile of the field of modes in the layered media in the framework of single self-consistent and rigorous procedure, allowing to

calculate the probability of spontaneous emission for modes characterized by a particular direction and polarization, without resorting to any assumptions.

We have developed the procedure of the quantization of the electromagnetic field in a layered inhomogeneous media, based on the analysis of the eigenvalues of the scattering matrix (S-matrix) [2, 3]. In contrast to traditional quantization procedure, based on the setting of periodic BC, S-quantization provides a rigorous and self-consistent description of modes of the electromagnetic field and the density of states, for example, for a finite BR the nonzero DOS in the PBG, figure 1(c). S-quantization provides the ability to rigorous calculation of the probability of spontaneous emission for certain directions and polarizations of the emission for arbitrary layered structures.

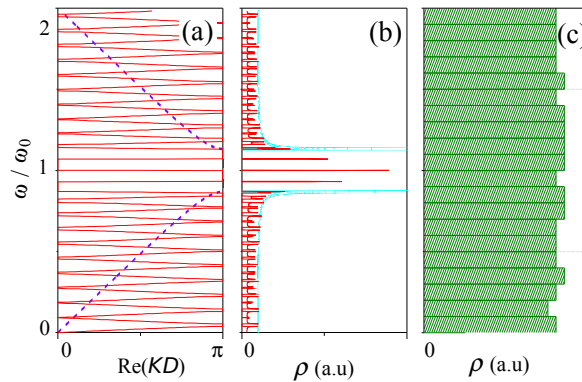


Fig. 1: (a) The dispersion relation, (b) the density of states obtained on the basis of periodical BC, and (c) the density of states obtained by the application of S-quantization BC for the structure that is a $\lambda/4$ Bragg reflector that is placed in a finite “quantization box”.

References

- [1] E. M. Purcell, *Phys. Rev.*, **69**, 11, p. 681 (1946).
- [2] M. A. Kaliteevski, *et al.*, *Optics and Spectroscopy*, **119**, 5, pp. 832–837 (2015).
- [3] M. A. Kaliteevski, *et al.*, Quantization of electromagnetic field and analysis of Purcell effect based on formalism of scattering matrix, submitted.

Strong emission of terahertz radiation from two dimensional arrays of nanostructures on Ge wafers

Chul Kang, Inhee Maeng, Chul Sik Kee

Integrated Optics Laboratory, Advanced Photonic Research Institute, GIST, Bukgu, Gwangju 61005 South Korea

e-mail: cskee@gist.ac.kr

Jung Woo Leem, Jae Su Yu

Department of Electronics and Radio Engineering, and Institute for Wearable Convergence Electronics, Kyung Hee University, Gyeonggi-do 446-701, South Korea

Tae Heon Kim, Jong Seok Lee

Department of Physics and Photon Science, GIST, Bukgu, Gwangju 61005 South Korea

Terahertz (THz) radiation has attracted considerable interest in recent years because it could be useful in nondestructive diagnosis, home security, and medical imaging. To realize the potential applications, an efficient and practical THz radiation source is necessary [1]. When semiconductors are illuminated by a femtosecond (fs) laser pulse, photo-carriers excited by the laser cause transient currents that generate THz radiation. Therefore, direct-gap semiconductors such as GaAs and InAs wafers are more efficient than indirect-gap semiconductors such as Ge and Si wafers in generating THz radiation [2].

In this presentation, we report strong emission of terahertz radiation from Ge wafers with two dimensional arrays of nanostructures. The power of the terahertz radiation from a Ge wafer with an array of nano-bullets is comparable to that from n-GaAs wafers, which have been widely used as a terahertz source. We find that the THz radiation from Ge wafers with the nano-bullets is even more powerful than that from n-GaAs for frequencies below 0.6 THz. Our results suggest that introducing properly designed nanostructure arrays on indirect band gap semiconductor wafers is a simple and cheap method to improve the terahertz emission efficiency of the wafers significantly.

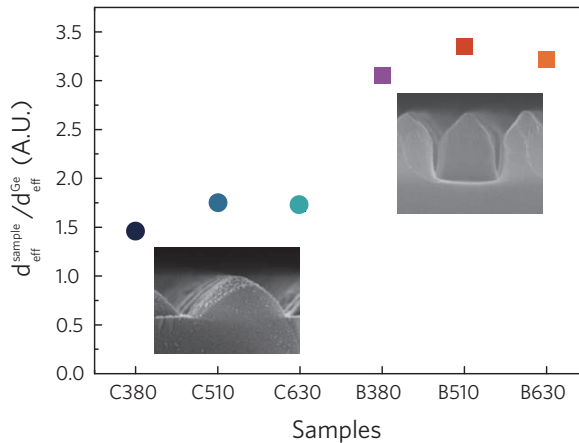


Fig. 1: The ratio of the effective separation distances of the six samples and a bare Ge wafer. The left-down (right-up) inset presents a part of the SEM image of C630 (B630) sample.

References

[1] Y.-S. Lee, *Principles of Terahertz Science and Technology*, Springer, New York (2009).
 [2] K. Sakai, *Terahertz Optoelectronics*, Topics in Applied Physics **97**, Springer-Verlag, Berlin Heidelberg (2005).

Bound state in the continuum nanophotonic laser

B. Kanté

Department of Electrical and Computer Engineering, University of California San Diego, La Jolla, CA 92093-0407, USA
 e-mail: bkante@ucsd.edu

We have designed a high quality factor cavity that is based on a bound state in the continuum at a metasurface and harnessed its properties to demonstrate a novel type of surface emitting laser. We have experimentally demonstrated lasing action in this compact nanophotonic laser at room temperature and for a very low threshold power.

In 1929, von Neumann and Wigner showed that Schrödinger’s equation can have, somewhat surprisingly, bound states above the continuum threshold [1]. These bound states represent the limiting case of quasi-bound states with an infinite lifetime, i. e., resonances that do not decay. It was recently realized that bound states in the continuum (BICs) are intrinsically a wave phenomenon and are thus not restricted to quantum mechanics. Since then, they have been shown to occur in many different fields of wave physics such as acoustics and photonics [2, 3].

In photonics’ terminology, BICs are eigenmodes of an open system with an infinite radiation quality factor, Q_{rad} . To take advantage of this unique property to design high quality resonant cavities, most investigations have focused on dielectric structures that, unlike their plasmonic counterparts, are not limited by their material quality factor, Q_{mat} [3–5]. To investigate the properties of BICs, various platforms have been used such as 1D gratings [3], waveguide arrays [4], 2D photonic crystal

slabs [5] and metamaterials [6]. In this contribution, we have designed a high quality cavity based on a BIC and harnessed its novel properties to achieve a compact low-threshold nanophotonic laser.

Our design consists of a 2D suspended array of nanoresonators (membrane) [7]. The membrane itself is composed of a square lattice of cylinders interconnected by a network of bridges as shown in the inset of Figure 1. This membrane contains epitaxially grown layers of InGaAsP which include quantum wells specially designed to operate around telecommunication wavelengths ($\lambda = 1550$ nm). Figure 1 shows the evolution of the total quality factor for the BIC mode in an infinite array with varying cylinder radius and for different Q_{mat} .

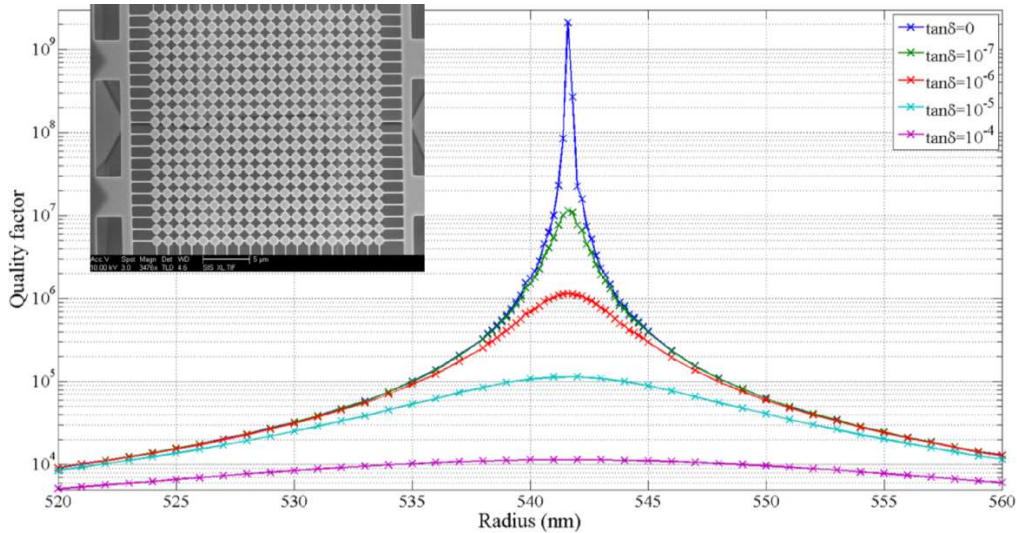


Fig. 1: (inset) scanning electron microscope (SEM) image of a finite 20×20 photonic crystal membrane; evolution of the total quality factor of the BIC eigenmode in an infinite array with varying radius for different material quality factors ($Q_{\text{mat}} = 1/\tan \delta$).

References

- [1] J. von Neumann, E. Wigner, On some peculiar discrete eigenvalues, *Phys. Z.*, **465** (1929).
- [2] C. Linton, P. McIver, Embedded trapped modes in water waves and acoustics, *Wave Motion*, **45**(1-2), 16–29 (2007).
- [3] D. C. Marinica, et al., Bound states in the continuum in photonics, *Phys. Rev. Lett.*, **100**, 183902 (2008).
- [4] Y. Plotnik, et al., Experimental observation of optical bound states in the continuum, *Phys. Rev. Lett.*, **107**, 183901 (2011).
- [5] C. W. Hsu, et al., Observation of trapped light within the radiation continuum, *Nature*, **499**, 188 (2013).
- [6] T. Lepetit, B. Kanté, Controlling multipolar radiation with symmetries for electromagnetic bound states in the continuum, *Phys. Rev. B*, **90**, 241103(R) (2014).
- [7] T. Lepetit, Q. Gu, A. Kodigala, B. Bahari, Y. Fainman, B. Kanté, Resonantly trapped bound state in the continuum laser, arXiv:1508.05164 [physics.optics] (2015).

Wireless power transfer system based on high-index dielectric resonators

Kapitanova P.V., Song M., Belov P.A.

Dept. of Nanophotonics and Metamaterials, ITMO University, Saint Petersburg 197101, Russia
e-mail: p.kapitanova@metalab.ifmo.ru

The recent need in wireless charging of portable devices such as cellphones, tablet, and laptop computers is driving the development of wireless powering and charging technologies [1, 2]. The main

targets to achieve are the increased efficiency, the extended operational distance, the WPT stability to the mutual orientation of transmitter and receiver in space, compact size and small weight [3]. Here we propose and experimentally verify an original approach to near field magnetic resonance wireless power transfer (WPT) using high index dielectric resonators. The results of numerical simulation and experimental investigation of the WPT systems based on spherical dielectric resonators with the permittivity $\varepsilon = 80$ and disk dielectric resonators with the permittivity $\varepsilon = 1000$ are reported. The WPT system based on spherical resonators operating at magnetic dipole mode and magnetic quadrupole mode was optimized for ISM band 2.4 GHz. The maximal measured efficiency of 60% and 80% was verified experimentally for magnetic dipole and magnetic quadrupole modes, respectively. The WPT system based on disk dielectric resonators with the permittivity $\varepsilon = 1000$ was optimized to operate at the frequency of 220 MHz. The measured efficiency of the WPT system is 50% at 7 cm distance between the resonators. The test with a real load was also performed.

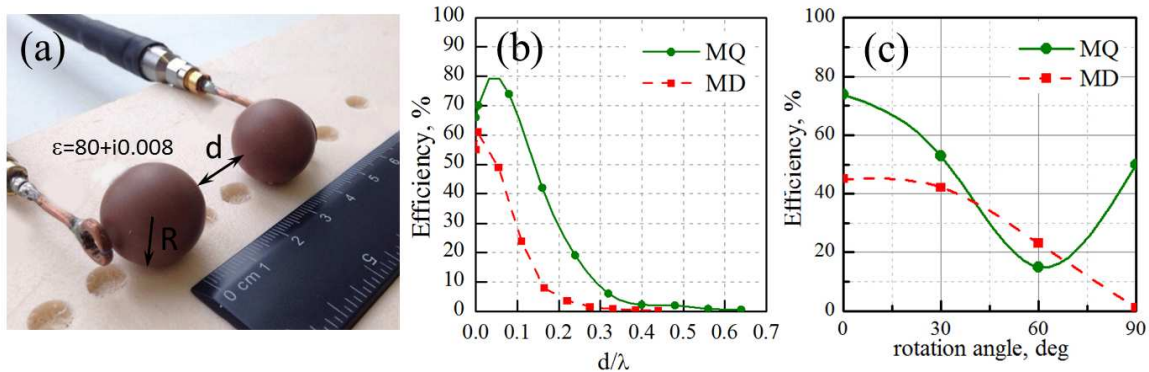


Fig. 1: WPT system based on high-index dielectric resonators separated by the distance d . (b) Measured WPT efficiency of the system operating at MD and MQ modes as a function of normalized distance.

References

- [1] W. C. Brown, *IEEE Trans. Microwave Theory and Techniques*, **32**, 1230–1242 (1984).
- [2] S. Y. R. Hui, W. Zhong, C. K. Lee, *IEEE Trans. Power Electron.*, **29**, 4500–4511 (2014).
- [3] A. Kurs, A. Karalis, R. Moffatt, J. D. Joannopoulos, P. Fisher, M. Soljacich, *Science*, **317**, 83–86 (2007).
- [4] M. Song, I. Iorsh, P. Kapitanova, E. Nenasheva, P. Belov, *Appl. Phys. Lett.*, **108**, 023902 (2016).

Reconfigurable and all-dielectric photonic topological insulators

Alexander B. Khanikaev

Department of Physics, Queens College of The City University of New York, Queens, NY 11367, USA;

Graduate Center of The City University of New York, New York, NY 10016, USA;

Department of Nanophotonics and Metamaterials, ITMO University, St. Petersburg 197101, Russia
e-mail: khanikaev@gmail.com

Following the footsteps of condensed matter topological systems, a significant progress has been recently made in understanding and realizing topological states of light [1]. Here I present the results demonstrating that that topological states protected by the electromagnetic duality can be engineered in 2D and 3D metacrystals. The duality, which is reflected in the symmetry of the Maxwell equations with respect to electric and magnetic field components, responsible for the SPT phase of the electromagnetic eigenmodes, otherwise broken by materials response [2, 3], is restored by careful design of building blocks of the 3D photonic lattice – meta-atoms. We demonstrate 2D and 3D

photonic metacrystals based on the meta-waveguide and all-dielectric metamaterial platform, which is thus free of very restrictive requirement earlier concepts of time-reversal violating systems, where magnets or temporal modulation are required [1].

Reconfigurable 2D photonic meta-crystals. Endowed with topological robustness, photonic edge modes can avoid back-reflection from structural imperfections and disordered regions. Although several successful experimental implementations of topological states of light with TR symmetry have been reported recently, one important property of true external fields available in condensed matter systems has evaded emulation in photonics—the control of topological states. The possibility of such control through reconfigurable synthetic gauge fields would usher in a broad range of practical applications from spin/helicity filtering to tunable photonic devices. Based on this idea, here we demonstrate experimentally that the electromagnetic radiation can be steered and delivered to any point within a reconfigurable topological metacrystal without back-reflection. This is achieved by exploiting adjustable gauge fields defining arbitrarily-shaped pathways for topological edge states.

Here, we realize a reconfigurable topological photonic lattice implemented in the parallel plate waveguide (PPW) shown in Figs. 1(a) and 1(b) [3]. The reconfigurable topological structure studied here is formed between two parallel copper plates through which holes are drilled to support a periodic triangular array of copper rods with ring collars. The rods can be moved up or down so that the collar of each rod can be positioned anywhere between the top and bottom plates. Lattices can be formed with the collar touching either the upper or lower copper plate and structures with arbitrarily-shaped domains of the two structures can be created.

The main property of topological edge states that differentiates them from their topologically trivial counterparts, such as Tamm states or modes of optical waveguides, is their robustness against defects and disorder. In order to test the robustness of photonic transport along reconfigurable pathways enabled by the design of the metacrystal, propagation was measured in samples with a variety of bends and shapes of the topological domain wall, as shown in Fig. 1c–f. The experimental spectra for different domain wall configurations exhibit high transmission mediated by the edge modes over the frequency range of the band gap. The high transmission observed for all domain wall contours, including an irregularly shaped wall with multiple bends, shows that transport is topologically robust.

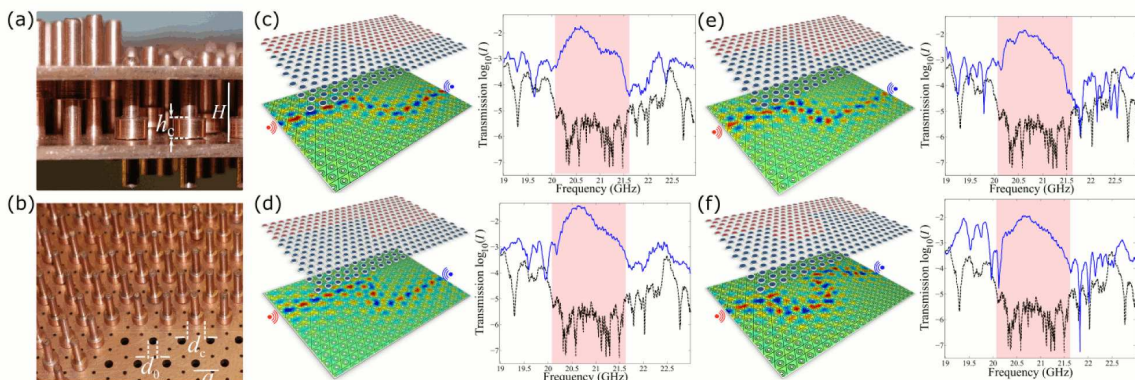


Fig. 1: (a) Geometric arrangement of metallic rods and collars inside the PPE. (b) The metacrystal without the top copper plate. (c–f) Domain walls with 60° , 90° , and 120° bends, and random shape, respectively.

Three-dimensional all-dielectric photonic topological insulators. In order to bring these ideas to three-dimensions, we introduce an all-dielectric topological photonic metacrystal shown in Fig. 2a. It represents a 3D hexagonal lattice of dielectric disks with the permittivity $\epsilon_d = 81$ embedded into a matrix of permittivity $\epsilon_b = 3$. The domain wall in such 3D photonic topological insulator concept represents an interface between two topological crystals inverted with respect to each other along the z -direction, which results in the reversal of bianisotropy. The schematic view of the corresponding structure is shown in Fig. 2a with the photonic band structure presented in Fig. 2(b,c). The surface states appear within the band gap region and cross it such that they

interconnect lower and upper bulk bands. The 3D band diagram shown in Fig. 2(c) exposes one of the Dirac cones corresponding to the surface states near K-point. The confinement of the surface states to the domain wall was confirmed by their field profiles for all directions within the domain wall plane. As in the case of 3D electronic topological insulators, the surface states in our system also have a property analogous to spin-locking which endows them with topological robustness.

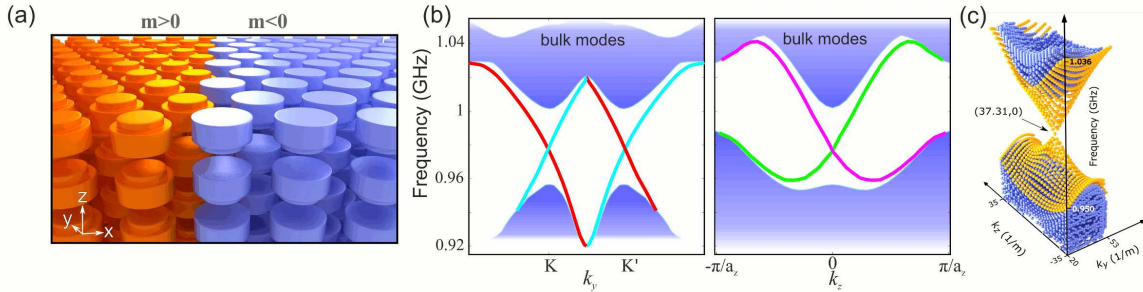


Fig. 2: (a) The schematics of the domain wall formed by the reversal of the mass term induced by the bianisotropy in the middle of the metacrystal. (b) Band diagrams of topological surface states supported by the domain wall. (c) The conical Dirac-like dispersion of the surface states.

In summary, we propose a photonic platform which can be used for implementation of reconfigurable and topologically robust 2D and 3D photonic circuitry in entire electromagnetic spectrum from microwave frequencies to optical domain. The proposed all-dielectric platform may allow avoiding undesirable effects of Ohmic loss unavoidable in metallic and plasmonic structures. In addition, the SPT order facilitates topological order in photonics-compatible materials, thus escaping technical difficulties associated with the use of magnetic materials, external magnets, and temporal modulation, which are required to induce topological order in systems with broken TR symmetry.

References

[1] L. Lu, J. D. Joannopoulos, M. Soljačić, *Nat. Photon.*, **8**, 821–829 (2014).
 [2] A. B. Khanikaev, S. H. Mousavi, W.-K. Tse, M. Kargarian, A. H. MacDonald, G. Shvets, *Nat. Mater.*, **12**, 233–239 (2013).
 [3] X. Cheng, C. Jouvaud, X. Ni, S. H. Mousavi, A. Z. Genack, A. B. Khanikaev, *Nat. Mater.* (2016), doi:10.1038/nmat4573.
 [4] A. Slobozhanyuk, S. H. Mousavi, X. Ni, D. Smirnova, Y. S. Kivshar, A. B. Khanikaev, arXiv:1602.00049 (2016).

All-dielectric resonant nanophotonics and metasurfaces

Yuri Kivshar

Nonlinear Physics Center, Australian National University, Canberra ACT 2601, Australia;
 ITMO University, St. Petersburg 197101, Russia
 e-mail: ysk@physics.anu.edu.au

Rapid progress in the fields of plasmonics and metamaterials is driven by their ability to enhance light-matter interaction and near-field effects with subwavelength localization of light, and many of such effects are usually associated with metallic nanoscale structures (“meta-atoms” and “meta-molecules”). Recently, we observe the emergence of a new branch of nanophotonics aiming at the manipulation of strong optically-induced electric and magnetic Mie-type resonances in dielectric and semiconductor nanostructures with high refractive index [1]. Unique advantages of dielectric resonant nanostructures over their metallic counterparts are low dissipative losses and the enhancement of both electric and magnetic fields that provide competitive alternatives for metal-based plasmonic structures including nanoantennas, nanoparticle sensors, and metasurfaces.

In this talk, we will review this new emerging field of nanophotonics and metamaterials and demonstrate that Mie-type resonances in dielectric nanoparticles and subwavelength-patterned dielectric structures can be exploited to boost performance of many nanophotonic metadevices. In addition, the co-existence of strong electric and magnetic resonances and resonant enhancement of magnetic field in dielectric nanoparticles bring new physics and entirely novel functionalities to simple geometries not much explored in plasmonic structures especially in the nonlinear regime.

In addition, we will discuss the basic properties of metasurfaces [2]. Optical metasurfaces are thin-layer subwavelength-patterned structures which interact strongly with light. Metasurfaces became the subject of several rapidly growing areas of research, being a logical extension of the field of metamaterials towards its practical applications. Metasurfaces demonstrate many useful properties of metadevices with engineered resonant electric and magnetic optical response combined with low losses of thin-layer structures. We will discuss the basic concepts of this rapidly growing research field that stems from earlier studies of frequency-selective surfaces in radio-physics, being enriched by the recent development of metamaterials and subwavelength nanophotonics. We will review the most interesting properties of photonic all-dielectric metasurfaces, demonstrating their useful functionalities such as frequency selectivity, wavefront shaping, polarization control, etc. We will discuss also the ways to achieve tunability of metasurfaces and also demonstrate that nonlinear effects can be enhanced with the help of metasurface engineering.

References

- [1] A. I. Kuznetsov, A. E. Miroshnichenko, M. L. Brongersma, Yu. S. Kivshar, B. Lukyanchuk, Optically resonant dielectric nanostructures, in preparation (2016).
- [2] A. E. Minovich, A. E. Miroshnichenko, A. Y. Bykov, T. V. Murzina, D. N. Neshev, Yu. S. Kivshar, Functional and nonlinear optical metasurfaces, *Laser & Photonics Rev.*, **9**, 195–213 (2015).

Influence of fs-laser modification on coupling effects between hybrid nanoparticles

Kolodny S.A.¹, Yali Sun², Zuev D.A.¹, Makarov S.V.¹, Milichko V.A.¹, Starikov S.V.³, Mukhin I.S.^{1,4}, Morozov I.A.⁴, Belov P.A.¹, Krasnok A.E.¹

¹ITMO University, St. Petersburg, 197101, Russia

²Huazhong University of Science and Technology, Wuhan, Hubei, 430074, China

³Joint Institute for High Temperatures of the Russian Academy of Sciences, Moscow 125412, Russia

⁴St. Petersburg Academic University, St. Petersburg 197101, Russia

e-mail: s.kolodny@metalab.ifmo.ru

Hybrid nanophotonics based on metal-dielectric nanostructures unifies the advantages of plasmonics and all-dielectric nanophotonics providing strong localization of light, magnetic optical response and specifically designed scattering properties. Recently, we have demonstrated a novel type of hybrid nanostructures fabricated by femtosecond laser reshaping of ordered arrays of metal-dielectric (Au/Si) nanoparticles created by lithographical methods [1]. Local laser heating of individual hybrid nanoparticles is applied for selective reshaping of the metal components without affecting dielectric ones, thus engineering both electric and magnetic optical resonances of the nanoparticle. We have confirmed our conclusions on the femtosecond laser reshaping of the metal component by the molecular dynamics simulation. The laser reshaping of gold component in a Au/Si nanoparticle allows to modify optical properties of the nanodimer. To understand the coupling effects in hybrid nanostructures under different degree of fs-laser reshaping, we have performed numerical simulation of hybrid nanostructures pairs. We have investigated scattering spectra and local field distribution of nanoparticles.

Thus, this work represents a next step in understanding of interaction among hybrid nanoparticles in array. The results of the work can be applied in optical properties engineering of metasurfaces for perspective nanophotonic devices.

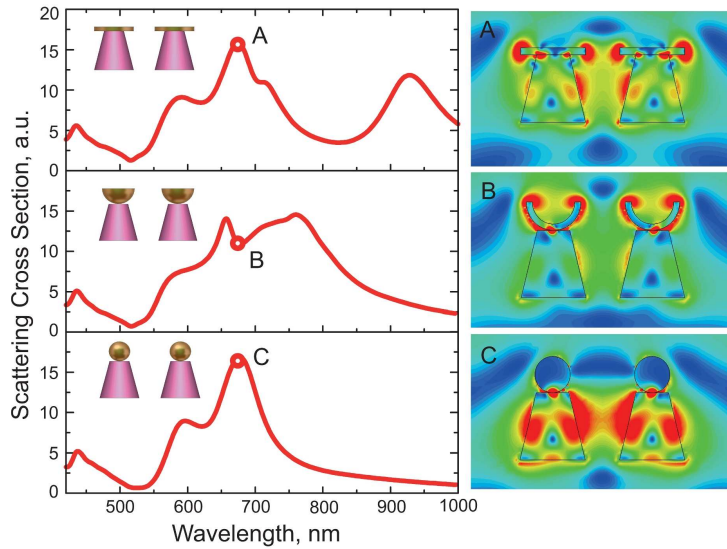


Fig. 1: Numerical modeling of scattering spectra of hybrid dimer nanoantennas with different value of fs-laser reshaping. On the right, the distributions of local E-field for wavelength of 670 nm.

References

[1] D. A. Zuev, S. V. Makarov, I. S. Mukhin, V. A. Milichko, S. V. Starikov, I. A. Morozov, I. I. Shishkin, A. E. Krasnok, P. A. Belov, Fabrication of hybrid nanostructures via nanoscale laser-induced reshaping for advanced light manipulation, *Adv. Mater.*, doi:10.1002/adma.201505346 (2016, accepted).

Optical chirality of 2D- and 3D-chiral metal hole arrays

Kondratov A.V., Gorkunov M.V., Darinskii A.N.

Shubnikov Institute of Crystallography, Russian Academy of Sciences, 119333 Moscow, Russia
 e-mail: kondratov@crys.ras.ru

Chiral plasmonic nanostructures can be generally classified into two types: truly chiral, consisting of 3D-chiral elements, and 2D-chiral, i.e., with only in plane broken mirror symmetry. While the former has its inherent optical chirality due to the geometrical asymmetry [1], for the latter any optical chirality is forbidden by the top-bottom mirror symmetry [2]. One can break this symmetry with different top and bottom substrates. Then 2D-chiral structure elements respond differently to left and right circular polarized (LCP and RCP) waves, but this difference is weak compared to the overall transmission. Therefore, such structures still exhibit rather low values of optical chirality [3].

We show that chiral Fano resonance of 3D twisted holes (Fig. 1a) provides a transmission dip where even a tiny split of response to LCP and RCP light leads to an extreme optical chirality (Fig. 1d). The use of 2D-chiral holes instead of 2D-chiral elements reduces the background transmission, which leads to a similar Fano resonance. We model an array of twisted cross holes (Fig. 1b) and find that a small refractive index deviation close to one side of the structure gives rise to notable values of optical chirality (Fig. 1d). Importantly, the optical chirality is much more sensitive to the dielectric environment changes than other observable quantities, e.g. transmittance. The local field enhancement has a strong top-bottom asymmetry (Fig. 1c), which provides conditions for a nonlinear chiral symmetry breaking. We discuss the related possibilities of enhanced optical chiral sensing and tunable chirality of metamaterials.

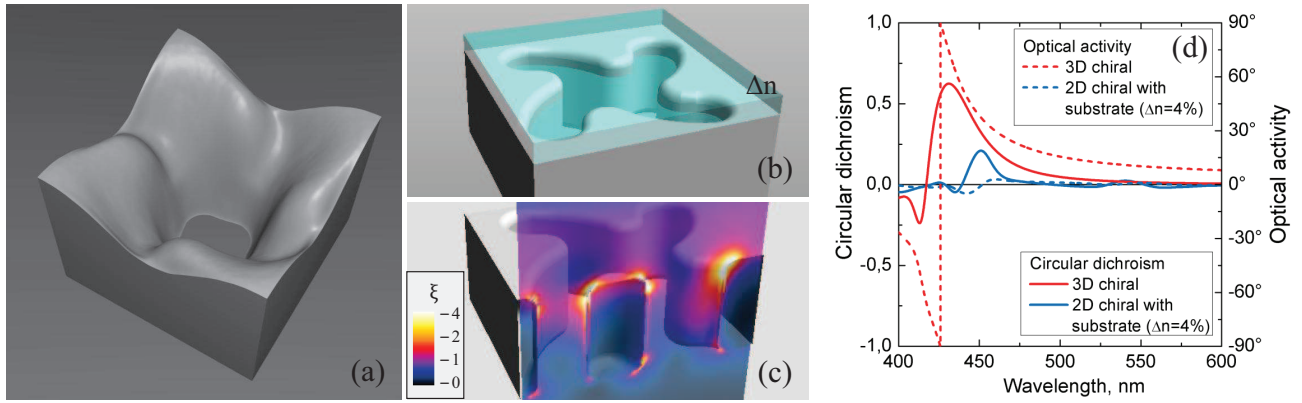


Fig. 1: 2D- and 3D-chiral holes in metal film. (a): Model of the 3D twisted hole. (b): Model of the hole of the twisted cross shape covered by a thin dielectric substrate with the refractive index slightly different from the background. (c): Cross section of the distribution of the root mean square of the absolute value of electric field normalized by the amplitude of the LCP incident wave. (d): Circular dichroism and optical activity spectra of the 2D- and 3D-chiral holes obtained by the FDTD simulation.

The work was supported by the Russian Science Foundation (project 14-12-00416).

References

- [1] M. V. Gorkunov, A. A. Ezhov, V. V. Artemov, O. Y. Rogov, S. G. Yudin, *Applied Physics Letters*, **104**, 221102 (2014).
- [2] S. I. Maslovski, D. K. Morits, S. A. Tretyakov, *J. Opt. A: Pure Appl. Opt.*, **11**, 074004 (2009).
- [3] M. Kuwata-Gonokami, N. Saito, Y. Ino, M. Kauranen, *et al.*, *Phys. Rev. Lett.*, **95**, 227401 (2005).

About dipole moment in doped carbon nanotubes

Konobeeva N.N.^{1,2}, Ten A.V.¹, Belonenko M.B.^{1,2}

¹Volgograd State University, Volgograd, Russia

²Volgograd Institute of Business, Volgograd, Russia

e-mail: yana_nn@inbox.ru, pak.anastasia@gmail.com, mbelonenko@yandex.ru

Carbon nanotubes (CNT) [1] are rolled into a cylinder of a carbon atoms layer arranged in a hexagonal lattice sites. They are perspective in terms of the modern nanoelectronics element base.

However, until now been neglected questions concerning the propagation of waves in nanotubes. In particular, the questions connected to the consideration of two-dimensional model, taking into account the dipole polarization in the study of the electromagnetic waves dynamics, etc. Impurity CNTs are considered because they are more realistic objects in terms of their experimental preparation.

In the present work was carried out theoretical study of nonlinear response of the isolated CNT type zig-zag on the laser intensity.

The wave equation describing the system behavior in two dimensions based on the electric dipole moment of the impurities P , which is changing under the electric field E influence is given by expression:

$$\frac{\partial^2 E}{\partial x^2} + \frac{\partial^2 E}{\partial y^2} - \frac{\varepsilon_0}{c^2} \frac{\partial^2 E}{\partial t^2} + \frac{4\pi}{c} \frac{\partial j}{\partial t} = \alpha \frac{\partial^2 P}{\partial t^2}, \quad (1)$$

where ε_0 is dielectric constant, $\alpha = 4\pi/c^2$, c is speed of light in vacuum.

Evolution of ultrashort optical pulses is presented in Figure 1.

This study was supported by the Ministry of Education and Science of the Russian Federation, project no. MK-4562.2016.2.

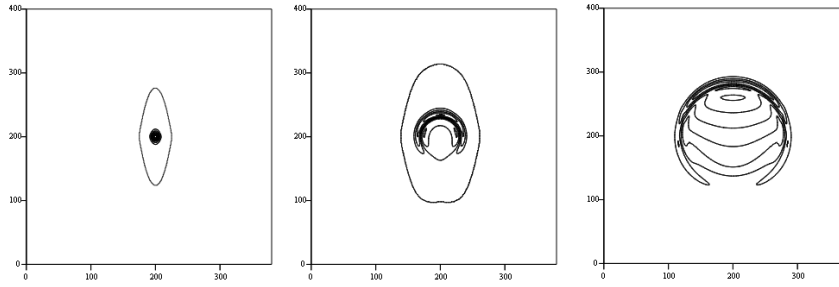


Fig. 1: The intensity of 2D optical pulse at the different times: a) $t = 0$ s; b) $t = 2.0 \cdot 10^{-13}$ s; c) $t = 5.0 \cdot 10^{-13}$ s. Dipole moment $r = 0.1$.

References

[1] R. Saito, M.S. Dresselhaus, G. Dresselhaus, *Physical properties of carbon nanotubes*, Imperial College Press (1999).

Hypersensitive transport in asymmetric photonic layered media

Kononchuk R.¹, Smith K.¹, Chabanov A.A.¹, Makri E.², Kottos T.², Vitebskiy I.³

¹University of Texas at San Antonio, One UTSA Circle, San Antonio, TX 78249, USA

²Wesleyan University, Department of Physics, Middletown, CT 06459, USA

³Air Force Research Laboratory, Sensors Directorate, Wright Patterson AFB, OH 45433, USA

e-mails: rdnbox@gmail.com, ksmith1281@gmail.com, andrey.chabanov@utsa.edu

eleana.makri@weslyan.edu, tkottos@weslyan.edu, ilya.vitebskiy@us.af.mil

A localized mode in a photonic layered medium can develop nodal points (nodal planes) where the oscillating electric field is negligible. Placing a thin metallic layer at such a nodal point leads to the phenomena of induced transmission, whereas shifting the nodal point away from the metallic layer results in the suppression of the localized mode along with the resonant transmission [1]. Here we show that if the nodal point is not a point of symmetry of the layered medium, an abrupt transition from the resonant transmission to broadband opacity can be brought about by a tiny alteration of the permittivity in the vicinity of the metallic layer. Applications of this hypersensitive transport to microwave and optical limiting and switching will be discussed.

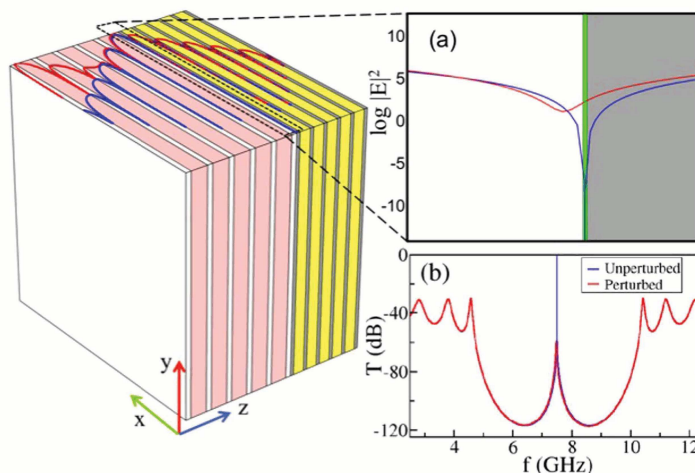


Fig. 1: Metal-dielectric layered structure consisting of two Bragg gratings (BG) with different constitutive bi-layers (white and orange for the left BG and grey and yellow for the right BG). The blue and the red curves in the upper facet of the structure show the resonant field profiles for the unperturbed and perturbed structures, respectively. (a) A magnified view of the

asymmetric cavity. The cavity consists of two dielectric layers (white and gray) separated by a metallic layer (green). The field distributions (blue and red curves corresponding to the unperturbed and perturbed structures) are also plotted. Notice the shift of the nodal point in the red curve leads to engaging the metallic layer and suppression of the resonant transmission, as shown in (b). (b) Transmission spectra of the unperturbed (blue curve) and perturbed (red curve) structures. The field profiles at the resonance frequency f_r are shown for both the unperturbed and perturbed structures. Here the structural perturbation is a 2% decrease in the dielectric constant of one of the cavity layers.

References

- [1] E. Makri, K. Smith, A. Chabanov, I. Vitebskiy, T. Kottos, *Scientific Reports*, **6**, 22169 (2016).

Slow light in nonlocal anisotropic metamaterials

K.L. Koshelev, A.A. Bogdanov

ITMO University, St. Petersburg 197101, Russia

e-mails: ki.koshelev@gmail.com, bogdanov@ioffe.mail.ru

We analyse and compare the effects of the spatial dispersion and structural anisotropy on the spectrum of a metamaterial slab. Dielectric function of the slab we describe within Drude–Lorentz approximation. Anisotropy of the slab is introduced through the anisotropy of plasma frequencies corresponding to the different component of the permittivity tensor. Nonlocal electromagnetic response is described within hydrodynamical approximation which is suitable for a wide range of spatially dispersive systems. We show that mutual effect of spatial dispersion and anisotropy can bring light to a complete stop at certain frequencies.

Electromagnetic response of many metamaterials (wire media, plasmonic metamaterials, multi-layer structures, etc) is described by an effective permittivity ε . Resonance response of meta-atoms provides good description of $\hat{\varepsilon}(\omega, \mathbf{k})$ in the framework of Drude–Lorentz approach [1]:

$$\varepsilon(\omega) = \varepsilon_\infty \left(1 - \frac{\Omega^2}{\omega(\omega + i\gamma)} \right). \quad (1)$$

Here, ε_∞ is the permittivity of a host material, γ is the damping parameter, Ω is the resonance frequency (plasma frequency) of a metamaterial.

Resonance frequencies of metamaterial can be degenerated due to a specific symmetry of the lattice or form-factor of the meta-atoms forming metamaterial. The degeneracies can be lifted, for example, by a structural anisotropy appeared because of the lattice geometry. Along with a structural anisotropy it is possible to distinguish a dynamical anisotropy induced by an incident wave due to the effects of nonlocality. Therefore, effects of the spatial dispersion, as well as a structural anisotropy, can lift the degeneracy of eigenmodes in metamaterials and dramatically change their optical properties.

We study spectrum of plasma (Langmuir) modes of metamaterial slab in detail and show that in contrast to the case of an isotropic slab in which Langmuir modes are degenerated and represent pure electric standing waves, anisotropy leads to nonzero magnetic field component and nonzero flux of electromagnetic energy, which direction is defined by nature of anisotropy. On the other hand, we show that nonlocality also removes the degeneracy of Langmuir modes, and in this case energy flux has purely electric component, accumulated by electron gas due to its compression and expansion. Spatial dispersion and anisotropy make oppositely directed contributions into the energy flow for the Langmuir modes. Therefore, the flows of electromagnetic and mechanic energy can completely compensate each other and bring the Langmuir mode to a complete stop, forming a so-called “slow light” [2].

This work has been supported by RFBR (16-37-60064, 14-02-01223), by the President of Russian Federation (MK-6462.2016.2), the Federal Programme on Support of Leading Scientific Schools (NSh-5062.2014.2), and by program of Fundamental Research in Nanotechnology and Nanomaterials of the Russian Academy of Science.

References

- [1] S. A. Maier, *Plasmonics: fundamentals and applications*, Springer Science & Business Media (2007).
- [2] T. Baba, Slow light in photonic crystals, *Nature Photonics*, Vol. **2**(8), 465–473 (2008).

Wire media for molding electromagnetic fields

Kosulnikov S. Yu.^{1,2}, Vovchuk D. A.³, Filonov D. S.¹, Glybovski S. B.¹, Mirmoosa M. S.², Nefedov I. S.², Tretyakov S. A.², Belov P. A.¹, Simovski C. R.^{1,2}

¹ITMO University, Kronverkskiy pr. 49, St. Petersburg 197101, Russia

²Department of Radio Science and Engineering, School of Electrical Engineering, Aalto University, P.O. Box 13000, Aalto FI-00076, Finland

³Department of Radio Engineering and Information Security, Yuriy Fedkovych Chernivtsi National University, Chernivtsi 58000, Ukraine

e-mail: serg.kosulnikov@phoi.ifmo.ru

Metamaterials performed as lattices of aligned metallic wires with subwavelength periods have been actively studied for a wide range of applications during last years. An important property of wire media (WM) is their strong spatial dispersion, which enables many interesting electromagnetic effects. Recently, in our group we studied theoretically and experimentally enhancement of power radiated by small (dipole) sources submerged into WM [1]. This enhancement results from two effects: the transformation of evanescent waves into propagating modes and the so-called hyperlensing [1].

If a finite-size structure of parallel metallic wires comprises an embedded dipole source, the radiation to free space is enhanced only within quite narrow frequency bands. Besides these Fabry–Perot resonances the enhancement is absent because the internal reflection blocks the radiation and in the system with negligible absorption restricts it on the same level as the radiation of the same dipole in the absence of the wire medium [1, 2]. However, if the interfaces of the slab are modified e. g. by closely located dielectric layers the internal reflection can dramatically reduce. In this report we demonstrate broadband transfer of power through a WM slab connecting two waveguides [2]. Here the waveguide open end plays the role of a dielectric interface. Next, we present two other WM structures which allow broadband enhancement of radiation from subwavelength sources. The first one is a WM hyperlens of truncated conical shape, which grants this enhancement to the sources located near its apex. Another one is the so-called irregular WM brush which offers a similar enhancement to the sources located in a large area because the overall shape of the sample is a flat layer. All our claims are accompanied by extensive simulations and validated experimentally.

We believe that the presented results are important for many prospective applications. WM can be realized in many frequency ranges, and in all of them have basically the same electromagnetic properties. For example, the revealed broadband power transfer in WM slabs though was confirmed at microwaves is a conceptual confirmation of the idea of enhanced radiative heat transfer through a thermophotovoltaic microcavity filled with nanowires operating in the mid infrared frequency band. Our structures can find applications from radio frequencies (imaging microwaves noises in electronic chips) to ultrafast (radiative) cooling of hot microscopic objects, which is a challenging problem of nanophotonics.

References

- [1] C. Simovski, S. Maslovski, I. Nefedov, S. Kosulnikov, P. Belov, S. Tretyakov, Hyperlens makes thermal emission strongly super-Planckian, *Phot. Nano. Fund. Appl.*, **13**, 31–41 (2015).

- [2] D. Vovchuk, S. Kosulnikov, I. S. Nefedov, S. A. Tretyakov, C. Simovski, Multi-mode broadband power transfer through a wire medium slab, *Prog. Electromagn. Res.*, **154**, 171–180 (2015).

Optically asymmetric structures for transparent electrodes

Kovrov A.E.^{1*}, Kadochkin A.S.^{1,2}, Mukhin I.S.³, Voroshilov P.M.^{1,4}, Simovski C.R.⁴, Shalin A.S.¹

¹ITMO University, 49, Kronverkskiy pr., St. Petersburg, 197101, Russia

²Ulyanovsk State University, 42, Leo Tolstoy Str., Ulyanovsk, 432017, Russia

³St. Petersburg Academic University, 8/3 Khlopina Str, St. Petersburg, 194021, Russia

⁴School of Electric and Electronic Engineers, Aalto University, Aalto, 00076, Finland

e-mail: *a.kovrov@metalab.ifmo.ru

Recently a great interest emerged to optically asymmetric structures with different transmission in opposite directions. Such structures can find application in optical data processing and light trapping [1–3].

We numerically studied two structures with different optical transmission in opposite directions. The first is based on conical holes in metal foil and another employs microlenses layer to improve optical transmission in one direction. It was shown that in both systems asymmetry effect is broadband.

Both systems were optimized in terms of forward transmission and asymmetry coefficient (ratio of forward transmission to backward one). Here forward transmission means transmission for light incidence from large radius of conical holes (first structure) or from the side of microlenses (second structure). For conical holes based system asymmetry coefficient exceeds 3 while forward transmission oscillates between 0.05 and 0.25 and for microlenses based system it is possible to reach asymmetry coefficient 5–6 for forward transmission about 90–94% or asymmetry coefficient around 10 for 50% direct transmission. Both structures are easy to produce by conventional lithography methods.

It was shown that transmission asymmetry is caused by asymmetric diffraction. For backward light incidence zero-order diffraction is pronounced the most, and for forward light incidence a number of higher order diffraction lobes are involved.

Calculation was performed in frequency domain using commercial program packages Comsol Multiphysics and CST Microwave Studio.

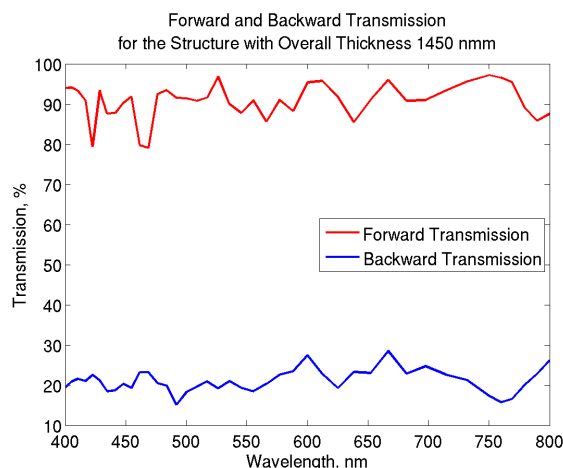


Fig. 1: Forward and backward transmission for microlenses-based structure.

References

- [1] J. Xu, C. Cheng, M. Kang, J. Chen, Z. Zheng, Y.-X. Fan, H.-T. Wang, *Opt. Lett.*, vol. **36**, no. 10, pp. 1905–1907, 2011.
- [2] N. Peng, X. Li, W. She, *Opt. Express*, vol. **22**, no. 14, pp. 17546–17552, 2014.
- [3] K. Tvingstedt, S. D. Zilio, O. Inganäs, M. Tormen, *Opt. Express*, vol. **16**, pp. 21608–21615, 2008.

Identifying microwave magnetic response of chiral elements through reflection for new applications

G.A. Kraftmakher, V.S. Butylkin, Yu.N. Kazantsev, V.P. Mal'tsev

Kotelnikov Institute of Radioengineering & Electronics RAS, Moscow, Russia

e-mail: gkraft@ms.ire.rssi.ru

It has been suggested a method for identifying and separating magnetic and electric microwave resonance responses of chiral conductive elements through reflection in standing- and travelling wave regime. Unique properties of metamaterials are mainly connected with magnetic resonance, which finds an application for creation of magnetic metamaterials and left handed media. So, separating magnetic and electric resonances and identifying magnetic resonance are important having regard to many different kinds of inclusions and great number of different types resonances, as well difficulties of direct measurements of permeability and permittivity. Going methods are based on transmission T analyzes [1, 2]. Separation of magnetic and electric resonances has been suggested and implemented from comparison of T in cutoff and conventional waveguides [1]. Authors [2] separate double split Ring Resonance (RR) and Dipole Resonance (DR) by comparison of T for DSR and closed rings and do not separate magnetic and electric resonances due to ring currents.

In this paper it has been experimentally observed in waveguide and numerically confirmed for free space that magnetic and electric resonances in metamaterial elements show dramatically different resonance curves of reflection R (module and phase) [3]. These distinctions allow to identifying the magnetic resonance as applied to different kinds of inclusions and offer perspective of new applications in the field of broadband matching of absorbers by no traditional quarter-wave effects. Matching layer is array of meta-inclusions excited by microwave magnetic field. Use of varactor (photo varactor) – loaded resonant elements opens a possibility of electric (light) control of absorbers matching.

References

- [1] G. Kraftmakher, New realization and microwave properties of double negative material, *Int. J. of Applied Electromagnetics and Mechanics*, V. **19**(1-4), 57–61, 2004.
- [2] N. Katsarakis, T. Koschny, M. Kafesaki, E. N. Economou, C. M. Soukoulis, Electric coupling to the resonance of split ring resonators, *Appl. Phys. Lett.*, V. **84**(15), 2943–2945, 2004.
- [3] Yu. N. Kazantsev, G. A. Kraftmakher, V. P. Mal'tsev, Identifying and separation magnetic and electric microwave responses of chiral elements, *Tech. Phys. Lett.*, Vol. **42**(3), 238–242, 2016.

Nanoscale conductive filaments and quantized optical properties of plasmonic nanoarrays

V.G. Kravets, F. Schedin, O.P. Marshall, A.N. Grigorenko

School of Physics and Astronomy, University of Manchester, Manchester, M13 9PL, UK

e-mail: vasy1.kravets@manchester.ac.uk

Atomic scale conductive bridges are fabricated by harnessing powerful collective plasmonic modes within a metal–insulator–metal structure. The enhanced plasmonic fields of a regular array of gold nanodots provide a straightforward means of forming conductive CrO_x filaments within a thin chromium oxide barrier between the nanodots and an underlying metallic Cr layer. These filaments consistently exhibit sizes around of few nanometers and can be considered as a nonvolatile memory cells. Furthermore, the electrical state of the filaments is determined optically, using the quantised transmission and absorption of infrared light, well away from the fundamental plasmonic modes at visible wavelengths. It was shown that electromagnetic theory modified by quantum-corrected approach correctly predicts the optical properties of arrays Au dots. The results presented here establish a new connection between the plasmonic responses of metal nanostructures and quantum

transport phenomena, thus bringing a new perspective to the emerging field of quantum plasmonic, which may enable the development of new applications in nanophotonics and optoelectronics.

Broadband all-dielectric metasurfaces for polarization control with near-unity efficiency

Kruk S.S.¹, Hopkins B.¹, Kravchenko I.², Miroshnichenko A.¹, Neshev D.N.¹, Kivshar Yu.S.¹

¹Nonlinear Physics Center, The Australian National University, Canberra, ACT 0200, Australia

²Center for Nanophase Materials Sciences, Oak Ridge National Laboratory, Oak Ridge, TN 37831, USA

e-mail: sergey.kruk@anu.edu.au

The concept of metasurfaces as artificial ultra-thin electromagnetic planar structures composed of subwavelength constituent elements, emerged recently as a novel concept for engineering arbitrary optical elements [1–3]. Metasurfaces based on all-dielectric nanostructures supporting both electric and magnetic Mie-type resonances have resulted in the best efficiency to date for functional optics with only one disadvantage: a narrow operational bandwidth. Here we demonstrate experimentally broadband transparent all-dielectric metasurfaces for highly efficient polarization manipulation. We utilize the generalized Huygens' principle with a superposition of the contributions from several electric and magnetic multipolar modes of the constituent meta-atoms to achieve destructive interference in reflection over a large spectral bandwidth. By employing this concept, we demonstrate reflection-less ($\sim 90\%$ transmission efficiency) half-wave plates, quarter-wave plates, and vector beam q -plates that all can operate across multiple telecom bands with $\sim 99\%$ polarization conversion efficiency.

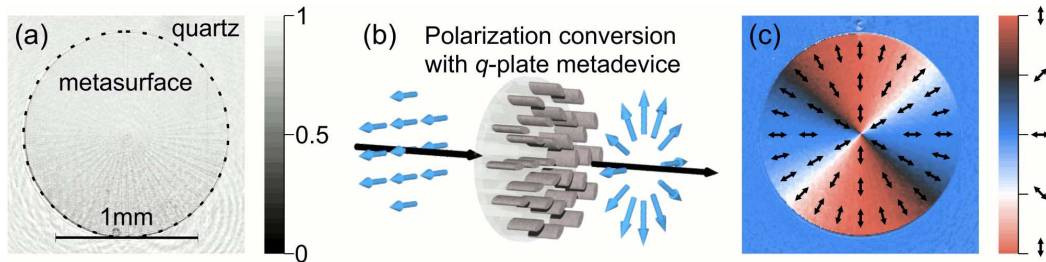


Fig. 1: (a) Optical image of a q -plate taken in transmission with a broadband light source illumination (C & L telecom bands at around $1.5 \mu\text{m}$ wavelength) Metadvice is nearly transparent, and it is hardly distinguishable from a quartz substrate. (b) Schematic of functionality of the q -plate: conversion of a linearly polarized beam into a radially polarized beam. (c) Experimentally retrieved polarization of light passed through the q -plate.

Demonstrated metadvice outperform conventional elements made of both natural birefringent crystals and liquid crystals. For example, in our metadvice (both half-wave plates and q -plates), the π phase difference is accumulated over 850 nm device thickness at 1550 nm wavelength, being equivalent to $\Delta n = (n_o - n_e) \approx 0.9$. The highest values of Δn for conventional materials do not exceed 0.3 . The size of a unit cell in our metasurfaces is 750 nm , i.e. our gradient q -plate has subdiffraction resolution which is at least 10^4 higher than the resolution of pixelated liquid crystal devices. In addition, unlike liquid crystal devices, dielectric metasurfaces can withstand high light intensities and therefore may be used in high-power laser systems.

Acknowledgement. The authors acknowledge a support of the Australian Research Council and thank F. Capasso, T. Krauss, and S. Turitsyn for stimulating discussions. A portion of this research was conducted at the Center for Nanophase Materials Sciences, which is a DOE Office of Science User Facility.

References

- [1] N. I. Zheludev, Y. S. Kivshar, *Nature Materials*, **11**, 917-924 (2012).

- [2] N. Yu, F. Capasso, *Nature Materials*, **13**, 139–150 (2014).
 [3] A. Minovich, et al., *Laser & Photonics Reviews*, **9**, 195–213 (2015).

Magnetic hyperbolic dispersion in optical metamaterials

Kruk S.S.¹, Wong Z.J.², Pshenay-Severin E.^{1,3}, O’Brien K.², Neshev D.N.¹, Zhang X.^{2,4}, Kivshar Yu.S.¹

¹Nonlinear Physics Center, The Australian National University, Canberra, ACT 0200, Australia

²NSF Nanoscale Science and Engineering Center, University of California, Berkeley, CA 94720, USA

³Institute of Applied Physics, Abbe Center of Photonics, Friedrich-Schiller-Universität Jena, 07743 Jena, Germany

⁴Materials Sciences Division, Lawrence Berkeley National Laboratory, Berkeley, CA 94720, USA

e-mail: sergey.kruk@anu.edu.au

Strongly anisotropic media where the principal components of electric permittivity or magnetic permeability tensors have opposite signs are defined as hyperbolic media [1–3]. Such media support propagating electromagnetic waves with extremely large wave vectors exhibiting unique optical properties. However, in all artificial and natural optical structures studied to date the hyperbolic dispersion originates solely from the electric response. This restricts functionality of these materials to one polarization of light (TM) and inhibits free-space impedance matching. Such restrictions can be overcome in media having components of opposite signs for both electric and magnetic tensors. Here we present the first experimental demonstration of three-dimensional metamaterials with the magnetic hyperbolic dispersion.

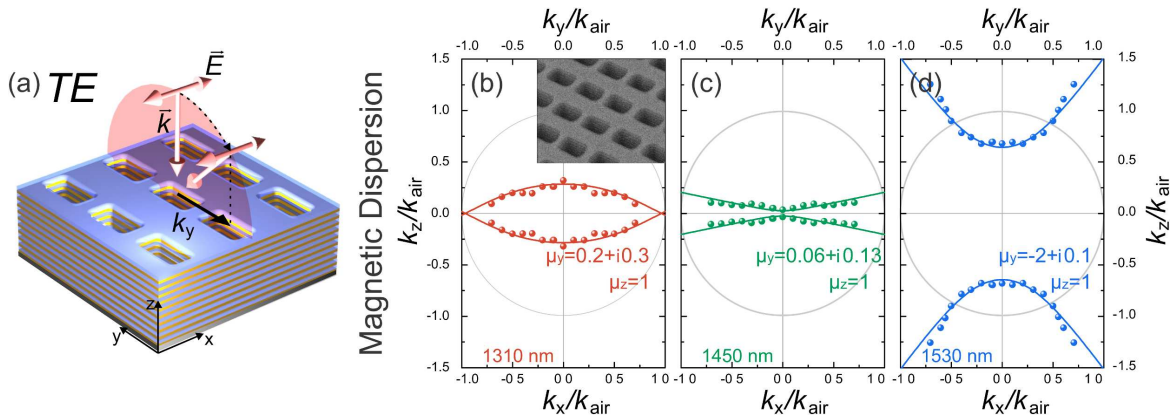


Fig. 1: (a) Schematic of metamaterial sample under illumination. The sample consists of 21 metal and dielectric layers nanopatterned at a sub-wavelength scale. (b–d) Experimentally measured (dots) and analytically retrieved (lines) isofrequency dispersion curves showing transition from elliptic regime at 1310 nm wavelength (b) to hyperbolic regime at 1530 nm (d) via a region of optical topological transition at 1450 nm (c). Numbers μ_y and μ_z indicate corresponding values of the magnetic permeability components. The inset shows an SEM image of the fabricated sample.

We measure metamaterial dispersion, observe and characterize the topological phase transition between the regimes of the elliptic and hyperbolic dispersions. We demonstrate in experiment that the magnetic hyperbolic dispersion enhances thermal emission being directional, coherent and polarized. Our findings show the possibilities for realizing impedance-matched hyperbolic media for unpolarised light.

References

- [1] D. Smith, D. Schurig, *Phys. Rev. Lett.*, **90**, 077405 (2003), (2010).
 [2] Z. Krishnamoorthy, et al., *Science*, **336**, 205 (2012).
 [3] A. Poddubny, I. Iorsh, P. Belov, Y. Kivshar, *Nature Photon.*, **7**, 948 (2013).

Locally resonant metamaterials beyond homogenization: subwavelength control of waves, negative refraction and other exotic phenomena

Lemoult F., Kaina N., Fink M., Lerosey G.

Institut Langevin, ESPCI Paris and CNRS, 1 rue Jussieu, 75005 Paris, France

e-mail: fabrice.lemoult@espci.fr

In this talk, we show how going beyond the homogenization paradigm usually introduced in the context of locally resonant metamaterials permits to enrich the physics associated with them in a drastic way. Starting from the very simple example of a soda can metamaterial in acoustics and the wire medium microwaves (Figure 1), we first underline that their physics can be entirely understood at the light of polaritons in solid state physics. We show, using a microscopic approach based on the transfer matrix that the metamaterials properties are strictly governed by interferences and propagation effects [1]. Namely, the physics of the system solely depend on Fano interferences between the scattered and the unscattered, and multiple scattering of waves between the unit cells of the metamaterial.

We then demonstrate how this observation allows one to tailor this kind of composite media at the scale of the unit cell, hence going much further than the homogenization approximation. Specifically, we show how this allows one to design various components such as cavities, waveguides, filters, that present deep subwavelength dimensions, much smaller than that of their phononic crystal counterparts [1]. We discuss the possibility to slow down waves drastically using this kind of components, through a comparison with recent microwave experiments [2].

Starting again from our microscopic approach of locally resonant metamaterials, we show how it can underline new effects that are totally hidden by other ones. In particular, we explain how a single negative metamaterial can be turned on a double negative medium thanks to multiple scattering, provided that it is rightly structured [3].

Finally, to conclude, we present a few exotic ideas that are direct consequences of the previous results and of a relatively new understanding of the physics of locally resonant metamaterials. For instance, we show how a 2D soda can metamaterials can be turned into a sheet of “acoustic graphene” whose Dirac cone can be positioned at will within a given frequency range.

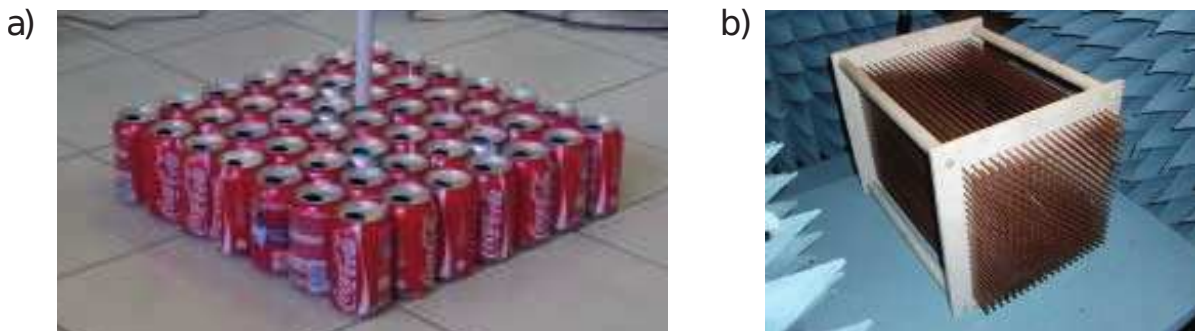


Fig. 1: Two examples of locally resonant metamaterials: (a) an acoustic example based on Helmholtz resonators (the soda cans), and (b) a microwave one based on half-wavelength-long copper wires.

References

- [1] F. Lemoult, N. Kaina, M. Fink, G. Lerosey, *Nature Physics*, **9**, 55–60 (2013).
- [2] N. Kaina, A. Causier, M. Fink, T. Berthelot, G. Lerosey, *submitted* (2015).
- [3] N. Kaina, F. Lemoult, M. Fink, G. Lerosey, *Nature*, **525**, 77–81 (2015).

Efficient absorption of light by nanoparticles designed by a stochastic optimizer

Ladutenko K.S.^{1,2*}, Belov P.A.¹, Peña O.³, Mirzaei A.⁴, Miroshnichenko A.E.⁴, Shadrivov I.V.⁴

¹ITMO University, St. Petersburg, Russian Federation

²Ioffe Institute, St. Petersburg, Russian Federation

³Instituto de Fusión Nuclear, Madrid, Spain

⁴The Australian National University, ACT, Australia

e-mail: k.ladutenko@metalab.ifmo.ru*

Nanoparticles have a fundamental limit as to how much light they can absorb. This limit is based on the finite number of modes excited in the nanoparticle at a given wavelength and maximum absorption capacity per mode. The enhanced absorption can be achieved when each mode supported by the nanoparticle absorbs light up to the maximum capacity. Using stochastic optimization algorithm, we design multilayer nanoparticles, in which we can make several resonant modes overlap at the same frequency resulting in *superabsorption*. We further introduce the *efficiency of the absorption* for a nanoparticle, which is the absorption normalized by the physical size of the particle, and show [1] that efficient absorbers are not always operating in the superabsorbing regime.

References

[1] K. Ladutenko, et al., *Nanoscale*, **7**, 18897–18901 (2015).

On the convergence from finite size and discrete structure towards homogeneous metamaterials

Mikhail Lapine

School of Mathematical and Physical Sciences, University of Technology Sydney, Australia

e-mail: mlapine@physics.usyd.edu.au

In this contribution, I report new findings related to the effect of a discrete structure of practical metamaterials, as opposed to the homogenised treatment assumed in the effective medium treatment. It is well known that effective medium description of metamaterials requires much caution [1], even for strongly subwavelength systems. One of the newly found aspects is that boundary effects play a dramatic role in finite metamaterial samples with discrete structure [2], making their observable properties quite different from the predictions of effective medium theory. We now analyse the convergence of the actual properties of discrete structures towards a homogenised response, taking a spherical shape of metamaterial sample (a cubic lattice, truncated to a shape as close to a sphere as possible). For small spheres with just a few unit cells along the diameter the shape is remarkably ragged, however larger spheres appear reasonably smooth overall.

We directly calculate the response of this structure to applied field, taking all the mutual interactions between the loops into account [3]. We have observed that the calculated magnetisation curves (Fig. 1) for small discrete samples show remarkable deviations and less trivial frequency dependence, however the convergence towards the continuous model improves with size and becomes a clear trend for sizes above 11, and the results for the spheres of 16 and larger appear very similar to each other. Although we have no computational tools to calculate much larger samples, the analysis of the convergence trend toward the effective medium theory allows us to conclude that eventually the difference between a discrete sphere and a continuous one can be eliminated to good precision.

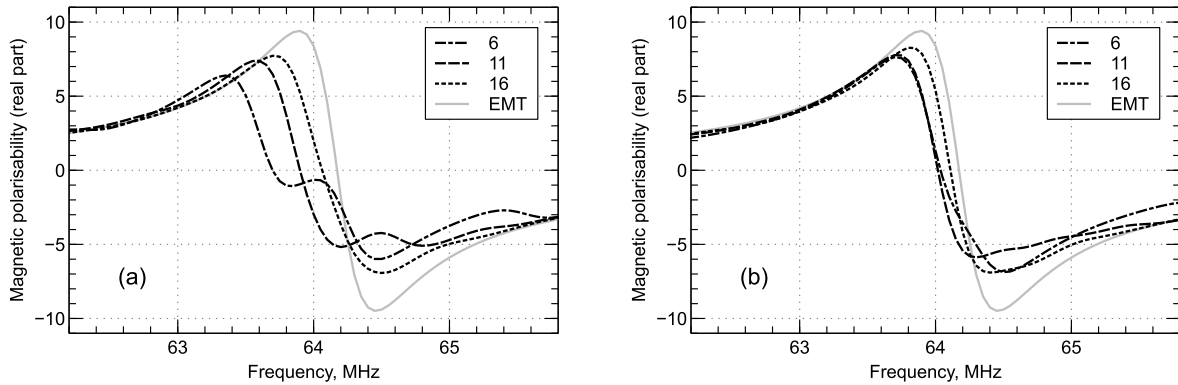


Fig. 1: Frequency dependence of the real part of the magnetic polarisability of the quasi-spherical metamaterial samples truncated from (a) “flat” or (b) “ragged” configuration of the initial boundary of the cubes. The sizes of the spheres, in terms of unit cells per diameter, is indicated by the numbers in the insets. The grey solid curve shows the polarisation theoretically calculated for a homogeneous sphere with the effective permeability [4] corresponding to the considered metamaterial structure.

References

- [1] C. Simovski, On electromagnetic characterization and homogenization of nanostructured metamaterials, *J. Opt.*, **13**(1), 013001 (2011).
- [2] M. Lapine, L. Jelinek, R. Marqués, Surface mesoscopic effects in finite metamaterials, *Opt. Express*, **20**(16), 18297–18302 (2012).
- [3] M. Lapine, L. Jelinek, R. Marqués, M. Freire, Exact modelling method for discrete finite metamaterial lens, *IET Microw. Antenn. Propag.*, **4**, 1132–1139 (2010).
- [4] J.D. Baena, L. Jelinek, R. Marqués, M. Silveirinha, Unified homogenization theory for magnetoinductive and electromagnetic waves in split-ring metamaterials, *Phys. Rev. A*, **78**, 013842 (2008).

Tuning of hybrid oligomers via fs-laser reshaping at nanoscale

Lepeshov S.I.¹, Zuev D.A.¹, Makarov S.V.¹, Miroshnichenko A.E.², Krasnok A.E.¹, Belov P.A.¹

¹ITMO University, St. Petersburg, 197101, Russia

²Nonlinear Physics Centre, Australian National University, Canberra, ACT, Australia

e-mail: s.lepeshov@gmail.com

Metal-dielectric (hybrid) nanostructures and metasurfaces combining advantages of plasmonic and all-dielectric ones open a wide range of perspective applications in medicine, photonics, photovoltaics, etc [1]. Recently, the novel concept of asymmetric hybrid nanoparticles and method of such type nanostructures fabrication were developed [2]. This hybrid nanodimer includes silicon (Si) nanocone and gold (Au) nanodisc that can be reshaped to nanosphere via fs-laser modification at nanoscale. Such hybrid nanostructure has electric dipole resonance of Au nanoparticle as well as magnetic dipole and electric dipole Mie resonances of Si nanocone. Therefore, optical properties of the nanostructure depend on interplay of resonances. It has demonstrated that fs-laser reshaping of Au nanodisc to nanosphere shifts electric dipole resonance of Au nanoparticle to the shorter wavelength region and changes scattering spectrum of hybrid nanodimer.

Here we discuss the possibility to tune optical properties of hybrid oligomers consisting of such hybrid nanodimers by numerical modeling.

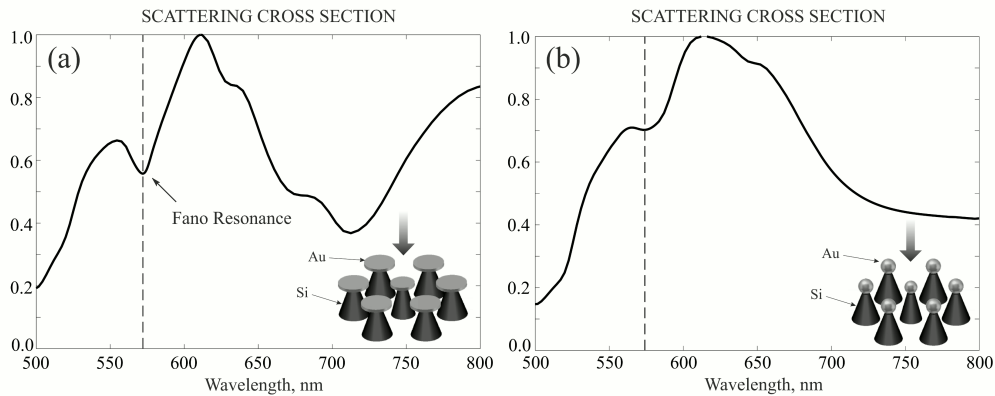


Fig. 1: Numerical modeling of scattering spectra of (a) unreshaped and (b) reshaped hybrid oligomers. Direction of incident wave is shown by an arrow.

We have observed that hybrid oligomers exhibit a Fano resonance in the visible range (Fig. 1a). This Fano resonance is caused by interference of two wave processes. The first process is collective magnetic resonance that is excited in Si nanocones of hybrid nanodimers ring and characterised with the broad spectral width. The second process (spectrally narrow magnetic dipole resonance of the central nanocone with a smaller diameter of the base) is shifted relative to collective magnetic resonance of the ring.

After fs-laser reshaping of hybrid oligomers electric dipole resonances of Au nanoparticles drive to shorter wavelength. It leads to increasing of scattered power at the wavelength of Fano resonance and overlapping of Fano resonance with electric dipole resonance of Au nanosphere (Fig. 1b).

Thus, we have found that this effect demonstrates the opportunity of Fano resonance tuning in hybrid oligomers via fs-laser reshaping of Au nanoparticles at nanoscale. The conducted investigation opens a way for experimental realization of Fano resonances engineering in hybrid oligomers for developing of new switchable nanophotonic devices.

References

- [1] N. Fahim, B. Jia, Z. Shi, M. Gu, *Optics Express*, **20**, A694 (2012).
- [2] D. Zuev, S. Makarov, V. Milichko, S. Starikov, I. Mukhin, I. Morosov, I. Shishkin, A. Krasnok, P. Belov, *Advanced Materials*, DOI: 10.1002/adma.201505346 (2016, accepted).

Chiral near-field formation with all-dielectric nanoantennas

Li S.V.¹, Baranov D.G.^{1,2}, Krasnok A.E.¹, Belov P.A.¹

¹ITMO University, 49 Kronverksky pr., St. Petersburg, 197101, Russia

²Moscow Institute of Physics and Technology, 9 Institutskiy per., Dolgoprudny, 141700, Russia

e-mail: s.li@metalab.ifmo.ru

Nanophotonics has paved the way towards unprecedented level of an optical near-field manipulation at the nanoscale by means of plasmonic and rarer dielectric resonant nanostructures [1]. This became possible after the emergence of optical antennas (or nanoantennas). Currently, nanoantennas have been used to control the local density of optical states, for single nanocrystal and molecule excitation, precise positioning at the nanoscale [2], controlling the scattering directivity, and for the efficient generation of higher optical harmonics [3]. Recently, study of nanoantennas for formation of chiral distributions of the near-field has gained considerable interest.

Here, we study the asymmetric excitation of high-index dielectric subwavelength nanoantenna by a point source, located in the notch at the nanoantenna surface [4]. The nanoantenna (Fig. 1a) is a spherical nanoparticle made of a dielectric material with a high dielectric constant. We observe

the generation of the chiral near-field distribution (Fig. 1b), which is similar to that of a circularly polarized or rotating dipole. Using numerical simulations, we show that this effect is the result of a higher multipole modes excitation within the nanoparticle. Further, we employ this effect for the unidirectional launching of guide modes in the dielectric and plasmonic waveguides. Our results are important for the integrated nanophotonics and quantum information processing systems.

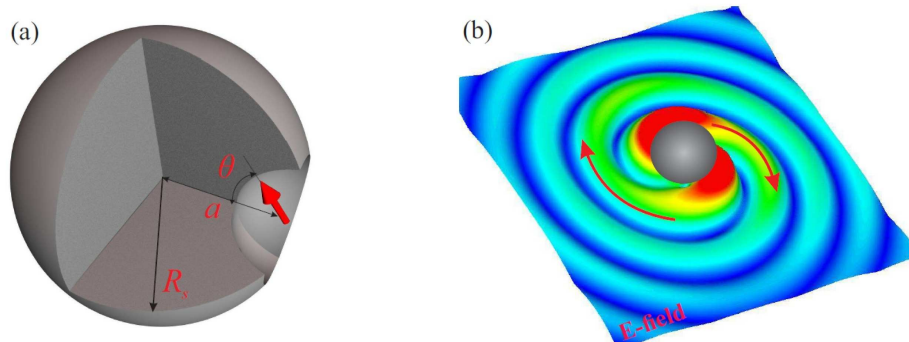


Fig. 1:(a) General view of the considered all-dielectric nanoantenna and orientation of the dipole source (red arrow). (b) The resulting distribution of the electric field at fixed moment of time.

References

- [1] A. Krasnok, S. Makarov, M. Petrov, R. Savelev, P. Belov, Y. Kivshar, *SPIE Opt. and Optoelectr.*, **9502**, 950203 (2015).
- [2] G. Cosa, *Nature Chemistry*, **5**, 159 (2013).
- [3] M. Celebrano, X. Wu, M. Baselli, S. Grobmann, P. Biagioni, A. Locatelli, C.D. Angelis, G. Cerullo, R. Osellame, B. Hecht, L. Duo, F. Ciccacci, M. Finazzi, *Nature Nanotechnology*, **10**, 412 (2015).
- [4] S. Li, D. Baranov, A. Krasnok, P. Belov, *Appl. Phys. Lett.*, **107**, 171101 (2015)

Terahertz all-dielectric magnetic mirror metasurface

Zhijie Ma

NUS Graduate School for Integrative Sciences & Engineering (NGS), National University of Singapore, 117456, Singapore
e-mail: mazhijie@u.nus.edu

Stephen Hanham

Department of Materials, Imperial College London, London SW7 2AZ, UK
e-mail: s.hanham@imperial.ac.uk

Pablo Albella, Stefan Maier

Department of Physics, Imperial College London, London SW7 2AZ, UK
e-mails: p.albella@imperial.ac.uk, s.maier@imperial.ac.uk

Minghui Hong

Department of Electrical and Computer Engineering, National University of Singapore, 117576, Singapore
e-mail: elehnh@nus.edu.sg

We demonstrate an all-dielectric metasurface operating in the terahertz band that is capable of engineering a reflected beam's spatial properties with high efficiency. The metasurface is formed from an array of subwavelength silicon cube resonators which simultaneously support electric and magnetic dipolar Mie resonances. The samples are fabricated by photolithography and deep reactive ion etching

(DRIE) and characterized by a THz time-domain spectroscopy. By controlling the interference between these modes, the amplitude and phase of a reflected wave can be arbitrarily controlled over a sub-wavelength area. We show theoretically and experimentally how the metasurface can produce a high-efficiency all-dielectric magnetic mirror in the terahertz band, which has maximum electric field intensity at the interface for further applications such as in improving the near-field light matter interaction. Additionally, we demonstrate the flexibility and utility of this metasurface by optimizing the surface to produce anomalous reflection and several reflected beam types including vortex and Bessel beams; the latter being useful for diffraction-free point-to-point terahertz communications.

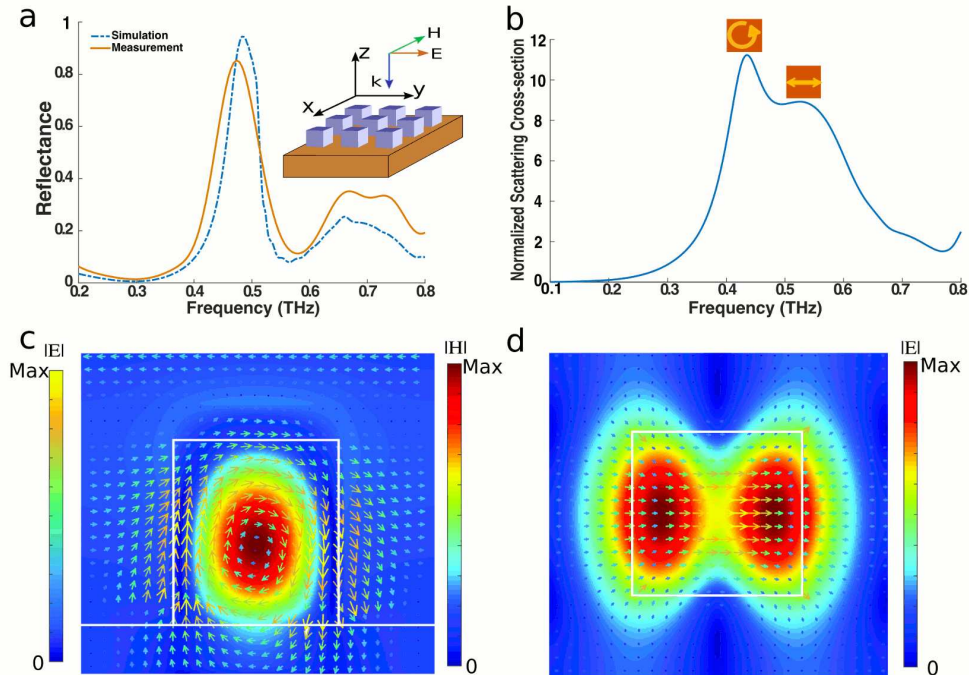


Fig. 1: The reflection spectra and mode profiles in the silicon resonators.

References

- [1] C. Bohren, D. Huffman, *Absorption and scattering of light by small particles*, WILEY-VCH Verlag GmbH (1998).
- [2] S. Mikhail, et al., *Nano Letters*, **15**, 6261–6266 (2015).

Applications of plasmonic and dielectric nanoantennas in nanophotonics

Stefan A. Maier

Imperial College London, London SW7 2AZ, UK
 e-mail: s.maier@imperial.ac.uk

Plasmonic and dielectric nanoantennas allow the concentration of electromagnetic energy from the visible to the mid-infrared regime of the optical spectrum. A variety of new research results will be presented, including (i) the tailoring of the vibrational spectrum of plasmonic nanoantennas via the careful placement of oxide bridges, pinning parts of the antenna strongly to the substrate and hence influencing the amplitudes of acoustic oscillations; (ii) super-resolution mapping of plasmonic hotspots using fluorescence microscopy, elucidating the interplay between enhanced absorption and coupled re-emission; (iii) dielectric nanoantennas for use in low-loss surface-enhanced spectroscopies.

Optical nanoantennas based on metallic nanostructures enable the controlled focusing of light from the far field to highly confined volumes below the diffraction limit, and furthermore form the

basis of implementations of metamaterials and metasurfaces operating in the optical regime of the spectrum.

Upon excitation of the plasmon oscillation, parts of the energy get dissipated via electron/hole pair formation, leading ultimately to dissipation into phonon modes. Here, we show how the vibrational frequencies of these modes can be controlled on the nanoscale, at the level of an individual nanoantenna [1]. This is achieved via pinning certain parts of the antenna stronger to the substrate, utilizing oxide bar layers. Comprehensive finite element modelling combined with degenerate fs pump probe spectroscopy allows us to determine the ratio of the amplitudes of the underlying vibrational normal mode, demonstrating the tailoring. We believe that this work could be the start of a new avenue for control over electromagnetic-acoustic coupling in optical metasurfaces.

We further demonstrate the mapping of plasmonic hot spots using super-resolution far-field fluorescence spectroscopy, including a de-coupling of enhanced absorption and emission processes. The crucial role of the latter in determining the position of the emitter with respect to the antenna will be elucidated. Finally, we will present applications of dielectric nanoantennas for surface-enhanced spectroscopies [2], including antennas operating via localized surface phonon-polarion modes [3].

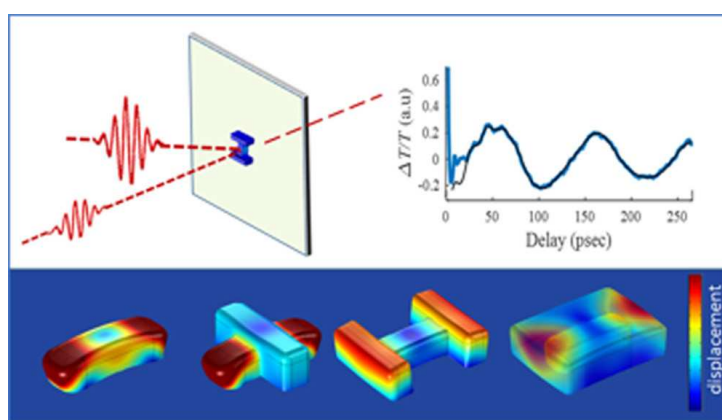


Fig. 1: Controlling the vibrational modes of a plasmonic nanoantenna via oxide bridges [1].

References

- [1] F. Della Picca, et al., *Nano Letters*, **16**, 1428 (2016).
- [2] M. Caldarola, et al., *Nature Communications*, **6**, 7915 (2015).
- [3] J.D. Caldwell, et al., *Nano Letters*, **13**, 3690 (2013).

Chirality of planar G-shaped metamaterials evidenced by polarization-resolved SHG microscopy

Mamonov E.A., Kolmychek I.A., Maydykovskiy A.I., Magnitskiy S.A., Murzina T.V.

Department of Physics, Moscow State University, 119991, Moscow, Russia, Leninskie Gory, 1
e-mail: mamonov@shg.ru

Nonlinear-optical response of planar chiral nanostructures can be significantly influenced by sample's chirality. Different chirality related nonlinear-optical effects have been revealed such as circular dichroism in second harmonic generation (SHG) [1] and asymmetric SHG [2]. The latter shows unusual interaction of linearly polarized light with a macroscopic array of chiral G-shaped nanostructures, as well as chirality related SHG peculiarities from G-shaped metasurface. The studies of microscopic SHG response of these structures with SHG microscopy method have shown that SHG sources (hotspots) within G-elements are strongly localized, their spatial distribution being different for the two G-shaped enantiomers [3]. At the same time, up to now there have been no studies of SHG polarization resolved microscopy of chiral nanostructures.

In the SHG microscopy studies the output of a Ti-Sapphire laser (800 nm wavelength, pulse duration of 30 fs, pulse frequency of 80 MHz) focused on the sample by an objective with the numerical aperture of 0.7. SHG from the sample was collected by the same objective and separated from the fundamental beam by a dichroic mirror. SHG polarization was analyzed using quarter- and half-wave plates and polarization beam splitter, so that all Stokes parameters were determined. The samples were planar gold G-shaped and mirror-G-shaped nanostructures on SiO₂/Si substrate with the lateral size of a single G-element of 1 μm .

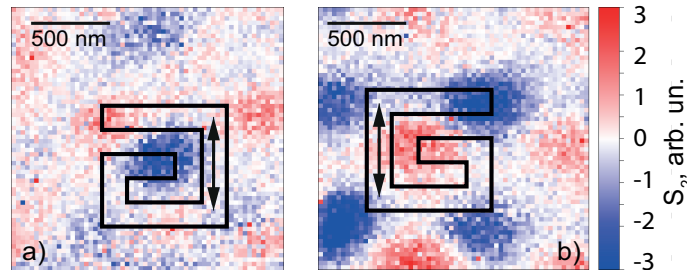


Fig. 1: Spatial distribution of Stokes parameter S_2 at SHG wavelength for mirror-G-shaped (a) and G-shaped (b) nanostructures, its sign governs SHG polarization plane rotation direction. The direction of the linear fundamental beam polarization is shown by the arrows.

SHG intensity map showed the existence of similar peculiarities as described before [3]: two almost equal in amplitude SHG hotspots for the fundamental beam polarization parallel to one of the sample's sides, and one hotspot for the orthogonal beam polarization. We found that the SHG polarization in hotspots is determined by the chirality of the sample. In case of two equal hotspots SHG polarization plane is rotated clockwise in one of the hotspots and counterclockwise in another hotspot (Fig. 1). Absolute value of the rotation angle for both hotspots is about 30°. For the enantiomorphous structure the rotation directions are opposite. The SHG ellipticity is almost equal for both hotspots of one structure and has different sign for enantiomorphs ($\pm 5^\circ$). We proved that these results can be described in terms of the chirality-modified charge density oscillations' direction at fundamental frequency, by corresponding calculations made using CST Microwave Studio software.

References

- [1] V. K. Valev, N. Smisdom, A. V. Silhanek, et al., *Nano Letters*, **9**, 3945–3948 (2009).
- [2] V. K. Valev, A. V. Silhanek, N. Verellen, et al., *Phys. Rev. Lett.*, **104**, 127401 (2010).
- [3] V. K. Valev, A. V. Silhanek, N. Smisdom, et al., *Opt. Express*, **18**, 8286–8293 (2010).

Metamaterial thermal superemitters and superabsorbers

Maslovski S.I.

Instituto de Telecomunicações, DEEC FCTUC Polo II, 3030-290 Coimbra, Portugal
e-mail: stas@co.it.pt

A problem of maximization of the radiative heat transfer (at a given wavelength) between a body and its environment (Fig. 1) is considered theoretically. Given the known electromagnetic characteristics of the environment — the distribution of complex material parameters such as permittivity $\bar{\epsilon}(\mathbf{r})$ and permeability $\bar{\mu}(\mathbf{r})$ — a closed form relation for the material parameters of a body which is optimally matched to the environment and achieves maximal spectral density of emitted power at a given wavelength is formulated. The fact that the material parameters of the optimal emitters can be deduced from the known material parameters of the environment opens a way for physical realization of far-field thermal superemitters and superabsorbers.

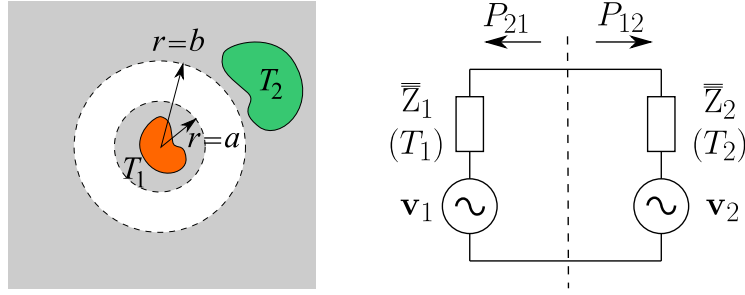


Fig. 1: Left: A body at the temperature T_1 located at $r < a$ exchanges radiative heat with the environment at the temperature T_2 located at $r > b$. Right: Equivalent circuit for the radiative heat exchange.

The spectral density of radiative heat power is expressed through the dyadic impedance operators of the emitter $\bar{\bar{Z}}_1$ and its environment $\bar{\bar{Z}}_2$, which correspond to the equivalent circuit shown in Fig. 1:

$$\frac{dP_{1,2}}{d\nu} = 4\text{Tr} \left[\left(\bar{\bar{Z}}_1^\dagger + \bar{\bar{Z}}_2^\dagger \right)^{-1} \cdot \bar{\bar{R}}_2 \cdot \left(\bar{\bar{Z}}_1 + \bar{\bar{Z}}_2 \right)^{-1} \cdot \bar{\bar{R}}_1 \right] \frac{h\nu}{e^{k_B T_{1,2}} - 1}, \quad \bar{\bar{R}}_{1,2} = \frac{\bar{\bar{Z}}_{1,2} + \bar{\bar{Z}}_{1,2}^\dagger}{2}. \quad (1)$$

The spectral density of the emitted power $dP_{1,2}/d\nu$ is maximized under the conjugate impedance matching condition $\bar{\bar{Z}}_1 = \bar{\bar{Z}}_2^\dagger$. It is shown that there are cases when the spectral density of radiated power can exceed the black body limit, resulting in super-Planckian radiative heat exchange at characteristic distances significantly greater than the wavelength. In fact, it is shown that there is no theoretical upper limit on the spectral density of thermal radiation produced by finite-size bodies, and that it is possible to realize super-Planckian emitters using passive metamaterials [1]. This result refutes the widespread belief that Planck's law itself sets an upper limit for the spectral density of thermal radiation emitted by a macroscopic finite-size object.

Probably the most exciting possible applications of the proposed conjugate-impedance matched superemitters are in creating narrowband super-Planckian thermal emitters for future thermophotovoltaic systems. Such emitters, if realized, have a potential to revolutionize this technology.

References

- [1] S.I. Maslovski, C.R. Simovski, S.A. Tretyakov, Overcoming black body radiation limit in free space: metamaterial superemitter, *New J. Phys.*, vol. **18**, no. 1, p. 013034 (2016).

Unidirectional second-harmonic generation from silicon nanoparticles

Melik-Gaykazyan E.V., Zubyuk V.V., Shorokhov A.S., Kroychuk M.K., Shcherbakov M.R., Dolgova T.V., Fedyanin A.A.

Lomonosov Moscow State University, Faculty of Physics, 119991, Moscow, Russia
e-mail: melik@nanolab.phys.msu.ru

Choi D.-Y.

The Australian National University, Laser Physics Centre, Canberra 2601 ACT, Australia

Neshev D.N., Kivshar Y.S.

The Australian National University, Nonlinear Physics Centre, Canberra 2601 ACT, Australia

Metal metamaterials with optical magnetism possess considerable Ohmic losses, which is even more crucial when considering their interaction with strong electromagnetic fields, particularly, for nonlinear optical applications. On the other hand, Mie scattering theory predicts highly localized optical modes in nanostructured high-index materials. Silicon nanostructures based on nanospheres [1, 2] or nanodisks [3] reveal the electric and magnetic dipolar response in the visible

and near-IR. The nonlinear, third-harmonic optical and ultrafast response of resonant all-dielectric nanostructures has been recently considered [4, 5], whereas the property of unidirectionality [3] was not studied sufficiently.

In this work we have investigated the features of second-harmonic-generation (SHG) process in silicon nanodisks. In the case of simultaneous excitation of electric dipolar and magnetic dipolar modes of the disk we observe unidirectional second-harmonic radiation. Reflected and transmitted SHG was calculated by using the model of oscillating point electric dipoles in nanodisk surface layers with the help of the *FDTD Solutions* software by *Lumerical Solutions, Inc.*

Experimentally, we address the arrays of amorphous silicon nanodisks by nonlinear spectroscopy conducting and comparing the transmitted and reflected SHG intensities. The results reveal a considerable improvement of the SHG front-to-back ratio, which could be utilized for novel subwavelength unidirectional light sources.

References

- [1] A. I. Kuznetsov, A. E. Miroshnichenko, Y. H. Fu, J. Zhang, B. Luk'yanchuk, *Scientific Reports*, **2**, 492 (2012).
- [2] A. B. Evlyukhin, S. M. Novikov, U. Zywietz, R. L. Eriksen, C. Reinhardt, S. I. Bozhevolnyi, B. N. Chichkov, *Nano Letters*, **12**, 3749–3755 (2012).
- [3] I. Staude, A. E. Miroshnichenko, M. Decker, N. T. Fofang, S. Liu, E. Gonzales, J. Dominguez, T. S. Luk, D. N. Neshev, I. Brener, Y. Kivshar, *ACS Nano*, **7**, 7824–7832 (2013).
- [4] M. R. Shcherbakov, D. N. Neshev, B. Hopkins, A. S. Shorokhov, I. Staude, E. V. Melik-Gaykazyan, M. Decker, A. A. Ezhov, A. E. Miroshnichenko, I. Brener, A. A. Fedyanin, Y. S. Kivshar, *Nano Letters*, **14**, 6488–6492 (2014).
- [5] M. R. Shcherbakov, P. P. Vabishchevich, A. S. Shorokhov, K. E. Chong, D.-Y. Choi, I. Staude, A. E. Miroshnichenko, D. N. Neshev, A. A. Fedyanin, Y. S. Kivshar, *Nano Letters*, **15**, 6985–6990 (2015).

Self-averaging of effective refractive index in layered system

Merzlikin A.M.^{1,2,3}, **Puzko R.S.**^{1,3}

¹All-Russia Research Institute of Automatics, ul. Sushchevskaya 22, Moscow 127055, Russia

²Institute for Theoretical and Applied Electromagnetics, Russian Academy of Sciences, ul. Izhorskaya 13, Moscow 125412, Russia

³Moscow Institute of Physics and Technology, Institutskiy per. 9, Dolgoprudny, Moscow Region, 141700, Russia

e-mails: merzlikin_a@mail.ru, roman998@mail.ru

The problem of the propagation of electromagnetic waves through inhomogeneous layered system traditionally attracts attention of researchers [1, 2, 3, 4]. However, the complexity of the problem for inhomogeneous media with large number of inclusions makes impossible precise solution. For solving this problem the inhomogeneous media might be described in term of homogeneous one but with effective material parameters. Introduction of effective parameters is called homogenization.

It should be noted, that the homogenization for cases of static and dynamic electromagnetic field is different. In the static case, Maxwell equations are divided into independent electric and magnetic parts. Therefore introducing of the effective dielectric and magnetic parameters is reasonable. However, this approach is not valid for dynamics, because the amplitude of electric field is connected to the amplitude of magnetic field by impedance. For periodical layered media at longwave regime the effective impedance (retrieved from reflection and transmission) strongly depends on the thickness of the system and thus may describe just the certain sample instead of the media [5]. At the same time, for longwave regime it was shown that the effective refractive index n_{eff} tends to a constant at the increasing of the system and thus n_{eff} can be used for describing of electromagnetic wave propagation through inhomogeneous media.

This communication is devoted to investigation of the properties of n_{eff} for layered system. It is shown that the n_{eff} is a self-averaged quantity at any relation between wavelength and thickness of layer and it is self-averaged quantity for disordered system as well as for periodical one. Moreover the corresponding effective wave vector possesses Kramers–Kronig relation, which results in Herbert–Jones–Thouless [6, 7] relation in the case of disordered layered system.

References

- [1] A. Reuss, *ZAMM-Journal of Applied Mathematics and Mechanics / Zeitschrift für Angewandte Mathematik und Mechanik*, **9**(1), 49–58 (1929).
- [2] W. Voigt, *Lehrbuch der Kristallphysik*, Teubner, Leipzig (1908).
- [3] S. M. Rytov, *Akust. Zh*, **11**, 71–83 (1956).
- [4] A. V. Chebykin, A. A. Orlov, A. V. Vozianova, S. I. Maslovski, Y. S. Kivshar, P. A. Belov, *Physical Review B*, **84**(11), 115438 (2011).
- [5] A. P. Vinogradov, A. M. Merzlikin, *Journal of Experimental and Theoretical Physics*, **94**(3), 482–488 (2002).
- [6] D. J. Thouless, *Journal of Physics C: Solid State Physics*, **5**(1), 77 (1972).
- [7] D. C. Herbert, R. Jones, *Journal of Physics C: Solid State Physics*, **4**(10), 1145 (1971).

Large-scale mechanical metamaterials for seismic wave shielding

Miniaci M.

University of Le Havre, Laboratoire Ondes et Milieux Complexes, UMR CNRS 6294, 76600 Le Havre, France

e-mail: marco.miniaci@gmail.com

Krushynska A.O., Bosia F.

Department of Physics and Nanostructured Interfaces and Surfaces Centre, University of Turin, Via Pietro Giuria 1, 10125, Turin, Italy

e-mails: akrushynska@gmail.com, federico.bosia@unito.it

Pugno N.M.

Laboratory of Bio-Inspired and Graphene Nanomechanics, Department of Civil, Environmental and Mechanical Engineering, University of Trento, 38123, Trento, Italy

e-mail: nicola.pugno@unitn.it

For several decades, many researchers have focused on designing civil infrastructural objects capable of withstanding vibrational events. This is of particular importance for strategic facilities such as hospitals, skyscrapers, long span bridges, historical heritage objects, etc. Among all possible natural and man-made hazards inducing building vibrations, earthquakes are the most devastating events. Although a variety of passive and active isolation systems were developed, a universally accepted risk mitigation procedure has been not proposed yet [1]. Most approaches are based on isolation of structures from seismic waves rather than on remote shielding of incoming waves.

This work proposes and numerically investigates large-scale mechanical metamaterials as a passive isolation strategy for seismic waves. Detailed analysis of the influence of geometric and mechanical parameters on the wave mitigation potential of feasible phononic crystals and locally resonant metamaterial structures is performed for typically recorded frequency and intensity ranges of seismic waves, taking into account crucial soil visco-elasticity. Inhibited frequency ranges are determined by means of finite-element modal analysis for 3D representative metamaterial unit cells accounting for a layered structure of the Earth. These results are confirmed by dynamic transient simulations for both surface and guided seismic waves. The guidelines for practical realization of the proposed structures are also provided.

The proposed remote shielding approach may open up new perspectives in the field of seismology and contribute to developing metamaterial-based earthquake-proof barriers. Numerical results indicate that the proposed seismic isolation strategy is theoretically effective and as well as technically feasible. Experimental validation of the efficiency of metamaterial-based barriers has also been obtained recently [2]. Moreover, the performed parametric study highlights a possibility of tuning inhibited frequency ranges by adjusting them to mechanical parameters of a soil type, in which protected structures are located [3].

References

- [1] R. Villaverde, *Fundamental Concepts of Earthquake Engineering*, Taylor & Francis Group, London-New York (2009).
- [2] S. Brûlé, E. H. Javelaud, S. Enoch, S. Guenneau, *Phys. Rev. Lett.*, **112**, 133901 (2014).
- [3] M. Miniaci, A. O. Krushynska, F. Bosia, N. M. Pugno, *Sci. Rep.*, (submitted). (2016).

Magnetic Purcell factor in polaritonic wire media

Mirmoosa M.S., Simovski C.R.

Department of Radio Science and Engineering, School of Electrical Engineering, Aalto University, P.O. Box 13000, FI-00076 AALTO, Finland

e-mails: mohammad.mirmoosa@aalto.fi, konstantin.simovski@aalto.fi

Arrays of parallel metallic wires, known as standard wire media, have been in a considerable attention since metamaterials have been introduced [1]. These media are uniaxially anisotropic and they have been presented through an effective permittivity tensor as

$$\bar{\epsilon} = \begin{pmatrix} \epsilon_{\perp} & 0 & 0 \\ 0 & \epsilon_{\perp} & 0 \\ 0 & 0 & \epsilon_{\parallel} \end{pmatrix}. \tag{1}$$

Here, ϵ_{\perp} and ϵ_{\parallel} are the perpendicular and parallel components with respect to the wires axis. It is well known: if the wires are made from metal, the perpendicular component (ϵ_{\perp}) of the effective medium permittivity is positive, whereas the parallel component (ϵ_{\parallel}) is negative [1]. Then the TM-polarized waves have open isofrequency surfaces close to a hyperboloid [1]. Such kind of dispersion surface gives high-density electromagnetic states and results in high Purcell’s factor (enhancement of the radiation of embedded sources). This factor is especially high in the frequency region, where ϵ_{\parallel} changes the sign and the so-called topological transition holds. Meanwhile, the isofrequency of the TE-waves is a simple sphere and the TE-waves practically do not interact with the medium. It is so because in metallic wire media the effective permeability tensor ($\bar{\mu}$) is equal to unity. Recently, in Ref. [2] one studied a medium for which the effective permeability allows both hyperbolic and elliptic types of the isofrequency for TE-waves. However, this medium in Ref. [2] is not a wire medium, it is the so-called spiral medium — a racemic array of helical metallic wires operating at microwave frequencies.

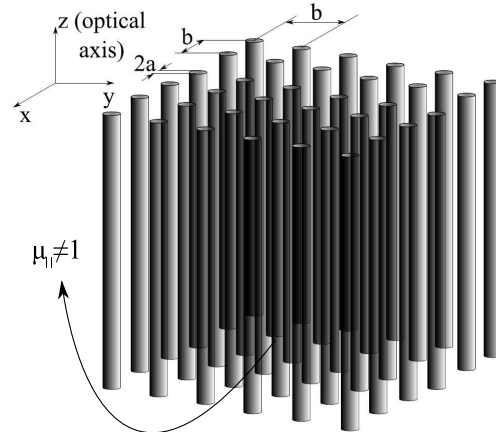


Fig. 1: Dielectric wire medium: \mathbf{z}_0 is the optical axis unit vector, b and a are the lattice constant and the wire radius, respectively ($4a < b \ll \lambda$).

In this work we report similar phenomena for wire media performed of ceramic materials (at microwaves) and polaritonic ones (at mid-infrared frequencies). Due to the Mie resonances in a high-index dielectric cylinder, the magnetic polarizability of an individual wire is resonant and determines the optical properties. We calculate the parallel component of the effective permeability of such a wire medium and study the topological transition of the medium dispersion. In the frequency region where this component (μ_{\parallel}) changes its sign, the huge Purcell factor is expected for a magnetic dipole located in the medium. These theoretical expectations are confirmed by exact numerical simulations.

References

- [1] C. R. Simovski, P. A. Belov, A. V. Atrashchenko, Y. S. Kivshar, Wire metamaterials: physics and applications, *Adv. Mater.*, **24**, 4229–4248 (2012).
- [2] T. A. Morgado, J. T. Costa, M. G. Silveirinha, Magnetic uniaxial wire medium, *Phys. Rev. B*, **93**, 075102 (2016).

THz near-field microscopy: application to spectroscopy of sub-wavelength resonators

O. Mitrofanov^{1,2}, I. Khromova^{3,4}, T. Siday¹, R.J. Thompson¹, I. Brener², T.S. Luk², J.L. Reno²

¹Electronic and Electrical Engineering Department, University College London, London, UK

²Center for Integrated Nanotechnologies, Sandia National Laboratory, USA

³Physics Department, Kings College London, London, UK

⁴ITMO University, St. Petersburg, Russia

e-mail: o.mitrofanov@ucl.ac.uk

We developed terahertz (THz) photoconductive detectors based on hybrid photoconductive optical cavities with plasmonic nano-antenna arrays. These THz detectors are embedded in THz near-field probes to enhance their sensitivity and spatial resolution. We will discuss the design principles and demonstrate practical THz near-field probes with $\lambda/100$ subwavelength apertures.

We demonstrate applications of the THz near-field probes for THz time-domain spectroscopy and imaging of the electric dipole and magnetic dipole modes in metallic and dielectric sub-wavelength THz resonators for metamaterials applications. Temporal evolution of the THz field detected in the near-field zone illustrates the excitation of THz resonances. The THz field distribution in space and local THz spectroscopy allows us to identify the nature of excited resonances.

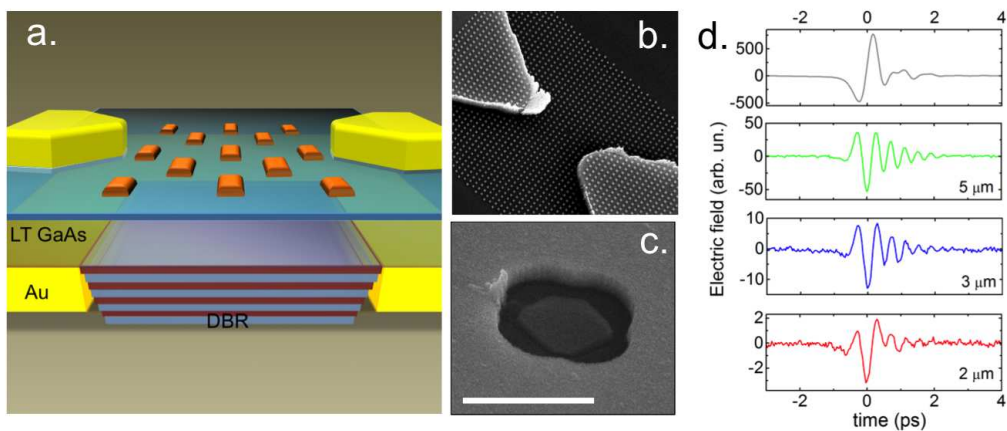


Fig. 1: A schematic diagram of the subwavelength aperture THz near-field probes with embedded photoconductive THz detector. SEM micrographs showing (b) the embedded photoconductive THz detector with the nanoantenna array and (c) the 2 μm input aperture of the probe (the scale bar: 2 μm). (d) THz pulse waveforms detected by the near-field probes with 2 (red), 3 (blue), and 5 μm (green) input apertures. The incident pulse is shown in the top panel (black).

References

- [1] O. Mitrofanov, I. Brener, T.S. Luk, J.L. Reno, Photoconductive terahertz near-field detector with a hybrid nanoantenna array cavity, *ACS Photonics*, **2**(12), 1763 (2015).
- [2] O. Mitrofanov, I. Khromova, T. Siday, R. J. Thompson, A. N. Ponomarev, I. Brener, J. L. Reno, Near-field spectroscopy and imaging of subwavelength plasmonic terahertz resonators, *IEEE Trans. on Terahertz Science and Technology* (2016).

Estimation of attenuation of EM waves propagating through interface biological tissue/free space

I. Munina, P. Turalchuk, E. Kunakovskaya, I. Vendik

Department of Microelectronics and Radio Engineering, St. Petersburg Electrotechnical University "LETI", St. Petersburg, Russia

e-mail: irina.munina@gmail.com

Michail Derkach

JSC "Radar MMS", St. Petersburg, Russia

e-mail: derkach_mm@radar-mms.com

The biological medium surrounding the implanted device is characterized by a high dielectric permittivity and a loss factor, resulting in a degradation of the electromagnetic signal. The high dielectric constant of the biological medium results in a strong wave reflection from the interface. The phenomena of total internal reflection at the interface between biological tissue and air is under consideration. The influence of additional matching layer on wave propagation on interface of biological tissue/free space was studied analytically and by using full wave simulation. Additionally, analysis of the influence of the dielectric properties and the thickness of the substrate of the implanted antenna on the antenna efficiency was performed. Realization of a miniature dipole antenna with SAW resonator was suggested for wireless remote temperature monitoring. Practical implementation was confirmed by the results of the experiment.

Surface and leaky waves in a waveguide, filled with graphene-based hyperbolic metamaterial

Nefedov I.S.

Laboratory Nanooptomechanics, ITMO University, St. Petersburg, 197101, Russia

e-mail: isnefedov@gmail.com

Boardman A.D.

Materials Research Centre, University of Salford, Greater Manchester, M5 4WT, UK

e-mail: a.d.boardman@salford.ac.uk

Layers of hyperbolic metamaterials with optical axes, tilted with respect to interfaces, possess unique properties such as a total absorption in an optically ultra-thin layer [1] and strong dependence of eigenwave spectra on orientation of the optical axis [2, 3]. Nevertheless, there are no published papers devoted to wave propagation in hyperbolic waveguides with arbitrary oriented optical axes, excepting [2, 3]. In this work, as an example of hyperbolic metamaterial, filling the waveguide, we consider periodically arranged graphene sheets, tilted to the layer interfaces on the angle ϕ , as in [1]. The parallel-plate waveguide is PEC-backed on one side and open on the other side. Effective permittivity tensor for the graphene-based metamaterial was obtained by using the Kubo model of graphene surface conductivity. The waves propagate along the x -axis with propagation constant k_x .

Dispersion of some surface and leaky modes, calculated for different tilt angles ϕ , is shown in Fig. 1. Two lowest backward modes and one forward mode are shown. Above the cutoff frequency for $\phi = 0$ (around 34.8 THz) the metamaterial becomes not hyperbolic and leaky waves propagate (only real part of k_x/k_0 is shown). In vicinities of frequencies ≈ 33.7 THz for $\phi = 25^\circ$ and ≈ 34.4 THz for $\phi = 15^\circ$ the wavevector component, normal to slab interfaces, becomes huge. Within these frequency bands (whose location depends on the tilt angle ϕ), exists a large number modes which are not shown here. Thus, changing the orientation of the axis, we can engineer waveguides with required spectra of modes, which, additionally, can be controlled by changing the chemical potential.

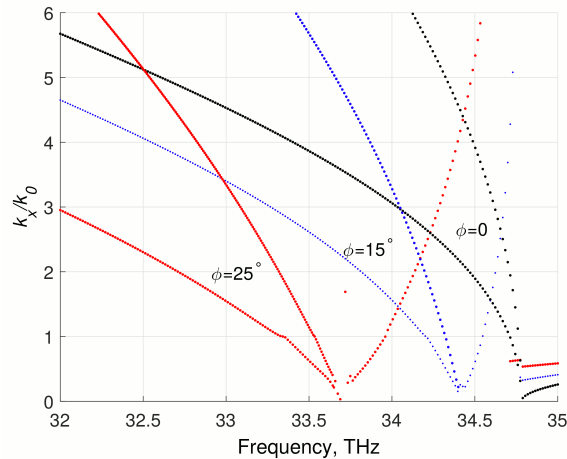


Fig. 1: Dispersion of eigenmodes, calculated at different tilt angles ϕ , where $\phi = 0$ corresponds to graphene sheets, parallel to the layer interfaces. Thickness of the layer is of 400 nm, period of graphene lattice is of 3 nm, and the chemical potential of graphene $\mu_c = 0.2$ eV.

References

- [1] I. S. Nefedov, C. A. Valaginnopoulos, L. A. Melnikov, *Journal of Optics*, **15**, 114003 (2013).
- [2] S. M. Hashemi, I. S. Nefedov, M. Soleimani, *Photonics Letters of Poland*, **5**, 72–74 (2013).
- [3] A. D. Boardman, P. Egan, M. McCall, *EPJ Applied Metamaterials*, **2**, 11 (2015).

Tuning and matching of antennas for preclinical MRI with metamaterial structures

A. Nikulin, S. Glybovski, I. Melchakova, P. Belov

ITMO University, St. Petersburg 197101, Russia

e-mail: a.v.nikulin@live.ru

B. Larrat, E. Georget

CEA-Saclay, DRF/I2BM/Neurospin/UNIRS, 91191 Gif-sur-Yvette Cedex, France

S. Enoch, R. Abdeddaim

Aix Marseille Université, CNRS, Centrale Marseille, Institut Fresnel, UMR 7249, 13013 Marseille, France

In the present work we propose, design and experimentally study a new class of metamaterial-inspired antennas for preclinical magnetic resonance imaging (MRI) for scanners with the permanent magnetic field of 7 Tesla. In contrast to conventional antenna designs (see e. g. the review paper [1]), where tuning and matching of a small magnetic loop is achieved by the use of lumped capacitive circuits, in the proposed approach we employ near-field coupling to passive metamaterial structures. These structures being resonators with high quality factors and multiple hybridized resonances are composed of near-half-wavelength metal wires and/or electrically short wires loaded by capacitive

patches [2]. The proposed antennas, therefore, require no expensive tunable non-magnetic capacitors, which makes the design much cheaper.

The considered metamaterial-inspired antennas are based on an electrically small loop coupled to one or several periodic arrays of thin copper strips, each one realized as a printed-circuit board. Such arrays of printed wires, when being half-wavelength, support multiple resonances of hybridized eigenmodes. Recently it was shown that coupling of an electrically-small loop feed to these eigenmodes improves the near-field homogeneity and the signal-to-noise ratio in preclinical MRI [3].

In our approach we employ the hybridized eigenmodes of resonant periodic wire structures to tune and match the loop feed at one or several separate frequencies, which corresponds to the antennas for single- and multi-nuclei MRI. Moreover, preferring one of the available eigenmodes (their number is determined by the number of wires), it is possible to optimize the distribution of the radiofrequency magnetic field inside a scanned subject.

In this works we demonstrate the experimentally realized metamaterial-inspired antennas for phosphorus and hydrogen imaging at 7 Tesla operating at one and two frequencies. We compare the obtained results of numerical simulations and measurements demonstrating the single- and double-frequency operation, including S-parameters and the transmit field distributions inside an MRI bore.

References

- [1] F. D. Doty, G. Entzminger, J. Kulkarni, K. Pamarthy, J. P. Staab, Radio frequency coil technology for small-animal MRI, *NMR in Biomedicine*, Vol. **20**, pp. 304325 (2007).
- [2] S. B. Glybovski, A. V. Shchelokova, A. V. Kozachenko, A. P. Slobozhanyuk, I. V. Melchakova, P. A. Belov, A. V. Sokolov, A. Yu. Efimtsev, V. A. Fokin, Capacitively-loaded metasurfaces and their application in magnetic resonance imaging, *Radio and Antenna Days of the Indian Ocean (RADIO)*, pp. 1–2, 21–24 (2015).
- [3] C. Jouvaud, R. Abdeddaim, B. Larrat, J. de Rosny, Volume coil based on hybridized resonators for magnetic resonance imaging, *Applied Physics Letters*, Vol. **108**, p. 023503 (2016).

Full broadband absorption of perovskite solar cells with plasmonic nanoparticles

Mikhail Omelyanovich^{1,2}, Sergey Makarov², Valentin Milichko², Constantin Simovski^{1,2}

¹Aalto University, P.O. 13000, FI-00076, Finland

²ITMO University, 197043, St. Petersburg, Russia

e-mail: mikhail.omelyanovich@aalto.fi

Synthetic perovskites with photovoltaic properties open a new era in solar photovoltaics. Their synthesis is a cheap low-temperature chemical process [1]. Since the initial work [2], where the record (for that time) efficiency was obtained for a dye-sensitized solar cell (where a perovskite played the role of dye), the efficiency of perovskite-based solar cells has grown by an order of magnitude [3]. This huge progress achieved in 6 years allows researchers to claim a new era in solar photovoltaics when the solar energy is becoming a really mass product due to perovskites [4].

Due to high optical absorption perovskite-based thin-film solar cells are usually considered as fully absorbing solar radiation on condition of ideal blooming. However, it is not really so. The analysis of the literature data has shown that the absorbance of all photovoltaic perovskites has the spectral hole at infrared frequencies where the solar radiation spectrum has a small local peak (Fig. 1). This absorption dip results in the decrease of the optical efficiency of thin-film perovskite solar cells and close the ways of utilise them at this range for any other applications. In our work we show that to cure this shortage is possible complementing the basic structure by an inexpensive plasmonic array. Perovskite compounds are mechanically amorphous [1] and by using a novel technology of laser ablation we will be able to put the array of nanoparticles inside the photovoltaic layer of a perovskite solar cell in order to achieve a full broadband absorption.

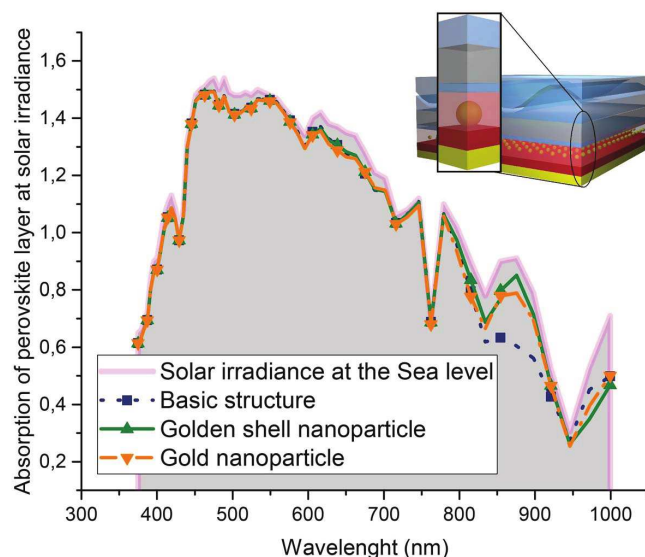


Fig. 1: Absorption in the perovskite layer for several variants of our solar cell (basic structure, the structure enhanced by solid nanospheres, and that enhanced by nanoshells) taking into account the solar irradiance spectrum.

References

- [1] A. Ecija, K. Vidal, A. Larranaga, L. Ortega-San-Martín, M. I. Arriortua, Synthetic methods for perovskite materials — structure and morphology, in *Advances in Crystallization Processes*, Ed. Y. Mastai, InTech Publisher, Rieka–Shanghai, 486–506 (2012).
- [2] A. Kojima, K. Teshima, Y. Shirai, T. Miyasaka, Organo-metal halide perovskites as visible-light sensitizers for photovoltaic cells, *J. Am. Chem. Soc.*, **131**, 6050–6051 (2009).
- [3] H.S. Jung, N.-G. Park, Perovskite solar cells: From materials to devices, *Small*, **11**(1), 10–25 (2015).
- [4] B. Wang, X. Xiao, T. Chen, Perovskite photovoltaics: a high-efficiency newcomer to the solar cell family, *Nanoscale*, **6**, 12287–12297 (2014).

Electrically controlled porous polymer films filled with liquid crystals: new possibilities for photonics and THz applications

Sergey Pasechnik, Dina Shmeliova, Anton Chopic, Denis Semerenko, Semen Charlamov, Alexander Dubtsov

Moscow Technological University (MIREA), Moscow, Russia

e-mail: pasechnik@mirea.ru

Liquid crystals (LC) have found the outstanding application in display industry due to unique properties such as a strong anisotropy of optical (Δn), dielectric ($\Delta \epsilon$) and viscous-elastic parameters, which provides an effective control (usually via electric fields) of light beams. It also makes possible to use these materials in electrically controlled devices of photonics like shutters, attenuators, phase retarders, polarization controllers etc., characterized by high efficiency, low control voltages and suitable operating times [1].

In this report we present the results of optical and rheological investigations of composite LC material, which consists of a polymer polyethylene terephthalate (PET) porous films filled with a liquid crystal pentyl-cyano-bepnyl (5CB) and subjected to the action of electric field. In experiments, the samples of track-etched membranes of micrometer thickness with randomly distributed open-end pores of diameters d in the range 100–5000 nm were studied. It was found, that the dynamics of

the electro-optic response essentially depends on the voltage shape. In particular, at application of video pulses of a different polarity the strong negative peaks in the intensity of light, passed through the samples, at moments, corresponding to the change of the polarity of an applied voltage, were registered. The threshold voltage and operating times for this effect as functions of the pore's diameter were established. Different possible mechanisms, responsible for the observed phenomenon, like the dielectric torque, the ion motion and the electro-osmotic flow were considered. The existence of the latter mechanism was confirmed by the direct investigations of electro-kinetic phenomena in porous films filled with LC [2]. It made possible to estimate the relative contributions of the different mechanisms mentioned above in the electro-optical response.

The prospects of usage of the obtained results in photonic applications were considered. In particular, electro-osmotic flow may be effective for a control of orientational structure of LC in pores of a relatively large diameter (more, than 1 μm). It mechanism can be perspective for THz range where the wavelengths are much larger than the pores' diameter. It opens the ways for an elaboration of the terra fluidic devices of different types.

References

- [1] V. Chigrinov, *Liquid Crystal Photonics*, Nova Science Publishers Inc. (2014).
- [2] S. V. Pasechnik, A. P. Chopik, D. V. Shmeliova, E. M. Drovnikov, D. A. Semerenko, A. V. Dubtsov, W. Zhang, V. G. Chigrinov, Electro-kinetic phenomena in porous PET films filled with liquid crystals, *Liquid Crystals*, **42**(11), 1–6 (2015).

Refraction angle of electromagnetic wave on a wired structure prism

Dmitrii Pavlov*, Leonid Butko, Anton Anzulevich

Chelyabinsk State University, Chelyabinsk, Russia

e-mail: *metam.chelsu@yandex.ru

In this work, we considered wired structure as an effective medium that can be described by electromagnetic properties μ_{eff} , ϵ_{eff} and n_{eff} . The samples under investigation were dielectric prisms consisting of periodically arranged with the lattice constant $a = 7 \text{ mm}$ conductive wires. It was obtained in [1] that given medium has $n_{\text{eff}} \sim 1$ at frequency 12 GHz. According to this, we fabricated and investigated samples with various angles of the facet of the prism (fig. 1a) to prove that specified wired structure is an effective medium at frequency 12 GHz and electromagnetic wave passes without deviation for various angles. All the measurements were performed on the angular spectrometer (fig. 1b) described in details in [1]. The results of refraction dependencies on the angle are shown on the fig. 2.

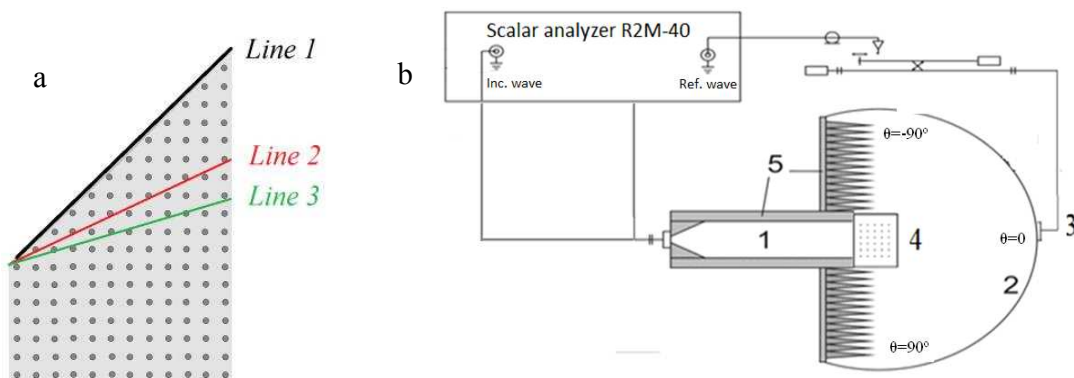


Fig. 1: Fabricated prisms with several angles of facet (a): Line 1 – 45°; Line 2 – 26°; Line 3 – 14°. Experimental setup (b).

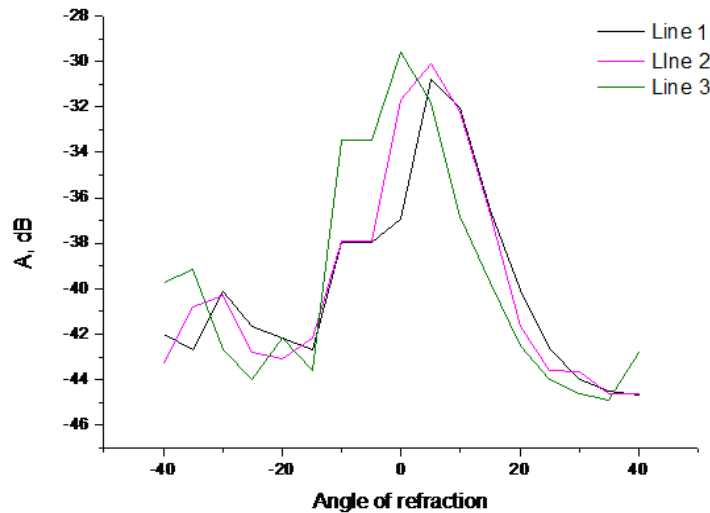


Fig. 2: Angular dependencies of refraction index at frequency 12 GHz on the prisms with various angles of the facet.

References

- [1] D. A. Pavlov, L. N. Butko, A. A. Fedyi, A. P. Anzulevich, I. V. Bychkov, V. D. Buchel'nikov, V. G. Shavrov, Wire structure with a negative effect refraction at microwave frequencies, *Journal of Radioelectronics*, **11** (2015).

Tungsten based metamaterials and photonic crystals for selective thermal emitters

Alexander Yu. Petrov^{1,2}, Pavel N. Dyachenko¹, Slawa Lang¹, Elisabeth W. Leib³, Jefferson do Rosario⁴, Sean Molesky⁵, Zubin Jacob^{5,6}, Tobias Krekeler⁷, Martin Ritter⁷, Michael Störmer⁸, Tobias Vossmeier³, Horst Weller^{3,9}, Gerold Schneider⁴, Manfred Eich¹

¹Institute of Optical and Electronic Materials, Hamburg University of Technology (TUHH), Eißendorfer Straße 38, 21073 Hamburg, Germany

²ITMO University, 49 Kronverkskii Ave., 197101, St. Petersburg, Russia

³Institute of Physical Chemistry, University of Hamburg, Grindelallee 117, D-20146 Hamburg, Germany

⁴Institute of Advanced Ceramics, TUHH, Denickestraße 15, 21073 Hamburg, Germany

⁵University of Alberta, Department of Electrical and Computer Engineering, 9107 - 116 Street, T6G 2V4, Edmonton, Canada

⁶Birk Nanotechnology Center, School of Electrical and Computer Engineering, Purdue University, West Lafayette, IN 47906, USA

⁷Electron Microscopy Unit, TUHH, Eissendorfer Strasse 42, 21073 Hamburg, Germany

⁸Institute of Materials Research, Helmholtz-Zentrum Geesthacht Centre for Materials and Coastal Research, Max-Planck-Straße 1, 21502 Geesthacht, Germany

⁹Department of Chemistry, Faculty of Science, King Abdulaziz Univ., Jeddah, Saudi Arabia
e-mail: a.petrov@tuhh.de

In order to tailor thermophotovoltaic emitters to match specific photovoltaic receivers we realized spectrally selective emitters that have close to black body emission at short wavelengths and substantially reduced emission at long wavelengths. To emit significant power at the wavelengths usable for photovoltaic conversion (below 2 μm) the far-field emitter should be heated to high temperatures. The development of such thermally stable selective emitters requires strong cooperation between material science and optics, which was possible in the frame of the Hamburg based Collab-

orative Research Center SFB 986 “Tailor-Made Multi-Scale Materials Systems” in cooperation with external partners. We demonstrate selective band-edge emitters based on a W-HfO₂ refractive metamaterial [1] and a ZrO₂ opal monolayer on tungsten both stable up to 1000°C [2]. The metamaterial exhibits almost angle independent selective emission due to a topological transition of its isofrequency surface. The monolayer approach, on the other hand, allows keeping the tungsten unstructured and thus demonstrates exceptional emission suppression at longer wavelengths. The physics behind the selective emission of the demonstrated concepts and an outlook for further improved selectivity as well as further enhanced thermal stability will be presented.

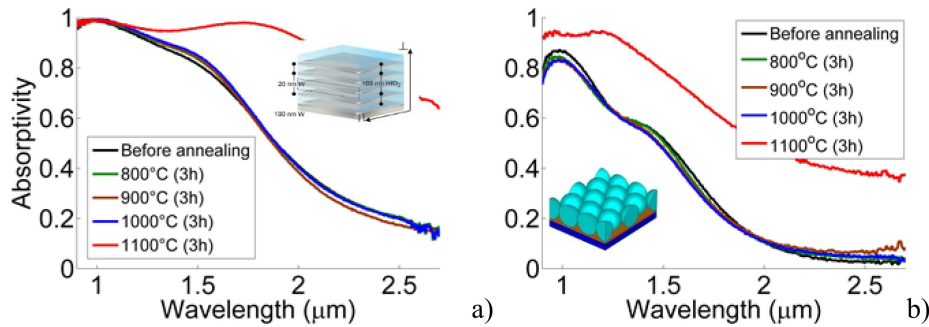


Fig. 1: (a) Absorptivity of the tungsten based metamaterial after tempering in vacuum. Schematic inset shows the layered structure of W-HfO₂ (20–100 nm) metamaterial. (b) Absorptivity of the tungsten emitter coated by a monolayer of ZrO₂ microparticles (660 nm diameter) after tempering in vacuum. Schematic inset shows the structure geometry. (dark blue — W, orange — HfO₂, light blue — ZrO₂).

References

- [1] P. N. Dyachenko, et al, Refractory epsilon-near-zero metamaterials: Controlling thermal emission with topological transitions, *Nat. Comm.*, accepted (2016).
- [2] P. N. Dyachenko, et al, Tungsten band edge absorber/emitter based on a monolayer of ceramic microspheres, *Opt. Exp.*, **23**, A1236 (2015).

Wide-aperture superabsorption of terahertz radiation by plasmonic periodic array of graphene nanoribbons

Polischuk O.V., Popov V.V.

Kotelnikov Institute of Radio Engineering and Electronics (Saratov Branch), Russian Academy of Sciences, Saratov 410019, Russia

e-mails: polischuk.sfir@mail.ru, glorvv@gmail.com

Melnikova V.S.

Saratov State University, Saratov 410012, Russia

e-mail: melnikovaveronica@yandex.ru

Graphene exhibits strong plasmon response at THz frequencies due to both the high density and low collective dynamic mass of free carriers in graphene [1]. Using the plasma oscillations of charge carriers in graphene is attractive, because it allows for concentrating the electromagnetic field near graphene, which significantly enhances the efficiency of interaction of THz radiation with graphene. This is important from both points of view of studying the physical properties of graphene and creating new types of THz graphene-based devices.

In this paper, we consider a periodic array of graphene nanoribbons, located on the surface of a dielectric (THz prism) with a high refractive index (Si in our case). External THz wave is incident on the array of graphene nanoribbons from inside the prism at an angle θ . The direction of the

periodicity of the array of graphene nanoribbons coincides with the plane of incidence of the plane p-polarized THz wave. The optical problem of interaction of THz wave with the periodic array of graphene nanoribbons has been solved by using of a self-consistent electromagnetic approach. The response of graphene is described by the complex dynamic surface conductivity [2].

The calculations were performed for realistic parameters of graphene at room temperature. It is shown (Fig. 1) that the total absorption can be reached in the total internal reflection (TIR) regime in a wide range of the incidence angles $\theta > \theta_R$, where θ_R is the angle of the total internal reflection. Note that the effect of the total absorption of the incident THz radiation is possible at the frequencies of the plasmon resonance when the balance between dissipative and radiative losses is realized. Dissipative losses are determined by the phenomenological scattering rate while the radiative losses depend on the concentration of free carriers and are determined by the position of the Fermi level.

This work was supported by the Russian Foundation for Basic Research (Grant 16-02-00814).

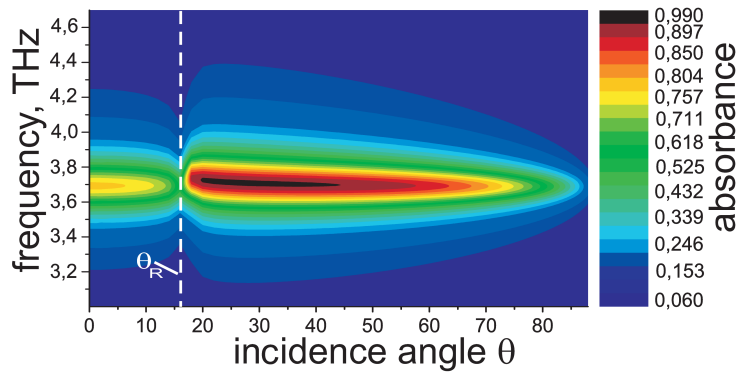


Fig. 1: Absorbance spectrum in the TIR regime at the fundamental plasmon resonance in the graphene nanoribbon array with period 1,6 μm and nanoribbon width 800 nm as a function of frequency and angle of incidence of the external wave for the Fermi energy value 200 meV.

References

- [1] J. Chen, M. Badioli, et al, *Nature*, **77**, 487 (2012).
- [2] L. A. Falkovsky, A. A. Varlamov, *Eur. Phys. J.*, **56**, 281 (2007).

Bianisotropic effective medium for subwavelength multilayers

Popov V.V., Novitsky A.V.

Belarusian State University, Department of Theoretical physics and Astrophysics, 4, Nezavisimosti avenue, 220030, Minsk, Republic of Belarus

e-mails: physics.vlad@gmail.com, andreyvnovitsky@gmail.com

For the metamaterials (artificial subwavelength structures) the concept of the material homogenization is crucial. In electromagnetism, the homogenization method implies the replacing of an inhomogeneous periodic structure, the unit cell of which is subwavelength, with an effective medium, which electromagnetic material parameters are spatially uniform. It is important to have a correct effective medium approximation to adequately predict the properties of the inhomogeneous structures.

In this paper we deal with the simplest case of inhomogeneous structures namely a set of alternating layers with dielectric permittivities ε_1 and ε_2 of thicknesses d_1 and d_2 , respectively. Thicknesses of layers are assumed to be much smaller than the vacuum wavelength. In accordance with the Maxwell-Garnet approach the structure can be treated as a nonmagnetic uniaxial crystal which optical axis is orthogonal to the interfaces of the layers (see for instance [1]). The applicability of the effective medium approach to structures under consideration has hardly ever been questioned.

However, in Refs. [2, 3] the breakdown of effective medium approximation for all-dielectric structures under certain circumstances was demonstrated theoretically and observed experimentally [4]. In spite of the fact that layers are deeply subwavelength it turns out that the multilayer structure and the corresponding effective medium can have significantly different transmission spectra when the incidence angle is close to the critical angle of the total internal reflection. Additionally, it was shown that transmission becomes sensitive to both the order of layers in the stack and its subwavelength features. All these and other facts fundamentally contradict to the effective medium predictions. As all-dielectric structures do not support surface waves in contrast to metal-dielectric structures it makes the breakdown of effective medium a crucial drawback of Maxwell–Garnet approach.

We develop a more precise definition of effective medium approximation (EMA) for subwavelength multilayer structures in order to overcome anomalous behavior of the ordinary Maxwell–Garnet effective medium for all-dielectric subwavelength multilayers. To that end homogenization technique for multilayers based on covariant operator methods [5] is used. We reveal that the correct effective medium should possess both magnetic and gyrotropic properties, and reveal spatial dispersion. As it should be expected the effective medium parameters depend on both the thickness of the layer pair and order of the layers in the multilayer (i. e. 1212...12 or 2121...21). We show that the transmission through this effective medium well matches with that of the generic multilayer in the cases when the ordinary effective medium fails.

References

- [1] P. Shekhar, et al., *Nano Convergence*, **1**, 14 (2014).
- [2] H. H. Sheinfux, et al., *Physical Review Letters*, **113**, 243901 (2014).
- [3] A. Andryieuski, et al. *Nanotechnology*, **26**, 184001 (2015).
- [4] S. Zhukovsky, et al., *Physical Review Letters*, **115**, 177402 (2015).
- [5] A. N. Borzdov, *Advances in Electromagnetics of Complex Media and Metamaterials*, 259–269 (2002).

Ultra-wideband antenna with single- and dual-band notched characteristics based on electric ring resonator

Alexander Rusakov¹, Irina B. Vendik¹, Komsan Kanjanasit², Jiasheng Hong², Dmitry Filonov³

¹Microwave Microelectronics Laboratory, Department of Microelectronics and Radio Engineering, St. Petersburg Electrotechnical University, St. Petersburg, Russia

²Department of Electrical, Electronic and Computer Engineering, School of Engineering and Physical Sciences, Heriot-Watt University, Edinburgh, U.K.

³Department of Photonics and Optical Information Technology, National Research University of Information Technologies, Mechanics and Optics, St. Petersburg, Russia

e-mails: sanyarus@bk.ru, ibvendik@rambler.ru, kk184@hw.ac.uk, j.hong@hw.ac.uk, dmitriy.filonov@phoi.ifmo.ru

The ultra-wideband (UWB) monopole antenna is designed as the circular patch fed by a coplanar waveguide (CPW). This antenna provides the impedance bandwidth of the wideband response from 2.5 GHz to 12 GHz with the gain of about 4–5 dB in the working frequency range. To achieve the notched characteristics at desirable frequencies, the electric ring resonator (ERR) incorporated into the CPW feed line is used. The notched frequency band is controlled by dimensions of the ERR structure. The single-notched band is obtained by placing a single ERR consisting of a square ring with the capacitive element inside beneath the CPW structure. For implementation of the dual-notched band, a cascaded connection of various ERRs with different resonant frequencies is examined. Moreover, modified structure of the dual-mode ERR providing dual band-notched characteristics is suggested and analyzed. Two single band-notched UWB monopole antennas loaded by the single ERR were designed for 5.8 GHz and 7.5 GHz notch responses. Additionally, two dual band-notched

UWB antennas were designed for 5.8 GHz and 7.5 GHz notched bands: antenna including cascaded connection of various ERR, and antenna contains the dual-mode ERR. The results of simulations and measurements are in good agreement.

Measurements of polarisation dependent Purcell factor in microwave metamaterials

Rustomji K.^{1,2}, **Abdeddaim R.**¹, **Kuhlmeiy B.**², **Enoch S.**¹

¹Aix-Marseille Université, CNRS, Centrale Marseille, Institut Fresnel, UMR 7249, 13013 Marseille, France

²Centre for Ultrahigh-bandwidth Devices for Optical Systems (CUDOS), University of Sydney NSW 2006, Australia

e-mails: kaizad.rustomji@fresnel.fr, redha.abdeddaim@fresnel.fr,
boris.kuhlmeiy@sydney.edu.au, stefan.enoch@fresnel.fr

Hyperbolic metamaterials [1] have attracted interest due to the possibility of a high broadband Purcell factor. We shall present measurements of electric and magnetic Purcell factor for a microwave metamaterial [2] between 5–15 GHz. Using electric and magnetic dipole antennas it will be shown that the polarisation dependent dispersion relations affect the Purcell factor.

We shall present the iso-frequency surfaces and present a method to calculate the density of states (DOS). Comparison shall be made between the measurements of Purcell factor using the impedance of an antenna [3, 4] and the local density of states (LDOS) of the periodic metamaterial unit cell.

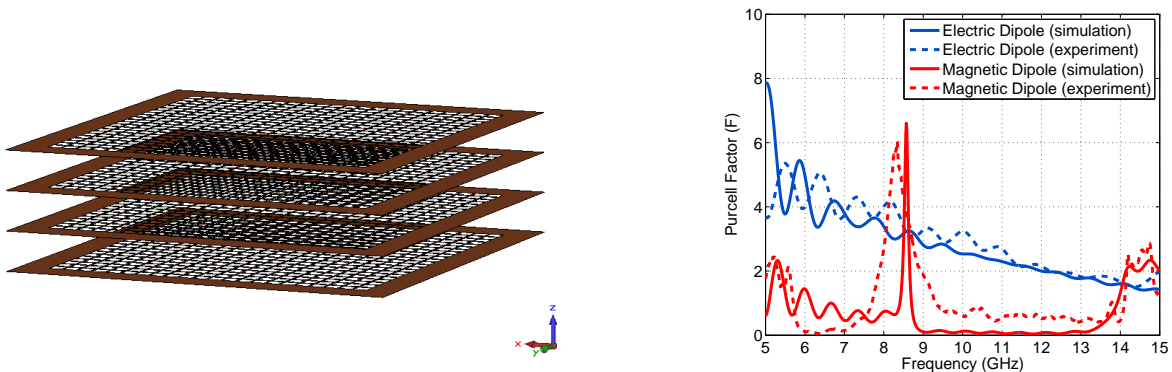


Fig. 1: (a) Metamaterial structure used for measurements, made of copper grids of periods 5.8 mm in x - y direction. (b) Electric and magnetic Purcell factor measured inside the metamaterial. The electric dipole emits in the transverse magnetic (TM) polarisation and Purcell factor is enhanced due to hyperbolic dispersion relations. The magnetic dipole emits in the transverse electric (TE) polarisation and magnetic Purcell factor is close to zero below the plasma frequency, because the dispersion relation does not allow any propagating solutions.

References

- [1] A. Poddubny, I. Iorsh, P. Belov, Y. Kivshar, *Nature Photonics*, **7**, 948–957 (2013).
- [2] S. Enoch, G. Tayeb, P. Sabouroux, N. Guérin, P. Vincent, *Physical Review Letters*, **89**, 213902 (2002).
- [3] J.-J. Greffet, M. Laroche, F. Marquier, *Physical Review Letters*, **105**, 117701 (2010).
- [4] A. Krasnok, A. Slobozhanyuk, C. Simovski, S. Tretyakov, A. Poddubny, A. Miroshnichenko, Y. Kivshar, P. Belov, *Scientific Reports*, **5**, 12956 (2015).

Concept of phase transitions between photonic crystals and all-dielectric metamaterials

M.V. Rybin^{1,2}, D.S. Filonov¹, K.B. Samusev^{1,2}, P.A. Belov¹, Y.S. Kivshar^{1,3}, **M.F. Limonov^{1,2}**

¹Department of Nanophotonics and Metamaterials, ITMO University, St. Petersburg 197101, Russia

²Ioffe Institute, St. Petersburg 194021, Russia

³Nonlinear Physics Center, Research School of Physics and Engineering, Australian National University, Canberra ACT 2601, Australia

e-mail: m.limonov@mail.ioffe.ru

We discuss transition between two different classes of artificial media i. e. photonic crystals and dielectric metamaterials and introduce the concept of a phase diagram, based on the physics of Mie and Bragg resonances [1]. For a square lattice of dielectric circular rods, we calculate: (i) spectra of the Mie scattering by an isolated circular rod; (ii) photonic band structure of a two-dimensional square lattice composed of circular rods; (iii) transmittance spectra of a PhC slab composed of 5 layers. We demonstrate that the calculated photonic band structure and transmission spectra depend dramatically on the dielectric contrast, structure filling ratio, and light polarization.

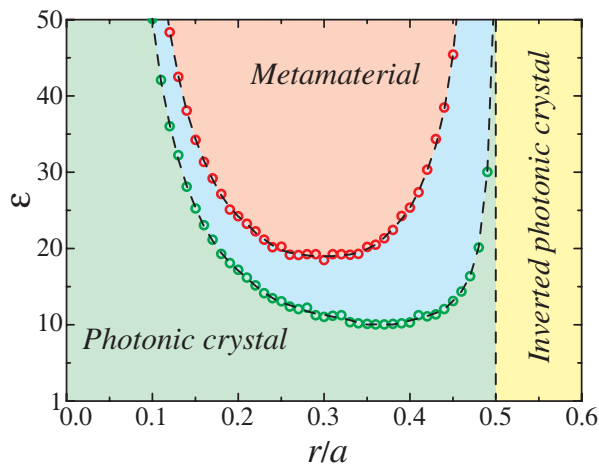


Fig. 1: Phase diagram for 2D square lattice of circular rods. The lower set of circles indicates the points of the collapse of the pure lowest Bragg gap in the calculated photonic band structure. The upper set of circles indicates the points where the TE_{01} Mie dispersion curve becomes completely flat at the $\Gamma \rightarrow X$ direction of the first Brillouin zone.

At low permittivity ϵ of the rods, the lowest TE_{01} Mie band has a higher energy than the lowest Bragg gap. With increasing ϵ , the Mie resonances demonstrate a strong shift from higher to low frequencies. In the p -polarization at a certain value of the dielectric contrast TE_{01} Mie band approaches and crosses the Bragg gaps. With further increase in ϵ , the TE_{01} Mie band splits off from the Bragg band becoming the lowest stop-band in the structure. This point indicates the birth of a metamaterial phase. Thus, we reveal that a transition between photonic crystals and dielectric metamaterials phase can be identified through the switching of the position of the Mie and Bragg resonances in the energy spectrum. Such switching makes possible the homogenization of the periodic dielectric structure with the negative effective permeability ($\mu < 0$) at higher values of ϵ .

This work was supported by the Russian Foundation for Basic Research (grant No. 15-02-07529).

References

- [1] M. V. Rybin, D. S. Filonov, K. B. Samusev, P. A. Belov, Y. S. Kivshar, M. F. Limonov, *Nature Commun.*, **6**, 10102 (2015).

Complex photonic band diagram and \mathcal{PT} -symmetry in periodic media

Mikhail V. Rybin^{1,2}, Mikhail F. Limonov^{1,2}

¹Ioffe Institute, St. Petersburg 194021, Russia

²Department of Nanophotonics and Metamaterials, ITMO University, St. Petersburg 197101, Russia
e-mail: m.rybin@mail.ioffe.ru

The ability to accurately calculate photonic properties is required for designing novel devices, while the photonic band diagram, i. e., frequency ω vs. wave vector \mathbf{k} , being the most important inherent property of periodic media. The common approach to the problem consists in reducing Maxwell's equations to the standard eigenproblem for the frequency as an eigenvalue. However these techniques are not practical, when we need to analyze evanescent modes or structures with frequency dependent dielectric functions. To overcome these problems we suggest an inverse dispersion method that calculates wave vector k in dependence on frequency ω [1].

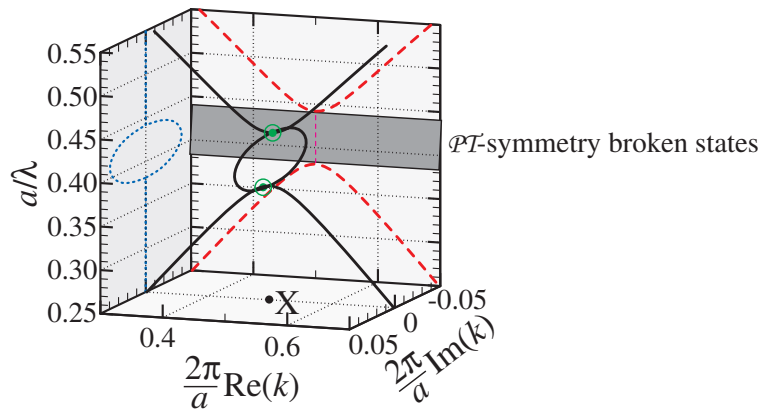


Fig. 1: Complex band diagram for TE-polarized electromagnetic wave in square lattice of dielectric cylinders. Solid curves are eigenmodes. Dashed curves are projection on the real plane, dotted curve are projection on the imaginary plane. Bandgap where evanescent modes are in \mathcal{PT} -symmetry broken state is shaded.

Using this method we reduce Maxwell's equations to the form of non-Hermitian eigenproblem for wave vector k , while the frequency ω is the parameter of operator. Let us consider TE-polarized electromagnetic wave in square lattice of dielectric cylinders of radius $r = 0.3a$ (a is the lattice constant) and dielectric permittivity $\varepsilon = 4$. Fig. 1 shows complex band diagram calculated by the inverse dispersion method. We obtain that the branches do not disappear after coalescence at the Brillouin zone surface, rather the wave vector k gains imaginary part. Inspired by the results obtained from non-Hermitian \mathcal{PT} -symmetric Hamiltonians [2] we assume that the wave vector operator possesses a certain symmetry. The symmetry \mathcal{T} is related to the time-reversal symmetry, while the parity \mathcal{P} should be applied to the fields represented in the k -space. The consequence from description of the problem by an operator with \mathcal{PT} -symmetry is that we should not consider the operator as a mathematical trick only and reject it as being unphysical, because it violates the axiom of Hermiticity. Conversely we do consider the operator as physical quantity that is related to the momentum of excitation in periodical media.

This work was supported by the Russian Foundation for Basic Research (15-02-07529).

References

- [1] M. V. Rybin, M. F. Limonov, *Phys. Rev. B* (2016).
- [2] C. M. Bender, *Rep. Prog. Phys.*, **70**, 947 (2007).

Purcell effect and Lamb shift for photonic modes

Mikhail V. Rybin^{1,2}, Sergei F. Mingaleev³, Mikhail F. Limonov^{1,2}, Yuri S. Kivshar^{2,4}

¹Ioffe Institute, St. Petersburg 194021, Russia

²Department of Nanophotonics and Metamaterials, ITMO University, St. Petersburg 197101, Russia

³VPI Development Center, Belarus Hi-Tech Park, Minsk 220037, Belarus

⁴Nonlinear Physics Center, Research School of Physics and Engineering, Australian National University, Canberra ACT 2601, Australia

e-mail: m.rybin@mail.ioffe.ru

Smart applications in photovoltaics, biosensing and integrated photonics require resonant elements with adjustable properties such as the quality factor (or lifetime), operation frequency, and lineshape. New approaches to the control of such properties are actively explored last years. Recently it was proposed [1] to adjust effective properties of the microcavity by modification of its environment, by an analogy with the Purcell effect well known for quantum systems, as well as oscillation of charged particles or loops of current [2]. The Purcell effect is observed as an increase of lifetime of an excited system due to the modification of zero-point oscillations that defined by a local density of states (LDOS). Besides, the zero-point oscillations affect the energy states of the system, known as the Lamb shift.

We consider a waveguide coupled to a side defect (a microcavity). Waveguide modes are modified by the Fabry–Perot resonator (FPR), and we study how FPR changes properties of pure photonic mode excited in the microcavity. We develop a phenomenological model and find that the microcavity lifetime is proportional to LDOS, in direct analogy with the quantum Purcell effect. Also we obtain the frequency shift being classical counterpart of the Lamb shift, however the shift is differ by factor 1/2.

To verify our phenomenological theory, we study numerically the system implemented in a photonic crystal, proposed in Ref. [3] as a system with asymmetrical Fano lineshape. By varying the position of the FPR reflectors, we modify electromagnetic eigenmodes between reflectors, and as a result change LDOS at microcavity. Numerical results show variation of the lifetime in 25 (Purcell effect) and the shift of microcavity frequency (Lamb shift) being in excellent agreement with phenomenological mode.

In summary, we observe three effects for a pure photonic mode in microcavity: (i) a change of the radiation rate caused by the Purcell effect; (ii) a change of the resonance frequency associated with the Lamb shift, and (iii) an asymmetric line-shape explained by the physics of the Fano resonances.

References

- [1] M. V. Rybin, S. F. Mingaleev, M. F. Limonov, Yu. S. Kivshar, *Sci. Rep.*, **6**, 20599 (2016).
- [2] A. E. Krasnok, A. P. Slobozhanyuk, C. R. Simovski, S. A. Tretyakov, A. N. Poddubny, A. E. Mi-roshnichenko, Yu. S. Kivshar, P. A. Belov, *Sci. Rep.*, **5**, 12956 (2015).
- [3] S. Fan, *Appl. Phys. Lett.*, **80**, 908–910 (2002).

Optical bound state in the continuum in one-dimensional photonic crystal slab: theory and experiment

Sadrieva Z.F.¹, Sinev I.S.¹, Samusev A.K.¹, Iorsh I.V.¹, Bogdanov A.A.¹, Lavrinenko A.V.²

¹ITMO University, St. Petersburg 197101, Russia

²DTU Fotonik, Technical University of Denmark, Kgs. Lyngby, Denmark

e-mail: zfsadrieva@corp.ifmo.ru

Optical bound states in the continuum (BIC) are infinitely high-Q states with energies lying above the light line of the surrounding space. The was firstly proposed for electrons in quantum

mechanics by von Neumann and Wigner in 1929 [1]. Optical analogue of BIC was firstly proposed by Marinica et al. [2]. Experimental observation of BIC was demonstrated in Ref. [3]. Such high-Q states are very promising for many potential applications ranging from on-chip photonics and optical communications to biological sensing and photovoltaics.

In this work we experimentally realized CMOS-compatible one-dimensional photonic structure based on silicon-on-insulator wafer with optical BIC at telecommunication wavelengths. Excitation of optical BIC from free space is possible due to sample imperfections which are always present. The design of the structure and the dispersion of the leaky mode are shown in Fig. 1(a). Figure 1(b) shows the dependence of Q-factor of the leaky mode on wavenumber. The sharp peak corresponds to optical BIC.

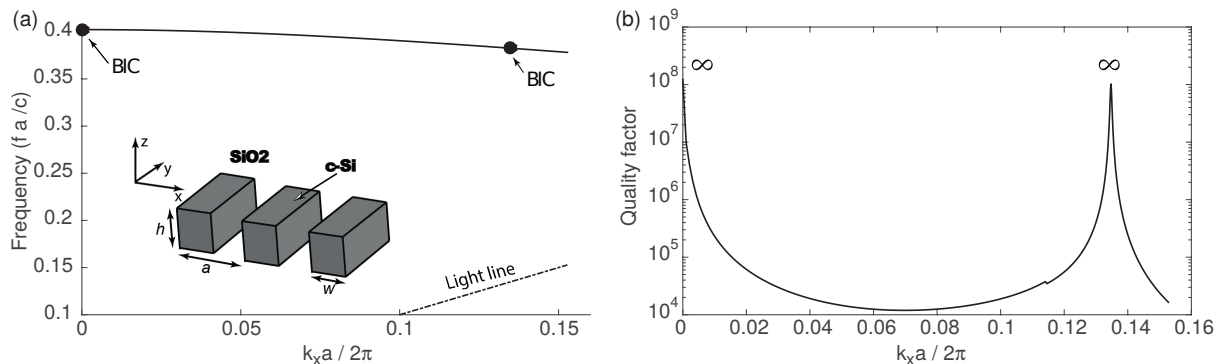


Fig. 1: (a) Dispersion of the leaky mode in 1D photonic structure. The insets show design of the structure. (b) Dependence of Q-factor of the leaky mode on the wavenumber. Both figures show results of simulations.

This work has been supported by RFBR (16-37-60064), by the President of Russian Federation (MK-6462.2016.2). Numerical simulations, and optical experiments have been supported by the Russian Science Foundation (Grant 15-12-20028).

References

- [1] J. von Neumann, E. Wigner, *Physikalische Zeitschrift*, **30**, 465 (1929).
- [2] D. C. Marinica, A. G. Borisov, S. V. Shabanov, *Physical Review Letters*, **100**, 183902 (2008).
- [3] Y. Plotnik, O. Peleg, F. Dreisow, M. Heinrich, S. Ntote, A. Szameit, M. Sergeev, *Physical Review Letters*, **107**, 183901 (2011).

Transition from photonic crystals to metasurfaces in optical Laue diffraction

K.B. Samusev^{1,2}, A.D. Sinelnik¹, M.V. Rybin^{1,2}, S.Y. Lukashenko^{2,3}, Y.S. Kivshar^{1,4}, M.F. Limonov^{1,2}

¹Department of Nanophotonics and Metamaterials, ITMO University, St. Petersburg 197101, Russia

²Ioffe Institute, St. Petersburg 194021, Russia

³Nanotechnology department, Institute for Analytical Instrumentation RAS, St. Petersburg, 198095, Russia

⁴Nonlinear Physics Center, Research School of Physics and Engineering, Australian National University, Canberra ACT 2601, Australia

e-mail: k.samusev@mail.ioffe.ru

In this study, we use a direct laser writing technique to fabricate 2D photonic structures as periodic arrays of submicron dielectric particles or their inverted counterparts with the square C_{4v} and orthogonal C_{2v} lattice symmetry. We study experimentally optical Laue diffraction from fabricated structures and observe on a screen placed after the sample diffraction patterns.

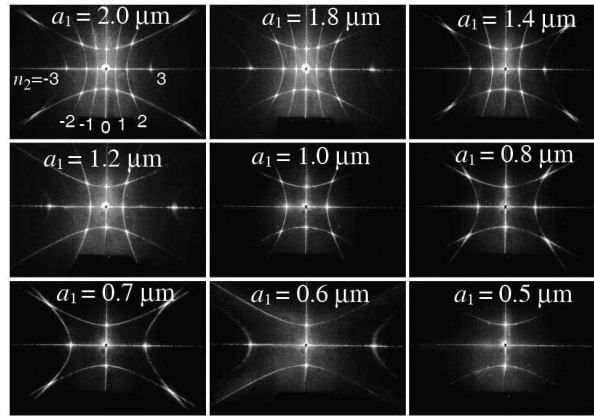


Fig. 1: Experimental diffraction patterns obtained from 2D structures with varied lattice parameter $0.5 \mu\text{m} \leq a_1 \leq 2 \mu\text{m}$ and constant parameter $a_2 = 1.0 \mu\text{m}$. The patterns observed on a flat screen positioned behind the sample. $\lambda = 0.53 \mu\text{m}$.

We demonstrated both experimentally and theoretically that the diffraction processes along mutually perpendicular \mathbf{a}_1 and \mathbf{a}_2 directions are completely independent for both square and rectangular 2D samples. The possibility of the experimental observation of a certain order of diffraction n is determined by the lattice constant a to wavelength λ ratio. Using a set of samples with orthogonal C_{2v} lattice symmetry and variable lattice parameter along \mathbf{a}_1 , we observed experimentally a transition between two regimes of Laue light diffraction, i. e. the regime of multi-order diffraction which is characteristic for photonic crystals ($a > \lambda$) and the regime where only the zero-order ($n = 0$) diffraction can be observed under condition $a < \lambda$ that is a fingerprint of metasurfaces (Fig. 1). As to the diffraction axis \mathbf{a}_2 with constant lattice parameter, the patterns remain unchanged for all samples: one pair of the first-order cones ($n_2 = \pm 1$) and horizontal zero-order plane ($n_2 = 0$) are observed.

This work was supported by the Russian Science Foundation (No. 15-12-00040).

Transducer of light to longitudinal electric field in sub-wavelength volume

Sarychev A.K.

Institute for Applied and Theoretical Electrodynamics of RAS, Moscow, 125412, Russia

e-mail: sarychev_andrey@yahoo.com

Vergeles S.S.

Institute for Theoretical Physics of RAS, Chernogolovka, 142432, Russia

e-mail: vergeles@gmail.com

Tartakovsky G.

Advanced Systems and Technologies, Inc., Irvine, CA 92618, USA

e-mail: gtartakov@gmail.com

We propose a novel all-dielectric near field transducer, which focuses the light, pumped through the waveguide, into a hot spot, which is much smaller than the wavelength, without dissipative loss inevitable in the plasmonic nanoantennae. Therefore, the detrimental thermal effects almost vanish, which gives an opportunity to use our light concentrator for the heat-assisted magnetic recording (HARM) [1].

In the proposed new device [2], the electric field is much enhanced at the vertex of the dielectric tip attached to the specially tuned dielectric resonator as it is shown in Fig. 1. The electric field enhancement and concentration is achieved by longitudinal polarization of the vertex, which is exposed to the resonator field. Concentration of light into nanospots much smaller than the wavelength is crucial for HAMR, but it is much beneficial for various applications: biomedical imaging and sensing, optical microscopy with single-molecule resolution, QED studies, nanolasing, etc. Until now,

plasmonic metal nanoantennae or metallic near field concentrators have been used for this purpose. Optical field enhancement and concentration is achieved by the excitation of the surface plasmons. The main advantage of the metal nano-antennae is their capabilities to localize plasmonic modes, which can be excited by the incident transverse em wave. Yet, a metal nanoparticles have large optic loss. The proposed novel all-dielectric transducer allows us to focus light into a hot spot much smaller than the wavelength without the dissipative loss.

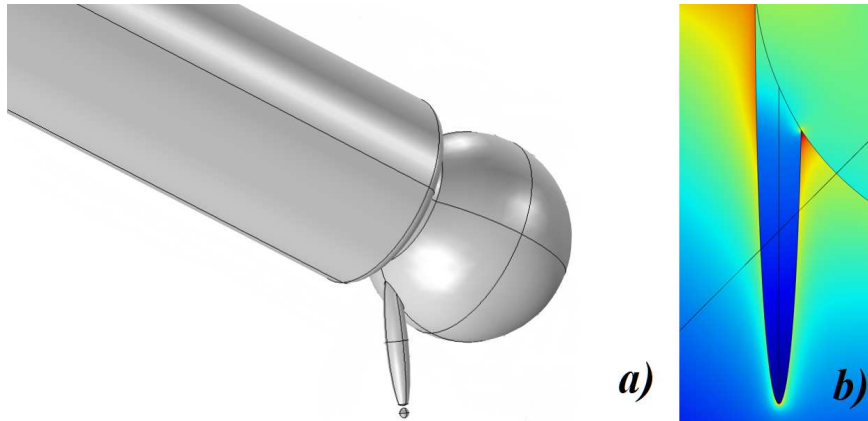


Fig. 1: a) Near field transducer consisting of cylindrical silicon waveguide, spherical resonator, and prolate ellipsoidal nanotip; b) numerical simulation of electric field which is pumped in the resonator through the waveguide; magnetic dipole resonance is excited in the spherical resonator; electric field of the resonance excites the vertical nanotip.

The longitudinal electric field enhancement at the tip's vertex can be achieved for any optically dense material, including a transparent dielectric. The problem is how to convert the incident light into a longitudinal electric field. A simple waveguide does not produce a considerably localized longitudinal electric field, which is necessary to excite the tip. In the recently proposed metal Fresnel lens, the specially designed plasmonic lens produce the longitudinal electric field [3]. In contrast to the previous works we propose to excite the dielectric nanotip through the waveguide ended by the optic resonator. The waveguide is matched with the resonator, which accumulates em energy. The em field, pumped in the resonator, effectively excites the tip.

References

- [1] S. Vedantam, H. Lee, J. Tang, J. Conway, M. Staffaroni, E. Yablonovitch, *Nano Lett.*, **9**, 3447 (2009).
- [2] S.S. Vergeles, A.K. Sarychev, *Metadevices and Metasystems*, Eds. N. Engheta, M. A. Noginov, I. N. Zheludev, SPIE **9544**, 954415 (2015).
- [3] Y. Wang, Z. Du, Y. Park, C. Chen, X. Zhang, L. Pan, *Optics Letters*, **40**, 3918 (2015).

Solitary waves in chains of silicon nanoparticles

Savelev R.S., Yulin A.V., Krasnok A.E.

ITMO University, Saint-Petersburg, Russia, 197101

e-mail: r.savelev@metalab.ifmo.ru

Modern tendency to replace the components of electronic integrated circuits with optical ones by means of minituarizing the latter requires very small interconnecting elements — relatively short waveguides with subwavelength cross-section sizes. One of the promising realizations of such waveguides is the chain of dielectric nanoparticles with high refractive index, e.g. silicon nanoparticles [1, 2]. Linear properties of silicon nanoparticles and structures composed of them were extensively

studied in the last several years. However, despite the apparent interest in their nonlinear properties, quite a few works were addressing this issue [3–5]. In these studies either nonlinear scattering of light by silicon nanoparticles and structures or third-harmonic generation was studied.

Here we consider theoretically the pulse propagation in the waveguide composed of silicon nanoparticles with nonlinear Kerr-like response. We show that despite the low quality factor of a single silicon nanoparticle, very high group velocity dispersion of the nanoparticle waveguide and the relatively low nonlinear refractive index in silicon, the compensation of pulse broadening with nonlinearity in the dielectric discrete waveguide can be achieved at the lengths of several tens of micrometers in optical frequency range. This is possible to achieve by exploiting the properties of the silicon nanodisks with the parameters providing close magnetic and electric dipole resonance frequencies. In contrast to the chain of silicon nanospheres having negative dispersion $\omega'' = d^2\omega/d\beta^2$ at all frequencies, the chain of appropriately arranged nanodisks has positive ω'' in a certain frequency range, i. e. it has the same sign as nonlinear refractive index of silicon, which allows to obtain a soliton in nanodisks waveguide at realistic level of intensities $\lesssim 5 \text{ GW/cm}^2$.

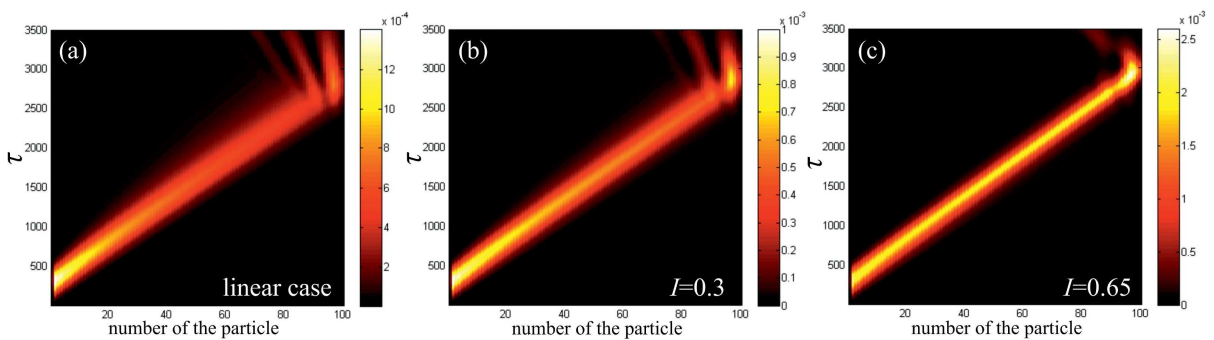


Fig. 1: Dynamics of the 100 fs pulse propagating in the chain of nanodisks (a) in the linear regime, (b, c) in the nonlinear regime with dimensionless intensities (b) $I = 0.3$, (c) $I = 0.65$.

References

- [1] J. Du, S. Liu, Z. Lin, J. Zi, S. T. Chui, *Phys. Rev. A*, **83**, 035803 (2011).
- [2] R. S. Savelev, *et al.*, *Phys. Rev. B*, **89**, 035435 (2014).
- [3] M. R. Shcherbakov, *et al.*, *Nano Lett.*, **14**, 6488–6492 (2014).
- [4] S. Makarov, *et al.*, *Nano Lett.*, **15**, 6187–6192 (2015).
- [5] M. R. Shcherbakov, *et al.*, *ACS Photon.*, **2**, 578–582 (2015).

Liquid metamaterials

Shadrivov, I.V.

Nonlinear Physics Centre, Research School of Physics and Engineering, Australian National University, Canberra ACT 2601, Australia
 e-mail: ilya.shadrivov@anu.edu.au

We present a new type of metamaterial, a meta liquid crystal (MLC) [1], with a structure inspired by conventional nematic liquid crystals. Our MLC consists of elongated particles containing meta-atoms, which are encapsulated in a dielectric and dispersed in a liquid. These elements, which we call “meta-mesogens”, work as anisotropic dipoles in the electrostatic limit and can reorient in response to a bias electric field, thus tuning the electromagnetic response of the whole MLC composite. In comparison to conventional liquid crystals, the electrodynamic response of MLCs is defined by the anisotropic meta-atoms instead of the whole mesogen, thus there is considerable freedom to prescribe the electromagnetic properties through the design of the meta-atom geometry, and the electrodynamic

and electrostatic responses can differ greatly. For example, apart from anisotropic electric response, one can also achieve magnetic, chiral/bianisotropic responses, or even more complicated spectral features such as electromagnetic induced transparency and Fano resonances. Importantly, the liquid nature of such metamaterials allows them to flow and fill in spaces or cover surfaces of arbitrary three-dimensional shapes, which would significantly widen the field where metamaterials can be employed.

As a proof of concept study, we design three different types of meta-mesogens with pure electric response around 0.5 THz. Two of them are based on electric split-ring resonators and one is based on I-beam resonators. The meta-mesogens work as electric dipoles in the electrostatic limit and all three designs have similar response time in the same host liquid. However, their THz responses are very different due to the distinct current distributions involved. To verify the prediction, we fabricate the meta-mesogens on silicon substrates with standard UV lithography, where metallic meta-atoms are encapsulated in polyimide; the meta-mesogens are then lifted off and dispersed in paraffin oil; finally the MLC composite is injected into a cylindrical PTFE (polytetrafluoroethylene) sample chamber and sealed with quartz slides, so that we can observe the morphology change and measure the transmission spectrum under a biased electric field. We have experimentally observed electromagnetic behaviour of the meta liquid crystals that matches our predictions.

References

- [1] M. Liu, K. Fan, W. Padilla, D. A. Powell, X. Zhang, I. V. Shadrivov, *Adv. Materials*, **28**, 1553 (2016).

Metasurfaces for magnetic resonance imaging

Shchelokova, A.V., Melchakova, I.V., Belov, P.A.

ITMO University, St. Petersburg, Russia

e-mails: alena.schelokova@phoi.ifmo.ru, belov@phoi.ifmo.ru

Slobozhanyuk, A.P.

Nonlinear Physics Center, Australian National University, Canberra, Australia

e-mail: aleksei.slobozhaniuk@anu.edu.au

We reveal that the unique properties of ultrathin metasurface resonators can improve dramatically magnetic resonance imaging (MRI) [1]. We place a metasurface formed by an array of metallic wires inside a scanner under the studied object and achieve a substantial enhancement of the radiofrequency magnetic field by means of subwavelength near-field manipulation with metasurface, also allowing to improve scanner sensitivity, signal-to-noise ratio, and image resolution.

The detail study of the different eigenmodes of the metasurface and its impact on the signal-to-noise ratio enhancement will be discussed.

Our proposal bridges a gap between the fundamental ideas of metamaterials and applications spanning the research fields from electromagnetic engineering to medical diagnostics: we show how a metasurface can boost the functionality of the magnetic resonance imaging devices that are widely available in hospitals and directly demonstrate a dramatic imaging enhancement for a commercial magnetic resonance scanner and a biological tissue sample [1].

References

- [1] A. P. Slobozhanyuk, A. N. Poddubny, A. J. E. Raaijmakers, C. A. T. van den Berg, A. V. Kozachenko, I. A. Dubrovina, I. V. Melchakova, Yu. S. Kivshar, P. A. Belov, *Advanced Materials*, **28**, 1832–1838 (2016).

Ultrafast semiconductor metasurfaces: all-optical switching beyond free carriers

Shcherbakov, M.R., Vabishchevich, P.P., Shorokhov, A.S., Fedyanin, A.A.

Faculty of Physics, Lomonosov Moscow State University, 119991 Moscow, Russia

e-mail: shcherbakov@nanolab.phys.msu.ru

Chong, K.E., Choi, D.-Y., Staude, I., Miroshnichenko, A.E., Neshev, D.N., Kivshar, Yu.S.

Nonlinear Physics Centre and Laser Physics Centre, Research School of Physics and Engineering, The Australian National University, Canberra, ACT 0200, Australia

All-optical signal processing is one of the most important directions of photonics aimed toward fast optical communications and high-performance optical computing. In nanophotonics it has been suggested that strong optical field enhancement by means of spatial confinement effects can result in smaller mode sizes and larger modulation depths [1–3]. However, many of such structures suffer from low efficiency and losses, especially when metallic elements are used for the nanoscale light confinement. Recently, high-permittivity all-dielectric nanoparticles and nanostructures have emerged as a promising alternative to metallic structures for a wide range of nanophotonic applications. These nanoparticles utilize localized magnetic resonant Mie modes, which were observed experimentally in the entire visible spectral range [4, 5]. Nanostructures and metasurfaces fabricated of all-dielectric nanoparticles benefit from both very low intrinsic losses and localized Mie-type modes that make them favorable candidates for improving nonlinearities [6]. Despite the apparent prospects of utilizing all-dielectric Mie-resonant nanostructures for ultrafast all-optical switching, neither pump–probe nor self-action experiments have been reported.

In this paper we demonstrate experimentally ultrafast all-optical switching in subwavelength nonlinear dielectric nanostructures exhibiting localized magnetic Mie resonances. We employ amorphous silicon nanodisks to achieve strong self-modulation of femtosecond pulses with a depth of 60% at picojoule-per-disk pump energies. In the pump-probe measurements, we reveal that switching in the nanodisks can be governed by pulse-limited 65 fs-long two-photon absorption being enhanced by a factor of 80 with respect to the unstructured silicon film. We also show that undesirable free-carrier effects can be suppressed by a proper spectral positioning of the magnetic resonance, making such a structure the fastest all-optical switch operating at the nanoscale [7].

References

- [1] D. Mazurenko, et al., *Phys. Rev. Lett.*, **91**, 213903 (2003).
- [2] K. F. MacDonald, et al., *Nat. Photonics*, **3**, 55–58 (2009).
- [3] H. Thyrestrup, et al., *Appl. Phys. Lett.*, **105**, 111115 (2014).
- [4] A. B. Evlyukhin, et al., *Nano Lett.*, **12**, 3749–3755 (2012).
- [5] A. I. Kuznetsov, et al., *Sci. Rep.*, **2**, 492 (2012).
- [6] M. R. Shcherbakov, et al., *Nano Lett.* **12**, 6488–6492 (2014).
- [7] M. R. Shcherbakov, et al., *Nano Lett.* **15**, 6985–6990 (2015).

Canonical quantization of surface plasmon polaritons

Shishkov V. Yu.^{1,2,3}, Andrianov E.S.^{1,3}, Pukhov A.A.^{1,2,3}, Vinogradov A.P.^{1,2,3}

¹Moscow Institute of Physics and Technology, 9 Institutskiy per., 141700 Dolgoprudny, Moscow reg., Russia

²Institute for Theoretical and Applied Electromagnetics RAS, 13 Izhorskaya, Moscow 125412, Russia

³All-Russia Research Institute of Automatics, 22 Sushchevskaya, Moscow 127055, Russia

e-mail: vladislavmipt@gmail.com

The canonical quantization of plasmon polariton of sphere in vacuum is performed. The permittivity of the sphere is modeled by the Lorentz oscillators. It is shown that the quant of the near

electric field of the plasmon depends only on its permittivity, defined for the bulk Lorentz dielectric. The developed formalism in low loss limit gives the same quant of the near electric field of the plasmon as the phenomenological quantization, widely used before [1–3].

In the Columb gauge the medium oscillations are quantized with accounting the influence of the scalar potential. Independently the vector potential is quantized. These quantum systems interact because of the multiple moments of the sphere. The excitation of one of the quantum subsystems leads to the excitation of the second one. The fact is closely relates to the retardation of the electromagnetic field. Finally we replace the model permittivity with the one of real materials (gold and silver), so the quant of the near electric field of plasmon is calculated for those materials.

References

- [1] E. S. Andrianov, A. A. Pukhov, A. P. Vinogradov, A. V. Dorofeenko, A. A. Lisyansky, *Photonics and Nanostructures — Fundamentals and Applications*, **12**, 387 (2014).
- [2] F. Alpeggiani, L. Andreani, *Plasmonics*, **9**, 965 (2014).
- [3] A. Archambault, F. Marquier, J.-J. Greffet, C. Arnold, *Physical Review B*, **82**, 035411 (2010).

Third-harmonic generation spectroscopy of magnetic Fano resonances in oligomers of silicon nanoparticles

Shorokhov A.S., Melik-Gaykazyan E.V., Shcherbakov M.R., Fedyanin A.A.

Lomonosov Moscow State University, Moscow

e-mail: shorokhov@nanolab.phys.msu.ru

Smirnova D.A., Hopkins B., Chong K.E., Choi D.-Y., Miroshnichenko A.E., Neshev D.N., Kivshar Y.S.

The Australian National University, Canberra

The study of Fano resonances in nanophotonic structures has recently attracted a lot of attention due to many applications that can benefit from sharp spectral features and extreme field localization [1, 2]. In plasmonic systems optical Fano resonances have been observed through the interference of purely electric modes. However, the recent studies of Fano resonances in all-dielectric nanoparticle oligomers [3] revealed that subwavelength metamolecule oligomers consisting of closely spaced dielectric nanoparticles can support both electric and magnetic Fano resonances at optical frequencies. This has opened opportunities for studies of magnetic-type Fano resonances that can exhibit novel interesting optical properties [4]. It also has been shown that magnetic type optical resonances strongly enhance nonlinear optical response with respect to the electric-type resonances [5]. However, the optical nonlinearities originated from the all-dielectric nanostructures possessing magnetic Fano resonance have not been studied to date.

In this work we study both experimentally and numerically nonlinear optical response of oligomers of silicon nanoparticles in the vicinity of their magnetic Fano resonance. The proposed structure are fabricated by electron-beam lithography and reactive-ion etching techniques out of a hydrogenated amorphous silicon (a-Si:H) film on a SiO₂ substrate. The samples consist of arrays of symmetric clusters of four a-Si:H nanodisks with different sizes. Experimental results of the third-harmonic generation (THG) spectroscopy demonstrate the two-orders enhancement of the THG signal in the vicinity of the magnetic Fano resonance of such structures in comparison with the initial silicon thin film. We believe these results will pave a way to establishing novel platforms of nanoscale resonant nonlinear optical composite media driven by optically induced collective magnetic response of low-loss nanoparticles.

References

- [1] B. Luk'yanchuk, N. I. Zheludev, S. A. Maier, N. J. Halas, P. Nordlander, H. Giessen, C. T. Chong, The Fano resonance in plasmonic nanostructures and metamaterials, *Nature Materials*, **9**, 707–715 (2010).

- [2] A. E. Miroshnichenko, S. Flach, Yu. S. Kivshar, The Fano resonance in plasmonic nanostructures and metamaterials, *Rev. Mod. Phys.*, **82**, 2257–2298 (2010).
- [3] K. E. Chong, B. Hopkins, I. Staude, A. E. Miroshnichenko, J. Dominguez, M. Decker, D. N. Neshev, I. Brener, Y. S. Kivshar, Observation of Fano resonances in all-dielectric nanoparticle oligomers, *Small*, **10**, 1985–1990 (2014).
- [4] B. Hopkins, D. S. Filonov, A. E. Miroshnichenko, F. Monticone, A. Alu, Yu. S. Kivshar, Interplay of magnetic responses in all-dielectric oligomers to realize magnetic Fano resonances, *ACS Photonics*, **2**, 724–729 (2015).
- [5] M. R. Shcherbakov, D. N. Neshev, B. Hopkins, A. S. Shorokhov, I. Staude, E. V. Melik-Gaykazyan, M. Decker, A. A. Ezhov, A. E. Miroshnichenko, I. Brener, A. A. Fedyanin, Y. S. Kivshar, Enhanced third-harmonic generation in silicon nanoparticles driven by magnetic response, *Nano Lett.*, **14**, 6488–6492 (2014).

Magnetically induced transparency of superconducting qubits array

K.V. Shulga^{1,5,6}, M.V. Fistul^{2,1}, I. Besedin^{1,5}, S. Butz³, E. Il'ichev^{4,5}, A.V. Ustinov^{3,1,5}

¹National University of Science and Technology MISIS, 119049 Moscow, Russia

²Theoretische Physik III, Ruhr-Universität Bochum, D-44801 Bochum, Germany

³Physikalisches Institut, Karlsruhe Institute of Technology, D-76131, Karlsruhe, Germany

⁴Institute of Photonic Technology, PO Box 100239, D-07702 Jena, Germany

⁵Russian Quantum Center, 143025 Moscow region, Russia

⁶Moscow Institute of Physics and Technology, Dolgoprudny, 141700 Moscow region, Russia

e-mail: ustinov@kit.edu

The coherent quantum phenomena are expected to govern the electrodynamics of a quantum metamaterial, e. g., an artificially fabricated medium composed of two-level systems acting as artificial atoms. The electromagnetic wave propagation through such a medium is accompanied by excitation of intrinsic quantum transitions within individual meta-atoms and modes corresponding to the interactions between them.

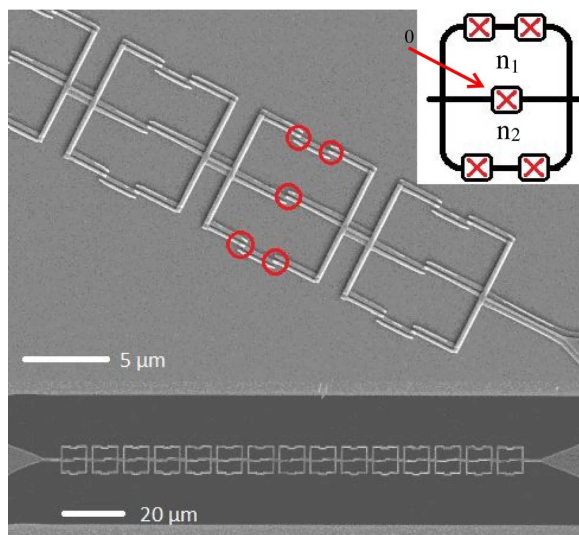


Fig. 1: The superconducting metamaterial containing an array of 15 mirror-type flux qubits embedded in the transmission line. The enlarged SEM image of a few qubits (above) and the SEM image of a whole superconducting metamaterial (below) are presented. The insert shows the schematic of a single qubit, which is composed of two superconductive loops with one common central Josephson junction and four identical Josephson junctions located on the outer sides of the loops (marked in red).

We experimentally and theoretically explore the propagation of electromagnetic waves through a superconducting quantum metamaterial in a strong coupling limit. Meta-atoms that we employ are two-cell superconducting flux qubits featuring tunneling between mirror-symmetric fluxoidal states. In a broad frequency range, the microwave transmission coefficient S_{21} periodically depends on the external dc magnetic flux Φ applied through the qubit loop and is suppressed by more than 15 dB at $\Phi \simeq \Phi_0/2$, where Φ_0 is the magnetic flux quantum. Simultaneously, in a narrower frequency range, we observe a large resonant enhancement of the transmission up to about 10 dB above zero flux level. These strong variations of the metamaterial transparency are explained by magnetic flux localization and tunneling between metastable states in the mirror-type flux qubits forming the metamaterial. Our theoretical analysis taking into account two-level quantum dynamics of meta-atoms is in good accord with experimental observations. We anticipate possible applications of the observed transparency tunability by dc magnetic field in superconducting quantum circuits.

Electromagnetic characterization of $p - m$ metasurfaces

Simovski C.R.^{1,2}, Albooyeh M.¹, Tretyakov S.A.¹

¹Aalto University, School of Electrical Engineering, FI00076, Finland

²ITMO University, Kronverkski 47, St. Petersburg, Russia

e-mail: konstantin.simovski@aalto.fi

In this work, we present a general methodology for electromagnetic homogenization and characterization of bianisotropic metasurfaces formed by regular or random arrangements of small arbitrary-shaped particles located at the interface of two different isotropic media. Particles can be fully emerged in the top medium, e.g. free space, or partially and even completely submerged into the substrate. Moreover, they can be placed in a special host layer. The array in what concerns the arrangement of particles can be either regular or random, even amorphous. The only approximation beyond the optical density of the array is the assumption that higher multipole moments except electric (\mathbf{p}) and magnetic (\mathbf{m}) moments are absent in the polarization response of these particles to the external plane-wave excitation. These dipole moments can be related to both electric and magnetic local fields, i.e. the case of bianisotropy is covered by our model. Both substrate-induced bianisotropy, inherent to plasmonic arrays [1], and intrinsic bianisotropy of particles, inherent to Ω or chiral particles are covered by this new model.

In our interpretation, a $p - m$ metasurface can be electromagnetically homogenized via the averaging of the fields and polarizations over each unit cell. It is possible even if the unit cell area is a stochastic parameter under the assumption that the maximal cell sizes are sufficiently small compared to the operational wavelength. At the same time, the whole metasurface array is assumed to be extended enough, so that the characteristic parameters do not depend on the transversal sizes of the array. We also assume that the particles of the array are identical and differ only in their arrangement including the inter-particle distance and orientations. The incident plane waves can illuminate this array from top or bottom sides. The approach unites and generalizes the earlier theories of such arrays developed independently by two joint research groups: that of profs. Holloway and Kuester and that of profs. Simovski and Tretyakov. The main generalization is the account of the substrate whose presence may dramatically change the overall response of the metasurface in both transmission and reflection. We analyze the features of both involved formalisms and discuss their peculiarities in several example cases. Our theory can be used in the analysis and synthesis of a wide spectrum of metasurfaces operating at different frequencies from microwaves to visible range.

We have re-derived the boundary conditions for such a metasurface and have shown that they are equivalent to so-called GSTC by Holloway and Kuester [2]. We have demonstrated how the electric and magnetic macroscopic fields on both sides of the plane $z = 0$ are related to each other through the surface polarizations. The equivalence of the description in terms of collective polarizabilities (Simovski and Tretyakov) with the description in terms of surface susceptibilities (Holloway and

Kuester) is proved. Moreover, we have finalized the circuit model, started by [3]. In this model the arbitrary $p - m$ metasurface is described via the impedance matrix. In the present work, we have resolved the problem with the normal component of Holloway and Kuester’s electric surface susceptibilities which seemingly makes their model not equivalent to the impedance matrix model (involving only tangential electromagnetic fields and polarizations). The normal component of the metasurface electric susceptibility can be expressed through elements of the impedance matrix as well. This is so, because normal components of the electric and magnetic fields are uniquely related to the tangential components. Finally, we have presented the reflection and transmission dyadic coefficients in terms of either effective surface susceptibilities or collective polarizabilities.

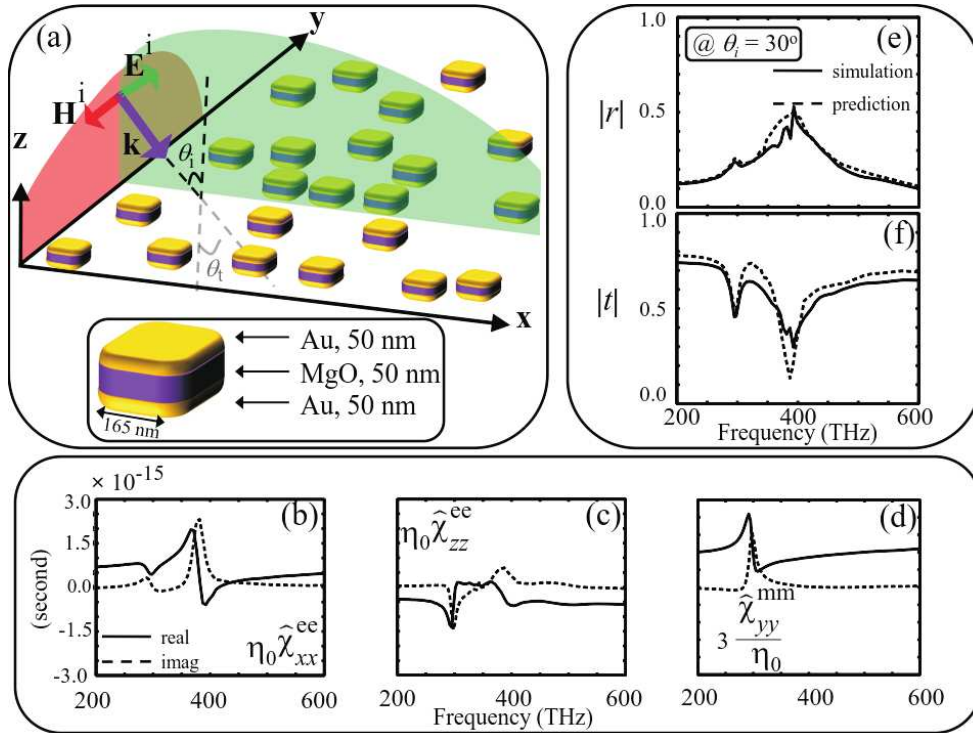


Fig. 1: (a) A planar disordered array of gold plasmonic coupled nano-patches located at the xy -plane on top of a fused silica substrate with the refractive index of $n = 1.5$. The patches are separated by a dielectric spacer of MgO with the refractive index of $n = 1.72$. The array is excited by a TM-polarized electromagnetic plane wave. (b) Tangential electric (c) Normal electric and (d) Tangential magnetic effective susceptibility components of the metasurface retrieved from the reflection and transmission data at $\theta_i = 0$ and 45° from numerical FDTD (Finite Difference Time Domain) method. (e) Predicted and simulated results for the amplitude of the reflection coefficient of the proposed metasurface for an incidence of $\theta_i = 30^\circ$. (f) The same plot as in (e) for the amplitude of the transmission coefficient. The average unit cell size of the array is 510 nm.

Two types of plasmonic metasurfaces — a random one formed by gold nano-patches (see Fig. 1) and a regular array of so-called split-ring resonators, both operating at frequencies of the visible light, are studied as examples of the applicability of our methodology – our approximate theory is confirmed by full-wave simulations.

To conclude this summary: We believe that the developed general homogenization framework can be successfully used in modeling and design of metasurfaces for various applications in different frequency ranges.

References

[1] M. Albooyeh, C. R. Simovski, *J. Opt.*, **13**, pp. 105102, 1–10 (2011).

- [2] C. L. Holloway, E. F. Kuester, J. A. Gordon, J. O'Hara, J. Booth, D. R. Smith, *IEEE Antennas Propag. Mag.*, **54**(2), pp. 10–35 (2012).
- [3] M. Albooyeh, R. Alaei, C. Rockstuhl, C. R. Simovski, *Phys. Rev. B*, **91**(19), pp. 195304, 1–11 (2015).

Light scattering and localization by silicon nanoparticle on metal

Sinev I.S.¹, Iorsh I.V.¹, Bogdanov A.A.¹, Permyakov D.V.¹, Komissarenko F.E.¹, Mukhin I.S.^{1,2}, Samusev A.K.¹, Miroschnichenko A.E.³, Kivshar Y.S.^{1,3}

¹ITMO University, 197101 St. Petersburg, Russia

²St. Petersburg Academic University, 194021 St. Petersburg, Russia

³Australian National University, Canberra ACT 0200, Australia

e-mail: i.sinev@metalab.ifmo.ru

High refractive index dielectric nanoparticles are attracting significant attention due to their unique properties that stem from the presence of both magnetic and electric dipole responses in the visible spectral range [1, 2]. The interplay of these resonances in combination with inherently low level of losses has already inspired all-dielectric-based solutions for superdirective nanoantennas, sensors, metasurfaces for efficient wavefront control and beam shaping, metadevices granting giant enhancement of non-linear effects, etc. Still, high radiative losses limit the maximum Q-factor of the low-order resonances of dielectric nanoparticles. This forces to use higher order modes for applications requiring field enhancement, which means the increase of the resonator size. Therefore, an efficient way to control the quality-factor of the dipole resonances of high-index nanoparticles could open new possibilities for integration of dielectric nanoparticles in nanophotonic devices.

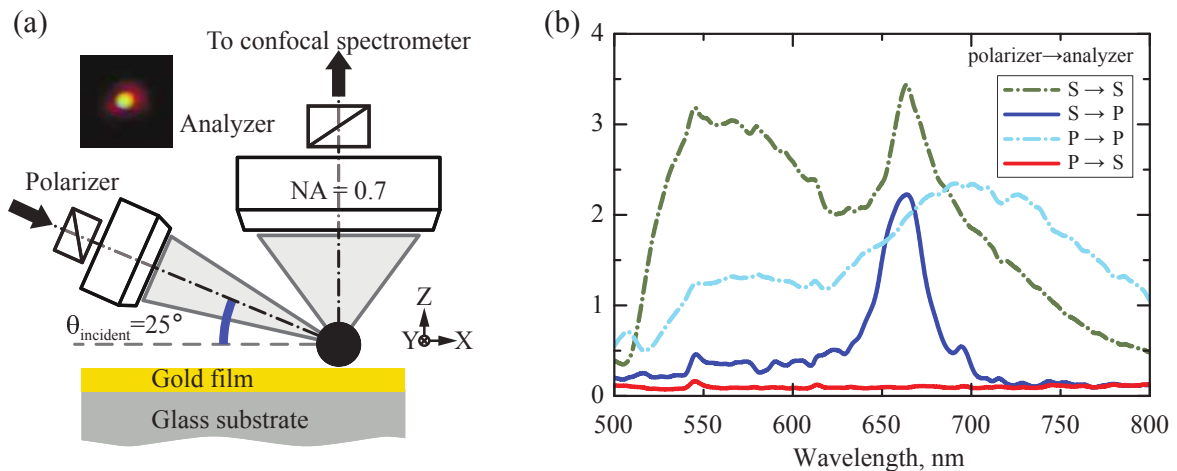


Fig. 1: (a) Experimental setup for the polarization-resolved dark-field spectroscopy. The sample is excited by polarized white light from its side at oblique incidence. (b) Experimental spectra for a 170 nm silicon sphere deposited on 40 nm gold film on glass substrate. Different curves correspond to different combinations of polarizer and analyzer orientations.

In this work, we discover remarkable modifications of *normal* (perpendicular to the substrate surface) magnetic and electric dipole responses of a silicon nanosphere driven by gold substrate. We study the scattering properties of a 170 nm silicon nanoparticle deposited onto a 40 nm gold film using a polarization-resolved dark-field microscope with independent excitation (side) and collection (upper) optical channels [3], Fig. 1a. Importantly, by introducing a linear polarizer in the collection channel (see Fig. 1a), we perform selective detection the scattering signal from the induced normal dipole components. The experimental results are presented in Fig. 1b, which shows the dark-field scattering spectra for all four combinations of the orientations of polarizer and analyzer. These spectra reveal both drastic substrate-driven modification of the quality factor of normal magnetic

dipole response (solid blue line in Fig. 1b) and reduction of the radiation losses of normal electric dipole mode (light blue dashed line in Fig. 1b). We find the measured spectra to be in excellent agreement with the analytical results obtained via the Green's function approach [4] and the data from full-wave numerical simulations. The latter also reveals strong field enhancement associated with both normal magnetic and normal electric dipole modes, which can be utilized for enhanced sensing and augmentation of nonlinear processes.

Acknowledgements. Analytical modelling, numerical simulations, nanoparticle transfer and dark-field spectroscopy measurements carried out at ITMO University were supported by the Russian Science Foundation (Grant #15-12-20028). The authors at ANU were supported by the Australian Research Council. We thank V. Valuckas for the fabrication of nanospheres. We are grateful to Andrey B. Evlyukhin, Alexander E. Krasnok and Arseniy I. Kuznetsov for fruitful discussions and comments.

References

- [1] A. B. Evlyukhin, et al., *Nano Letters*, **12**, 3749 (2012).
- [2] A. I. Kuznetsov, et al., *Scientific Reports*, **2**, 492 (2012).
- [3] D. Permyakov, et al., *Applied Physics Letters*, **106**, 171110 (2015).
- [4] A. E. Miroshnichenko, et al., *ACS Photonics*, **2**, 1423 (2015).

Rotation method for the reconstruction of anisotropic electromagnetic characteristics of metamaterials

Smirnov Yu.G., Derevyanchuk E.D.

Department of Mathematics and Supercomputer Modeling, Penza State University, 40, Krasnaya street, Penza, Russia

e-mails: smirnovyug@mail.ru, katyader11@yandex.ru

In the last few decades a lot of different artificial materials were produced, such as composite, metamaterials and others. As a rule, the effective electromagnetic characteristics of artificial materials cannot be measured. Therefore, to solve this problem numerical-analytical methods have been developed.

This work is devoted to the rotation method for the reconstruction of metamaterial electromagnetic characteristics in microwave band. The technique of the method consists in diaphragm rotation with regard to the rectangular waveguide. Using this approach and numerical-analytical method presented in earlier papers [1, 2], we reconstruct permittivity and permeability of diagonal tensors.

Numerical results are presented for the case of metamaterials.

The obtained solution can be applied in metamaterials research.

References

- [1] Yu. G. Smirnov, Yu. V. Shestopalov, E. D. Derevyanchuk, Permittivity reconstruction of layered dielectrics in a rectangular waveguide from the transmission coefficient at different frequencies, *Inverse Problems and Large-Scale Computations, Series: Springer Proceedings in Mathematics and Statistics*, Vol. **52**, No. 12, 169–181, 2013.
- [2] Yu. G. Smirnov, Yu. V. Shestopalov, E. D. Derevyanchuk, Solution to the inverse problem of reconstructing permittivity of an n-sectional diaphragm in a rectangular waveguide, *Algebra, Geometry and Mathematical Physics, Springer Proceedings in Mathematics and Statistics*, Vol. **85**, Ser. 10533-2014, 555–567, 2014.

Numerical analysis of 2D approximate cloaking problem with using M layered shell

Spivak Yu.E.

Far Eastern Federal University, D(20), pen. Ayaks, i. Russky, Vladivostok, 690922, Russia
e-mail: u3l3i3y3a3@mail.ru

Recently, invisibility and cloaking are extensively discussed in scientific community, this fact is confirmed by number of publications about mentioned subject (see, e. g., [1, 2]). Transformation optics method is the most known cloaking method [2]. In fact, this is the mathematical method that enables to design suitable material structures (metamaterials) that when placed around the object may drastically suppress its scattering. We note that solutions obtained with the help of this method possess a drawback: components of the permittivity and permeability tensors (ε, μ) always have singularities at the inner boundary. This complicates technical realization of obtained solutions. In order to overcome this drawback we study the scattering properties of cloaked cylinder as in [3] with the help of a combination of approximate cloaking together with discretizing by $2M$ layers the cloaking shell using pairs of homogeneous isotropic sub-layers. The special parameter δ is introduced which describes the degree of approximation of exact cloaking problem by an approximate one. This discretization reduces the level of scattering as the number of layers increases. Each anisotropic layer can be replaced by a pair of equivalent homogeneous isotropic sub-layers A and B which have parameters ε_A and ε_B related to original permittivities.

The solution of the corresponding cloaking problem under study is obtained by solving the 2D Helmholtz equation using cylindrical functions expansion. The coefficients of these expansions are determined by solving system of $4M + 3$ linear algebraic equations with ill-conditioned matrix A . Here M is a number of layers. It is found that the determinant of matrix A is not zero for each value of $\delta > 0$, but the condition number of A sharply increases when δ is decreasing. A numerical algorithm for solving the approximate cloaking problem is developed, which is based on using the singular value decomposition of matrix A . The properties of this algorithm are studied and the results of numerical experiments are discussed. It is shown, in particular, that the scattering from the cloaked cylinder decreases when a number M of layers increases or the parameter δ decreases. We also note that there is an alternative approach that consists of using optimization method for finding solutions of approximate cloaking problems [4, 5]. Based on optimization method we develop an efficient numerical algorithm of solving cloaking problems and discuss results of numerical experiments.

This work is supported by the Russian Foundation for Basic Research (project no 16-01-00365-a).

References

- [1] L. S. Dolin, *Izvestiya Vuzov. Radiofizika*, **4**, 964–967 (1961).
- [2] J. B. Pendry, D. Shurig, D. R. Smith, *Science*, **312**, 1780–1782 (2006).
- [3] H. Zamel, E. El-Diwany, H. El-Hennawy, *J. of El. Syst. and Inf. Technology*, **1**, 82–93 (2014).
- [4] G. V. Alekseev, *Dokl. Phys*, **58**, 147–151 (2013).
- [5] Z. Yu., Y. J. Feng, X. F. Xu, J. M. Zhao, T. Jiang, *J. Phys. D: Appl. Phys.*, **44**, 185102 (2011).

Application of the matrix homogenization method to the Maxwell equations

Ivan A. Starkov

Nanotechnology Center, St. Petersburg Academic University, Russian Academy of Sciences,
Khlopin st. 8/3, St. Petersburg, Russia, 194021

e-mail: starkov@spbau.ru

Alexander S. Starkov

National Research University of Information Technologies, Mechanics and Optics, Kronverksky pr. 49,
St. Petersburg, Russia, 197101

e-mail: ferroelectrics@ya.ru

The paper presents an illustrative application of the matrix homogenization [1] method to estimate the effective parameters of layered structures. The model effectiveness is demonstrated for the Maxwell equations by means of the comparison of the analytical solution and simulated data. For this purpose, CST Microwave Studio, a full wave electromagnetic simulator [2], has been employed. The considered method can be rigorously justified in contrast to the existing models. Moreover, the homogenization procedure is extremely simple and just matrix operations are involved, but is only possible for equations of the special form. In other words, the main computational effort of the used method is to reduce the problem to the required form. Finally, the developed approach can be easily extended on block and cylindrical structures.

The reported study was funded by RFBR, according to the research project No. 16-32-60189 mol_a_dk.

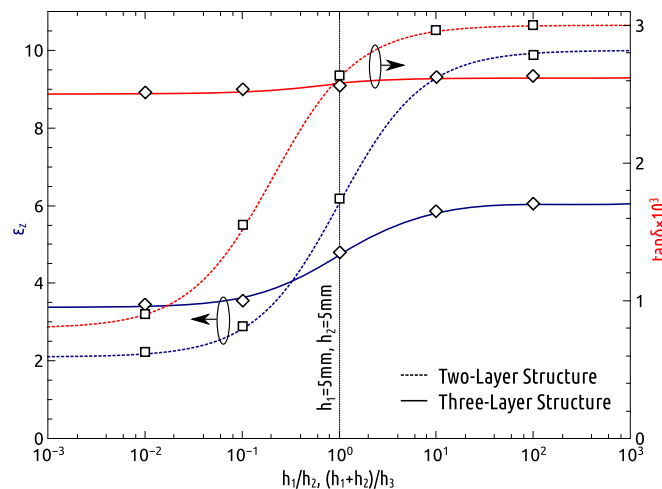


Fig. 1: The dependence of the effective relative dielectric permittivity and electric loss tangent of the two- and three-layer systems on the ratio of the layer thicknesses. Lines: analytical calculations. Symbols: CST Microwave Studio simulations.

References

- [1] A. S. Starkov, I. A. Starkov, *J. Exp. Theor. Phys.*, **119**, 861–869 (2014).
- [2] *CST Microwave Studio Users Guide*. Available at www.cst.com.

Emission of cyanine dye embedded in nanopores of anodic alumina matrix

A. A. Starovoytov¹, T. A. Vartanyan¹, V. I. Belotitskii², Yu. A. Kumzerov², A. A. Sysoeva², N. O. Alexeeva³, V. G. Solovyev³

¹Laboratory of Surface Photophysics, ITMO University, St. Petersburg, Russia

²Laboratory of Physics of Anisotropic Materials, Ioffe Institute, St. Petersburg, Russia

³Department of Physics, Faculty of Physics and Mathematics, Pskov State University, Lenin Square 2, Pskov 180000, Russia

e-mail: anton.starovoytov@gmail.com

The composite system and metamaterials based on an organic dye that embedded in a solid matrix has attracted wide interest because of its useful applications, such as light concentrators in solar cells, optical waveguides, lasers, sensors and nonlinear optical components.

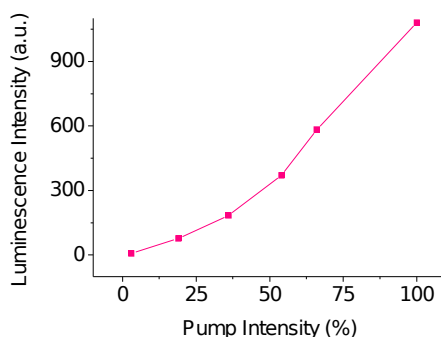
The absorption and the luminescence of cyanine dye embedded in a regular arrangement of cylindrical nanopores in Al_2O_3 (por Al_2O_3) that form a two-dimensional nanopore system were studied.

Self-assembled porous alumina structures (por Al_2O_3) have been prepared by two-step anodization. The cyanine dye was embedded in nanopores of host matrix by dipping por Al_2O_3 in dye solution in ethanol.

Since the samples are opaque, the reflectance spectra of pure por Al_2O_3 and por Al_2O_3 with dye were compared, and the absorption spectrum of the dye embedded in pore was determined. The absorption and fluorescence spectra of dye in por Al_2O_3 and solution have the similar shapes, but the spectral shape of dye in por Al_2O_3 is broadened and the maximum has bathochromic shift of 4 nm. So we conclude that organic molecules in pore are well-isolated as monomer and free from aggregation.

We investigated the fluorescence decay lifetime of dye molecules in por Al_2O_3 and solution. For asbestos samples the lifetime is longer due to the decrease of the nonradiative decay process. The main pathway of this process for cyanine is photostereoisomerization, which is hindered in pores.

Stimulated emission of the cyanine in the por Al_2O_3 was obtained in the long-wavelength band of the fluorescence spectrum. Dependence of the luminescence intensity of the sample versus the pump energy density of stimulated emission was obtained (see figure). The narrowing of the emission band with increasing of excitation intensity indicates the prevalence of stimulated emission over the spontaneous emission, and reveals that the system passes into generation mode.



Luminescence intensity of the sample versus the pump intensity. Pump energy is 3 mJ, the wavelength is 520 nm.

These results demonstrate the potential use of the por Al_2O_3 activated by cyanine dye for developing of active elements of quantum electronics.

The financial support from EU project “LIMACONA” (IRSES-GA-2013-612600) and state contract no. 2014/190, project 2350 are acknowledged.

Opto-mechanical interactions in silicon nanoparticles

Yue Sun, Andrey E. Miroschnichenko, Andrey A. Sukhorukov

Nonlinear Physics Centre, Research School of Physics and Engineering, Australian National University, Acton, ACT 2601

e-mail: yue.s@anu.edu.au

We demonstrate that strong opto-mechanical interactions appear in silicon nanoparticles in the vicinity of magnetic dipolar resonance driven by radiation pressure and electrostriction. Simulations show that both acoustic monopolar and quadrupolar modes strongly interact with magnetic dipolar resonance and the interference between electric and magnetic dipoles enhances the detection sensitivity of such interaction when monitoring either forward or backward scattering.

A single dielectric nanoparticle supports both electric (ED) and magnetic (MD) dipolar resonances [1–4]. In the vicinity of magnetic dipole resonance, optical field is concentrated inside the particle [2, 3], approaches the ideal absorption limit [5] and can drive mechanical vibrations by scattering and electrostrictive forces. Moreover, the interference and its resulting directionality provide the possibility of additional enhancement to the opto-mechanical (OM) interaction and its detection sensitivity. In this work, we predict a potential for highly efficient OM interactions in silicon nanospheres.

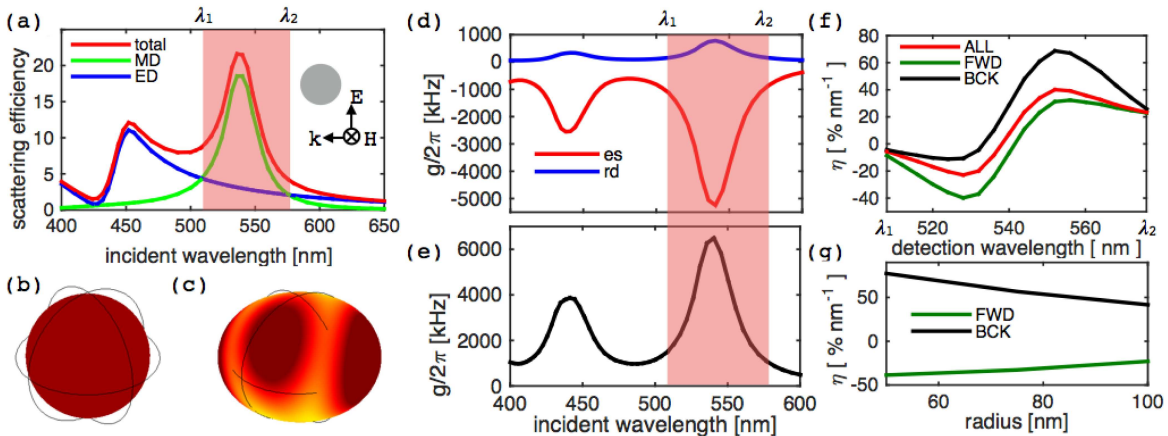


Fig. 1: (a) Optical scattering efficiency spectrum with mode decomposition. Total deformation of (b) Monopolar and (c) quadrupolar vibrations in contrast to the original boundary (black curves). (d) OM coupling rate $g/2\pi$ to monopolar vibration contributed by radiation pressure (blue curve) and electrostriction (red curve). (e) Total OM coupling rate to quadrupolar vibrations. (f) Detection sensitivity η of monopolar vibration by monitoring scattering in forward (green), backward (black) and all (red) directions. (g) Maximum detection sensitivity as a function of the radius of silicon spheres.

The multiple decomposition of total scattering for a silicon sphere of radius $r = 63$ nm, shown in Fig. 1(a), indicates the ED and MD interfere destructively at λ_1 and constructively at λ_2 , respectively. Between these two extremes, the optical field strongly interacts with acoustic monopolar and quadrupolar modes whose deformations are shown in Figs. 1(b) and (c), respectively. Fig. 1(d) shows that the OM coupling rate to the monopolar vibration has contributions from radiation pressure and electrostriction both of which peak at MD resonant wavelength. Fig. 1(e) shows that the optical MD resonance can efficiently excite the quadrupolar vibration. Such vibrations can be detected through backward scattering, with the maximum sensitivity around $70\% \cdot \text{nm}^{-1}$ as shown in Fig. 1(f), exceeding the effect on forward scattering as shown in Fig. 1(g).

Our results show strong OM interaction in silicon spheres through radiation pressure and electrostriction, paving the path to study OM interactions in more sophisticatedly nanostructured dielectric metamaterials which allow finer control of light in the near field and thus stronger coupling between optical and mechanical modes.

References

- [1] J. C. Ginn, et al, Realizing optical magnetism from dielectric metamaterials, *Phys. Rev. Lett.*, **108**, 097402 (2012).
- [2] P. Spinelli, et al, Broadband omnidirectional antireflection coating based on subwavelength surface Mie resonators, *Nat. Commun.*, **3**, 692 (2012).
- [3] A. B. Evlyukhin, et al, Demonstration of magnetic dipole resonances of dielectric nanospheres in the visible region, *Nano Lett.*, **12**, 3749 (2012).
- [4] Y. H. Fu, et al, Directional visible light scattering by silicon nanoparticles, *Nat. Commun.*, **4**, 1527 (2013).
- [5] V. Grigoriev, et al, Optimizing nanoparticle designs for ideal absorption of light, *ACS Photonics*, **2**, 263 (2015).

Magneto-optical nonreciprocity of the waveguide modes of photonic crystals in transverse magnetic field

Sylgacheva D.A.^{1,2}, Khokhlov N.E.^{1,2}, Kalish A.N.^{1,2}, Belotelov V.I.^{1,2}, Dagesyan S.A.¹, Shaposhnikov A.N.³, Berzhansky V.N.³

¹Faculty of Physics, M. V. Lomonosov Moscow State University, Leninskie gori 1, bld. 2, Moscow 119991, Russia

²Russian Quantum Center, Skolkovo, Moscow Region 143025, Russia

³Faculty of Physics, V. I. Vernadsky Crimean Federal University, Simferopol 95007, Russia

e-mail: sylgacheva.darjja@physics.msu.ru

We represent theoretical and experimental study of the waveguide modes of one-dimensional magneto-photonic crystals magnetized in layers plane. It is shown the propagation constants of TM waveguide modes are sensitive to the transverse magnetization reversal and, as a consequence, magneto-optical Kerr effect has resonant features at the modes frequencies. Comparison of the effect in the nonmagnetic photonic crystal with additional magnetic layer on top and a magneto-photonic crystal with altering magnetic layers shows the effect is greater for the first case due to the higher asymmetry of the claddings of the magnetic layer. Experimental observations show resonant features at optical and magneto-optical spectra for considered types of magneto-photonic crystals. Experimental angular dispersions of the resonances are in good agreement with the theoretical ones

The work is supported by RFBR (projects No. 14-02-01012, 16-02-01065) and the Russian Presidential Grant (project No. MD-5763.2015.2).

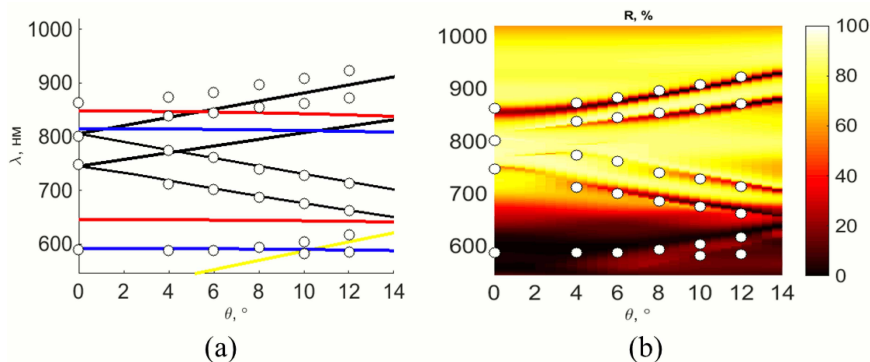


Fig. 1: (a) Colored lines represent the dispersions of waveguided modes calculated from transfer matrix approach taking into account the magnetization of the layers, (b) contour plot of the reflection of photonic crystal via wavelength and angle of incidence at the TM-polarization obtained with Rigorous Coupled Wave Analysis (RCWA) numerical method. Circles point out the positions of the experimental resonances.

References

- [1] P. Yeh, A. Yariv, *J. Opt. Soc. Amer.*, **67**(4), 423–438 (1977).
- [2] V. N. Berzhansky, *et al.*, *Solid State Phenom.*, **200**(233), 233–238 (2013).
- [3] N. E. Khokhlov, *et al.*, *J. Phys. D: Appl. Phys.*, **48**, 095001 (2015).
- [4] D. A. Sylgacheva, *et al.*, *Optics Lett.*, submitted.

**Induced transmission and enhanced Faraday rotation
in ferromagnetic thin films**

Treviño C.¹, Kononchuk R.¹, Smith K.¹, Vitebskiy I.², Chabanov A.A.¹

¹University of Texas at San Antonio, One UTSA Circle, San Antonio, TX 78249, USA

²Air Force Research Laboratory, Sensors Directorate, Wright Patterson AFB, OH 45433, USA

e-mails: christianantrevino@hotmail.com, rdnbox@gmail.com, ksmith1281@gmail.com,
ilya.vitebskiy@us.af.mil, andrey.chabanov@utsa.edu

Metals like iron or cobalt, despite being powerful magnets, are not commonly used in nonreciprocal photonic devices such as optical isolators and circulators. The reason for this is that, due to strong electric conductivity, a film made of a metallic ferromagnet is either too thick to transmit light or too thin to produce any measurable Faraday rotation. Here we demonstrate experimentally that placing of a ferromagnetic metal nanolayer in a resonant cavity can result in the phenomenon of nearly perfect induced transparency accompanied by strong resonant enhancement of Faraday rotation. In our experiment, a 150-nm thick CoFe film placed in a resonant cavity produced a 45-degree Faraday rotation with nearly 100% transmission at frequency of 9.3 GHz. This is the first known observation of such an effect in metallic ferromagnets. Similar effect can be realized at different frequencies starting from microwave and up to the far infrared.

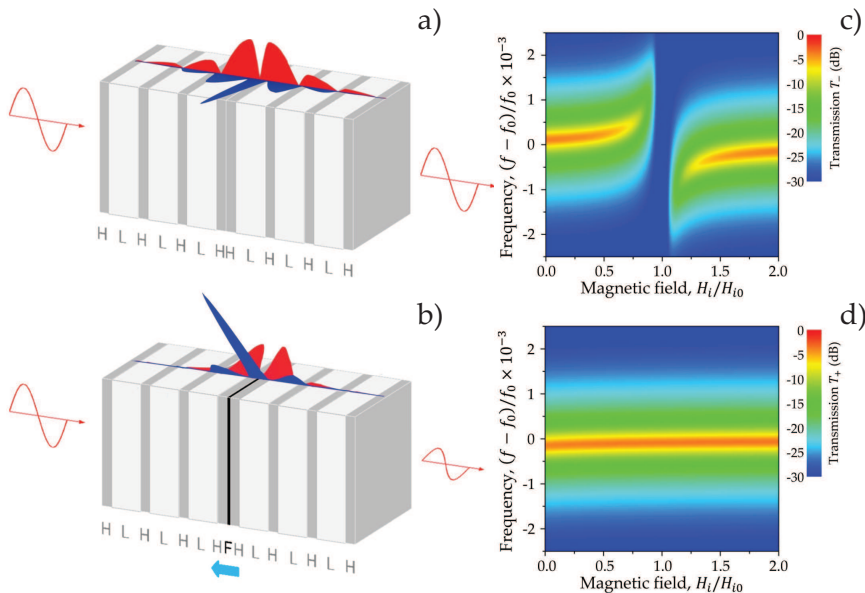


Fig. 1: Faraday rotation enhancement scheme [1]. (a) Bragg resonator $(HL)^3HH(LH)^3$ of high (H) and low (L) refractive index dielectric layers, incident and transmitted waves, and spatial distributions of the electric (red) and magnetic (blue) fields at a resonance frequency f_0 . (b) Placing a ferromagnetic metal layer F in the resonator at the position of a node (antinode) of the electric (magnetic) field suppresses ohmic losses and enhances magnetic Faraday rotation in the F layer. The Faraday rotation enhancement is determined by the applied magnetic field (blue arrow) and the cavity Q -factor. (c) & (d) Left-handed and right-handed wave transmission, T_- and T_+ , as a function of wave frequency f and internal magnetic field H_i .

References

- [1] K. Smith, T. Carroll, J. D. Bodyfelt, I. Vitebskiy, A. A. Chabanov, *Journal of Physics D: Applied Physics*, **46**, 165002 (2013).

Light scattering by particles with high refractive index

Tribelsky M.I.

Lomonosov Moscow State University, Moscow, 119991, Russia;
 Moscow Technological University MIREA, Moscow 119454, Russia
 e-mail: tribelsky@mirea.ru

Miroshnichenko A.E.

Nonlinear Physics Centre, Australian National University, Acton, ACT 2601, Australia
 e-mail: andrey.miroshnichenko@anu.edu.au

Light scattering by high refractive index (HRI) sphere is studied in detail based upon the exact Mie solution. It is shown, that the process is characterized by sharp, high-Q resonances affecting both the scattered field outside the particle and the one within it. However, the manifestation of the resonances in the former and later cases is quite different. For the scattered field outside the particle each partial mode exhibits an infinite cascade of the Fano resonances [1], see also [2]. Regarding the field within the particle, in contrast to the common believe that for a HRI particle this field is weak, it is shown that the resonances may give rise to a giant concentration of the electromagnetic field within the particle [1]. Examples of this concentration for a sphere of GaP is presented in Fig. 1.

The obtained results are readily generalized to the case of a HRI cylinder and other exactly solvable cases. Qualitatively they remain valid for a HRI scatterer of any shape. These features of the light scattering problem provide physical grounds for numerous applications, especially those related to the design and engineering of high nonlinear heterogeneous nanostructures and cloaking metamaterials

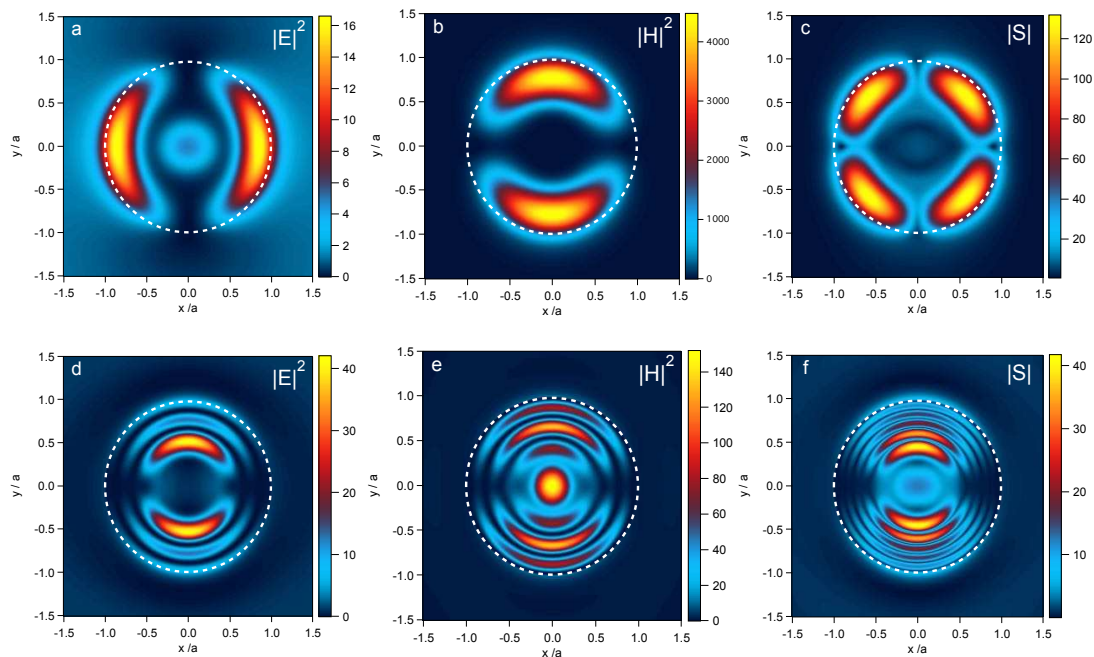


Fig. 1: Distribution of the electromagnetic field and the Poynting vector $|S|$ in plane $z = 0$ within a GaP sphere with radius R irradiated in a vacuum by a plane linearly polarized electromagnetic wave with $\lambda = 532$ nm. Calculations according to the exact Mie solution. The wave propagates along z -axis with vector \mathbf{E} directed along x -axis. The fields are normalized over the amplitude of the electric field of the incident wave. The boundary of the sphere is shown as white dashed line. The size parameter $2\pi R/\lambda$ for panels a–c equals 2.318, for d–f it is 5.380.

References

- [1] M. I. Tribelsky, A. E. Miroshnichenko, ArXiv:1511.02931v1 [physics.optics]; *Phys. Rev. A*, in press.
- [2] M. V. Rybin, et al, *Optics Express*, **21**, 30107 (2013); *Sci. Rep.*, **5**, 8774 (2015).

Two-mode loop antenna with doubled gain

Pavel Turalchuk¹, Irina Munina¹, Vladimir Yashenko¹, Orest Vendik²

¹Department of Microelectronics and Radio Engineering, St. Petersburg Electrotechnical University, St. Petersburg, Russia

²Department of Electronics, St. Petersburg Electrotechnical University, St. Petersburg, Russia
e-mails: pavel.turalchuk@mwlab.spb.ru, ogvendik@rambler.ru

In this paper an original design of a low-profile loop antenna with increased directivity is proposed. Odd- and even-mode currents excitation in the loop allows providing two times higher gain than the gain of a single loop or dipole. The special design of a power dividing network in order to excite odd- and even-mode currents with the amplitude equality and 90° phase difference between modes is suggested. The antenna designed as planar thin-film structure is intended for radio frequency identification systems application.

Radio frequency identification (RFID) systems are of great practical interest for various applications: industry, trade, transport service, biological and medical practice [1]. A typical back-scattered RFID system consists of a base station (also called reader) with a transmitting/receiving antenna and a transponder (also called tag or label), which is placed on the object to be identified. The reader transmits a modulated RF signal to the tag consisting of an antenna and an integrated circuit chip (RFIC) connected directly with antenna terminals. Tag responds by varying RFIC input impedance and thus modulating the backscattered signal. The most of commercially available passive RFID tags for ultra-high frequency (UHF, 860–960 MHz) and microwave (2.4 GHz and 5.8 GHz) applications are long-range systems which use electromagnetic waves propagating between reader and tag antennas [2].

Typically loop antennas are used to link with the implanted wireless sensors [3], tags immersed inside the liquids [4], and etc. In this case magnetic coupling between the tag loop and the reader loop in near field is preferable due to minimization of the effect of the dielectric properties of the dielectric medium.

At the same time, the loop could be successfully used as the reader antenna in order to interrogate conventional tags in the far-field zone. Thus the antenna with improved gain to maximize the tag read range is of interest. For this purpose, a combination of dipole and loop allows providing cardioid radiation pattern in the far-field region with zero radiation in the direction opposite to the main lobe radiation [5]. The gain of such an antenna is two times higher than the gain of a single loop or dipole. In this paper we present a novel doubled-gain antenna design consisting of the only planar loop with two-mode excitation. In order to excite odd- and even-mode currents along the loop wires a power dividing network design is proposed.

The reader antenna for UHF RFID applications were designed as a thin film planar structure on a dielectric substrate. As a result of modeling of the suggested antenna the cardioid (hemispherical) radiation pattern with gain 5.5 dB have been achieved.

Generation of photon pairs through spontaneous four-wave mixing in nonlinear waveguides with the account of losses

Vavulin D.N.

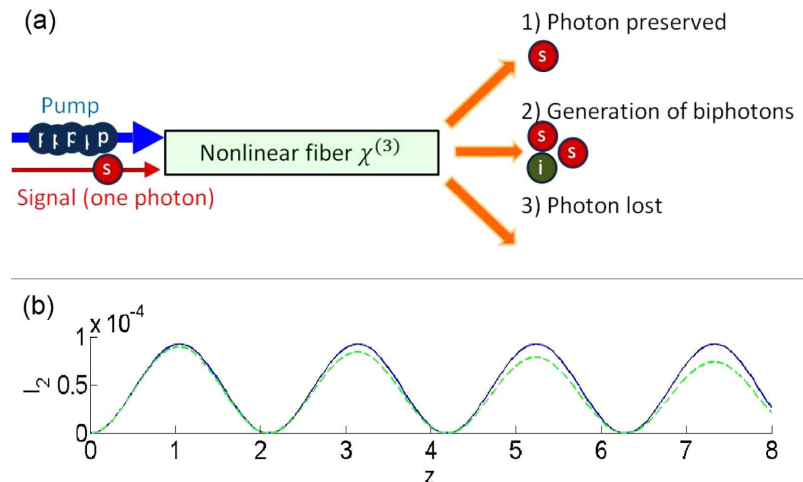
ITMO University, 49 Kronverksky Ave., St.Petersburg, 197101, Russia
e-mail: dima-vavulin@mail.ru

Sukhorukov A.A.

Nonlinear Physics Centre, Research School of Physics and Engineering, Australian National University, Canberra, ACT 2601, Australia
e-mail: andrey.sukhorukov@anu.edu.au

Modern quantum communication schemes, including quantum teleportation [1, 2] and quantum cryptography [3, 4], are based on the creation of entangled photon pairs for the transmission of quantum information. Most modern systems of quantum communication are using the effect of spontaneous parametric down-conversion (SPDC) as a source of photon pairs [5, 6]. The generation of biphotons through effect of SPDC in quadratic-nonlinear fibers has been described in detail in [7]. However, this effect requires the fibers with the quadratic nonlinearity, whose crystal lattice has no inversion center [8]. Thus, the production of such fibers is entailed with certain difficulties. Therefore, we consider the generation of biphotons through the effect of spontaneous four-wave mixing (SFWM), which occurs in standard fiber-optic communication lines, with cubic nonlinearity.

The focus of our attention is on three cases (Fig. 1(a)): 1. The signal photon propagates in the fiber without generating of biphotons; 2. The photon pair is generated; 3. The photon is lost in the fiber.



(a) Possible cases of signal photon propagation through cubic-nonlinear fiber with losses in presence of pumping. (b) Normalized number of signal photons with biphotons generated through SFWM $I_2(z)$ in a single waveguide vs the propagation distance z for $A = 0.12$, and different losses: solid line — $\gamma_p = \gamma_s = \gamma_i = \gamma = 0$, dashed line — $\gamma_p = \gamma_s = \gamma_i = \gamma = 0.005$. Phase mismatch $\Delta\beta = 3$.

In this paper we have performed analytical and numerical analysis of the effect of linear losses on spontaneous four-wave mixing in cubic nonlinear fiber, considering in detail single-photon, triple-photon (single-photon + biphoton) and without photon outputs under a different distances and phase mismatching. In particularly, we provide a detail analysis of a case with small losses by perturbation theory, and obtain an expressions for max and min of intensities of triple-photon states and find distances which satisfy to this expressions.

In Fig. 1(b) we show a characteristic example of evolution of the normalized number of signal photons with biphotons generated through SFWM $I_2(z)$ in a single waveguide vs the propagation

distance z for $A = 0.12$, and different losses: solid line — $\gamma_p = \gamma_s = \gamma_i = \gamma = 0$, dashed line — $\gamma_p = \gamma_s = \gamma_i = \gamma = 0.005$. Phase mismatch $\Delta\beta = 3$.

We also have find a speed of growth of triple photon states intensity at initial distances in an assumption of a small losses.

References

- [1] D. Bouwmeester, J. W. Pan, K. Mattle, M. Eibl, H. Weinfurter, A. Zeilinger, Experimental quantum teleportation, *Nature*, **390**, 575–579 (1997).
- [2] D. Boschi, S. Branca, F. De Martini, L. Hardy, S. Popescu, Experimental realization of teleporting an unknown pure quantum state via dual classical and Einstein–Podolsky–Rosen channels, *Phys. Rev. Lett.*, **80**, 1121–1125 (1998).
- [3] A. K. Ekert, J. G. Rarity, P. R. Tapster, G. M. Palma, Practical quantum cryptography based on 2-photon interferometry, *Phys. Rev. Lett.*, **69**, 1293–1295 (1992).
- [4] M. Giustina, et al., Bell violation using entangled photons without the fair-sampling assumption, *Nature*, **497**, 227–230 (2013).
- [5] S. Tanzilli, H. De Riedmatten, W. Tittel, H. Zbinden, P. Baldi, M. De Micheli, D. B. Ostrowsky, N. Gisin, Highly efficient photon-pair source using periodically poled lithium niobate waveguide, *Electronics Letters*, **37**, 26–28 (2001).
- [6] K. Banaszek, A. B. U'Ren, I. A. Walmsley, Generation of correlated photons in controlled spatial modes by downconversion in nonlinear waveguides, *Optics Letters*, **26**(17), 1367–1369 (2001).
- [7] D. A. Antonosyan, A. S. Solntsev, A. A. Sukhorukov, Effect of loss on photon-pair generation in nonlinear waveguide arrays, *Physical Review A*, **90**, 043845 (2014).
- [8] G. P. Agrawal, *Nonlinear fiber optics*, Academic Press (2007).

Modeling and experimental investigations of on-body electromagnetic wave propagation

Irina Vendik, Orest Vendik, Vladimir Pleskachev, Vitaly Kirillov

St. Petersburg Electrotechnical University

e-mails: ibvendik@rambler.ru, ibvendik@yandex.ru

Development of wearable wireless systems is highly challenged due to a wide spectrum of applications such as personal communication, medicine, firefighting, military, and radio frequency identification (RFID) [1]. The lightweight, low fabrication cost, easy manufacturing, and the availability of inexpensive materials make the wearable electronics very attractive. A new branch of wireless system technology is connected with the Wireless Body Area Network (WBAN). Such systems in combination with personal area networks provide monitoring of biological systems (human body) in real time. For an adequate estimation and control of the data transfer of electromagnetic (EM) waves over the body surface, it is necessary to describe properly the wave propagation.

Interface between the air and the body surface supports three basic EM wave modes [2]: surface wave, leaky wave and creeping wave. The first two modes are well studied [3, 4] while the latter [5] exhibits a specific property of rounding curved parts of the body and penetrating into shadow regions. This property of the creeping wave is of high importance for the body networks making non line-of-sight communications possible. Analytic studies of the creeping wave properties was suggested in [5, 6], as applied to wave propagation over a uniform cylinder.

In this paper, we present results of numerical/analytical simulations and experimental studies of the EM wave propagating over plane and curved surfaces of a human body. The main attention is paid to properties of a creeping wave. Surface waves are also under consideration.

References

- [1] P. S. Hall, Y. Hao, *Antennas and Propagation For Body-Centric Wireless Communications*, Artech House, Norwood MA (2012).

- [2] R. Paknys, D. R. Jackson, The relation between creeping waves, leaky waves, and surface waves, *IEEE Trans. on Antennas and Propag.*, vol. **53**(3), pp. 898–907 (2005).
- [3] R. E. Collin, *Field Theory of Guided Waves*, McGraw-Hill, New York (1960).
- [4] F. Monticone, A. Alu, Leaky-wave theory, techniques, and applications: from microwaves to visible frequencies, *IEEE Proc.*, vol. **103**(5), pp. 793–821 (2015).
- [5] R. Paknys, N. Wang, Creeping wave propagation constant and modal impedance for dielectric coated cylinder, *IEEE Trans. on Antennas and Propag.*, vol. **34**(5), pp. 674–680 (1986).
- [6] G. A. Conway, W. G. Scanlon, S. L. Cotton, M. J. Bentum, An analytical path-loss model for on-body radio propagation, *IEEE. URSI Intern. Symp. on Electromagnetic Theory*, pp. 353–356 (2010).

Third harmonic generation from the silicon self-organized nanostructured surface

Voytova T.A.¹, Makarov S.V.¹, Tsytkin A.N.¹, Milichko V.A.¹, Mukhin I.S.^{1,2}, Yulin A.V.¹, Putilin S.E.¹, Baranov M.A.¹, Krasnok A.E.¹, Belov P.A.¹

¹ITMO University, St. Petersburg, 197101, Kronverksky pr. 49, Russia

²St. Petersburg Academic University, St. Petersburg, 194021, Khlopina 8/3, Russia

e-mail: t.voytova@phoi.ifmo.ru

In recent time nonlinear optical processes in nanoscale dielectric systems attract great attention of scientists. The dielectric nanostructure, in contrast to the plasmonic one, have low optical losses, high nonlinearity and higher damage threshold as compared to plasmonic nanostructures. The use of the strong spatial localization of the field in the particles at the resonant frequencies allows enhancing nonlinear optical effects.

In recent work we consider the enhanced third-harmonic generation from the self-organized silicon nanostructured surface. To produce the periodically arranged arrays of silicon nanoparticles we use pumping pulse at the optical frequency (800 nm). The obtained surface inhomogeneities have a size of 130 nm × 330 nm and arranged with periodicity 260 nm in one direction and 700 nm in another. As a result in the experiment we observed 1.3 nJ femtosecond pulses at the ultraviolet frequency 266 nm. Resulting enhancement of conversion efficiency obtained up to 10⁻⁶. The obtained third harmonic generation efficiency was compared to the same in the case of smooth silicon film. We found 2.5-fold enhancement of TH conversion efficiency as compared to the resonant 100 nm silicon film and 30-fold enhancement as compared to the 170 nm nonresonant film. So this process of third harmonic generation in the considered nanostructures can be used for the development of nanoscale sources of ultraviolet light.

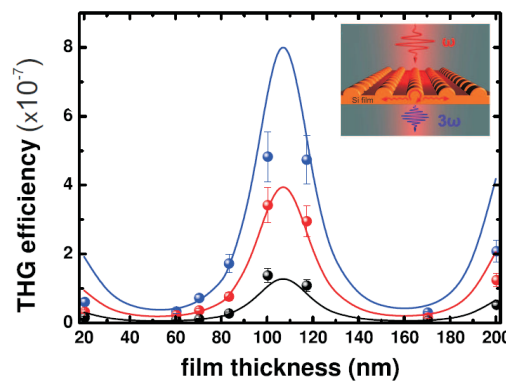


Fig. 1: Experimental (circles) and theoretical (lines) dependencies of third harmonic generation (THG) efficiency on a-Si:H film thickness at various pump intensities: 20 GW/cm² (black), 35 GW/cm² (red), 55 GW/cm² (blue). Schematic sketches of third harmonic generation from smooth nanostructured Si film on the inset.

References

- [1] M. R. Shcherbakov, D. N. Neshev, B. Hopkins, et al., *Nano Letters*, **14**, 6488 (2014).
- [2] S. Makarov, S. Kudryashov, I. Mukhin, et al., *Nano Letters*, **15**, 6187 (2015).
- [3] A. E. Miroshnichenko, A. B. Evlyukhin, Y. F. Yu, et al., *Nature Communications*, **6** (2015).
- [4] Y. Yang, W. Wang, A. Boulesbaa, et al., *Nano Letters*, **15**, 7388 (2015).
- [5] R. M. Bakker, D. Permyakov, Y. F. Yu, et al., *Nano Letters*, **15**, 2137 (2015).

New degrees of freedom of spin-optonics implemented by using hybrid surface waves localized at hyperbolic metasurface

Yermakov O.Y.¹, Bogdanov A.A.¹, Iorsh I.V.¹, Lavrinenko A.V.²

¹The International Research Centre for Nanophotonics and Metamaterials, ITMO University, St. Petersburg 197101, Russia

²DTU Fotonik, Technical University of Denmark, Oersteds pl. 343, DK-2800 Kongens Lyngby, Denmark

e-mail: oe.yermakov@gmail.com

The possibilities of spin angular momentum tuning and opportunities to support various configurations of surface waves polarization have been theoretically considered recently [1]. We propose to implement the polarization control using surface waves propagating along hyperbolic metasurface. We describe our hyperbolic metasurface within effective medium approximation in terms of anisotropic conductivity. Such metasurface can be implemented by using an array of graphene strips [2] or of dielectric subwavelength antennas [3]. The spectrum of surface waves consists of two hybrid TE-TM polarized surface waves. Anisotropy of metasurface and different propagation directions lead to a mixing of TE and TM surface plasmons, what makes their polarization structure very miscellaneous.

It is convenient to characterize the spin properties with the quantity known as helicity σ , which is the projection of spin angular momentum on the direction of motion. Photon can possess only two spin states $\sigma = \pm 1$ corresponding to the right and left circular polarizations. It means that spin angular momentum of photon is always parallel or antiparallel to propagation direction. Spin of surface plasmon-polariton is always transverse, because at any fixed frequency the interface supports the surface wave of the fixed linear polarization. Therefore, helicity of surface plasmon-polariton is equal to 0. For the perspective nanophotonic applications, it would nevertheless be desirable to be able to tailor the helicity continuously in the range $[-1; 1]$. In contrast to surface plasmon-polariton propagating along metal-dielectric interface, hyperbolic plasmons possess longitudinal component of spin angular momentum. Consequently, the direction of spin angular momentum can be arbitrary and helicity can change continuously from -1 to 1 . It exhibits a continuous transition from the transverse spin angular momentum as for the conventional surface plasmon-polariton to the longitudinal spin angular momentum as for the left and right circularly polarized bulk electromagnetic mode.

These findings open new routes for the optomechanical manipulation of the nanoobjects and perspectives for the effective optical control over the spin currents in solid state systems, which is the subject of rapidly emerging field of spin-optonics.

This work has been supported by RFBR (16-37-60064, 14-02-01223), by the President of Russian Federation (MK-6462.2016.2), the Federal Programme on Support of Leading Scientific Schools (NSh-5062.2014.2), and by program of Fundamental Research in Nanotechnology and Nanomaterials of the Russian Academy of Science. Numerical simulations, and optical experiments have been supported by the Russian Science Foundation (Grant 15-12-20028).

References

- [1] K. Y. Bliokh, A. Y. Bekshaev, F. Nori, *Nature Communications*, **5**, 3300 (2014).
- [2] J. S. Gomez-Diaz, M. Tymchenko, A. Alù, *Physical Review Letters*, **114**, 233901 (2015).

- [3] O. Y. Yermakov, A. I. Ovcharenko, M. Song, A. A. Bogdanov, I. V. Iorsh, Y. S. Kivshar, *Physical Review B*, **91**, 235423 (2015).

Enrichment of few-cycle pulse spectrum by non-linear interaction with medium

Zagursky D.Yu., Trofimov V.A., Zakharova I.G.

Moscow State University, Russia, 119991, Moscow, GSP-1, Leninskiye Gory
e-mails: zagurski@physics.msu.ru, vatro@cs.msu.ru, zaharova@phys.msu.ru

The contemporary development of THz sources has conditioned the introduction of nonlinear interactions to terahertz frequency range [1, 2, 3].

Given that the pulse of THz frequency range has greater photon concentration than the optical pulse of comparable amplitude, the THz pulse has greater potential of introducing significant disturbances to populations of energy levels which it may excite. Thus, taking into account the development of high-intensity terahertz sources, the nonlinear regime of interaction may become of high interest in relation to terahertz spectroscopy.

Computer simulations were used to study 1D case of the process of non-linear interaction of few-cycle electromagnetic pulse with medium described by multilevel Maxwell–Bloch system of equations also known as semi-classical model. These equations describe the medium with nonlinear non-instant response to the electromagnetic field. Gaussian envelope with cosine filling defined the incident pulse shape. The width of pulse envelope was chosen so that only a few (5–6) oscillations were contained in it.

The simulated pulses had intensities sufficiently high to notably alter the energy level populations in medium from their equilibrium values. Due to that the nonlinearity of the medium polarization becomes significantly pronounced and can result in various frequency transformations in spectrum including the generation of higher harmonics and combination frequencies.

This study was made under support of the Russian Science Foundation (Grant No. 14-21-00081).

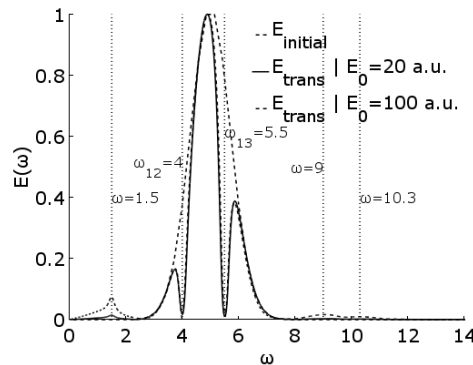


Fig. 1: Comparison of spectrum of incident pulse with the spectra of pulses with different initial amplitudes through three-level medium in nonlinear regime. Spectra are normalized to 1. Vertical lines mark positions of spectral absorption lines of medium (ω_{12} , ω_{13} and positions of additional peaks appearing due to nonlinearity.

References

- [1] I. Al-Naib, M. Poschmann, M. M. Dignam, Optimizing third-harmonic generation at terahertz frequencies in graphene, *Phys. Rev. B*, **91**, 205407 (2015).
 [2] K. E. Hamilton, A. A. Kovalev, A. De, L. P. Pryadko, Continuous third harmonic generation in a terahertz driven modulated nanowire, *J. Appl. Phys.*, **117**, 213103 (2015).
 [3] C. Zhang, B. Jin, J. Han, I. Kawayama, H. Murakami, et al., Terahertz nonlinear superconducting metamaterials, *Appl. Phys. Lett.*, **102**, 081121 (2013).

On the influence of the thermal disorientation of meta-atoms on electromagnetic properties of liquid metacrystals

Zharov A.A.¹, Zharov A.A. Jr.¹, Zharova N.A.²

¹Institute for Physics of Microstructures, Russian Academy of Sciences, Nizhny Novgorod 603950, Russia

²Institute of Applied Physics, Russian Academy of Sciences, Nizhny Novgorod 603950, Russia
e-mail: zharov@ipm.sci-nnov.ru

Recently suggested liquid metacrystals (LMCs) [1] (or meta-liquid crystals [2]) is a novel type of resonant metamaterials that bodes potentially a number of unique properties, such as high tunability and very strong nonlinearity, at least in microwave and THz domains. From general view, LMC is an array of anisotropic macroscopic oscillators (meta-atoms) suspended in viscous liquid that can be oriented along any chosen axis by an external static electric (or magnetic) field. Thereby, the effective LMC medium acquires anisotropic electromagnetic properties. The anisotropy axis can be managed via the changing of direction and/or the strength of the external static field. In turn, high frequency electric (magnetic) field aspires to re-orient meta-atoms along the field, that provides nonlinear properties of LMC media [3].

Thermal motion tends to disorient meta-atoms, thus leading to the suppression of LMC anisotropic properties.

Here we report the influence of the thermal spread on the electromagnetic properties of LMC in equilibrium and weakly nonequilibrium cases.

The stationary distribution function for meta-atoms' orientation has been found. It allowed to obtain the effective LMC permittivity tensor as a function of temperature for different values of static controlling field and different frequency ranges (from microwaves up to visible domain). In the analysis of the the resonant LMC properties we used model meta-atoms such as metal subwavelength particles of special shape in microwave/THz range and metal plasmonic nanoparticles in the shape of ellipsoid of revolution in IR and visible bands.

We show that the phase transition of the second kind is possible at some critical temperature when elliptical-type LMC medium turns into hyperbolic one with decreasing temperature. We also estimate the value of nonlinear characteristic field as a function of temperature.

References

- [1] A. A. Zharov, A. A. Zharov, N. A. Zharova, *JOSA B*, **31**, 559–564 (2014).
- [2] M. Liu, K. Fan, W. Padilla, D. A. Powell, X. Zhang, I. V. Shadrivov, *Adv. Mater.*, **28**, 1525 (2016).
- [3] A. A. Zharov, A. A. Zharov, N. A. Zharova, *Phys. Rev. A*, **90**, 023207 (2014).

Manipulations with surface plasmon excitation via the scattering of light by a nanoparticle: scanning and switching

Alexander A. Zharov Jr., Alexander A. Zharov

Institute for Physics of Microstructures, Russian Academy of Sciences, Nizhny Novgorod, Russia
e-mail: azharov@ipmras.ru

Nina A. Zharova

Institute of Applied Physics, Russian Academy of Sciences, Nizhny Novgorod, Russia

We study an excitation of surface plasmons (SPs) due to the scattering of plane light wave by a dipole nanoparticle located nearby flat air/metal interface. It is well-known that such a scattering can reveal asymmetric behavior of excited SP regarding the plane of incidence of light [1]. This asymmetric SP excitation which takes place at, in particular, the incidence of elliptically polarized light

is often attributed to so-called photonic spin Hall effect [2]–[4] caused by interplay between rotating polarization of nanoparticle and intrinsic angular momentum of SP. We show that this photonic spin Hall effect may be applied for the SP excitation control that allows to manage the directivity pattern of SP and its amplitude. On the base of analytical solution and numerical simulations we demonstrate that the dominant direction of SP propagation and whole directivity pattern can be effectively managed by means of the angle of incidence of light, light polarization and the nanoparticle position above the interface. The possibility of SP control can also be extended using nanoparticles with anisotropic polarizability. We believe that manipulations with SP at nanometer scale may broaden the field of possible plasmonic applications.

References

- [1] D. O. O'Connor, P. Ginzburg, F. J. Rodriguez-Fortino, G. A. Wurtz, A. V. Zayats, *Nat. Commun.*, **5**, 5327 (2014).
- [2] K. Y. Bliokh, D. A. Smirnova, F. Nori, *Science*, **348**, 1448 (2015).
- [3] J. Petersen, J. Volz, A. Rauschenbentel, *Science*, **346**, 67 (2014).
- [4] B. Le Feber, N. Rotenberg, L. Kuipers, *Nat. Commun.*, **6**, 6695 (2015).

Spectral diffusion of light in deformed (conformally squeezed and stretched) hyperbolic metamaterial

Zharova N.A.¹, **Zharov A.A.**², **Zharov A.A., Jr.**²

¹Institute of Applied Physics, RAS, Nizhny Novgorod, Russia

²Institute for Physics of Microstructures, RAS, Nizhny Novgorod, Russia

e-mail: zhani@appl.sci-nnov.ru

Exotic and interesting material features of hyperbolic metamaterials (HM) cause their intensive study [1]. In literature, characteristic properties of HM are often related to very high (ideally, infinite) density of photonic states in certain propagation directions (along the resonance cone). This property of hyperbolic media may be useful in particular for heating and cooling applications, since high density of photonic states ensures effective radiative heat transfer and allows to build nano-sized cooling devices on the base of HM.

Different applications have been proposed based on absorbing properties of HM. In particular, HMs can be used in design of absorbers. Indeed, launching a wave beam from free space into HM at a proper angle leads to propagation of this radiation along the resonance cone generatrix. The wavenumber k will be very large in this case, and this extremely small-scale radiation will be strongly and effectively absorbed in HM medium. However, this launching scheme is not simple to implement, and the absorptivity of the HM will be very sensitive to the incidence angle.

In this report, we propose a way to overcome this problem via deformation of the HM slab: The wave propagated in such a deformed — nonuniform — HM medium scatters, and it leads to the diffusion of radiation in \mathbf{k} space. Since the density of photonic states in HM tends to infinity (in ideal case) for wave vectors along the resonance cone, then one can expect the concentration of the scattered radiation in this direction without precise control of the incident beam.

We consider a special — conformal — kind of HM slab deformation. Application of methods of Transformational Optics in this case simplifies the statement of the problem. This allows to find approximate analytical solution which is confirmed by numerical calculations. The analysis also helps to explain specific character of spectral diffusion in HM: it is shown analytically and numerically that besides the conventional diffusion spreading, a spectral drift of the radiation takes place, and the waves scattered in this way keep coherence.

References

- [1] L. Ferrara, C. Wu, et al., *Progress in Quantum Electronics*, **40**, 1–40 (2015).
- [2] I. S. Nefedov, C. A. Valagiannopoulos, S. M. Hashemi, E. I. Nefedov, *Sci. Rep.* **3**, 2662 (2013).

A perfectly absorbing mushroom metasurface for two arbitrary angles of incidence

D.V. Zhirihin, S.B. Glybovski, P.A. Belov

ITMO University, St. Petersburg 197101, Russia

e-mail: zhirihin_dmitry@mail.ru

C.R. Simovski, S.A. Tretyakov

Aalto University, FI-00076 Aalto, Finland

Previously many designs of optically thin perfect absorbers have been proposed based on metasurfaces, which are usually two-dimensional arrays of engineered unit cells with subwavelength periodicity. Among other designs, e.g. reviewed in [1], there were so-called perfect absorbers based on grounded arrays of metal patches [2] and mushroom structures [3]. The term ‘perfect’ generally means total absorption of an incident plane electromagnetic wave with a given polarization at one frequency and only one angle of incidence. A lot of efforts have been made on extension of the frequency and angular ranges of thin absorbers. With the aim to improve the angular stability of absorption in [4] it was proposed to use the combination of two resonances in the lossy mushroom structure.

In this work we have theoretically investigated the way to obtain ideal absorption of TM-polarized plane waves coming from two different angles. We have proposed an appropriate absorber design, which is based on the mushroom metasurface having two kinds of losses: in lumped impedances connecting the wires of patches to the ground plane and in the structure’s dielectric substrate. The above mentioned losses in the metasurface can be controlled independently, which allows to reach perfect absorption of TM-waves with the absorption factor theoretically equal to unity at two given angles of incidence. The effect relies on the birefringence in the wire-medium layer, which is a part of the mushroom structure.

We demonstrate our results of analytical calculations of the reflection coefficient using a non-local homogenization model of the mushroom structure with the generalized additional boundary conditions and compare them to the numerical simulations. The proposed approach can be extended to the case of both polarizations.

References

- [1] Y. Ra’di, C. R. Simovski, S. A. Tretyakov, Thin perfect absorbers for electromagnetic waves: theory, design, and realizations, *Phys. Rev. Applied*, **3**, 037001 (2015).
- [2] H. Mosallaei, K. Sarabandi, A one-layer ultra-thin meta-surface absorber, *IEEE Antennas and Propagation Society International Symposium*, pp. 615–618 (2005).
- [3] C. S. R. Kaipa, A. B. Yakovlev, S. I. Maslovski, M. G. Silveirinha, Mushroom-type high-impedance surface with loaded vias: homogenization model and ultra-thin design, *IEEE Antennas and Wireless Propagation Letters*, vol. **10**, pp. 1503–1506 (2011).
- [4] O. Luukkonen, F. Costa, C. R. Simovski, A. Monorchio, S. A. Tretyakov, A thin electromagnetic absorber for wide incidence angles and both polarizations, *IEEE Transactions on Antennas and Propagation*, vol. **57**(10), pp. 3119–3125 (2009).

Novel method for fabrication of high-index metal-dielectric core-shell nanoparticles for advanced optical applications

Zograf G.P.^{1,2}, Makarov S.V.¹, Zuev D.A.¹, Milichko V.A.¹, Mukhin I.A.^{1,3}, Krasnok A.E.¹, Belov P.A.¹

¹ITMO University, 49 Kronverksky Pr., St. Petersburg, 197101, Russia

²Ioffe Institute, 26 Politekhnicheskaya, St. Petersburg 194021, Russia

³St. Petersburg Academic University, 8/3 Khlopina Str, St. Petersburg, 194021, Russia

e-mail: g.zograf@metalab.ifmo.ru

Plasmonic nanoparticles have wide range of applications, including optics and biomedicine [1], due to their ability to enhance field. However, metallic particles have some limitations related to high dissipative losses and presence of only electric resonances in simple shape structures (spheres, rods, etc.). On the other hand, dielectric nanoparticles of high refractive index and low extinction coefficient maintain a strong electric and magnetic resonances in the visible range [2]. In comparison with the plasmonic particles, dielectric have low-losses and can be used for superdirective scattering [3]. Our goal is to combine benefits from both types of nanoantennas.

Recently, it has been demonstrated that spherical high-index crystalline silicon nanoresonators can be fabricated by femtosecond laser ablation of amorphous films [4]. Here we are applying this technique to create core-shell structures from thin gold and silicon films. Resonant core-shell properties depend on the size of the nanostructure. This size can be precisely controlled via thickness of Au/Si films layers.

A strong advantage of our method is that femtosecond laser-induced printing makes possible to obtain nanoparticles with plethora of sizes. Numerical calculations showed the influence of the size of the core and the shell on the optical properties of the particles. These results are in good agreement with series of experimental dark-field scattering spectra. The ability to tune resonances provides the opportunity to use core-shell as a platform for biosensing, directional nanolasers and other applications.

References

[1] A. E. Krasnok, *et al.*, *Physics-Uspekhi*, **56**, 539–564 (2013).

[2] A. I. Kuznetsov, *et al.*, *Sci. Rep.*, **2**, 492 (2012).

[3] A. E. Krasnok, *et al.*, *Nanoscale*, **6**, 7354–7361 (2014).

[4] P. A. Dmitriev, *et al.*, *Nanoscale*, **8**, 5043 (2016).

Reversible and non-reversible tuning of hybrid optical nanoresonators

Zuev D.A.¹, Makarov S.V.¹, Milichko V.A.¹, Krasnok A.E.¹, Belov P.A.¹, Baranov D.G.², Miroshnichenko A.E.³, Mukhin I.S.⁴, Morozov I.A.⁴

¹ITMO University, St. Petersburg 197101, Russia

²Moscow Institute of Physics and Technology, 9 Institutskiy per., Dolgoprudny 141700, Russia

³Nonlinear Physics Centre, Research School of Physics and Engineering, The Australian National University, Canberra, ACT 0200, Australia

⁴St. Petersburg Academic University, St. Petersburg 194021, Russia

e-mail: zuewda@gmail.com

The combination of plasmonics and all-dielectric nanophotonics in the concepts of metal-dielectric (hybrid) nanophotonics has allowed to utilize the advantages of both these directions (strong local-

ization of light, artificial magnetic optical response and unique scattering properties) in the form of hybrid nanostructures (nanoantennas and metasurfaces) [1, 2]. The unique properties of hybrid nanostructures mostly depend on the spectral overlapping of their optical modes in metal and dielectric nanoparticles. Therefore, the ability to tune optical properties of nanosystems is the key factor towards development of all-optical data-processing components for integration in optical circuits.

Recently, we have proposed a novel method for fabrication of ordered asymmetric metal-dielectric (Au/Si) nanoparticles [3]. Here, we present a original concepts of reversible and non-reversible precise manipulation by the optical properties of the hybrid nanostructures. The feasibility of both concepts is confirmed by numerical modeling and demonstrated experimentally. The non-reversible tuning of hybrid nanostructures is attained via selective laser-induced reshaping of the metal components without affecting the dielectric ones. We apply this approach for the demonstration of the local optical properties tuning of hybrid metasurfaces by shifting of spectral position of resonant transmittance on 250 nm. The reversible technique is based on electron-hole plasma generation in the dielectric component of the hybrid nanodimer, leading to modification of its optical properties. This technique was recently demonstrated as a means of optical tuning of all-dielectric nanostructures [4]. Here, we experimentally demonstrate 15% tuning of transmittance of a single hybrid nanodimer by femtosecond laser pulses. The received results are in good agreement with predictions of developed analytical model.

Our investigations open a possibility for application of hybrid nanophotonics in advanced optical and biomedical applications as well as creation of storage elements for optical computer systems.

References

- [1] H. Wang, P. Liu, Y. Ke, Y. Su, L. Zhang, N. Xu, S. Deng, H. Chen, *ACS Nano*, **9**, 436–448 (2015).
- [2] R. Jiang, B. Li, C. Fang, J. Wang, *Advanced Materials*, **26**, 5274–5309 (2014).
- [3] D. A. Zuev, S. V. Makarov, V. A. Milichko, S. V. Starikov, I. S. Mukhin, I. A. Morozov, I. I. Shishkin, A. E. Krasnok, P. A. Belov, *Advanced Materials*, doi: 10.1002/adma.20150534 (2016, accepted).
- [4] S. Makarov, S. I. Kudryashov, I. Mukhin, A. Mozharov, V. Milichko, A. Krasnok, P. A. Belov, *Nano Letters*, **15**(9), 6187–6192 (2015).

Laser printed nanoparticles to control light on the nanoscale

U. Zywietz, T. Fischer, T. Birr, A.B. Evlyukhin, C. Reinhardt, B.N. Chichkov

Laser Zentrum Hannover e. V., Hollerithallee 8, 30419 Hannover

e-mail: u.zywietz@lzh.de

Spherical nanoparticles with radii of 50–150 nm provide unique optical properties. They are characterized by strong Mie resonances within the visible range [1]. In a precise arrangement they can be used as building blocks of more complex optical elements. We developed a novel laser printing technique for the controlled fabrication of highly ordered nanoparticle arrays [2, 3]. This technique allows to generate precisely designed ultra-flat lenses on the the basis of spherical nanoparticles. A sophisticated design was developed using Mie calculations to control and optimize the focussing effect. A schematic drawing is given in Figure 1. Each individual nanoparticle within this lens contributes to the focussing effect. Experimental realization has been carried out by a combination of prestructured material films and subsequent laser transfer.

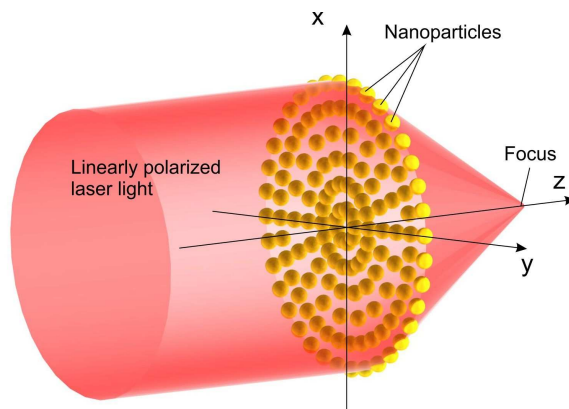


Fig. 1: Schematic representation of an ultra-flat nanoparticle lens.

References

- [1] A. B. Evlyukhin, S. M. Novikov, U. Zywietz, R. L. Eriksen, C. Reinhardt, S. I. Bozhevolnyi, B. N. Chichkov, Demonstration of magnetic dipole resonances of dielectric nanospheres in the visible region, *Nano Letters*, vol. **12**(1), pp. 3749–3755 (2012).
- [2] U. Zywietz, A. B. Evlyukhin, C. Reinhardt, B. N. Chichkov, Laser printing of silicon nanoparticles with resonant optical electric and magnetic responses, *Nature Communications*, vol. **5** (2014).
- [3] U. Zywietz, M. K. Schmidt, A. B. Evlyukhin, C. Reinhardt, J. Aizpurua, B. N. Chichkov, Electromagnetic resonances of silicon nanoparticle dimers in the visible, *ACS Photonics*, vol. **2**(7), pp. 913–920 (2015).

Author index

- Abdeddaim, R., 208, 216
Abramian, A.K., 19
Abramochkin, E.G., 19, 108
Aero, E.L., 20
Albella, P., 198
Albooyeh, M., 228
Aleksandrov, A.A., 160
Alekseev, G.V., 133
Alexandrov, A.A., 57
Alexeeva, N.O., 234
Alodjants, A.P., 143
Altaisky, M.V., 21, 134
Andrianov, E.S., 225
Andronov, I.V., 21
Andryieuski, A., 134
Angermann, L., 22
Anikin, A.Yu., 22
Anzulevich, A.P., 141, 211
Arlova, H.S., 90
Astrakhantseva, A.A., 23
Avdonin, S.A., 24
Bab
Babnikov, M.B., 25
Babicheva, V.E., 135
Badanin, A.V., 73
Baena, J.D., 136
Bagaev, A.A., 26
Bagmutov, A.S., 27
Baranov, A.V., 162
Baranov, D.A., 137
Baranov, D.G., 153, 197, 248
Baranov, M.A., 162, 242
Baryshnikova, K.V., 135, 138
Baskin, L.M., 28
Basova, T.V., 140
Beginin, E.N., 168
Belonenko, M.B., 118, 186
Belotelov, V.I., 236
Belotitskii, V.I., 234
Belov, P.A., 135, 136, 153, 180,
184, 189, 195–197, 208, 217,
224, 242, 247, 248
Belyaev, A.K., 28
Belyaeva, N.A., 104
Belyayev, Yu.N., 29, 30
Benimetskiy, F.A., 140
Bentivegna, F.F.L., 148, 149
van den Berg, C.A.T., 172
Berzhansky, V.N., 236
Besedin, I., 227
Bezus, E.A., 155
Bichurin, M.I., 149
Bigall, N., 143
Bilous, P.Yu., 21
Birr, T., 139, 143, 159, 249
Blagoveshchensky, A.S., 24, 31, 32
Blokhin, A.M., 32
Boardman, A.D., 207
Boes, A., 85
Bogdanov, A.A., 137, 164, 165,
188, 219, 230, 243
Bogomolov, Ya.L., 33
Bolotova, A., 131
Bonod, N., 141
Borodov, M.A., 33
Borzov, V.V., 34
Bosia, F., 204
Boumaza, H., 34
Bozhok, E.V., 29
Bratov, V.A., 35
Brener, I., 206
Budylin, A.M., 35, 36
Bulatov, V.V., 36
Bulygin, A.N., 20
Burmak, L.I., 88
Butko, L.N., 141, 211
Butylkin, V.S., 142, 191
Butz, S., 227
Bykov, D.A., 155
Cardinali, A., 47
Castillo-Pérez, R., 78
Chabanov, A.A., 187, 237
Chang, T.-C., 37
Charlamov, S., 210
Charukhchyan, M.V., 143
Chebotarev, A.Yu., 23, 38, 73
Chen, A.L., 57
Chernykh, G.A., 46
Chestnov, I.Yu., 143
Chhantyal, P., 143
Chichkov, B.N., 143, 159, 249
Choi, D.-Y., 202, 225, 226
Chong, K.E., 225, 226
Chopic, A.P., 210
Choque Rivero, A., 24
Chou, Y.-H., 37, 144
Chubchev, E.D., 145
Chugainova, A.P., 39
Chukov, V.N., 40
Churikov, D.V., 76
Clark, S.J., 174, 176
Colombi, A., 145
Craster, R.V., 145
Dadoenkova, N.N., 147–149
Dadoenkova, Yu.S., 147–149
Dagesyan, S.A., 236
Dai, J., 157
Damaskinsky, E.V., 34
Damdinov, B.B., 150
Danaeifar, M., 150
Danek, T., 42
Darinskii, A.N., 185
Delitsyn, A.L., 42
Dembelova, T., 150
Demidchik, V.I., 152
Demin, A.S., 150
Demin, D.B., 43
Denisov, D.V., 176
Denisova, I.V., 44
Derevyanchuk, E.D., 231
Derkach, M., 207
Despres, B., 45
Dmitriev, P.A., 153
Dmitrieva, L.A., 46
Dobrokhotov, S.Yu., 46–48
Dolgaleva, K., 70
Dolganov, P.V., 153, 154
Dolganov, V.K., 153, 154
Dolgova, T.V., 202
Dorodnyi, M.A., 49
Doskolovich, L.L., 155
Drachev, V.P., 156
Dubtsov, A.V., 210
Dyachenko, P.N., 212
Dyakov, S.A., 157
Dyankov, G., 130
Edemskii, D., 103
Efimova, A.I., 166
Eglit, M.E., 50
Egorov, A.Yu., 176
Egorov, O.A., 143
Eich, M., 212
Enoch, S., 208, 216
Evlyukhin, A.B., 138, 159, 249
Evstigneev, R.O., 50
Faleeva, M.P., 51
Fan, S., 158
Fedotov, A.A., 51, 52
Fedyanin, A.A., 202, 225, 226
Filippenko, G.V., 52
Filonov, D.S., 189, 215, 217
Fink, M., 158, 194
Firsova, N., 158
Fischer, T., 159, 249
Fistul, M.V., 227
Fiziev, P., 53
Fomenko, S.I., 57, 160
Fritzen, C.-P., 58
Friziuk, K.S., 161, 162
Gallant, A.J., 174
Galyamin, S.N., 163
Garbuzov, F.E., 53
Gavrilov, S.N., 54
Georget, E., 208
Gerasimov, D.A., 55
Ginzburg, P., 164, 175

- Gippius, N.A., 157
 Girshova, E.I., 174
 Glushkov, E.V., 56
 Glushkova, N.V., 56
 Glybovski, S.B., 136, 172, 189, 208, 247
 Golenitskii, K.U., 165
 Golovan, L.A., 166
 Golub, M.V., 57, 58
 Goray, L.I., 59, 176
 Gordeev, S.O., 154
 Gorkunov, M.V., 185
 Gorlach, M.A., 167
 Grachev, A.A., 168
 Grange, R., 169
 Granpayeh, N., 150
 Grenkin, G.V., 38
 Grigorenko, A.N., 191
 Grigoriev, D., 60
 Gubaydullin, A.R., 177
 Gula, I.A., 53
 Gusev, V.A., 61
Hakobyan, M.V., 64
 Hanham, S., 198
 Hartmann, M., 169
 Hasan, M., 170
 He, S., 62
 Hernandez-Juarez, J., 106
 Heuberger, A., 169
 Hong, J., 215
 Hong, K.-B., 61, 62
 Hong, M., 198
 Hopkins, B., 192, 226
 Huang, S.-C., 62
 Hurshkainen, A.A., 172
Il'ichev, E., 227
 Il'iasov, Kh.Kh., 63
 Imbert-Gerard, L.M., 45
 Iorsh, I.V., 137, 170, 219, 230, 243
 Ishkhanyan, A.M., 64
 Ishkhanyan, T.A., 64
 Ivanov, A.V., 173
 Ivanov, K.A., 174, 176, 177
 Ivinskaya, A.N., 164, 175
Jacob, Z., 212
Kabardov, M.M., 28
 Kadochkin, A.S., 190
 Kaina, N., 194
 Kalish, A.N., 236
 Kaliteevski, M.A., 174, 176, 177
 Kang, C., 178
 Kanjanasit, K., 215
 Kanté, B., 179
 Kapitanova, P.V., 134, 180
 Kaplunov, J., 35
 Kaputkina, N.E., 134
 Karchevskii, E.M., 121
 Katranchev, B., 130
 Kazakov, A.Ya., 65
 Kazantsev, Yu.N., 142, 191
 Kee, C.S., 178
 Khanikaev, A.B., 181
 Khokhlov, N.E., 236
 Kholodov, M.M., 166
 Kholodova, S.E., 65, 98
 Khromova, I.A., 138, 206
 Khusnutdinova, K.R., 66
 Kim, T.H., 178
 Kirillov, V., 241
 Kirpichnikova, A.S., 67
 Kirpichnikova, N.Ya., 67
 Kiselev, A.D., 68
 Kiselev, A.P., 31, 120
 Kislin, D.A., 69
 Kivshar, Yu.S., 134, 153, 183, 192, 193, 202, 217, 219, 220, 225, 226, 230
 Kleev, A.I., 43
 Klevin, A., 47
 Klushin, A.M., 70
 Kniazev, M.A., 70
 Kobayashi, K., 71
 Kolmychek, I.A., 200
 Kolodny, S.A., 184
 Kolonitskii, S.B., 72
 Komissarenko, F.E., 230
 Komissarova, M.V., 91
 Kondratov, A.V., 185
 Konobeeva, N.N., 118, 186
 Kononchuk, R., 187, 237
 Koptelov, Ya.Yu., 35
 Kornev, R.V., 152
 Korolkov, A.I., 115
 Korotyayev, E.L., 73, 111
 Koshelev, K.L., 188
 Kosulnikov, S.Yu., 189
 Kottos, T., 187
 Kovrov, A.E., 190
 Kovtanyuk, A.E., 23, 38, 73
 Kozitskiy, S.B., 73, 124
 Kozlov, S.A., 69, 70, 105
 Kozlov, V.A., 74, 75
 Krafft, C., 79, 127
 Kraftmakher, G.A., 142, 191
 Krasnok, A.E., 153, 161, 162, 184, 196, 197, 222, 242, 248
 Krasnov, I.P., 75
 Kravchenko, I., 192
 Kravchenko, O.V., 76
 Kravchenko, V.F., 76
 Kravchenko, V.V., 77, 78
 Kravets, V.G., 191
 Krawczyk, M., 147
 Krekeler, T., 212
 Kretushev, A., 131
 Krivtsov, A.M., 25
 Kroychuk, M.K., 202
 Kruk, S.S., 192, 193
 Krushynska, A.O., 204
 Krylov, V.A., 134
 Kshevetskii, S.P., 92, 127
 Kuchyanov, A.S., 140
 Kudrin, A.V., 79
 Kuhlmeier, B., 216
 Kumzerov, Yu.A., 234
 Kunakovskaya, E., 207
 Kuperin, Yu.A., 46
 Kurin, V.V., 70
 Kurseeva, V.Yu., 80
 Kuzmina, E.A., 81
 Kuznetsov, E.V., 81
 Kuznetsov, N.G., 82, 83
 Kuznetsova, S.M., 134
 Kyurkchan, A.G., 43, 83
Ladutenko, K.S., 195
 Lafitte, O., 34, 45
 Lagarkov, A.N., 173
 Lagovsky, B.A., 84
 Lai, Y.-Y., 37
 Lang, S., 212
 Lapine, M., 195
 Larkina, O.S., 133
 Larrat, B., 208
 Lavrinenko, A.V., 134, 137, 219, 243
 Lee, J.S., 178
 Lee, Y.P., 148
 Leem, J.W., 178
 Leib, E.W., 212
 Lemoult, F., 194
 Lepeshov, S.I., 196
 Lerosey, G., 194
 Levin, S.B., 35, 36
 Li, S.V., 197
 Limonov, M.F., 217–220
 Lin, C.-C., 144
 Lin, T.-R., 144
 Liu, T., 85
 Lobachev, A.M., 28
 Lobanov, A.V., 133
 Louati, H., 86
 Lu, T.-C., 37, 61, 62, 86, 144
 Luk, T.S., 206
 Lukashenko, S.Y., 220
 Lyalinov, M.A., 88
 Lyubchanskii, I.L., 147–149
Ma, X., 143
 Ma, Z., 198
 Machikhin, A.S., 88
 Maeng, I., 178

- Magnitskiy, S.A., 200
 Maier, S.A., 198, 199
 Makarov, S.V., 153, 162, 184, 196, 209, 242, 248
 Makin, R.S., 90
 Makin, V.S., 90
 Makri, E., 187
 Mal'tsev, V.P., 142, 191
 Malureanu, R., 137
 Maly, S.V., 90
 Malyshkin, D.S., 29, 30
 Mamaikin, M.S., 91
 Mamonov, E.A., 200
 Manenkov, S.A., 83
 Marchenko, S.V., 117
 Marshall, O.P., 191
 Masajada, J., 102
 Maslovski, S.I., 201
 Maximov, V.V., 92
 Maydykovskiy, A.I., 200
 Mazlin, V.A., 177
 Medvedik, M.Yu., 50
 Melchakova, I.V., 172, 208, 224
 Melik-Gaykazyan, E.V., 202, 226
 Melnikov, A.S., 93
 Melnikova, V.S., 213
 Merzlikin, A.M., 81, 203
 Miakisheva, O.A., 56
 Mikhaylov, V.S., 24
 Milichko, V.A., 153, 162, 184, 209, 242, 248
 Mingaleev, S.F., 219
 Miniaci, M., 204
 Mirmoosa, M.S., 189, 205
 Miroshnichenko, A.E., 192, 195, 196, 225, 226, 230, 235, 238, 248
 Mirzaei, A., 195
 Mitchell, A., 85
 Mitrofanov, O., 206
 Mochalova, Yu.A., 54
 Modestov, V.S., 28
 Molesky, S., 212
 Morozov, I.A., 184, 248
 Moskaleva, M.A., 50
 Motygin, O.V., 83
 Mukhin, I.S., 153, 162, 184, 190, 230, 242, 248
 Müller, F.M., 93
 Müller, I., 58
 Munina, I., 207, 239
 Murzina, T.V., 200
 Nakonechny, A.G., 95
 Naskar, S., 143
 Nazaikinskii, V.E., 48, 63
 Nazarov, S.A., 95
 Neely, S.T., 96
 Nefedov, I.S., 189, 207
 Nefedov, V.I., 84
 Neshev, D.N., 85, 192, 193, 202, 225, 226
 Neskoronnaya, A.V., 166
 Nikitina, E.V., 176
 Nikulin, A., 208
 Novitsky, A.V., 214
 O'Brien, K., 193
 Odit, M., 134
 Omelyanovich, M., 209
 Panasenko, G.P., 97
 Panyaev, I.S., 147
 Parkhomenko, R.G., 140
 Pasechnik, S.V., 210
 Pastukhova, S., 98
 Pavlov, D.A., 141, 211
 Pavlov, Yu.V., 20
 Peña, O., 195
 Peregudin, S.I., 65, 98
 Perel, M.V., 99
 Pereskokov, A.V., 100
 Permyakov, D.V., 230
 Peshkov, A.A., 163
 Pestov, Yu.I., 90
 Petrov, A.Yu., 212
 Petrov, G.I., 166
 Petrov, M., 130
 Petrov, M.I., 135, 161, 162
 Petrov, P.S., 100
 Petrov, R.V., 149
 Petrova, T.N., 100
 Petrova, Y.P., 101
 Pileckas, K., 97
 Pirogov, E.V., 176
 Pis'mak, Yu.M., 26
 Plachenov, A.B., 120
 Plamenevskii, B.A., 101
 Plekhanov, A.I., 140
 Pleskachev, V., 241
 Płociniczak, Ł., 102
 Plutenko, D.O., 68
 Poddubny, A.N., 167
 Podlipenko, Y.K., 95
 Podymaka, F.N., 32
 Polischuk, O.V., 213
 Polyakov, N.K., 176
 Polyanskaya, S.V., 88
 Polyanskiy, V.A., 28
 Popiolek-Masajada, A., 102
 Popov, A.I., 55
 Popov, A.V., 103
 Popov, I.Yu., 27, 51, 55, 119
 Popov, M.M., 67
 Popov, V.V., 213, 214
 Poretskii, A.S., 101
 Pozina, G., 176
 Presnov, D.E., 166
 Prikazchikov D.A., 35
 Prokhorov, I.V., 38, 73
 Prokopovich, I., 103
 Prozorova, E.V., 104
 Pryanishnikova, E.A., 104
 Pshenay-Severin, E., 193
 Pugno, N.M., 204
 Pukhov, A.A., 145, 225
 Putilin, S.E., 242
 Puzko, R.S., 203
 Puzyrev, D.N., 105
 Qiu, M., 157
 Raaijmakers, A.J.E., 172
 Rabinovich, V., 106
 Rasetshwane, D.M., 96
 Rastegaev, N.V., 107
 Razueva, E.V., 19, 108
 Reinhardt, C., 143, 159, 249
 Reinitz, J., 60
 Reno, J.L., 206
 del Risco, J.P., 136
 Ritter, M., 212
 do Rosario, J., 212
 Rouleux, M., 86
 Rozhleys, I. A., 147
 Rudnitsky, A.S., 109
 Rusakov, A., 215
 Rushchitsky, J.J., 110
 Rustomji, K., 216
 Rybin, M.V., 217–220
 Saburova, N.Yu., 111
 Sadovnikov, A.V., 168
 Sadrieva, Z.F., 219
 Samokhin, A.B., 84, 112
 Samokhina, A.S., 112
 Samsonov, A.M., 53
 Samusev, A.K., 137, 153, 219, 230
 Samusev, K.B., 217
 Samusev, S.F., 220
 Sannikov, D.G., 147
 Saritskaya, Zh.Yu., 112
 Sarychev, A.K., 173, 221
 Savelev, R.S., 222
 Schedin, F., 191
 Schneider, G., 212
 Schühler, M., 169
 Schwab, Ch., 93
 Sedaikina, V., 113
 Sekerzh-Zen'kovich, S.Ya., 63
 Semenov, A.A., 53
 Semenov, A.S., 28
 Semerenko, D.A., 210
 Semtchenok, N.N., 67
 Sergeev, S.A., 113
 Shadrivov, I.V., 195, 223

- Shafarevich, A.I., 114
 Shalin, A.S., 138, 164, 175, 190
 Shanin, A.V., 114, 115
 Shaposhnikov, A.N., 236
 Sharaevskii, Yu.P., 168
 Sharkova, N.M., 28
 Shchelik, G.S., 116
 Shchelokova, A.V., 224
 Shcherbakov, M.R., 202, 225, 226
 Shchetka, E., 51
 Shelykh, I.A., 170
 Shereshevskii, I.A., 70, 93
 Sheshukova, S.E., 168
 Shestakov, P.Yu., 117
 Shestopalov, Y.V., 81, 95
 Shishkina, E.V., 54
 Shishkov, V.Yu., 225
 Shmeliova, D.V., 210
 Shorokhov, A.S., 202, 225, 226
 Shpak, A.N., 58
 Shtukin, L.V., 28
 Shulga, K.V., 227
 Siday, T., 206
 Sidorenko M.S., 99
 Simovski, C.R., 189, 190, 205, 209, 228, 247
 Sinelnik, A.D., 220
 Sinev, I.S., 219, 230
 Skvortsov, D.S., 118
 Slawinski, M.A., 42
 Slobozhanyuk, A.P., 136, 224
 Sloushch, V.A., 119
 Smetanin, N.M., 46
 Smirnov, Yu.G., 231
 Smirnova, D.A., 226
 Smith, K., 187, 237
 Smolkina, M.O., 119
 So, I.A., 120
 Sofronov, I.L., 116
 Solntsev, A.S., 85
 Solonnikov, V.A., 44
 Solovyev, V.G., 234
 Song, M., 180
 Spiridonov, A.O., 121
 Spivak, Yu.E., 232
 Starikov, S.V., 184
 Starkov, A.S., 122, 233
 Starkov, I.A., 122, 233
 Starovoytov, A.A., 234
 Staude, I., 225
 Stelmakh, L.S., 104
 Stolin, A.M., 104
 Störmer, M., 212
 Sukhorukov, A.A., 85, 235, 240
 Sun, Y., 184, 235
 Suslina, T.A., 49, 123
 Sylgacheva, D.A., 236
 Sysoeva, A.A., 234
 Takayma, O., 137
 Tartakovskiy, G., 221
 Ten, A.V., 186
 Terekhov, P.D., 138
 Thielecke, J., 169
 Thompson, R.J., 206
 Timoshenko, V.Yu., 166
 Tirozzi, B., 47, 48
 Tkachev, D.L., 32
 Tolchennikov, A.A., 63
 Torba, S.M., 78
 Tranter, M.R., 66
 Tretyakov, D.A., 28
 Tretyakov, S.A., 189, 228, 247
 Treviño, C., 237
 Tribelsky, M.I., 238
 Trofimov, M.Yu., 73, 124
 Trofimov, V.A., 244
 Tsupak, A.A., 50
 Tsvetkov, D.V., 25
 Tsvetkova, A.V., 114
 Tsypkin, A.N., 242
 Turalchuk, P., 207, 239
 Tyukhtin, A.V., 163
 Ul'yanov S.V., 125
 Ustinov, A.V., 227
 Utkin, A.B., 125
 Vabishchevich, P.P., 225
 Vakulenko, S.A., 19, 60, 75
 Valovik, D.V., 80
 Vartanyan, T.A., 234
 Vasilchuk, V., 126
 Vavulin, D.N., 240
 Vdovicheva, N.K., 70, 93
 Vendik, I.B., 207, 215, 241
 Vendik, O., 239, 241
 Vergeles, S.S., 221
 Vialov, V., 128
 Vinogradov, A.P., 145, 225
 Vitebskiy, I., 187, 237
 Vladimirov, Yu.V., 36
 Voogt, I.J., 172
 Voroshilov, P.M., 190
 Vossmeier, T., 212
 Vovchuk, D.A., 189
 Voytova, T.A., 242
 Vyshenskaya, T., 131
 Wang, Y.S., 57
 Weber, A., 60
 Weisgerber, L., 169
 Weller, H., 212
 Wennergren, U., 75
 Wohler, M., 169
 Wojda, P., 127
 Wong, Z.J., 193
 Yakovlev, V.V., 166
 Yakovlev, Yu.A., 28
 Yakubenko, A.E., 50
 Yakubenko, T.A., 50
 Yan, M., 157
 Yang, C.-C., 61
 Yashenko, V., 239
 Yashina, N.F., 127
 Yatsyk, M.V., 22
 Yatsyk, V.V., 22
 Yermakov, O.Y., 243
 Yu, J.S., 178
 Yulin, A.V., 222, 242
 Yunakovskiy, A.D., 33
 Yurchuk, V.N., 110
 Zaboronkova, T.M., 79, 127
 Zabotnov, S.V., 166
 Zagurskiy, D.Yu., 244
 Zaitseva, A.S., 79
 Zakharenko, A.D., 73, 124
 Zakharova, I.G., 91, 244
 Zalipaev, V., 128
 Zavorokhin, G.L., 129
 Zhang, Ch., 57
 Zhang, X., 193
 Zharov, A.A., 245, 246
 Zharov, A.A., Jr., 245, 246
 Zharova, N.A., 245, 246
 Zhelyazkova, K., 130
 Zhibalova, Yu.A., 30
 Zhirihin, D.V., 247
 Zhuchkova, M.G., 130
 Zhukovskiy, S.V., 134
 Zograf, G.P., 248
 Zubyuk, V.V., 202
 Zuev, D.A., 162, 184, 196, 248
 Zverzhcovskiy, V., 131
 Zywietz, U., 143, 159, 249